

Volume 174S1 October 2022

ISSN 0959-8049

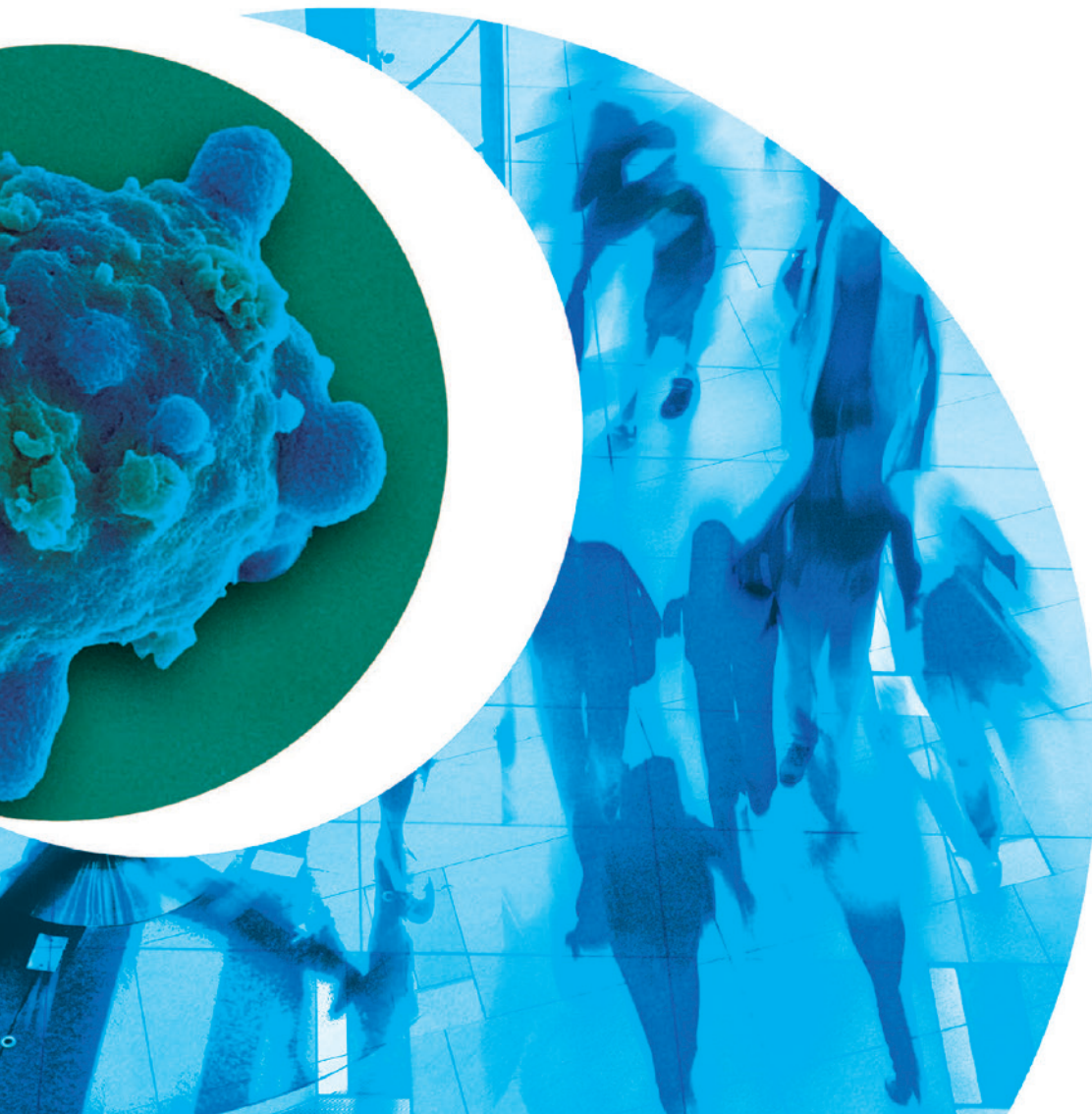
# EJC

EUROPEAN JOURNAL OF CANCER

**34th EORTC-NCI-AACR Symposium on Molecular  
Targets and Cancer Therapeutics**

**26–28 October 2022  
Barcelona, Spain**

**ABSTRACT BOOK**



*The future of cancer therapy*



# European Journal of Cancer

## 34th EORTC-NCI-AACR Symposium on Molecular Targets and Cancer Therapeutics 26–28 October 2022 Barcelona, Spain

### Abstract Book



Publication of this supplement was supported by the EORTC



# European Journal of Cancer

## Editor-in-Chief:

Alexander M.M. Eggermont  
Princess Máxima Center for Pediatric Oncology & University Medical Center Utrecht,  
Utrecht, Netherlands

## Editors:

Preclinical Cancer Research: Ulrich Keilholz, Berlin, Germany  
Epidemiology and Prevention: Valery E.P.P. Lemmens, Utrecht, The Netherlands  
Tumour Immunotherapy: Aurélien Marabelle, Villejuif, France  
Breast Cancer: Giuseppe Curigliano, Milan, Italy  
Suzette Delalogue, Villejuif, France  
Gastrointestinal Cancers: Volker Heinemann, Munich, Germany  
Michel Ducreux, Villejuif, France  
Genitourinary Cancers: Karim Fizazi, Villejuif, France  
Head and Neck Cancer: J.P. Machiels, Brussels, Belgium  
Hemato-Oncology: Roch Houot, Rennes, France  
Lung Cancer: Joachim Aerts, Rotterdam, The Netherlands  
Martin Schuler, Essen, Germany  
Gynaecological Cancers: Ignace Vergote, Leuven, Belgium  
Endocrine, Sarcomas and Other Rare Tumours: Hans Gelderblom, Leiden, The Netherlands  
Melanoma: Dirk Schadendorf, Essen, Germany  
Neuro-Oncology: Martin van den Bent, Rotterdam, The Netherlands  
Paediatric Oncology: Rob Pieters, Utrecht, The Netherlands

## Founding Editor:

Henri Tagnon

## Past Editors:

Michael Peckham, London, UK; Hans-Jörg Senn, St Gallen, Switzerland; John Smyth, Edinburgh, UK

## Editorial Office:

Elsevier, The Boulevard, Langford Lane, Kidlington, Oxford OX5 1GB, UK  
Tel: +44 (0) 1865 843590, Email: [ejcancer@elsevier.com](mailto:ejcancer@elsevier.com)

## EDITORIAL BOARD

### CLINICAL ONCOLOGY

R. Baird (UK)	J.C. Horiot (Switzerland)	D. Nam (Korea)
N. Brügger (Denmark)	D. Jäger (Germany)	J. Perry (Canada)
R. Califano (UK)	A. Katz (Brazil)	J. Ringash (Canada)
E. Calvo (Spain)	C. Le Tourneau (France)	A. Rody (Germany)
F. Cardoso (Portugal)	Y. Loriot (France)	M. Schmidinger (Austria)
E. de Vries (The Netherlands)	C-C. Lin (Taiwan)	S. Sleijfer (The Netherlands)
A. Dicker (USA)	P. Lorigan (UK)	S. Stacchiotti (Italy)
R. Dummer (Switzerland)	C. Massard (France)	C. Sternberg (Italy)
S. Erridge (UK)	K. McDonald (Australia)	A. van Akkooi (The Netherlands)
H. Gelderblom (The Netherlands)	F. Meunier (Belgium)	E. Van Cutsem (Belgium)
B. Geoerger (France)	A. Miller (Canada)	G. Velikova (UK)
B. Hasan (Belgium)	T. Mok (Hong Kong)	E. Winquist (Canada)
		T. Yap (UK)

### BASIC SCIENCE, PRECLINICAL AND TRANSLATIONAL RESEARCH

P. Allavena (Italy)	J.M. Irish (USA)	S. Singh (Canada)
J. Anderson (UK)	H.E.K. Kohrt (USA)	J. Stagg (Canada)
M. Brogini (Italy)	J. Lunec (UK)	A. Virós (UK)
C. Catapano (Switzerland)	A.M. Müller (USA)	B. Weigelt (USA)
C. Caux (France)	D. Olive (France)	T. Yap (UK)
J. Carreras (Spain)	A.G. Papavassiliou (Greece)	N. Zaffaroni (Italy)
E. Garattini (Italy)	V. Rotter (Israel)	
R. Giavazzi (Italy)	V. Sanz-Moreno (UK)	

### EPIDEMIOLOGY AND PREVENTION

B. Armstrong (Australia)	D. Forman (France)	P. Peeters (The Netherlands)
P. Autier (France)	A. Green (Australia)	S. Sanjose (Spain)
V. Bataille (UK)	K. Hemminki (Germany)	M.K. Schmidt (The Netherlands)
J.M. Borrás (Spain)	C. Johansen (Denmark)	I. Soerjomataram (France)
C. Bosetti (Italy)	L.A. Kiemeny (The Netherlands)	H. Storm (Denmark)
H. Brenner (Germany)	I. Lansdorp-Vogelaar (The Netherlands)	L.V. van de Poll-Franse (The Netherlands)
L.E.M. Duijm (The Netherlands)	E. Lynge (Denmark)	H.M. Verkooijen (The Netherlands)
J. Faivre (France)	M. Maynadié (France)	E. de Vries (The Netherlands)
S. Franceschi (France)	H. Möller (UK)	R. Zanetti (Italy)

### PAEDIATRIC ONCOLOGY

C. Bergeron (France)	G. Chantada (Argentina)	L. Sung (Canada)
A. Biondi (Italy)	F. Doz (France)	M. van den Heuvel-Eibrink (The Netherlands)
E. Bouffet (Canada)	A. Ferrari (Italy)	M. van Noessel (The Netherlands)
M. Cairo (USA)	M.A. Grootenhuis (The Netherlands)	
H. Caron (The Netherlands)	K. Pritchard-Jones (UK)	

# European Journal of Cancer

## Aims and Scope

The *European Journal of Cancer* (EJC) integrates preclinical, translational, and clinical research in cancer, from epidemiology, carcinogenesis and biology through to innovations in cancer treatment and patient care. The journal publishes original research, reviews, previews, editorial comments and correspondence.

The EJC is the official journal of the European Organisation for Research and Treatment of Cancer (EORTC) and the European Society of Breast Cancer Specialists (EUSOMA).

For a full and complete Guide for Authors, please go to <http://www.ejcancer.com>

**Advertising information.** Advertising orders and inquiries can be sent to: USA, Canada and South America: Bill Hipple Advertising Department, Elsevier Inc., 230 Park Avenue, Suite 800, New York, NY 10169-0901, USA; phone: (+1) 646-671-0385; fax: (+1) (212) 633 3820; e-mail: [b.hipple@elsevier.com](mailto:b.hipple@elsevier.com). Europe and ROW: Advertising Sales: Elsevier Pharma Solutions; 125 London Wall, London, EC2Y 5AS, UK; Tel.: +48 500 259 970; fax: +44 (0) 20 7424 4433; e-mail: [k.lach.1@elsevier.com](mailto:k.lach.1@elsevier.com).

**Publication information:** *European Journal of Cancer* (ISSN 0959-8049). For 2022, volumes 160–177 (18 issues) are scheduled for publication. Subscription prices are available upon request from the Publisher or from the Elsevier Customer Service Department nearest you or from this journal's website (<http://www.elsevier.com/locate/ejca>). Further information is available on this journal and other Elsevier products through Elsevier's website (<http://www.elsevier.com>). Subscriptions are accepted on a prepaid basis only and are entered on a calendar year basis. Issues are sent by standard mail (surface within Europe, air delivery outside Europe). Priority rates are available upon request. Claims for missing issues should be made within six months of the date of despatch.

**Orders, claims, and journal inquiries:** Please visit our Support Hub page <https://service.elsevier.com> for assistance.

### Author inquiries

You can track your submitted article at <http://www.elsevier.com/track-submission>. You can track your accepted article at <http://www.elsevier.com/trackarticle>. You are also welcome to contact Customer Support via <http://support.elsevier.com>.

**Language (usage and editing services).** Please write your text in good English (American or British usage is accepted, but not a mixture of these). Authors who feel their English language manuscript may require editing to eliminate possible grammatical or spelling errors and to conform to correct scientific English may wish to use the English Language Editing service available from Elsevier's WebShop <http://webshop.elsevier.com/languageediting/> or visit our customer support site <http://support.elsevier.com> for more information.

### Illustration services

Elsevier's WebShop (<http://webshop.elsevier.com/illustrationservices>) offers Illustration Services to authors preparing to submit a manuscript but concerned about the quality of the images accompanying their article. Elsevier's expert illustrators can produce scientific, technical and medical-style images, as well as a full range of charts, tables and graphs. Image 'polishing' is also available, where our illustrators take your image(s) and improve them to a professional standard. Please visit the website to find out more.

**Funding body agreements and policies.** Elsevier has established agreements and developed policies to allow authors whose articles appear in journals published by Elsevier, to comply with potential manuscript archiving requirements as specified as conditions of their grant awards. To learn more about existing agreements and policies please visit <http://www.elsevier.com/fundingbodies>.

© 2022 Elsevier Ltd. All rights reserved

This journal and the individual contributions contained in it are protected under copyright, and the following terms and conditions apply to their use in addition to the terms of any Creative Commons or other user license that has been applied by the publisher to an individual article:

**Photocopying.** Single photocopies of single articles may be made for personal use as allowed by national copyright laws. Permission is not required for photocopying of articles published under the CC BY license nor for photocopying for non-commercial purposes in accordance with any other user license applied by the publisher. Permission of the publisher and payment of a fee is required for all other photocopying, including multiple or systematic copying, copying for advertising or promotional purposes, resale, and all forms of document delivery. Special rates are available for educational institutions that wish to make photocopies for non-profit educational classroom use.

**Derivative Works.** Users may reproduce tables of contents or prepare lists of articles including abstracts for internal circulation within their institutions or companies. Other than for articles published under the CC BY license, permission of the publisher is required for resale or distribution outside the subscribing institution or company.

For any subscribed articles or articles published under a CC BY-NC-ND license, permission of the publisher is required for all other derivative works, including compilations and translations.

**Storage or Usage.** Except as outlined above or as set out in the relevant user license, no part of this publication may be reproduced, stored in a retrieval system or transmitted in any form or by any means, electronic, mechanical, photocopying, recording or otherwise, without prior written permission of the publisher.

**Permissions.** For information on how to seek permission visit [www.elsevier.com/permissions](http://www.elsevier.com/permissions).

**Author rights.** Author(s) may have additional rights in their articles as set out in their agreement with the publisher (more information at <http://www.elsevier.com/authorsrights>).

**Notice.** Practitioners and researchers must always rely on their own experience and knowledge in evaluating and using any information, methods, compounds or experiments described herein. Because of rapid advances in the medical sciences, in particular, independent verification of diagnoses and drug dosages should be made. To the fullest extent of the law, no responsibility is assumed by the publisher for any injury and/or damage to persons or property as a matter of products liability, negligence or otherwise, or from any use or operation of any methods, products, instructions or ideas contained in the material herein.

Although all advertising material is expected to conform to ethical (medical) standards, inclusion in this publication does not constitute a guarantee or endorsement of the quality or value of such product or of the claims made of it by its manufacturer.

♻️ The paper used in this publication meets the requirements of ANSI/NISO Z39.48-1992 (Permanence of Paper).

# Peer Review Policy for the *European Journal of Cancer (EJC)*

The practice of peer review is to ensure that only good science is published. It is an objective process at the heart of good scholarly publishing and is carried out by all reputable scientific journals. Our reviewers therefore play a vital role in maintaining the high standards of the *European Journal of Cancer (EJC)* and all manuscripts are peer reviewed following the procedure outlined below.

## Initial manuscript evaluation

The Editors first evaluate all manuscripts. In some circumstances it is entirely feasible for an exceptional manuscript to be accepted at this stage. Those rejected at this stage are insufficiently original, have serious scientific flaws, have poor grammar or English language, or are outside the aims and scope of the journal. Those that meet the minimum criteria are passed on to experts for review.

Authors of manuscripts rejected at this stage will be informed within 2 weeks of receipt.

## Type of Peer Review

The EJC employs single blind review, where the reviewer remains anonymous to the authors throughout the process.

## How the reviewer is selected

Reviewers are matched to the paper according to their expertise. Our reviewer database contains reviewer contact details together with their subject areas of interest, and this is constantly being updated.

## Reviewer reports

Reviewers are asked to evaluate whether the manuscript:

- Is original
- Is methodologically sound
- Follows appropriate ethical guidelines
- Has results which are clearly presented and support the conclusions
- Correctly references previous relevant work

Reviewers are not expected to correct or copyedit manuscripts. Language correction is not part of the peer review process. Reviewers are requested to refrain from giving their

personal opinion in the “Reviewer blind comments to Author” section of their review on whether or not the paper should be published. Personal opinions can be expressed in the “Reviewer confidential comments to Editor” section.

## How long does the peer review process take?

Typically the manuscript will be reviewed within 2-8 weeks. Should the reviewers’ reports contradict one another or a report is unnecessarily delayed a further expert opinion will be sought. Revised manuscripts are usually returned to the Editors within 3 weeks and the Editors may request further advice from the reviewers at this time. The Editors may request more than one revision of a manuscript.

## Final report

A final decision to accept or reject the manuscript will be sent to the author along with any recommendations made by the reviewers, and may include verbatim comments by the reviewers.

## Editor’s Decision is final

Reviewers advise the Editors, who are responsible for the final decision to accept or reject the article.

## Special Issues / Conference Proceedings

Special issues and/or conference proceedings may have different peer review procedures involving, for example, Guest Editors, conference organisers or scientific committees. Authors contributing to these projects may receive full details of the peer review process on request from the editorial office.

## Becoming a Reviewer for the *EJC*

If you are not currently a reviewer for the *EJC* but would like to be considered as a reviewer for this Journal, please contact the editorial office by e-mail at [ejcancer@elsevier.com](mailto:ejcancer@elsevier.com), and provide your contact details. If your request is approved and you are added to the online reviewer database you will receive a confirmatory email, asking you to add details on your field of expertise, in the format of subject classifications.

## Contents

---

### Late Breaking Abstracts

**28 October 2022**

Plenary Session 7 S1

### Oral Abstracts

**27 October 2022**

Plenary Session 3 S3

**28 October 2022**

Plenary Session 6 S5

Plenary Session 7 S7

### Posters Spotlight Abstract

**27 October 2022**

Posters in the Spotlight session  
Poster in the Spotlight 1 S9

**28 October 2022**

Posters in the Spotlight session  
Poster in the Spotlight 2 S10

### Poster Abstracts

**26 October 2022**

Poster Session

Angiogenesis and Vascular Disrupting Agents	S11
Animal Models	S12
Cellular Therapies	S15
Molecular Targeted Agents 1	S15
New Agents for Pediatric Oncology	S28
New Drugs	S29
Preclinical Models	S41
Radiation Interactive Agents	S45
Tumour Immunology and Inflammation	S45
Other	S48

**27 October 2022**

Poster Session

Apoptosis inducers	S50
Combination Therapies	S52

Cytotoxics (including Antimetabolites, Anthracyclin, Alkylating agents, Aurora kinases, Polo-like kinase, Topoisomerase inhibitors, Tubulin-binding compounds)	S65
Epigenetic Modulators (HDAC Bromodomain modulators, EZH2)	S67
Immune Checkpoints	S69
Molecular Targeted Agents 2	S71

## **28 October 2022**

### **Poster Session**

Antibody-drug Conjugates	S86
Cancer Genomics	S94
Functional Genomics	S98
DNA Repair Modulation (including PARP, CHK, ATR, ATM)	S99
Drug Delivery	S101
Drug Design	S103
Drug Resistance and Modifiers	S105
Drug Screening	S113
Molecular Profiling	S116
New Therapies in Immuno Oncology	S122
Novel Clinical Trial Design	S128
Oncolytic Viruses and Vaccination	S128

### **Author Index**

**S129**

28 October 2022

15:00–16:30

PLENARY SESSION 7

## Late Breaking and Proffered Papers

## 1LBA

Late Breaking

**A Phase I trial of BI 1810631, a HER2 tyrosine kinase inhibitor (TKI), as monotherapy in patients (pts) with advanced/metastatic solid tumors with HER2 aberrations**

F. Opdam<sup>1</sup>, J. Heymach<sup>2</sup>, M. Barve<sup>3</sup>, Y.L. Wu<sup>4</sup>, N. Gibson<sup>5</sup>, B. Sadrolhefazi<sup>6</sup>, J. Serra<sup>7</sup>, K. Yoh<sup>8</sup>, N. Yamamoto<sup>9</sup>. <sup>1</sup>The Netherlands Cancer Institute, Department of Clinical Pharmacology, Amsterdam, Netherlands; <sup>2</sup>MD Anderson Cancer Center- University of Texas, Department of Thoracic/Head and Neck Medical Oncology- Division of Cancer Medicine, Houston, USA; <sup>3</sup>Mary Crowley Cancer Research, Chief Medical Officer, Dallas, USA; <sup>4</sup>Guandong Provincial People's Hospital, Department of Medical Oncology, Guangzhou, China; <sup>5</sup>Boehringer Ingelheim Pharma GmbH & Co. KG, Department of Translational Medicine and Clinical Pharmacology, Biberach, Germany; <sup>6</sup>Boehringer Ingelheim Pharmaceuticals- Inc., Department of Oncology, Ridgefield, USA; <sup>7</sup>Boehringer Ingelheim España S.A., Department of Clinical Development & Operations, Barcelona, Spain; <sup>8</sup>National Cancer Center Hospital East, Department of Thoracic Oncology, Kashiwa, Japan; <sup>9</sup>National Cancer Center Hospital, Department of Thoracic Oncology, Tokyo, Japan

**Background:** There is an unmet need for effective TKIs against HER2 mutations in solid tumors, particularly in NSCLC. BI 1810631 is a HER2 selective TKI that covalently binds to both wild-type and mutated HER2 receptors, including exon 20 insertions, whilst sparing EGFR signaling; preclinical data suggest good tolerability and efficacy. This Phase Ia/Ib, open-label, non-randomized study aims to determine the safety, MTD, PK, pharmacodynamics and preliminary efficacy of BI 1810631 in pts with HER2 aberration-positive solid tumors (NCT04886804). Here, we present results of Phase 1a.

**Materials and Methods:** In Phase Ia, pts with HER2 aberration-positive (overexpression, gene amplification, somatic mutation, or gene rearrangements) advanced/unresectable/metastatic solid tumors refractory/unsuitable for standard therapy were enrolled. Pts received escalating doses of BI 1810631 BID (starting dose: 15 mg) or BI 1810631 QD (starting dose: 60 mg). Phase Ib will initially include 30 pts with advanced HER2 tyrosine kinase domain mutation-positive, pre-treated NSCLC. Additional cohorts may be included in the future. Primary endpoints: MTD based on number of DLTs; number of pts with DLTs (Phase Ia); objective response (Phase Ib). Secondary endpoints: number of pts with DLTs throughout entire treatment period and PK parameters (Phase Ia/Ib); duration of response, disease control, duration of disease control and PFS (Phase Ib).

**Results:** As of 14 September 2022, 26 patients have been treated in the US, The Netherlands, Japan and China. Patients had NSCLC (n = 15), colorectal cancer (n = 2), other tumors (n = 7) or unreported tumor type (n = 2). Most patients had a pathological HER2 mutation (n = 15). Patients received BI 1810631 15, 30, 60, 100, 150 mg BID (n = 3/3/4/4/3) or 60, 120 mg QD (n = 5/4). Median number of cycles was 4 (range 1–11). Treatment is ongoing in 16 patients. To date, one DLT has been observed (grade 2 edema in the 60 mg BID cohort). The MTD has not been reached with either schedule. Treatment-related adverse events (TRAEs) have been reported in 13 pts (50%). The most common TRAEs were diarrhea (n = 6), increased alkaline phosphatase (n = 2) and hypoalbuminemia (n = 2). There were no grade ≥3 TRAEs. In 19 patients evaluable for response the ORR (regardless of confirmation) was 37% (n = 7, all PRs; NSCLC: n = 5; esophagus, cholangiocarcinoma: n = 1). The DCR was 84%. In 11 NSCLC patients evaluable for response, the ORR was 45% and the DCR was 91%.

**Conclusions:** These preliminary data indicate that BI 1810631 is well tolerated and shows encouraging anti-tumor activity in patients with HER2 aberration-positive solid tumors. Recruitment into Phase Ia is ongoing.

**Conflict of interest:**

Advisory Board:

John Heymach reports participating in an advisory board for AstraZeneca, EMD Serono, Boehringer-Ingelheim, Catalyst, Genentech, GlaxoSmithKline, Hengrui Therapeutics, Eli Lilly, Spectrum, Sanofi, Takeda, Mirati Therapeutics, BMS, BrightPath Biotherapeutics, Janssen Global Services, Nexus Health Systems, Pneuma Respiratory, RefleXion, Chugai Pharmaceuticals. Noboru Yamamoto reports participating in an advisory board for Eisai, Takeda, Boehringer Ingelheim, Cimic, Chugai Pharma.

**Board of Directors:**

John Heymach reports participating in a board of directors for Rexnana Foundation.

**Corporate-sponsored Research:**

John Heymach reports receiving corporate-sponsored research fees from AstraZeneca, Boehringer-Ingelheim, Spectrum and Takeda. Yi-Long Wu reports receiving corporate-sponsored research fees from AstraZeneca, BMS, Pfizer.

**Other Substantive Relationships:**

Frans Opdam reports other substantive relationships with Boehringer Ingelheim, Astra Zeneca, GSK, Cytovation, InteRNA technologies, Merus, Taiho, and Pierre-Fabre. John Heymach reports receiving royalties and licensing fees from Spectrum. Minal Barve reports other substantive relationships with Texas Oncology physician Associates Mary Crowley Cancer Research. Yi-Long Wu reports receiving speaker fees from AstraZeneca, Boehringer Ingelheim, BMS, Eli Lilly, Hengrui, MSD, Pfizer, Sonofi, Roche. Neil Gibson, Behbood Sadrolhefazi, and Josep Serra report being employed with Boehringer Ingelheim. Kiyotaka Yoh reports other substantive relationships with AstraZeneca, Boehringer Ingelheim, Bristol-Myers Squibb, Chugai, Daiichi sankyo, Janssen, Kyowa kirin, Lilly, Novartis, Taiho, Abbvie, AstraZeneca, Daiichi sankyo, Lilly, MSD, Pfizer, Taiho, Takeda. Noboru Yamamoto reports other substantive relationships with Chugai Pharma, Ono Pharmaceutical, Lilly Japan, Sysmex, Daiichi Sankyo/UCB Japan, Eisai, Chiome Bioscience, Otsuka, Taiho pharmaceutical, Astellas Pharma, Novartis, Daiichi Sankyo, Takeda, Kyowa Hakkō Kirin, Bayer, Pfizer, Janssen, MSD, Abbvie, Bristol-Meyers Squibb, Merck Serono, GlaxoSmithKline, Sumitomo Dainippon, Carma Biosciences, Genmab/Seattle Genetics, Shionogi, Toray Industries.

## 2LBA

Late Breaking

**Pivotal topline data from the phase 1/2 TRIDENT-1 trial of repotrectinib in patients with ROS1+ advanced non-small cell lung cancer (NSCLC)**

B.C. Cho<sup>1</sup>, J. Lin<sup>2</sup>, D.R. Camidge<sup>3</sup>, V. Velcheti<sup>4</sup>, B. Solomon<sup>5</sup>, S. Lu<sup>6</sup>, K.H. Lee<sup>7</sup>, S.W. Kim<sup>8</sup>, S. Kao<sup>9</sup>, R. Dziadziuszko<sup>10</sup>, M. Beg<sup>11</sup>, M. Nagasaka<sup>12</sup>, E. Felip<sup>13</sup>, B. Besse<sup>14</sup>, C. Springfeld<sup>15</sup>, S. Popat<sup>16</sup>, J. Wolf<sup>17</sup>, D. Trone<sup>18</sup>, S. Stopatschinskaja<sup>19</sup>, A. Drilon<sup>20</sup>. <sup>1</sup>Yonsei Cancer Center- Yonsei University College of Medicine, Department of Internal Medicine, Seoul, South Korea; <sup>2</sup>Massachusetts General Hospital- Harvard Medical School, Hematology/Oncology, Massachusetts, USA; <sup>3</sup>University of Colorado Denver- Anschutz Medical Campus, Medical Oncology, Aurora, USA; <sup>4</sup>NYU Perlmutter Cancer Center, Department of Medicine at NYU Grossman School of Medicine, New York, USA; <sup>5</sup>Peter MacCallum Cancer Center, Department of Medical Oncology, Melbourne, Australia <sup>6</sup>Shanghai Chest Hospital, Oncology Department, Shanghai, China; <sup>7</sup>Chungbuk National University Hospital, Department of Internal Medicine, Cheongju-si, South Korea; <sup>8</sup>Asan Medical Center, Department of Oncology, Seoul, South Korea; <sup>9</sup>The Chris O'Brien Lifehouse, Oncology Department, Camperdown, Australia; <sup>10</sup>Medical University of Gdansk- Early Clinical Trials Centre, Department of Oncology & Radiotherapy, Gdansk, Poland; <sup>11</sup>UT Southwestern Medical Center, Oncology Department, Dallas, USA; <sup>12</sup>University of California Irvine- School of Medicine, Hematology/Oncology, Irvine, USA; <sup>13</sup>Vall d'Hebron University Hospital- Vall d'Hebron Institute of Oncology VHIO, Oncology Department, Barcelona, Spain; <sup>14</sup>Paris-Saclay University- Gustave Roussy Cancer Center, Cancer Medicine, Villejuif, France; <sup>15</sup>Heidelberg University Hospital- National Center for Tumor Diseases, Department of Medical Oncology, Heidelberg, Germany; <sup>16</sup>The Royal Marsden NHS Foundation Trust, Oncology Department, London, United Kingdom; <sup>17</sup>Centrum für Integrierte Onkologie - Uniklinik Köln, Oncology Department, Köln, Germany; <sup>18</sup>Turning Point Therapeutics Inc, Biostatistics and Programming, San Diego, USA; <sup>19</sup>Turning Point Therapeutics Inc, Clinical Development, San Diego, USA; <sup>20</sup>Memorial Sloan Kettering Cancer Center- Weill Cornell Medical College, Early Drug Development Service, New York, USA

**Background:** Repotrectinib is a next-generation ROS1 tyrosine kinase inhibitor (TKI) currently under evaluation in the global phase 1/2 TRIDENT-1 trial (NCT03093116). We report updated results in TKI-naïve and -pretreated patients with advanced, ROS1 fusion-positive (ROS1+) NSCLCs.

**Materials and methods:** Patients were assigned to one of four expansion cohorts (EXP). The primary endpoint was objective response rate (ORR) by Blinded Independent Central Review (BICR) using RECIST v1.1. Secondary endpoints included duration of response (DOR), clinical benefit rate (CBR), progression-free survival (PFS), overall survival (OS), intracranial objective response rate (iORR) in patients with measurable brain metastases, ORR in TKI-pretreated cancers with ROS1 G2032R, safety, and patient reported outcomes. Efficacy included pooled data from phase 1 (all dose levels



meeting pooling criteria) and phase 2 (RP2D of 160 mg QD x 14 days followed by 160 mg BID) and safety included all patients who received 1 dose of repotrectinib.

**Results:** As of June 20, 2022, the primary efficacy population included 71 TKI-naïve patients (EXP-1) and 56 TKI-pretreated patients with no prior chemotherapy (CT; EXP-4). ORR was 79% (95% CI 68,88) in EXP-1 and 38% (95% CI 25,52) in EXP-4. DOR (95% CI) by KM estimate was 86% (76,96) at 12 months in EXP-1 and 80% (62,98) at 6 months in EXP-4. Median duration of treatment in EXP-1 and -4 was 13.3 (0.8,60.6+) and 8.25 (0.5,24.8) months, respectively. ORR in pooled patients (EXP-2 to -4) with ROS1 G2032R (n=17) was 59%; six-month DOR by KM estimate was 70% (95% CI 42,98). Additional efficacy data are shown in the table. In the overall safety population of 444 patients, most treatment-related adverse events (AE) were grade 1-2. All-grade treatment-emergent AEs reported in >20% of patients were dizziness (61%), dysgeusia (49%), constipation (37%), anemia (35%), paresthesia (32%), dyspnea (29%), fatigue (24%), nausea (21%), and ALT increase (21%). Dose reductions and drug discontinuation were required in 34.0% and 9.7% of patients, respectively.

#### TRIDENT-1: Repotrectinib in ROS1+ advanced NSCLC

	EXP-1 ROS1 TKI-naïve n = 71	EXP-4 1 prior ROS1 TKI + no prior CT n = 56	EXP-2 1 prior ROS1 TKI + 1 platinum- based CT n = 26	EXP-3 2 prior ROS1 TKIs + no prior CT n = 18
ORR % (95% CI)	79 (68,88)	38 (25,52)	42 (23,63)	28 (10,54)
iORR % (95% CI)	88 (47,100) n = 8	42 (15,72) n = 12	50 (7,93) n = 4	0 n = 2
Landmark DOR % (95% CI)				
6-mo	91 (83,99)	80 (62,98)	64 (35,92)	60 (17,100)
12-mo	86 (76,96)	60 (36,83)	40 (8,72)	30 (0,77)
Landmark PFS % (95% CI)				
6-mo	91 (84,98)	67 (54,81)	39 (19,58)	22 (3,41)
12-mo	80 (70,90)	44 (29,59)	15 (0,33)	7 (0,21)

**Conclusions:** Repotrectinib achieves durable activity, including intracranial responses, in TKI-naïve and TKI-pretreated patients with ROS1+ advanced NSCLC, and those with ROS1 G2032R. Repotrectinib safety is well characterized, manageable, and compatible with long-term use.

#### Conflict of interest:

Ownership:  
DT, SS Turning Point Therapeutics Employee and Stock or Stock Options Advisory Board:  
BCC- (Scientific Advisory Board) KANAPH Therapeutic Inc, Brigebio therapeutics, Cyrus therapeutics, Guardant Health, Joseah BIO Board of Directors:  
BCC- Gencurix Inc, Interpark Bio Convergence Corp.  
Corporate-sponsored Research:  
BCC- (Research funding) Novartis, Bayer, AstraZeneca, MOGAM Institute, Dong-A ST, Champions Oncology, Janssen, Yuhan, Ono, Dizal Pharma, MSD, Abbvie, Medpacto, Glnnovation, Eli Lilly, Blueprint medicines, Interpark Bio Convergence Corp.  
JL (Research funding) Hengrui Therapeutics, Turning Point Therapeutics, Neon Therapeutics, Relay Therapeutics, Bayer, Elevation Oncology, Roche, Linnaeus Therapeutics, Nuvalent, and Novartis  
SL (Research funding) AstraZeneca, Hutchison, BMS, Heng Rui Beigene and Roche, Hansoh  
Other Substantive Relationships:  
BCC -(Founder) DAAN Biotherapeutics, (Consulting role) Novartis, AstraZeneca, Boehringer-Ingelheim, Roche, BMS, Ono, Yuhan, Pfizer, Eli Lilly, Janssen, Takeda, MSD, Medpacto, Blueprint medicines

#### 3LBA Late Breaking NMS-01940153E, an MPS1 inhibitor with anti-tumor activity in relapsed or refractory unresectable Hepatocellular carcinoma

M. Reig<sup>1-4</sup>, S. Damian<sup>5</sup>, D. Roberti<sup>6</sup>, S. Maruzzelli<sup>6</sup>, P. Crivori<sup>6</sup>, L. Gianellini<sup>7</sup>, M.T. De Pietro<sup>6</sup>, N. Personeni<sup>8-9</sup>, M. Sanduzzi-Zamparelli<sup>1</sup>, M. Duca<sup>5</sup>, L. Disconzi<sup>10</sup>, A. Montagnoli<sup>11</sup>, A. Galvani<sup>7</sup>, E. Ardini<sup>11</sup>, A. Isacchi<sup>12</sup>, E. Colajori<sup>6</sup>, C. Davite<sup>6</sup>, L. Mahnke<sup>6</sup>, L. Rimassa<sup>8-9</sup>, <sup>1</sup>Hospital Clínica Barcelona, Liver Oncology Unit, Barcelona, Spain; <sup>2</sup>BCLC group, FUNDACIO/IDIBAPS, Barcelona, Spain; <sup>3</sup>CIBEREHD, Madrid, Spain; <sup>4</sup>Universitat de Barcelona, Barcelona, Spain; <sup>5</sup>Fondazione IRCCS Istituto

Nazionale dei Tumori, Medical Oncology Unit, Milan, Italy; <sup>6</sup>Nerviano Medical Sciences S.r.l., Global Clinical Development, Nerviano – Milan, Italy; <sup>7</sup>Nerviano Medical Sciences S.r.l., Discovery Pharmacology, Nerviano – Milan, Italy; <sup>8</sup>IRCCS Humanitas Research Hospital, Medical Oncology and Hematology Unit, Rozzano – Milano, Italy; <sup>9</sup>Humanitas University, Department of Biomedical Sciences, Pieve Emanuele, Milan, Italy; <sup>10</sup>IRCCS Humanitas Research Hospital, Radiologia Diagnostica, Rozzano – Milano, Italy; <sup>11</sup>Nerviano Medical Sciences S.r.l., Global Asset Leadership, Nerviano – Milan, Italy; <sup>12</sup>Nerviano Medical Sciences S.r.l., Oncology – Discovery, Nerviano – Milan, Italy

**Background:** Monopolar Spindle 1 (MPS1) kinase is overexpressed in several tumors, including hepatocellular carcinoma (HCC) where it correlates with tumor features and poor overall and disease-free survival. NMS-01940153E is a highly potent and selective inhibitor of MPS1 kinase with strong preclinical anti-tumor activity in different tumor types. It was previously tested in a FIH study, CL1-81694-001 (EudraCT 2014-002023-10), where activity in HCC patients was detected. The Sponsor, Nerviano Medical Sciences S.r.l., further explored preclinical activity and initiated a Phase 1-2 study, MPSA-153-001 (EudraCT 2020-001002-26), in patients with HCC undergone more than one systemic therapy.

**Materials and Methods:** Preclinically, a panel of HCC cell lines was assessed for antiproliferative activity. In the phase 1, a 3+3 escalation design started at 100 mg/m<sup>2</sup>/wk, with planned dose-increment of 25-35%, to determine MTD and RP2D. Secondary objectives were safety, PK, and preliminary anti-tumor activity. NMS-01940153E was administered IV, on days 1, 8 and 15 every 4 wks.

**Results:** Here we present results from the phase 1 part of the trial and supporting pre-clinical data. In HCC lines NMS-01940153E showed ~2-Log higher anti-proliferative activity compared to sorafenib, lenvatinib, and regorafenib. Twelve HCC patients were evenly enrolled. Median age was 64 years, median number of prior systemic therapies was 2 (range 1-3). At the data cut-off date, 16-AUG-2022, 10 patients had discontinued treatment, 7 due to disease progression (PD). Two DLTs (neutropenia G4 with either sepsis G4 or urinary tract infection G2) occurred at 135 mg/m<sup>2</sup>/wk. Overall, most frequent (≥10%) any grade drug-related TEAE were neutropenia (50% in the overall population, 2 out of 6 patients at 100 mg/m<sup>2</sup>/wk, all G≥3), chromaturia and thrombocytopenia/platelet count decrease (25%, 1/6 and 0/6), anemia, asthenia, diarrhea, and injection site reaction (16.7%, 0/6, 1/6, 0/6 and 0/6).

Out of 11 patients evaluable for efficacy, two (one for each dose level) had confirmed investigator-assessed PR with duration of 11.1 and 40.3 wks (2.5 and 9.3 months); both discontinued treatment due to PD at 6.5 and 11.1 months from treatment start, respectively. Two further patients, one for each dose level, had long-lasting SD, still on treatment at cycles 18 and 11. Three patients, two with PR and one with SD, showed AFP down-modulation. The PK profiles of parent and metabolite showed an increase in exposure with the dose with approximately 4-day half-life for the parent drug; the metabolite accounted for 3% of the parent drug exposure.

**Conclusion:** NMS-01940153E showed preclinical and clinical activity in HCC with manageable safety features. This MPS1 inhibitor is currently under evaluation in the phase 2 part of the study in patients with unresectable HCC previously treated with standard-of-care systemic therapy.

#### Conflict of interest:

Corporate-sponsored Research:  
M. Reig: Bayer, Ipsen  
L. Rimassa: Agios, ARMO BioSciences, AstraZeneca, BeiGene, Eisai, Exelixis, Fibrogen, Incyte, Ipsen, Lilly, MSD, Nerviano Medical Sciences, Roche, Zymeworks.  
N. Personeni: Basilea, Merck Serono, Servier  
Other Substantive Relationships:  
M. Reig: consulting fees and/or travel support: AstraZeneca, Bayer, BMS, Eli Lilly, Geneos, Ipsen, Merck, Roche, Universal DX Lecture fees: AstraZeneca, Bayer, BMS, Eli Lilly, Gilead, Roche  
L. Rimassa: consulting fees from Amgen, ArQule, AstraZeneca, Basilea, Bayer, BMS, Celgene, Eisai, Exelixis, Genenta, Hengrui, Incyte, Ipsen, IQVIA, Lilly, MSD, Nerviano Medical Sciences, Roche, Sanofi, Servier, Taiho Oncology, Zymeworks lecture fees from AbbVie, Amgen, Bayer, Eisai, Gilead, Incyte, Ipsen, Lilly, Merck Serono, Roche, Sanofi travel expenses from Astra Zeneca  
N. Personeni: consulting fees from Amgen, Merck Serono, Servier lectures fees from AbbVie, Gilead, Lilly, Sanofi travel expenses from Amgen, ArQule

27 October 2022

10:00–11:30

PLENARY SESSION 3

## Proffered Papers

1

Oral

**A radiohaptent capture system for CAR T cells that tracks them *in vivo* and improves efficacy**

K. Kurtz<sup>1</sup>, L. Eibler<sup>2</sup>, M. Dacek<sup>1</sup>, L. Carter<sup>3</sup>, S. Cheal<sup>4</sup>, D. Veach<sup>2</sup>, S. Qureshy<sup>5</sup>, J. Han<sup>1</sup>, E. Reynaud<sup>2</sup>, S. Verma<sup>1</sup>, M. McDevitt<sup>6</sup>, B. Punzalan<sup>1</sup>, D.B. Vargas<sup>1</sup>, B.H. Santich<sup>7</sup>, S. Monette<sup>8</sup>, A. Kesner<sup>9</sup>, N.K. Cheung<sup>7</sup>, S. Larson<sup>2</sup>, D. Scheinberg<sup>10</sup>, S. Krebs<sup>2</sup>. <sup>1</sup>Memorial Sloan Kettering, Molecular Pharmacology, New York, USA; <sup>2</sup>Memorial Sloan Kettering, Radiology, New York, USA; <sup>3</sup>Memorial Sloan Kettering, Medicine, New York, USA; <sup>4</sup>Weill Cornell Medicine, Radiology, New York, USA; <sup>5</sup>Weill Cornell Medicine, Medicine, New York, USA; <sup>6</sup>Memorial Sloan Kettering, Radiology, Radiology, USA; <sup>7</sup>Memorial Sloan Kettering, Pediatrics, New York, USA; <sup>8</sup>Memorial Sloan Kettering, Research Facilities, New York, USA; <sup>9</sup>Memorial Sloan Kettering, Medical Physics, New York, USA; <sup>10</sup>Memorial Sloan Kettering, Memorial Kettering, New York, USA

**Background:** CAR T cell therapy has become an important therapeutic tool for the treatment of B-cell neoplasms. However, the development of CAR T cell therapy outside of hematologic malignancies has stalled. As such, there is an unmet need to understand why CAR T cell therapy fails, which would be aided through the creation of tools to track them *in vivo*. Additionally, endowing CAR T cells with potent orthogonal anti-tumor activity has emerged as a strategy to improve upon CAR T cell efficacy. To accomplish both goals, we engineered a class of theranostic “THOR” CAR T cells that express a membrane-bound scFv, huC825, that binds DOTA-radiohaptens with pM affinity; these haptent chelands can be conjugated with radionuclides with therapeutic potential or diagnostic imaging capabilities.

**Methods:** We engineered 19BBZ anti-CD19 CAR T cells to express huC825 (THOR CAR T cells) and confirmed transduction of these cells with flow cytometry. To assess the cytolytic ability and effector function of THOR CAR T cells, we used the Matador co-culture assay and measured the cytokine secretion of these co-cultures. We tested the potential to track THOR CAR T cells *in vivo* using PET/CT following intravenous DOTA-based radiohaptent tracer administration in immunodeficient (NSG) mice bearing subcutaneous CD19+ Raji tumors. We also tested the ability of THOR CAR T cells to synergize with therapeutic radionuclide therapy. We evaluated the anti-tumor efficacy using whole animal bioluminescence imaging, tumor size measurements, and median animal survival.

**Results:** We successfully transduced THOR CAR T cells, which demonstrated similar *in vitro* anti-tumor effects and cytokine secretion as parent 19BBZ CAR T cells. *In vivo* tracking experiments with 86Y-DOTA-Bn radiotracer showed that THOR CAR T cells can be observed at day 7 post T cell administration, peak at day 14, and persist until at least day 28. 86Y-DOTA-Bn uptake was specific to THOR CAR T cells, as minimal uptake was observed in mice transplanted with 19BBZ CAR T cells. Importantly, we noted rapid renal clearance of unbound tracer resulting in high contrast images. In efficacy assays *in vivo*, we demonstrated the synergy between 225Ac-Proteus-DOTA and THOR CAR T cells, as shown by a significant decrease in tumor burden and increase in median survival (THOR CAR treated = 26 days, treated with THOR CAR plus 225Ac-Proteus-DOTA = 32 days,  $p = .04$ ,  $n = 6$  per group). In contrast, mice receiving 19BBZ CAR T cells with or without 225Ac-Proteus-DOTA showed no improvements in anti-tumor efficacy.

**Conclusions:** We show the pharmacokinetics of THOR CAR T cells can be probed *in vivo* following systemic administration of radiotracer using serial PET/CT imaging. Furthermore, we demonstrate a CAR T cell can be potentiated by systemically administered cytotoxic radionuclide that are then delivered selectively to tumors by the THOR cells.

**Conflict of interest:**

Ownership: MSK has filed for patent protection on behalf of M.M.D., S.M.C., D.R.V., B.H.S., N.K.C., D.A.S., S.M.L. and S.K. for inventions related to this work.

Advisory Board: N.K.C. is an advisor to, or owns equity in Abpro, Alexs Lemonade Stand Foundation, Biotec Pharmacon, Eureka Therapeutics, Keystone Symposia, Partner Therapeutics, St. Jude-VIVA Forum, and Y-mAbs Therapeutics that may work in areas related to this study.

Other Substantive Relationships: S.M.C. has licensed IP to Y-mAbs.

2

Oral

**ROS induction as a strategy to target persist cancer cell metabolism**

O. Eichhoff<sup>1</sup>, C. Stoffel<sup>1</sup>, L. Briker<sup>1</sup>, P. Turko<sup>1</sup>, G. Karsai<sup>2</sup>, V. Paulitschke<sup>3</sup>, N. Zamboni<sup>4</sup>, Z. Balazs<sup>5</sup>, A. Tastanova<sup>1</sup>, R. Wegmann<sup>4</sup>, J. Mena<sup>4</sup>, V. Viswanathan<sup>6</sup>, C. TuPro<sup>1</sup>, M. Krauthammer<sup>5</sup>, S. Schreiber<sup>6</sup>, T. Hornemann<sup>2</sup>, M. Distel<sup>7</sup>, B. Snijder<sup>4</sup>, R. Dummer<sup>1</sup>, M. Levesque<sup>1</sup>. <sup>1</sup>University Hospital Zurich, Dermatology, Zurich, Switzerland; <sup>2</sup>University Hospital Zurich, Clinical Chemistry, Zurich, Switzerland; <sup>3</sup>Medical University of Vienna, Dermatology, Vienna, Austria; <sup>4</sup>Swiss Federal Institute of Technology, Institute for Molecular Systems Biology, Zurich, Switzerland; <sup>5</sup>University Hospital Zurich, Biomedical Informatics, Zurich, Switzerland; <sup>6</sup>Harvard University, Broad Institute, Cambridge, USA; <sup>7</sup>St. Anna Children's Cancer Research Institute, Pediatric Cancer Research, Vienna, Austria

**Background:** Metastatic melanoma is the most aggressive form of skin cancer and is raising in incidence every year. The MAPK pathway plays a key role in melanoma development making it an important therapeutic target. FDA-approved kinase inhibitors targeting the mutated BRAF kinase have shown excellent clinical response rates. However, there are limited treatment options for melanomas with mutations in the NRAS kinase. Inhibition of downstream effector molecules (e.g. MEK) have been shown to have limited efficacy. Therefore, the discovery of small molecules that target NRAS-mutated melanoma cells and overcome resistance to MEK inhibitors is a high medical priority.

**Material and methods:** We have used multi-omics analysis to decipher the energetic phenotype of drug-resistant melanoma cells and uncover novel vulnerabilities. We have performed high-throughput screening (HTS) of small molecules to discover novel compounds that target these cellular phenotypes. We used *ex vivo* pharmacology to investigate the drug responses of 62 tumors from metastatic patients. We performed xenograft experiments to test HTS compounds in combination with MEK inhibitors and analyzed the tumors by scRNA sequencing. We profiled the CCLE panel of 486 cancer cell lines to extend our findings to other cancer types and correlated cell susceptibility with available omics data analyses.

**Results:** Metabolic reprogramming is an emerging hallmark of resistance and melanoma cells with a mesenchymal transcriptional profile adopt a quiescent metabolic program to resist the cellular stress response triggered by MEK inhibitor resistance. We identified ionophoric copper-chelators (ICC) to target metabolically quiescent melanoma cells resistant to MEK inhibition by increasing reactive oxygen species (ROS). *In vivo* experiments and scRNA sequencing have shown that heterogeneity within the tumor requires the combination of a ROS inducer and a MEK inhibitor to inhibit tumor growth and metastasis. By *ex vivo* screening of tumors we found that MEK inhibitor-resistant tumors benefited significantly from treatment with ICC alone or in combination with the MEK inhibitor binimetinib. Finally, we profiled the CCLE cell line panel and revealed that oxidative stress responses and translational depression are biomarkers for ROS-inducer sensitivity, independent of cancer indications.

**Conclusion:** We found that persist cells with low metabolic activity withstand drug treatment but have elevated intracellular ROS levels. This intracellular susceptibility can be used to target melanoma cells. Profiling of the CCLE panel revealed that oxidative stress responses and translational repression are biomarkers of susceptibility to ROS inducers, independent of cancer indication. These results link transcriptional plasticity to a metabolic phenotype that can be inhibited by ROS inducers in melanoma and other cancers.

**Conflict of interest:**

Ownership: Ossia Eichhoff, Luzia Briker, Corinne Stoffel, Reinhard Dummer and Mitch Levesque are co-authors of a patent claiming the use of ionophoric copper-chelators with MEK inhibitors in the use of cancer.

3

Oral

**Integrated molecular and clinical analysis of BRAF-mutant glioma in adults**

K. Schreck<sup>1</sup>, P. Langat<sup>2</sup>, T. Li<sup>3</sup>, V. Bhav<sup>2</sup>, C. Pratilas<sup>4</sup>, C. Eberhart<sup>5</sup>, W.L. Bi<sup>6</sup>. <sup>1</sup>Johns Hopkins University School of Medicine, Neurology and Oncology, Baltimore, USA; <sup>2</sup>Harvard School of Medicine, Medicine, Boston, USA; <sup>3</sup>Johns Hopkins School of Medicine, Biomedical Engineering, Baltimore, USA; <sup>4</sup>Johns Hopkins University School of Medicine, Pediatrics and Oncology, Baltimore, USA; <sup>5</sup>Johns Hopkins University School of Medicine, Pathology, Baltimore, USA; <sup>6</sup>Brigham and Women's Hospital, Neurosurgery, Boston, USA

**Background:** The significance of *BRAF* alterations in adult glioma is increasingly acknowledged given their potential therapeutic implications.

While the spectrum of *BRAF* alterations in pediatric glioma is well-characterized, the implications of *BRAF* alterations on the clinical course and response to treatment in adult glioma remain unclear. In this study, we characterize a large (300 patient) multi-institutional, retrospective cohort of adults with *BRAF*-mutated gliomas by functional class. We identify the clinical phenotypes, genomic signatures, and molecular features associated with each *BRAF* alteration functional class to assess prognostic implications and guide therapeutic approaches.

**Materials and Methods:** 206 adults with *BRAF*-mutated gliomas—along with a pediatric sub-cohort—were identified from Dana-Farber/Brigham Cancer Center, Johns Hopkins Hospital, GENIE, and TCGA. Patients were grouped into cohorts based on the putative activation mechanism of their *BRAF* alteration: Class I (RAS-independent/ dimerization-independent), II (RAS-independent/ dimerization-dependent), III (RAS-dependent/ dimerization-dependent), as well as rearrangements, amplifications, and other unclassified alterations.

**Results:** Adult *BRAF*-mutant gliomas harbor distinct clinical and molecular features from pediatric, with a higher prevalence of *BRAF*<sup>V600E</sup> (Class I) and *BRAF*-fusions in pediatric tumors. Class II/III, gains and unclassified alterations are almost exclusively present in adult glioma. Other genomic associations observed within functional classes (NF1 loss with Class II/III; *EGFR* with unclassified) are consistent with their putative mechanism of ERK-activation. *BRAF*<sup>V600E</sup> alterations are associated with improved survival in adults with glioma compared with other *BRAF* alterations, though not in glioblastoma, while increased age is associated with inferior survival. A subset of additional alterations is associated with better (K1AA1549 HR 0.48;  $p < 0.02$ ) or worse (CDKN2A/B loss, *TERT*-promoter, *PTEN*;  $p < 0.01$ ) survival. Moreover, glioma with *BRAF*<sup>V600E</sup> alterations expressed higher levels of transcripts associated with MEK inhibitor sensitivity. In 13 patients treated with targeted therapy (6 PXA, 4 GBM, 2 PA, 1 other astrocytoma), 6 had a clinical benefit. Median time to progression was 5 months and overall survival was 165 months (53 months in glioblastoma).

**Conclusions:** This large cohort of *BRAF*-altered adult glioma demonstrates a broad range of alterations. Molecular alterations and clinical outcomes varied across *BRAF* classes, suggesting distinct biological characteristics.

#### Conflict of interest:

Corporate-sponsored Research: Dr. Schreck's laboratory receives research support from Springworks Therapeutics.

4

Oral

#### Improved outcomes in women with *BRAF*-mutant melanoma treated with *BRAF*/*MEK*-targeted therapy across randomized clinical trials. A systematic review and meta-analysis

L. Pala<sup>1</sup>, T. De Pas<sup>1</sup>, E. Pagan<sup>2</sup>, C. Catania<sup>3</sup>, V. Bagnardi<sup>4</sup>, F. Conforti<sup>1</sup>.  
<sup>1</sup>European institute of oncology, Division of Melanoma- Sarcomas and Rare Tumors- European Institute of Oncology, Milan, Italy; <sup>2</sup>University of Milan-Bicocca- Milan- Italy, Department of Statistics and Quantitative Methods- Milan, Italy; <sup>3</sup>European Institute of Oncology, Division of Thoracic Oncology- European Institute of Oncology- IRCCS, Milan, Italy; <sup>4</sup>University of Milan-Bicocca- Milan- Italy, Department of Statistics and Quantitative Methods, Milan, Italy

**Background:** Preclinical and clinical evidence suggests that patients' sex could be associated with the outcome of patients with advanced *BRAF* V600-mutant melanoma, treated with the combination of B-RAF and MEK-inhibitors. We performed a systematic review and meta-analysis of all RCTs testing the combination of *BRAF* and MEK inhibitors, to assess the interaction between treatment effect and patients' sex.

**Material and Methods:** We systematically searched PubMed, Embase, and Scopus, up to Jan 30, 2022, for RCTs testing the combination of *BRAF* and MEK-inhibitors versus monotherapy with B-RAF inhibitors, in patients with *BRAF* V600-mutant, advanced, cutaneous melanoma, that had available hazard ratios (HRs) for progression or death according to patients' sex.

The primary endpoint was to assess the difference in treatment efficacy between men and women, measured in terms of the difference in progression-free survival (PFS) log(HR). The secondary endpoint was the difference in overall survival (OS) log(HR). We calculated the pooled PFS and OS HRs and 95% CI in men and women using a random-effects model, and assessed the heterogeneity between the two estimates using an interaction test.

**Results:** Four phase III and one phase II RCTs trials and 2113 patients were included in the analysis.

925 (44%) patients were female and 1494 (71%) had ECOG PS of 0. 110 patients (5%) had tumors in stage III, 302 (14%) M1a, 367 (17%) M1b and 1232 (58%) M1c.

The majority of patients had normal LDH blood values at baseline (1192; 56%) and a tumor harboring a *BRAF* V600E mutation (1763; 83%).

In experimental arms, twenty-nine percent of patients (617) received dabrafenib + trametinib (D + T) combination, 12% (247) vemurafenib + cobimetinib (V+C) and 9% (192) encorafenib + binimetinib (E + B).

In control arms, 13% (266) received dabrafenib monotherapy (D) and 37% (791) vemurafenib monotherapy (V).

In women, the combination of *BRAF* and MEK-inhibitors halved the risk of progression or death as compared with *BRAF*-inhibitor monotherapy (pooled PFS-HR: 0.50, 95%CI 0.41–0.61). In men, the benefit obtained with *BRAF* and MEK inhibitors combination was significantly smaller (pooled PFS-HR: 0.63, 0.54–0.74;  $p^{\text{heterogeneity}} = 0.05$ ).

There was no substantial inter-study heterogeneity among single-study estimates neither in women ( $I^2 = 18.3\%$ ), nor in men ( $I^2 = 0.0\%$ ).

A similar trend was observed for OS: the pooled OS-HR was 0.59 (95% CI, 0.48–0.74) in women and only 0.75 (95% CI, 0.63–0.88) in men ( $p^{\text{heterogeneity}} = 0.13$ ).

There was no substantial inter-study heterogeneity among single-study estimates neither in women ( $I^2 = 13.3\%$ ), nor in men ( $I^2 = 0.0\%$ ).

**Conclusion:** These results demonstrate meaningful sex-based heterogeneity of response to combination targeted therapy in patients with advanced B-RAF mutant melanoma, that should be taken into account by future research aimed to improve treatment effectiveness.

#### No conflict of interest.

5

Oral

#### Lineage plasticity in prostate cancer depends on *FGFR* and *JAK/STAT* inflammatory signaling

J. Chan<sup>1</sup>, S. Zaidi<sup>2</sup>, J. Love<sup>2</sup>, J. Zhao<sup>2</sup>, M. Setty<sup>3</sup>, K. Wadosky<sup>4</sup>, A. Gopalan<sup>5</sup>, Z.N. Choo<sup>3</sup>, S. Persad<sup>6</sup>, O. Chaudhary<sup>3</sup>, T. Xu<sup>3</sup>, I. Masilionis<sup>3</sup>, M. Morris<sup>7</sup>, L. Mazutis<sup>8</sup>, R. Chaligne<sup>3</sup>, Y. Chen<sup>2</sup>, D. Goodrich<sup>4</sup>, W. Karthaus<sup>9</sup>, D. Pe'er<sup>3</sup>, C. Sawyers<sup>2</sup>. <sup>1</sup>Memorial Sloan Kettering Cancer Center, Thoracic Oncology, New York, USA; <sup>2</sup>Memorial Sloan Kettering Cancer Center, Human Oncology and Pathogenesis Program, New York, USA; <sup>3</sup>Memorial Sloan Kettering Cancer Center, Program for Computational and Systems Biology, New York, USA; <sup>4</sup>Roswell Park Cancer Institute, Department of Pharmacology and Therapeutics, Buffalo, USA; <sup>5</sup>Memorial Sloan Kettering Cancer Center, Pathology, New York, USA; <sup>6</sup>Columbia University, Computer Science, New York, USA; <sup>7</sup>Memorial Sloan Kettering Cancer Center, Genitourinary Oncology, New York, USA; <sup>8</sup>Vilnius University, Institute of Biotechnology, Vilnius, Lithuania; <sup>9</sup>EPFL, Swiss Institute for Experimental Cancer Research, Lausanne, Switzerland

**Background:** The inherent plasticity of tumor cells provides a mechanism of resistance to molecularly targeted therapies, exemplified by adeno-to-neuroendocrine lineage transitions in prostate and lung cancer. Here we investigate the root cause of lineage plasticity following *Trp53* and *Rb1* loss in genetically engineered mouse models, murine and patient-derived organoid cultures, and patient biospecimens with castrate-resistant prostate cancer.

**Materials and methods:** We performed single-cell transcriptomic analysis in time-course experiments in murine prostate organoids and genetically engineered mouse models following *Trp53* and *Rb1* deletion. We conducted additional single-cell profiling in an independent cohort of patients with metastatic castrate-resistant prostate cancer. Genetic and pharmacological studies in murine and patient-derived organoids served as functional validation.

**Results:** In time-course experiments following *Trp53* and *Rb1* loss, we observe rapid collapse of cell-type fidelity with the emergence of a mixed luminal and basal phenotype with additional EMT-like features. To quantify dynamic changes in plasticity, we develop scBLender, a suite of computational methods that measure basal-luminal mixing as a proxy for plasticity. We leverage these plasticity metrics to identify *Fgfr* and *Jak-Stat* inflammatory signaling as putative drivers of plasticity that are activated early in the time-course prior to any corresponding morphological changes as well as under therapeutic pressure. Genetic and pharmacologic inhibition of *Jak1/2* combined with *Fgfr* blockade in murine and patient-derived organoids not only reversed the plastic state to wild-type morphology, but also restored sensitivity to antiandrogen therapy in models with residual AR expression. Single-cell analysis of clinical biospecimens confirms the presence of mixed basal-luminal cells with elevated *JAK/STAT* and *FGFR* signaling in a subset of patients with metastatic disease, with implications for stratifying patients for clinical trials.

**Conclusions:** Collectively, we show that lineage plasticity initiates quickly as a cell-autonomous process that is further increased in the *in vivo* setting, and through newly developed computational approaches, we identify a pharmacological strategy that restores lineage identity using clinical grade inhibitors of the *JAK/STAT* and *FGFR* pathways.

**Conflict of interest:**

Other Substantive Relationships: C.S. is on the board of directors of Novartis, is a cofounder of ORIC Pharmaceuticals, and is a coinventor of the prostate cancer drugs enzalutamide and apalutamide, covered by U.S. patents 7,709,517, 8,183,274, 9,126,941, 8,445,507, 8,802,689, and 9,388,159 filed by the University of California. C.S. is on the scientific advisory boards of the following biotechnology companies: Agios, Beigene, Blueprint, Column Group, Foghorn, Housey Pharma, Nextech, KSQ Therapeutics, Petra Pharma, and PMV Pharma, and is a cofounder of Seragon Pharmaceuticals, purchased by Genentech/Roche in 2014. D.P. is on the scientific advisory board of Insitro. W. K. is a coinventor of organoid technology.

28 October 2022

11:30–13:30

## PLENARY SESSION 6

**New drugs on the horizon**

6

Oral

**STAR0602, a novel TCR agonist antibody, demonstrates potent anti-tumor activity in refractory solid tumor models through the expansion of a novel, polyclonal effector memory T cell subset**

J.L. Gulley<sup>1</sup>, A. Bayliffe<sup>2</sup>, R. Donahue<sup>1</sup>, Y.T. Tsai<sup>1</sup>, K. Liu<sup>3</sup>, M. Katraggada<sup>2</sup>, J. Hsu<sup>2</sup>, L.L. Siu<sup>4</sup>, E.J. Wherry<sup>5</sup>, R. Chopra<sup>3</sup>, J. Schlom<sup>1</sup>, Z. Su<sup>3</sup>. <sup>1</sup>National Cancer Institute- NIH, Center for Immuno-Oncology, Bethesda, USA; <sup>2</sup>Marengo Therapeutics, Research, Cambridge, USA; <sup>3</sup>Marengo Therapeutics, Clinical Development, Cambridge, USA; <sup>4</sup>University of Toronto, Princess Margaret Cancer Center, Toronto, Canada; <sup>5</sup>University of Pennsylvania, Systems Pharmacology & Translational Therapeutics, Philadelphia, USA

**Background:** Limitations with agents that activate endogenous T cell responses to cancer, particularly in the setting of solid tumors, supports the study of alternative mechanisms. STAR0602 is a bifunctional antibody—fusion molecule that selectively activates and expands a sub-set of human  $\alpha\beta$  T cells expressing the germline—encoded variable b6 and b10 regions of the T cell receptor (TCR). STAR0602 simultaneously engages a novel, direct TCR activation with a cis-binding cytokine co-stimulation through the fusion of IL-2 to an inactivated Fc domain bearing an anti-TCR Vb6/Vb10 Fab.

**Methods:** The effects of STAR0602 on healthy human and cancer patient T cells was assessed *in vitro* by flow cytometry and NanoString. A murine surrogate (mSTAR0602) was tested as a monotherapy in multiple murine syngeneic tumor models (including PD1-insensitive and refractory), with tumor re—challenge and cellular depletion studies to assess long-term protection and cell—specific activities, respectively. EMT6 tumors were excised for IHC staining and phenotyping of tumor-infiltrating lymphocytes (TILs) using flow cytometry and scRNAseq/TCRseq.

**Results:** STAR0602 induced expansion of Vb6/Vb10T cell subsets preferentially in CD8<sup>+</sup> T cells over CD4<sup>+</sup> T cells. Compared to controls and anti-CD3 mAbs, STAR0602—stimulated T cells adopted a novel, highly activated phenotype with markers of both effector and central memory T cells ( $T_{EM}/T_{CM}$ ). STAR0602 also boosted the *ex vivo* expansion of antigen-specific T cells from HPV<sup>+</sup> individuals (both healthy donor and cancer patient). Consistently across multiple syngeneic murine tumor models, mSTAR0602 monotherapy either eradicated tumors, or led to substantial tumor regressions. mSTAR0602-cured mice also demonstrated long-term protection from tumor re-challenge. *In vivo* anti-tumor activity was shown to be dependent on the accumulation of Vb6/Vb10T cells, and analysis of murine TILs showed expanded Vb6/Vb10 T cells were almost exclusively polyclonal  $T_{EM}$  or  $T_{CM}$  cells, with almost no exhausted or regulatory T cells.

**Conclusions:** STAR0602 is a first-in-class T cell activator that selectively targets subsets of the “germline TCR repertoire.” *In vitro*, STAR0602 promotes the expansion of a novel T cell phenotype with hallmarks of both effector and long-lived memory cells, and *in vivo* mSTAR0602 demonstrates potent and durable single-agent anti-tumor activity in PD1—insensitive solid tumor models, that is dependent on Vb6/Vb10 memory T cells. The modulation of the TME, striking increase in TCR diversity, and functional immune memory observed in murine models suggests that STAR0602 could promote a fundamental remodelling of adaptive immune responses to solid tumors via a PD1-independent mechanism, and thus represents a novel therapeutic strategy for patients. A phase 1/2 trial of STAR0602 in patients with advanced solid tumors is planned to commence in 2022.

**Conflict of interest:**

Ownership: Marengo Therapeutics.  
Advisory Board: Marengo Therapeutics.  
Board of Directors: Marengo Therapeutics.

7

Oral

**Dose escalation study of OMO-103, a first in class Pan-MYC-inhibitor in patients (pts) with advanced solid tumors**

E. Garralda<sup>1</sup>, V. Moreno<sup>2</sup>, G. Alonso<sup>3</sup>, E. Corral<sup>4</sup>, T. Hernandez-Guerrero<sup>5</sup>, J. Ramon<sup>4</sup>, B. Doger de Spéville<sup>5</sup>, E. Martinez<sup>6</sup>, L. Soucek<sup>7</sup>, M. Niewel<sup>8</sup>, E. Calvo<sup>9</sup>. <sup>1</sup>Vall d'Hebron Institute of Oncology VHIO, Director- Early Drug Development Unit, Barcelona, Spain; <sup>2</sup>START Madrid-FJD- Hospital Fundación Jiménez Díaz, Director Clinical Research Phase 1 Trials Unit, Madrid, Spain; <sup>3</sup>Vall d'Hebron Institute of Oncology VHIO, Clinical Investigator- Early Drug Development Unit, Barcelona, Spain; <sup>4</sup>START Madrid-CIOCC- Centro Integral Oncológico Clara Campal, Clinical Investigator- Phase 1 Trials Unit, Madrid, Spain; <sup>5</sup>START Madrid-FJD- Hospital Fundación Jiménez Díaz, Clinical Investigator- Phase 1 Trials Unit, Madrid, Spain; <sup>6</sup>Vall d'Hebron Institute of Oncology VHIO, SC- Phase I Clinical Trials, Barcelona, Spain; <sup>7</sup>Peptomyc- SL, Founder, Barcelona, Spain; <sup>8</sup>Peptomyc- SL, Chief Medical Officer, Barcelona, Spain; <sup>9</sup>START Madrid-CIOCC- Centro Integral Oncológico Clara Campal, Director of Clinical Research- START Madrid-HM CIOCC Early Phase Program, Madrid, Spain

**Background:** MYC has a key role in driving and maintaining human tumors. However, MYC has long been perceived as an “undruggable” target and, to date, there is still no MYC inhibitor approved for clinical use. Omomyc is a MYC dominant negative mini-protein, previously used to inhibit MYC function both *in vitro* and *in vivo*, demonstrating a potent therapeutic impact in various mouse models of cancer. Here we present the dose escalation results of a Phase 1 study testing OMO-103, an Omomyc-based mini-protein developed by Peptomyc S.L.

**Material and Methods:** Phase I dose escalation study used the conventional 3 + 3 design, with 6 dose levels ranging from 0.48 to 9.72 mg/kg, as a weekly 30-min *i.v.* infusion. The primary objectives were safety and tolerability, while secondary ones were preliminary efficacy according to RECIST 1.1, PK and RP2D. Tumor biopsies were collected at screening and at the end of the dose limiting toxicity (DLT) period (3 weeks) to assess MYC-levels, Ki67, CC3 and transcriptomics, among other indicators.

**Results:** 22 patients with advanced solid tumors were included. 50% women and men, pts had a range of 3–13 prior treatment lines. ECOG 0 and 1 were equally distributed. The most common treatment related adverse events (TRAE) were mainly grade 1 infusion related reactions (IRR) like chills, fever, nausea, rash, hypotension. 58 TRAEs (80.5%) were grade 1, 12 (16.6%) grade 2 and 1 (1.4%) grade 3. Higher dose levels were associated with more IRRs but easily treated with (pre)medication. 1 DLT was observed: grade 2 pancreatitis (DL 5), 18 SAE, only one considered related. At the time of data cut-off (June22) 4 patients were non evaluable for response. 7 patients achieved SD. 2 pts with PDAC, 2 CRC, 1 NSCLC, 1 Sarcoma, 1 Salivary Gland Carcinoma. Remarkably, 1 PDAC patient stayed in the study for more than 6 months with tumor shrinkage of 8% of target lesions and a reduction of ctDNA. A sarcoma patient was on treatment for more than 7 months and the salivary gland carcinoma patient is still ongoing after 11 months.

The PK analysis revealed a plasma half-life of approximately 50 h. No ADAs were detected in any of the patients, even after long term treatment. Drug activity is supported by a strong association of stable disease with a distinctive dose-dependent cytokine signature. Moreover, patients responding to the drug display modulation of the *bona fide* MYC target CD47 as well as of anti-tumor immune related markers such as calprotectin and OX-40. Further intratumoral PK data and target engagement evidence will be presented.

**Conclusion:** OMO-103 demonstrates a favorable safety profile, with early signs of activity that merit further investigation. RP2D has been determined to be DL5 with 6.48 mg/kg. Dose expansion cohorts (Phase 2a) are already planned.

**Conflict of interest:**

Ownership: M. Niewel: Peptomyc S.L. L. Soucek: Peptomyc S.L. E. Calvo: START and OnCoart Associated.

Advisory Board: E. Garralda has Consulting fees from: Roche/Genentech - F. Hoffmann/La Roche, Ellipses Pharma, Neomed Therapeutics1 Inc, Boehringer Ingelheim, Janssen Global Services, SeaGen, Alkermes, Thermo Fisher, Bristol-Mayers Squibb, MabDiscovery, Anaveon, F-Star Therapeutics, Hengrui, Lilly and Novartis. V. Moreno from: Roche, Bayer, BMS, Janssen and Basilea. E. Calvo from: Nanobiotix, ansen-Cilag, Roche/Genentech, TargImmune Therapeutics, Servier, Bristol-Myers Squibb, Amunix, Adcendo, Anaveon, AstraZeneca/MedImmune, Chugai Pharma, MonTa, MSD Oncology, Nouscom, Novartis, OncoDNA, T-Knife, Elevation Oncology, PharmaMar, Ellipses Pharma.

Board of Directors: E. Calvo: START, PharmaMar, EORTC, Sanofi, BeiGene, Novartis.

Corporate-sponsored Research: E.Garralda has institutional research funding from: Novartis/Roche/Thermo Fisher/AstraZeneca/Taiho/BeiGene. E.Calvo has personal research funding from: START.

Other Substantive Relationships: PI or Co-PI, institutional. E.Garralda: Novartis/Roche/Thermo Fisher/AstraZeneca/Taiho/BeiGene. V.Moreno: AbbVie, AceaBio, Adaptimmune, ADC Therapeutics, Aduro, Agenus, Amcure, Amgen, Astellas, AstraZeneca Bayer Beigene BioInvent International AB, BMS, Boehringer, Boehringer, Boston, Celgene, Daiichi Sankyo, DEBIOPHARM, Eisai, e-Terapeutics, Exelixis, Forma Therapeutics, Genmab, GSK, Harpoon, Hutchison, Immunet, Incyte, Inovio, Iovance, Janssen, Kyowa Kirin, Lilly, Loxo, MedSir, Menarini, Merck, Merus, Millennium, MSD, Nanobiotix, Nektar, Novartis, Odonate Therapeutics, Pfizer, Pharma Mar, PharmaMar, Principia, PsiOxus, Puma, Regeneron, Rigotec, Roche, Sanofi, Sierra Oncology, Synthon, Taiho, Takeda, Tesaro, Transgene, Turning Point Therapeutics, Upshersmith.

8

Oral

### Safety and preliminary clinical activity of NVL-520, a highly selective ROS1 inhibitor, in patients with advanced ROS1 fusion-positive solid tumors

A. Drilon<sup>1</sup>, B. Besse<sup>2</sup>, D.R. Camidge<sup>3</sup>, S.H.I. Ou<sup>4</sup>, S.M. Gadgeel<sup>5</sup>, M.L. Johnson<sup>6</sup>, A. Calles<sup>7</sup>, M.J. de Miguel<sup>8</sup>, A.I. Spira<sup>9</sup>, E. Felip<sup>10</sup>, G. Lopes<sup>11</sup>, A.J. van der Wekken<sup>12</sup>, Y.Y. Elamin<sup>13</sup>, J. Green<sup>14</sup>, Y. Sun<sup>15</sup>, J. Soglia<sup>16</sup>, V.W. Zhu<sup>14</sup>, J.J. Lin<sup>17</sup>. <sup>1</sup>Memorial Sloan Kettering Cancer Center, Early Drug Development Service, New York, USA; <sup>2</sup>Institut Gustave Roussy, Cancer Medicine, Villejuif, France; <sup>3</sup>University of Colorado Cancer Center- Anschutz Medical Campus, Thoracic Oncology, Aurora, USA; <sup>4</sup>University of California Irvine Medical Center, Medicine, Orange, USA; <sup>5</sup>Henry Ford Cancer Institute, Internal Medicine, Detroit, USA; <sup>6</sup>Sarah Cannon Research Institute, Oncology, Nashville, USA; <sup>7</sup>Hospital Universitario Gregorio Marañón, Medical Oncology, Madrid, Spain; <sup>8</sup>START Madrid- HM CIOCC, Medical Oncology, Madrid, Spain; <sup>9</sup>NEXT Oncology - Virginia Cancer Specialists, Thoracic and Phase I Program, Fairfax, USA; <sup>10</sup>Hospital Vall d'Hebron, Oncology, Barcelona, USA; <sup>11</sup>Sylvester Comprehensive Cancer Center- University of Miami Miller School of Medicine, Medical Oncology- Thoracic Medical Oncology, Miami, USA; <sup>12</sup>University of Groningen and University Medical Centre Groningen, Pulmonary Oncology, Groningen, Netherlands; <sup>13</sup>MD Anderson Cancer Center, Thoracic Head & Neck Medical Oncology, Houston, USA; <sup>14</sup>Nuvalent Inc., Clinical Development, Cambridge, USA; <sup>15</sup>Nuvalent Inc., Biology, Cambridge, USA; <sup>16</sup>Nuvalent Inc., Translational Development, Cambridge, USA; <sup>17</sup>Massachusetts General Hospital, Medicine, Boston, USA

**Background:** Oncogenic ROS1 fusions drive various malignancies, including 1–3% of non-small cell lung cancers (NSCLC). Rationally designed ROS1 tyrosine kinase inhibitors (TKIs) that surpass the limitations of FDA/EMA-approved (crizotinib/entrectinib) or other investigational agents are a medical need. The novel ROS1 TKI NVL-520 is highly selective and designed to avoid the neurologic toxicities associated with ROS1 TKIs that concurrently inhibit TRK (entrectinib/repotrectinib/taletrectinib). Furthermore, NVL-520 is brain-penetrant and targets a diverse array of ROS1 fusions and recalcitrant resistance mutations, including the ROS1 G2032R solvent-front mutation.

**Materials and Methods:** ARROS-1 (NCT05118789) is a global, tumor-agnostic, phase 1/2 trial of NVL-520. In the ongoing phase 1 dose escalation, patients are required to have a previously treated ROS1 fusion-positive solid tumor, including NSCLC treated with  $\geq 1$  prior ROS1 TKI. Primary objectives are to determine the recommended phase 2 dose (RP2D) and, if applicable, the maximum tolerated dose. Additional objectives include safety, pharmacokinetics (PK), pharmacodynamics, and preliminary activity. Response (RECIST v1.1) was investigator assessed. Data cut: June 13, 2022.

**Results:** Twenty patients (19 NSCLC, 1 pancreatic cancer) have received NVL-520 orally at dose levels of 25–100 mg once daily. Patients received a median of 3 (range: 1–9) prior anticancer therapies, including any ROS1 TKI (100%); investigational ROS1 TKI (85%, including lorlatinib in 55%, repotrectinib in 40%);  $\geq 2$  ROS1 TKIs (75%); any chemotherapy (80%);  $\geq 2$  lines of chemotherapy (50%). At baseline, 55% had CNS metastases and 45% had ROS1 G2032R. No dose-limiting toxicities (DLTs), dose reductions, or drug-related treatment discontinuations have been reported. All treatment-related adverse events (TRAEs) were grade 1. The only TRAE in  $>1$  patient was nausea ( $n = 2$ ). NVL-520 PK analyses demonstrated dose-dependent exposure. Among 12 efficacy-evaluable patients with ROS1+ NSCLC treated at 25–75 mg QD, 6 confirmed partial responses (PRs) were achieved. Shrinkage or resolution of intracranial metastases were observed; no patients had intracranial progression. A PR was achieved in most ( $n = 5/7$ ) ROS1 G2032R-mutant cancers, including lorlatinib or repotrectinib pre-treated tumors. Circulating tumor DNA analyses showed reductions of ROS1

variant allele frequency. The RP2D has not been identified and dose escalation continues.

**Conclusions:** NVL-520 has been well-tolerated up to 100 mg daily with favorable pharmacokinetics. Activity has been demonstrated in heavily pretreated patients (of whom 70% received  $\geq 2$  prior ROS1 TKIs plus chemotherapy), including those with brain metastases and the G2032R mutation.

#### Conflict of interest:

Ownership: Treeline Bio (AD) Nuvalent (JG, JS, YS, VZ) Turning Point Therapeutics, Elevation Oncology (SO).

Advisory Board: Ignity/Genentech/Roche, Loxo/Bayer/Lilly, Takeda/Ariad/Millennium, TP Therapeutics, AstraZeneca, Pfizer, Blueprint Medicines, Helsinn, Beigene, BergenBio, Hengrui Therapeutics, Exelixis, Tyra Biosciences, Verastem, MORE Health, Abbvie, 14ner/Elevation Oncology, ArcherDX, Monopteros, Novartis, EMD Serono, Medendi, Repare RX, Nuvalent, Merus, Chugai Pharmaceutical, Remedica Ltd, mBrace, AXIS, EPG Health, Harborside Nexus, Liberum, RV More, Ology, Amgen, TouchIME, Janssen, Entos, Treeline Bio, Prelude, Applied Pharmaceutical Science, Inc, AiCME, i3 Health, MonteRosa (AD).

Amgen, Astra Zeneca, Bayer, Bristol-Myers Squibb, Daiichi Sankyo, Eli Lilly, F. Hoffmann-La Roche, Glaxo Smith Kline, Janssen, Merck Sharp & Dohme, Merck Serono, Novartis, Peptomyc, Pfizer, Sanofi, Takeda (EF) Genentech/Roche, Pfizer (SG) AbbVie, Amgen, Astellas, AstraZeneca, Axelia Oncology, Black Diamond, Boehringer Ingelheim, Bristol-Myers Squibb, Calithera Biosciences, Checkpoint Therapeutics, CytomX Therapeutics, Daiichi Sankyo, EcoR1, Editas Medicine, Eisai, EMD Serono, G1 Therapeutics, Genentech/Roche, Genmab, Genocoe Biosciences, GlaxoSmithKline, Gritstone Oncology, Ideaya Biosciences, iTeos, Janssen, Lilly, Merck, Mirati Therapeutics, Novartis, Oncorus, Regeneron Pharmaceuticals, Revolution Medicines, Ribon Therapeutics, Sanofi-Aventis, Turning Point Therapeutics, VBL Therapeutics, WindMIL (MJ) Pfizer, Nuvalent, C4 Therapeutics, Turning Point Therapeutics, Elevation Oncology, Novartis, Mirati Therapeutics, Bayer, Genentech, Blueprint Medicines (JL) Syneos health, cell therapy program (MM) Elevation Oncology (SO).

Board of Directors: Grifols (EF).

Corporate-sponsored Research: Pfizer, Exelixis, GlaxoSmithKlein, Teva, Taiho, PharmaMar (AD) 4D Pharma, Abbvie, Amgen, Aptitude Health, AstraZeneca, BeiGene, Blueprint Medicines, Boehringer Ingelheim, Celgene, Cergentis, Chugai pharmaceutical, Cristal Therapeutics, Daiichi-Sankyo, Eli Lilly, Eisai, Genzyme Corporation, GSK, Invitae, IPSEN, Janssen, Onxeo, OSE immunotherapeutics, Pfizer, Roche-Genentech, Sanofi, Takeda, Tolero Pharmaceuticals, Turning Point Therapeutics (BB) Nuvalent (RC, GL, AS) Merck Healthcare KGAA, Fundación Merck Salud (EF) AbbVie, Acerta, Adaptimmune, Amgen, Apexigen, Arcus Biosciences, Array BioPharma, Artios Pharma, AstraZeneca, Atreca, BeiGene, BerGenBio, BioAtla, Boehringer Ingelheim, Calithera Biosciences, Checkpoint Therapeutics, Corvus Pharmaceuticals, Curis, CytomX, Daiichi Sankyo, Dracen Pharmaceuticals, Dynavax, Lilly, Elicio Therapeutics, EMD Serono, Erasca, Exelixis, Fate Therapeutics, Genentech/Roche, Genmab, Genocoe Biosciences, GlaxoSmithKline, Gritstone Oncology, Guardant Health, Harpoon, Helsinn Healthcare SA, Hengrui Therapeutics, Hutchison MediPharma, IDEAYA Biosciences, IGM Biosciences, Immunocore, Incyte, Janssen, Jounce Therapeutics, Kadmon Pharmaceuticals, Loxo Oncology, Lycera, Memorial Sloan-Kettering, Merck, Merus, Mirati Therapeutics, Neolmmune Tech, Neovia Oncology, Novartis, Numab Therapeutics, Nuvalent, OncoMed Pharmaceuticals, Pfizer, PMV Pharmaceuticals, RasCal Therapeutics, Regeneron Pharmaceuticals, Relay Therapeutics, Revolution Medicines, Ribon Therapeutics, Rubius Therapeutics, Sanofi, Seven and Eight Biopharmaceuticals/Birdie Biopharmaceuticals, Shattuck Labs, Silicon Therapeutics, Stem CentRx, Syndax Pharmaceuticals, Takeda Pharmaceuticals, Tarveda, TCR2 Therapeutics, Tempest Therapeutics, Tizona Therapeutics, TMUNITY Therapeutics, Turning Point Therapeutics, University of Michigan, Vyriad, WindMIL, Y-mAbs Therapeutics (MJ) Hengrui Therapeutics, Turning Point Therapeutics, Novartis, Neon Therapeutics, Bayer, Roche/Genentech, Pfizer, Elevation Oncology, Relay Therapeutics, Linnaeus Therapeutics, Nuvalent (JL) Roche, Novartis, MSD, Pharmamar, Cytomex, Abbvie, Achilles, Astra Zeneca, Basilea, Bayer, Biontech, Catalym, Dizal, Fameway, Genentech, Janssen, Menarini, Regeneron and Seattle (MM) Pfizer, Daiichi Sankyo, Revolution Medicine, Merus, Roche, Mirati, BluePrint Medicines, JNJ/Jassen (SO).

Other Substantive Relationships: Medscape, OncLive, PeerVoice, Practitioner Education Resources, Targeted Oncology, Research to Practice, Axis, Peervoice Institute, Paradigm Medical Communications, WebMD, MJH Life Sciences, Med Learning, Imedex, Answers in CME, Clinical Care Options, EPG Health, JNCC/Harborside, Liberum, Remedica Ltd., Wolters Kluwer, Merck, Puma, Merus, Boehringer Ingelheim, Astra Zeneca, Eli Lilly (AD).

Amgen, Astra Zeneca, Bristol-Myers Squibb, Eli Lilly, F. Hoffmann-La Roche, Janssen, Medscape, Merck Sharp & Dohme, PeerVoice, Pfizer, Medical

Trends, Merck Serono, Sanofi, Takeda, TouchONCOLOGY (EF) Pfizer, OncoLive, Northwell Health, Medstar Health (JL) JNJ/Jassen, BeiGene, Pfizer, Lilly, DAVA Oncology LLP, Caris Life Science (SO).

28 October 2022

15:00–16:30

PLENARY SESSION 7

## Late breaking and Proffered Papers

9

Oral

**NCI10329: Phase Ib Sequential Trial of Agents against DNA Repair (STAR) Study to investigate the sequential combination of the Poly (ADP-Ribose) Polymerase inhibitor (PARPi) olaparib (ola) and WEE1 inhibitor (WEE1i) adavosertib (ada) in patients (pts) with DNA Damage Response (DDR)-aberrant advanced tumors, enriched for BRCA1/2 mutated and CCNE1 amplified cancers**

T.A. Yap<sup>1,2</sup>, N. Ngoi<sup>1</sup>, E.E. Dumbrava<sup>1</sup>, D.D. Karp<sup>1</sup>, J. Rodon Ahnert<sup>1</sup>, S. Fu<sup>1</sup>, D.S. Hong<sup>1</sup>, A. Naing<sup>1</sup>, S. Pant<sup>1</sup>, S.A. Piha-Paul<sup>1</sup>, V. Subbiah<sup>1</sup>, A.M. Tsimberidou<sup>1</sup>, D. Dufner<sup>1</sup>, J. Rhudy<sup>1</sup>, S. Gore<sup>3</sup>, S.P. Ivy<sup>4</sup>, Y. Yuan<sup>5</sup>, S.N. Westin<sup>6</sup>, G.B. Mills<sup>7</sup>, F. Meric-Bernstam<sup>1</sup>. <sup>1</sup>The University of Texas MD Anderson Cancer Center, Department of Investigational Cancer Therapeutics, Houston, USA; <sup>2</sup>The University of Texas MD Anderson Cancer Center, Khalifa Institute for Personalized Cancer Therapy, Houston, USA; <sup>3</sup>National Institutes of Health- National Cancer Institute, Cancer Therapy Evaluation Program CTEP, Bethesda, USA; <sup>4</sup>Cancer Therapy Evaluation Program CTEP, National Institutes of Health- National Cancer Institute, Bethesda, USA; <sup>5</sup>The University of Texas MD Anderson Cancer Center, Department of Biostatistics, Houston, USA; <sup>6</sup>The University of Texas MD Anderson Cancer Center, Department of Gynecologic Oncology and Reproductive Medicine, Houston, USA; <sup>7</sup>Knight Cancer Institute, Oregon Health Sciences University, Portland, USA

**Background:** Combination PARPi plus WEE1i (PARPi + WEE1i) induces replication stress (RS), DNA damage, and abrogates the G2 cell cycle checkpoint. Concurrent PARPi + WEE1i administration effectively inhibits tumor growth but is poorly tolerated. Sequential PARPi+WEE1i administration in vivo mirrors concurrent dosing in cells with high basal RS, while normal cells with low basal RS are protected from DNA damage, improving tolerability while preserving efficacy (Fang et al., Cancer Cell 2019). Based on these compelling preclinical data, the NCI CTEP-sponsored STAR study investigated sequential ola+ada in pts with DDR aberrant advanced tumors (NCT04197713).

**Materials and Methods:** Pts with advanced cancer with actionable DDR variants were enrolled. Prior PARPi was allowed. Dose escalation followed Bayesian Optimal Interval Design; Dose Level (DL) 1: ola 300 mg BID days (D) 1–5, 15–19 + ada 250 mg QD D8–12, 22–26; DL 2: ola 300 mg BID D1–5, 15–19 + ada 300 mg QD D8–12, 22–26; Q28 days. Primary objectives were safety and recommended phase 2 dose (RP2D). Secondary objectives were antitumor activity, PK, PD and biomarkers of response/resistance. Serial tumor and blood sampling were obtained for tumor whole exome and RNA sequencing, RAD51-IF, multiplex IHC and ctDNA NGS.

**Results:** 13 pts (M:F 2:11; ECOG PS 0:1: 4/9; mean age: 50y (35–72) with breast (n = 5), ovarian (n = 5), colorectal, gastric, prostate (n = 1) cancers were enrolled. Actionable genomic alterations included BRCA1/2 (n = 8), CCNE1 amplification (n = 3), ARID1A (n = 2), ATM (n = 1), PALB2 (n = 1). 10/13 pts had ≥3 lines of prior systemic therapy; 7/13 had progressed on prior PARPi. 3/13 pts were treated with sequential ola+ada at DL 1, 10/13 at DL 2. Common toxicities: grade (G) 1/2 nausea (10/13), anemia (7/13), fatigue (7/13), vomiting (7/13), and diarrhea (4/13). No DLTs occurred. Non-DLT ≥G3 myelosuppression occurred in 2/13 pts who were heavily pre-treated (≥5 prior lines). Dose reduction occurred in only 1/13 pts even with long term follow-up. 3/12 evaluable pts had RECIST1.1 PR and/or GCIG CA125 response, and 5/12 pts had SD ≥4 mths for 66.7% (8/12) disease control rate; 4 of these 8 pts had progressed on prior PARPi. RECIST1.1 PRs were seen in BRCA2m ER+ breast cancer pt (–57%, 17 wks) and BRCA2m PARPi-resistant ovarian cancer pt (–50%; 26 wks) who had BRCA2m reversion at baseline. A CCNE1 amp ovarian cancer pt had GCIG CA125 response and SD 20 wks. Translational analyses are ongoing.

**Conclusion:** The novel sequential dosing schedule of ola + ada is well tolerated at full monotherapy dosing of each drug, with antitumor activity in pts with post-PARPi DDR aberrant tumors. RP2D was ola 300 mg BID D1–5,

15–19 + ada 300 mg OD D8–12, 22–26; Q28 days. Planned expansion cohorts include (1) pts with BRCA1/2m tumors with intrinsic PARPi resistance and (2) pts with DDR mutated tumors with acquired PARPi resistance.

### Conflict of interest:

Ownership: T.A.Y holds stocks in Seagen.

Advisory Board: T.A.Y has received fees for consulting from AbbVie, AstraZeneca, Acrivon, Adagene, Almac, Aduro, Amphista, Artios, Athena, Atrin, Avoro, Axiom, Baptist Health Systems, Bayer, Beigene, Boxer, Bristol Myers Squibb, C4 Theapeutics, Calithera, Cancer Research UK, Clovis, Cybrea, Diffusion, EMD Serono, F-Star, Genmab, Glenmark, GLG, Globe Life Sciences, GSK, Guidepoint, Idience, Ignyta, I-Mab, ImmuneSensor, Institut Gustave Roussy, Intellisphere, Jansen, Kyn, MEI pharma, Merco, Merck, Natera, Nexys, Novocure, OHSU, OncoSec, Ono Pharma, Pegascy, PER, Pfizer, Piper-Sandler, Prolynx, Repare, resTORbio, Roche, Schrodinger, Theragnostics, Varian, Versant, Viiblome, Xinthera, Zai Labs and ZielBio.

Board of Directors: N/A.

Corporate-sponsored Research: T.A.Y has received research support (paid to his institution) from Acrivon, Artios, AstraZeneca, Bayer, Beigene, BioNTech, Blueprint, BMS, Clovis, Constellation, Cyteir, Eli Lilly, EMD Serono, Forbius, F-Star, Artios, GlaxoSmithKline, Genentech, Haihe, ImmuneSensor, Ionis, Ipsen, Jounce, Karyopharm, KSQ, Kyowa, Merck, Mirati, Novartis, Pfizer, Ribon Therapeutics, Regeneron, Repare, Rubius, Sanofi, Scholar Rock, Seattle Genetics, Tesaro, Vivace and Zenith.

Other Substantive Relationships: N/A.

10

Oral

**CBX-12-101: A first-in-human study of CBX-12, an alphalex peptide drug conjugate (PDC) in patients with advanced or metastatic solid tumors**

F. Meric-Bernstam<sup>1</sup>, J.P. Eder<sup>2</sup>, A. Vandross<sup>3</sup>, M. Gara<sup>4</sup>, S. Gayle<sup>4</sup>, P. Pearson<sup>4</sup>, A. DeCillis<sup>4</sup>, A. Tolcher<sup>5</sup>. <sup>1</sup>University of Texas, MD Anderson Cancer Center, Houston, USA; <sup>2</sup>Yale University, Smilow Cancer Center, New Haven, USA; <sup>3</sup>NEXT Oncology, Medical Oncology, Austin, USA; <sup>4</sup>Cybrea Therapeutics, Inc, Biology, New Haven, USA; <sup>5</sup>NEXT Oncology, Clinical Research, San Antonio, USA

**Background:** Tumor-targeted drug delivery technologies are urgently needed to overcome lack of tumor selectivity, a major drawback of conventional chemotherapy. The acidic intercellular microenvironment in solid tumors traps weak acid/base chemotherapy agents, preventing necessary intracellular concentrations in tumor cells. An alphalex conjugate, which contains a pH-low insertion peptide (pHLIP), a linker, and a payload, was designed to overcome these limitations. Unlike antibody drug conjugates, alphalex PDCs target tumors in an antigen-agnostic manner. At pH ≥7.0, the peptide is unstructured. In the low-pH tumor microenvironment the peptide forms an alpha helix and inserts directionally into the tumor cell membrane delivering the linker and payload intracellularly where the linker is cleaved releasing the payload in the cytosol. CBX-12 consists of the pH-sensitive peptide, a self-immolating linker, and the topoisomerase 1 (TOP1) inhibitor exatecan.

**Method:** In a Phase 1 trial, cohorts of patients were treated with escalating doses of CBX-12 in a 3 + 3 design on three dosing schedules: Daily × 5 every 3 weeks (Schedule A), daily × 3 every 3 weeks (Schedule B) or once weekly (Schedule C). NCT04902872. The primary objectives are safety, tolerability, and to determine the MTD and/or RP2D. Secondary and exploratory objectives include evaluation of plasma PK and intratumoral levels of CBX-12 and exatecan, anti-tumor activity per RECIST v1.1, and measurement of anti-drug antibodies.

**Results:** As of 28 June 2022, 24 patients have been treated in the following schedules/cohorts (dose; n): A1 (0.25 mg/kg; 1), A2 (0.50 mg/kg; 3), B1 (20 mg/m<sup>2</sup>; 3), B2 (30 mg/m<sup>2</sup>; 3), B3 (45 mg/m<sup>2</sup>; 7), B4 (60 mg/m<sup>2</sup>; 2), C1 (20 mg/m<sup>2</sup>; 5). The most common treatment-related AEs (TRAEs) were nausea (11), diarrhea (8), vomiting (8), anemia (8), and WBC/ANC decrease and fatigue (7 each), dehydration (4), AST increased (3) and alopecia (3). The most common Gr3/4 TRAEs (Gr: n) were ANC decrease (Gr3:2, Gr4:3), anemia (Gr3:4), platelet (Plt) count decrease (Gr4:3), and WBC decrease (Gr3:1, Gr4:2). One patient in Cohort A2 had DLTs of ANC and Plt decrease. Two patients in Cohort B4 had DLTs including febrile neutropenia (2), ANC and Plt decrease (2) and sepsis (1). The best response for 14 response-evaluable patients were 1 CR (ovarian), 1 PR (breast) and 9 SD. The preliminary PR2D in Part B is 45 mg/m<sup>2</sup>. Dose escalation continues in Part C. Plasma CBX-12 and free exatecan concentrations increased in a dose-

proportional manner. Intratumoral CBX-12 and exatecan levels will be presented.

**Conclusions:** In this FIH study of a pH-targeting alphalectin PDC, CBX-12 demonstrated good tolerability, single-agent anti-tumor activity including 2 confirmed responses, and an AE profile consistent with the TOP1 payload, exatecan. Phase 2 cohort expansions are planned in patients with ovarian and SCLC.

**Conflict of interest:**

Advisory Board: Funda Meric-Bernstam: Black Diamond, Biovica, Eisai, FogPharma, Immunomedics, Inflection Biosciences, Karyopharm Therapeutics, Loxo Oncology, Mersana Therapeutics, OnCusp Therapeutics, Puma Biotechnology Inc., Seattle Genetics, Sanofi, Silverback Therapeutics, Spectrum Pharmaceuticals, Zentalis.

Corporate-sponsored Research: Funda Meric-Bernstam: Aileron Therapeutics, Inc. AstraZeneca, Bayer Healthcare Pharmaceutical, Calithera Biosciences Inc., Curis Inc., CytomX Therapeutics Inc., Daiichi Sankyo Co. Ltd., Debiopharm International, eFFECTOR Therapeutics, Genentech Inc., Guardant Health Inc., Klus Pharma, Takeda Pharmaceutical, N ovartis, Puma Biotechnology Inc., Taiho Pharmaceutical Co.

Andrea Vandross: Mabwell (Shanghai), Abbvie, Astra Zeneca, Aminex Therapeutics, Ascentage Pharma, Asana Bio, BioOneCure, BJ Bioscience Inc, Elpiscience Biopharma, Nanjing Immunophage Biotech, Chugai Pharmaceuticals, Lyngen Biopharma, NGMBio, Zhuhai Yufan Biotechnologies, siRNAomics, Sorrento therapeutics, Exelixis, Xilio, ZielBio. Anthony Tolcher: AbbVie Inc, ABL Bio Inc, Adagene Inc, ADC Therapeutics SA, Agenus Inc, Aminex Therapeutics Inc, Amphivena Therapeutics Inc, Apros Therapeutics Inc, Arcellx Inc, ARMO Biosciences, Arrys Therapeutics Inc, Artios Pharma Limited, Asana BioSciences LLC, Ascentage Pharma Group Inc, Astex Pharmaceuticals, Basilea Pharmaceutica International Ltd, Biolnvent International AB, BioNTech RNA Pharmaceuticals GmbH, Birdie Biopharmaceuticals HK Ltd, Boehringer Ingelheim Pharmaceutical, Inc., Boston Biomedical Inc, Calgent Biotechnology Co Ltd, Codiak BioSciences Inc, CStone Pharmaceuticals (Suzhou) Co., Ltd., Cybrexa Therapeutics, Inc., Daiichi Sankyo Inc., Deciphera Pharmaceuticals, LLC, eFFECTOR Therapeutics, Inc, Eli Lilly and Company, EMD Serono, Gilead Sciences, Inc., GlaxoSmithKline Research & Development Limited, Haihe Biopharma Co., Ltd., Heat Biologics, IDEAYA Biosciences, ImmuneOncia Therapeutics, Inc., IMPACT Therapeutics, Inc., Inhibrx, Inc., Innate Pharma SA, Janssen Research & Development, K-Group Beta, Inc., KeChow Pharma, Inc., Kirilys Therapeutics, Kiromic Biopharma, Inc, Mabspace Biosciences (Suzhou) Co., Limited, Merck Sharp & Dohme Corp., a subsidiary of Merck & Co. Inc., Mersana Therapeutics, Inc., Mirati Therapeutics, Inc., NatureWise Biotech & Medicals Corporation, Navire Pharma Inc., NBE-Therapeutics AG, NextCure, Inc, Nitto BioPharma, Inc., Odonate Therapeutics, Inc., ORIC Pharmaceuticals, Pelican Therapeutics, Inc., Petra Pharma, Pfizer, Inc., Pieris Pharmaceuticals, Inc., PMV Pharmaceuticals, Inc., Qilu Puget Sound Biotherapeutics Corporation, Samumed, LLC, Seattle Genetics, Inc., Spring Bank Pharmaceuticals, Inc., Sunshine Guojian Pharmaceutical (Shanghai) Co., Ltd., Symphogen A/S, Syndax Pharmaceuticals Inc., Synthorx, Inc., Takeda, Tizona Therapeutics, VRISE Therapeutics, Zymeworks Inc.

Other Substantive Relationships: Funda Meric-Bernstam (consultant): AbbVie, Aduro BioTech Inc., Alkermes, AstraZeneca, Daiichi Sankyo Co. Ltd., Debiopharm, eFFECTOR Therapeutics, F. Hoffman-La Roche Ltd., Genentech Inc., Harbinger Health, IBM Watson, Infinity Pharmaceuticals, Jackson Laboratory, Kolon Life Science, Lengo Therapeutics, Origimed, PACT Pharma, Parexel International, Pfizer Inc., Protai Bio Ltd, Samsung Bioepis, Seattle Genetics Inc., Tallac Therapeutics, Tyra Biosciences, Xencor, Zymeworks.

J. Paul Eder (consultant): Parthenon, Artis, Hillstream, Roche Diagnostic. Michelle Gara (consultant): Cybrexa Therapeutics Inc, Heat Biologics, Pyramid.

Paul Pearson (consultant): Acurastem, Ariagen Pharmaceuticals, Blueprint Medicines, Cybrexa Therapeutics, Epizon, Erasca, ESSA Pharmaceuticals, Evommune, Inipharm, National Institute of Health (NINDS), NIDO Biosciences, Lengo Therapeutics, Monopteros, Tetra Therapeutics.

Arthur DeCillis (consultant): Ariagen, Bright Peak, Codiak, Genocera, Lumeda, Monopteros, Osmol, Pyramid.

Arthur DeCillis (employee): Cybrexa Therapeutics Inc.

Sophia Gayle (employee): Cybrexa Therapeutics Inc.

11

Oral

**Ipatasertib in Patients with Tumors with AKT Mutations: Results from the NCI-MATCH ECOG-ACRIN Trial (EAY131) Sub-protocol Z1K**

K. Kalinsky<sup>1</sup>, W. Zihan<sup>2</sup>, C. McCourt<sup>3</sup>, E.P. Mitchell<sup>4</sup>, J.J. Wright<sup>5</sup>, L.A. Doyle<sup>6</sup>, R.J. Gray<sup>7</sup>, V. Wang<sup>7</sup>, L.M. McShane<sup>8</sup>, L.V. Rubinstein<sup>8</sup>, D. Patton<sup>9</sup>, P.M. Williams<sup>10</sup>, S.R. Hamilton<sup>11</sup>, B.A. Conley<sup>12</sup>, C.A. Arteaga<sup>13</sup>, L.N. Harris<sup>12</sup>, P.J. O'Dwyer<sup>14</sup>, A.P. Chen<sup>15</sup>, K.T. Flaherty<sup>16</sup>. <sup>1</sup>Emory University at Winship Cancer Institute, Hematology and Medical Oncology, Atlanta, USA; <sup>2</sup>Dana Farber Cancer Institute – ECOG-ACRIN Biostatistics Center, Biostatistics, Boston, USA; <sup>3</sup>Washington University School of Medicine, Gynecology, Saint Louis, USA; <sup>4</sup>Thomas Jefferson University Hospital, Hematology and Medical Oncology, Philadelphia, USA; <sup>5</sup>Investigational Drug Branch- Division of Cancer Treatment and Diagnosis- National Cancer Institute, Cancer Treatment and Diagnosis, Bethesda, USA; <sup>6</sup>Cancer Therapy Evaluation Program- Division of Cancer Treatment and Diagnosis- National Cancer Institute, Cancer Therapy and Diagnosis, Bethesda, USA; <sup>7</sup>Dana Farber Cancer Institute – ECOG-ACRIN Biostatistics Center, Biostatistics, Boston, USA; <sup>8</sup>Biometric Research Program- Division of Cancer Treatment and Diagnosis- National Cancer Institute, Cancer Treatment and Diagnosis, Bethesda, USA; <sup>9</sup>Center for Biomedical Informatics & Information Technology- National Cancer Institute, Center for Biomedical Informatics & Information Technology, Bethesda, USA; <sup>10</sup>Frederick National Laboratory for Cancer Research, Frederick National Laboratory for Cancer Research, Frederick, USA; <sup>11</sup>City of Hope National Medical Center, Pathology, Duarte, USA; <sup>12</sup>Cancer Diagnosis Program- Division of Cancer Treatment and Diagnosis- National Cancer Institute, Cancer Treatment and Diagnosis, Bethesda, USA; <sup>13</sup>Univ of TX Southwestern Medical Center, Hematology and Medical Oncology, Dallas, USA; <sup>14</sup>University of Pennsylvania, Hematology and Medical Oncology, Philadelphia, USA; <sup>15</sup>Division of Cancer Treatment and Diagnosis- National Cancer Institute, Cancer Treatment and Diagnosis, Bethesda, USA; <sup>16</sup>Massachusetts General Hospital, Hematology and Medical Oncology, Boston, USA

**Background:** In the NCI-MATCH trial, pts receive agents based on the genetic alterations in their tumors. In sub-protocol EAY131-Z1K, pts with AKT1 E17K mutant metastatic tumors received the pan-AKT inhibitor ipatasertib.

**Methods:** Pts received ipatasertib orally once daily in a 28-day cycle until progression or unacceptable toxicity. Pts with well-controlled diabetes were eligible, unless baseline fasting glucose >160 mg/dL, Hemoglobin A1C ≥7.5%, on >2 oral hypoglycemics, or on insulin. Pts with known KRAS, NRAS, HRAS, or BRAF mutations were not eligible, as these mutations may lead to limited response due to resistance. Prior PI3K and mTOR inhibitors were allowed, including in the metastatic setting. Prior AKT inhibitors were excluded. Tumor assessments were repeated every 2 cycles. The primary endpoint was objective response rate (ORR). Secondary endpoints included progression-free survival (PFS), 6-month PFS, and toxicity.

**Results:** Of the 35 pts enrolled between August 2019–November 2020, 1 never started ipatasertib and 2 were ineligible due to prior therapy within 4 weeks of starting treatment (tx). Of the 32 evaluable pts, 29 were female (91%); 24 were Caucasian (75%), 3 were African American (9%), and 2 were Hispanic (6%); 11 had an ECOG PS of 0 (34%). The majority had >3 lines of prior tx for metastatic disease [21/32 (66%)]. The most prevalent cancers were breast (BC) [n = 20: 63%; 15 HR+/HER2–, 3 HR–/HER2–, 1 HR+/HER2+] and gynecologic (n = 7: 22%; 3 endometrioid endometrial adenocarcinoma). The confirmed partial response (PR) rate was 22% (n = 7) [90% confidence interval (CI): 11%–37%] in all analyzable pts. Of those with PR, 4 pts had BC (3 HR+/HER2– and 1 HR+/HER2+), 1 endometrioid adenocarcinoma, 1 squamous cell of the anus, and 1 salivary gland cancer, with a median duration of response of 9.9 months. The best confirmed responses for pts achieving less than a PR included 18 with stable disease (56%), 3 with progressive disease (PD: 9%), and 4 not evaluable (13%). The estimated 6-month PFS rate was 44% (90% CI: 29%, 58%). The most common reason for tx discontinuation was PD (78%), followed by adverse events (3%). Most common grade 1–2 tx related adverse events (TRAEs, n = 34) included diarrhea (65%), nausea (35%), anorexia (18%), AST increase (18%), creatinine increase (18%), hyperglycemia (21%), vomiting (15%), and fatigue (15%). Grade 3 TRAEs included diarrhea (9%), vomiting (6%), and maculopapular rash (6%). At this time, 2 pts remain on study, at 19 and 26 months.

**Conclusions:** Ipatasertib demonstrated clinically significant activity in heavily pretreated patients with various tumors harboring AKT1 E17K mutations with an ORR of 22%. E131-Z1K met its primary endpoint. Toxicities included hyperglycemia, fatigue, and gastrointestinal TRAEs. Additional studies are warranted with ipatasertib in patients with AKT1 E17K mutations. NCT02465060.

**Conflict of interest:**

Advisory Board: Eli-Lilly, Pfizer, Novartis, AstraZeneca, Daiichi Sankyo, Puma, 4D Pharma, Oncosec, Immunomedics, Puma, Merck, Seattle Genetics, Mersana, and Cyclocel (KK).

Other Substantive Relationships: Employment/Stock: Spouse - EQRX, Grail (Prior Employee) Institutional Research Funding: Genentech/Roche, Novartis, Eli-Lilly, AstraZeneca, Daiichi Sankyo, Ascentage (KK).

27 October 2022

13:30–14:00

## POSTERS IN THE SPOTLIGHT SESSION

## Poster in the Spotlight 1

15

(PB001)

**Impact of orthotopic versus subcutaneous implantation on patient-derived xenograft transcriptomic profile**

Y. Sheng<sup>1</sup>, W. Qian<sup>1</sup>, S. Guo<sup>1</sup>. <sup>1</sup>Crown Bioscience, Inc., Data Science and Bioinformatics, San Diego, USA

**Background:** Patient-derived xenografts (PDXs) have become the leading model system in oncology drug discovery. Depending on their site of implantation, PDX models from solid tumors can be divided into two categories: subcutaneous (s.c.) and orthotopic (ortho). The advantage of s.c. implantation is that tumor size can be easily monitored, allowing fast validation of drug efficacy. However, since the s.c. microenvironment is likely different from the tissue of origin for most tumor types, there is concern that s.c. PDXs may not fully recapitulate the complexities of human cancer. Understanding how the site of implantation impacts the PDX transcriptome is essential for selecting suitable models for an oncology study. In this study the transcriptome of 49 ortho/s.c. pairs from five different cancer types were analyzed.

**Methods:** Cryopreserved or fresh PDX tumor tissues (~2–3 mm in diameter) were transplanted into NOD/SCID or BALB/c nude mice. In total, RNA-seq data was obtained for 98 PDX samples (49 ortho/s.c. pairs) from five cancer types, including breast, colorectal, gastric, liver, pancreatic. Sequencing reads were aligned to both human and mouse reference genomes and the species origin of each read was assigned based on which alignment yielded fewer mismatches. Following post-alignment quality control for transcript integrity, transcript abundance was quantified using the Kallisto software tool. Paired comparisons between s.c. and ortho samples were carried out in R package sleuth.

**Results:** Overall, the gene expression profiles were highly similar for matched ortho/s.c. pairs, with a median gene-wise Spearman correlation coefficient of 0.85. Using a <0.05 cut-off for false discovery rate, 211 differentially expressed genes were identified. For most of these genes, the magnitude of change was less than two-fold. Gene set enrichment analysis suggested that gene sets related to extracellular matrix functions were significantly enriched in top-ranked genes. Considering that samples from different cancer types were pooled in this analysis, the results represent common patterns across the cancer types examined in this study. In a separate preliminary analysis, additional genes were significantly impacted by the site of implantation in a cancer type-specific manner.

**Conclusions:** Although the tumor transcriptomes of matched ortho/s.c. PDX pairs were highly similar, the subtle differences identified may prove relevant in certain scenarios, especially if the experimental drug targets a molecule involved in one of the pathways impacted by the implantation site. Aside from the mechanism of action, these preliminary results also suggest that the choice of whether to use s.c. or ortho PDX models should depend on the cancer type of interest.

No conflict of interest.

16

(PB002)

**Predicting response to naratuximab emtansine, an anti-CD37 antibody-drug conjugate (ADC), in combination with rituximab in Diffuse Large B Cell Lymphoma (DLBCL), by analyzing the spatial arrangement of CD37 and CD20 positive cells using deep learning**

A. Pokorska-Bocci<sup>1</sup>, S. Micallef<sup>2</sup>, M. Dymkowska<sup>3</sup>, Y. Gabay<sup>4</sup>, R. Gluskin<sup>4</sup>, Y. Blum<sup>4</sup>, A. Laniado<sup>5</sup>, E. Dicker<sup>5</sup>, A. Bart<sup>5</sup>, T. Dicker<sup>5</sup>, I. Rotbein<sup>5</sup>, A. Achtenberg<sup>4</sup>, O. Zelichov<sup>5</sup>. <sup>1</sup>Debiopharm International SA, Personalized medicine, Lausanne, Switzerland; <sup>2</sup>Debiopharm International SA, Biostatistics, Lausanne, Switzerland; <sup>3</sup>Debiopharm International SA, Clinical Development, Lausanne, Switzerland; <sup>4</sup>Nucleai, Research, Tel Aviv, Israel; <sup>5</sup>Nucleai, Medical, Tel Aviv, Israel

**Background:** DLBCL is the most common type of Non-Hodgkin's lymphoma, accounting for 30–40% of cases. Despite improvements in survival with standard of care treatment, up to 40% of patients have relapsed and/or refractory (R/R) disease. A phase 2 study (NCT02564744) evaluated the efficacy of naratuximab emtansine, an anti-CD37 ADC, in combination with rituximab, in 80 patients with R/R DLBCL. We performed an exploratory analysis of the study to find pathology-based biomarkers predictive of response. Deep learning (DL) models were used to extract spatial features from whole slide images (WSI) stained with CD37 and CD20 and their predictive role was evaluated.

**Material and methods:** A cohort of 47 DLBCL patients from the study were selected based on availability of CD20 and CD37 IHC stainings and were used for analysis. Patient characteristics of the analyzed cohort were similar to those of the full study cohort. Overall response rate (ORR) of the cohort was 44.7%, similar to the ORR of the full study cohort. For each patient, two WSI from a pre-treatment biopsy, one stained for CD20 and one for CD37, were analyzed. DL models were used to classify cells as positive or negative to the two markers and CD20+CD37+ co-expression was assessed using an image alignment model to better predict potential synergy of the drug combination. Over 140 spatial features were pre-defined based on biological hypotheses and were calculated for each patient using the cell classifications. Due to the small cohort size, a repeated 5-fold cross-validation analysis was performed to identify features predictive of objective response.

**Results:** Two spatial features related to the proximity of CD37 and CD20 positive cells, demonstrated a significant correlation with clinical outcome. Each feature identified patients in the cohort as having either a positive or a negative response. Feature performance was estimated using multiple repetitions of 5-fold cross-validation. One feature classified on average 21% of patients as responders. Patients positive for this feature had an average ORR of 78% (95% CI 64%–82%), an increase of 34% in ORR relative to the original cohort ( $p < 0.05$ ). The second feature classified on average 35% of patients as positive. Patients positive for this feature had an average ORR of 67% (95% CI 62%–71%), an increase of 23% in ORR relative to the original cohort ( $p < 0.05$ ). In a covariate analysis, the two spatial features remained predictive after stratification to prognostic factors such as LDH and IPI score.

**Conclusions:** DL analysis of the co-expression and spatial arrangement of CD37 and CD20 positive cells in pre-treatment biopsies of DLBCL patients could potentially be used as a predictive biomarker for a response to a combination treatment of naratuximab emtansine and rituximab in DLBCL, and may improve patient stratification for further clinical trials.

**Conflict of interest:**

Other Substantive Relationships: Anna Pokorska-Bocci, Sandrine Micallef and Mariola Dymkowska are employees of Debiopharm, who sponsored this work. Yuval Gabay, Roman Gluskin, Yoav Blum, Avi Laniado, Efrat Dicker, Amit Bart, Tomer Dicker, Ifat Rotbein, Albert Achtenberg and Ori Zelichov are employees of Nucleai who performed the analysis.

17

(PB003)

**BA7 2927088: The first non-covalent, potent, and selective tyrosine kinase inhibitor targeting EGFR exon 20 insertions and C797S resistance mutations in NSCLC**

F. Siegel<sup>1</sup>, S. Siegel<sup>2</sup>, K. Graham<sup>3</sup>, G. Karsli-Uzunbas<sup>4</sup>, D. Korr<sup>5</sup>, J. Schroeder<sup>5</sup>, U. Boemer<sup>6</sup>, R.C. Hillig<sup>7</sup>, J. Mortier<sup>8</sup>, M. Niehues<sup>9</sup>, S. Golfier<sup>10</sup>, V. Schulze<sup>2</sup>, S. Menz<sup>11</sup>, A. Kamburov<sup>12</sup>, M. Hermsen<sup>13</sup>, A. Cherniak<sup>4</sup>, K. Eis<sup>14</sup>, A. Eheim<sup>1</sup>, M. Meyerson<sup>15</sup>, H. Greulich<sup>1</sup>. <sup>1</sup>Bayer, Research & Early Development-Precision Molecular Oncology, Cambridge, USA; <sup>2</sup>Bayer, Drug Discovery Sciences, Berlin, Germany; <sup>3</sup>Boehringer Ingelheim, Medicinal Chemistry, Berlin, Germany; <sup>4</sup>Broad Institute of MIT and Harvard, Cancer Program, Cambridge, USA; <sup>5</sup>nuvisan, Therapeutic Research, Berlin, Germany; <sup>6</sup>nuvisan, Biochemistry, Berlin, Germany; <sup>7</sup>nuvisan, Structural Biology, Berlin, Germany; <sup>8</sup>Bayer, Computational Chemistry, Berlin, Germany; <sup>9</sup>nuvisan, Structure & Sample Analytics, Berlin, Germany; <sup>10</sup>nuvisan, Translational Research, Berlin, Germany; <sup>11</sup>Bayer, DMPK Modeling & Simulation, Berlin, Germany; <sup>12</sup>Bayer, Biomedical Data Science, Berlin, Germany; <sup>13</sup>Instituto de Investigación Sanitaria del Principado de Asturias ISPA, Department of Head and Neck Cancer, Oviedo, Spain; <sup>14</sup>Bayer, Drug Discovery Sciences, Cambridge, USA; <sup>15</sup>Dana Farber Cancer Center, Center for Cancer Genome Discovery, Boston, USA

**Background:** EGFR exon 20 insertion mutations represent a distinct subset of EGFR-mutant lung cancer with poor prognosis generally associated with resistance to several EGFR tyrosine kinase inhibitors. Despite the recent advances with the approval of amivantamab and mobocertinib, there remains a high unmet need for more effective and better tolerated agents



targeting exon 20 insertions that can improve response rates and response durability.

**Results:** Here we present BAY 2927088, the first reversible small molecule inhibitor selectively targeting EGFR exon 20 insertion mutations.

BAY 2927088 is highly potent against EGFR exon 20 insertions in biochemical and cellular assays, and displays strong, ~40-fold selectivity for EGFR exon 20 insertion mutants relative to wild-type EGFR. Both potency and selectivity were validated *in vivo* in cell line-derived xenografts as well as in patient-derived xenograft models carrying different EGFR exon 20 insertion mutations.

BAY 2927088 is also highly active against the classical EGFR exon 19 del and L858R activating mutations with >1000-fold selectivity vs. wild-type EGFR in Ba/F3 cellular models. Importantly, BAY 2927088 retains potent activity in the presence of the EGFR C797S resistance mutation due to its non-covalent binding mode.

**Conclusions:** The strong potency and improved selectivity of BAY 2927088 offer the prospect of a wider therapeutic window in the clinic and potentially a favorable safety profile with improved combinability compared to available EGFR exon 20 insertion targeted therapies.

BAY 2927088 is currently being evaluated in a first-in-human, phase I clinical trial in patients with EGFR mutant NSCLC (NCT05099172). The study will evaluate safety, tolerability, pharmacokinetics, pharmacodynamics, and preliminary anti-tumor activity of BAY 2927088.

#### Conflict of interest:

Ownership: shareholder of Bayer.

Corporate-sponsored Research: employee of Bayer.

28 October 2022

14:00–14:30

### POSTERS IN THE SPOTLIGHT SESSION

## Poster in the Spotlight 2

19

(PB005)

### DNA Damage Response (DDR) Basket of Baskets (D-BOB) Trial: Phase 1/2 Study of the ATR inhibitor (ATRI) berzosertib and PD-L1 inhibitor avelumab in patients (pts) with advanced solid tumors with DDR molecular alterations

N. Ngoi<sup>1</sup>, P.G. Pilie<sup>2</sup>, S.A. Piha-Paul<sup>1</sup>, E.E. Dumbrava<sup>1</sup>, S. Fu<sup>1</sup>, D.S. Hong<sup>1</sup>, D.D. Karp<sup>1</sup>, A. Naing<sup>1</sup>, S. Pant<sup>1</sup>, J. Rodon Ahnert<sup>1</sup>, V. Subbiah<sup>1</sup>, A.M. Tsimberidou<sup>1</sup>, C. Salguero<sup>1</sup>, C.V. Brown<sup>1</sup>, W.E. Hoadley<sup>1</sup>, A. Johnson<sup>3</sup>, Y. Yuan<sup>4</sup>, S.N. Westin<sup>5</sup>, F. Meric-Bernstam<sup>1</sup>, T.A. Yap<sup>1</sup>. <sup>1</sup>The University of Texas MD Anderson Cancer Center, Department of Investigational Cancer Therapeutics, Houston, USA; <sup>2</sup>The University of Texas MD Anderson Cancer Center, Department of Genitourinary Medical Oncology, Houston, USA; <sup>3</sup>The University of Texas MD Anderson Cancer Center, Khalifa Institute for Personalized Cancer Therapy, Houston, USA; <sup>4</sup>The University of Texas MD Anderson Cancer Center, Department of Biostatistics, Houston, USA; <sup>5</sup>The University of Texas MD Anderson Cancer Center, Department of Gynecologic Oncology and Reproductive Medicine, Houston, USA

**Background:** ATR is a central kinase involved in the DDR and replication stress response (RSR) and innate immune activation. This is the first report of the investigator-initiated phase 1/2 D-BOB trial (NCT04266912), funded by EMD Serono (CrossRef Funder ID: 10.13039/100004755).

**Materials and Methods:** Pts with advanced cancers and actionable variants in ≥1 DDR gene (*ARID1A*, *ATM*, *ATR*, *ATRX*, *BAP1*, *BARD1*, *BRCA1/2*, *BRIP1*, *CDK12*, *CHEK2*, *FANCA*, *MRE11A*, *MSH2*, *NBN*, *PALB2*, *RAD51*, *RAD51C/D*, *SMARCB1*, *VHL*) were enrolled. Prior immunotherapy (IO), but not ATRI, was allowed. Dose escalation was conducted using Bayesian optimal interval design (dose level (DL) 1: berzosertib 240 mg/m<sup>2</sup>; DL2: berzosertib 480 mg/m<sup>2</sup> weekly, plus avelumab 800 mg 2-weekly), followed by dose-expansion of pts with *ATM* mutated cancers. Primary objectives were safety and recommended phase 2 doses (RP2D). Secondary objectives were antitumor activity. Exploratory objectives assessed biomarkers of response/resistance through serial tumor and blood sampling for tumor whole exome, RNA sequencing and RPPA, RSR scores, immune biomarkers and ctDNA NGS.

**Results:** 17 pts (7:10 M:F; mean age 56y (37–80y); ECOG PS 0:1 1:16) with advanced breast (n = 3), colorectal (n = 3), pancreas (n = 3), prostate (n = 2) and other (n = 6) cancers were enrolled. Pts had actionable germline/somatic DDR mutations in *ATM* (n = 7), *ARID1A* (n = 5), *ATRX* (n = 3), *BRCA1/2* (n = 3), *CHEK2* (n = 2), *CDK12* (n = 1), *MSH2* (n = 1), *PALB2* (n = 1), *RAD51* (n = 1). 6/17 pts had prior PARP inhibitors; 6/17 had prior IO. 13/17 pts were treated in dose-escalation (DL 1: 7/13, DL 2: 6/13), 4/17 pts in

dose-expansion. Common all-grade toxicities were chills (2/17), diarrhea (2/17), rash (2/17), thrombocytopenia (2/17). 2/17 pts had grade ≥3 transaminitis related to avelumab, 1 was a DLT. 2 RECIST 1.1 responses were observed (1 CR, 1 PR). 2 further pts had SD as best response, including a germline *ATM*-mutated pancreatic cancer pt treated at DL1 for 6 months and an *ATM*-mutated colorectal cancer pt treated at DL2. A *RAD51/ATRX* co-mutated PD-L1+ vaginal cancer pt treated at DL1 had a CR for 84+ weeks; a *MSH2* mutated colorectal cancer pt treated at DL1 had PR (~30%) for 91+ weeks. In total, 19 tumor and 52 ctDNA samples were obtained longitudinally for ongoing analyses.

**Conclusions:** The berzosertib plus avelumab combination was well tolerated with preliminary efficacy in genomically-selected cancers. RP2D was berzosertib 480 mg/m<sup>2</sup> weekly plus avelumab 800 mg 2-weekly. DDR-aberrant doublet cohorts and triplet cohorts with peposertib (DNA-PK inhibitor) are planned.

#### Conflict of interest:

Ownership: T.A.Y holds stocks in Seagen.

Advisory Board: T.A.Y has received fees for consulting from AbbVie, AstraZeneca, Acrivon, Adagene, Almac, Aduro, Amphista, Artios, Athena, Atrin, Avoro, Axiom, Baptist Health Systems, Bayer, Beigene, Boxer, Bristol Myers Squibb, C4 Therapeutics, Calithera, Cancer Research UK, Clovis, Cybrexa, Diffusion, EMD Serono, F-Star, Genmab, Glenmark, GLG, Globe Life Sciences, GSK, Guidepoint, Idience, Ignyta, I-Mab, ImmuneSensor, Institut Gustave Roussy, Intellisphere, Jansen, Kyn, MEI pharma, Merco, Merck, Natera, Nexys, Novocure, OHSU, OncoSec, Ono Pharma, Pegascy, PER, Pfizer, Piper-Sandler, Prolynx, Repare, restORbio, Roche, Schrodinger, Theragnostics, Varian, Versant, Vibliome, Xinthera, Zai Labs and ZielBio.

Board of Directors: N/A.

Corporate-sponsored Research: T.A.Y has received research support (paid to his institution) from Acrivon, Artios, AstraZeneca, Bayer, Beigene, BioNTech, Blueprint, BMS, Clovis, Constellation, Cyteir, Eli Lilly, EMD Serono, Forbius, F-Star, Artios, GlaxoSmithKline, Genentech, Haihe, ImmuneSensor, Ionis, Ipsen, Jounce, Karyopharm, KSQ, Kyowa, Merck, Mirati, Novartis, Pfizer, Ribon Therapeutics, Regeneron, Repare, Rubius, Sanofi, Scholar Rock, Seattle Genetics, Tesaro, Vivace and Zenith. Other Substantive Relationships: N/A.

21

(PB007)

### HER2 as a therapeutic target in bladder cancer

Z. Chen<sup>1</sup>, X. Tang<sup>1</sup>, J.R. Christin<sup>2</sup>, S.P. Gao<sup>1</sup>, C.E. Chu<sup>3</sup>, M.F. Berger<sup>4</sup>, N.D. Schultz<sup>4</sup>, M.M. Shen<sup>2</sup>, H.A. Al-Ahmadi<sup>5</sup>, G. Iyer<sup>6</sup>, K. Kim<sup>3</sup>, D.B. Solit<sup>1</sup>. <sup>1</sup>Memorial Sloan Kettering Cancer Center, Human Oncology and Pathogenesis Program, New York, USA; <sup>2</sup>Columbia University, Irving Medical Center, New York, USA; <sup>3</sup>Memorial Sloan Kettering Cancer Center, Department of Surgery, New York, USA; <sup>4</sup>Memorial Sloan Kettering Cancer Center, Marie-Josée and Henry R. Kravis Center for Molecular Oncology, New York, USA; <sup>5</sup>Memorial Sloan Kettering Cancer Center, Department of Pathology, New York, USA; <sup>6</sup>Memorial Sloan Kettering Cancer Center, Department of Medicine, New York, USA

**Background:** HER2 (encoded by the *ERBB2* gene) is a non-ligand-binding member of this family that exerts its activity through homo- or heterodimerization with other ERBB proteins. While multiple HER2-targeted therapies are FDA-approved for breast cancer, the clinical utility of targeting HER2 in bladder cancer patients remains undefined. Therefore, we leveraged a prospective sequencing initiative and a new collection of patient-derived organoid (PDO) and xenograft (PDX) models to explore the prevalence and biologic role of HER2 in bladder cancer pathogenesis and the potential clinical utility of HER2-targeted therapies.

**Material and methods:** To define the landscape of HER2 alterations in bladder cancer patients, we leveraged data generated by The Cancer Genome Atlas (TCGA), and 2230 bladder cancer patients enrolled in a prospective tumor genomic profiling initiative at Memorial Sloan Kettering Cancer Center (MSK).

We generated 41 PDOs that genetically and phenotypically reflect the human disease. Those proprietary models were characterized through various genomic sequencing and used to understand HER2 activation potential and sensitivity to multiple anti-HER2 targeted agents.

**Results:** 17% of bladder cancer patients in TCGA and 16% in the prospective MSK bladder cancer cohorts had oncogenic HER2 mutations and/or gene amplification. HER2 alterations were more common in tumors of higher grade and stage, and also varied significantly as a function of histology with the highest frequency in the micropapillary subtype (37% vs 19% in UC, NOS). Analysis of 119 patients with paired primary/metastatic tumors noted discordance in 37.5% of patients with HER2 alterations. Compared to breast cancer patients, the mean *ERBB2* copy number in HER2 amplified bladder cancers was significantly lower (2.69 vs 3.30, p-value = 0.004), with a lower

correlation between *ERBB2* linear copy number and mRNA expression. Of 41 PDX/PDO models, we identified HER2 alterations in 10. HER2 altered PDX models were significantly more sensitive to the antibody-drug conjugate (ADC) trastuzumab deruxtecan (T-DXd) than the HER kinase inhibitor neratinib. Neratinib resistance was associated with lacking AKT dependence on upstream HER2 activation.

**Conclusion:** In sum, HER2 mutations/amplification in bladder cancer are associated with higher grade and stage and enriched in patients with micropapillary histology. In addition, we observed frequent discordance in HER2 status between primary/metastatic pairs and a lower correlation between HER2 expression and gene copy number versus breast cancers. Preclinical evaluation of HER2 altered PDX/PDOs indicated significantly greater sensitivity to the HER2-directed ADC T-DXd compared to the HER kinase inhibitor neratinib, which provided justification for clinical trials of HER2 ADCs in bladder cancer patients.

**Conflict of interest:**

Advisory Board: D.B.S. has served as a consultant for/received honorarium from Pfizer, Loxo/Lilly Oncology, Vividion Therapeutics, Scorpion Therapeutics, Fore Therapeutics and BridgeBio. H.A.A provided consultation to AstraZeneca, Janssen Biotech, Bristol-Myers-Squibb and Paige.ai. M.B. has served as a consultant for Eli Lilly and PetDx.

22

(PB008)

**Detection of myeloid malignancies through cfDNA profiling in patients with advanced stage cancer**

M. Tagliamento<sup>1</sup>, M. Aldea<sup>1</sup>, V. Verge<sup>2</sup>, A. Bayle<sup>3</sup>, F. Blanc-Durand<sup>1</sup>, A. Marinello<sup>1</sup>, J. Hadoux<sup>1</sup>, Y. Lorient<sup>3</sup>, D. Vasseur<sup>2</sup>, C. Nicotra<sup>3</sup>, C. Smolenschi<sup>1</sup>, P. Martin-Romano<sup>3</sup>, A. Hollebecque<sup>3</sup>, S. Ponce<sup>3</sup>, L. Lacroix<sup>2</sup>, E. Rouleau<sup>2</sup>, C. Marzac<sup>2</sup>, A. Italiano<sup>3</sup>, B. Besse<sup>1</sup>, J.B. Micol<sup>4</sup>.  
<sup>1</sup>Gustave Roussy, Department of Medical Oncology, Villejuif, France;  
<sup>2</sup>Gustave Roussy, Department of Medical Biology and Pathology, Villejuif, France;  
<sup>3</sup>Gustave Roussy, Drug Development Department DITEP, Villejuif, France;  
<sup>4</sup>Gustave Roussy, Department of Hematology, Villejuif, France

**Background:** Clonal hematopoiesis (CH) is frequently incidentally found in liquid biopsy and may reveal a risk situation for developing myeloid malignancy or uncover occult hematologic disease.

**Material and methods:** Adult patients with treatment-naïve or pre-treated advanced solid cancer enrolled in the Gustave Roussy Cancer Profiling study (STING, NCT04932525) underwent at least one liquid biopsy with next-generation sequencing of cfDNA performed by FoundationOne Liquid CDx. The Gustave Roussy Molecular Tumor Board reviewed molecular reports. Potential CH alterations were registered, and patients referred to hematology consultation in case of identified mutation in *JAK2* or *MPL*, irrespective of the variant allele frequency (VAF), or mutation with VAF  $\geq 10\%$  in at least one gene between *DNMT3A*, *TET2*, *ASXL1*, *IDH1*, *IDH2*, *SF3B1*, *U2AF1*. On the contrary, mutations in *TP53* were discussed on a case-by-case basis, excluding cases with somatic alteration identified by tumor tissue testing. Objective of the study was to determine the diagnostic rate of myeloid malignancies following the incidental finding of high-risk CH via liquid biopsy for cfDNA detection.

**Results:** Between March and October 2021, 1416 patients underwent at least one liquid biopsy. Overall, 113 patients (8%) met the identified criteria and carried at least one CH mutation considered at high-risk for developing myeloid hematologic disorders (*JAK2* = 27, *MPL* = 3, *DNMT3A* = 32, *TET2* = 19, *ASXL1* = 18, *IDH1* = 4, *IDH2* = 3, *SF3B1* = 5, *U2AF1* = 2). Indication for hematology consultation followed in 45 cases, taking into account also patient's and cancer disease's characteristics. Five out of these selected patients had a confirmed diagnosis of malignant myeloid disorder: one chronic myelomonocytic leukemia, two myelodysplastic syndrome, two essential thrombocythemia.

**Conclusions:** Incidental finding of CH via liquid biopsy may trigger additional hematological tests revealing risk for developing myeloid malignancy or uncovering occult disease. This attitude should follow a multidisciplinary case-by-base evaluation.

**Conflict of interest:**

Other Substantive Relationships: No conflict of interest related to this study.

26 October 2022

12:00–20:00

POSTER SESSION

**Angiogenesis and Vascular Disrupting Agents**

30

(PB021)

**Taxanes act as vascular disrupting agents and increase rate of metastasis when combined with angiogenic therapy**

E. Henke<sup>1</sup>, R. Nandigama<sup>1</sup>, S. Das<sup>2</sup>, M. Kallius<sup>1</sup>, H. Katherina<sup>3</sup>, H. Mohamed<sup>1</sup>, D. Scheld<sup>4</sup>, S. Herterich<sup>4</sup>, A. Zerneck<sup>5</sup>, O. Penack<sup>6</sup>, K. Camphausen<sup>7</sup>, D. Ascheid<sup>1</sup>, U. Shankavaram<sup>2</sup>, K. Heinze<sup>3</sup>, F. Escorcía<sup>8</sup>.  
<sup>1</sup>Institute of Anatomy and Cell Biology, Universität Würzburg, Würzburg, Germany; <sup>2</sup>Bioinformatics core- Radiation Oncology Branch, National Cancer Institute, Bethesda, USA; <sup>3</sup>Molecular Microscopy, Universität Würzburg, Würzburg, Germany; <sup>4</sup>Zentrallabor, Universitätsklinikum Würzburg, Würzburg, Germany; <sup>5</sup>Institute of Experimental Biomedicine, Universitätsklinikum Würzburg, Würzburg, Germany; <sup>6</sup>Medizinische Klinik mit Schwerpunkt Hämatologie- Onkologie und Tumormimmunologie, Universitätsklinikum Charité, Berlin, Germany; <sup>7</sup>Radiation Oncology Branch, National Cancer Institute, Bethesda, Germany; <sup>8</sup>Molecular Imaging Branch, National Cancer Institute, Bethesda, USA

**Background:** Taxanes are known to have a profound effect on endothelial cells (ECs) and the vasculature, even at low doses. Neither the mechanism behind this anti-angiogenic effect nor its clinical implication is well understood. For late stage disease management in certain cancers, taxanes are combined with anti-angiogenic therapeutics like bevacizumab, with significant improvement in PFS but marginal effects on OS. We were interested in investigating the effects of this vessel co-targeting both on the tumor vasculature and on disease progression in general.

**Methods:** We examined the acute effects of taxanes on the tumor vasculature in various murine models of metastatic cancer, using (immuno-) histology, mRNA expression analysis and 3D-time resolved high resolution angiography. This studies were supplemented with *in vitro* experiments, including impedance-based EC barrier assessment and fluorescence life cell imaging. Finally, to investigate if our preclinical models recapitulated a true clinical phenomenon, we analyzed gene expression data from clinical trials, that compared use of taxanes versus a combination of taxanes with bevacizumab.

**Results:** We were able to demonstrate that taxanes rather than being anti-angiogenic agents display vascular disrupting properties at nanomolar and therapy-relevant doses. In contrast to classic vascular disrupting agents the effect of taxanes was reversible *in vitro*. Utilizing mouse models, we found that this reversible effect nevertheless results in rapid vascular collapse *in vivo*. Tumors consequently experienced acute hypoxic stress. Combining taxane treatment with application of anti-angiogenic drugs (VEGF-sequestering antibodies or VEGF-R-directed TKIs) blocked vasculogenic rescue mechanisms, prolonged hypoxic stress and resulted in the upregulation of pro-metastatic programs, a surge of circulating tumor cells and a strong increase in metastasis. Analyzing gene expression data from clinical trials, we found that addition of bevacizumab to a taxane-based regimen increases signatures for angiogenesis, hypoxia, invasiveness, EMT and metastasis in patients. Moreover, it is correlated with a gene signature predictive of reduced survival.

**Conclusion:** Applying anti-VEGF drugs in combination with taxanes, as is routine practice in the management of certain metastatic malignancies, significantly increases further metastatic spread. Our data indicates that adjusting drug scheduling could improve efficacy and ameliorate the pro-metastatic effects. Importantly, we were also able to show that taxanes exert their vascular disruptive effect through mechanisms that can be pharmacologically inhibited. This might allow blocking this undesirable effect, thereby improving patient outcome of this combination therapy.

**No conflict of interest.**

31 (PB021)  
**6-gingerol Suppresses Angiogenesis and Promotes T-cell cytotoxicity in Mice Model of Colorectal Cancer**

B. Ajayi<sup>1</sup>, A. Adeshina<sup>2</sup>. <sup>1</sup>Ajayi Crowther University, Oncopreventives and System Oncology Biochemistry, Oyo, Nigeria; <sup>2</sup>All Saints School of Medicine Dominican, Medicine, Roseau, Dominican Republic

**Background:** Colorectal cancer (CRC) is the second most common adult cancer in women and the third most common in men, and it is the fourth leading cause of cancer death worldwide. Angiogenesis is a critical step in CRC progression and metastasis. Immune checkpoint proteins (ICP) such as programmed cell death 1 (PD1), PD1 ligand 1 (PD-L1) and cytotoxic T lymphocyte antigen 4 (CTLA4) act as inhibitory immunoreceptors that prevent cytotoxic T-cells from killing tumor cells. Several studies have reported the contribution of angiogenesis and ICP to anti-tumor immunity. Indeed, targeting angiogenesis and use of immune checkpoint protein blockage have revolutionized colorectal cancer treatment and improved patients' survival. However, the use of immune checkpoint inhibitors has been shown to induce immune-related adverse reactions such as colitis. 6-gingerol (6G), the most pharmacologically active compound discovered in *Zingiber officinale* (ginger). We have reported the anti-tumor and anti-inflammatory effects of 6-gingerol. However, there is a lack of information on the effect of 6G on angiogenic drivers and T-cell cytotoxicity in a mouse model of CRC. Herein, we investigated the effects of 6G angiogenesis and cytotoxic T-cell signaling in mice model of CRC.

**Method:** Male BALB/c mice were divided into three groups of 20 mice each. Group 1 mice served as controls Group 2 (CRC model) mice received a single dose of azoxymethane (AOM) 10 mg/kg and, after one week, they received three cycles of dextran sulfate sodium (DSS) 4% in drinking water. Group 3 mice received 6G 10 mg/kg/day by oral gavage in combination with AOM and three cycles of 4% DSS (W/V) in drinking water. The colons of the mice in the CRC group and treated group were observed daily for tumor development, and the experiment was terminated after confirmation of colorectal adenocarcinoma.

**Results:** Tumor burden was observed to be decreased in CRC mice treated with 6G. Also, 6G decreases the expression of collagen (type I and II), vascular endothelial growth factor (VEGF), VEGF receptor, epidermal growth factor (EGF), and EGF receptor in mice with CRC when compared with control. Furthermore, mice administered 6G+AOM/DSS had increased expression of cluster of differentiation (CD) 4 and CD8+ T-cells and decreased expression of tumor necrosis factor (TNF- $\alpha$ ), cyclooxygenase-2 (COX-2), PD1, PD-L1, and CTLA4 when compared to mice with CRC. Using computational oncology, we observed a high binding affinity of 6G with VEGF, VEGFR, EGF, EGFR, PD1, PD-L1, and CTLA4.

**Conclusion:** The result obtained from this study showed that 6-gingerol suppresses angiogenic drivers and promotes T-cell cytotoxicity in mice model of colorectal cancer.

No conflict of interest.

POSTER SESSION

**Animal Models**

32 (PB022)  
**Humanized mouse models for preclinical evaluation of novel immune therapies, checkpoint inhibitors and immune cell engagers**

M. Stecklum<sup>1</sup>, B. Brzezicha<sup>1</sup>, S. Rhein<sup>1</sup>, W. Walther<sup>1,2</sup>, J. Hoffmann<sup>1</sup>. <sup>1</sup>EPO – Experimental Pharmacology & Oncology Berlin-Buch GmbH, Immuno-Oncology, Berlin, Germany; <sup>2</sup>Universitätsmedizin Berlin - corporate member of Freie Universität Berlin and Humboldt Universität zu Berlin, ECRC Experimental and Clinical Research Center, Berlin, Germany

**Background:** The preclinical evaluation of novel immune therapies demands humanized mouse models with functional human immune cells. In previous studies we have established a humanized immune system with functional T- B- and NK cells, as well as monocytes in immunodeficient mice by transfer of hematopoietic stem cells (HSCs) or peripheral blood mononuclear cells (PBMC). By transplantation of cell-line-derived (CDX) or patient-derived (PDX) tumor xenografts on humanized mice, we successfully generated a full human tumor-immune-cell model for different tumor entities. Finally, we validated the functionality of these models using checkpoint inhibitors or immune cell engagers.

**Methods:** HSC-humanized mice were generated by single i.v. transplantation of CD34+ stem cells to immunodeficient NOG mice. Engraftment of immune cells was monitored by FACS analysis of blood samples. CDX and

PDX from different entities were transplanted on the humanized mice. PBMC or isolated T- or NK-cell preparations were used to humanize mice by single or multiple i.v. injections into tumor-bearing mice or with simultaneous tumor cell transplantation. These models were used to evaluate immune checkpoint inhibitors. Blood and tumor samples were analysed by FACS and immunohistochemistry for immune cell infiltration and activation.

**Results:** The transplanted HSCs engrafted in mice and established a functional human differentiated immune system with proliferating immune cells. Up to 20% of the human immune cells in the blood were functional T cells, characterized by a high PD-1 expression 14 weeks after HSC inoculation. Selected CDX and PDX tumors successfully engrafted on humanized mice without significant differences in tumor growth compared to non-humanized mice. Checkpoint inhibitor treatments induced tumor growth delay in selected models. FACS analysis of xenograft tumors revealed an increased percentage of tumor-infiltrating T cells. In addition, we identified a set of CDX and PDX models without interference with parallel injection of PBMC, T- or NK-cell preparations for the evaluation of immune cell engagers and other immune therapeutics.

**Conclusions:** We established human tumor-immune-cell models of different entities using CDX or PDX in combination with different donor derived immune cell subsets as effector cells. We demonstrated successful engraftment of HSCs on immunodeficient mouse strains generating mice with a functional human hematopoiesis. These models have been employed for preclinical evaluation of novel checkpoint inhibitors and immune cell engagers. Our human tumor-immune-cell models allow preclinical, translational studies on tumor immune biology as well as evaluation of new therapies, drug combinations and biomarker identification and validation.

No conflict of interest.

33 (PB023)  
**Establishment and characterization of a preclinical platform of subcutaneous renal cell carcinoma (RCC) patient-derived xenograft models to evaluate novel treatment strategies**

D. Kobelt<sup>1</sup>, D. Gürgen<sup>1</sup>, M. Becker<sup>1</sup>, M. Dahlmann<sup>1</sup>, S. Flechsig<sup>1</sup>, E. Schaeffeler<sup>2</sup>, F.A. Büttner<sup>2</sup>, C. Schmees<sup>3</sup>, R. Bohnert<sup>2</sup>, J. Bedke<sup>4</sup>, M. Schwab<sup>5</sup>, J.J. Wendler<sup>6</sup>, M. Schostak<sup>6</sup>, B. Jandrig<sup>6</sup>, W. Walther<sup>1</sup>, J. Hofmann<sup>1</sup>. <sup>1</sup>Experimental Pharmacology and Oncology Berlin-Buch GmbH EPO, Experimental Pharmacology and Oncology Berlin-Buch GmbH EPO, Berlin, Germany; <sup>2</sup>Dr. Margarete Fischer-Bosch Institute of Clinical Pharmacology, Dr. Margarete Fischer-Bosch Institute of Clinical Pharmacology, Stuttgart, Germany; <sup>3</sup>Natural and Medical Sciences Institute NMI at the University of Tübingen, Natural and Medical Sciences Institute NMI at the University of Tübingen, Reutlinger, Germany; <sup>4</sup>Department of Urology- University Hospital Tübingen, Department of Urology- University Hospital Tübingen, Tübingen, Germany; <sup>5</sup>Departments of Clinical Pharmacology- and Pharmacy and Biochemistry- University of Tübingen, Departments of Clinical Pharmacology- and Pharmacy and Biochemistry- University of Tübingen, Tübingen, Germany; <sup>6</sup>Department of Urology- University Medical Center Magdeburg, Department of Urology- University Medical Center Magdeburg, Magdeburg, Germany

**Background:** Renal cell carcinoma (RCC) is a cancer type with an onset mainly during the sixth or seventh decade of the patient's life. Patients with advanced or metastasized RCC have a poor prognosis. The majority of patients develop drug resistance towards Standard of Care (SoC) drugs within months. Tyrosine kinase inhibitors (TKI) are used in first-line therapy and have been combined with immune checkpoint inhibitors recently. The development of novel therapies targeting acquired TKI resistance mechanisms in advanced and metastatic RCC remains an urgent medical need. To promote novel personalized therapies, preclinical models with high translational relevance are needed. It has been demonstrated that patient-derived xenograft (PDX) models represent a valuable tool for the preclinical evaluation of novel targeted therapies and their combinations.

**Material and methods:** Use of patient tissue was approved by the responsible local ethics committees. RCC tissue from 167 patients was transplanted into mice within 24 h after surgery. Local authorities approved all procedures involving animals. PDX were characterized by immunohistochemistry using human Ki-67, CD31, Pax2 and Pax8 antibodies. Further, gene expression, copy number variations and mutational analyses were performed. For in vivo drug response testing of RCC PDX models, mice transplanted with PDX tumors were treated i.p. with bevacizumab or p.o. with everolimus, sorafenib, or sunitinib. The anti-tumor activity of the tested compounds in RCC PDX models was classified using the adopted clinical response criteria for solid tumors (RECIST). Additionally, next generation panel sequencing data and transcriptome analysis was performed to compare primary tumors and metastases.

**Results:** We established and molecularly characterized a comprehensive panel of subcutaneous RCC PDX models with well-conserved molecular and pathological features over multiple passages. Similar to observations in patients, drug screening towards four SoC drugs, targeting the VEGF and PI3 K/mTOR pathway, revealed individual and heterogeneous response profiles in the PDX. As unique features, our cohort includes PDX models from metastatic RCC and multi-tumor regions from one patient, allowing extended studies on intra-tumor heterogeneity. The PDX models are further used as source to develop corresponding *in vitro* cell culture models, thus enabling advanced high throughput drug screening in a personalized context. Next generation sequencing enabled the characterization of cancer-relevant features including driver mutations or cellular processes in the PDX models.

**Conclusion:** In summary, we report a newly established and molecularly characterized panel of RCC PDX models with high relevance for translational preclinical research.

**No conflict of interest.**

35

(PB025)

### Therapeutic inhibition of the SRC-kinase HCK facilitates T cell tumor infiltration, restricts the development and metastasis of solid malignancies and improves their response to immunotherapy

M. Ernst<sup>1</sup>, A. Poh<sup>1</sup>. <sup>1</sup>Olivia Newton-John Cancer Research Institute, Cancer & Inflammation, Heidelberg, Australia

**Background:** Although immunotherapy has revolutionized cancer treatment, many immunogenic tumors remain refractory to treatment. This can be largely attributed to an immunologically “cold” tumor microenvironment characterized by an accumulation of immunosuppressive myeloid cells and exclusion of activated T cells.

**Material & Methods:** We use orthopic syngeneic mouse models for colon cancer (MC38 cells) and pancreatic ductal adenocarcinoma (KPT cells) using either wild-type hosts, hosts that are lacking expression of HCK or wild-type hosts treated with a small molecule HCK-inhibitor.

**Results:** We demonstrate that genetic ablation or therapeutic inhibition of the myeloid-specific hematopoietic cell kinase (HCK) in mice enables activity of antagonistic anti-PD1, anti-CTLA4, or agonistic anti-CD40 immunotherapies in otherwise refractory Pancreatic ductal adenocarcinomas, and augments response in treatment-susceptible colon tumors. Mechanistically, HCK ablation reprograms tumor-associated macrophages and dendritic cells toward an inflammatory endotype and enhances CD8+ T cell recruitment and activation when combined with immunotherapy in mice. Meanwhile, therapeutic inhibition of HCK in humanized mice engrafted with patient-derived xenografts counteracts tumor immunosuppression, improves T cell recruitment, and impairs tumor growth.

**Conclusions:** Our results suggest that therapeutic targeting of HCK activity enhances response to immunotherapy by simultaneously stimulating immune cell activation and inhibiting the immunosuppressive tumor microenvironment.

**No conflict of interest.**

36

(PB026)

### HER2 distribution in tumour and blood of mice with xenograft human cancer

A. Antos<sup>1</sup>, M. Świtalska<sup>2</sup>, A. Topolska-Woś<sup>1</sup>, M. Woś<sup>1</sup>, A. Mitura<sup>1</sup>, M. Staniszweska<sup>1,3</sup>. <sup>1</sup>SDS Optic S. A., Research and Development Department, Lublin, Poland; <sup>2</sup>Ludwik Hirsfeld Institute of Immunology and Experimental Therapy Polish Academy of Sciences, Department of Experimental Oncology, Wrocław, Poland; <sup>3</sup>The John Paul II Catholic University of Lublin, Faculty of Science and Health, Lublin, Poland

**Background:** HER2 is well established diagnostic and therapeutic target of the malignant tumors. It is important to precisely determine HER2 status of a tumor to achieve the best therapeutic outcome. This transmembrane receptor is shed by proteolytic cleavage and secreted as the soluble extracellular domain (ECD) of ~97–115 kDa circulating in a patient blood. The data on HER2 protein distribution within a tumor are scarce. Therefore, our goal was to quantify the HER2 protein associated with cells and cell-free tissue fluids of tumor. In addition, we aimed to compare the level of ECD circulating in blood with the tumor associated HER2 using the developed ELISA.

**Material and methods:** Xenograft mouse model included two groups of SCID mice. Animals were inoculated with SK-OV-3 (HER2+) and MDA-MB-231 (HER2-) cells, Group A and B respectively, to trigger tumor mass formation. Animals were euthanized for serum and tumor tissue collection. One part of the tumor sample was fixed for immunohistochemistry (IHC) and

stained for typical cancer biomarkers (including HER2). The second part was processed for PBS and RIPA buffer extraction for analysis of the tumor-released and cell-integral proteins, respectively. Presence of HER2 in the resulting tissue homogenates was confirmed by Western Blotting (WB). The developed ELISA was used for HER2 quantification in mouse tissue and serum. Statistical analysis on the obtained data was performed with R 4.1.2 software.

**Results:** IHC of the tumor sections confirmed malignant pathology in all studied mice. Intermediate HER2 staining (corresponding to score 2+ or 3+) was observed in mice receiving SK-OV-3 cells but not in mice with MDA-MB-231 tumor (negative staining). There was variable expression of other typical cancer markers like CK8/18, ER, and PR. WB with anti-HER2 antibody of the RIPA buffer homogenates (cell-associated fraction) showed presence of the full length HER2 protein in SK-OV-3 but not in MDA-MB-231 homogenates. Reactivity of the 75–110 kDa proteins (corresponding to ECD) was observed for the SK-OV-3 tumors. In the same mice the blood level of HER2 reached on average 152.56 ng/ml (129.47–166.1 ng/ml) in animals with SK-OV-3 tumors or was under detection in mice with MDA-MB-231 tumors. In cell-free tumor homogenates there was on average 47 235.33 ng/mL (10 102.92–80 825.03 ng/ml) of HER2 protein.

**Conclusions:** The level of HER2 released from tumor in tissue homogenates was of a magnitude higher compared to the serum HER2 concentration in the same mice. It suggests significant accumulation of the shed HER2 protein around the tumor microenvironment and points out to the attractive diagnostic site for detection of the HER2, especially in the low expressing tumors.

**Funds:** National Centre for Research and Development, Strategmed II (No. STRATEGMEDII/269364/5/NCBR/2015); EU, Horizon 2020 SME Instrument (No. 783818).

**No conflict of interest.**

37

(PB027)

### Establishment and characterization of HPV+ metastatic squamous cell anal carcinoma XPDX models in athymic nude mice

J. Flores<sup>1</sup>, C. Moreno<sup>1</sup>, A. Moriarty<sup>1</sup>, K. Papadopoulos<sup>2</sup>, R. Drengler<sup>3</sup>, L. Rodriguez<sup>3</sup>, H. Salih<sup>3</sup>, D. Rasco<sup>2</sup>, A. Patnaik<sup>2</sup>, M. Wick<sup>1</sup>. <sup>1</sup>XenoSTART, Translational Research, San Antonio, USA; <sup>2</sup>START, Ph1 Research, San Antonio, USA; <sup>3</sup>START Center, Medical Oncology, San Antonio, USA

**Background:** Squamous cell carcinoma of the anus (SCCA) is a rare malignancy comprising less than 3% of all gastrointestinal cancers in the United States. While over 90% of SCCA have been found human papilloma virus positive (HPV+), a majority of cases present locally and can be cured with definitive therapy. However, metastatic SCCA is less treatable and poorly understood in part due to the lack of relevant preclinical models. To this end we have established four HPV+ XenoSTART ethnically and gender diverse Patient-Derived Xenograft (XPDX) models of metastatic SCCA designated ST4808, ST5678, ST5872 and ST6058. These models were established in athymic nude mice and characterized for receptor expression, genomic alterations, and *in vivo* drug sensitivity.

**Methods:** ST4808 was established from biopsy collected from a 51-year-old Hispanic male with recurrent anal cancer following initial resection. ST5678 was established from a liver biopsy collected from a 55-year-old Hispanic male with newly-diagnosed SCCA. ST5872 was established from a liver biopsy collected from a 70-year-old Hispanic female with recurrent SCCA following prior treatment with 5-FU, mitomycin and radiation. ST6058 was established from a lung biopsy collected from a 55-year-old Caucasian female with recurrent SCCA following treatment with 5-FU/mitomycin/radiation, carboplatin/gemcitabine, and investigational therapies. The resulting models were passaged and characterized using immunohistochemistry and genomic analysis including WES and RNA<sub>seq</sub>. *In vivo* studies were performed testing various chemotherapy and targeted agents; study endpoints included tumor volume and time from treatment initiation with % T/C values and tumor regression reported at study completion; a %T/C of £20 versus control was considered sensitive. Tumor regression (%T/C < 0) versus Day 0 tumor volume was also reported.

**Results:** Immunohistochemistry analysis of each model confirmed disease similar to corresponding patient's cancer using archival clinical samples. WES/RNA<sub>seq</sub> analysis identified E2H2 and STK11 variants in ST4808, ERBB2 and PIK3CA mutations in ST5678, an FGFR3-TACC3 fusion in ST5872 and KDM6A and CYLD variants in ST6058. *In vivo*, ST4808 demonstrated sensitivity to platinum chemotherapy while ST5678 was resistant to tucatinib, neratinib and apelisib but not platinum. ST5872 reported modest sensitivity to erdafitinib and ST6058 was resistant to tested therapies.

**Conclusion:** We have established and characterized four models of HPV+ metastatic SCCA cancer and benchmarked chemotherapy and relevant

targeted therapies in each model. These models are valuable tools for evaluating potential therapies for metastatic anal cancer.

**No conflict of interest.**

38 (PB028)

**Establishment and characterization of a panel of BRAFV600E colorectal XPDX models from patients with acquired resistance to targeted therapies**

A. Moriarty<sup>1</sup>, J. Flores<sup>1</sup>, A. Peskin<sup>2</sup>, M. Lynch<sup>2</sup>, K. Papadopoulos<sup>3</sup>, N. Lakhani<sup>4</sup>, M. Sharma<sup>4</sup>, R. Drengler<sup>5</sup>, J. Szender<sup>5</sup>, D. Rasco<sup>3</sup>, A. Patnaik<sup>3</sup>, A. Bucheit<sup>5</sup>, M. Wick<sup>1</sup>. <sup>1</sup>XenoSTART, Translational Research, San Antonio, USA; <sup>2</sup>XenoSTART, Translational Research, Grand Rapids, USA; <sup>3</sup>START, Ph1 Research, San Antonio, USA; <sup>4</sup>START Midwest, Ph1 Research, Grand Rapids, USA; <sup>5</sup>START Center, Medical Oncology, San Antonio, USA

**Background:** The BRAF V600E mutation occurs in up to 20% of patients with metastatic colorectal cancer (CRC). Combination of the BRAF inhibitor encorafenib with the EGFR inhibitor cetuximab was recently approved for V600E-mutated metastatic CRC cancer as second-line therapy. While this treatment provides needed benefit to BRAF<sup>V600E</sup>-mutated CRC patients, some patients will progress on therapy with few viable options. To this end we have established four XenoSTART Patient-Derived Xenograft (XPDX) models from CRC BRAF<sup>V600E</sup> patients clinically refractory to targeted therapies. These models, designated ST5111, ST5986, STM054 and STM110C, were characterized for receptor expression, genomic alterations, and in vivo drug sensitivities toward multiple chemotherapies and targeted agents.

**Methods:** ST5111 was established from a liver biopsy collected from a 69-year-old Caucasian female following treatment with FOLFOX (2 m), dabrafenib/trametinib (21 m), encorafenib /binimetinib (14 m) and radiation. ST5986 was established from a vaginal biopsy collected from a 72-year-old Hispanic female following treatment with capecitabine (9 m), pembrolizumab (6 m), and encorafenib/panitumumab (9 m). STM054 was established from fluid collected from a 53-year-old female following treatment with FOLFOX/beva (3 m), FOLFOXIRI (4 m) and encorafenib/binimetinib/cetuximab (10 m). STM110C was established from fluid collected from a 52-year-old male following treatment with FOLFOX/beva (3 m), FOLFIRI (3 m), encorafenib/cetuximab (2 m) and an investigation therapy plus encorafenib/cetuximab (7 m). The resulting models were passaged and characterized using genomic analysis including WES and RNA<sub>seq</sub>. In vivo studies were performed testing therapies; study endpoints included tumor volume and time from treatment initiation with %T/C values and tumor regression reported at study completion; a %T/C of E20 versus control was considered sensitive. Tumor regression (%T/C < 0) versus Day 0 tumor volume was also reported.

**Results:** Genomic analysis of models confirmed BRAF<sup>V600E</sup> in all models as well as several co-mutations including BRCA2<sup>T2685fs</sup> in ST5986, MCL1<sup>E110del</sup> in STM054 and PIK3CA<sup>Q546E</sup> in STM110C. In vivo models were resistant to encorafenib plus binimetinib but adding cetuximab significantly improved response. Single agent trametinib but not binimetinib was active in two of four models and dabrafenib alone or in combination did not provide benefit in any model. Sacituzumab and alpelisib alone reported some activity towards STM110C but HER2 therapies T-DM1 or DS-8201a were not effective.

**Conclusion:** We established and characterized a panel of four CRC BRAF<sup>V600E</sup> models from patients with acquired resistance to BRAF/MEK/EGFR targeted therapies. These models are useful for evaluating next generation therapies and elucidating mechanisms of resistance to targeted therapies in V600E CRC.

**No conflict of interest.**

39 (PB029)

**Sodium-glucose cotransporter 2 (SGLT2) inhibition improves alpelisib (ALP)-induced hyperglycemia in Zucker diabetic fatty (ZDF) rats**

C. Schnell<sup>1</sup>, T. Ferrat<sup>1</sup>, A. Schwarzmueller<sup>1</sup>, J. Gao<sup>2</sup>, C. Fritsch<sup>1</sup>. <sup>1</sup>Novartis Institutes for Biomedical Research, Oncology Research, Basel, Switzerland; <sup>2</sup>Novartis Institutes for Biomedical Research, Cardiovascular & Metabolic Diseases, Cambridge, USA

**Background:** In the Phase III SOLAR-1 trial (NCT02437318), the PI3K $\alpha$  selective inhibitor ALP + fulvestrant (FULV) significantly improved progression-free survival vs FULV alone in patients (pts) with HR+/HER2-ABC with PIK3CA mutations. Hyperglycemia is an on-target adverse effect of ALP (PI3 K inhibition affects insulin sensitivity and glucose metabolism) that led to 6% of pts in the ALP arm discontinuing treatment (tx) in SOLAR-1. SGLT2

inhibition is known to reduce PI3 K inhibition-induced blood glucose and insulin increase. In 6 SOLAR-1 pts, the addition of an SGLT2 inhibitor to metformin (MET) stabilized blood glucose levels, allowing pts to continue ALP + FULV tx. In a study (Schnell C, et al. EORTC 2021. P137) in healthy 10- to 12-week-old Brown Norway rats, we showed that a repeated daily dose of MET + dapagliflozin (DAPA) + ALP normalized ALP-induced increase in blood glucose levels over the 24 h dosing period and was well tolerated. In this study, we investigated if this positive interaction would persist in an obese animal model used in type 2 diabetes research, the ZDF rat, which represents aspects of a pt population at high risk for developing hyperglycemia.

**Methods:** The ZDF rat was used to investigate the degree of glucose and insulin control achievable upon tx with ALP and an SGLT2 inhibitor DAPA + MET. Freely feeding (Purina 5008 rat chow) male rats (mild diabetic stage) at 8 to 11 weeks of age were selected for the study.

**Results:** In ZDF rats with mild diabetes, repeated daily doses of DAPA at 1 mg/kg with MET at 350 mg/kg and ALP at 12.5 mg/kg po (ALP 12.5–25 mg/kg is considered the clinically relevant dose in rats) normalized blood glucose levels over the 24 h dosing period and was well tolerated. This effect was maintained when the dose of ALP was increased to 30 and 40 mg/kg. ALP (40 mg/kg) as a single agent induced hyperinsulinemia at 4 h post tx, confirming the mild diabetic stage of our ZDF rats. When combined with DAPA + MET, a lower incidence of hyperinsulinemia was observed compared to ALP as a single agent. ALP (40 mg/kg) as a single agent induced a mild increase in ketone levels at 4 h post tx. When combined with DAPA + MET, a smaller increase in ketone levels was observed compared to ALP as a single agent. No modulations of blood lactate levels were observed in any groups. When combined with DAPA + MET, no differences in ALP blood levels at C<sub>max</sub> (4 h post tx) were observed compared with ALP as a single agent, indicating low likelihood of drug-drug interactions.

**Conclusions:** DAPA + MET significantly reduced hyperglycemia and improved hyperinsulinemia induced by ALP in mild diabetic ZDF rats. The Phase II EPIK-B4 trial (NCT04899349) is currently assessing the safety and efficacy of the combination of DAPA + MET compared with MET during tx with ALP + FULV in pts with HR+/HER2- ABC with PIK3CA mutations and prior endocrine therapy.

**Conflict of interest:**

Ownership: Mr. Schnell reports stock ownership from Novartis, during the conduct of the study Mr. Ferrat reports stock ownership from Novartis, during the conduct of the study Mr. Schwarzmueller reports stock ownership from Novartis, during the conduct of the study Ms. Gao reports stock ownership from Novartis, during the conduct of the study Ms. Fritsch reports stock ownership from Novartis, during the conduct of the study. Other Substantive Relationships: Mr. Schnell reports employment from Novartis, during the conduct of the study Mr. Ferrat reports employment from Novartis, during the conduct of the study Mr. Schwarzmueller reports employment from Novartis, during the conduct of the study Ms. Gao reports employment from Novartis, during the conduct of the study Ms. Fritsch reports employment from Novartis, during the conduct of the study.

40 (PB030)

**Genome-wide mapping of cancer dependency and genetic modifiers of chemotherapy using a high-risk hepatoblastoma genetic model**

J. Yang<sup>1</sup>. <sup>1</sup>St Jude Children's Research Hospital, Surgery, Memphis, USA

A lack of genetic models hampers our understanding of hepatoblastoma pathogenesis and the development of new therapies for this neoplasm. We have developed a liver-specific MYC-driven murine model that faithfully recapitulates the pathological features of human hepatoblastoma, with transcriptomics resembling the high-risk gene signatures of the human disease. Single-cell RNA-sequencing and spatial transcriptomics identified distinct subpopulations of hepatoblastoma cells. After deriving cell lines from the mouse model, we mapped the cancer dependency genes using CRISPR-Cas9 screening and identified druggable targets conserved in human hepatoblastoma. Our screen also revealed oncogenes and tumor suppressor genes in hepatoblastoma that engage multiple, druggable cancer signaling pathways. A genome-wide mapping of doxorubicin response by CRISPR-Cas9 screening identified modifiers whose loss-of-function synergizes with or antagonizes with the effect of chemotherapy. A novel combination therapy based on the screening greatly enhances therapeutic efficacy. These studies have provided a useful set of resources for high-risk hepatoblastoma including disease models, cancer dependency genes, potential therapeutic targets and more effective therapies.

**No conflict of interest.**

## POSTER SESSION

## Cellular Therapies

41 (PB031)  
**CAR-T cell engineering strategies aimed at safe and effective targeting of solid tumors**

S. Das<sup>1</sup>, S. Dharani<sup>1</sup>, J. Valton<sup>2</sup>, P. Duchateau<sup>3</sup>, L. Poirot<sup>4</sup>. <sup>1</sup>Collectis Inc, Innovation-Immunology, New York, USA; <sup>2</sup>Collectis, Gene Therapy, Paris, France; <sup>3</sup>Collectis, Gene Editing, Paris, France; <sup>4</sup>Collectis, Innovation-Immunology, Paris, France

Adoptive cell therapy based on chimeric antigen receptor-engineered T (CAR-T) cells has proven to be life-saving for many cancer patients. However, its therapeutic efficacy has so far been restricted to only a few malignancies, with solid tumors proving to be especially recalcitrant to efficient therapy. Poor intra-tumor infiltration by T cells and “T cell dysfunction” due to an immunosuppressive microenvironment are key barriers against CAR-T cell success against solid tumors. Furthermore, low level expression of CAR-directed tumor-associated antigens (TAA) in normal tissues can result in “on-target off-tumor” cytotoxicity, raising potential safety concerns. Using our best-in-class TALEN®-based gene editing platform, we present here innovative T cell engineering strategies that can combat some of the challenges posed by CAR-T cell development for solid tumors. These allogeneic ‘Smart CAR-T’ cells are designed to integrate locus-specific synthetic genes that respond to cues localized to the solid tumor microenvironment. The subsequent expression of these genes increases CAR-T cell persistence and anti-tumor activity while staying restricted to the tumor milieu. Thus, our proof-of-concept study demonstrates the feasibility of developing CAR-T cell engineering strategies that can improve solid tumor targeting while mitigating potential safety risks, encouraging us to bring them to the clinic.

No conflict of interest.

42 (PB032)  
**Utilizing Targeted Therapy to Block Triple-negative Breast Cancer Cell Colonization**

C. Zhang<sup>1</sup>, L. Wang<sup>1</sup>, R. Liu<sup>1</sup>. <sup>1</sup>University of Alabama at Birmingham, Genetics, Birmingham, USA

Triple-negative (estrogen receptor [ER]/progesterone receptor [PR]/human epidermal growth factor receptor 2 [HER2]-negative) breast cancer (TNBC) is a highly aggressive subtype of breast cancer. Approximately 34% of patients will experience distant recurrence within 3 years and eventually develop the chemotherapy-resistant, incurable disease. Therefore, the development of novel treatments is necessary. Accumulating data demonstrate that microRNA (miR)-146a, which is part of the miR-146 family, inhibits cancer cell proliferation, invasion, and metastasis in human cancers, including breast cancer, suggesting that miR-146a functions as a tumor suppressor in tumor cells. Our group demonstrated that miR-146a negatively regulates NF- $\kappa$ B activation to inhibit tumor growth and metastasis in TNBC. Furthermore, our data suggested that miR-146a suppresses TNBC colonization through the cellular transfer of miR-146a by exosomes at distant sites, highlighting a miR-146a-mediated crosstalk between TNBC cells and the microenvironment that inhibits tumor colonization. The data from our studies not only provide a novel therapeutic approach to prevent tumor metastasis in TNBC but also identify a new signaling pathway responsible for tumor metastasis. Since our studies support the suppressive role of miR-146a in tumor metastasis, thus, miR-146a may have the potential to block TNBC cell colonization at distant sites. We seek to test the therapeutic value of miR-146a in the prevention or treatment of TNBC metastasis.

No conflict of interest.

43 (PB033)  
**Unclustering Centrosomes and Induction of Multipolarity: Selective Killing Method to Cancer Cells**

B. Kalkan<sup>1</sup>, C. Özcan<sup>2</sup>, E. Çiçek<sup>1</sup>, C. Açılan Ayhan<sup>3</sup>. <sup>1</sup>Koç University, Graduate School of Health Sciences, Istanbul, Turkey; <sup>2</sup>Koç University, Research Center for Translational Medicine, Istanbul, Turkey; <sup>3</sup>Koç University, School of Medicine, Istanbul, Turkey

**Background:** The chemotherapeutics used today mostly suffer from selectively targeting tumor cells. Unlike normal cells, cancer cells frequently exhibit extra centrosomes, which tend to form multipolar spindles (MPS), triggering cell death. Nevertheless, cancer cells divide successfully by clustering their extra centrosomes into two poles. Nek2 kinase is a key molecule regulating mitotic processes, including centrosome cycle, kinetochore attachment, microtubule organization, and spindle assembly checkpoint. In our studies, we showed that while disruption of Nek2 results in clustering and bipolar divisions, its overexpression can uncluster centrosomes leading to MPS and consequent cell death. Therefore, revealing the molecular mechanism and targeting Nek2 in cells with supernumerary centrosomes may be an alternative strategy for targeted therapies.

**Material and methods:** Cell viability, apoptosis and competition assays were performed to investigate the effect of Nek2 overexpression inducing MPS. To investigate how and through which molecules Nek2 accomplishes its unclustering activity, we started with known Nek2 targets with relevant function and assessed their involvement in centrosomal unclustering. Known Nek2 targets (C-NAP1, Rootletin, Trf1, Hec1, Gas2L1) were tested using knock out or siRNAs in cells with extra centrosomes. We then identified the cell cycle specific interactome of Nek2 using TurboID labelling system.

**Results:** Cells with extra centrosomes were depleted from the population upon Nek2 overexpression as determined via competition assays. Apoptosis was induced following Nek2 overexpression as judged by the increase in caspase activity and Annexin V staining. Known Nek2 targets revealed no effect on centrosome clustering. Furthermore, the effect of Nek2 overexpression on MPS was additive with other known unclustering factors, such as the molecular motor protein HSET, suggestive of independent mechanism of action. We identified several proteins using TurboID labelling system, which were previously known to bind to Nek2 confirming the specificity of the assay. NuMA - also shown to uncluster centrosomes, was significantly enriched in our samples. Interestingly, while NuMA did not co-immunoprecipitate (co-IP) with Nek2, its knockdown was able to revert its unclustering activity. Another significantly enriched protein, Kif2C - a microtubule dependent motor protein known to localize to centrosomes, not only reverted Nek2 activity, but also co-IP'ed with Nek2.

**Conclusions:** We assigned a novel function for Nek2 in centrosome clustering. We are currently elucidating the detailed mechanism of action for how target proteins interact with Nek2 regulating its centrosome unclustering activity in cancer cells. Understanding the mechanism will provide new translational approaches for cancer-specific treatment.

No conflict of interest.

## POSTER SESSION

## Molecular Targeted Agents 1

45 (PB035)  
**Discovery of novel MTA-cooperative PRMT5 inhibitors as targeted therapeutics for MTAP deleted cancers**

A. Bartosik<sup>1</sup>, A. Radzimiński<sup>1</sup>, O. Levenets<sup>1</sup>, A. Bobowska<sup>1</sup>, A. Stachowicz<sup>1</sup>, K. Kuś<sup>1</sup>, K. Michalik<sup>1</sup>, K. Banaszak<sup>1</sup>, D. Krzemień<sup>1</sup>, M. Madej<sup>1</sup>, M. Skoda<sup>1</sup>, I. Tomczyk<sup>1</sup>, P. Podkalicka<sup>1</sup>, K. Gluza<sup>1</sup>, G. Satała<sup>1</sup>, A. Gondela<sup>1</sup>, M. Sowińska<sup>1</sup>, N. Boutard<sup>1</sup>, K. Brzózka<sup>1</sup>, M. Nowak<sup>1</sup>. <sup>1</sup>Ryvü Therapeutics, Research and Development, Krakow, Poland

Targeting PRMT5 in MTAP-deleted tumors in a synthetic lethal approach represents a promising antitumor strategy across many tumor types. Metabolic gene *MTAP* is localized at the 9p21 chromosome in the close proximity to *CDKN2A* tumor-suppressor locus. Co-deletion of *MTAP* may be observed in 80–90% of all tumors harboring homozygous deletion of *CDKN2A*, which represents 10–15% of all human tumors.

*MTAP* deletion results in a massive accumulation of methylthioadenosine (MTA) in cells. MTA in high concentrations is a selective inhibitor of PRMT5 type II methyltransferase. PRMT5 conjugated with WD-repeat containing proteins (MEP50/WDR77) forms methylosome, which regulates essential cellular functions via symmetric dimethylation (SDMA) of target proteins involved in regulation of gene expression, RNA splicing, signal transduction,

metabolism and other functions. Accumulation of MTA in cells with MTAP deletion causes a partial inhibition of the methylation activity of PRMT5, which in turn reduces the level of symmetric arginine dimethylation of the whole proteome, and thus an increased sensitivity of cells to modulation of the methylome activity. Therapeutic targeting of PRMT5 in homozygous MTAP-deleted cancers constitute a promising strategy of selective killing of genetically defined cancer cells. Here we present MTA-cooperative PRMT5 inhibitors, which selectively inhibit the growth of MTAP-deleted cancer cells.

Ryvu has identified a series of MTA-cooperative PRMT5 inhibitors which have good drug-like physicochemical properties and block methyltransferase activity with nanomolar IC50 values. Structurally enabled hit generation and optimization allowed quick expansion and delivery of several generations of compounds with novel IP, high target engagement in cells and selective potency in MTAP-deleted cell lines. Ryvu compounds selectively inhibit growth of MTAP-deleted cancer cells in prolonged 3D culture, which strongly correlates with inhibition of PRMT5-dependent protein symmetric dimethylation (SDMA) in those cells. Selectivity between effects observed in MTAP-deleted and WT cells exceeds 100-fold both for SDMA and growth inhibition. The DMPK profile of these compounds allows for oral administration, which enables testing dose-dependent antitumor activity in MTAP null tumor xenograft-bearing mice. Efficacy studies with our lead compound resulted in demonstration of tumor growth inhibition in MTAP<sup>-/-</sup> model, accompanied by significant inhibition of target proximal PD biomarker.

Overall, these studies provide a rationale for the further optimization of our chemical series of MTA-cooperative PRMT5 inhibitors towards a clinical candidate.

**No conflict of interest.**

46 (PB036)

#### Superior efficacy of a dual EGFR-DNA targeting combi-molecule “ZR2002” in comparison with its analogues 6-mono-alkylamino- and 6,6-dialkylaminoquinazoline in a human osteosarcoma xenograft model

C. Facchin<sup>1</sup>, A.L. Larroque<sup>1</sup>, A. Alliga<sup>1</sup>, A. Fraga Timiraos<sup>1</sup>, B. Jean-Claude<sup>1</sup>. <sup>1</sup>Cancer Drug Research Laboratory- The Research Institute of the McGill University Health Center/Glen Hospital, Department of Medicine- Division of Medical Oncology, Montreal, QC H4A 3J1, Canada

**Background:** We and others demonstrated the feasibility of one single molecule capable of inhibiting the epidermal growth factor receptor (EGFR) and capable of inducing DNA damage. ZR2002 is a combi-molecule carrying a chloroethyl at the 6-position of the quinazoline ring and it does not require hydrolysis to inhibit EGFR and alkylate the DNA. ZR2002, despite its good pharmacokinetics, is metabolized *in vivo* into deschloroethyl metabolite, losing the DNA damage activity. More recently, we undertook a comparative study to test whether N,N-disubstituted analogues of ZR2002 (JS84 and JS61) could behave as its stable prodrugs and maintain stronger dual-activity *in vivo*. We compared the efficacy, metabolism and mechanism of action of ZR2002 and the selected analogues.

**Material and Methods:** Tumor xenografts were obtained by unilateral and subcutaneous injection of Saos-2 cell line into immunodeficient NSG male mice. Mice were randomly divided into 4 groups: one treated with ZR2002 (N = 7), the other treated with JS84 (N = 7), another treated with JS61 (N = 7) and the last treated with vehicle (VEH) (N = 7). Mice were treated every other day for 20 days, receiving a total of 10 doses by oral gavage (80 mg/kg). In addition to caliper measurement, at the end of the study tumor burden was measured by CT-imaging and drug metabolism by LC-MS. The levels of EGFR phosphorylation (P-EGFR) and  $\gamma$ -H2AX phosphorylation (P-H2AX) for DNA damage were quantified by western blot and immunohistochemistry.

**Results:** ZR2002 caused a significant antitumor activity *in vivo* ( $p < 0.05$ ). JS84 induced an apparent tumor delay ( $p > 0.05$ ) and JS61 was inactive. Metabolic analysis by LC-MS revealed that the disubstituted molecule JS84 remains partially intact, partially deschloroethylated or demethylated ZR2002. Likewise, JS61 remained partially intact and deschloroethylated to give ZR2002 and other metabolites. However, none of these prodrugs yielded greater concentrations of ZR2002 than when the latter was administered intact. ZR2002-treated tumors showed 4-folds stronger inhibition of P-EGFR and enhanced levels of P-H2AX than the VEH. JS84 and JS61-treated tumors did not exhibit decreased levels P-EGFR or increased P-H2AX in comparison with VEH or ZR2002.

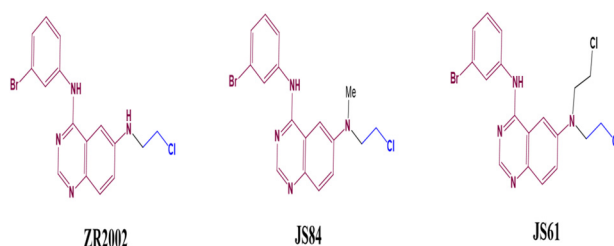


**Figure 1** Structure formula of the combi-molecules ZR2002, JS84 and JS61.

**Conclusions:** The results *in toto* suggest that intratumoral concentrations of intact ZR2002 are correlated with the highest inhibition of P-EGFR and induction of DNA damages. ZR2002 intact structure is required for an optimal activity *in vivo* and represents a good drug candidate for the treatment of EGFR-overexpressing osteosarcoma.

**No conflict of interest.**

47 (PB037)

#### TYRA-200: Potent Against FGFR2 Fusions, Molecular Brake Mutations and Gatekeeper Resistance

E. Allen<sup>1</sup>, A. Balcer<sup>1</sup>, D. Bensen<sup>1</sup>, T. Burn<sup>1</sup>, I. Hoffman<sup>1</sup>, R. Hudkins<sup>2</sup>, S. Iyer<sup>1</sup>, M. Neal<sup>1</sup>, K. Nelson<sup>1</sup>, C. Occhino<sup>2</sup>, P. Patel<sup>2</sup>, J. Starrett<sup>1</sup>, R. Swanson<sup>1</sup>, Q. Ye<sup>1</sup>. <sup>1</sup>Tyra Biosciences, Biology, Carlsbad, USA; <sup>2</sup>Tyra Biosciences, Chemistry, Carlsbad, USA

**Background:** Approved pan-FGFR (fibroblast growth factor receptor) inhibitors and those in late-stage clinical development (pemigatinib, infigratinib, and futibatinib) have demonstrated a clinical benefit in metastatic FGFR2-fusion or rearranged intrahepatic cholangiocarcinoma (ICC). However, inhibition of emerging polyclonal on-target acquired resistance mutations remains a critical unmet need. TYRA-200 is an FGFR1/2/3 inhibitor that was designed to specifically address these clinically observed acquired resistance mutations within the kinase domain of FGFR2. A significant therapeutic benefit may be achieved from this precision approach for FGFR2-driven cancers.

**Materials and Methods:** TYRA-200 was evaluated in enzymatic assays and cell lines driven by FGFR2 fusions and mutations. *in vivo* tumor growth inhibition with TYRA-200 was tested in several FGFR2-driven models.

**Results:** In enzymatic assays, TYRA-200 maintained potent inhibition for the gatekeeper mutants V565L/F and the molecular brake mutants N550D/H/K and E566A. Cellular potency for these mutants was confirmed in a panel of Ba/F3 cell lines expressing wild type FGFR2 and variants N550 K, V565F, V565I, K660E and K660N. Additionally, TYRA-200 maintained potency *in vitro* in an endometrial cancer cell line AN3CA, which harbors the molecular brake mutation N550 K. *in vivo* tumor regressions were achieved in both the AN3CA and Ba/F3 FGFR2 V565F models. In the AN3CA xenograft model 80% tumor regression was achieved, while in the Ba/F3 FGFR2 V565F allograft model, a 64% tumor regression was seen, whereas tumor regression was not observed with futibatinib.

**Conclusions:** TYRA-200 is currently under development for FGFR2-altered advanced solid tumors, including ICC. Importantly, the data demonstrates that TYRA-200 retains potency across multiple resistance mutations which emerge during therapy, including gatekeeper and molecular brake mutations.

**Conflict of interest:**

Ownership: Tyra Biosciences shareholders.

48 (PB038)  
**NMS-173, a potent, covalent second generation IDH1/IDH2 inhibitor**

P. Magnaghi<sup>1</sup>, F. Casuscelli<sup>2</sup>, E. Ardini<sup>3</sup>, A. Parazzoli<sup>4</sup>, S. Troiani<sup>1</sup>, B. Valsasina<sup>1</sup>, G. Texido<sup>5</sup>, E. Casale<sup>2</sup>, N. Avanzi<sup>1</sup>, P. Orsini<sup>2</sup>, S. Nuvoletti<sup>2</sup>, B. Salom<sup>2</sup>, A. Lombardi Borgia<sup>2</sup>, E. Salsi<sup>2</sup>, G.S. Saturno<sup>6</sup>, S. Re Depaolini<sup>1</sup>, C. Stellato<sup>5</sup>, A. Montagnoli<sup>3</sup>, A. Galvani<sup>5</sup>, A. Isacchi<sup>7</sup>. <sup>1</sup>Nerviano Medical Sciences srl, Biotech Sciences, Nerviano MI, Italy; <sup>2</sup>Nerviano Medical Sciences srl, Medicinal Chemistry & Drug Design, Nerviano MI, Italy; <sup>3</sup>Nerviano Medical Sciences srl, Global Asset Leadership, Nerviano MI, Italy; <sup>4</sup>Accelera, Preclinical Development, Nerviano MI, Italy; <sup>5</sup>Nerviano Medical Sciences srl, Discovery Pharmacology, Nerviano MI, Italy; <sup>6</sup>Nerviano Medical Sciences srl, Global Asset Leadership srl, Nerviano MI, Italy; <sup>7</sup>Nerviano Medical Sciences srl, Oncology Discovery, Nerviano MI, Italy

**Background:** IDH1 and IDH2 (isocitrate dehydrogenase 1 and 2) are metabolic enzymes mutated in subsets of solid and hematological tumors. Mutations in IDH1 or IDH2 generate high levels of the 2-HG (2-hydroxyglutarate) oncometabolite that promotes de-differentiation, stemness and tumorigenesis. Inhibition of mutant IDH1 or IDH2 decreases 2-HG production and induces re-differentiation of tumor cells. First generation IDH inhibitors received FDA approval for the treatment of subsets of AML and cholangiocarcinoma patients, but extent and duration of response are limited in these patients and no targeted options are available for the other IDH1/IDH2 mutant solid tumors.

NMS-173 is a second-generation potent, covalent dual inhibitor of mutant IDH1 and IDH2, with preclinical features expected to result in improved and long-lasting clinical efficacy compared to first-generation IDH inhibitors.

**Methods:** NMS-173 was profiled in biochemical and cellular assays related to different IDH1 and IDH2 mutants. ADME properties and pharmacokinetic (PK) parameters in rodent and non-rodent species were evaluated. Pharmacodynamic (PD) studies measuring target engagement and 2-HG modulation were conducted in tumor tissue and PBMC samples from mice bearing solid and hematological human tumor xenografts, including models with different IDH mutants. A complete IND-enabling package was prepared, submitted and approved by the FDA.

**Results:** NMS-173 specifically derivatized Cys269 of IDH1 and Cys308 of IDH2 *in vitro* and displayed a time-dependent biochemical activity with (t = 2 h) IC50 s in the low nanomolar range on IDH1 R132X and IDH2 R172 K mutants. NMS-173 completely inhibited the production of 2-HG in several IDH1 and IDH2 mutant cell lines, with no direct antiproliferative effects. In preclinical PK/PD studies, oral treatment with NMS-173 consistently suppressed production of the 2-HG oncometabolite in tumors and corresponding plasma samples by >90% in different IDH1 mutant xenograft and PDX models (HT-1080 fibrosarcoma, HCCC-9810 cholangiocarcinoma, BT-142 orthotopic glioma, LEXFAM 2734 AML) at well-tolerated doses. NMS-173 induced stronger and more durable efficacy than ivosidenib in the HCCC-9810 IDH1 mutant cholangiocarcinoma xenograft model and increased the survival of mice bearing the LEXFAM2734 IDH1 mutant PDX AML line, with a better disease control compared to ivosidenib. NMS-173 was very well tolerated upon repeated administration in different species with a wide therapeutic window in non-GLP and GLP tox studies.

**Conclusions:** NMS-173 is a second generation, dual IDH1/IDH2 inhibitor with a covalent mode of action, inducing abrogation of 2-HG production and anti-tumor efficacy in IDH mutant mouse models superior to competitors. NMS-173 has the potential for better efficacy compared to FDA approved drugs and has received authorization to start phase I clinical studies.

**No conflict of interest.**

49 (PB039)  
**Combined inhibition of SHP2 and CDK4/6 is active in NF1-MPNST**

J. Wang<sup>1</sup>, A. Calizo<sup>1</sup>, K. Pollard<sup>1</sup>, L. Zhang<sup>1</sup>, J. Gross<sup>2</sup>, C. Pratiias<sup>1</sup>. <sup>1</sup>Johns Hopkins, Oncology, Baltimore, USA; <sup>2</sup>Johns Hopkins, Pathology, Baltimore, USA

**Background:** NF1 is an essential negative regulator of RAS activity and its function is lost in nearly 90% of malignant peripheral nerve sheath tumors (MPNST). Additional recurrent molecular changes include loss of function alterations in *CDKN2A*, *TP53*, *EED* and *SUZ12*, but molecular targeting of these genomic events represents a unique challenge. We previously reported that the efficacy of MEK inhibitor is limited by adaptive activation of receptor tyrosine kinases and the adaptor protein SHP2, and that combined inhibition of MEK and SHP2 is effective in MPNST. However, the clinical potential of combination MEK and SHP2 inhibitors may be limited by the overlapping toxicity induced by ERK pathway inhibition. Loss of *CDKN2A*, inactivation of RB1, and hyperactivation of cyclin dependent kinases (CDK) in MPNST also suggest that small-molecule CDK4/6

inhibitors (CDK4/6i) may be a potential therapeutic strategy, but monotherapy with CDK4/6i also demonstrates limited activity. We hypothesize that the anti-tumor response of SHP2i may be potentiated by agents targeting the cell cycle in combination.

**Methods:** The effects of shRNA-mediated inducible SHP2 knockdown on RAS signaling, short-term and long-term cell growth, and response to CDK4/6i were examined using immunoblotting, high throughput proliferation assays, and colony formation assays. Combined effects of SHP2i plus CDK4/6i on signaling, cell cycle, apoptosis, cell and *in vivo* tumor growth were assessed. Pharmacodynamic (PD) assays were performed on tumors extracted following drug treatment in patient-derived xenograft (PDX) models of MPNST.

**Results:** Despite a modest effect of SHP2 knockdown on ERK signaling, shPTPN11 reduced MPNST cell growth. SHP2 knockdown or SHP2i treatment alleviated activation of ERK signaling and cyclin D1 expression induced by CDK4/6i, and enhanced the sensitivity to CDK4/6i. Combination benefit was observed in *in vitro* cell growth and *in vivo* PDX. Although some PDX models demonstrated similar responses to SHP2i alone or SHP2i + CDK4/6i during the initial four weeks on treatment, we found sustained tumor growth inhibition exerted by the combination on longer therapy. PD studies demonstrated a decrease in p-ERK levels in tumors treated with either SHP2i alone or the SHP2i/CDK4/6i combination, as well as a synergistic suppression of cell cycle regulators by the combination.

**Conclusions:** Our preliminary data demonstrate that the combined inhibition of SHP2 and CDK4/6 is active and produces deep and durable response in models of NF1-associated MPNST. This combination strategy may represent a novel treatment approach for patients with MPNST.

**Conflict of interest:**

Other Substantive Relationships: Grant support, Novartis Institute for Biomedical Research

50 (PB040)

**A phase 1/2, open-label, multicenter study to investigate the safety, pharmacokinetics, and efficacy of fadraciclib (CYC065), an oral CDK2/9 inhibitor, in subjects with advanced solid tumors and lymphoma**

S. Piha-Paul<sup>1</sup>, D.Y. Oh<sup>2</sup>, E. Garralda<sup>3</sup>, M. Vieito<sup>4</sup>, J. Huang<sup>5</sup>, M. Kirschbaum<sup>5</sup>, M. Villanona-Calero<sup>6</sup>. <sup>1</sup>MD Anderson Cancer Center, Investigational Cancer Therapeutics, Houston, USA; <sup>2</sup>Seoul National University Hospital, Medical Oncology, Seoul, South Korea; <sup>3</sup>Vall d'Hebron Institute of Oncology, Medical Oncology - Early Drug Development, Barcelona, Spain; <sup>4</sup>Vall d'Hebron Institute of Oncology, Medical Oncology, Barcelona, Spain; <sup>5</sup>Cyclacel, Clinical Development, Berkeley Heights, USA; <sup>6</sup>City of Hope National Medical Center, Medical Oncology and Therapeutic Research, Duarte, USA

**Background:** Fadraciclib is a highly selective, orally- and intravenously-available, 2nd generation amino-purine inhibitor of CDK2 and CDK9. Translational biology supports the development of fadraciclib as a therapeutic agent for cancers dependent on MCL1 and MYC through the inhibition of CDK9, and for cancers associated with CCNE1 amplification, a known resistance factor for trastuzumab and CDK4/6 inhibitors, through the inhibition of CDK2. By inhibiting CDK2 and 9, fadraciclib causes apoptotic death of cancer cells at sub-micromolar concentrations. In an earlier Phase 1 study of IV fadraciclib, confirmed CR has been achieved in a subject with MCL1-amplified endometrial cancer. Oral fadraciclib is highly bioavailable allowing flexibility of dosing and schedule.

**Methods:** Fadraciclib is being evaluated in a global, open-label, non-randomized, dose-escalation (phase 1) study in subjects with advanced solid tumors or lymphoma, and proof of concept (phase 2) in subjects with targeted indications, designated CYC065-101, (NCT04983810). Phase 1 explores both schedule and dose of oral fadraciclib monotherapy in 28-day cycles to identify MTD and/or RP2D. Once RP2D is established, phase 2 will enroll 12 to 40 subjects in seven specific tumor-type groups and a basket cohort, utilizing a Simon two-stage optimal design to evaluate clinical activity. Phase 2 groups include endometrial or ovarian cancer, biliary tract cancer, hepatocellular carcinoma, breast cancer, B-cell lymphoma, T-cell lymphoma, metastatic colorectal cancer and a basket cohort for tumors with MCL1, MYC or CCNE1 amplification/overexpression.

**Results:** CYC065-101 study started enrolling subjects in July 2021 and is ongoing at City of Hope National Cancer Center, MD Anderson Cancer Center, Seoul National University Hospital, and Vall d'Hebron Institute of Oncology. As of June 2022, 17 subjects have received fadraciclib at dose levels 1 to 5. Fadraciclib was well tolerated at all dose levels with no DLT and no SUSAR observed. Preliminary efficacy data are available for 16 patients. One patient with CTCL showed PR per mSWAT response criteria. At dose level 5, a patient with endometrial cancer showed 15% reduction of target lesions after first cycle of treatment, and a patient with Angioimmunoblastic



T-Cell Lymphoma (AITL) showed extensive reduction in multiple lesions after first cycle of treatment. PK, PD, and PGx including NGS and RNA-Seq are being evaluated in phase 1 subjects. Preliminary PK analysis suggests dose dependent exposure. Studies on MYC, MCL1, and PPP1R10 mRNA in peripheral blood samples after fadraciclib treatment will be shown.

**Conclusion:** Based on data from the CYC065-101 study, fadraciclib appears to be well tolerated from dose levels 1 to 5. No drug related SAEs, SUSAR or DLTs were reported. The trial is ongoing with a primary endpoint of defining MTD and RP2D.

#### Conflict of interest:

Advisory Board: D. Oh: AstraZeneca, Novartis, Genentech/Roche, Merck Serono, Bayer, Taiho, ASLAN, Halozyme, Zymeworks, BMS/Celgene, BeiGene, Basilea, Turning Point, Yuhan, Arcus Biosciences, IQVIA

M. Villanona-Calero: Eli Lilly

Corporate-sponsored Research: S. Piha-Paul: AbbVie, ABM Therapeutics, Acepodia, Alkermes Aminex Therapeutics Amphivena Therapeutics, BioMarin Pharmaceutical, Boehringer Ingelheim Bristol Myers Squibb Cerulean Pharma, Chugai Pharmaceutical, Curis, Cyclacel Pharmaceuticals Daiichi Sankyo Eli Lilly ENB Therapeutics Five Prime Therapeutics F-Star Beta Limited F-Star Therapeutics Gene Quantum Genmab A/S Gilead Sciences, GlaxoSmithKline Helix BioPharma, HiberCell, Immunomedics, Incyte, Jacobio Pharmaceuticals, Lytix Biopharma AS Medimmune, Medivation, Merck Sharp and Dohme, Novartis Pharmaceuticals Pieris Pharmaceuticals, Pfizer Phanes Therapeutics Principia Biopharma, Puma Biotechnology, Purinomia Biotech, Rapt Therapeutics, Seattle Genetics Silverback Therapeutics Synlogic Therapeutics Taiho Oncology Tesaro, TransThera Bio ZielBio, NCI/NIH, P30CA016672 – Core Grant (CCSG Shared Resources) Consulting: CRC Oncology

D. Oh: Research Grant: AstraZeneca, Novartis, Array, Eli Lilly, Servier, BeiGene, MSD, Handok

E. Garralda: Research: Novartis/Roche/Thermo Fisher/AstraZeneca/Taiho/BeiGene Consultant/Advisor: Roche/Genentech - F.Hoffmann/La Roche/Ellipses Pharma/Neomed Therapeutics 1 Inc/Boehringer Ingelheim/Janssen Global Services/SeaGen/Alkermes/Thermo Fisher/Bristol-Mayers Squibb/MabDiscovery/Anaveon/F-Star Therapeutics/Hengrui Speakers Bureau: Merck Sharp & Dohme/Roche/Thermo Fisher/Lilly/Novartis Clinical Trials PI or Co-PI (Institution): Affimed GmbH - Amgen SA - Anaveon AG - AstraZeneca AB - Biontech GmbH - Catalym GmbH - Cytomx - F.Hoffmann La Roche Ltd - F-Star Beta Limited - Genentech Inc - Genmab B.V. - Hutchison Medipharma Limited - Icon - Imcheck Therapeutics - Immunocore Ltd - Janssen-Cilag SA - Medimmune Lic - Merck Kgga - Novartis Farmacéutica, S.A - Peptomyc - Ribon Therapeutics - Roche Farma SA - Seattle Genetics Inc - Symphogen A/S - Taiho Pharma Usa Inc

M. Vieito: Travel grants: Roche, EMD/Serono Consulting: Roche, Debiopharm

M. Villanona-Calero: Speakers Bureau: Amgen

Other Substantive Relationships: J. Huang: Employee of Cyclacel, the trial sponsor

M. Kirschbaum: Employee of Cyclacel, the trial sponsor

M. Villanona-Calero: Stocks: Moderna

#### 51 (PB041) HX301 (ON123300) shows broad antitumor activity in preclinical mantle cell lymphoma models, inclusive of those resistant to BTKi

Z. Jiao<sup>1</sup>, H. Ke<sup>2</sup>, F. Zhang<sup>2</sup>, H. Li<sup>2</sup>, J. Wang<sup>1</sup>. <sup>1</sup>Crown Bioscience Inc., San Diego, USA; <sup>2</sup>Hanx Biopharmaceuticals Inc., Oceanside, California, USA

**Background:** Mantle cell lymphoma (MCL) is a subtype of non-Hodgkin lymphoma (NHL) of a mature B cell malignancy, which accounts for ~6% of NHLs. It is hallmarked with the chromosomal translocation t(11;14)(q13;q32). MCL is considered difficult to treat, with frequent relapse after effective conventional chemotherapy, contributing to a short median survival of 5–7 years and thus warranting the development of new therapeutics. Although the recent approval of Bruton tyrosine kinase inhibitor (BTKi) therapy has greatly improved the treatment of MCL, patients exhibiting primarily (intrinsic) resistance or BTKi-induced resistance, have few treatment options. HX301 (ON123300) is a clinical-stage multi-kinase inhibitor (CDK4/6, ARK5 and PI3K- $\delta$ ), potent against MCL via its dual targeting mechanism of action (MoA) against CDK4 and PI3K- $\delta$ , as demonstrated through *in vitro* activities on two MCL cell lines (Granta519, Z138C), a couple of primary patient samples and *in vivo* activity in a Z138C cell line-derived xenograft (CDX) model. To test the hypothesis that HX301 has broad activity against MCL, an expanded panel of preclinical MCL models including patient-derived xenograft (PDX) and BTKi-resistant tumors were examined.

**Methods:** Xenograft panels including three PDX models (LY9615, LY9607, LY9604), two cancer CDX models (Granta-519 and Jeko-1), and two BTKi-induced resistant lines (REC-1 BTK C481S and ibrutinib-R-Mino

[FBP6]) were subcutaneously transplanted. When tumors reached ~200 mm<sup>3</sup> in size, the tumor-bearing mice were randomized into control and treatment groups and subjected to daily dosing of 100 mg/kg of HX301. The tumor growth kinetics and body weight of the models were monitored twice weekly.

**Results:** Our preliminary results confirmed that both CDX models responded well to HX301, consistent with previous observations for the Z138C model. Additionally, our data demonstrated that the three PDX models, with heterogeneity, genomic landscape and histopathology better mimicking MCL patients', also responded to HX301, superior to the current standards of care, lenalidoamine and the BTKi, ibrutinib. Together, HX301 showed broad anti-MCL activity in preclinical models, 100% to date. Most interestingly, the induced resistant models also responded, including the BTK-C481S MCL model. Our data suggest that MCL could be a potential indication for the clinical development of HX301, particularly for BTKi-resistant patients, either primary refractory or induced resistance.

**Conclusions:** Due to its complete distinct MoA from BTKi, HX301 may be a new treatment option for primary BTKi resistance as well as BTKi-induced resistance in MCL, warranting further clinical investigation.

No conflict of interest.

#### 52 (PB042) The RAF/MEK clamp VS-6766 shows strong anti-tumor activity across multiple MAPK pathway alterations, with a preferential effect on KRAS G12V

S. Coma<sup>1</sup>, M. Musteanu<sup>2</sup>, A. Mira<sup>3</sup>, C. Caffarra<sup>3</sup>, D. Morrison<sup>4</sup>, C. Ambrogio<sup>3</sup>, M. Barbacid<sup>2</sup>, J. Pachter<sup>1</sup>. <sup>1</sup>Verastem Oncology, Preclinical Research, Needham, USA; <sup>2</sup>Centro Nacional de Investigaciones Oncológicas, Biochemistry and Molecular Biology, Madrid, Spain; <sup>3</sup>University of Torino, Molecular Biology, Torino, Italy; <sup>4</sup>NCI-Frederick, Laboratory of Cell and Developmental Signaling, Frederick, USA

**Background:** KRAS is the most frequently mutated RAS/RAF family member (mutated in 15% of cancers), followed by BRAF (5%) and NRAS (3%). Several BRAF and MEK inhibitors (MEKi) are approved for BRAF V600E cancers, and the G12C inhibitor sotorasib is approved for KRAS G12C non-small cell lung cancer (NSCLC). However, there is still a need for agents targeting other RAS/RAF mutations (mt), including KRAS G12V which is mutated in ~7%, ~9% and ~19% of NSCLC, colorectal and pancreatic cancers, respectively.

VS-6766 is a unique RAF/MEK clamp that potently inhibits MEK kinase activity and induces a dominant negative RAF-MEK complex preventing phosphorylation of MEK by ARAF, BRAF and CRAF. This unique mechanism allows VS-6766 to block MEK signaling without the compensatory re-activation of MEK that appears to limit the efficacy of MEKi.

**Material and Methods:** *In vitro* assays were performed to evaluate the anti-proliferative activity of VS-6766 in human tumor cell lines with MAPK pathway alterations and in RAS-less mouse embryonic fibroblasts (MEFs) stably transfected with various KRAS variants. The anti-tumor activity of VS-6766 was assessed in genetically engineered mouse models (GEMM) of KRAS G12V/Trp53 KO and KRAS G12C/Trp53 KO NSCLC.

**Results:** VS-6766 showed strong anti-proliferative potency across tumor cell lines carrying KRAS, BRAF, CRAF, NRAS or NF1 alterations. Among KRAS mt cell lines, the anti-proliferative potency of VS-6766 differed by KRAS variant, with greatest potency observed with G12V > G12C > G12D, which is consistent with G12V signaling through CRAF/MEK/ERK and G12D signaling more through PI3K/AKT/mTOR. Similarly, in MEFs stably transfected with different KRAS variants, VS-6766 showed best potency with KRAS G12V and G12C, and least potency with G12D and KRAS wildtype. Accordingly, in the KRAS G12V NSCLC GEMM model, previously shown to be CRAF-dependent, VS-6766 monotherapy induced stronger tumor regression than in a corresponding G12C NSCLC GEMM model. Strikingly, the combination of VS-6766 with FAK inhibition conferred tumor regressions in 87% (27/31) and 71% (36/51) of all tumors in the KRAS G12V and KRAS G12C NSCLC models, respectively. Clinically, objective responses to VS-6766 monotherapy occurred mainly in patients with KRAS G12V with 4 out of the 7 responders bearing KRAS G12V (Guo, 2020). In KRAS mt NSCLC patients treated with VS-6766 in combination with the FAK inhibitor defactinib, a G12V preference was also observed with confirmed responses in 2/2 patients with KRAS G12V and tumor reduction in 4/6 patients with KRAS G12C (Krebs, 2021).

**Conclusions:** These data support the ongoing registration-directed study evaluating VS-6766 ± defactinib for patients with KRAS G12V NSCLC (NCT04620330), as well as the clinical combinations of VS-6766 with the KRAS G12C inhibitors sotorasib (NCT05074810) or adagrasib (NCT05375994) for KRAS G12C NSCLC.

No conflict of interest.

53 (PB043)

**The TBL1 inhibitor, Tegavivint, suppresses tumour growth and enhances T-cell infiltration in preclinical murine  $\beta$ -Catenin mutant hepatocellular carcinoma**

T. Drake<sup>1</sup>, E.H. Tan<sup>1</sup>, A. Georgakopoulou<sup>1</sup>, S. May<sup>1</sup>, M. Mueller<sup>1</sup>, S. Horrigan<sup>2</sup>, K. Holloway<sup>2</sup>, J. Chang<sup>2</sup>, R. Aras<sup>2</sup>, T. Bird<sup>1</sup>. <sup>1</sup>CRUK Beatson Institute, Liver Disease and Regeneration Laboratory, Glasgow, United Kingdom; <sup>2</sup>Iterion Therapeutics, Iterion Therapeutics, Houston, TX, USA

**Background:** Up to 40% of hepatocellular carcinoma (HCC) patients have tumours driven by activating  $\beta$ -Catenin and canonical Wnt pathway mutations. Activated  $\beta$ -Catenin/canonical Wnt signalling is associated with primary resistance to standard of care immune checkpoint blockade mediated through immune cell excluded 'cold' tumour microenvironment. Recruitment of  $\beta$ -Catenin to canonical-Wnt target genes requires transducer beta-like protein 1 (TBL1) to activate transcription. The aim of this study was to test if small molecule inhibition of the TBL1: $\beta$ -Catenin interaction is a tractable therapy in activated  $\beta$ -Catenin/canonical Wnt HCC and characterise its immunomodulatory effects upon the 'cold' immune microenvironment.

**Materials and methods:** Using a genetically engineered C57BL/6J mouse model (GEMM) of  $\beta$ -Catenin<sup>exon3</sup> mutant HCC, we tested the effects of TBL1 inhibition with the small molecule inhibitor, Tegavivint in either early or late stage disease. Littermates were randomised to receive either Tegavivint or vehicle control. We measured tumour number, volume and used immunohistochemistry to characterise the immune microenvironment and the expression of TBL1 and canonical Wnt target genes.

**Results:** In untreated,  $\beta$ -Catenin<sup>exon3</sup> mutant HCC GEMMs, TBL1 expression was identified specifically in tumour epithelium at early and late stages of tumour development. Inhibition of TBL1 in early-stage disease significantly reduced the number of tumour initiating clones identified by markers of canonical Wnt activation (Glutamine Synthetase, GS) compared with vehicle controls. Treatment of established  $\beta$ -Catenin<sup>exon3</sup> activated tumours with Tegavivint inhibited tumour growth and resulted in a reduced tumour burden compared with vehicle controls. Furthermore, in mice with established tumours, Tegavivint treatment increased CD3<sup>+</sup> T-lymphocyte tumour infiltration, with prominent increases in intratumoural CD8<sup>+</sup> T-cells. Tegavivint treatment of mice with activated  $\beta$ -Catenin<sup>exon3</sup> signalling throughout the entire liver significantly inhibited upregulation of canonical Wnt target genes (Glul, Axin2, Notum). In intestinal tissue, which depends on canonical Wnt signalling to maintain tissue homeostasis, we did not observe off target effects.

**Conclusions:** Overall, this study suggests the TBL1: $\beta$ -Catenin interaction is critical in the initiation of and maintaining growth of  $\beta$ -Catenin<sup>exon3</sup> mutant HCC. Tegavivint therapy reduced tumour growth and lead to increased T-lymphocyte infiltration into the previously 'immune-cold' tumour microenvironment. Taken together, disruption of TBL1 and  $\beta$ -Catenin may provide a new precision therapy for  $\beta$ -Catenin mutant HCC. Further studies are underway to identify whether Tegavivint may be a useful therapy for immune checkpoint inhibitor refractory HCC.

**Conflict of interest:**

Corporate-sponsored Research: Iterion therapeutics supplied the compound for this study.

Other Substantive Relationships: Kimberly Holloway, Stephen Horrigan, Jean Chang and Rahul Aras are employees of Iterion Therapeutics.

54 (PB044)

**Non-clinical identification and characterization of KRAS G12D inhibitors**

A. Brooun<sup>1</sup>, J.H. Bae<sup>1</sup>, H. Chen<sup>2</sup>, P. Li<sup>2</sup>, B. Lin<sup>1</sup>, P. Fagan<sup>1</sup>, A. Irimia<sup>2</sup>, R. Nevarez<sup>1</sup>, J. Zhang<sup>1</sup>, P. Chen<sup>2</sup>, D. Olaharski<sup>3</sup>, G. Chiang<sup>1</sup>, J.M. Vernier<sup>2</sup>, R. Shoemaker<sup>4</sup>. <sup>1</sup>Erasca, Biology, San Diego, USA; <sup>2</sup>Erasca, Chemistry, San Diego, USA; <sup>3</sup>Erasca, Toxicology, San Diego, USA; <sup>4</sup>Erasca, Research, San Diego, USA

KRAS G12D is the most prevalent KRAS oncogenic mutant and occurs frequently in pancreatic ductal adenocarcinoma (PDAC), colorectal adenocarcinoma (CRC), and non-small cell lung cancer (NSCLC; 37%, 12% and 4%, respectively). KRAS G12D cycles between inactive (GDP) and active (GTP) states to regulate the RAS/MAPK pathway. Although the rate of intrinsic and GAP (GTPase activating protein) mediated hydrolysis is significantly slower in KRAS G12D than in KRAS wild-type (KRAS WT), we were able to build upon success of targeting the GDP state of KRAS G12C and designed novel KRAS G12D lead compounds with promising *in vitro* and *in vivo* activity.

Our KRAS G12D inhibitors preferentially bind to KRAS G12D GDP as indicated by differential scanning fluorimetry (DSF), block KRAS G12D

SOS1-mediated nucleotide exchange, and inhibit KRAS G12D binding to the RAS binding domain of C-RAF (RAF-RBD) with single digit nanomolar potency. Our leads effectively inhibit ERK1/2 phosphorylation (pERK) in AsPC-1 PDAC cells and inhibit cell proliferation in 3-dimensional Cell-Titer Glo assays in a panel of KRAS G12D mutant PDAC, CRC, and NSCLC cell lines.

This *in vitro* activity translates *in vivo* where robust pharmacodynamic modulation in the PDAC AsPC-1 CDX model was induced. Tumor growth inhibition studies in this model revealed robust dose-dependent tumor growth inhibition and tumor regression in the absence of overt toxicity.

In summary, we have identified potent and selective KRAS G12D inhibitors with robust dose-dependent tumor growth inhibition and regression activity in a PDAC CDX model. Lead optimization is ongoing with the aim of identifying a development candidate.

**No conflict of interest.**

56 (PB046)

**Discovery and functional characterization of potent, balanced AXL/MER inhibitors using a novel MER X-Ray crystal structure**

C. McCarthy<sup>1</sup>, P. Finan<sup>2</sup>, M. Garrett<sup>2</sup>, E. Campbell<sup>2</sup>, E. Walker<sup>3</sup>, E. Beaumont<sup>4</sup>, I. Cade<sup>4</sup>, L. Mooney<sup>5</sup>, J. Kendrick<sup>5</sup>, D. Schwarz<sup>6</sup>, V. Schuster<sup>6</sup>, A. Domingo<sup>6</sup>, N. Holliday<sup>7</sup>, V. Patel<sup>7</sup>, F. Garcia Raposo<sup>7</sup>, T. Gorman<sup>3</sup>, B. Aillard<sup>3</sup>, S. Hewison<sup>3</sup>, J. Ehler<sup>8</sup>, J. Lauterwasser<sup>8</sup>. <sup>1</sup>Kinsensus Ltd, Medicinal Chemistry, Childrey, United Kingdom; <sup>2</sup>Kinsensus, Biology, Childrey, United Kingdom; <sup>3</sup>Evotec, Medicinal Chemistry, Abingdon, United Kingdom; <sup>4</sup>Evotec, X-Ray Crystallography, Abingdon, United Kingdom; <sup>5</sup>Sygnature Discovery, In vivo Pharmacology, Alderley Edge, United Kingdom; <sup>6</sup>Advanced Cellular Dynamics, Cell Biology, Seattle, USA; <sup>7</sup>Excellerate Bioscience, Molecular and Cellular Pharmacology, Nottingham, United Kingdom; <sup>8</sup>Reaction Biology Europe GmbH, Cellular Pharmacology, Freiburg, Germany

The TAM family of kinases consist of AXL, MER and TYRO3. The aim of our program is to design potent inhibitors of this family that demonstrate excellent kinase selectivity and good PK properties for probing the role of these kinases in immune evasion, resistance, tumour cell growth and survival.

A novel construct of MER was designed including the juxtamembrane domain which was used for X-ray crystallography. X-rays of MER in the fully active conformation were obtained for the first time. Additionally, contrasting crystal structures of a type 2 inhibitor KIN101222 were generated using both this novel construct and the previously reported truncated construct. This juxtamembrane domain containing construct afforded novel insight into designing optimal kinase selectivity

Derived compounds were profiled *in vitro* in biochemical assays, TAM driven Ba/F3 proliferation, inhibition of pAXL in a murine embryonal fibroblast cell line over-expressing AXL and a 125 cell panel of human cancer cell lines. Finally, preferred compounds were profiled *in vivo* in a mechanistic model in which AXL and MER expressing Ba/F3 cells were implanted into mice.

The compounds collectively evaluated in this study demonstrated potent inhibition of a Ba/F3 cell line derivative expressing a recombinant AXL kinase, with IC<sub>50</sub> values <10 nM, 3–5 fold cellular selectivity over a similar recombinant MER assay, and excellent broader kinase selectivity. The activity of a representative molecule from this series shows a markedly different activity profile to the clinical AXL inhibitor Bemcentinib in the human cancer cell line panel. When dosed *in vivo* in the mechanistic model, a number of the compounds tested induced either stasis or regression at doses which were well tolerated. In some examples e.g. KIN101433, stasis/regression was observed at doses of 5 mg/kg QD and below.

In summary, selective type 2 AXL/MER inhibitors are well tolerated in mice and show a remarkably benign profile in a broad human cancer cell line panel. Further profiling is ongoing oriented towards investigating the role of these molecules in modulating the immune system and more detailed investigation of their toxicological properties.

**No conflict of interest.**

57 (PB047)

**Regulation of BIM by cooperative Src and MAPK signaling**

M. Rose<sup>1</sup>, V. Sharma<sup>1</sup>, V. Espinoza<sup>1</sup>, M.C. Hoffman<sup>2</sup>, R. Schweppe<sup>1</sup>. <sup>1</sup>University of Colorado, Endocrinology, Aurora, USA; <sup>2</sup>MD Anderson, Department of Endocrine Neoplasia & Hormonal Disorders, Houston, USA

**Background:** Thyroid cancer is the most common endocrine malignancy with poor survival rates for patients with advanced and anaplastic thyroid cancer due to lack of effective therapies. We have previously demonstrated that combined Src and MAPK inhibition results in synergistic inhibition of

growth *in vitro* and *in vivo*, and increased apoptosis in *BRAF*- and *RAS*-mutant cells, while *PIK3CA*-mutants are resistant. Using a proteomics approach, here we show that the pro-apoptotic protein, BIM, is increased in cells that are sensitive to combined Src and MAPK inhibition compared to cells that are resistant. Thus, we hypothesize that inhibition of growth and induction of apoptosis induced by combined Src and MEK1/2 inhibition is mediated by the upregulation of BIM.

**Materials/Methods:** Reverse Phase Protein Array (RPPA) was performed on a panel of authenticated thyroid cancer cell lines (7 sensitive 3 resistant) with varying mutations treated with the Src inhibitor, dasatinib (Srci), with or without the MEK1/2 inhibitor, trametinib (MEKi). The role of BIM was tested using siRNA and overexpression approaches. The role of AKT was determined by expressing a constitutively active myr-AKT1 (mAKT). Western blotting was performed to assess signaling responses, growth assays were performed using CellTiter Glo, and apoptosis assays were performed using Annexin V/PI or Cleaved Caspase 3/7 Glo. All cells were treated with clinically relevant doses of dasatinib and trametinib.

**Results:** RPPA showed that sensitive cells exhibited a ~2-fold induction of BIM in response to combined Srci and MEKi ( $p < 0.0001$ ), whereas this response was blunted in resistant cells. Accordingly, western blots showed a 6-fold induction of BIM in sensitive cells treated with Srci/MEKi and only a 1.5- to 3-fold induction of BIM in resistant cells treated with Srci/MEKi. Knockdown of BIM in the sensitive cells promoted resistance and increased the IC50 of combined Src/MEKi by 2-fold, but exhibited little to no effect on apoptosis. Overexpression of BIM in resistant cells sensitized them to growth inhibition induced by Srci/MEKi, however did not affect apoptosis. These data suggest a non-canonical role of BIM in regulating growth. Inhibition of AKT is key for the effects induced by Srci and MEKi, as expression of mAKT in cells demonstrated increased resistance to growth inhibition (11-fold increase in IC50) and apoptosis induction (3-fold decrease,  $p < 0.008$ ) driven by combined Srci/MEKi in *BRAF*-mutant cells, which correlated with a 3-fold reduction in BIM.

**Conclusion:** Dual inhibition of Src and MEK1/2 synergistically inhibits growth and induces apoptosis through Src/FAK, MEK/ERK, and AKT; and BIM is a key protein cooperatively regulated by the Src and the MAPK pathways.

**No conflict of interest.**

58 (PB048)

#### HIF-2 $\alpha$ inhibitor AB521 modulates erythropoietin levels in healthy volunteers following a single oral dose

K. Liao<sup>1</sup>, P. Foster<sup>2</sup>, L. Seitz<sup>3</sup>, T. Cheng<sup>3</sup>, K. Gauthier<sup>4</sup>, K. Lawson<sup>5</sup>, L. Jin<sup>6</sup>, E. Paterson<sup>2</sup>. <sup>1</sup>Arcus Biosciences, Clinical Pharmacology, Hayward, USA; <sup>2</sup>Arcus Biosciences, Clinical Development, Hayward, USA; <sup>3</sup>Arcus Biosciences, Translational Sciences, Hayward, USA; <sup>4</sup>Arcus Biosciences, Biology, Hayward, USA; <sup>5</sup>Arcus Biosciences, Chemistry, Hayward, USA; <sup>6</sup>Arcus Biosciences, DMPK & Bioanalytics, Hayward, USA

**Background:** Hypoxia-inducible factor (HIF)-2 $\alpha$  is a transcription factor that is an oncogenic driver in clear cell renal cell carcinoma (ccRCC). The post-translational regulation of the HIF-2 $\alpha$  protein is oxygen-dependent and, in hypoxic or pseudohypoxic conditions, results in the stabilization of HIF-2 $\alpha$  and downstream transcription of tumor-inducing genes. HIF-2 $\alpha$  inhibition has been shown to mitigate tumor growth in ccRCC cases with mutation or dysregulation of the von Hippel-Lindau tumor suppressor gene.

**Material and Methods:** AB521 is a potent small molecule HIF-2 $\alpha$  inhibitor that is in Phase 1 clinical development (ClinicalTrials.gov Identifier: NCT05117554). The safety, tolerability, pharmacokinetics (PK), and pharmacodynamics (PD; erythropoietin hormone) of AB521 are being investigated in a randomized, placebo-controlled single and multiple ascending dose study in healthy volunteers. This study is ongoing, and safety, PK and PD data continue to be collected.

**Results:** A total of 32 healthy volunteers have been enrolled in the study to date and received single oral doses of either AB521 (3, 10, 30, or 100 mg) or placebo at a 3:1 ratio. At these dose levels, minimal toxicity was observed. Following single ascending doses AB521 up to 30 mg, median  $T_{max}$  ranged from 1 to 3 hours. The mean terminal half-life was 18–20 hours, which supports once daily dosing. Exposure ( $AUC_{\infty}$ ) increased in an approximately dose proportional manner in this dose range. Dose-dependent reductions in serum erythropoietin (EPO) were observed following single doses at 10–100 mg, with mean maximum reduction up to approximately 85%, demonstrating potent HIF-2 $\alpha$  inhibition *in vivo*.

**Conclusions:** In this first-in-human study, AB521 demonstrated PK/PD properties that are consistent with a potential best-in-class HIF-2 $\alpha$  profile.

**Conflict of interest:**

Ownership: N/A  
Advisory Board: N/A  
Board of Directors: N/A

Corporate-sponsored Research: This work was sponsored by Arcus Biosciences.

Other Substantive Relationships: All authors are employees of Arcus Biosciences and own Arcus stocks and/or stock options.

59 (PB049)

#### PIN-A1, a novel Casein Kinase 1 $\alpha$ -selective molecular glue degrader, demonstrates strong antitumor activity via activation of the p53 pathway in preclinical models of AML with a favorable safety profile

J. Jung<sup>1</sup>, J. Park<sup>1</sup>, S. Mohanty<sup>1</sup>, Y. Kim<sup>1</sup>, D. Levy<sup>2</sup>, J. King-Underwood<sup>3</sup>, M. Deninno<sup>2</sup>, J. Baek<sup>1</sup>, W. Choi<sup>4</sup>, S. Lee<sup>4</sup>, D. Lee<sup>1</sup>, H. Kang<sup>1</sup>, T. Brotz<sup>1</sup>, N. Terrett<sup>2</sup>, H. Jo<sup>1</sup>, Y. Kim<sup>1</sup>. <sup>1</sup>Pin Therapeutics Inc., Bioscience, Seoul, South Korea; <sup>2</sup>Pin Therapeutics Inc., Medicinal Chemistry, Seoul, South Korea; <sup>3</sup>Pin Therapeutics Inc., Computational Chemistry, Seoul, South Korea; <sup>4</sup>Pin Therapeutics Inc., Biophysics, Seoul, South Korea

Casein kinase 1 $\alpha$  (CK1 $\alpha$ ) reportedly promotes tumor growth by increasing the negative effects of MDM2 and MDMX on p53. Unlike in many other cancer types, the frequency of *TP53* mutations is relatively low (<20%) in acute myeloid leukemia (AML). Therefore, activating the p53 pathway has been considered an attractive strategy to treat the disease with wild-type (WT) *TP53*. However, promising preclinical activities of p53 activators represented by MDM2 inhibitors have not been fully translated into clinical efficacy, partly due to their on-target hematological toxicities. To develop a drug targeting CK1 $\alpha$ , we screened a series of compounds hijacking cereblon (CRBN) E3 ligase and identified a novel CK1 $\alpha$ -selective molecular glue degrader (MGD), PIN-A1. Here, we report its robust pharmacological activities in various preclinical models of AML and its superior safety profile to MDM2 inhibitors. First, PIN-A1's activity against CK1 $\alpha$  as a MGD was demonstrated by the formation of ternary complex of PIN-A1-CK1 $\alpha$ -CRBN using TR-FRET assay and with the inhibitors of proteasome/neddylation, respectively. Selective degradation of CK1 $\alpha$  by PIN-A1 was also confirmed by global proteomics analysis. As predicted, PIN-A1 induced rapid degradation of CK1 $\alpha$  protein in human AML MV-4-11 cells with WT *TP53*, which was followed by increases in the levels of p53 protein and its downstream target genes, ultimately leading to apoptotic cell death. Consistent with these results, screening in a broad panel of liquid cancer cell lines demonstrated preferential sensitivity of AML cells with WT *TP53* to the CK1 $\alpha$  degrader. When combined with cytarabine or other targeted therapies in AML such as venetoclax (Bcl2i), AMG232 (MDM2i), or gilteritinib (FLT3i), PIN-A1 displayed strong synergistic effects in cell killing. To evaluate its pharmacological activity *in vivo*, PIN-A1 was tested in a *s.c* xenograft model of MV-4-11 and a dissemination model of MOLM-14, respectively. Systemic administration of PIN-A1 alone *via i.p* resulted in robust antitumor activity with >90% CK1 $\alpha$  degradation in tumors, which was comparably achieved at a much lower dose in combo treatments. Importantly, animals remained tumor-free (5/8) in the MV-4-11 model or survived longer in the MOLM-14 model even after they were off the combination treatment of PIN-A1 with AMG232. Lastly, while PIN-A1 had minimal effects on the viability and the p53 pathway in human PBMC at efficacious doses for MV-4-11 (Therapeutic index [TI] = >8000) despite >90% CK1 $\alpha$  degradation, AMG232 induced the p53 pathway and reduced viability to a similar extent in both cell types (TI = 4). Taken together, these results suggest that a CK1 $\alpha$  MGD with its favorable safety profile has a potential to become an effective treatment option for advanced AML. Current activities are focused on more advanced MGD analogs with superior oral systemic exposure.

**No conflict of interest.**

60 (PB050)

#### Combination of MDM2 inhibition with milademetan and MEK inhibition leads to improved anti-tumor activity in cancer models harboring WT TP53

V. Tirunagaru<sup>1</sup>, K. Singh<sup>1</sup>, X. Pei<sup>1</sup>, R.C. Doebele<sup>1</sup>. <sup>1</sup>Rain Therapeutics, Research, Newark, USA

**Background:** Loss of p53 activity is important for tumor initiation and progression. While approximately 50% of tumors lose p53 activity through inactivating mutations in *TP53*, tumors harness other mechanisms to inactivate p53, including MDM2, an E3 ligase that targets p53 for proteasomal degradation. Milademetan is an MDM2 inhibitor currently being evaluated in clinical trials. The MAPK pathway is commonly activated in tumors by mutations in the RTK-RAS-RAF-MAPK axis or other mechanisms to sustain proliferative signaling, growth, and survival. Here we evaluated whether inhibition of the MAPK pathway using the MEK1/2 inhibitor trametinib could further enhance milademetan antitumor activity.

**Materials and Methods:** We evaluated multiple cancer models derived from different tumor types (including lung cancer, renal cell carcinoma, melanoma, colorectal cancers and sarcomas) based on three genetic categories that represent varying levels of potential MDM2 dependence: *MDM2* gene amplification (and WT *TP53*), *CDKN2A* homozygous loss (and WT *TP53*), or WT *TP53* alone. We evaluated the effects of milademetan, trametinib or the combination on cell signaling pathways, *in vitro* cell proliferation including synergy indices (Loewe, Bliss and HSA), and *in vivo* tumor growth.

**Results:** Milademetan induced p53 reactivation as measured by induction of p21 and PUMA proteins whereas trametinib inhibited MAPK activation as measured by pERK1/2 in cancer cell models representing cancers with *MDM2* gene amp (~1–4% of solid tumors, depending on copy number cutoff), *CDKN2A* loss (6.2% of solid tumors that also harbor WT *TP53*, Tirunagaru et al., ASCO 2022), or WT *TP53* only (~40% of solid tumors). The majority of cancer models tested demonstrated *in vitro* synergy with the combination of milademetan and trametinib, including models with known oncogenic drivers such as RAS and RAF activating mutations. *In vivo* xenograft experiments in A549 (lung adenocarcinoma with *CDKN2A* loss, *KRAS* G12S, and WT *TP53*) and HT1197 (urothelial carcinoma with *NRAS* Q61R and WT *TP53*) demonstrated that the combination of milademetan plus trametinib was superior to either agent alone.

**Conclusions:** The combination of milademetan and trametinib demonstrated synergy *in vitro* and combinatorial superiority *in vivo*. These data support the exploration of combination of milademetan and MAPK inhibition in patients whose tumors harbor selected genetic alterations, including *MDM2* amplification, *CDKN2A* loss or WT *TP53*.

#### Conflict of interest:

Ownership: Authors are employees and shareholders of Rain Therapeutics.

### 61 (PB051) Capmatinib response in patients with advanced non-small cell lung cancer (NSCLC) harboring focal MET amplifications: Analysis from the phase 2, multicohort GEOMETRY mono-1 study

J. Wolf<sup>1</sup>, E.B. Garon<sup>2</sup>, H.J.M. Groen<sup>3</sup>, D.S.W. Tan<sup>4</sup>, S. Le Mouhaer<sup>5</sup>, M. Riestler<sup>6</sup>, L. Ji<sup>7</sup>, A. Robeva<sup>7</sup>, L. Fairchild<sup>8</sup>, A. Boran<sup>7</sup>, R.S. Heist<sup>9</sup>. <sup>1</sup>Center for Integrated Oncology- University Hospital of Cologne, Department of Internal Medicine, Cologne, Germany; <sup>2</sup>University of California Los Angeles, Department of Medicine, Los Angeles, USA; <sup>3</sup>University Medical Center Groningen and University of Groningen, Department of Pulmonary Diseases, Groningen, Netherlands; <sup>4</sup>National Cancer Centre Singapore, Department of Medical Oncology, Singapore, Singapore; <sup>5</sup>Novartis Pharma S.A.S, Global Drug Development, Rueil Malmaison, France; <sup>6</sup>Novartis Institutes for BioMedical Research, Oncology Data Science, Cambridge, USA; <sup>7</sup>Novartis Pharmaceuticals Corporation, Global Drug Development, East Hanover, USA; <sup>8</sup>Massachusetts General Hospital, Department of Medical Oncology, Boston, USA

**Background:** *MET* amplifications (*METamp*) occur in 1–6% of patients (pts) with NSCLC and are associated with a poor prognosis. Capmatinib is a highly selective and potent *MET* inhibitor (METi) with antitumor activity in pretreated and treatment-naïve pts with *MET*-amplified (gene copy number [GCN]  $\geq 10$ ) NSCLC. Focal *METamp* are associated with a relatively high *MET* GCN and may be a predictor of benefit from METi. In this retrospective analysis from GEOMETRY mono-1 (NCT02414139), we aimed to determine the response to capmatinib according to focality of *METamp* detected in cell-free DNA (cfDNA) using a blood-based assay.

**Materials and Methods:** Pretreated (1 or 2 prior lines) pts with EGFR wild-type, *ALK*-negative, *MET* exon 14 skipping-negative, stage IIIB/IV NSCLC were grouped into cohorts C1a, C1b, C2, and C3 based on different levels of *MET* GCN amp by FISH on tumor tissue. Pts received capmatinib 400 mg twice daily. cfDNA isolated from blood plasma samples collected at baseline was enriched using RNA-bait-based hybrid capture and analyzed using next-generation sequencing (PanCancer assay 1.0, NGDx, Novartis). Focal *METamp* were defined using the PureCN pipeline that estimates a gene-level log-ratio relative to normal samples, adjusting for probe signal variation. *MET* was called focally amplified if gene-level *P* value was  $<0.001$  and gene-level log-ratio reached 90th percentile of all genes. The overall response rate (ORR) by Blinded Independent Review Committee was descriptively compared between pts with focal vs nonfocal *METamp* (data cutoff, August 2021).

**Results:** 195 pts across the 4 cohorts had *METamp* by FISH. Of these, baseline cfDNA samples from 113 pts were successfully analyzed (C1a [n = 29], C1b [n = 32], C2 [n = 31], C3 [n = 21]). Baseline characteristics were comparable between pts who were analyzed by cfDNA (n = 113) vs not analyzed (n = 82) and between pts with focal (n = 18) vs nonfocal (n = 95) *METamp*. Of all pts with focal *METamp*, most were in high *MET*-amplified C1a (14 of 18 pts [78%]). In C1a, the distribution of GCN by FISH was similar

in pts with focal vs nonfocal *METamp* but more responders were found in pts with focal vs nonfocal *METamp* (ORR, 57% vs 13%). In C1b, 3 of 32 pts (9%) had focal *METamp*; 2 were responders (Table).

Cohort	<i>MET</i> GCN by FISH	Parameter	Focal <i>METamp</i>	Nonfocal <i>METamp</i>	Pts analyzed	All pts in cohort
C1a	$\geq 10$	N	14	15	29	69
		ORR, n (%)	8 (57)	2 (13)	10 (34)	20 (29)
C1b	$\geq 6$ and $< 10$	N	3	29	32	42
		ORR, n (%)	2 (67)	1 (3)	3 (9)	5 (12)
C2	$\geq 4$ and $< 6$	N	0	31	31	54
		ORR, n (%)	-	2 (6)	2 (6)	5 (9)
C3	$< 4$	N	1	20	21	30
		ORR, n (%)	0 (0)	1 (5)	1 (5)	2 (7)

**Conclusions:** *METamp* status, including focal *METamp*, was successfully determined using cfDNA isolated from blood. For pts with high *MET*-amplified NSCLC by FISH, a numerically higher proportion of responders to capmatinib was observed in pts with focal vs nonfocal *METamp*. Given the small sample size, a larger study is needed to verify this result.

#### Conflict of interest:

Ownership: Juergen Wolf: None  
Markus Riestler, Lexiang Ji, Anna Robeva, Aislyn Boran: Novartis stock  
Advisory Board: Juergen Wolf: Consulting or advisory role for Abbvie, AstraZeneca, Bristol-Myers Squibb, Boehringer Ingelheim, Chugai Pharma, Ignyta, Lilly, MSD Oncology, Novartis, Pfizer, Roche, Janssen, Loxo/Lilly, Blueprint Medicines, Amgen, Takeda, Bayer, Daiichi Sankyo Europe GmbH, Seattle Genetics  
Edward B. Garon: Consultant and/or advisor for Abbvie, ABL-Bio, AstraZeneca, Boehringer-Ingelheim, Bristol Myers Squibb, Dracen Pharmaceuticals, EMD Serono, Eisai, Eli Lilly, Gilead, GlaxoSmithKline, Merck, Natera, Novartis, Personalis, Regeneron, Sanofi, Shionogi, and Xilio.  
Daniel S. W. Tan: Consulting/advisory role for Pfizer, Novartis, Takeda, Boehringer Ingelheim, Merck, Amgen, AstraZeneca, DKSH, Roche, C4 Therapeutics, GSK  
Board of Directors: Juergen Wolf: None  
Corporate-sponsored Research: Juergen Wolf: Research funding from Bristol-Myers Squibb, Novartis, Pfizer, Janssen  
Edward B. Garon: Grant/research support from ABL-Bio, AstraZeneca, Bristol Myers Squibb, Dynavax Technologies, Eli Lilly, EMD Serono, Genentech, Iovance Biotherapeutics, Merck, Mirati Therapeutics, Neon, and Novartis  
Daniel S. W. Tan: Research funding (payments to institution) from AstraZeneca, Pfizer, ACM Biolabs, Amgen  
Rebecca S. Heist: To institution (not to self) from Agios, Abbvie, Lilly, Novartis, Turning Point, Daichii Sankyo, Mirati, Corvus, Exelixis, Erasca  
Other Substantive Relationships: Juergen Wolf: Honoraria from Abbvie, AstraZeneca, Bristol-Myers Squibb, Boehringer Ingelheim, MSD, Novartis, Roche, Amgen, Bayer, Blueprint Medicines, Chugai Pharma Europe, Daiichi Sankyo Europe GmbH, Ignyta, Janssen, Lilly, Loxo, Loxo/Lilly, Pfizer, Seattle Genetics, Takeda  
Sylvie Le Mouhaer, Markus Riestler, Lexiang Ji, Anna Robeva, Lauren Fairchild, Aislyn Boran: Employment at Novartis  
Rebecca S. Heist: Consulting for Novartis, Daichii Sankyo, EMD Serono

### 62 (PB052) p53 mRNA rescue of tumor suppressor function prevents tumor growth and restores PARPi sensitivity in p53-deficient cancers *in vitro* and *in vivo*

G. Divita<sup>1</sup>, E. Czuba<sup>1</sup>, A. Grunenberger<sup>1</sup>, M. Guidetti<sup>2</sup>, V. Jossierand<sup>2</sup>, N. Desai<sup>3</sup>. <sup>1</sup>DIVINCELL, Molecular Therapy, Nimes, France; <sup>2</sup>IAB, Optimal, Grenoble, France; <sup>3</sup>Aadigen LLC, Aadigen, Pacific Palisades, USA

**Background:** Loss of function in tumor suppressor genes is commonly associated with the onset/progression of cancer and the development of therapeutic resistance. The p53 tumor suppressor mutations resulting in loss of function are common across variety of tumors and control tumor cell proliferation in more than 50% of cancers. p53 null mutations are present in about 10% of p53 driven cancers. However, to date there is no effective treatment for rescuing p53 function in cancers. We have developed a new potent strategy combining p53 mRNA with a tumor selective nanocarrier, to rescue p53 tumor suppressor function as potential therapeutic approach in cancers.

**Methods:** ADGN-technology is based on short amphipathic peptides that form stable neutral nanoparticles with mRNA. ADGN-531 nanoparticles containing full length p53-mRNA were evaluated on 20 different cancer cell

lines (osteosarcoma, pancreas, colorectal, ovarian, lung, breast and prostate cancers) harboring different types of p53 mutations (null, deletion, nonsense, missense). Cell proliferation, cell cycle level and apoptosis activation were determined by flow cytometry, Elisa and Tunel assay. *In-vivo* efficacy of IV-administered ADGN-531 nanoparticles (0.5 mg/kg) was evaluated on colorectal SW403 (p53 deleted) and osteosarcoma SaOs2 (p53 null) mouse xenografts. Sensitivity to Veliparib (PARPi) following ADGN-531 treatment *in vitro* was evaluated on PARPi resistant SUM-149PT and OVCAR-8 cells and on PARPi sensitive MDA-MB436 cells.

**Results:** ADGN-531 NPs markedly delay the growth of a large panel of cancer cells harboring p53-null or nonsense mutations, by inducing cell cycle arrest in G1 due to p21 upregulation and apoptosis following PUMA activation. We demonstrated that ADGN-531 mediated p53 function rescue is directly correlated to the type and level of p53 mutation in the cancer cells. ADGN-531 induces 60% to 80% cell proliferation inhibition in p53 null or nonsense mutated cells and 20 to 50% in p53 missense mutated cells. Intravenous-administration ADGN-531 containing wild type p53-mRNA (0.5 mg/kg) resulted in tumor growth inhibition of 90% and 70% in SaOs2 and SW403 xenografted mouse model, respectively. ADGN-531 NPs treatments are well tolerated, without inducing clinical toxicity or inflammatory response. We demonstrated that ADGN-531 mediated p53 rescue markedly improves (200 fold) and restores the sensitivity of ovarian and breast cancer cells to the PARPi veliparib.

**Conclusions:** ADGN-531 nanoparticles are effective in rescuing P53 functions both *in vitro* and *in vivo*. Our study provides a proof-of-concept that restoration of tumor suppressor function by the ADGN-531 NP targeted delivery strategy could be combined together with other therapies for potent combinatorial cancer treatment.

**No conflict of interest.**

63 (PB053)

#### Exposure-response relation in metastatic colorectal cancer organoids after high-dose short-term tyrosine kinase inhibitor exposure

K. Iyer<sup>1</sup>, A. Miggelenbrink<sup>1</sup>, D. Poel<sup>1</sup>, E. van den Hombergh<sup>2</sup>, L. de Jong<sup>2</sup>, N. van Erp<sup>2</sup>, D. Tauriello<sup>3</sup>, H. Verheul<sup>4</sup>. <sup>1</sup>Radboudumc, Medical Oncology and Cell Biology, Nijmegen, Netherlands; <sup>2</sup>Radboudumc, Pharmacy, Nijmegen, Netherlands; <sup>3</sup>Radboudumc, Cell Biology, Nijmegen, Netherlands; <sup>4</sup>Radboudumc, Medical Oncology, Nijmegen, Netherlands

A better understanding of the molecular basis of metastatic colorectal cancer (mCRC), has led to interest in small molecule tyrosine kinase inhibitors (TKIs) as its treatment option. However, most of the TKIs tested for mCRC in their standard dosing regimen, fail in early-phase clinical trials due to lack of efficacy or excessive toxicity. TKIs are known to have a broader kinase inhibitory potency at higher concentrations. Optimizing TKI dosing regimens aims at improved antitumor efficacy with acceptable toxicity. Knowledge of the TKI concentrations required to elicit response, achieving those levels in the tumor, and understanding the mechanism of action can potentially increase the clinical success of TKIs for mCRC.

To test this hypothesis, we established patient-derived organoids (PDTOs) from mCRC biopsies, as this form of 3D cell culture best maintains the genetic architecture of the patient's tumor. Based on favorable physico-chemical and pharmacokinetic properties, 3 TKIs (sunitinib, cediranib and osimertinib) were selected to investigate the antitumor effect of high-dose, short-term exposure (HDSE) using viability assays. Five PDTOs were exposed at various timepoints to high drug dose (20 µM). In parallel, intratumoroid TKI concentrations were determined using a validated LC/MS-MS method.

The tested PDTOs were most sensitive for osimertinib. Comparable sensitivity was observed between sunitinib and cediranib, although we identified PDTOs that were generally more sensitive or least sensitive. Further, the pharmacokinetic analysis after HDSE revealed differences in intra-tumoroid TKI concentrations in these PDTOs. After 6 hours of treatment, we observed that the most sensitive PDTO had a significant higher intra-tumoroid concentration of sunitinib as compared to the least sensitive PDTO. Similarly, the most sensitive PDTO had a significantly higher amount of cediranib after 3 hours of exposure as compared to the least sensitive PDTO. Lastly, we found a significant correlation between the response of the PDTOs towards HDSE TKI treatment and their intra-tumoroid concentrations for both sunitinib and cediranib.

We established and validated a method to reliably determine intra-tumoroid TKI concentrations in mCRC PDTOs. The sensitivity towards the HDSE treatment was found to be positively correlated with intra-tumoroid TKI concentrations. In future experiments, we can use this integration of functional assays and *in vitro* pharmacology to further dissect the mechanism of action, as well as further the clinical translation of HDSE of TKIs, including informing patient selection.

Abstracts, 34th EORTC-NCI-ACR Symposium

**No conflict of interest.**

64 (PB054)

#### BDTX-1535, a fourth generation EGFR inhibitor, targeting intrinsic and acquired resistance mutations in NSCLC

M. Lucas<sup>1</sup>, M. Merchant<sup>2</sup>, M. O'Connor<sup>3</sup>, S. Smith<sup>4</sup>, A. Trombino<sup>4</sup>, N. Waters<sup>4</sup>, S. Eathiraj<sup>2</sup>, E. Buck<sup>5</sup>. <sup>1</sup>Black Diamond Therapeutics, Discovery, Cambridge, USA; <sup>2</sup>Black Diamond Therapeutics, Clinical Development, Cambridge, USA; <sup>3</sup>Black Diamond Therapeutics, Translational Biology, New York, USA; <sup>4</sup>Black Diamond Therapeutics, Non-clinical Development, Cambridge, USA; <sup>5</sup>Black Diamond Therapeutics, Research Biology, New York, USA

**Background:** The classical mutations of the epidermal growth factor receptor (EGFR) in NSCLC are the exon 19 del and exon 21 (L858R) mutations. The 3rd generation EGFR tyrosine kinase inhibitor (TKI), osimertinib, has become the first-line treatment of choice for NSCLC patients with these mutations.

Resistance to 3rd generation TKIs can be driven by gain of secondary EGFR alterations, e.g., substitution at cysteine-797 to serine (C797S). Real world evidence shows that in addition to C797S, other EGFR alterations are also acquired upon osimertinib treatment, including kinase domain mutations (e.g., S768I), extracellular domain alterations (e.g., EGFRVIII, A289X), and EGFR amplification.

In addition to the classical mutations, NSCLC tumors express a wide spectrum of primary kinase domain mutations including G719X in exon 18, S768I in exon 20, and L861Q in exon 21, which confer intrinsic resistance to approved TKIs. NCCN guidelines recommend the use of afatinib or osimertinib, however, there remains a need for an EGFR TKI that targets these mutations with high potency, good tolerability, and CNS penetration.

Our MAP platform allowed us to select MasterKey inhibitor BDTX-1535, a 4th-generation CNS penetrant EGFR TKI, that potently and selectively targets multiple intrinsic and acquired resistance EGFR alterations.

**Materials and Methods:** BDTX-1535 preclinical exposure was evaluated across species, and PK and K<sub>puu</sub> values were calculated in brain and plasma. Antitumor activity was assessed across a broad range of mouse PDX and allograft models.

**Results:** BDTX-1535 is a potent and selective, CNS penetrant, wild type sparing, irreversible EGFR TKI targeting Exon 18–21 alterations which are associated with intrinsic or acquired resistance to 3rd generation EGFR inhibitors. These include a broad range of kinase domain EGFR mutations (e.g., C797S, L718Q, G724S, S768I), extracellular domain alterations (e.g., EGFRVIII, A289X), and EGFR amplification. Mouse xenograft and allograft studies showed that BDTX-1535 consistently achieves regression of tumors carrying these mutations at well tolerated doses without significant EGFR wild type associated toxicities. BDTX-1535 is orally bioavailable with a CNS K<sub>puu</sub> of 0.55 and 0.48 in rat and dog, respectively, and active in an intracranial PDX model.

**Conclusions:** BDTX-1535 is a 4th generation CNS penetrant EGFR TKI discovered using the MAP platform which allows MasterKey targeting of EGFR alterations associated with intrinsic or acquired resistance to 3<sup>rd</sup> generation EGFR TKIs, while sparing wild type EGFR. This broad spectrum coverage of resistance mutations in conjunction with CNS penetration properties allows BDTX-1535 to address a key unmet medical need in EGFR mutant lung cancer. BDTX-1535 is currently under phase I clinical investigation (NCT05256290).

**Conflict of interest:**

Ownership: Black Diamond Therapeutics

65 (PB055)

#### Discovery and characterization of ABSK071, a novel and potent small-molecule covalent inhibitor for KRAS-G12C

F. Guo<sup>1</sup>, Y. Zhao<sup>2</sup>, H. Yu<sup>2</sup>, Y. Xu<sup>3</sup>, Z. Chen<sup>1</sup>, S. Yang<sup>1</sup>. <sup>1</sup>Abbisko Therapeutics, Biology, Shanghai, China; <sup>2</sup>Abbisko Therapeutics, Medicinal Chemistry, Shanghai, China; <sup>3</sup>Abbisko Therapeutics, Chief Executive Officer, Shanghai, China

KRAS is frequently mutated in human cancers, including pancreatic (~90%), colorectal (~35%), and lung cancer (~25%). The KRAS<sup>G12C</sup> mutation (single amino acid substitution of cysteine for glycine at position 12) accounts for ~14% of lung cancer, ~4% of colorectal cancer, and ~2% of pancreatic cancer. Recently, covalent inhibitors such as sotorasib have been designed to target the mutated cysteine in codon 12 and have achieved clinical benefit for these patients. Here, we describe the discovery and characterization of ABSK071, a novel and highly potent small-molecule inhibitor that irreversibly modifies and inhibits KRAS<sup>G12C</sup> *in vitro* and *in vivo*. In cellular experiments,

Poster Session (26 October 2022)

ABSK071 treatment inhibited KRAS signaling across a panel of KRAS<sup>G12C</sup> mutant cancer cell lines, as measured by the phosphorylation of ERK1/2 (p-ERK). The treatment of ABSK071 resulted in significantly impaired cell viability at nanomolar concentration, which is superior to the approved KRAS<sup>G12C</sup> inhibitor sotorasib. Further, *in vivo* pharmacodynamic study demonstrated the dose- and time-dependent inhibition of KRAS signaling by ABSK071. *in vivo* efficacy studies showed that ABSK071 has higher antitumor potency than sotorasib at the same dose in multiple xenograft models. Together, these data demonstrated the antitumor activity of ABSK071 towards KRAS<sup>G12C</sup>-dependent cancers.

**Conflict of interest:**

Ownership: All co-authors are stock owners of Abbisko Therapeutics.

**66 (PB056)**  
**Anti-tumor activity of BDTX-1535, an irreversible CNS penetrant inhibitor of multiple EGFR extracellular domain alterations, in preclinical glioblastoma models**

M. Lucas<sup>1</sup>, M. Merchant<sup>2</sup>, M. O'Connor<sup>3</sup>, S. Smith<sup>4</sup>, A. Trombino<sup>4</sup>, N. Waters<sup>4</sup>, S. Eathiraj<sup>2</sup>, J. Ball<sup>5</sup>, A. Breschi<sup>5</sup>, K. Igartua<sup>5</sup>, M. Kang<sup>5</sup>, E. Buck<sup>6</sup>. <sup>1</sup>Black Diamond Therapeutics, Discovery, Cambridge, USA; <sup>2</sup>Black Diamond Therapeutics, Clinical Development, Cambridge, USA; <sup>3</sup>Black Diamond Therapeutics, Translational Biology, New York, USA; <sup>4</sup>Black Diamond Therapeutics, Non-clinical Development, Cambridge, USA; <sup>5</sup>Tempus Labs, Research, Chicago, USA; <sup>6</sup>Black Diamond Therapeutics, Research Biology, Cambridge, USA

**Background:** EGFR genetic alterations, including mutation and amplification, are very common in glioblastoma multiforme (GBM), however, no targeted therapy has been approved for this disease. EGFR oncogenic mutations in GBM promote EGFR oncogenic covalent homodimer formation which leads to paradoxical activation and renders reversible inhibitors ineffective. An effective EGFR inhibitor in GBM must meet four conditions:

1. Highly potent and selective against a broad range of extracellular domain mutations and amplified EGFR,
2. Wild-type EGFR sparing,
3. Irreversible binding to circumvent paradoxical activation,
4. High CNS penetration.

Our MAP discovery platform led to the identification of MasterKey inhibitor BDTX-1535, an irreversible 4th-generation CNS penetrant EGFR tyrosine kinase inhibitor (TKI) that potently and selectively targets a broad range of EGFR alterations in GBM.

**Materials and Methods:** BDTX-1535 preclinical exposure was evaluated in multiple species in plasma and brain. Antitumor activity was assessed across a broad range of mouse PDX and allograft models, including an intracranial PDX. 2540 tumors were sequenced with the Tempus xT NGS assay. Mutational frequencies and co-expression status of oncogenic EGFR variants were assessed. The relationship between treatment history and oncogenic EGFR mutational frequency was analyzed.

**Results:** BDTX-1535 is a small molecule that irreversibly inhibits a spectrum of EGFR alterations expressed in GBM together with EGFR amplification, while sparing inhibition of normally expressed wild type EGFR. BDTX-1535 avoids efficacy limiting paradoxical activation that can occur with reversible EGFR inhibitors. BDTX-1535 exhibits good oral bioavailability and a CNS K<sub>puu</sub> of 0.55 and 0.48 in rat and dog, respectively, comparing favorably with other CNS penetrant TKIs. Tumor regression and survival advantage were observed across all tumor models with EGFR amplification or mutation, including in an intracranial PDX model. EGFR mutations and amplification are commonly expressed in GBM. Consistent with published data, EGFR mutations, variants, and copy number gain were frequently co-expressed. For example, among tumors expressing EGFR<sup>WT</sup>, ~95% co-expressed at least one other variant, and among tumors expressing EGFR<sup>VI</sup>, ~45% co-expressed at least one other variant. Within a subset of GBM patients with longitudinal sequencing data, oncogenic EGFR mutations were expressed and persisted following front-line treatment.

**Conclusions:** BDTX-1535 is a potent, CNS penetrant, irreversible small molecule EGFR inhibitor that shows efficacy against a broad range of extracellular domain mutations and EGFR amplification found in GBM patients. RWE findings demonstrate a heterogeneous EGFR mutational profile in GBM patients, with persistent prevalence over time. BDTX-1535 is currently in a phase I clinical study (NCT05256290).

**Conflict of interest:**

Ownership: Black Diamond Therapeutics  
Tempus Labs

**67 (PB057)**  
**Phase I/II trial of RVU120, a CDK8/CDK19 inhibitor in patients with relapsed/refractory metastatic or advanced solid tumors**

R. Dziadziuszko<sup>1</sup>, E. Garralda Cabanas<sup>2</sup>, K. Rojas<sup>2</sup>, M. Chelstowska<sup>3</sup>, M. Blaszowska<sup>1</sup>, R. Dudziak<sup>4</sup>, T. Rzymiski<sup>5</sup>, N. Angelosanto<sup>4</sup>, P. Littlewood<sup>6</sup>, H. Noga<sup>4</sup>, V. Boni<sup>7</sup>, I. Lugowska<sup>3</sup>. <sup>1</sup>Medical University of Gdansk, Early Clinical Trials Centre, Gdansk, Poland; <sup>2</sup>Vall d'Hebron Institute of Oncology VHIO, Early Drug Development Unit UITM, Barcelona, Spain; <sup>3</sup>Maria Skłodowska-Curie National Research Institute and Oncology Centre MSCI, Early Phase Clinical Trials Unit and Department of Soft Tissue Bone Sarcoma and Melanoma, Warsaw, Poland; <sup>4</sup>Ryvu Therapeutics, Clinical Development, Krakow, Poland; <sup>5</sup>Ryvu Therapeutics, Department of Biology, Krakow, Poland; <sup>6</sup>Ryvu Therapeutics, Department of Drug Metabolism and Pharmacokinetics, Krakow, Poland; <sup>7</sup>Universitary Hospital Quironsalud, NEXT Oncology Madrid, Madrid, Spain

**Background:** CDK8 and CDK19 are kinases involved in transcriptional regulation via the mediator complex. A variety of cancer cells hijack CDK8 and CDK19 to maintain stemness and undifferentiated state and to prevent apoptotic cell death. Targeting cancer-specific gene transcription via CDK8/19 inhibition has potential for the treatment of solid tumors. RVU120 is a CDK8/19 inhibitor with high selectivity and potency. Preclinical data indicate efficacy of RVU120 in hematologic malignancies and a variety of solid tumor types (Rzymiski et al. 2017).

**Methods:** RVU120 is currently being tested in patients with solid tumors in an ongoing Phase I/II clinical trial (NCT05052255). Patients with metastatic or advanced solid tumors who have exhausted available standard treatments receive increasing doses of RVU120 as a single oral dose every other day (QOD) for a total of 7 doses on Days 1, 3, 5, 7, 9, 11 and 13, in a 3-week treatment cycle. Primary objectives of the Phase I part are safety/tolerability of RVU120 as a single agent and determination of the recommended Phase II dose (RP2D) using a 3 + 3 dose escalation design. Secondary objectives include preliminary anti-tumor response as assessed by RECIST v1.1 and PK of RVU120.

**Results:** As of 30JUN 2022, 9 pts have been enrolled into the trial at doses of 75 mg, 100 mg, and 125 mg. The median age was 62 years, all patients were heavily pre-treated with a median of 3 prior lines of systemic therapy. None of the pts experienced a DLT, drug-related SAE, or drug-related AE of Grade 3 or higher. The majority of TEAEs were mild or moderate. TEAEs that occurred in at least 2 patients were vomiting, cold, itching, constipation, asymptomatic increased NT-proBNP, increased CRP. All these events were Grade 1 or 2, non-serious and assessed as unrelated to study drug, except one AE of vomiting and one AE of itching, which were assessed as possibly related to study drug. There were no Grade 4 or Grade 5 events. 6 pts discontinued treatment: 5 due to progressive disease and one patient withdrew consent. As of the cut-off date, 6 patients had at least one post-baseline disease assessment. The best response was stable disease in 2 patients (gastro-esophageal junction cancer, 18 weeks; adenoid cystic carcinoma, ongoing after 33 weeks) and progressive disease in 4 patients (thymic carcinoma, pancreatic cancer, 2 patients with breast cancer). 1 patient (breast cancer) withdrew consent prior to the first post-baseline assessment, and in 2 patients (testicular cancer, colorectal cancer) the first assessment is pending.

**Conclusion:** RVU120 demonstrates a favorable safety profile at the tested dose levels. In a heavily pretreated, unselected all-comer population, disease stabilization was observed in 2 patients. Available data warrant continuation of dose escalation and collection of additional clinical data.

**Conflict of interest:**

Ownership: Ryvu Therapeutics (TR, HN, NA, PL)

68

(PB058)

**MYC inhibition by Omomyc as a therapeutic strategy for (KRAS-mutated) colorectal cancer**

J. Kaur<sup>1</sup>, S. Martínez-Martín<sup>2</sup>, L. Foradada<sup>2</sup>, S. López-Estévez<sup>2</sup>, E. Serrano<sup>1</sup>, G. Martín-Fernández<sup>1</sup>, H. Thabusot<sup>3</sup>, V. Castillo Cano<sup>3</sup>, S. Casacuberta-Serra<sup>4</sup>, M.F. Zacarías-Fluck<sup>1</sup>, J. Grueso<sup>1</sup>, M.E. Beaulieu<sup>5</sup>, J.R. Whitfield<sup>1</sup>, L. Soucek<sup>1,5,6,7</sup>. <sup>1</sup>Vall d'Hebron Institute of Oncology, Models of Cancer Therapies Group, Barcelona, Spain; <sup>2</sup>Peptomyc S.L., Biomarkers, Barcelona, Spain; <sup>3</sup>Peptomyc S.L., Protein Production Platform, Barcelona, Spain; <sup>4</sup>Peptomyc S.L., Immuno Oncology, Barcelona, Spain; <sup>5</sup>Peptomyc S.L., Peptomyc, Barcelona, Spain; <sup>6</sup>Institució Catalana de Recerca i Estudis Avançats, Icrea, Barcelona, Spain; <sup>7</sup>Universitat Autònoma de Barcelona, Department of Biochemistry and Molecular Biology, Bellaterra, Spain

**Background:** Colorectal cancer (CRC) is the 4th leading cause of cancer-related deaths and is in dire need of new therapeutics. Deregulation of MYC function, a proto-oncogene involved in tumorigenesis, is a feature common to most malignancies including CRC. However, no MYC inhibitor has obtained clinical approval yet. In this study, we pre-clinically validated in CRC the efficacy of Omomyc mini-protein, a MYC inhibitor developed by Dr. Soucek (Principal Investigator), which is currently in Phase I/IIa clinical trial. Importantly, as KRAS-mutated CRC (~45% of CRC cases) is resistant to anti-EGFR therapy, the first line treatment for CRC, we investigated if Omomyc (and MYC inhibition by extension) could serve as a potential therapeutic agent for KRAS-mutated CRC.

**Materials and methods:** We investigated the efficacy of Omomyc in both *in vitro* and *in vivo* preclinical CRC models. We made use of a panel of commercially available CRC cell lines bearing wild-type or mutated KRAS gene for *in vitro* assays investigating the effect of Omomyc on their proliferation as well as cell cycle. Additionally, to compare the efficacy of Omomyc in KRAS-mutated vs -wild-type background in the same cellular context, we made use of isogenic cell lines that are wild-type or mutated for KRAS. We then tested the efficacy of intravenous-administered Omomyc *in vivo* using KRAS-mutated cell line-derived xenograft (CDX) and patient-derived xenograft (PDX) subcutaneous mouse models.

**Results:** We observed that, in the *in vitro* setting, Omomyc significantly impeded cell growth across the panel of KRAS-mutated and -wild-type cell lines. Furthermore, we observed that the presence of KRAS mutations did not affect the efficacy of Omomyc, which caused perturbations in the cycle across the cell line panel, irrespective of their KRAS mutational status. Finally, in the *in vivo* models, we observed that Omomyc, administered intravenously once a week for the duration of the experiment, resulted in significantly reduced relative tumour volume at end point in both CDX and PDX CRC models.

**Conclusions:** Our data suggest that MYC inhibition by Omomyc is a promising potential strategy for the treatment of CRC, especially but not limited to KRAS-mutated cases, hence paving the way for its clinical development as a therapeutic for CRC.

**Conflict of interest:**

Other Substantive Relationships: S. Martínez-Martín reports personal fees from Peptomyc S.L. during the conduct of the study personal fees from Peptomyc S.L. outside the submitted work. S. López-Estévez reports personal fees from Peptomyc S.L. during the conduct of the study personal fees from Peptomyc S.L. outside the submitted work. L. Foradada reports personal fees from Peptomyc S.L. during the conduct of the study personal fees from Peptomyc S.L. outside the submitted work. V. Castillo Cano reports other from Peptomyc S.L. outside the submitted work. S. Casacuberta-Serra reports personal fees from Peptomyc S.L. during the conduct of the study personal fees from Peptomyc S.L. outside the submitted work in addition, S. Casacuberta-Serra has a patent to EP19382194 pending. M.F. Zacarías Fluck reports other from Peptomyc S.L. outside the submitted work. M. Beaulieu is a cofounder and shareholder of Peptomyc, a company focused on developing Myc inhibitors for cancer treatment. J.R. Whitfield reports Shareholder in Peptomyc. Soucek reports personal fees from Peptomyc S.L. personal fees from Peptomyc S.L. outside the submitted work in addition, L. Soucek has a patent to EP13382167.8 issued.

69

(PB059)

**Transcriptomic profiling to identify key players of Ewing Sarcoma metastasis**

S. Sánchez-Serra<sup>1</sup>, M. Chicón-Bosch<sup>1</sup>, S. Maqueda-Marcos<sup>1</sup>, P. Monaco<sup>1</sup>, L. Santana-Viera<sup>1</sup>, R. López-Aleman<sup>1</sup>, O.M. Tirado<sup>1,2,3</sup>. <sup>1</sup>Bellvitge Biomedical Research Institute IDIBELL, Oncobell Program- Sarcoma Research Group, Hospitalet de Llobregat, Spain; <sup>2</sup>ICO, Catalan Oncology Institute, Hospitalet de Llobregat, Spain; <sup>3</sup>CIBERONC, Carlos III Institute of Health ISCIII, Madrid, Spain

**Background:** Metastasis at diagnosis is the most adverse prognostic factor in Ewing Sarcoma (ES), drastically decreasing patients' overall survival down to <30%. However, mechanisms leading to metastasis in this disease remain poorly understood. There is thus an urgent need to better understand the metastatic process in this disease, which will hopefully lead to better treatment strategies and improved survival rates for these patients.

**Materials and methods:** To deepen our knowledge on the main players in ES metastasis, microarray (Clariom™ D Array, Affymetrix) analysis was performed on primary tumours (n = 5) and metastases (n = 12) samples from a spontaneous metastatic ES mouse model. After bioinformatics analysis a list of differentially expressed genes between the 2 sample groups was obtained.

Candidates were validated by qPCR and Western Blot. Phenotypic characterisation of these genes' transient loss-of-function (using siRNAs and inhibitors) was performed by MTT, clonogenic and migration assays.

**Results:** Several genes of interest, including LOXHD1 and Gene 2 confirmed to be overexpressed in metastases samples compared to primary tumours as identified by microarray analysis and qPCR/Western Blot validation.

LOXHD1 showed upregulation in sphere-growing ES cells, validating its role in ES hypoxia and metastasis as demonstrated previously. LOXHD1 being in the list as one of the most differentially expressed genes between tumours and metastasis further validates the strength and reliability of our spontaneous metastatic mouse model.

Gene 2 transient loss-of-function significantly impaired metastatic ability of ES cells, as seen by migration assays. Development of a stable knock-out cell line for this gene using CRISPR-Cas9 technology is being carried out for further validation and elucidation of the mechanism by which this gene plays a role in ES metastasis.

**Conclusions:** Studying the profile of paired tumours and metastases provides a unique tool to decipher the mechanisms of tumour progression. Fully understanding the metastatic process will ultimately lead to the development of better targeted therapies and thus to improved outcomes for ES patients.

Next steps: Further experiments include stable knock-in of Gene 2 and its characterisation. Additionally, both knock-out and knock-in stable models will be studied *in vivo* using our spontaneous metastatic mouse model. Finally, clinical relevance of these targets will be explored in several cohorts of patients by immunohistochemistry on Tissue Microarrays. Proteomic and epigenomic approaches have also been performed to have the complete picture of differences between tumours and metastases. Also, these same steps are being followed in our laboratory for Rhabdomyosarcoma, another developmental tumour with discouraging overall survival rates for metastatic patients (<30%).

**No conflict of interest.**

71

(PB061)

**Identification of the mechanism of action of CYT-0851, an inhibitor of monocarboxylate transporter (MCT) mediated lactate transport**

B. Bradley<sup>1</sup>, M.A. Belmonte<sup>1</sup>, S. Kansara<sup>1</sup>, J.L. Blank<sup>1</sup>, L. Cryan<sup>1</sup>, N.M. Reilly<sup>1</sup>, V. Murali<sup>1</sup>, D.H. Miller<sup>1</sup>, J.P. Secrist<sup>1</sup>. <sup>1</sup>Cyteir Therapeutics, Research & Development, Lexington MA, USA

CYT-0851 was discovered using a phenotypic screen and rapidly advanced to a phase 1 clinical trial where responses in solid tumor and lymphoma patients have been observed. To elucidate the mechanism of action (MOA) of CYT-0851, extensive bioinformatic, functional genomic, and molecular characterization was performed. This preclinical work demonstrated that CYT-0851 disrupts lactate transport via inhibition of monocarboxylate transporter (MCT) activity. In rapidly proliferating cancers, lactate is produced during glycolysis and is exported primarily by MCT1 and MCT4, which provide functional redundancy when co-expressed.

**Methods:** CYT-0851 sensitivity data across 439 cell lines was cross-compared with available DepMap gene essentiality data and gene expression data. A genome-wide CRISPR screen identified genes that significantly influenced sensitivity to CYT-0851. MDCKII cells expressing human MCT1 were treated with CYT-0851 and transport of the MCT1

substrate, 2-thiophene-glyoxylic acid, was quantified by LC-MS. CYT-0851-mediated reversal of cytotoxicity induced by 3-bromopyruvate, an MCT1 substrate, was measured in Daudi human lymphoma cells. Lactate was measured using Lactate-Glo. Extracellular acidification and O<sub>2</sub> consumption were measured by Seahorse.

**Results:** Bioinformatic analysis revealed that CYT-0851 treatment most closely phenocopied genetic loss of MCT1 and was most effective at inhibiting the growth of cell lines with low MCT4 expression. A CRISPR dropout screen consistently identified genomic loss of MCT4 as a significant sensitizer to CYT-0851. CYT-0851 dose-dependently inhibited MCT1 transporter activity with an IC<sub>50</sub> of 134 nM and protected cells from the cytotoxic effects of 3-bromopyruvate. Intracellular lactate levels increased dose-dependently with CYT-0851 and strongly correlated with CYT-0851 cytotoxicity in 10 cell lines. CYT-0851 rapidly induced a metabolic shift from glycolysis to mitochondrial respiration as measured by reduced extracellular acidification rate and increased O<sub>2</sub> consumption. CYT-0851 cytotoxicity was enhanced by inhibitors of oxidative phosphorylation. Additional orthogonal studies validating MCT1 inhibition have been completed.

**Conclusions:** Rapidly proliferating cancers rely on lactate-producing glycolysis which necessitates lactate export through MCTs. CYT-0851 inhibition of MCT-mediated lactate transport in glycolytic cancer cells results in intracellular lactate accumulation, disruption of cellular metabolism and energetics, and cytotoxicity. Given the highly glycolytic nature of many cancers, MCTs are an attractive target for cancer therapies. CYT-0851 is in a phase 1/2 trial as monotherapy and in combination with chemotherapy. Translational analyses of patient samples are ongoing to confirm pharmacodynamic effects consistent with the MOA and test predictive biomarker hypotheses.

#### Conflict of interest:

Ownership: Cyteir Therapeutics

72

(PB062)

#### Differential off-target pharmacology between the PARP inhibitor rucaparib and its major metabolite

H. Hu<sup>1</sup>, A. Llebaria<sup>2</sup>, C. Serra<sup>2</sup>, A. Antolin Hernandez<sup>1</sup>. <sup>1</sup>The Institute of Cancer Research, Cancer Therapeutics, London, United Kingdom; <sup>2</sup>Institut de Química Avançada de Catalunya IQAC Consejo Superior de Investigaciones Científicas CSIC, Medicinal Chemistry and Synthesis MCS Laboratory, Barcelona, Spain

**Background:** Drug metabolites are generally more soluble, achieve lower concentrations in human plasma and can be excreted more easily than their parent drugs. Accordingly, drug metabolites are rarely characterized comprehensively in preclinical models and their on- and off-target activity is often overlooked. However, drug metabolites can play significant roles in the efficacy and safety of their parent drugs and help us explain clinical observations. Four PARP inhibitors have been approved by the FDA as cancer therapeutics, namely, olaparib, rucaparib, niraparib and talazoparib. The four drugs have largely similar PARP family inhibition profiles, but several differences at the molecular and clinical level have been reported that cannot be explained by their different kinase polypharmacology and remain poorly understood.

**Results:** Here, we use experimental and computational methods to synthesize and comprehensively characterize the off-target kinase landscape of Rucaparib's main metabolite, M324. We demonstrate that M324 has a unique polypharmacological profile across the kinome, different from rucaparib. M324 inhibits GSK3B and PLK2 at submicromolar concentrations – none of which is significantly inhibited by rucaparib (IC<sub>50</sub> > 1 μM). Moreover, we also demonstrate intracellular target engagement of PLK2 at clinically achievable low micromolar concentrations. The inhibition of PLK2 by M324 could help explain some of the unique side effects observed with rucaparib and could contribute to improve the precise and personalized use of this drug in selected cancer populations.

**Conclusion:** In summary, we demonstrate that rucaparib and its main metabolite M324 have a differential kinase polypharmacology. This different profile should be investigated further to clarify its potential implications for efficacy and safety in the clinic and to help tailoring this drug to cancer patients.

#### Conflict of interest:

Other Substantive Relationships: HH and AAA are/were employees of The Institute of Cancer Research (ICR), which has a commercial interest in a range of drug targets including PARP inhibitors. The ICR operates a Rewards to Inventors scheme whereby employees of the ICR may receive financial benefits following the commercial licensing of a project. AAA has been instrumental in the development of canSAR, Probe Miner and The Chemical Probes Portal. AAA is/was a consultant of Darwin Health. CSC and AL declare no conflict of interest.

73

(PB063)

#### Results from the NCI-MATCH ECOG-ACRIN Trial (EAY131) - Phase 2 Study of MLN0128 (TAK-228) in Patients with Tumors with TSC1 or TSC2 Mutations: Sub-protocol EAY131-M

J. Hays<sup>1</sup>, Z. Song<sup>2</sup>, P. Paik<sup>3</sup>, G. Iyer<sup>3</sup>, E. Mitchell<sup>4</sup>, J. Wright<sup>5</sup>, L. Doyle<sup>5</sup>, R. Gray<sup>2</sup>, V. Wang<sup>2</sup>, L. McShane<sup>6</sup>, L. Rubinstein<sup>6</sup>, D. Patton<sup>7</sup>, M. Williams<sup>8</sup>, S. Hamilton<sup>9</sup>, B. Conley<sup>10</sup>, C. Arteaga<sup>11</sup>, L. Harris<sup>10</sup>, P. O'Dwyer<sup>12</sup>, A. Chen<sup>13</sup>, K. Flaherty<sup>14</sup>. <sup>1</sup>The Ohio State University, James Comprehensive Cancer Center, Columbus Ohio, USA; <sup>2</sup>Dana Farber Cancer Institute, ECOG-ACRIN Biostatistics Center, Boston, USA; <sup>3</sup>Memorial Sloan Kettering Cancer Center, Medical Oncology, New York, USA; <sup>4</sup>Thomas Jefferson University Hospital, Medical Oncology, Philadelphia, USA; <sup>5</sup>National Cancer Institute, Investigational Drug Branch- Division of Cancer Treatment and Diagnosis, Bethesda, USA; <sup>6</sup>National Cancer Institute, Biometric Research Program- Division of Cancer Treatment and Diagnosis, Bethesda, USA; <sup>7</sup>National Cancer Institute, Center for Biomedical Informatics & Information Technology, Bethesda, USA; <sup>8</sup>Frederick National Laboratory for Cancer Research, Molecular Characterization Laboratory, Frederick, USA; <sup>9</sup>City of Hope National Medical Center, Department of Pathology, Duarte, USA; <sup>10</sup>National Cancer Institute, Cancer Diagnosis Program- Division of Cancer Treatment and Diagnosis, Bethesda, USA; <sup>11</sup>UT Southwestern Medical Center, Harold C. Simmons Comprehensive Cancer Center, Dallas, USA; <sup>12</sup>University of Pennsylvania, Abramson Cancer Center, Philadelphia, USA; <sup>13</sup>National Cancer Institute, Early Clinical Trials Development Program- Division of Cancer Treatment and Diagnosis, Bethesda, USA; <sup>14</sup>Massachusetts General Hospital, Mass General Cancer Center, Boston, USA

**Background:** The NCI-MATCH trial was designed to assess the clinical efficacy of select targeted therapies in pts with specific mutations in a tumor agnostic fashion. Loss of function mutations in the tumor suppressor genes TSC1 and TSC2 have been shown to activate the mTORC1 pathway constitutively. TAK-228 is an orally available potent inhibitor of both TORC1 and TORC2 complexes. Subprotocol M is a phase 2 study to determine the effects of TAK-228 on pts whose tumors harbor TSC1 or TSC2 alterations.

**Materials and Methods:** Patients with advanced metastatic solid tumors or lymphomas who progressed following at least 1 prior systemic therapy were accrued to NCI-MATCH for tumor molecular profiling, and those with functionally curated somatic TSC1 or TSC2 alterations were offered participation in sub-protocol M. Patients received TAK-228 3 mg daily for 28-day cycles until progression or intolerable toxicity.

**Results:** 49 pts were enrolled on arm M with 4 pts deemed ineligible or never starting treatment, leaving 45 evaluable pts. The primary analysis includes 34 pts with centrally confirmed mutations (CM), 7 from the MATCH screening cohort assay and 27 from approved outside laboratories. Of the 34 CM pts, 17 were female (50%), median age 62 (22–87), 21 had received 3 or more lines of prior therapy (61.7%), all had ECOG PS 0-1. Tumor types included urothelial (4), renal (2), prostate (2), colorectal (6), pancreas (1), HCC (1), ovary (3), endometrial stromal sarcoma (2), cervical adenocarcinoma (1), TNBC (1), squamous lung (2), PEComa (2), spindle cell sarcoma (1), PNET (1), angiosarcoma of spleen (1), osteosarcoma (1), melanoma (1), and undifferentiated carcinoma (2). TSC2 alterations made up 17 of the CM pts and 25 of the evaluable pts. Of the 34 CM pts, there were 5 PR for a 14.7% ORR (90% CI 6.0%- 28.5%), 13 SD, 12 PD and 4 were unevaluable. The estimated 6-month PFS rate is 28.7% (90% CI 17.3%–47.5%) in CM pts. The five responders were endometrial stromal sarcoma (1), high grade angiosarcoma of the spleen (1), PNET (1), HCC (1), and renal clear cell carcinoma (1). 4/5 responders had TSC2 alterations. Two pts with squamous NSCLC had clinical benefit for greater than 6 mo. Most common emergent adverse events among the 45 evaluable pts included hyperglycemia, fatigue, nausea, anemia and diarrhea. Grade 3–4 treatment-related adverse events (TRAE) included creatinine increase (4), TTP (4), dysphagia (4), pruritis (4). No grade 5 TRAE were reported. Six pts came off study due to adverse events.

**Conclusions:** While the primary endpoint of 6/34 (17.6% ORR) CM responses was not met, TAK-228 therapy had modest clinical activity in pts with various solid tumors exhibiting TSC1 or TSC2 alterations. The observation that 4/17 (23.5%) tumors harboring confirmed TSC2 alterations responded in this heavily pretreated population merits further investigation. NCT02465060.

No conflict of interest.



74

(PB064)

**Molecular characterization of primary and secondary resistance to RET inhibitors in patients with advanced NSCLC and RET fusions**

A. Marinello<sup>1</sup>, D. Vasseur<sup>2</sup>, N. Conci<sup>3</sup>, C. Lindsay<sup>4</sup>, G. Metro<sup>5</sup>, R. Ferrara<sup>6</sup>, A. Eisert<sup>7</sup>, F. Citarella<sup>8</sup>, V. Fallet<sup>9</sup>, C. Audugier-Valette<sup>10</sup>, S. Cousin<sup>11</sup>, F. Tabbò<sup>12</sup>, A. Russo<sup>13</sup>, A. Calles Blanco<sup>14</sup>, P. Irazo Gomez<sup>15</sup>, M. Tagliamento<sup>1</sup>, L. Mezquita<sup>16</sup>, S. Ponce<sup>17</sup>, B. Besse<sup>1</sup>, M. Aldea<sup>1</sup>. <sup>1</sup>Institut Gustave Roussy, Department of Cancer Medicine- Thoracic Unit, Villejuif, France; <sup>2</sup>Institut Gustave Roussy, Biopathology, Villejuif, France; <sup>3</sup>IRCCS-Azienda Ospedaliero-Universitaria di Bologna, Medical Oncology, Bologna, Italy; <sup>4</sup>The Christie NHS Foundation Trust, Department of Medical Oncology, Manchester, United Kingdom; <sup>5</sup>Azienda Ospedaliera di Perugia, Medical Oncology, Perugia, Italy; <sup>6</sup>Fondazione IRCCS Istituto Nazionale dei Tumori, Medical Oncology, Milano, Italy; <sup>7</sup>University Hospital of Cologne, Lung Cancer Group Cologne- Department I of Internal Medicine, Cologne, Germany; <sup>8</sup>Campus Bio-Medico University of Rome, Medical Oncology Department, Rome, Italy; <sup>9</sup>Hôpital Tenon- AP-HP, Service de Pneumologie et Oncologie Thoracique, Paris, France; <sup>10</sup>Hôpital Saint Musse- Toulon, Service de Pneumologie, Toulon, France; <sup>11</sup>Institut Bergonié, Medical Oncology, Bordeaux, France; <sup>12</sup>University of Turin- S. Luigi Gonzaga Hospital, Medical Oncology, Orbassano TO, Italy; <sup>13</sup>A.O. Papardo, Medical Oncology, Messina, Italy; <sup>14</sup>Hospital General Universitario Gregorio Marañón, Medical Oncology, Madrid, Spain; <sup>15</sup>Vall d'Hebron University Hospital & Vall d'Hebron Institute of Oncology, Oncology Department, Barcelona, Spain; <sup>16</sup>Hospital Clinic, Department of Medical Oncology, Barcelona, Spain; <sup>17</sup>Hospital Universitario 12 de Octubre, Department of Medical Oncology, Madrid, Spain

**Background:** RET fusions are a known tumor driver in 1–2% of patients with advanced non-small cell lung cancer (aNSCLC). The advent of selective RET inhibitors (RETi) significantly improved prognosis, but around 20% of patients show primary resistance. Moreover, secondary resistance inevitably occurs and molecular mechanisms are still incompletely characterized.

**Methods:** This multicentric retrospective study included 24 centres. Eligible patients had a RET-rearranged aNSCLC, received treatment with a RETi and had at least one molecular profile by next-generation sequencing (NGS), performed before and/or after RETi, on tissue and/or plasma samples. Primary resistance under RETi was defined as disease progression (PD) within 6 months of therapy.

**Results:** 95 patients were included with 112 biopsies: 93 performed at baseline, 19 at PD. 17 patients had paired NGS (baseline and PD). Median age was 65 years (range 56–72); 62% were female, 54% were never smokers, 17% presented with brain metastasis (BM) at diagnosis. 55 patients received pralsetinib, 36 selpercatinib, 4 other RETi. Overall, median progression-free survival (PFS) under RETi was 17.1 months (95%CI 12.6–28). Primary resistance to RETi occurred in 22 (23%) patients. Primary resistant did not show statistically significant differences when compared to durable responders to RETi in terms of histology (adenocarcinoma vs other, 9% vs 46%,  $p = 0.61$ ), smoking history (57% vs 40%,  $p = 0.21$ ), BM (5% vs 21%,  $p = 0.1$ ), TP53 co-mutations (37% vs 22%,  $p = 0.23$ ). KRAS G12 V mutation and SMARCA4 alterations were found only in poor responders (4.5% vs 0%,  $p = 0.2$ ; and 25% vs 0%,  $p = 0.04$ , respectively).

Considering biopsies at PD (N = 19, 13 liquid and 6 tissue biopsies), 7/13 (54%) liquid biopsies failed due to insufficient ctDNA. Among 12 evaluable patients, 3 (25%) acquired secondary RET mutations (G810S in two cases, S904F in one case), and 3 (25%) patients had off-target alterations, consisting in 2 MET amplification and 1 MYC amplification. Three patients (25%) developed novel TP53 mutations, while 3 (25%) had no novel identifiable alterations at PD.

**Conclusions:** SMARCA4 and KRAS baseline co-mutations may have a role in primary resistance to RETi. Secondary RET mutations and MET/MYC amplifications were identified after treatment with RETi.

**Conflict of interest:**

Ownership: none

Advisory Board: Viatris, Takeda, AstraZeneca, Boehringer-Ingelheim, Pfizer, Roche/Genentech, Eli Lilly and Company, Novartis, Merck Sharp & Dohme, Bristol Myers Squibb, AMGEN, GSK, Sanofi

Board of Directors: none

Corporate-sponsored Research: Merck Sharp & Dohme, Abbvie, Amgen, AstraZeneca, Biogen, Blueprint Medicines, BMS, Celgene, Eli Lilly, GSK, Ignyta, IPSEN, Merck KGaA, Nektar, Onxeo, Pfizer, Pharma Mar, Sanofi, Spectrum Pharmaceuticals, Takeda, Tiziana Pharma.

Other Substantive Relationships: none

75

(PB065)

**Biochemical characterization of TNG908 as a novel, potent MTA-cooperative PRMT5 inhibitor for the treatment of MTAP-deleted cancers**

W. Zhang<sup>1</sup>, S. Gong<sup>1</sup>, K. Cottrell<sup>2</sup>, K. Briggs<sup>3</sup>, M. Tonini<sup>3</sup>, L. Gu<sup>1</sup>, D. Whittington<sup>1</sup>, H. Yuan<sup>1</sup>, D. Gotur<sup>1</sup>, H. Jahic<sup>1</sup>, A. Huang<sup>3</sup>, J. Maxwell<sup>2</sup>, W. Mallender<sup>1</sup>. <sup>1</sup>Tango Therapeutics, Biochemistry, Cambridge, USA; <sup>2</sup>Tango Therapeutics, Chemistry, Cambridge, USA; <sup>3</sup>Tango Therapeutics, Biology, Cambridge, USA

TNG908 is a clinical stage MTA-cooperative PRMT5 inhibitor that leverages the synthetic lethal interaction between PRMT5 inhibition and MTAP deletion. PRMT5 is a type II arginine methyltransferase that regulates multiple essential cellular functions via symmetric dimethylation of arginine in target proteins. SAM is an essential co-factor for PRMT5, serving as the methyl donor when bound to a PRMT5-substrate protein complex. MTA is structurally similar to SAM but lacks the amino-carboxy terminus, therefore functions as an intrinsic inhibitor of PRMT5 when bound to a PRMT5-substrate protein complex. MTA is rapidly metabolized by MTAP in normal cells but accumulates in MTAP-deleted cancer cells to levels 10–100 times greater than MTAP WT cells. MTA-PRMT5 complexes are the predominant form in MTAP deleted cancer cells and present a unique and selective precision oncology target. We have discovered small molecules that exhibit MTA-cooperative PRMT5 binding and selectively kill MTAP-deleted cancer cells compared to MTAP WT cells. Here we present biochemical and orthogonal binding assay data to demonstrate that our clinical candidate, TNG908, is a potent, reversible, peptide substrate competitive inhibitor with a novel MTA-cooperative binding mechanism that binds selectively to the MTA-PRMT5 complex, with 15X selectivity for MTAP-deleted cell lines vs isogenic MTAP WT cell lines. We further propose a working model describing the mechanism of MTA-cooperative inhibition of PRMT5 by TNG908.

**Conflict of interest:**

Ownership: All authors are full-time employees of Tango Therapeutics and have stock and/or stock options.

77

(PB067)

**Discovery of I-0436650, a potent and selective SHP2 allosteric inhibitor for the treatment of RAS driven solid tumors**

F. Puca<sup>1</sup>, V. Fodale<sup>1</sup>, P. Randazzo<sup>2</sup>, D. Fabbrini<sup>2</sup>, A. Missineo<sup>1</sup>, M. Bisbocci<sup>3</sup>, S. Esposito<sup>4</sup>, M. Nibbio<sup>4</sup>, J. Amaudrut<sup>2</sup>, F. Colaceci<sup>5</sup>, R. Sasso<sup>5</sup>, F. Scalabrini<sup>1</sup>, S. Loponte<sup>1</sup>, C. Alli<sup>3</sup>, V. Pucci<sup>4</sup>, C. Montalbetti<sup>2</sup>, R. Di Fabio<sup>2</sup>, A. Petrocchi<sup>2</sup>, A. Carugo<sup>1</sup>, C. Toniatti<sup>1</sup>. <sup>1</sup>IRBM S.p.A., Biology, Rome, Italy; <sup>2</sup>IRBM S.p.A., Small Molecules R&D, Rome, Italy; <sup>3</sup>IRBM S.p.A., Translational Research, Rome, Italy; <sup>4</sup>IRBM S.p.A., Experimental Pharmacology, Rome, Italy; <sup>5</sup>IRBM S.p.A., In Vivo Pharmacology, Rome, Italy

**Background:** SHP2 (Src homology region 2-containing protein tyrosine phosphatase 2) is a target of interest for cancer therapy due to its key role in the regulation of RAS/MAPK signal transduction downstream of Receptor Tyrosine Kinases (RTKs). We report here the identification of I-0436650, a novel, highly potent, orally available SHP2 allosteric inhibitor, with potential for the treatment of tumors with dysregulated RTK/RAS/ERK signaling pathways.

**Material and Methods:** High-throughput biological, biochemical and pharmacodynamic (PD) assays were used to inform Structure Activity Relationship studies which led to the identification of a chemical series of potent SHP2 inhibitors. Iterative optimization of physicochemical and pharmacological properties resulted in the identification of I-0436650, an orally available SHP2 inhibitor with excellent drug-like properties. The therapeutic potential of I-0436650 was tested in a series of ex vivo and in vivo experiments.

**Results:** I-0436650 is a potent inhibitor of the SHP2 enzyme in vitro (IC50 = 5 nM) with a very slow koff rate (2.42E-05 1/s). When tested in cell line, it strongly inhibits pERK, a downstream marker of MAPK pathway activity, in a dose dependent manner. I-0436650 exhibits significant anti-proliferation activity against multiple RAS or EGFR mutant cancer cell lines alone and/or in combination with different FDA approved drugs. Further, I-0436650 effectively inhibits tumor growth in vivo in SHP2 dependent human xenograft models.

**Conclusions:** I-0436650 is a potent, selective orally available SHP2 inhibitor with potential for once-a-day dosing in humans. Of note, its predicted brain permeability in humans makes it a potential therapeutic agent against SHP2i responsive brain tumors and metastases.

**No conflict of interest.**

78

(PB068)

**Vepafestib is effective in preclinical models of sarcomas with RET fusion including a brain metastasis model**

L. Odintsov<sup>1</sup>, A. Liu<sup>2</sup>, I. Khodos<sup>3</sup>, Q. Chang<sup>3</sup>, C. Giuliano<sup>4</sup>, M. Mattar<sup>2</sup>, M. Vojnic<sup>5</sup>, A. Bonifacio<sup>6</sup>, E. De Stanchina<sup>3</sup>, E. Lovati<sup>4</sup>, M. Ladanyi<sup>2</sup>, R. Somwar<sup>2</sup>. <sup>1</sup>Brigham and Women's Hospital, Pathology, Boston, USA; <sup>2</sup>Memorial Sloan Kettering Cancer Center, Pathology, New York, USA; <sup>3</sup>Memorial Sloan Kettering Cancer Center, Anti-tumor Assessment Core Facility, New York, USA; <sup>4</sup>Helsinn Health Care SA, Preclinical Drug Development, Lugano, Switzerland; <sup>5</sup>Northwell Health Cancer Institute, Medicine, New York, USA; <sup>6</sup>Helsinn Health Care, Preclinical Drug Development, Lugano, Switzerland

**Background:** RET fusions are found in an increasing number of undifferentiated pediatric sarcomas, with many tumors occurring in the infantile fibrosarcoma spectrum. Vepafestib (TAS0953/HM06) is a brain-penetrant 2nd generation RET-selective inhibitor that is also effective against RET solvent front (G810) and gatekeeper (V804) mutations. We evaluated the brain penetrability and efficacy of vepafestib in preclinical sarcomas models with RET fusion.

**Methods:** We established several novel preclinical models of RET fusion-driven sarcomas: 1) PDX model and cell line from sarcoma tissue with SPECC1L::RET fusion (SR-Sarc-0001); 2) Isogenic cell line models where SPECC1L::RET was introduced into human mesenchymal stem cells using CRISPR-Cas9 (HMSC-RET); 3) A brain metastasis model where HMSC-RET cells labeled with luciferase to facilitate bioluminescence imaging was injected into the cerebellum of mice. Inhibitor level in the brain was assessed by pharmacokinetic profiling in the prefrontal cortex (PFC), cerebrospinal fluid (CSF) and plasma in freely-moving male Han Wistar rats following single-dose oral administration of 3, 10 and 50 mg/kg vepafestib.

**Results:** Treatment of SR-Sarc-0001 and HMSC-RET cells with vepafestib resulted in dose- and time-dependent loss of RET, ERK1/2, AKT, STAT3 and S6 phosphorylation, changes in core mediators of cell cycle regulation (p27 upregulation, CCND1 downregulation), suppressed MYC expression and induction of pro-apoptosis proteins (c-PARP, BIM). Vepafestib blocked growth of SR-Sarc-0001 (IC<sub>50</sub>: 0.09 μM, 95% CI: 0.03–0.2) and HMSC-RET (IC<sub>50</sub>: 0.09 μM, 95% CI: 0.06–0.1) cells and activated caspase 3/7. Control HMSC cells were refractory to the inhibitor. In all *in vitro* assays vepafestib was more effective than vandetanib and as effective as the FDA-approved RET inhibitors selipratinib and pralsetinib. Treatment of SR-Sarc-0001 PDX model with vepafestib (50 mg/kg BID) resulted in tumor shrinkage of 64.8 ± 0.5%. Importantly, no PDX tumor regrew after cessation of vepafestib treatment for 46 days. In contrast, after cessation of selipratinib (10 mg/kg BID) or pralsetinib (15 mg/kg BID) treatment, 1/5 and 3/5 tumors, respectively, regrew. Vepafestib was more effective than selipratinib at blocking growth of HMSC-RET brain xenograft tumors (p = 0.001) and increasing survival (p = 0.0001). Following administration and equilibration between body fluid compartments, the concentration ratio of vepafestib in the PFC, CSF and plasma free fraction was approximately 1:1:1.

**Conclusions:** Our preclinical results suggest that vepafestib is more effective than selipratinib in the brain and represents a therapeutic strategy for RET-driven sarcomas. Vepafestib is currently in phase 1/2 clinical trials for adult patients with advanced solid tumors with RET alterations (margaRET, NCT 04683250).

**Conflict of interest:**

Advisory Board: M. Ladanyi has received advisory board compensation from Boehringer Ingelheim, AstraZeneca, Bristol-Myers Squibb, Takeda, Bayer, and Paige.AI  
Corporate-sponsored Research: R. Somwar and M.Ladanyi received research funding from Helsinn Health Care that partially supposed this study. Vepafestib is being developed by Helsinn Health Care.  
Other Substantive Relationships: E. Lovati, C. Giuliano and A. Bonifacio are employees of Helsinn Healthcare. Vepafestib is being developed by Helsinn Health Care.

79

(PB069)

**Tumor-selective, chaperone-mediated protein degradation (CHAMP) of the bromodomain transcription factor BRD4**

K. Foley<sup>1</sup>, Y. Dai<sup>2</sup>, Q. Ding<sup>3</sup>, F. Du<sup>4</sup>, J. Li<sup>5</sup>, C. Lv<sup>4</sup>, T. Prince<sup>6</sup>, Y. Sun<sup>3</sup>, M. Wang<sup>3</sup>, R. Wang<sup>2</sup>, X. Yang<sup>3</sup>, Y. Wang<sup>2</sup>, Z. Wang<sup>5</sup>, L. Ma<sup>7</sup>, L.Y. Long Ye<sup>8</sup>, W.Y. Wei Yin<sup>5</sup>, C.Y. Chenghao Ying<sup>1</sup>, M.Y. Min Yu<sup>9</sup>, Y. Zhu<sup>3</sup>, W. Ying<sup>9</sup>. <sup>1</sup>Ranok Therapeutics, Biology, Waltham, USA; <sup>2</sup>Ranok Therapeutics, Biology, Shanghai, China; <sup>3</sup>Ranok Therapeutics, Biology, Hangzhou, China; <sup>4</sup>Ranok Therapeutics, Preclinical Development, Hangzhou, China; <sup>5</sup>Ranok Therapeutics, Chemistry, Hangzhou, China; <sup>6</sup>Ranok Therapeutics, Biology, Danville, USA; <sup>7</sup>Ranok Therapeutics, Chemistry, Shanghai, China; <sup>8</sup>Ranok

Therapeutics, Preclinical Development, Shanghai, China; <sup>9</sup>Ranok Therapeutics, Chemistry, Lexington, USA

**Background:** The HSP90 chaperone complex has an important role in facilitating folding of newly synthesized substrate proteins, but can also mediate degradation of misfolded proteins through interaction with ubiquitin E3 ligases. Additionally, the HSP90 complex is often activated in cancer cells, which is associated with HSP90-binding agents displaying unusual tumor-selective pharmacokinetics *in vivo*. Taking advantage of these characteristics of the HSP90 chaperone complex, chaperone-mediated protein degraders (CHAMPs) are hetero-bifunctional small molecules that bind to a target protein of interest and direct its interaction with the HSP90 chaperone complex, thereby inducing degradation of the target protein via the ubiquitin proteasome system. The BET bromodomain transcription factor BRD4 is a promising cancer target due to its role in regulating expression of a number of important cancer-associated genes, including MYC. In order to chemically induce BRD4 degradation, a BRD4-CHAMP compound was synthesized by covalently coupling HSP90- and BET-binding moieties through a short linker.

**Materials and methods:** CHAMPs were synthesized using standard medicinal chemistry techniques. CHAMP-induced degradation of BRD4 and biological activity was studied *in vitro* in cancer cell lines and *in vivo* in tumor xenograft models.

**Results:** *In vitro*, BRD4-CHAMP treatment of cancer cell lines induced degradation of BRD4, leading to cell growth inhibition and apoptosis. BRD4 in complex with HSP90 could be immune-precipitated from CHAMP-treated cells, and LC-MS/MS proteomics detected multiple ubiquitin E3 ligases associated with the complex. Consistent with this, BRD4 degradation was blocked by treatment with a proteasome inhibitor. Although BRD4-CHAMP displayed pan-BET binding selectivity in biochemical bromodomain binding assays, BRD4 was selectively degraded relative to the closely related family members, BRD2 and BRD3, perhaps due to different protein-protein interactions with HSP90. In mouse xenograft tumor models, consistent with activation of HSP90 in tumors, the concentration of BRD4-CHAMP in tumors was dramatically elevated relative to plasma and normal tissues for up to 7 days following a single dose. Treatment with BRD4-CHAMP on a once weekly dosing schedule induced prolonged ~90% BRD4 degradation, resulting in significant tumor growth inhibition, and depending on the model, tumor regression. *In vivo* BRD4-CHAMP displayed greater efficacy than a clinical-stage BET inhibitor at tolerated doses, suggesting that tumor-selective, BRD4-specific degradation has a superior therapeutic index relative pan-BET inhibition.

**Conclusions:** Based on these findings, we have initiated a Phase 1/2 clinical of the BRD4-CHAMP compound RNK05047 in solid tumors and lymphoma patients.

**Conflict of interest:**

Ownership: Stock in Ranok Therapeutics

80

(PB070)

**Human EGFR (HER) family ligands as targets in Cancer and Autoimmune Disease**

H.M. Shepard<sup>1</sup>. <sup>1</sup>Enosi Therapeutics, Translational Research, Eugene, USA

**Background:** Solid tumors and rheumatoid arthritis have overlapping mechanisms of pathogenesis. Both diseases are characterized by a hyperproliferative component, hypoxia, excessive angiogenesis, and inflammation. First-line treatments also overlap. Examples are methotrexate and cyclophosphamide which are used to treat many different malignancies as well as being first-line treatments for rheumatoid arthritis. The hyperproliferative component of RA is the pannus, which is a fibroblastic mass that expands in the affected joint and provides a home to immune cells which produce inflammatory cytokines, much like the biology of the tumor extracellular matrix. A significant amount of research has shown the increased presence of HER family ligands in many tumors and in RA joints. These growth factors have proliferative effects resulting in tumor growth and angiogenesis. The work described here shows the potential for a EGFR-Fc/HER3-Fc heterodimer in the treatment of both diseases.

**Material and Methods:** The extracellular ligand-binding domains of EGFR and HER3 were optimized to provide transmembrane-like affinity for 9 of the 11 EGFR/HER3-binding growth factors (Jin et al., Mol Med 15: 11, 2009). *In vitro* and *In vivo* methods for evaluating the anticancer effects of the EGFR-Fc/HER3-Fc are also described in Jin et al. Methods related to experiments in the collagen-induced arthritis model are described in Gompels et al., Arthritis Research and Ther 13: R161, 2011). The EGFR-Fc/HER3-Fc was engineered not to bind Heregulin/neuregulin-4 to minimize effects on HER4, which has many non-cancer physiological roles, such as survival of cardiac myocytes.

**Results:** In vitro and in vivo studies showed that EGFR-Fc/HER3-Fc was effective in inhibiting human tumor cell growth in vitro and in vivo and in nude mice. Initial biomarker screening showed best in vitro growth inhibitory effects were dependent upon the presence of the EGFR, HER2 and HER3 and HRG expression. In vivo studies in the collagen-induced arthritis model showed regression of arthritis in animals treated with the combination of EGFR-Fc/HER3-Fc plus etanercept. Immunohistochemistry showed inhibition of angiogenesis in affected joints.

**Conclusions:** The extension of anti-receptor antibodies from oncology to autoimmune disease has been slowed because of unwanted toxicity of reagents like gefitinib or cetuximab. This toxicity is due to the presence of the EGFR on many tissues and therefore in discriminating between normal and disease tissues. The EGFR-Fc/HER3-Fc instead acts as a ligand trap, which can remove excess growth factors from diseased tissues, thus starving diseased cells and preserving normal cell function. This principal can possibly be applied to both cancer and rheumatoid arthritis.

**Conflict of interest:**

Ownership: HMS owns shares in Enosi Therapeutics, Inc.

POSTER SESSION

**New Agents for Pediatric Oncology**

81 (PB071)

**A novel and potent strategy for blocking the Hedgehog pathway to treat rhabdomyosarcoma**

P. Zarzosa<sup>1</sup>, N. Navarro<sup>2</sup>, J. Sansa-Girona<sup>1</sup>, G. Pons<sup>1</sup>, G. Gallo-Oller<sup>1</sup>, A. Magdaleno<sup>1</sup>, M.F. Segura<sup>1</sup>, J. Sánchez de Toledo<sup>3</sup>, S. Gallego<sup>4</sup>, L. Moreno<sup>4</sup>, J. Roma<sup>1</sup>. <sup>1</sup>Fundació Hospital Universitari Vall d'Hebron - Institut de Recerca VHIR, Childhood Cancer and Blood Disorders Group, Barcelona, Spain; <sup>2</sup>IDIBAPS-Hospital Clinic, Gastrointestinal and Pancreatic Oncology Group, Barcelona, Spain; <sup>3</sup>Institut Català d'Oncologia ICO, Relacions Institucionals, Barcelona, Spain; <sup>4</sup>Fundació Hospital Universitari Vall d'Hebron - Institut de Recerca VHIR, Oncologia y Hematología Pediátrica, Barcelona, Spain

**Background:** This study identifies the Hedgehog pathway coreceptor CDO as a new molecular target in rhabdomyosarcoma and initiates preclinical drug development of the first experimental anti-CDO compound, a novel small molecule with high therapeutic potential.

**Material and methods:** The expression of specific molecular markers was determined by real time PCR and Western Blot.

Genetic inhibition of CDO and BOC was performed by shRNA systems.

*In silico* (molecular docking approach) and *in vitro* (proliferation assay) anti-CDO small molecule screening.

Anti-CDO small molecules were screened both *in silico* (molecular docking approach) and *in vitro* (proliferation assay).

*In vitro* (proliferation, apoptosis, invasion, differentiation) and *in vivo* (orthotopic primary tumor growth in mice) experiments assessed the functional and molecular effects of CDO and BOC genetic or pharmacologic inhibition.

**Results:** CDO and BOC Hh coreceptors are ubiquitously overexpressed in rhabdomyosarcoma tumors compared to normal muscle tissue. *In vitro* BOC genetic downregulation ruled out an essential oncogenic role in rhabdomyosarcoma cells. Conversely, genetic inhibition of CDO caused strong lethality. Together with the biotechnology company SELABTEC from LEITAT group, we developed and patented (EP3586847) the first CDO inhibitory compound worldwide. The new compound showed impressive antioncogenic efficacy in the most aggressive rhabdomyosarcoma cell lines (PAX3/FOXO1 translocated), emerging as a new therapeutic hope for high-risk patients. Specifically, CDO inhibition compromised cell viability and invasion and induced apoptosis and differentiation. Additionally, our anti-CDO small molecule has superior *in vitro* antiproliferative potency than the classical HH inhibitors (Vismodegib and Sonidegib). Finally, an *in vivo* murine model confirmed the antioncogenic efficacy of the new compound without apparent toxicity.

**Conclusions:** In conclusion, we describe for the first time the oncogenic role of the CDO coreceptor in rhabdomyosarcoma. Furthermore, we developed a promising new compound targeting CDO that shows potent therapeutic efficacy *in vitro* and *in vivo*.

**Conflict of interest:**

Other Substantive Relationships: Authors (Zarzosa P, Sánchez de Toledo J, Gallego S, and Roma J) and their institution (Fundació Hospital Universitari Vall d'Hebron - Institut de Recerca (VHIR)) share the intellectual property of the new anti-CDO compound with INSTITUT UNIV. DE CIÈNCIA I

TECNOLOGIA, S. A. (E.C. Patent Application No. EP19733520A, U.S. Patent Application No. US201917256837A, and Japan Patent Application No. JP2021500159A).

82 (PB072)

**Phase I dose-escalation study of the pan-PI3 K inhibitor copanlisib in children and adolescents with relapsed/refractory solid tumors**

M. Macy<sup>1</sup>, T. Cash<sup>2</sup>, N. Pinto<sup>3</sup>, J.G. Pressey<sup>4</sup>, L. Szalontay<sup>5</sup>, W.L. Furman<sup>6</sup>, A. Bukowski<sup>7</sup>, J.H. Foster<sup>8</sup>, G.K. Friedman<sup>9</sup>, J. HaDuong<sup>10</sup>, E. Fox<sup>6</sup>, B.J. Weigel<sup>11</sup>, J. Grevel<sup>12</sup>, F. Huang<sup>13</sup>, C. Phelps<sup>14</sup>, B.H. Childs<sup>15</sup>, J. Chung<sup>15</sup>, S. Chaturvedi<sup>16</sup>, A. Schulz<sup>17</sup>, S.G. DuBois<sup>18</sup>. <sup>1</sup>University of Colorado and Center for Cancer and Blood Disorders- Children's Hospital Colorado, Department of Pediatrics, Aurora, USA; <sup>2</sup>Aflac Cancer and Blood Disorders Center- Children's Healthcare of Atlanta and Emory University, Department of Pediatrics, Atlanta, USA; <sup>3</sup>Seattle Children's Hospital, Hematology and Oncology, Seattle, USA; <sup>4</sup>Cincinnati Children's Hospital Medical Center, Cancer and Blood Diseases Institute, Cincinnati, USA; <sup>5</sup>Columbia University Medical Center, Department of Pediatrics, New York, USA; <sup>6</sup>St. Jude Children's Research Hospital, Department of Oncology, Memphis, USA; <sup>7</sup>UPMC Children's Hospital of Pittsburgh, Department of Hematology/Oncology, Pittsburgh, USA; <sup>8</sup>Texas Children's Hospital, Division of Hematology and Oncology- Department of Pediatrics, Houston, USA; <sup>9</sup>University of Alabama at Birmingham, Department of Pediatrics- Division of Hematology/Oncology, Birmingham, USA; <sup>10</sup>Children's Hospital of Orange County, Division of Oncology- Hyundai Cancer Center, Orange, USA; <sup>11</sup>University of Minnesota Masonic Cancer Center, Department of Pediatrics, Minneapolis, USA; <sup>12</sup>BAST Inc. Limited, Clinical Statistics, Leicester, United Kingdom; <sup>13</sup>Bayer HealthCare Pharmaceuticals, Clinical Pharmacology, Whippany, USA; <sup>14</sup>Bayer HealthCare Pharmaceuticals, Clinical Statistics, Whippany, USA; <sup>15</sup>Bayer HealthCare Pharmaceuticals, Clinical Development, Whippany, USA; <sup>16</sup>Bayer HealthCare Pharmaceuticals, Precision Medicine, Whippany, USA; <sup>17</sup>Bayer AG, Pharmaceuticals Division, Berlin, Germany; <sup>18</sup>Dana-Farber/Boston Children's Cancer and Blood Disorders Center, Pediatric Hematology and Oncology, Boston, USA

**Background:** The pan-PI3 K inhibitor copanlisib is approved as monotherapy in adult patients (pts) with relapsed follicular lymphoma. While PI3 K activation is often observed in high-risk pediatric cancers, copanlisib had not been studied in this setting. We report the results of a trial sponsored by Bayer AG and conducted in collaboration with the Children's Oncology Group on the safety, efficacy, and pharmacokinetics (PK) of copanlisib in pediatric pts with relapsed/refractory solid tumors (NCT03458728).

**Methods:** Pts were aged 6 months to 21 years, with a confirmed histologic diagnosis of malignancy with no standard curative or effective therapy after  $\geq 1$  line of therapy. Copanlisib was given i.v. over 1 hour on days 1, 8, and 15 of a 28-day cycle. Primary endpoints were safety and the determination of the maximum tolerated dose (MTD) and/or recommended Phase II dose (RP2D); secondary endpoints included PK, response, and analysis of biomarkers including % pAKT. Dose-limiting toxicity (DLT) criteria were amended to exclude non-clinically significant laboratory abnormalities after 5 pts were treated at 28 mg/m<sup>2</sup>.

**Results:** 23 pts received copanlisib: 16 at 28 mg/m<sup>2</sup> and 7 at 35 mg/m<sup>2</sup>. Median age was 14 years (range 7–19) and median number of prior anti-cancer therapies was 4 (range 2–18). The most common tumor types were neuroblastoma (26%) and osteosarcoma (22%). DLTs were observed in 1/8 pts in the 28 mg/m<sup>2</sup> cohort (hyperuricemia) and in 2/7 pts in the 35 mg/m<sup>2</sup> cohort (decreased platelet count [n = 1]; transient grade 3 hypertension and fever [n = 1]). The MTD/RP2D was 28 mg/m<sup>2</sup>; 3 additional pts were treated at the MTD with no DLTs. The most common treatment-emergent adverse events (TEAEs) were hyperglycemia (70%), nausea (61%), and decreased white blood cell count (52%). Grade 3/4 TEAEs were observed in 56%/25% and 86%/0% of pts in the 28 and 35 mg/m<sup>2</sup> cohorts, respectively, with no grade 5 TEAEs. Copanlisib exposure at 28 mg/m<sup>2</sup> was ~80% of the adult exposure at the 60 mg dose. No objective responses occurred (22 evaluable pts); best response was stable disease (3 pts, 14%) and progressive disease (19 pts, 86%); 2 pts received >2 treatment cycles. A significant decrease in % pAKT from baseline to 3 hours after dosing occurred in surrogate tissue of platelet-rich plasma on day 15 of cycle 1 (p < 0.001), consistent across samples and copanlisib dose, irrespective of response (mean inhibition 75%; median inhibition 77%).

**Conclusions:** The RP2D of single-agent copanlisib in pediatric pts was 28 mg/m<sup>2</sup> i.v. on days 1, 8, and 15 of a 28-day cycle; the PK expansion cohort is ongoing. No unexpected toxicities were observed. The PK profile and pharmacodynamic effects were similar to those seen in adults, but no

evidence of efficacy as monotherapy was observed. Studies of copanlisib plus other active agents may be warranted.

#### Conflict of interest:

Ownership: Margaret Macy: stock in Johnson & Johnson.

Funan Huang: stock in Bayer.

Charles Phelps: stock in Bayer, Johnson & Johnson, Pfizer, Amgen, and Eli Lilly and Company.

Advisory Board:

Thomas Cash: Y-mAbs Therapeutics.

Elizabeth Fox: de minimis compensation from Moffit Cancer Center Sunshine Project.

Board of Directors: Elizabeth Fox: leadership or fiduciary role in other board, society, committee or advocacy group, paid or unpaid, with Children's Oncology Group/Pediatric Early Phase Clinical Trial Network, ACCELERATE, and CureSearch.

Corporate-sponsored Research: Margaret Macy: salary support and institutional support for this abstract from Bayer HealthCare Pharmaceuticals, Inc.

Thomas Cash: institutional grants or contracts from Celgene/BMS and F. Hoffman-La Roche/Genentech.

Joseph G. Pressey: grants or contracts from the Jeff Gordon Foundation.

Gregory K. Friedman: grants or contracts from Eli Lilly and Company, Pfizer, and Eisai.

Joachim Grevel: institutional support for this abstract from Bayer Germany.

Stephen G. DuBois: support for this abstract from Bayer.

Other Substantive Relationships: Margaret Macy: consulting fees from Y-mAbs Therapeutics.

Thomas Cash: payment or honoraria for lectures, presentations, speaker bureau, manuscript writing or educational events, and support for attending meetings and/or travel, from EUSA Pharma.

Joseph G. Pressey: payment or honoraria for lectures, presentations, speaker bureau, manuscript writing or educational events from General Dynamics.

Gregory K. Friedman: patent pending related to oncolytic virotherapy for brain tumors, and receipt of equipment, materials, drugs, medical writing, gifts or other services from Treovir LLC, who provided G207 for an investigator-initiated trial related to brain cancer treatment.

Joachim Grevel: consulting fees from BAST Inc Ltd.

Funan Huang: employee of Bayer HealthCare Pharmaceuticals, Inc.

Charles Phelps: employee of Bayer HealthCare Pharmaceuticals, Inc.

Barrett H. Childs: employee of Bayer HealthCare Pharmaceuticals, Inc.

John Chung: employee of, and support for attending meetings and/or travel from, Bayer HealthCare Pharmaceuticals, Inc.

Shalini Chaturvedi: employee of Bayer HealthCare Pharmaceuticals, Inc.

Anke Schultz: employee of Bayer AG.

Steven G. DuBois: consulting fees from Amgen, Bayer, Jazz, and Loxo Oncology, and travel expenses from Loxo Oncology, Roche, and Salarius.

Navin Pinto, Luca Szalontay, Wayne L. Furman, Jennifer H. Foster, Josephine HaDuong, Andrew Bukowski, and Brenda J. Weigel have no conflicts of interest to declare.

83

(PB073)

#### Novel Casein Kinase II (CK2) inhibitor BMS-135 shows significant *in vivo* anti-leukemia effect

C. Gowda<sup>1</sup>, A. Purandare<sup>2</sup>, K. Mercer<sup>1</sup>, K. Duke<sup>1</sup>, S. Dovat<sup>1</sup>. <sup>1</sup>Pennsylvania State University College of Medicine, Pediatrics, Hershey, USA; <sup>2</sup>Bristol Myers Squibb, Research and Development, New Jersey, USA

**Introduction:** Targeting CK2 to achieve anti-leukemia effect has been validated in various leukemia models. Even though several CK2 inhibitors have been tested in animal models for over two decades, only one small molecule inhibitor has reached human trial. Here we report a novel and potent small molecule inhibitor of CK2 BMS-135 that has excellent *in vivo* leukemia inhibition and favorable toxicity profile in patient derived xenograft models of high-risk B cell acute lymphoblastic leukemia (B-ALL).

**Methods:** Various cell lines (n = 6) representing B-cell as well as primary leukemia cells (n = 6) from high risk B-ALL were treated with serial dilution of BMS-135 for 24 to 48 hrs and cell viability was measured using calorimetric (WST) assay. Similarly treated cells were analyzed for cell cycle distribution, apoptosis and colony formation. We measured mRNA and protein level of known CK2 targets. RNA sequencing and gene expression analysis was done to evaluate gene expression changes following treatment with BMS-135. Patient derived xenografts of B-ALL were treated with BMS-135 at dose 7.5 mg/kg intraperitoneal for 21 days or vehicle.

**Results:** Combined *in vitro* and *in vivo* experiments establish efficacy of BMS-135. Cytotoxicity at inhibitory concentrations of 30–1200 nM, G0-G1 cell cycle arrest, increased apoptosis and poor colony formation following treatment was noted consistently in all cells tested. Single drug treatment with

BMS-135 achieved 50–80% leukemia inhibition and significantly prolonged survival in treated mice after 3 weeks of therapy. Following *in vivo* treatment with BMS-135, we confirmed inhibition of known CK2 targets in B-ALL, at mRNA and protein level (Akt, PI3 K, Bcl-xl). No significant myelosuppression or organ toxicity was noted in BMS-135 treated NRG tumor bearing mice compared to vehicle treated mice. BMS-135 show synergistic cytotoxic activity with daunorubicin.

**Conclusions:** BMS-135 is a novel, selective inhibitor of CK2 which is significantly more potent than currently available CK2 small molecule inhibitors. BMS-135 shows *in vivo* therapeutic efficacy in acute leukemia models. BMS-135 showed dose depended *in vivo* target inhibition and favorable toxicity profile. These results support further pre-clinical characterization and clinical development of BMS-135.

No conflict of interest.

## POSTER SESSION

### New Drugs

84

(PB074)

#### Identification of STX-721, an EGFR exon 20 mutant inhibitor with superior selectivity and a potential best-in-class profile

R. Pagliarini<sup>1</sup>, B.C. Milgram<sup>1</sup>, D.R. Borrelli<sup>1</sup>, N. Brooijmans<sup>1</sup>, M.R. Huff<sup>1</sup>, T. Ito<sup>1</sup>, P. Jonsson<sup>1</sup>, B. Ladd<sup>1</sup>, E. O'Hearn<sup>1</sup>, W. Wang<sup>1</sup>, P. Kuzmic<sup>2</sup>, J. Bellier<sup>3</sup>, A.N. Hata<sup>3</sup>, A. Guzman-Perez<sup>1</sup>, D.D. Stuart<sup>1</sup>. <sup>1</sup>Scorpion Therapeutics, Oncology, Boston, MA, USA; <sup>2</sup>BioKin Ltd., President, Watertown, MA, USA; <sup>3</sup>Massachusetts General Hospital- Harvard Medical School, Department of Medicine, Charlestown, MA, USA

**Background:** EGFR mutations are well validated clinical targets in NSCLC. Osimertinib, a highly selective EGFR mutation-targeted drug, achieves an objective response rate (ORR) of >70% against cancers with L858R or exon 19 deletion. In contrast, patients with EGFR exon 20 insertion mutations have ORRs to currently approved or investigational therapies between 28 and 45%. This suggests suboptimal selectivity of existing EGFR inhibitors for exon 20 mutants versus wild-type EGFR.

**Materials and methods:** The apparent *in vitro* selectivity of EGFR inhibitors is dependent on the model systems used, limiting the predictive value of these systems for drug discovery. To address this issue, we optimized drug potency and selectivity across a broad panel of exon 20 mutant cell lines, including engineered Ba/F3 cells as well as NSCLC cells with endogenous or isogenic knock-in exon 20 mutations. Osimertinib selectivity in EGFR T790M mutant cells was used as a benchmark for mutant selectivity. Compounds were tested in proliferation, cell signaling, and biochemical assays. Finally, we examined inhibitor efficacy, pharmacodynamics, pharmacokinetics, and tolerability in novel patient-derived EGFR exon 20 mutant xenograft (PDX) mouse models.

**Results:** STX-721, representing novel chemical matter, demonstrated strong *in vitro* potency and selectivity for EGFR exon 20 mutations approaching the selectivity of Osimertinib in EGFR T790M mutant cells. Importantly, the superior selectivity of STX-721 was preserved across several human exon 20 mutant human cancer cell models. Excellent STX-721 *in vitro* selectivity was observed across cell proliferation, signaling (pEGFR, pERK), biochemical, and kinome profiling assays. Once-daily dosing of STX-721 resulted in tumor regression in multiple exon 20 mutant PDX models. All doses used were well-tolerated, including doses above the minimal fully efficacious dose. The observed selectivity of STX-721 exceeds that seen by head-to-head benchmarking of approved and investigational EGFR Exon 20 inhibitors.

**Conclusions:** STX-721 demonstrates EGFR exon 20 mutant selectivity approaching the selectivity of Osimertinib in EGFR T790M mutants, warranting further exploration of this potential best-in-class exon 20 inhibitor in the clinic.

#### Conflict of interest:

Corporate-sponsored Research: ANH receives research funding from Scorpion, Amgen, Pfizer, Eli Lilly, Novartis, Bristol-Myers Squibb, Genentech, Blueprint Medicines, Nuvalent, BridgeBio, and C4 Therapeutics. Other Substantive Relationships: RP, BCM, DRB, NB, MRH, TI, PJ, BL, EO, WW, AGP, and DDS are employees of Scorpion Therapeutics. ANH is a consultant for Nuvalent, Engine Biosciences, Tolremo Therapeutics, and TigaTx. PK is a consultant for Scorpion Therapeutics.

Table (abstract: 84 (PB074))

	Ba/F3: proliferation selectivity vs. EGFR WT		Human cells: proliferation selectivity (vs. EGFR WT NCI-H2073)							
	L858R/T790M	SVD	ASV	NCI-H1975 (L858R/ T790M)	NCI-H2073 (ASV knockin)	NCI-H2073 (SVD knockin)	CUTO14 (ASV)	CUTO17 (NPH)	SCCNC4 (SVD)	MGH10080 (GF)
Osimertinib	32x			6x						
Pozotinib		2x	2x		<1x	<1x	<1x	<1x	<1x	<1x
Mobocertinib		8x	10x		1x	1x	1x	<1x	1x	2x
BDTX-189		4x	4x		1x	2x	2x	1x	<1x	2x
CLN-081		8x	4x		<1x	3x	1x	1x	2x	5x
DZD-9008		10x	6x		1x	<1x	<1x	<1x	<1x	1x
STX-721		22x	24x		5x	9x	5x	4x	8x	8x

**85** (PB075)  
**ASP3082, a First-in-class novel KRAS G12D degrader, exhibits remarkable anti-tumor activity in KRAS G12D mutated cancer models**

T. Nagashima<sup>1</sup>, K. Inamura<sup>1</sup>, Y. Nishizono<sup>1</sup>, A. Suzuki<sup>2</sup>, H. Tanaka<sup>1</sup>, T. Yoshinari<sup>1</sup>, Y. Yamanaka<sup>3</sup>. <sup>1</sup>Targeted Protein Degradation, Astellas Pharma Inc., Tsukuba-shi, Ibaraki, Japan; <sup>2</sup>Immuno-Oncology, Astellas Pharma Inc., Tsukuba-shi, Ibaraki, Japan; <sup>3</sup>Applied Research & Operations, Astellas Pharma Inc., Tsukuba-shi, Ibaraki, Japan

**Background:** KRAS is one of the most frequently mutated oncogenes in various cancers. Among KRAS mutations, KRAS G12D is the most frequent driver mutation and is found in approximately 34% of pancreatic ductal adenocarcinoma (PDAC), 10% to 12% of colorectal cancer, 4% of lung adenocarcinoma and also in a subset of other solid tumors. However, there is no direct KRAS G12D-targeted inhibitors used in the clinical setting. Here, we identified ASP3082, a novel KRAS G12D degrader with high potency and selectivity.

**Methods:** We investigated (1) binding affinity of ASP3082 to KRAS G12D protein and an E3 ligase in the conditions of binary complex and ternary complex formation using surface plasmon resonance assay, (2) degradation activity of ASP3082 on KRAS G12D protein using western blotting or in-cell western method, (3) inhibitory effect of ASP3082 on the growth of human cancer cells harboring KRAS G12D mutation and KRAS wild-type, (4) specificity for ASP3082-mediated degradation using proteomics approach, (5) antitumor activity of ASP3082 in mice subcutaneously xenografted with KRAS G12D-mutated pancreatic cancer cells, (6) PK-PD profile of ASP3082 after a single intravenous administration in the xenograft model.

**Results:** ASP3082 directly bound to KRAS G12D-mutated protein and the E3 protein to form a ternary complex. Also, ASP3082 potently degraded KRAS G12D-mutated protein and inhibited phosphorylation of ERK in KRAS G12D-mutated pancreatic cancer cells. In addition, ASP3082 showed the growth inhibitory activity of KRAS G12D-mutated pancreatic cancer cells, but not of KRAS wildtype cancer cells. Furthermore, the quantitative proteomics analysis suggested that ASP3082 selectively degraded the KRAS G12D-mutated protein over other (>9000) proteins. *in vivo* experiment revealed that once-weekly intravenous administration of ASP3082 induced dose-dependent and significant growth inhibition of KRAS G12D PDAC tumors, resulting in profound tumor regression without body weight loss. ASP3082 showed sustained concentrations in the xenograft tumors after a single intravenous administration and decreased KRAS G12D-mutated protein levels according to the duration of the ASP3082 concentrations.

**Conclusions:** ASP3082 is a potential therapeutic agent for patients with tumors harboring the KRAS G12D mutation. Currently, Phase I clinical trial is underway (NCT05382559).

**Conflict of interest:**

Corporate-sponsored Research: All authors are employees of Astellas Pharma Inc.

**86** (PB076)  
**The novel, telomerase-directed, telomere-targeted, anticancer agent 6-thio-dG (THIO) demonstrates potent activity and induces antitumor immunity in hepatocellular carcinoma (HCC) models**

J. Shay<sup>1</sup>, I. Mender<sup>1</sup>, S. Siteni<sup>1</sup>, M. Obrocea<sup>2</sup>, V. Vitoc<sup>2</sup>, S. Gryaznov<sup>2</sup>. <sup>1</sup>UT Southwestern, Cell Biology, Dallas, USA; <sup>2</sup>Maia Biotechnology, Inc., Clinical Development, Chicago, USA

**Background:** HCC is one of the leading causes of cancer-related deaths worldwide. Low response rates with current treatments for HCC demonstrate an urgent unmet need for more effective systemic therapies. However, development of novel treatments for HCC has been challenging due to a lack of functionally druggable targets. The nucleoside prodrug analogue THIO is a first-in-class telomerase-directed, telomere-targeted, anticancer agent that has shown potent activity in other tumor types, including colorectal, lung, melanoma, and brain cancer models. In cancer cells, THIO is converted into the corresponding 5'-triphosphate, which is efficiently incorporated into telomeres by telomerase, activating DNA damage responses and proapoptotic pathways. We hypothesized that telomerase-targeting agents may be effective in HCC given the high rate of mutations in the telomerase reverse transcriptase (hTERT) promoter. Moreover, since >90% of HCCs reactivate telomerase to drive escape from senescence-induced growth arrest, treatment with THIO or second-generation telomere-targeted analogues is likely highly selective for telomerase-positive cancer cells relative to nonmalignant hepatocytes.

**Material and methods:** Activity of THIO and second-generation analogues was evaluated *in vitro* using telomerase-positive HCC cells and *in vivo* using syngeneic mouse models of aggressive HCC. HCC cells treated with or without THIO were analyzed for cell proliferation and stained with markers of replicative stress or cell cycle arrest, followed by confocal microscopy and/or flow cytometry. Immunophenotyping of tumor-infiltrating T cells in mice treated with THIO was performed by measuring the frequencies of MDSCs (Ly6C+Ly6G-), NK cells (NK1+), CD4 T cells (Ki67+/CD4+), and CD8 T cells (Ki67+/CD8+). Antitumor activity was assessed by serial measurements of tumor volume in mice sequentially treated with therapeutically relevant doses of THIO ± checkpoint inhibitors compared to control mice.

**Results:** THIO treatment induced replicative stress, followed by cell cycle arrest and apoptosis in telomerase-reactivated HCC cells. In syngeneic mouse models of aggressive HCC, treatment with THIO activated pathways associated with innate and adaptive immunity (eg, cGAS-STING pathway and infiltration of CD8+ T cells into the tumor microenvironment) and altered the immune-suppressive tumor microenvironment. THIO treatment enhanced the response to checkpoint inhibitors, yielding complete responses in some HCC model systems with no dose-limiting toxicities. Similar results were observed with second-generation THIO analogues.

**Conclusions:** Results of this study indicate that THIO, a first-in-class telomerase-directed, telomere-targeted agent, and its analogues may enhance the overall therapeutic efficacy of current immune checkpoint inhibitor-based treatments for HCC.

**Conflict of interest:**

Other Substantive Relationships: JW Shay: I have an interest in relation with one or more organizations that could be perceived as a potential conflict of interest in the context of this abstract. The relationship is summarized below: Scientific Advisory Board member and stock/stock options in MAIA Biotechnology, Inc. I am also a named inventor on several patents licensed to MAIA.

I Mender: I have an interest in relation with one or more organizations that could be perceived as a potential conflict of interest in the context of this abstract. The relationship is summarized below:

I am a named inventor on several patents licensed to MAIA.

S Siteni: I have no potential conflict of interest to disclose.

M Obrocea: I have an interest in relation with one or more organizations that could be perceived as a potential conflict of interest in the context of this abstract. The relationship is summarized below:

Full-time employee, officer (Chief Medical Officer), and stock/stock options in MAIA Biotechnology, Inc.

V Vitoc: I have an interest in relation with one or more organizations that could be perceived as a potential conflict of interest in the context of this abstract. The relationship is summarized below:

Full-time employment, officer (Founder and Chief Executive Officer), and stock/stock options in MAIA Biotechnology, Inc.

SM Gryaznov: I have an interest in relation with one or more organizations that could be perceived as a potential conflict of interest in the context of this abstract. The relationship is summarized below:

Full-time employment, officer (Chief Scientific Officer), and stock/stock options in MAIA Biotechnology, Inc.

87 (PB077)

### Optimal dosing of a novel PLK4 inhibitor nested in a phase II study of CFI-400945 in patients with Advanced/Metastatic Breast Cancer (MBC): Canadian Cancer Trials Group (CCTG) IND.237

M. Rushton<sup>1</sup>, D. Cescon<sup>2</sup>, J. Hilton<sup>3</sup>, P. Bedard<sup>2</sup>, P. Blanchette<sup>4</sup>, A. Bashir<sup>5</sup>, R. Pezo<sup>6</sup>, V. Kumar<sup>2</sup>, T. Ng<sup>3</sup>, A. Awan<sup>3</sup>, A. Lott<sup>6</sup>, J.A. Raphael<sup>4</sup>, L. Hagerman<sup>1</sup>, M. Bray<sup>7</sup>, L. Muyo<sup>2</sup>, J. Fuentes Antras<sup>2</sup>, L. Seymour<sup>1</sup>, D. Tu<sup>1</sup>, P.O. Gaudreau<sup>1</sup>. <sup>1</sup>Queen's University, Canadian Cancer Trials Group, Kingston, Canada; <sup>2</sup>University Health Network, Princess Margaret Cancer Centre, Cancer Clinical Research Unit CCRU, Toronto, Canada; <sup>3</sup>Ottawa Hospital Research Institute, Division of Medical Oncology, Ottawa, Canada; <sup>4</sup>London Regional Cancer Program, Division of Medical Oncology, London, Canada; <sup>5</sup>Allan Blair Cancer Centre, Medical Oncology, Regina, Canada; <sup>6</sup>Odette Cancer Centre, Sunnybrook Health Sciences Centre, Toronto, Canada; <sup>7</sup>Treadwell Therapeutics, Co-Founder- Chief Scientific Officer, Toronto, Canada

**Background:** CFI-400945 is a selective oral inhibitor of Polo-like Kinase 4 (PLK4), a controller of centriole duplication and mitotic progression. CFI-400945 was identified by functional screening of genomically unstable breast cancer (BC). The phase I study escalated doses from 3 to 96 mg/d in a 3 + 3 design; dose-dependent neutropenia (ANC) was noted, and the recommended phase 2 dose (RP2D) declared at 64 mg. IND.237 (NCT01954316) is a phase 2 study in MBC with 3 cohorts, 2 enriched for PTEN status. Enrollment started in 2018 at 64 mg. The initial patients had higher than expected grade 3/4 ANC.

**Materials and Methods:** The primary endpoint of the safety cohort was to confirm the RP2D for CFI-400945. Patients with MBC who met inclusion criteria for CCTG IND.237 were enrolled. A reverse 3 + 3 design was used, and patients enrolled at 64 mg, 48 mg, 40 mg and 32 mg dose levels (DL). In cycle (C)1, patients were treated 7 days on 7 days off for 28 d; for c2 onwards, CFI-400945 was administered continuously.

**Results:** The most common severe adverse event (AE) was dose dependent ANC (table 1). After 80% of the first 5 patients developed grade 3 or 4 ANC, accrual was held while the protocol was amended to add a dose exploration cohort with pharmacokinetics in a reverse dose-finding approach. Based on the frequency of ANC and dose intensity, 32 mg was declared the new RP2D for CFI-400945. There were no non-hematologic severe AEs. PK analysis confirmed similar AUC for the 32 mg DL compared to the PK from the phase I study RP2D.

Table 1: Frequency of severe neutropenia by DL during C1 and C2 of safety cohort of IND.237

DL	# Patients	Grade 3 ANC (n(%))	Grade 4 ANC (n(%))
64 mg	5	1 (20%)	3(60%)
48 mg	6	5 (50%)	2(33%)
40 mg	8	2 (25%)	2(25%)
32 mg	6	0 (0%)	0(0%)

Refinement of the manufacturing process used for IND.237 and subsequent studies incorporated a more stable polymorph of CFI-400945 drug substance had the unexpected property of higher exposure at a given dose and was hypothesized to be due to slightly faster dissolution of the new tablets in the acidic environment of the stomach.

**Conclusions:** The RP2D for CFI-400945 in patients with advanced breast cancer is 32 mg/day. This is 50% lower than the RP2D previously established in the phase I study due to an unexpected increase in exposure resulting from tablets containing a more stable polymorph of CFI-400945 drug substance.

**Acknowledgements:** Sponsored by CCTG. Research supported by a Stand Up to Cancer Canada (SU2C), Canadian Breast Cancer Foundation Breast Cancer Dream Team Research Funding, with supplemental support of the Ontario Institute for Cancer Research through funds provided by the Government of Ontario (Funding Award Number: SU2C-AACR-DT-18-15). Research funding is administered by the American Association for Cancer Research International - Canada, the scientific partner of SU2C Canada.

#### Conflict of interest:

Ownership: none

Advisory Board: Anthony Lott - Novartis, Eisai, Astra-Zeneca, Ipsen  
Terry Ng - Novartis, Knight Therapeutics, Boehringer-Ingelheim  
Arif Awan - AstraZeneca, Eli Lilly, Exact Sciences, Exactis, Novartis, Pfizer, Roche Honoraria: Apotex, Roche  
Rossanna Pezo - Merck, Novartis, Pfizer, Astra Zeneca, Lilly, BMS, Exact Sciences, Myriad Genomics, Mylan  
Philippe Bedard - Seattle Genetics, Lilly, Amgen, Merck, Gilead Sciences, BMS, Pfizer

John Hilton - Bristol-Myers-Squibb (BMS), AstraZeneca (AZ), Pfizer, Novartis, Eli Lilly, Puma, and Genomic Health

Jacques Antoun Raphael - Lilly, Merck, AstraZeneca and Novartis.

Moirá Rushton - Gilead, Pfizer, Viatris

David Cescon - Pfizer, AstraZeneca, Novartis, GlaxoSmithKline, Merck, Roche/Genentech,

Exact Sciences, Gilead Sciences, Eisai

Board of Directors: none

Corporate-sponsored Research: Terry Ng - Takeda Oncology

Rossanna Pezo - Merck and Novartis

Philippe Bedard - Bristol-Myers Squibb, Sanofi, AstraZeneca, Genentech/Roche, GlaxoSmithKline, Novartis, Nektar, Merck, Seattle Genetics, Immunomedics, Lilly, Amgen, Bicara, Zymeworks

David Cescon - Merck, Roche/Genentech, GlaxoSmithKline, Pfizer, Inivata, AstraZeneca, Gilead Sciences

Other Substantive Relationships: Terry Ng - Pharma-sponsored education session - ARIAD and Takeda Oncology

Arif Awan - Travel: Roche

Mark Bray - Full time employee of Treadwell Therapeutics

Lesley Seymour & Pierre-Olivier Gaudreau - Funding to CCTG from UHN to partially support trial conduct

Moirá Rushton - Medical Montior: Pharmamatrix, Edmonton, Alberta

David Cescon - Patent (US62/675,228) for methods of treating cancers characterized by a high expression level of spindle and kinetochore associated complex subunit 3 (ska3) gene. note CFI-402257 // CFI-400945 were developed at UHN

89 (PB079)

### Preliminary Clinical Data From Ongoing Phase 2 Study With Enhancer of Zeste Homolog 2 (EZH2) Inhibitor CPI-0209 in Patients With Advanced Solid Tumors or Hematologic Malignancies

H. Kindler<sup>1</sup>, R.D. Harvey<sup>2</sup>, L.R. Duska<sup>3</sup>, L. Gandhi<sup>4</sup>, R.J. Sullivan<sup>5</sup>, T. Gastinne<sup>6</sup>, M. Kwiatek<sup>7</sup>, A.M. García-Sancho<sup>8</sup>, N. Hadar<sup>9</sup>, L. Kann<sup>10</sup>, N. Faulhaber<sup>10</sup>, C. Drescher<sup>11</sup>. <sup>1</sup>The University of Chicago, Hematology and Oncology, Chicago, IL, USA; <sup>2</sup>Emory University School of Medicine and Winship Cancer Institute, Hematology and Medical Oncology, Atlanta, GA, USA; <sup>3</sup>University of Virginia, Obstetrics and Gynecology, Charlottesville, VA, USA; <sup>4</sup>Dana-Farber Cancer Institute, Center for Cancer Therapeutic Innovation, Boston, MA, United Kingdom; <sup>5</sup>Massachusetts General Hospital, Hematology Oncology, Boston, MA, USA; <sup>6</sup>CHU de Nantes, Clinical Hematology, Nantes, France; <sup>7</sup>Centrum Medyczne Pratia Poznań, Hematology, Skorzewo, Poland; <sup>8</sup>Hospital Universitario de Salamanca-IBSAL, Hematology, Salamanca, Spain; <sup>9</sup>MorphoSys US, Inc., Boston, MA, USA; <sup>10</sup>MorphoSys, Ag, Planegg, Germany; <sup>11</sup>Swedish Cancer Institute, Gynecologic Oncology, Seattle, WA, USA

**Background:** Enhancer of zeste homolog 2 (EZH2) is a histone-lysine N-methyltransferase enzyme and the catalytic subunit of polycomb repressive complex 2. ARID1A mutations have been linked to increased sensitivity to EZH2 inhibition. Inactivating BAP1 mutations in mesothelioma have been linked to dependency on EZH2 function. CPI-0209 is an investigational oral, small-molecule, second-generation, selective EZH2 inhibitor that shows durable and comprehensive target coverage based on findings in Phase 1 (NCT04104776; Lakhani, et al. ASCO 2021; Abstract #3104).

**Methods:** In the ongoing Phase 2 study, the antitumor activity and safety of CPI-0209 at the recommended Phase 2 dose (RP2D) of 350 mg once daily in

28-day cycles is being evaluated in six malignancies (M1: urothelial; M2: ovarian clear cell carcinoma; M3: endometrial carcinoma; M4: peripheral T-cell or diffuse large B-cell lymphoma; M5: mesothelioma; M6: metastatic castration-resistant prostate cancer); patients will be followed from first dose for 24 months. Each cohort will be enrolling 10–29 pts, including patients with *ARID1A* (M1, M2, M3) or *BAP1* (M5) mutations. Primary objective is to evaluate the antitumor activity of CPI-0209 in the selected tumor types (primary endpoint: objective response rate [ORR]).

**Results:** As of May 2, 2022, 37 pts (M2–M6) were enrolled and received  $\geq 1$  dose. 27/37 pts (73%) received  $\geq 2$  prior cancer treatment lines. Efficacy-evaluable pts (n = 26) received  $\geq 1$  dose of CPI-0209 at the RP2D and had  $\geq 1$  postbaseline tumor assessment. Median duration of follow-up was 70 days. Preliminary results of best unconfirmed responses of stage 1 of Simon's-2-Stage design are shown in the Table.

Table. Best unconfirmed responses

Cohort	Partial Response, n	Stable Disease, n	Progressive Disease, n
M2 (N = 9)	2	4	3
M3 (N = 3)	2	1	0
M4 (N = 0)	-	-	-
M5 (N = 9)	1	5	3
M6 (N = 5)	0	2	3

34/37 pts (92%) experienced  $\geq 1$  treatment-emergent adverse event (TEAE); Grade  $\geq 3$  TEAEs were observed in 21/37 pts (57%). The most frequently reported TEAEs included thrombocytopenia (43%; 27% Grade  $\geq 3$ ), diarrhea (43%; 19% Grade  $\geq 3$ ), fatigue (35%; 0% Grade  $\geq 3$ ), anemia (32%; 19% Grade  $\geq 3$ ), nausea (30%; 3% Grade  $\geq 3$ ), decreased appetite (27%; 0% Grade  $\geq 3$ ) and vomiting (24%, 3% Grade  $\geq 3$ ). 22/37 pts (60%) experienced TEAEs leading to dose modifications. 4/37 pts (11%) discontinued treatment due to TEAEs.

**Conclusions:** These preliminary data showed that heavily pretreated patients with multiple different tumor types may benefit from CPI-0209 treatment, encouraging further clinical investigations. The safety profile of CPI-0209 is consistent with the known mechanism of action and as expected in the underlying study population.

#### Conflict of interest:

Advisory Board: HK: Blueprint Genomics, Tempus, Deciphera  
LD: Genetech/Roche, Merck, Inovio Pharmaceuticals, CUE Biopharma, Regeneron

LG: Beigene, BMS, Xilio, Eisai, Mersana, Pliant, Tentaris

RS: Bristol Myers Squibb, Merck, Novartis, Pfizer

Board of Directors: LG: Bright Peak Therapeutics, Neximmune

Corporate-sponsored Research: RH: Abbisko, AbbVie, Actuate, Amgen, AstraZeneca, Bayer, Bristol-Myers Squibb, Boston Biomedical, Constellation, Genmab, GlaxoSmithKline, Infinity, InhibRx, Janssen, Merck, Mersana, Merx, Nektar, Novartis, Pfizer, Regeneron, Sanofi, Sutro, Takeda, Xencor

LD: Glaxo Smith Kline, Millenium, Bristol-Myers Squibb, Aeterna Zentaris, Novartis, Abbvie, Tesaro, Cerulean Pharma, Aduro Biotech, Advaxis, Syndax, Pfizer, Merck, Genetech/Roche, Morab, Morphotek, Ludwig Institute for Cancer Research, Leap Therapeutics

AG-S: Janssen, Teva

Other Substantive Relationships: RH: Consultant: Amgen, GlaxoSmithKline

LD: Data Safety Monitoring Committee for Inovio and Ellipse

LG: Honoraria: Tempus Stock ownership: Lilly

AG-S: Honoraria: Roche, BMS/Celgene, Janssen, Servier, Gilead/Kite, Takeda, Eusa Pharma, Novartis Consulting fees: Roche, BMS/Celgene, Kyowa Kirin, Clinigen, Eusa Pharma, Novartis, Gilead/Kite, Servier, Incyte, Lilly, Takeda, ADC Therapeutics America, Miltenyi Travel, accommodation, expenses: Gilead/Kite, Janssen, Roche, BMS/Celgene, Servier, Kern Pharma

LK: Employed by MorphoSys AG. Owns stock from MorphoSys AG

NH and NF: Employed by MorphoSys AG

90

(PB080)

#### The CNS-penetrant EGFR inhibitor, ERAS-801, shows promising nonclinical activity in a CNS metastases model of EGFR mutant NSCLC

J. Tsang<sup>1</sup>, E. Zhao<sup>1</sup>, R. Plawat<sup>1</sup>, T. Cloughesy<sup>1</sup>, D. Nathanson<sup>2</sup>. <sup>1</sup>UCLA, Molecular and Medical Pharmacology, Los Angeles, USA; <sup>2</sup>UCLA, Molecular and Medical Pharmacology, Los Angeles, USA

ERAS-801 is a highly CNS-penetrant small molecule ( $K_{p, brain, mouse} = 3.7$  and  $K_{p, uu, brain, mouse} = 1.2$ ) designed to reversibly inhibit EGFR alterations observed in GBM, including EGFR amplification and the EGFRvIII variant. It is currently being evaluated in recurrent GBM in the phase 1 clinical trial

THUNDERBOLT-1 (NCT05222802). ERAS-801 also shows in vitro activity against other EGFR alterations observed in NSCLC. Due to its high CNS penetration, an exploratory in vivo study was conducted to characterize ERAS-801's activity in a CNS metastases model of EGFR mutant NSCLC. Preliminary data suggest ERAS-801 shows superior nonclinical activity relative to osimertinib, which is the current standard of care treatment for patients with EGFR mutant NSCLC.

Secreted gaussia luciferase expressing PC9 cells, which were derived from EGFR exon 19 deletion NSCLC, were intracranially injected into female NSG mice and were randomized into the following treatment groups: vehicle, osimertinib at 10 and 25 mg/kg (mpk) and ERAS-801 at 10 and 25 mpk (n = 8 mice per group). 25 mpk was osimertinib's maximum tolerated dose. Dosing schedule was QD for 5 days followed by 2 days off. Relative light unit (RLU) intensity from tumor secreted gaussia luciferase was measured as a surrogate of intracranial tumor growth. RLU and body weight were measured 2x weekly until mice were taken down due to body weight loss, health observations, and/or study termination.

As of treatment day 91, ERAS-801 at both 10 and 25 mpk showed a 450% extension of survival relative to vehicle. Osimertinib at 10 and 25 mpk showed a 264% and >450% extension of survival relative to vehicle, respectively. The median survival for vehicle treatment was 16.5 days. Median survival for either ERAS-801 dose and osimertinib at 25 mpk has not been reached and the median survival for osimertinib at 10 mpk was 60 days. At either dose, ERAS-801 achieved significantly greater tumor growth inhibition than osimertinib at 25 mpk (p-value <0.05). Osimertinib at 10 and 25 mpk achieved a maximum tumor regression of 37% and 75% on treatment day 17, respectively. On this treatment day, ERAS-801 at 10 and 25 mpk achieved a significantly greater tumor regression of 89% and 94% relative to osimertinib at 25 mpk (p-values <0.05). At 25 mpk in a mouse PK study, ERAS-801 achieved an unbound brain peak concentration (C<sub>max</sub>) of 400 nM and osimertinib achieved 20 nM. In a 3-day cellular viability assay in the PC9 cell line, ERAS-801 had an IC<sub>50</sub> of 33 nM while osimertinib had an IC<sub>50</sub> of 31 nM.

ERAS-801 at 10 and 25 mpk achieved significantly greater tumor regressions than osimertinib in an intracranial EGFR mutant NSCLC PC9 CDX study. Exhibiting both potent activity against EGFR alterations and high CNS penetration, ERAS-801 shows promising nonclinical activity in cancers outside of GBM, such as CNS metastases of EGFR mutant NSCLC.

#### Conflict of interest:

Corporate-sponsored Research: This work was in part supported by corporate sponsored research funds.

Other Substantive Relationships: Inventor of IP related to this work.

91

(PB081)

#### A Ph-Ib study of TRK-950 combined with anti-cancer treatment regimens in patients with advanced solid tumors

D. Hanna<sup>1</sup>, P. Cassier<sup>2</sup>, A. Alistar<sup>3</sup>, S. Sharma<sup>4</sup>, M. Matrana<sup>5</sup>, B. George<sup>6</sup>, A.B. El-Khoueiry<sup>7</sup>, F. Okano<sup>8</sup>, D.D. Von Hoff<sup>9</sup>, J.Y. Blay<sup>10</sup>. <sup>1</sup>USC Norris Comprehensive Cancer Center, Medical Oncology, Los Angeles, CA, USA; <sup>2</sup>Center Leon Berard, Medical Oncology, Lyon, France; <sup>3</sup>Atlantic Health System/Morrisstown Medical Center, Medicine/Medical Oncology, Morrisstown, USA; <sup>4</sup>HonorHealth, Research Institute, Scottsdale, USA; <sup>5</sup>Ochsner Clinic Foundation, Ochsner Cancer Institute, New Orleans, USA; <sup>6</sup>Froedtert Hospital & Medical College of Wisconsin, Department of Medicine/Division of Hematology and Oncology, Milwaukee, USA; <sup>7</sup>USC Norris Comprehensive Cancer Center, Medicine/Medical Oncology, Los Angeles, USA; <sup>8</sup>Toray Industries Inc., New Frontiers Research Laboratories, Kamakura, Japan; <sup>9</sup>Translational Genomics Research Institute TGEN, Molecular Medicine Division, Phoenix, USA; <sup>10</sup>Center Leon Berard, Executive Management, Lyon, France

**Background:** TRK-950 is a first-in-class humanized antibody raised against CAPRIN-1 which we have identified as a novel and universal target for cancer therapies. TRK-950 strongly and specifically binds to various cancer cells and shows anti-tumor effects via engagement of immune cells. A series of pre-clinical studies demonstrates its potency and safety. In the phase I study of TRK-950 monotherapy (NCT02990481), it appears safe and well tolerated. No DLT was observed and MTD was not reached at doses of 3–30 mg/kg IV weekly. Here, we report on select cohorts of the ongoing, multicenter phase Ib study of TRK-950 combined with standard of care (SOC) regimens in patients (pts) with advanced cancers (NCT03872947).

**Materials and Methods:** Pts with colorectal cancer (CRC), cholangiocarcinoma (CCA), gastric/GEJ (GC) and ovarian cancer (OC) with measurable disease were enrolled in separate cohorts. Pts with CRC received FOLFIRI on D1, 15 of a 28-day cycle. Pts with CCA received Gemcitabine/Cisplatin on D1, 8 of a 21-day cycle. Pts with OC received Gemcitabine on D1, 8 and Carboplatin on D1 of a 21-day cycle. Pts with GC

received Paclitaxel on D1, 8, 15 and Ramucirumab on D1, 15 of a 28-day cycle. TRK-950 was given 10 mg/kg IV weekly in all cohorts. Each cohort consists of  $\geq 6$  pts and DLT was evaluated during the first cycle. Response was assessed every 2 cycles. Primary endpoint was safety and tolerability. Secondary endpoints incl. overall response rate (ORR), disease control rate (DCR) per RECIST v1.1. Tumor CAPRIN-1 expression was measured by IHC.

**Results:** A total of 75 pts have been enrolled and received at least 1 dose of TRK-950, incl. 44 pts with four representative solid tumors: 14 pts with CRC, 11 pts with CCA, 10 pts with OC, 9 pts with GC. Median age 60 yrs; Karnofsky performance status 70 (7%), 80 (23%), 90 (48%), 100 (23%); 52% male, 48% female. Most common all-grade treatment-related AEs (TRAEs) in  $\geq 10\%$  of all pts were fatigue (34%), nausea (27%), neutrophil count decreased (16%), diarrhea (11%), vomiting (11%) and white blood cell count decreased (11%). Most common grade  $\geq 3$  TRAE in  $\geq 10\%$  of pts was neutrophil count decreased (14%). In response evaluable pts, ORR was 21% in CRC, 27% in CCA, 33% in OC and 56% in GC. DCR was 57% in CRC, 82% in CCA, 78% in OC and 100% in GC.

**Conclusions:** TRK-950 binds to a newly described target, CAPRIN-1, and has an acceptable safety and tolerability profile when combined with SOC chemotherapy in multiple cancers. Preliminary clinical activity is demonstrated in pre-treated patients with encouraging response rates and high disease control rates, particularly in OC and GC. Further antitumor activity is being confirmed for cancer types for which such a notable response rate has been obtained.

#### Conflict of interest:

Other Substantive Relationships: Dr. Okano - Director of TORAY

## 92 (PB082)

### RP12146, a novel, selective, and potent small molecule inhibitor of PARP 1/2, synergizes with SOC therapy in preclinical models of solid tumors

S. Viswanadha<sup>1</sup>, S. Eleswarapu<sup>2</sup>, K. Karnam<sup>1</sup>, S. Vakkalanka<sup>3</sup>. <sup>1</sup>Incozen Therapeutics Pvt. Ltd., Biology, Hyderabad, India; <sup>2</sup>Incozen Therapeutics Pvt Ltd, Biology, Hyderabad, India; <sup>3</sup>Rhizen Pharmaceuticals AG, Management, Basel, Switzerland

**Background:** Poly (ADP-ribose) polymerase (PARP) activity involves synthesis of Poly-ADP ribose (PAR) polymers that recruit host DNA repair proteins leading to correction of DNA damage and maintenance of cell viability. Several PARP inhibitors have been approved for the treatment of BRCA-mutated ovarian, breast and pancreatic cancer. In addition to BRCA-mutated cancers, therapeutic role of PARP inhibitors as monotherapy agent or in combination with established therapy can be expanded to other types of solid tumors through 'synthetic lethality' mechanism. Herein, we describe the efficacy of RP12146 as a single agent and in combination with approved therapies in preclinical models of solid tumors.

**Material & Methods:** Enzymatic potency was evaluated using a PARP Chemiluminescent Activity Assay Kit (BPS biosciences). Cell growth was determined following incubation with RP12146 as a single agent or in combination with approved agents in various solid tumor cell lines. Apoptosis & Cell cycle was evaluated following incubation of cell lines with compound for 48 or 72 h, subsequent staining with Annexin-V-PE and 7-AAD or Propidium Iodide, and analysis by flow cytometry. Anti-tumor potential of RP12146 as a single agent or in combination with chemotherapeutic agents was tested in OVCAR-3 and NCI-H69 Xenografts. Expression of downstream markers were determined in cell lines and xenograft tumor samples by Western blotting.

**Results:** RP12146 inhibited PARP1 (0.6 nM) & PARP2 (0.5 nM) with equal potency with several fold selectivity over the other members of the PARP family. In addition, RP12146 demonstrated selective PARP1-Trapping with ~20-fold selectivity over PARP2. RP12146 caused a dose-dependent growth inhibition of both BRCA mutant and non-mutant cancer cell lines with  $GI_{50}$  in the range of 0.04  $\mu$ M to 9.6  $\mu$ M. Combination of RP12146 with Temozolomide, SN-38, Topotecan, and Lurbinectedin demonstrated either additive or synergistic effects manifested by an inhibition in growth, induction of apoptosis and cell cycle arrest in Breast, Gastric, Glioma, Lung Cancer, and Ovarian cancer cell lines. RP12146 exhibited anti-tumor potential with TGI of 28% and 21.8% as a single agent in OVCAR-3 and NCI-H69 Xenograft model respectively. In NCI-H69 xenograft model, RP12146 in combination with cisplatin exhibited TGI of 69.3%.

**Conclusion:** Data demonstrate the therapeutic potential of RP12146 as single agent and in combination in solid tumors. RP12146 is currently being evaluated in Phase 1 clinical trials in patients with locally advanced or metastatic solid tumors (NCT05002868).

No conflict of interest.

Poster Session (26 October 2022)

## 93 (PB083)

### Preclinical Profile of RP14042, a novel, selective, and potent small molecule inhibitor of PARP7

S. Viswanadha<sup>1</sup>, S. Eleswarapu<sup>1</sup>, K. Karnam<sup>1</sup>, S. Veeraraghavan<sup>2</sup>, A. Kota<sup>1</sup>, S. Vakkalanka<sup>3</sup>. <sup>1</sup>Incozen Therapeutics Pvt. Ltd., Biology, Hyderabad, India; <sup>2</sup>Incozen Therapeutics Pvt. Ltd., Pharmacokinetics, Hyderabad, India; <sup>3</sup>Rhizen Pharmaceuticals AG, Management, Basel, Switzerland

**Background:** Poly (ADP-ribose) polymerase (PARP)-7 is a member of PARP family and is classified as monoPARP as it catalyzes the transfer of single units of ADP-ribose (M<sup>A</sup>RYlation) onto its substrates to exert its physiological functions. It is involved in several cellular processes, including responses to hypoxia, innate immunity, and regulation of nuclear receptors. In addition, PARP7 is overexpressed/amplified in variety of cancers including Ovarian, Breast, Pancreatic ductal adenocarcinoma (PDAC), Non-small cell lung carcinoma (NSCLC) and Squamous cancers. PARP-7 acts as a negative regulator of nucleic acid sensing in tumor cells leading to suppression of Type I interferon (IFN) response. Preclinical studies have demonstrated that inhibition of PARP-7 restores Type I interferon (IFN) signaling leading to tumor cell growth inhibition and activation of the immune system, thereby contributing to tumor regression. Herein, we describe the preclinical profile of RP14042, a novel, selective, and potent small molecule inhibitor of PARP7.

**Material & Methods:** Enzymatic potency was evaluated using a PARP Chemiluminescent Activity Assay Kit (BPS biosciences). Cell growth was determined following incubation with RP14042 as a single agent in various solid tumor cell lines. Cell cycle was evaluated following incubation of cells with compound for 72 h, subsequent staining with Propidium Iodide, and analysis by flow cytometry. Expression of p-STAT1 and p-IRF3 were determined in NCI-H1373 cell line by Western blotting. Pharmacokinetic properties of the molecule were also evaluated.

**Results:** RP14042 inhibited PARP7 with an  $IC_{50}$  of 10.2 nM with selectivity over other members of the PARP family. Compound caused a dose-dependent growth inhibition of NCI-H1373, a PARP-7 overexpressing, cell line with an  $GI_{50}$  of 0.5  $\mu$ M without any effect on the growth in low PARP-7 expressing cell lines. Incubation of NCI-H1373 cells with RP14042 caused G<sub>0</sub>/G<sub>1</sub> cell cycle arrest. Inhibition of PARP7 by RP14042 in NCI-H1373 induced STAT1 and IRF3 phosphorylation suggesting restoration of Type I IFN signaling. Pharmacokinetic studies in rodents indicated high oral bioavailability with favorable plasma concentrations relevant for efficacy.

**Conclusion:** Data demonstrate the therapeutic potential of RP14042 in PARP7 overexpressing tumors

No conflict of interest.

## 94 (PB084)

### Novel inhibitors of the luminal lineage transcription factor peroxisome proliferator-activated receptor gamma (PPARG) durably eradicate tumors in urothelial cancer (UC) animal models

J. Mertz<sup>1</sup>, J. Stuckey<sup>1</sup>, J. Wilson<sup>1</sup>, W. Motley<sup>1</sup>, B. DeLaBarre<sup>1</sup>, J. Audia<sup>1</sup>, R. Sims III<sup>1</sup>. <sup>1</sup>Flare Therapeutics, Inc., Cambridge, USA

**Background:** Small molecule targeting of cell lineage-defining transcription factors is a demonstrated and effective therapeutic strategy in oncology, exemplified by estrogen receptor (ER) agents in luminal breast cancer. Two-thirds of advanced UC is classified as luminal and overexpression of PPARG is characteristic of this molecular subtype. Currently, there is a poor understanding of how recurrent missense mutations in PPARG and its obligate heterodimer retinoid X receptor alpha (RXRA) impact PPARG function; previous tool compounds designed to inhibit PPARG have minimal phenotypic activity in UC cell lines.

**Material and Methods:** The PPARG inhibitor FTX-6746 was evaluated in UC cell lines including UMUC9 (PPARG amplification) and HT1197 (RXRA-S427F hotspot mutation), which activate PPARG by different genetic mechanisms. *In vitro* analyses included clonogenic growth assays and assessment of target gene modulation after treatment. *In vivo* studies were performed in NCG or Balb/C nude mice with oral administration of FTX-6746 at doses indicated below.

**Results:** Our biochemical studies indicate that patient-derived missense mutations in PPARG and RXRA bias an active conformation of PPARG, mimicking an agonist-bound state. Addressing the limitations of previous tool compounds, we discovered novel inhibitors that drive a powerful repressive conformation of PPARG with high specificity (>100X selective over PPARG/PPARD). This results in robust PPARG target gene silencing in cells ( $IC_{50}$  = 5 nM), and *in vitro* growth inhibition preferentially observed in cell lines with activated PPARG signaling. Tumor growth inhibition or regression was observed in two xenograft models of UC at well-tolerated oral doses with no tumor regrowth upon cessation of treatment. Treatment of UMUC9 xenograft

Abstracts, 34th EORTC-NCI-AACR Symposium



tumors with 3, 10, 30 and 60 mg/kg twice daily of FTX-6746 resulted in up to 80% target gene suppression in tumor tissue at day 2 and up to >100% tumor growth inhibition at day 21. Similar efficacy was observed in HT1197 xenograft studies treated with 30 and 60 mg/kg twice daily of FTX-6746, with >45% target gene suppression at day 2 and 85–112% tumor growth inhibition at day 42.

Model	Dose (mg/kg)	Schedule	%Tumor Growth Inhibition	%Target Gene Suppression (D2)
UMUC9	3	BID*20	59	16
UMUC9	10	BID*20	70	ND
UMUC9	30	BID*20	83	73
UMUC9	30	BID*21	105	80
UMUC9	60	BID*21	108	ND
HT1197	30	BID*42	85	46
HT1197	60	BID*42	112	59

**Conclusions:** These collective results suggest that PPARG is a lineage-defining transcription factor in UC and small molecule PPARG inhibition will be an effective therapy for patients with advanced urothelial cancer harboring the luminal subtype.

**Conflict of interest:**

Ownership: All authors are shareholders in Flare Therapeutics.

95 (PB085)

**Preliminary results from FLAGSHIP-1: A Phase I dose escalation study of ERAS-601, a potent SHP2 inhibitor, in patients with previously treated advanced or metastatic solid tumors**

M. McKean<sup>1</sup>, M. Barve<sup>2</sup>, D. Hong<sup>3</sup>, A. Parikh<sup>4</sup>, E. Rosen<sup>5</sup>, J. Yang<sup>6</sup>, R. Picard<sup>6</sup>, J. Yi<sup>6</sup>, L. Brail<sup>6</sup>, D. Vecchio<sup>6</sup>, T. Meniawy<sup>7</sup>, T. John<sup>8</sup>, J. Wang<sup>9</sup>.  
<sup>1</sup>Sarah Cannon Research Institute, Drug Development Unit, Nashville, USA; <sup>2</sup>Mary Crowley Cancer Research, Research Oncology, Dallas, USA; <sup>3</sup>MD Anderson, Investigational Cancer Therapeutics ICT, Houston, USA; <sup>4</sup>Massachusetts General Hospital, Massachusetts General Hospital, Boston, USA; <sup>5</sup>Memorial Sloan Kettering Cancer Center, Medicine, New York, USA; <sup>6</sup>Erasca Inc., Erasca Inc., San Diego, USA; <sup>7</sup>Linear Clinical Research and University of Western Australia, Medical Oncology, Nedlands, Australia; <sup>8</sup>Peter MacCallum Cancer Centre, Medical Oncology, Melbourne, Australia; <sup>9</sup>Florida Cancers Specialists/Sarah Cannon Research Institute, Drug Development Unit, Sarasota, Sarasota, USA

**Background:** SHP2 is an oncogenic tyrosine phosphatase that transduces receptor tyrosine kinase signaling to the RAS/MAPK pathway via its phosphatase-mediated regulation of guanine nucleotide exchange factors. ERAS-601 is a potent, selective, and orally bioavailable allosteric inhibitor of SHP2 that has demonstrated robust anti-proliferative activity in vitro and in vivo as monotherapy and in combination in preclinical models of cancer harboring EGFR, KRAS, BRAF class III and NF1<sup>LOF</sup> mutations.

**Method:** FLAGSHIP-1 is the first-in-human, open-label, multicenter clinical study of ERAS-601 administered as monotherapy and in combination with cetuximab in patients with advanced or metastatic solid tumors. The primary objective of this study is to characterize the safety profile, determine the maximum tolerated dose (MTD)/recommended dose (RD), and characterize the pharmacokinetics (PK) profile of ERAS-601 as a monotherapy and in combination with cetuximab. Secondary objectives include tolerability and antitumor activity in solid tumors. Here we present results from monotherapy dose escalation cohorts in which patients received ERAS-601 continuously once a day (QD) or twice a day (BID) on a 28-day cycle.

**Results:** As of April 4, 2022, a total of 27 patients with previously treated advanced or metastatic solid tumors received ERAS-601 monotherapy on a 28-day cycle: 20–80 mg QD (n = 15); or 20–40 mg BID (n = 12). Monotherapy MTD was determined to be 40 mg QD and 40 mg BID. Dose-limiting toxicities (DLTs) occurred at 60 mg QD (two Grade 3 AST increase) and at 80 mg QD (one Grade 3 hypertension and one Grade 3 thrombocytopenia ≥5 days) dose levels. No DLTs were observed with the BID schedule. Treatment related adverse events (TRAEs) occurring in ≥20% of patients included thrombocytopenia and diarrhea (33.3%), AST and ALT increase (29.6%), and peripheral edema (25.9%). TRAEs were mostly Grade 1 and 2. Grade ≥3 TRAEs occurring in ≥10% of patients included AST increase (14.8%), thrombocytopenia (14.8%), and neutropenia (11.1%). A confirmed partial response was observed in a patient with a BRAF class III mutation. ERAS-601 exhibits rapid absorption, with C<sub>max</sub> generally achieved within 4 hours post dose. The PK exposure increased in a dose-

dependent manner over the dose range evaluated. Estimated half-life was approximately 15–22 hours, consistent with steady-state PK accumulation.

**Conclusions:** ERAS-601 shows promising preliminary safety and tolerability with reversible TRAEs that are manageable and consistent with the known mechanism of action for the SHP2 inhibitor class. Observed PK properties and AE profile support continued development in combination with other anti-cancer therapies, which continue to be investigated alongside additional intermittent dosing schedules.

**Conflict of interest:**

Ownership: Jennifer Yang, Roxana Picard, Jing Yi, Les Brail, Daniela Vecchio

Corporate-sponsored Research: Meredith McKean, Minal Barve, David Hong, Apama Parikh, Ezra Rosen, Tarek Meniawy, Thomas John, Judy Wang

96 (PB086)

**NP-G2-044, a First-in-Class Fascin Inhibitor, Inhibits Growth and Metastasis of Gynecologic Cancers**

V. Chung<sup>1</sup>, F. Tsai<sup>2</sup>, W. Chen<sup>3</sup>, D.D. Von Hoff<sup>2</sup>, E.G. Garmey<sup>4</sup>, J.J. Zhang<sup>4</sup>, X.Y. Huang<sup>4</sup>. <sup>1</sup>City of Hope, Medical Oncology, Duarte, USA; <sup>2</sup>Honor Health Research Institute, Medical Oncology, Scottsdale, AZ, USA; <sup>3</sup>Weill Cornell Medical College of Cornell University, Department of Physiology and Biophysics, New York, NY, USA; <sup>4</sup>Novita Pharmaceuticals, Inc., Medicine, New York, NY, USA

**Background:** Fascin is the primary actin cross-linker in filopodia, membrane protrusions that form upon remodeling of the cytoskeleton beneath the plasma membrane. Its role is critical in tumor cell migration, invasion and metastasis. Studies of human cancer demonstrate that high fascin levels correlate with lymph node and distant metastases, clinically aggressive phenotypes, poor prognosis and decreased survival. Deletion of the fascin gene delays onset of cancer development, slows tumor growth, reduces metastatic colonization and increases overall survival in cancer mouse models. NP-G2-044 is a novel, first in class, orally administered small molecule fascin inhibitor. In a completed phase 1 clinical trial, the drug appeared safe and well tolerated when dosed for 4 weeks on followed by 2 weeks off.

**Material and Methods:** This ongoing, multi-center phase 2A clinical trial is designed to determine the recommended phase 2 dose (RP2D) of continuously dosed NP-G2-044 as monotherapy and in combination therapy with anti-PD1 checkpoint inhibitors. Following the determination of RP2D, expansion cohorts will enroll additional patients to further evaluate efficacy, with a focus on gynecologic cancer patients for the monotherapy arm.

**Results:** Pre-clinical models demonstrate growth inhibition in gynecologic cancers and EGFR-high triple-negative breast cancers with a mechanism of action distinct from fascin-mediated inhibition of filopodial formation. Synergy was seen with both anti-PD-(L)1 immune checkpoint inhibitors and spindle assembly checkpoint inhibitors. The 2100 mg dosing cohort appears safe and well tolerated with mainly grade 1–2 gastrointestinal toxicities observed. Preliminary efficacy signals were observed in the completed phase 1 study and phase 2A studies for gynecologic cancer patients are ongoing.

**Conclusion:** Fascin represents a novel target for cancer therapy. NP-G2-044 acts simultaneously on tumor cells to block tumor metastasis and on intra-tumoral dendritic cells to reinvigorate anti-tumor immune response. These dual mechanisms of action may be ideally suited for long-term and well-tolerated maintenance therapy.

**Conflict of interest:**

Ownership: J. Jillian Zhang, Xin-Yun Huang

Advisory Board: Daniel D. Von Hoff

Other Substantive Relationships: Edward G. Garmey

97 (PB087)

**The ULK1 inhibitor ENV-201 impairs tumor growth in KRAS-driven flank xenografts as a single agent and in combination with the KRAS inhibitor adagrasib**

J. Pitman<sup>1</sup>, L. Dellamary<sup>1</sup>, S. Kc<sup>1</sup>, M. de los Rios<sup>1</sup>, J. Hood<sup>1</sup>. <sup>1</sup>Endeavor BioMedicines, Research & Development, San Diego, USA

**Background:** Lung cancer is the leading cancer cause of death in the US, and non-small cell lung cancers (NSCLCs) account for 85% of those cases. Among NSCLCs, mutations resulting in ectopic activation of the RAS signal transduction pathway account for at least a quarter of cases, and the activating KRAS<sup>G12C</sup> mutation is found in 11% of all NSCLC patient samples. When treated with RAS pathway-inhibiting therapeutics, KRAS-driven

tumors have been shown to become dependent on autophagy for continued survival. Simultaneous targeting of both the RAS pathway and autophagy therefore presents an opportunity to block multiple mechanisms of tumor growth and survival.

**Materials and methods:** We have demonstrated the added benefit of KRAS inhibition and autophagy inhibition in an animal model, using the NCI-H2122 cell line (homozygous for the activating KRAS<sup>G12C</sup> mutation) as flank xenografts in NOD/SCID mice. ENV-201 is a selective and potent antagonist of the autophagy-initiating kinase, ULK1, one which also inhibits the related ULK2. Mice were treated via daily oral dosing of (1) vehicle, (2) ENV-201 (20 mg/kg), (3) the KRAS<sup>G12C</sup>-specific inhibitor adagrasib (Mirati Therapeutics, 25 mg/kg), or (4) combination of both ENV-201 and adagrasib at the same doses. Treatment lasted 30 days, body weight was monitored daily, and tumor size was measured three times a week. All animal work was carried out at and met necessary approvals at Crown Bioscience.

**Results:** Both ENV-201 and adagrasib treatments resulted in significant tumor growth inhibition when either drug was used as a single agent (32% or 55% TGI, respectively). Significant additive tumor growth inhibition (78%) was also observed when animals were treated with both drugs in combination.

**Conclusions:** ENV-201-mediated ULK1 inhibition thus shows promise as both a single agent or in combination with a growth factor/RAS/MAPK pathway-targeting cancer treatment.

**Conflict of interest:**

Corporate-sponsored Research: All authors are employees of Endeavor BioMedicines.

**98** (PB088)

**Discovery and validation of biomarkers to support clinical development of NXP800: A first-in-class orally active, small-molecule HSF1 pathway inhibitor**

P. Workman<sup>1</sup>, P.A. Clarke<sup>2</sup>, R. Te Poole<sup>2</sup>, M. Powers<sup>2</sup>, G. Box<sup>2</sup>, E. De Billy<sup>2</sup>, A. De Haven Brandon<sup>2</sup>, A. Hallsworth<sup>2</sup>, A. Hayes<sup>2</sup>, H. McCann<sup>2</sup>, S. Sharp<sup>2</sup>, M. Valenti<sup>2</sup>, F.I. Raynaud<sup>2</sup>, S.A. Eccles<sup>2</sup>, M. Cheeseman<sup>2</sup>, K. Jones<sup>2</sup>. <sup>1</sup>The Institute of Cancer Research, UK Centre for Cancer Therapeutics, Sutton, United Kingdom; <sup>2</sup>The Institute of Cancer Research, CRUK Cancer Therapeutics Unit, London, United Kingdom

**Background:** Heat Shock Factor (HSF1) is a stress-inducible transcription factor that plays a key role in the activation of the eukaryotic heat shock response. HSF1 is hijacked by cancer cells to activate a set of genes that overlap with, but are not identical to, the classical heat shock response. Whereas the HSF1 pathway has been shown to play a key role in oncogenesis and multiple hallmark features of malignancy in experimental cancers, and its amplification/expression/activity correlates with poor clinical outcome, knockout of HSF1 does not impair viability in model organisms – suggesting a potential therapeutic window. Drug discovery has been limited as HSF1 is difficult to drug directly. Therefore, we sought to discover inhibitors of the HSF1 pathway using a phenotypic screening approach, from which we discovered the bisamide clinical development candidate NXP800. Here we describe the discovery and validation of biomarkers to support the clinical development of NXP800, forming a Pharmacological Audit Trail.

**Material and methods:** We searched for biomarkers that correlated with sensitivity in human tumour xenografts and human cancer cell line panels and used isogenic models to validate the key predictive biomarker. To identify pharmacodynamic markers we used a combination of gene expression and protein profiling, combining both screening and hypothesis-driven approaches.

**Results:** NXP800 (CCT361814) has good PK properties in mice, including oral bioavailability. Moreover, NXP800 exhibits impressive therapeutic activity in xenografts of human ovarian clear cell ovarian cancer (OCCC) and endometrioid ovarian cancer – two serious conditions of high unmet medical need with limited treatment options – including sustained tumour growth inhibition and regression at well-tolerated doses. The efficacy and tolerability data indicate a clear therapeutic window. We identified genetic loss of *ARID1A*, a component of the SWI/SNF chromatin remodelling complex, as predictive of greater therapeutic responsiveness. This correlation was confirmed in isogenic models. We have also observed promising therapeutic potential in additional cell lines including, gastric and small cell lung cancer, as well as haematological cancer. Gene expression profiling showed that NXP800 caused activation of the integrated stress response and inhibition of the heat shock response pathways. As PD biomarkers, we selected and validated CHAC1, ATF3, ATF4 and HSP27. We are currently investigating links between CHAC1, glutathione depletion and ferroptosis.

**Conclusions:** A Phase 1 trial (NCT05226507) of NXP800 is underway, incorporating the validated predictive, PK and PD biomarkers that constitute a Pharmacological Audit Trail. Future expansion cohorts will include patients

with *ARID1A* mutation, including ovarian clear cell carcinoma and ovarian endometrioid carcinoma.

**Conflict of interest:**

Ownership: Alterome Therapeutics, Black Diamond Therapeutics, Chroma Therapeutics, NextechInvest, Nuvectis Pharma, Storm Therapeutics Advisory Board: Alterome Therapeutics, Astex Pharmaceuticals, Black Diamond Therapeutics, CV6 Therapeutics, NextechInvest, Nuvectis Pharma, Storm Therapeutics, Vividion Therapeutics Board of Directors: Storm Therapeutics Corporate-sponsored Research: Astex Pharmaceuticals, AstraZeneca, BACIT, Cyclacel Pharmaceuticals, Merck KGaA, Nuvectis Pharma, Sixth Element Other Substantive Relationships: Chemical Probes Portal (non profit, Paul Workman, Executive Director)

**99** (PB089)

**Discovery of an allosteric small molecule inhibitor that can potently target SHP2 in vitro and in vivo**

M. Kim<sup>1</sup>, D. Park<sup>1</sup>, D. Kim<sup>1</sup>, M. Lee<sup>2</sup>, D. Jeon<sup>2</sup>, S. Jang<sup>2</sup>, J. Kim<sup>2</sup>, E. Kim<sup>2</sup>, K.J. Yoon<sup>1</sup>, S.K. Lim<sup>1</sup>, K. Lee<sup>2</sup>, S. Choi<sup>1</sup>. <sup>1</sup>Kanaph Therapeutics, Research, Seoul, South Korea; <sup>2</sup>Yungjin Pharm, Research, Suwon, South Korea

**Background:** SHP2 (Src homology region 2-containing protein tyrosine phosphatase 2) is the only known tumor-promoting phosphatase, that relays the signals from the diverse receptor tyrosine kinases to the RAS/MAPK pathway. Abnormal SHP2 activation and activating mutations are frequently observed in various cancers and accordingly genetic or pharmacological inhibition of SHP2 has been reported to suppress RTK/KRAS-mediated cancer progression. Moreover, SHP2 serves as a key component of the ERK re-activation in the resistance mechanism to KRAS pathway inhibitors. Therefore, SHP2 inhibitor has a great therapeutic potential in treating RTK/RAS-mediated cancer as monotherapy and in combination treatment.

**Material and methods:** Biochemical phosphatase assays were performed by detecting DiFMU which is converted by SHP2(WT or mutants) with various concentrations of compounds. For the cellular pERK analysis, compounds were treated into H358 cells followed by pERK measurement using the AlphaLISA system (PerkinElmer). Cell viability was measured by CellTiter-Glo (Promega) after 3-day treatment with compounds. For the in vivo tumor model, cancer cells were inoculated into the flank region of BALB/c nude mice. Once the tumor size reached 100 mm<sup>3</sup>, compounds were administered (P.O., Q.D). Tumor size was measured twice a week.

**Results:** Cpd1, an orally available and highly potent SHP2 inhibitor, profoundly suppressed SHP2 activity in vitro and KRAS-mutated tumor growth in mouse xenograft models, outcompeting the positive control TNO-155. In detail, Cpd1 potently inhibited SHP2(WT) and also the highly-active oncogenic SHP2 mutants. It impeded the proliferation of cancer cells encoding KRAS and/or SHP2 mutations. With an excellent PK profile, Cpd1 induced in vivo tumor regression in KRAS mutation-driven models.

**Conclusions:** Cpd1 is a potent and selective SHP2 allosteric inhibitor, with a great anti-tumor effect in vitro and in vivo. It may provide a novel therapeutic option for diverse cancers, including KRAS-driven tumors, as a monotherapy or in combination therapies.

**No conflict of interest.**

**100** (PB090)

**Synergy of the novel dual TTK/PLK1 mitotic checkpoint inhibitor (MCI) BAL0891 with paclitaxel and carboplatin in mouse models of human cancer**

P. Mcsheehy<sup>1</sup>, N. Forster-Gross<sup>2</sup>, K. Litherland<sup>3</sup>, L. Kellenberger<sup>4</sup>, H. Lane<sup>2</sup>. <sup>1</sup>Basilea Pharmaceutica International Ltd, Cancer Biology, Basel, Switzerland; <sup>2</sup>Basilea Pharmaceutica International, Cancer Biology, Basel, Switzerland; <sup>3</sup>Basilea Pharmaceutica International, DMPK & Clinical Pharmacology, Basel, Switzerland; <sup>4</sup>Basilea Pharmaceutica International, Research, Basel, Switzerland

**Background:** BAL0891 is a first-in-class dual inhibitor of threonine tyrosine kinase (TTK) and polo-like kinase 1 (PLK1). Both kinases collaborate in activating the spindle assembly checkpoint (SAC) to regulate chromosome alignment and segregation before the cell can exit mitosis. In vitro treatment of tumor cells with BAL0891 leads to rapid SAC disruption and accumulation of cells with aberrant chromosome numbers. The resultant genetic instability suggests a potential for combination effects with approved cytotoxic therapies, such as paclitaxel and carboplatin.

**Materials and Methods:** The patient-derived TNBC xenograft (PDX) model, BR1282, and the ovarian cell-derived (CDX) SKOV-3 model were

grown s.c. in female Balb/c mice. Mice were treated with BAL0891 (7 or 8 mg/kg, i.v., 2qw or qw) alone or combined with paclitaxel (15 mg/kg, i.v., qw) or carboplatin (60 mg/kg, i.v., qw) with BAL0891 administered 1, 2, 4 or 24 hr before or after the cytotoxic (8 mice per group). Mice were culled when tumors exceeded 1500 mm<sup>3</sup>, otherwise treatments continued for 5–6 weeks. Experiments were followed up to 14 weeks to confirm regressions. Implantation sites indicating complete tumor regression were ablated, embedded and assessed for remaining tumor cells by H&E staining. Efficacy was summarized as the endpoint  $\Delta T/C$  and statistical significance used one-way ANOVA at the initiation of culling or based on exponential fits of the tumor growth curves. The combination interaction was assessed using the Clarke-Combination-Index.

**Results:** In the BR1282 model, both BAL0891 and paclitaxel monotherapies significantly inhibited tumor growth:  $\Delta T/C$ s of 24–55% (two independent experiments). Combination of paclitaxel with BAL0891 at MTD-2qw or sub-MTD-qw caused prolonged tumor regressions, independent of the order or timing of drug administration. Regressions began 1–2 weeks post treatment-initiation and led to complete eradication of tumors in 38–88% of cases. In this model, carboplatin monotherapy was without activity and BAL0891 combined with carboplatin showed an additive effect only when carboplatin was administered first. However, in the SKOV-3 model, BAL0891 and carboplatin showed moderate activity as monotherapies ( $\Delta T/C$ s of 64–72%) but were synergistic in combination ( $\Delta T/C$ s of 20–32%). The most effective schedules of a 1 or 4 hr interval between dosing carboplatin and BAL0891 showed 13% complete regression. In all cases the combinations were as well tolerated as the monotherapies.

**Conclusions:** BAL0891 combined with paclitaxel *in vivo* showed strong reproducible synergy in the TNBC BR1282 model, with a high percentage of complete cures. Synergistic anti-tumor effects were also observed with carboplatin in the ovarian SKOV-3 model. Strong BAL0891 single agent activity was previously reported; the current data support BAL0891 combination strategies in the clinic.

**No conflict of interest.**

101

(PB091)

**Phase 1b results from OP-1250-001, a dose escalation and dose expansion study of OP-1250, an oral CERAN, in subjects with advanced and/or metastatic estrogen receptor (ER)-positive, HER2-negative breast cancer (NCT04505826)**

E. Hamilton<sup>1</sup>, J. Meisel<sup>2</sup>, C. Alemany<sup>3</sup>, B. Virginia<sup>4</sup>, N. Lin<sup>5</sup>, R. Wesolowski<sup>6</sup>, G. Mathauda-Sahota<sup>7</sup>, D. Makower<sup>8</sup>, J. Lawrence<sup>7</sup>, D. Faltaos<sup>7</sup>, Z. Mitri<sup>9</sup>, D. Sabanathan<sup>10</sup>, D. Clark<sup>11</sup>, T. Pluard<sup>12</sup>, R. Hui<sup>13</sup>, N. McCarthy<sup>14</sup>, M. Patel<sup>15</sup>. <sup>1</sup>Sarah Cannon Research Institute at Tennessee Oncology, Oncology, Nashville, USA; <sup>2</sup>Winship Cancer Institute at Emory University, Oncology, Atlanta, USA; <sup>3</sup>AdventHealth Cancer Institute, Oncology, Orlando, USA; <sup>4</sup>University of Colorado Cancer Center, Oncology, Denver, USA; <sup>5</sup>Dana Farber Cancer Institute, Oncology, Boston, USA; <sup>6</sup>The Ohio State University Comprehensive Cancer Center, Oncology, Columbus, USA; <sup>7</sup>Olema Oncology, Oncology, San Francisco, USA; <sup>8</sup>Albert Einstein College of Medicine, Oncology, New York, USA; <sup>9</sup>Knight Cancer Institute- Oregon Health and Science University, Oncology, Portland, USA; <sup>10</sup>MQ Health Cancer Services at Macquarie University Health Sciences Centre, Oncology, Sydney, Australia; <sup>11</sup>Icon Cancer Center- Cancer Research SA, Oncology, Adelaide, Australia; <sup>12</sup>Saint Luke's Cancer Institute Director- Koontz Center for Advanced Breast Cancer, Oncology, Kansas City, USA; <sup>13</sup>Westmead Hospital, Oncology, Westmead, Australia; <sup>14</sup>Icon Cancer Center- Wesley Medical Centre, Oncology, Auchenflower, Australia; <sup>15</sup>Florida Cancer Specialists and Research Institute, Oncology, Sarasota, USA

**Background:** OP-1250 is a small molecule oral complete estrogen receptor antagonist (CERAN) that binds the ligand binding domain of the ER and completely blocks ER driven transcriptional activity. OP-1250 potently inactivates both wild-type ER and mutant forms of ER that confer ligand independent activity and resistance to standard of care endocrine therapies. OP-1250 inhibits estrogen-driven breast cancer cell growth and induces degradation of the ER. In preclinical models, OP-1250 is active in the presence of wild-type ER, mutant ER (ESR1 activating mutations), and brain metastasis. OP-1250 is being developed for ER+, HER2- metastatic breast cancer (MBC) patients (pts). We previously reported Phase 1a (dose escalation) results, here we present data from the Phase 1b expansion portion of the clinical trial.

**Methods:** Following Phase 1a dose escalation of OP-1250 from 30 mg to 300 mg QD, a recommended phase 2 dose (RP2D) range was defined of 60 to 120 mg QD. Sixty pts are planned for Phase 1b enrollment, with 30 pts at each dose level (60 and 120 mg). In Phase 1b eligibility included measurable disease, 1–4 prior lines of hormonal therapy, and £1 prior line of

chemotherapy in the advanced setting. Pts were monitored for adverse events (AE) and tumor assessments (RECIST 1.1) were conducted every two 28-day cycles.

**Results:** As of May 13, 2022, 37 patients were assigned to either 60 mg or 120 mg dose levels. Pts were heavily pretreated: 62% had received 2 or more prior endocrine therapies in the advanced setting, 32% received chemotherapy, and 97% had received a prior CDK 4/6 inhibitor. More than half (57%) of pts who had ctDNA evaluated had an *ESR1* mutation. At 60 mg and 120 mg, OP-1250 demonstrated high oral bioavailability and dose proportional exposure. The most common treatment emergent adverse events reported ( $\geq 10\%$ ) in Phase 1b in the 60 mg/120 mg cohorts were nausea (28%/21%), vomiting (17%/16%), fatigue (17%/5%) and headache (11%/11%). Adverse events were Grade 1/2, with the exception of two Grade 3 events at 60 mg (diarrhea and anemia); no Grade 3 events occurred at 120 mg. There were no dose reductions or discontinuations due to an AE. Across Phase 1b, among pts eligible for at least one post-baseline scan (n = 24), 1 confirmed PR (cPR) was observed at 60 mg and 1 uPR was observed at 120 mg. Data continues to mature and updated data will be presented.

**Conclusions:** OP-1250 was well tolerated and showed promising safety and efficacy in Phase 1b pts treated at 60 mg and 120 mg daily. Based on safety and pharmacokinetic data, a RP2D will be selected. A Phase 2 evaluation will be initiated, and a Phase 3 monotherapy study is planned for 2023.

**Conflict of interest:**

Corporate-sponsored Research: Erika Hamilton: Abbvie, Acerta Pharma, Accutar Biotechnology, ADC Therapeutics, AKESOBIO Australia, Amgen, Aravive, ArQule, Artios, Arvinas, AstraZeneca, AtlasMedx, Black Diamond, Bliss BioPharmaceuticals, Boehringer Ingelheim, Cascadian Therapeutics, Clovis, Compugen, Cullen-Florentine, Curis, CytomX, Daiichi Sankyo, Dana Farber Cancer Inst, Dantari, Deciphera, Duality Biologics, EFFECTOR Therapeutics, Ellipses Pharma, Elucida Oncology, EMD Serono, Fochon, FujiFilm, G1 Therapeutics, H3 Biomedicine, Harpoon, Hutchinson MediPharma, Immunogen, Immunomedics, Incyte, Infinity Pharmaceuticals, InvestisBio, Jacobio, Karyopharm, Leap Therapeutics, Lilly, Lycera, Mabspace Biosciences, MacroGenics, MedImmune, Merck, Mersana, Merus, Millennium, Molecular Templates, Myraid Genetic Laboratories, Novartis, Nucana, Olema, OncoMed, Onconova Therapeutics, ORIC Pharmaceuticals, Orinove, Pfizer, Pharma Mar, Pieris Pharmaceuticals Pionyr, Immunotherapeutics, Plexikon, Radius Health, Regeneron, Relay Therapeutics, Repertoire, Immune Medicine, Rgenix, Roche/Genentech, SeaGen, Sermonix Pharmaceuticals, Shattuck Labs, Silverback, StemCentRx, Sutro, Syndax, Syros, Taiho, TapImmune, Tesaro, Tolmar, Torque Therapeutics, Treadwell Therapeutics, Verastem, Vincerx Pharma, Zenith Epigenetics, Zymework

Other Substantive Relationships: Erika Hamilton: Consulting Advisory Role (all to institution only): Arcus, Arvinas, AstraZeneca, Black Diamond, Boehringer Ingelheim, CytomX, Daiichi Sankyo, Dantari, Deciphera Pharmaceuticals, Eisai, Greenwich LifeSciences, H3 Biomedicine iTeosJanssen, Lilly, Loxo, Merck, Mersana, Novartis, Orum Therapeutics, Pfizer, Propella Therapeutics, Puma Biotechnology, Relay Therapeutics, Roche/Genentech, SeaGen, Silverback Therapeutics

102

(PB092)

**First-in-class heterobifunctional proteomimetic polymer capable of direct inhibition of Myc and target it for degradation**

M. Wang<sup>1</sup>, M. Trucia<sup>2</sup>, B. Gattis<sup>1</sup>, S. Abdulkadir<sup>2</sup>, N. Gianneschi<sup>1</sup>. <sup>1</sup>Northwestern University, Chemistry, Evanston, USA; <sup>2</sup>Northwestern University, Urology, Chicago, USA

**Background:** The proto-oncogene Myc is known to play critical roles in tumorigenesis and therapeutic resistance, being dysregulated in up to 70% of all human cancers. Heterodimerization with its binding partner Max is required for oncogenic transformation, yet the development of small molecule inhibitors has been hampered due to the lack of suitable binding pockets. Myc inhibitory peptides derived from the first helix (H1) of the bHLH-LZ region have been developed in efforts to address this limitation. However, poor pharmacokinetic profiles have precluded clinical translation of these approaches. Here, we use a novel platform technology referred to as the Protein-Like Polymer (PLP) for the development of more potent Myc inhibitors.

**Material and Methods:** PLPs were generated using ring-opening metathesis polymerization (ROMP) wherein peptides occupy every side chain, resulting in structures highly resistant to proteolysis. Characterization was done using HPLC, LC-MS, NMR, and GPC. Toxicity screening was performed in both neoplastic and benign cell lines. Taking advantage of the ability for the platform to multiplex different payloads in a sequence-controlled manner, heterofunctional PLPs were designed by incorporating secondary sequences imbuing desirable functionalities. Two specific

sequences were explored: a M1 nuclear localization sequence (NLS) and a degron sequence (RRRG) to engage endogenous cellular machinery for targeted protein degradation. Fluorescently labeled PLPs were used to quantify cellular uptake by confocal microscopy and FACS. Biophysical analysis was performed to confirm target engagement and protein degradation.

**Results:** A library of PLPs with narrow polydispersity and predetermined degrees of polymerization were generated. Cell assays revealed formulation-dependent antiproliferative effects with submicromolar IC50 values in a Myc-dependent manner. High levels of uptake were observed across formulations, with NLS and degron containing PLPs showing slightly elevated levels of nuclear accumulation. A EBox (Myc transcription binding site) luciferase reporter assay showed decreased luciferase signal only in Myc-targeted PLP treatments, suggesting Myc-specific effects. Western blotting showed minor reductions in Myc protein levels in H1-PLP and H1-NLS-PLP treatment groups, but significant decreases in protein level in H1-degron-PLPs. RNAseq showing selective overexpression of Myc pathway genes. Mice bearing transplanted Myc-CaP tumors showed delayed tumor growth following treatment with Myc-degrading PLPs with tumor analysis ongoing.

**Conclusion:** We present a novel peptide delivery platform that addresses the challenges inherent to peptide delivery approaches. The presented work demonstrates the feasibility of this platform in delivering Myc inhibitory peptides and provides rationale for further in vivo studies in Myc-dependent tumor models.

**No conflict of interest.**

### 103 (PB093)

#### Advances in the development of a targeted N-Terminal Domain androgen receptor (AR) degrader (ANITAC) for the treatment of prostate cancer

N.H. Hong<sup>1</sup>, B. Biannic<sup>1</sup>, P. Virsik<sup>1</sup>, H.J. Zhou<sup>1</sup>, R. Le Moigne<sup>1</sup>. <sup>1</sup>ESSA Pharma, South San Francisco Office, South San Francisco, USA

**Background:** Androgen receptor (AR) signaling is a main driver of prostate cancer progression and remains a crucial target for therapeutic intervention even in late stages of the disease. While current antiandrogen therapies that directly or indirectly target the AR ligand binding domain (LBD) are initially effective, resistance ultimately develops and new methods of inhibiting the AR pathway are needed. Recent advances in targeted protein degradation using the PROteolysis TArgeting Chimera (PROTAC) technology demonstrate that AR-LBD targeted PROTACs can selectively degrade AR but not splice variant forms of AR that are found in advanced castration-resistant prostate cancer (CRPC) patients. We recently demonstrated that targeting the N-terminal domain (NTD) of the AR by anitens (small molecule inhibitors) represents a novel method of blocking AR signaling that can bypass LBD-related drug resistance mechanisms. By developing an aniten-based bifunctional degrader (ANITAC™ for ANITen bAsed Chimera), our goal is to eliminate any forms of AR proteins found in CRPC patients including LBD mutants and LBD truncated variants that can potentially drive disease progression.

**Material and Methods:** Selective AR degradation was monitored by various in vitro assays. AR transcriptional activity and selectivity was assessed in cellular models expressing different forms of AR using reporter and cell viability assays. NanoString was used to qualitatively demonstrate ANITAC activity on AR signaling. In vivo efficacy was assessed using mouse xenograft models of prostate cancer.

**Results:** Herein we report the first series of AR degraders, ANITACs, which target the NTD of AR. ANITACs degrade AR in all cell lines tested through an E3 ligase dependent mechanism with an observed 50% degradation concentration (DC<sub>50</sub>) in the low nanomolar range measured using HiBiT assays. ANITACs degrade clinically relevant AR mutants and splice variants and show robust inhibition of AR transcriptional activity in multiple cell lines expressing different forms of AR including AR full length (AR-FL), AR-V7, and AR-V567es. In addition, AR degradation mediated by ANITACs effectively suppresses AR-regulated gene expression in both LNCaP and LNCaP95 cells and decreases prostate cancer cell viability. Moreover, ANITACs induce degradation of AR-FL and AR-V7 in vivo and induce tumor regression in castrated mice bearing VCaP tumor xenografts. In vitro ADME (Absorption, Distribution, Metabolism, and Excretion) studies show the compounds can be metabolically stable and exhibit favorable ADME properties needed for oral dosing.

**Conclusion:** ANITAC molecules are the first bifunctional degraders targeting the AR NTD that can be orally bioavailable and active against all forms of AR expressed in late stage CRPC patients.

**Conflict of interest:**

Other Substantive Relationships: All authors listed are shareholders/employees of ESSA Pharma.

### 104 (PB094)

#### A novel anti-cancer compound development targeting YAP-TEAD protein-protein interaction

J.S. Park<sup>1</sup>, Y.K. Shin<sup>2</sup>, E. Hong<sup>3</sup>, Y.H. Park<sup>3</sup>, J. Um<sup>4</sup>, D. Lee<sup>4</sup>, H.S. Kwon<sup>4</sup>, G. Issabayeva<sup>5</sup>, O.Y. Kang<sup>5</sup>, B.H. Lim<sup>5</sup>, S.J. Park<sup>5</sup>, H.J. Lim<sup>5</sup>, H.C. Jeung<sup>6,7</sup>. <sup>1</sup>Yonsei Cancer Center- Yonsei University College of Medicine, Cancer Prevention Center, Seoul, South Korea; <sup>2</sup>Yonsei University College of Medicine, Gangnam Severance Biomedical Research Center, Seoul, South Korea; <sup>3</sup>Daegu-Gyeongbuk Medical Innovation Foundation, New Drug Development Center, Daegu, South Korea; <sup>4</sup>Samjin Pharmaceuticals Co., Ltd., Research Center, Seoul, South Korea; <sup>5</sup>Korea Research Institute of Chemical Technology, Therapeutics & Biotechnology Division- Department of Drug Discovery, Daejeon, South Korea; <sup>6</sup>Gangnam Severance Hospital- Yonsei University College of Medicine, Division of Medical Oncology- Department of Internal Medicine, Seoul, South Korea; <sup>7</sup>Yonsei University College of Medicine, Songdang Institute for Cancer Research, Seoul, South Korea

**Background:** Dysregulation of the Hippo signaling pathway can result in tumorigenesis and overgrowth of cancer. A significant percentage of cancer patients present an overexpression of YAP (Yes Associated Protein) proteins. YAP transcriptional activity requires its binding to transcriptional enhanced associated domain (TEAD) transcription factors. Therefore, one attractive strategy for the targeting of YAP consists of preventing its interaction with TEAD using interfering peptides. Although several protein-protein interaction disruptors (PPID) have been developed to target inhibition of YAP-TEADs, drug candidates selectively targeting YAP-TEAD are still lacking.

**Material and methods:** We identified drug candidates screened from integrated 3D database, based on structural interface between YAP and TEADs. We identified a novel lead compound, and its pharmaco-chemical activity and antitumor activity were comprehensively validated in human colorectal cancer (CRC) model.

**Results:** A lead compound KYP-1104 harbored highly conserved molecular docking poses with TEAD1, TEAD4, and YAP1, and its disturbing activity of interaction of YAP-TEAD was validated by luciferase reporting system and immunoprecipitation assay. KYP-1104 harbored anti-proliferative activity of CRC cells in vitro and anti-tumor activity in vivo. Then, we showed that KYP-1104-related antitumor activity was also related to the inhibition of epithelial-to-mesenchymal transition and invasion, and by promotion of cell death. Additionally, KYP-1104 also presented time-dependent and dose-dependent inhibition of phosphatidylinositol-3-kinase signaling pathway and MAPK signaling pathway, and it suppressed transcription of major molecules such as BIRC, CTGF, PD-L1, and CCND1 assisted by YAP-TEADs binding. Finally, using integrative transcriptome analyses, CRC cells treated with KYP-1104 showed a YAP-conserved signature, and the responders had higher activity of E2F and Myc pathways than non-responders in which NF-κB and KRAS pathways was enriched.

**Conclusions:** We herein demonstrated that KYP-1104 is a potential PPID which selectively inhibits YAP-TEADs interaction. This drug compound is expected to have therapeutic efficacy to control Hippo pathway-dependent cancers by inhibiting YAP-TEAD-mediated transcription and its related pathways, especially in human CRC.

**No conflict of interest.**

### 105 (PB095)

#### KSQ-4279, a first-in-class USP1 inhibitor shows strong combination activity in BRCA mutant cancers with intrinsic or acquired resistance to PARP inhibitors

L. Cadzow<sup>1</sup>, P.C. Gokhale<sup>2</sup>, S. Ganapathy<sup>2</sup>, P. Sullivan<sup>3</sup>, S. Nayak<sup>3</sup>, S. Shenker<sup>4</sup>, M. Schlabach<sup>5</sup>, E. Tobin<sup>5</sup>, U.A. Matulonis<sup>6</sup>, J.F. Liu<sup>6</sup>, F. Stegmeier<sup>7</sup>, A. Wylie<sup>3</sup>. <sup>1</sup>KSQ Therapeutics Inc., Pharmacology, Cambridge, USA; <sup>2</sup>Dana-Farber Cancer Institute, Belfer Center for Applied Cancer Science, Boston, USA; <sup>3</sup>KSQ Therapeutics Inc., Oncology, Cambridge, USA; <sup>4</sup>KSQ Therapeutics Inc., Computational Biology, Cambridge, USA; <sup>5</sup>KSQ Therapeutics Inc., Target Discovery, Cambridge, USA; <sup>6</sup>Dana-Farber Cancer Institute, Department of Medical Oncology, Boston, USA; <sup>7</sup>KSQ Therapeutics Inc, Research, Cambridge, USA

Tumors harboring BRCA1/2 mutations and other homologous repair deficiencies (HRD) are sensitive to agents targeting pathways involved in DNA repair, and multiple molecules that target poly (ADP-ribose) polymerase (PARP), including Olaparib, have been approved for the treatment of BRCA mutant cancers. Despite the clinical benefit achieved with these drugs, many

patients achieve incomplete disease control and often develop resistance. By employing our proprietary CRISPRomics® technology to screen over 700 cancer cell lines, we identified the deubiquitinating enzyme USP1 as one of the top targets that displays selective anti-tumor activity in ovarian and triple negative breast cancers. Subsequent drug discovery efforts identified KSQ-4279 as a potent and highly selective first-in-class small molecule USP1 inhibitor that is now in clinical development. We previously demonstrated that KSQ-4279 displays monotherapy potential and combination activity in BRCA mutant cancers that are PARP inhibitor (PARPi) treatment naive. To further investigate the therapeutic potential of KSQ-4279 for treating patients who are either intrinsically resistant, or have developed acquired resistance to PARPi, we performed a number of pre-clinical studies in PARPi-resistant models. KSQ-4279 activity was evaluated in multiple PARPi-resistant, BRCA mutant, ovarian orthotopic PDX models generated from patient tumor samples that have relapsed after multiple rounds of chemotherapy and/or PARPi treatment. While these models did not respond to Olaparib as a monotherapy, the combination of KSQ-4279 and Olaparib led to strong and durable anti-tumor efficacy, including the induction of tumor regressions in several models. Additionally, when we tested KSQ-4279 in combination with Olaparib in PARPi-resistant, BRCA mutant, triple-negative breast cancer (TNBC)-derived PDX models, we observed significantly greater and more durable anti-tumor activity, including regressions, with the combination therapy compared to single agents. The combination of KSQ-4279 was well tolerated over the entire treatment period with no need for dosing holidays, even at the maximum tolerated dose of Olaparib, across all *in vivo* mouse studies. Our data supports the clinical testing of KSQ-4279 in combination with PARP inhibitors in patients harboring BRCA1/2 mutations that have developed intrinsic or acquired resistance to PARP inhibitors.

**No conflict of interest.**

106

(PB096)

**Omomyc mini-protein can be directly and continuously delivered to the brain to prevent glioblastoma in patient-derived xenograft mouse models**

J. Whitfield<sup>1</sup>, L. Foradada<sup>2</sup>, E. Serrano<sup>1</sup>, H. Thabusot<sup>2</sup>, S. López-Estévez<sup>2</sup>, G. Martín-Fernández<sup>1</sup>, J. Gruoso<sup>1</sup>, J. Bove<sup>3</sup>, J. Juanola<sup>1</sup>, V. Castillo Cano<sup>2</sup>, M. Squatrito<sup>4</sup>, A. Jimenez Schumacher<sup>5</sup>, M. Zacarias-Fluck<sup>1</sup>, M.E. Beaulieu<sup>2</sup>, L. Soucek<sup>1</sup>. <sup>1</sup>VHIO, Models of Cancer Therapies Lab, Barcelona, Spain; <sup>2</sup>Peptomyc, s.l., Barcelona, Spain; <sup>3</sup>VHIR, Neurodegenerative Diseases Research Group, Barcelona, Spain; <sup>4</sup>CNIO, Brain Tumor Group, Madrid, Spain; <sup>5</sup>Aragon Health Research Institute, Molecular Oncology Group, Zaragoza, Spain

**Background:** Myc is a 'hot target' in oncology and implicated in the development of glioblastoma multiforme (GBM), a cancer with a dire prognosis and limited treatment options. Standard of care involves surgery, radiotherapy and treatment of residual tumour with temozolomide. Very few other treatment options exist and they do not significantly affect overall survival, which stands at around 15 months.

In a proof of concept, we previously showed Myc inhibition to be a potential strategy against GBM using lentiviral-driven expression of Omomyc, a Myc dominant negative. Here, we address whether Omomyc can be directly administered *in vivo* as a mini-protein drug to treat GBM.

**Material and methods:** We use the Omomyc mini-protein (OMO-103), currently in early-phase clinical trials for all-comer solid tumours (NCT04808362, sponsored by Peptomyc). Different delivery methods were tested for *in vivo* treatments. Patient-derived GBM neurospheres were examined in culture and in orthotopic PDX models for their response to Omomyc and to combination with standard of care.

**Results:** We find that intravenous or intranasal delivery shows limited biodistribution to the brain, with some minimal therapeutic efficacy after intranasal treatment. We therefore employed osmotic pumps to directly deliver the mini-protein drug to the brain, avoiding any issues with crossing the BBB and enabling continuous, local administration. In this case, Omomyc prevented the growth of patient-derived GBM orthotopic xenografts.

Omomyc reduced proliferation and increased cell death in a panel of patient-derived GBM neurospheres in culture, showing efficacy regardless of their Myc levels, and had additive effects in combination with the standard of care, temozolomide.

**Conclusions:** These results extend the clinical applicability of the Omomyc mini-protein to GBM patients and provides an administration route to deliver the mini-protein drug to this hard-to-reach organ.

**Conflict of interest:**

Ownership: LS and MEB are co-founders and shareholders in Peptomyc. Other Substantive Relationships: LS, MEB, JW and LF are shareholders in Peptomyc.

Abstracts, 34th EORTC-NCI-ACR Symposium

107

(PB097)

**Preclinical characterization of TOS-358, a potent and selective covalent inhibitor of wild-type and mutant PI3K $\alpha$  with superior anticancer activity**

J. Macdougall<sup>1</sup>, J. Bradley<sup>1</sup>, S. Bader<sup>1</sup>, J. Blair<sup>2</sup>, N. Dhawan<sup>3</sup>, W. Chen<sup>4</sup>. <sup>1</sup>Totus Medicines, Biology, Emeryville, USA; <sup>2</sup>Totus Medicines, Platform Chemical Biology, Emeryville, USA; <sup>3</sup>Totus Medicines, Chief Executive Officer, Emeryville, USA; <sup>4</sup>Totus Medicines, Chief Scientific Officer, Emeryville, USA

Phosphoinositide 3-kinase alpha (PI3K $\alpha$ ) is the most frequently mutated oncogene in cancer, inferring a critical role for this protein in neoplasia. The molecular biology of PI3K $\alpha$  reveals it to be a protein that integrates a large and diverse set of cellular signals. In the development of small molecule inhibitors of this target protein it has been demonstrated that deep but also durable inhibition is critical to potent anti-cancer activity, an area traditionally challenging for reversible competitive and allosteric inhibitors. TOS-358 was developed to inhibit covalently both wild-type and mutant PI3K $\alpha$  with observed IC50s of 2.2 nM for WT PI3K $\alpha$  and 4.1 nM for mutant PI3K $\alpha$  (H1047R). TOS-358 is highly selective in a kinome-wide screen and selective for PI3K $\alpha$  over other isoforms. We confirmed covalent binding to PI3K $\alpha$  by NanoBRET in washout experiments, where it was observed that TOS-358 maintained 90% binding at 100 nM 6 hours after washout; in contrast, binding of Alpelisib at 100 nM was completely lost over the same time frame. Irreversible binding was further established using TR-FRET assay in which  $K_{inact}/K_I$  was found to be  $5.6 \times 10^7 \text{ M}^{-1} \text{ s}^{-1}$ . Importantly, we also noted that TOS-358 produced sustained inhibition of phosphorylated AKT(S473) to 48 hours while allosteric inhibitors lose >60% inhibition. TOS-358 mediated cell growth inhibition has been evaluated in a panel of 120 cell lines and compared with Alpelisib in the same panel. This analysis revealed approximately 50% more cell lines to be responsive to TOS-358 compared with Alpelisib. There was no strong association of response and PI3K $\alpha$  mutation status, and in fact for both TOS-358 and Alpelisib there was a higher frequency of WT PI3K $\alpha$  cell lines responding to either treatment. TOS-358 activity has been tested in multiple different cell-derived and patient-derived xenograft cancer models and was found to produce reproducible and substantial tumor growth inhibition. Indeed, in several PDX models, TOS-358 induced tumor regressions while the clinical stage molecules Alpelisib and Inavolisib were unable to generate similar tumor regressions despite pharmacokinetic exposures comparable to, or in excess of, TOS-358. Finally, TOS-358 generated little or no glucose impact in mice and dogs at exposures that produced superior efficacy in these cancer models. Taken together, our *in vitro* and *in vivo* data reveal TOS-358 to be a potent, selective covalent inhibitor of PI3K $\alpha$  with superior anticancer activity to comparator molecules.

**Conflict of interest:**

Ownership: The authors are employees of and may hold equity in Totus Medicines.

108

(PB098)

**MYC inhibition by Omomyc unveils a prognostic gene signature in Melanoma**

M. Zacarias-Fluck<sup>1</sup>, D. Massó-Vallés<sup>1</sup>, J. Kaur<sup>1</sup>, F. Giuntini<sup>1</sup>, S. Casacuberta-Serra<sup>2</sup>, T. Jauset<sup>1</sup>, G. Martín-Fernández<sup>1</sup>, M.E. Beaulieu<sup>2</sup>, J.R. Whitfield<sup>1</sup>, L. Soucek<sup>1</sup>. <sup>1</sup>Vall d'Hebron Institute of Oncology VHIO- Vall d'Hebron Barcelona Hospital Campus, Models of Cancer Therapy Group, Barcelona, Spain; <sup>2</sup>Peptomyc SL- Vall d'Hebron Barcelona Hospital Campus, Peptomyc, Barcelona, Spain

**Background:** Melanoma is one of the most frequent causes of cancer death and despite significant treatment improvements, non-responder patients and those who develop resistance constitute a significant proportion of patients still in dire need of alternative and improved therapeutic options. Omomyc is a MYC inhibitor designed by Dr. Soucek that is extensively preclinically validated and currently being tested in a Phase I/IIa Clinical Trial. We have seen potent antitumour and antimetastatic effects when Omomyc is transgenically expressed in melanoma cells.

**Material and methods:** We performed microarray analysis on BRAF-mutated A375 and BRAF wild-type SkMel147 human melanoma cells *in vivo* after one week of Omomyc expression and analysed them in R with Bioconductor. We assessed the overlap on transcriptional reprogramming exerted by Omomyc and investigated how these genes are associated with patient prognosis, by retrieving clinical and transcriptional data from the Skin Cutaneous Melanoma TCGA, PanCancer Atlas study in cBioPortal.

**Results:** We found 620 differentially expressed genes in common, 436 downregulated by Omomyc (DN) and 184 upregulated (UP). DN genes

Poster Session (26 October 2022)

cluster into Cell Cycle, RNA processing, Metabolism and Chromatin modification, organisation, and remodelling, while UP genes are related to Immune Response and several subcellular processes. Expression lower than the median of 45% of the DN genes or higher than the median of 54% of the UP genes are associated with significantly increased survival. We then generated a 6-gene signature combining DN and UP genes, that clearly separates patients in good and bad prognosis cohorts. Those with simultaneous low expression of these DN genes and high expression of these UP genes have significantly increased OS (205 (162-NA) vs. 42 (28–63) months,  $p = 7 \times 10^{-7}$ ). Additionally, 63% of UP genes are enriched in patients with Good Prognosis whereas 56% of DN genes are enriched in Poor Prognosis patients. Thus, Omomyc *in vivo*-regulated genes overlap considerably with those genes enriched in patients pointing to a reasonable similarity among *in vivo* results with Omomyc and clinical and transcriptional data from patients. Finally, pre-ranked GSEA in these patients showed that those with Good Prognosis have lower expression of MYC target genes and genes involved in melanoma relapse and metastases, and increased expression of Adaptive Immune Response.

**Conclusion:** We show that specific gene sets reflecting decreased MYC transcriptional activity, restricted metastatic capacity and increased immune response are identified in Omomyc-expressing melanoma xenografts and indicate patients with Good Prognosis. We can therefore define an Omomyc-derived gene signature that clearly discriminates patients with different prognoses, whose transcriptional signatures resemble those of vehicle or Omomyc-expressing tumours *in vivo*.

#### Conflict of interest:

Ownership: L. Soucek and M. Beaulieu are cofounders and shareholders of Peptomyc, a company focused on developing Myc inhibitors for cancer treatment. M.F. Zacarias Fluck, S. Casacuberta-Serra, and J.R. Whitfield are shareholders of Peptomyc S.L.

109

(PB099)

#### A novel dual PARP-HDAC inhibitor for treatment of Ewing sarcoma

S. Truong<sup>1</sup>, B. Zhai<sup>1</sup>, F. Ghaidi<sup>1</sup>, L. Ramos<sup>1</sup>, J. Joshi<sup>1</sup>, D. Brown<sup>1</sup>, N. Sankar<sup>1</sup>, J. Langlands<sup>1</sup>, J. Bacha<sup>1</sup>, W. Shen<sup>1</sup>, P. Sorensen<sup>2</sup>, M. Daugaard<sup>1</sup>.  
<sup>1</sup>Rakovina Therapeutics, Research, Vancouver, Canada; <sup>2</sup>University of British Columbia, Pathology & Laboratory Medicine, Vancouver, Canada

**Background:** Inhibition of poly-adenosine diphosphate-ribose polymerase (PARP) is an effective therapy against cancers with DNA damage repair (DDR) deficiencies, such as BRCA1 and BRCA2 defects. In preclinical studies, PARP inhibitors demonstrated potential therapeutic value in Ewing sarcoma (ES), but clinical trials with olaparib failed to show significant clinical benefit. A key regulatory event in DNA damage repair is acetylation and deacetylation of histones, controlled by histone acetyltransferases (HATs) and histone deacetylases (HDACs). Increased expression of HDACs correlate with more malignant phenotypes in sarcomas and inhibition of HDAC in pre-clinical models of ES inhibits tumor growth. HDAC inhibition combined with PARP inhibition has promising results *in vitro*, however clinically, combination therapies often require complicated sequential dosing protocols due to different pharmacokinetic profiles and overlapping toxicities, that severely limits clinical utility. Here, we report the efficacy of a novel bifunctional small-molecule compound designed to have both PARP and HDAC inhibition activity.

**Methods:** PARP1 and PARP2 activity was measured using the Trevigen Universal Colorimetric PARP Assay Kit, the BPS Bioscience PARP2 Colorimetric PARP2 Assay Kit, and by PARylation assays. HDAC activity was measured using HeLa cell nuclear extracts and a fluorogenic peptide-based biochemical assay. Cell survival EC50 s were determined using live cell imaging with an Incucyte S3 system and the CellTiter Glo viability assay. DNA damage was detected by western blot, immuno-fluorescence, and comet assays.

**Results:** A representative compound from the kt-3000 series showed potent inhibition of PARP1 and PARP2 with IC50 values in the low nM range, comparable to FDA-approved PARP inhibitors. The compound also showed inhibition of HDAC enzymes with IC50 values in the low  $\mu$ M range, slightly lower than the FDA-approved HDAC inhibitor, vorinostat. Cell survival EC50 values were superior to olaparib in ES cell lines *in vitro*. Treatment with the kt-3000 compound also resulted in increased DNA damage and S and G2/M cell cycle arrest as compared to olaparib.

**Conclusion:** Our kt-3000 compound shows potent inhibition of PARP1, PARP2, and HDAC, as well as induction of DNA damage and cell cycle arrest. Further development of these bifunctional single molecule inhibitors may offer a novel treatment opportunity for Ewing sarcoma and other solid tumors with limited responses to PARP1 monotherapies.

#### Conflict of interest:

Board of Directors: J. Bacha and D. Brown are directors of Rakovina Therapeutics.

Corporate-sponsored Research: S. Truong, B. Zhai, F. Ghaidi, L. Ramos, J. Joshi are employees of Rakovina Therapeutics. J. Langlands, M. Daugaard and W. Shen are consultants to Rakovina Therapeutics.

110

(PB100)

#### Characterization of differential metabolic phenotypes and PT-112-induced mitochondrial effects in human prostate cancer cells

R. Soler Agesta<sup>1</sup>, R. Moreno-Loshuertos<sup>1</sup>, J. Marco-Brualla<sup>1</sup>, C. Junquera<sup>2</sup>, R. Martínez De Mena<sup>3</sup>, J.A. Enriquez<sup>3</sup>, C.Y. Yim<sup>4</sup>, M.R. Price<sup>4</sup>, T.D. Ames<sup>4</sup>, J. Jimeno<sup>4</sup>, A. Anel<sup>1</sup>. <sup>1</sup>University of Zaragoza, Biochemistry and Molecular and Cell Biology, Zaragoza, Spain; <sup>2</sup>University of Zaragoza, Anatomy and Human Histology, Zaragoza, Spain; <sup>3</sup>Carlos III National Center for Cardiovascular Research, Genética Funcional del Sistema de Fosforilación Oxidativa, Madrid, Spain; <sup>4</sup>Promontory Therapeutics Inc., Research & Development, New York, USA

**Background:** PT-112 is the first pyrophosphate-platinum conjugate under phase 1/2 clinical development, with clinical activity against heavily pretreated solid tumors including metastatic castration-resistant prostate cancer (PC). Prior work has shown that PT-112 causes mitochondrial stress, may be selective to cancer cells with mitochondrial defects, and promotes robust immunogenic cell death. Here, we sought to explore if differential mitochondrial and metabolic status alters PT-112 sensitivity and better characterize the effects of PT-112 on mitochondria in a panel of human PC cell lines.

**Material and methods:** Human PC cell lines (LNCap, LNCap-C4, LNCap-C4-2, DU-145, 22Rv1, and PC-3) and the non-tumorigenic prostate cell line RWPE-1 were used to assess PT-112 sensitivity. Mitochondrial reactive oxygen species (mtROS) production and mitochondrial mass were analyzed using MitoSOX<sup>TM</sup> and MitoTracker<sup>TM</sup> Green labelling, respectively. Cell death was analyzed by flow cytometry using annexin-V-FITC and 7-AAD staining. Blue native gel electrophoresis was performed using mitochondrial extracts, followed by immunoblot analysis of respiratory complexes. Mitochondrial extracts were used to measure the activity of respiratory supercomplexes by spectrophotometry. Oxygen consumption rate and extracellular acidification rate were monitored using Seahorse<sup>TM</sup> technology. Finally, the effects on cell and mitochondria morphology were analyzed by transmission electron microscopy (TEM).

**Results:** Human PC cell lines exhibited different metabolic features compared to the healthy prostate cell line RWPE-1. Baseline mtROS levels and supercomplex expression/activity varied across the panel, with PT-112-sensitive cell lines often showing higher mtROS levels. In addition, using the Seahorse<sup>TM</sup> technology, we observed a preference for aerobic respiration over glycolysis across all cell lines. In the PT-112-sensitive cell line DU-145, PT-112 induced a large increase in mitochondrial mass and mtROS, and reduced the activity of mitochondrial complex I and complex IV while increasing that of supercomplexes involving complex III. Finally, we observed by TEM the loss of internal mitochondrial structure after brief durations of PT-112 exposure (1–6 hours).

**Conclusions:** PT-112 was broadly active across a variety of human PC cell lines, induced mitochondrial stress, and showed a degree of selectivity on the basis of different mitochondrial phenotypes. The increase in activity of complex III-containing supercomplexes could be involved in massive mtROS generation in sensitive cell lines, and the rapid effects on mitochondrial structure suggest the importance of this organelle in the anticancer activity of PT-112. These data warrant further studies on PT-112-induced mitochondrial effects and differential sensitivity, which may have clinical applications.

#### Conflict of interest:

Ownership: Dr. Ames, Mr. Price, Dr. Jimeno and Dr. Yim all have ownership interests in Promontory Therapeutics Inc., which holds the global rights to all uses of PT-112 in oncology.

Board of Directors: Mr. Price serves on the Board of Directors of Promontory Therapeutics Inc.

Corporate-sponsored Research: This work was sponsored by Promontory Therapeutics Inc.

Other Substantive Relationships: Promontory Therapeutics Inc. pays Dr. Ames, Mr. Price, Dr. Jimeno and Dr. Yim as part of consulting or employment relationships.

111

(PB101)

**IK930, a novel TEAD inhibitor, sensitizes KRAS and EGFR mutant tumors to oncogene targeted therapy**

M. Rajurkar<sup>1</sup>, M. Sanchez-Martin<sup>1</sup>, D. Hidalgo<sup>1</sup>, N. Young<sup>2</sup>, B. Amidon<sup>2</sup>, G. Punkosdy<sup>3</sup>, J. Ecsedy<sup>4</sup>, L. Xu<sup>1</sup>. <sup>1</sup>Ikena Oncology, Translational Research, Boston, USA; <sup>2</sup>Ikena Oncology, Molecular and Cellular Oncology, Boston, USA; <sup>3</sup>Ikena Oncology, In vivo Pharmacology, Boston, USA; <sup>4</sup>Ikena Oncology, Discovery Biology, Boston, USA

The Hippo signaling pathway plays a key role in the regulation of cell proliferation, survival, and tissue homeostasis. The transcription co-factors YAP and TAZ, the downstream effectors of this pathway, are phosphorylated by the LATS1/2 kinases in response to a signaling cascade initiated by the MST1/2 (Hippo) kinases. Upon phosphorylation, YAP/TAZ can be sequestered in the cytoplasm or targeted for degradation. In the absence of phosphorylation, YAP and TAZ translocate to the cell nucleus where they interact with members of the TEAD transcription factor family to activate target gene expression. Dysregulated Hippo signaling due to genetic alterations leading to constitutive YAP/TAZ activation, or crosstalk with other oncogenic pathways have been associated with tumorigenesis in multiple cancer types including Mesothelioma, Meningioma and Non-small cell Lung Cancer (NSCLC) among others. Additionally, inhibition of critical nodes in pathways such as EGFR, RAS, and MEK has been shown to induce YAP/TAZ/TEAD signaling, leading to continued tumor cell survival. Therefore, YAP/TAZ/TEAD activation is an important mechanism of resistance to oncogene targeted therapies. To investigate the mechanism of YAP/TAZ/TEAD activation upon treatment with targeted therapies, KRAS or EGFR mutant cell lines were engineered to express a TEAD-responsive luciferase reporter, and then treated with MEK and EGFR inhibitors. TEAD transcriptional activity was measured as changes in luciferase in response to MEKi or EGFRi treatment. These studies demonstrated that inhibition of MEK or EGFR with small molecules drives TEAD transcriptional activity in a concentration dependent manner, suggestive of TEAD pathway upregulation as an adaptive response to oncogene inhibition in cancer. Furthermore, treatment with multiple modalities of MEK inhibitors, or with EGFR inhibitors resulted in nuclear translocation of YAP, consistent with pathway activation, as demonstrated in immunofluorescence experiments. Importantly, the addition of the TEAD inhibitor IK-930, resulted in abrogation of TEAD-mediated transcription induced by MEK or EGFR inhibitors. Consistently, combination of IK-930 with MEKi and EGFRi resulted in apoptosis *in vitro* and led to strong antitumor activity *in vivo* in KRAS and EGFR mutant xenograft models of CRC and NSCLC.

Our findings provide a strong rationale for combined targeting of TEAD transcription factors with MEK and EGFR and support clinical evaluation of the combination of IK-930 with targeted therapies in oncogene driven solid tumors.

**No conflict of interest.**

112

(PB102)

**A family of novel TEAD palmitoylation site inhibitors with exceptional pre-clinical anti-neoplastic activity as a monotherapy and in combination with MAPK inhibitors**

F. Muller<sup>1</sup>, D. Warshaviak<sup>2</sup>, J. Gyuris<sup>3</sup>, R. Nir<sup>4</sup>, E. Baloglu<sup>5</sup>, S. Shacham<sup>3</sup>, A. Morley<sup>6</sup>, R. Depinho<sup>7</sup>. <sup>1</sup>SPOROS BIOVENTURES, Cancer Biology, Houston, USA; <sup>2</sup>SPOROS, Cancer Biology, Thousand Oaks, USA; <sup>3</sup>SPOROS, Cancer Biology, Boston, USA; <sup>4</sup>SBH Sciences, Director, Natick, USA; <sup>5</sup>Boston Biotech Consulting, Director, Boston, USA; <sup>6</sup>O2h, Director, Manchester, United Kingdom; <sup>7</sup>M.D. Anderson Cancer Center, Cancer Biology, Houston, USA

**Background:** The Hippo pathway (effected by the YAP/TAZ-TEAD transcriptional complex) is a major regulator of cell density and organ size, and is a major pro-growth, pro-survival pathway yet to be targeted in precision oncology. YAP/TAZ-TEAD transcription is hyperactivated by specific genetic events (e.g. YAP/TAZ oncofusions, NF2 mutations) and has been demonstrated as a key mechanism of resistance acquisition to MAPK pathway inhibition, as well as inhibition of its upstream inputs, such as EGFR and other receptor tyrosine kinases. While YAP/TAZ are globular proteins without obvious docking sites, the four TEAD family members share a highly conserved palmitoylation site suitable for inhibitor docking.

**Materials and Methods:** We developed a virtual structural model of the palmitoylation site of TEAD and generated a series of novel inhibitors. We evaluated direct TEAD binding by Isothermal titration calorimetry, and in cell-based assays using a luciferase reporter under a consensus TEAD-binding element. Finally, we evaluated selective killing of TEAD oncogene-addicted cell lines (H226, MSTO-211 h) *in vitro*, and anti-tumor activity in xenografts of

the same cell lines *in vivo*. We also evaluated interactions of TEAD inhibitors with inhibitors of other major oncogenic pathways.

**Results:** We identified two chemical families of TEAD inhibitors with low nM cytostatic activity against TEAD-dependent cancer cell lines *in vitro*. Both TEAD inhibitors and literature compounds required long treatment (6-days), low cell seeding to observe biological effects, which were limited to cytostatic and not cytotoxic effects. The lead TEAD inhibitor, SPR1-TE-0294, caused rapid and dramatic tumor regression even in very large (>800 mm<sup>3</sup>) xenografted tumors. Furthermore, SPOROS TEAD inhibitors strongly interacted with MAPK pathway inhibitors in both cell lines with obvious sensitization mutation (e.g. KRAS, BRAF) and those without.

**Conclusions:** TEAD inhibitors show exceptional anti-tumor effects in pre-clinical models *in vivo*, despite somewhat modest effects *in vitro*. We speculate that cell culture conditions (attachment, serum) minimize dependence on the Hippo pathway, and that TEAD inhibitors may have much broader utility than cell line-screening studies have suggested.

**Conflict of interest:**

Ownership: SPOROS Bioventures  
Advisory Board: SPOROS Bioventures  
Board of Directors: SPOROS Bioventures

113

(PB103)

**Pharmacological activation of the mitochondrial stress protease OMA1 reveals a therapeutic liability in Diffuse Large B-Cell Lymphoma**

A. Schwarzer<sup>1</sup>, M. Oliveira<sup>2</sup>, M.J. Kleppa<sup>1</sup>, M. Liesa<sup>3</sup>, M. Kostura<sup>4</sup>. <sup>1</sup>Hannover Medical School, Institute of Experimental Hematology, Hannover, Germany; <sup>2</sup>David Geffen School of Medicine, Department of Medicine-Endocrinology, Los Angeles, USA; <sup>3</sup>UCLA- David Geffen School of Medicine, Department of Medicine-Endocrinology, Los Angeles, USA; <sup>4</sup>Bantam Pharmaceutical, Drug Development, Durham, NC, USA

**Background:** Relapsed diffuse large B-cell lymphomas (DLBCL) are a clinical challenge, with poor outcomes in the growing number of patients not suitable for transplant and in patients who fail CAR-T-cells.

**Materials and Methods:** medicinal chemistry, cell culture- and animal models of lymphoma, gene expression analysis, electron microscopy, mitochondrial biology, functional genetics

**Results:** We describe BTM-3566, a first-in-class compound that activates the OMA1 dependent mitochondrial quality control pathway in DLBCL. BTM-3566 is a small molecule based on a pyrazolothiazol-backbone and induces apoptosis and complete cell killing in DLBCL lines with an IC<sub>50</sub> of ~300 nM, including ABC, GCB, and double-hit and triple-hit lymphoma lines. BTM-3566 has >50% of oral bioavailability and 6 hours of serum half-life. In a dose-finding study using the DLBCL line SUDHL-10, daily oral treatment with 20 mg/kg BTM-3566 for 21 days resulted in complete regression in all tumor-bearing animals. Expansion studies into human DLBCL PDX models harboring a range of high-risk genomic alterations, demonstrated response in 100% of the lines with complete tumor regression in 6 of 8 PDX models tested. Transcriptome analyses revealed that BTM-3566 activates the ATF4-integrated stress response (ISR) via HRI-Kinase (EIF2AK1). HRI is activated by mitochondrial-related stress which causes the activation of the mitochondrial stress sensing protease OMA1. We found that BTM-3566 activates OMA1 in a manner unrelated to changes in mitochondrial ATP synthesis, reactive oxygen species generation or electron transport chain inhibition. OMA1 activation was required for the therapeutic effect and CRISPR-Cas9 depletion of OMA1 eliminated BTM-3566's apoptotic activity. We show that downstream of OMA1 the apoptotic stress signal is relayed to HRI by DELE1, whereas OMA1-dependent OPA1 cleavage and mitochondrial fragmentation were dispensable for the therapeutic effect. Gene expression-based profiling of BTM-3566 sensitivity in over 400 cancer cell lines showed that FAM210B, a poorly characterized mitochondrial membrane protein, negatively correlated with response to BTM-3566. Intriguingly, FAM210B is not expressed in either germinal-center B-cells or germinal-center-derived lymphomas. Increased FAM210B expression in DLBCL cell lines blocks all effects of the compounds, revealing a fundamental intrinsic vulnerability of DLBCL.

**Conclusion:** We describe a novel antitumor mechanism in DLBCL, where BTM-3566 induces mitochondrial stress, activating the OMA1-DELE1-HRI-eIF2a-ATF4 pathway leading to apoptosis and tumor regression. An IND application in B-cell malignancies has been completed with initiation of first in human clinical trials planned in 2022.

**Conflict of interest:**

Ownership: Matthew Kostura (stock)  
Advisory Board: Adrian Schwarzer  
Corporate-sponsored Research: Adrian Schwarzer, Marc Liesa, Matthew Kostura

114 (PB104)

**Covalent pan-TEAD inhibitors for the treatment of cancers with Hippo pathway alterations**S. Guo<sup>1</sup>, C. Huang<sup>1</sup>, S. Shrishrimal<sup>1</sup>, J. Cui<sup>1</sup>, V. Zhang<sup>1</sup>, N. Deng<sup>1</sup>, I. Dong<sup>1</sup>, G. Wang<sup>1</sup>, C.G. Begley<sup>1</sup>, S. Luo<sup>1</sup>, P. Cao<sup>1</sup>, W. Wiedemeyer<sup>1</sup>. <sup>1</sup>BridGene Biosciences, Research and Development, San Jose, USA

The Hippo pathway is a tumor suppressor pathway with important functions in regulating cell proliferation, survival, and growth. Hippo signaling is mediated by sequential phosphorylation of kinases MST1/2 and LATS1/2, which results in phosphorylation and degradation of the transcriptional regulators, YAP and TAZ. In human cancers, the Hippo pathway is frequently deregulated, e.g. as a result of NF2 mutation, which culminates in constitutive activation of oncogenic YAP/TAZ signaling. In order to activate their transcriptional program, which include target genes involved in angiogenesis, survival and proliferation, YAP and TAZ depend on protein partners with a DNA binding domain. In this context, TEAD transcription factors have emerged as the main effectors of oncogenic YAP/TAZ signaling. Moreover, due to the absence of targetable oncogenic kinases in the Hippo pathway, TEAD proteins have been recognized as therapeutic targets in human cancers with Hippo pathway alterations, such as mesotheliomas and some soft tissue sarcomas.

We have applied our proprietary chemoproteomic platform IMTAC<sup>TM</sup> (Isobaric Mass Tagged Affinity Characterization), to perform a proteome-wide live cell screen using a covalent library of drug-like molecules. We identified three distinct hits that covalently bound to TEAD1 with nanomolar affinity and high proteomic selectivity. Subsequent mass spectrometry identified the binding site as cysteine 359, located within the central lipid binding pocket of TEAD1.

We have carried out structure activity relationship (SAR)-guided optimization of our hit molecules focusing on improving the pharmacokinetic (PK) properties *in vivo*, as well as potent activity against all four TEAD isoforms and efficient suppression of TEAD-mediated transcription via disruption of YAP binding. To this end, we established a TEAD reporter assay in MCF7 cells, a YAP ELISA assay, as well as a palmitoylation assay and proliferation assays in multiple cell lines to assess the potency and selectivity of our compounds. While our initial hits and early leads were selective TEAD1/3 inhibitors, SAR activities resulted in pan-TEAD inhibitors with single-digit nanomolar potency in the TEAD reporter assay and low double-digit efficacy in NF2-mutant mesothelioma cell lines *in vitro*, as well as excellent PK properties *in vivo*. Importantly, proteome-wide profiling of our lead compound by IMTAC revealed improved selectivity compared to the initial hit molecule and show no concerning off-target effects.

Our ultimate goal is to take our covalent TEAD inhibitor to the clinic for the treatment of cancers with Hippo pathway alterations, and as a potential combination agent in cancers with acquired drug resistance as a result of activated YAP/TAZ signaling.

No conflict of interest.

## POSTER SESSION

**Preclinical Models**

115 (PB105)

**New patient derived lymphoma xenograft (PDX) panel for drug development, immuno-oncology and translational research**

B. Brzezicha<sup>1</sup>, M. Becker<sup>2</sup>, M. Stecklum<sup>3</sup>, T. Conrad<sup>2</sup>, M. Janz<sup>4</sup>, A. Bittner<sup>5</sup>, C.A. Schmitt<sup>6</sup>, J. Hoffmann<sup>1</sup>. <sup>1</sup>EPO - Experimental Pharmacology & Oncology Berlin-Buch GmbH, Preclinical Oncology, Berlin, Germany; <sup>2</sup>EPO - Experimental Pharmacology & Oncology Berlin-Buch GmbH, Bioinformatic, Berlin, Germany; <sup>3</sup>EPO - Experimental Pharmacology & Oncology Berlin-Buch GmbH, Immunoncology, Berlin, Germany; <sup>4</sup>Max Delbrueck Center for Molecular Medicine and Charité- University Hospital Berlin- Campus Benjamin Franklin, Biology of Malignant Lymphomas, Berlin, Germany; <sup>5</sup>Charité Universitätsmedizin Berlin Campus Virchow-Klinikum, Medizinische Klinik m.S. Hämatologie- Onkologie und Tumorimmunologie, Berlin, Germany; <sup>6</sup>Charité Universitätsmedizin Berlin CVK- and Max-Delbrück-Center for Molecular Medicine, Hematology- Oncology- and Tumor Immunology, Berlin, Germany

Lymphomas represent a very heterogeneous group of hematological malignancies and, despite successful therapies, they are a major challenge in clinical practice. Lymphomas often develop resistance to treatment with standard of care drugs (SoC) and have a high relapse rate. Therefore, new

therapies are needed to improve long-term remission and patient survival. Recent advances in high-throughput molecular profiling have helped to identify genetic factors and genetic subtypes of diffuse large B-cell lymphoma (DLBCL). Validation of targets in drug development are highly dependent on appropriate preclinical models representing the different clinical subtypes. Therefore, we have generated and characterized a panel of diverse patient-derived xenografts (PDX) of non-Hodgkin's (NHL) and Hodgkin's (HL) lymphoma for preclinical research and immuno-oncological approaches.

Our lymphoma PDX models were generated from peripheral blood, lymph node extirpations or core needle biopsies and primarily transplanted subcutaneously into immune-deficient mice. For further characterisation, the established lymphoma PDX were treated with SoC such as cyclophosphamide, doxorubicine, vincristine and investigational drugs such as ibrutinib. In addition, growth of lymphoma PDX on humanised mice was investigated to create new models for the evaluation of novel immunotherapy approaches. For thorough molecular characterization of all lymphoma models, RNA sequencing was performed.

More than 20 PDX models of NHL (including 8 DLBCL) and HL were successfully established and characterised. Heterogeneous individual responses to treatments were observed. Analysis of RNA sequencing data confirmed the representation of clinical lymphoma subgroups in our PDX panel. Similarly, genetic subtypes of Cell of origin (COO) classes of DLBCL were confirmed by principal component analyses (PCA) and hierarchical clustering methods. Patterns of genetic driver mutations were identified.

Our newly and comprehensively characterised lymphoma PDX panel enables the evaluation of new targeted and immunological therapies in preclinical phase II studies. They provide an exceptional platform for the identification and validation of new targets and enable the preclinical screening of new combinations in translational research.

No conflict of interest.

116 (PB106)

**Preclinical activity for TPX-4589 (LM-302), an antibody-drug conjugate targeting tight junction protein CLDN18.2 in solid tumors**

W. Huang<sup>1</sup>, Y. Li<sup>1</sup>, Z. Liu<sup>1</sup>, L. Rodon<sup>2</sup>, S. Correia<sup>2</sup>, Y. Li<sup>1</sup>, R. Li<sup>1</sup>. <sup>1</sup>La Nova Medicines, Shanghai, China; <sup>2</sup>Turning Point Therapeutics Inc, San Diego, USA

**Background:** Claudin 18 isoform 2 (CLDN18.2) is a tight junction protein involved in the regulation of epithelial cell permeability, barrier function, and polarity. In healthy tissue, CLDN18.2 is selectively expressed in tight junctions of gastric epithelial tissue and hence largely inaccessible to intravenous antibodies. On malignant transformation, CLDN18.2 is exposed on the cancer cell surface and expressed in many solid tumors, including gastric cancer (GC) and pancreatic cancer (PC). CLDN18.2 expression is associated with tumor pathogenesis, proliferation, and metastasis, making it a promising target for cancer therapies. TPX-4589, a novel antibody-drug conjugate (ADC) coupled with cytotoxic payload monomethyl auristatin E (MMAE), was developed to target CLDN18.2.

**Materials and methods:** Preclinical studies were conducted to characterize TPX-4589 in CLDN18.2-positive cells, including binding affinity, antibody-dependent cell-mediated cytotoxicity (ADCC), cell proliferation inhibition, and *in vivo* efficacy in gastric and pancreatic tumor models.

**Results:** TPX-4589 bound to endogenous CLDN18.2 GC GAXC031 cells in a dose-dependent manner, with an EC50 of 47.25 nM. Internalization was shown in both high- and low-expressing CLDN18.2-positive cells, with superior internalization when compared to zolbetuximab, a monoclonal antibody (mAb) that specifically binds to CLDN18.2 (table). TPX-4589 showed strong concentration-dependent ADCC activity, with EC50 of 0.11 nM, and inhibited tumor cell proliferation *in vitro* with nanomolar potency in GAXC031 and PC MIA PaCa2-high CLDN18.2 cell lines. In a cell-line xenograft GC tumor model with high CLDN18.2 expression, TPX-4589 significantly reduced tumor volume in a dose-dependent manner and demonstrated superior efficacy to zolbetuximab. In a CLDN18.2-high patient-derived xenograft (PDX) PC tumor model, increasing doses of TPX-4589 demonstrated superior tumor growth inhibition compared to gemcitabine and LM-102, a compound with identical anti-CLDN18.2 mAb component as LM-302, and similar efficacy to LM-102 + gemcitabine in combination. In a PDX PC tumor model with low CLDN18.2 expression, TPX-4589 showed potent inhibition of tumor growth.

**Conclusions:** TPX-4589, a novel CLDN18.2-targeting ADC, showed potent inhibitory effects on tumor cell proliferation *in vitro* and reduced tumor volume in both high- and low-expressing CLDN18.2 tumor models, with superior internalization and efficacy to zolbetuximab in a GC tumor model. These data suggest that TPX-4589 is a promising therapeutic candidate that warrants further investigation in clinical studies.



Table. (abstract: 116 (PB106)). TPX-4589 internalization in CLDN18.2-positive cells

	Cell line	TPX-4589 (LM-102 conjugated with MMAE)	LM-102 (CLDN18.2 mAb)	Zolbetuximab	Control hlgG1
EC50 (nM)	CLDN18.2/MKN45.#1 (low CLDN18.2 expression)	22.4	4.8	NA	NA
EC50 (nM)	CLDN18.2/MKN45.#14 (high CLDN18.2 expression)	3.5	3.5	83.93	NA

**Conflict of interest:**

Ownership: Stephanie Correia, Laura Rodon Turning Point Therapeutics Employee and Stock or Stock Options  
 Other Substantive Relationships: Laura Rodon Turning Point Therapeutics Patents planned, issued or pending  
 Yifan Li: Nothing to disclose  
 Zhifang Liu: Nothing to disclose  
 Runsheng Li: Nothing to disclose  
 Yuan Li: Nothing to disclose  
 Wentao Huang: Nothing to disclose

### 117 (PB107) Response of Human and Canine Tumor Cell Lines to Pharmacologic and Genetic Autophagy Inhibition

K. Van Eaton<sup>1</sup>, C. Towers<sup>2</sup>, L. Viola<sup>1</sup>, D. Gustafson<sup>1</sup>. <sup>1</sup>Colorado State University, Flint Animal Cancer Center, Fort Collins, USA; <sup>2</sup>Salk Institute of Biological Studies, Molecular and Cell Biology, La Jolla, USA

**Background:** The intrinsic autophagy-dependence of human tumor cell lines has been demonstrated using CRISPR screens showing that some cell lines respond in similar ways to loss of core autophagy genes as they do to loss of an established essential gene such as proliferating cell nuclear antigen (PCNA). Pharmacologic inhibition of autophagy can be achieved using lysosomotropic agents such as hydroxychloroquine (HCQ) that interfere with fusion of the autophagosome to the lysosome thus preventing completion of the recycling process. The sensitivity of tumor cells to the antiproliferative and cytotoxic activity of HCQ is complicated by pH and the non-selective mechanism of action and thus determining autophagy-dependence based on HCQ sensitivity has not been explicitly established. The goal of the present study is to determine the sensitivity of canine osteosarcoma (cOSA) and human tumor cell lines (hTC) to antiproliferative and cytotoxic effects of lysosomal autophagy inhibitors (HCQ and LysoV), and to compare these results to the autophagy-dependence measured using a CRISPR/Cas9 live-cell imaging assay.

**Materials and Methods:** RFP labelled canine and human tumor cell line antiproliferative and cytotoxic response to HCQ and LysoV was determined using live cell imaging and YOYO-1 staining in buffered media in an INCUCYTE ZOOM<sup>®</sup>. CRISPR/Cas9 live cell imaging screen was done using species specific guide RNA's and transfection of reagents into cells that were dual RFP and GFP labelled. Guide RNA for GFP was included in CRISPR/Cas9 reagent mix with selection of RFP only cells indicating uptake of autophagy targeted guide RNA's (ATG7, FIP200, LAMP2, ULK2, ATG12, ATG13, STX17 or VPS34). Response to autophagy core genes was compared to response to an essential (PCNA) and non-essential (PTEN) gene.

**Results:** cOSA and hTC showed similar antiproliferative and cytotoxic responses to HCQ and LysoV with median lethal dose ( $D_m$ ) values ranging from 7.1–14.6  $\mu$ M and 1.1–5.2  $\mu$ M for measures of anti-proliferative response, respectively.  $D_m$  values for cell death ranged from 11.4–36.4  $\mu$ M for HCQ and 3.4–7.9  $\mu$ M for LysoV. Analysis of key autophagy genes showed varied responses within cell lines. A clear relationship was observed between antiproliferative response to HCQ and LysoV and VPS34 CRISPR score with HCQ and LysoV  $D_m$  values showing clear correlations with VPS34 response ( $r^2 = 0.9463$  and  $0.6395$ ) in a species independent manner.  $D_m$  values for cell death also showed VPS34 correlations although CRISPR scores for other autophagy genes (ATG7, ATG12, ATG13, FIP200) enhanced predictive ability.

**Conclusions:** Response of tumor cell lines to lysosomal autophagy inhibitors shows a strong correlation to response to VPS34 CRISPR knockout. This correlation is species and cell lineage independent and suggests variable cellular responses to knockout of select autophagy genes.

**No conflict of interest.**

### 118 (PB108) Standardization of viability assays and high-content live-cell imaging protocols for large-scale drug testing in prostate cancer PDX-derived organoids

A. Van Hemelryk<sup>1</sup>, S. Erkens-Schulze<sup>1</sup>, L. Lam<sup>1</sup>, D. Stuurman<sup>1</sup>, C.M.A. de Ridder<sup>1</sup>, P.J. French<sup>2</sup>, M.E. van Royen<sup>3</sup>, W.M. van Weerden<sup>1</sup>. <sup>1</sup>Erasmus MC Cancer Institute, Urology, Rotterdam, Netherlands; <sup>2</sup>Erasmus MC Cancer Institute, Cancer Treatment Screening Facility, Rotterdam, Netherlands; <sup>3</sup>Erasmus MC Cancer Institute, Pathology, Rotterdam, Netherlands

**Background:** Organoid-based studies have revolutionized *in vitro* preclinical research and hold great promise for the cancer research field, including prostate cancer (PCa). However, standardized drug testing procedures are generally lacking, introducing experimental variability that complicates reproducibility, both within and between institutions. Moreover, common viability assays are restricted to endpoint measurements and viability as the sole read-out, losing important information on key biological aspects that might be exclusive to 3D organoids and that may be impacted by the administered drugs. In this study, we aimed to standardize a viability-based drug testing procedure for organoids derived from PCa patient-derived xenografts (PDXs). In addition, we developed and optimized an image-based live/dead assay using high-content fluorescence live-cell imaging in living PCa organoids.

**Material and Methods:** To initiate PCa PDX-derived organoids (PDXOs), PDX tumors were dissected and digested enzymatically, passed through a 100  $\mu$ m cell strainer and resuspended in a synthetic, thermo-sensitive, hydrogel. Organoids were allowed to assemble in 24-well plates and harvested after 7 to 14 days by dissolving the hydrogel dome. Organoids were plated at a density of 5000–10 000 organoids per 8  $\mu$ L hydrogel domes in 96-well plates. Organoids were incubated with dose ranges of standard PCa chemotherapeutics (docetaxel and cabazitaxel) and of the anti-androgen enzalutamide. Organoid viability was measured with CellTiter-Glo (CTG) 3D (Promega). An optimized fluorescent dye combination of caspase 3/7, propidium iodide and Hoechst 33342 was used for imaging experiments. Confocal time-lapse imaging was performed with the Opera Phenix High Content Screening System (PerkinElmer). Staurosporine treatment was used as positive control, solvents as negative controls in both CTG assays and image-based drug tests.

**Results and Discussion:** We developed a standardized protocol for performing CTG-based drug tests in PCa PDXOs and found 3 factors to be crucial for accurate interpretation of viability assays in these PDXOs: presence of ROCK-inhibitor in organoid medium, organoid proliferation rate and treatment duration. Moreover, we generated an image-based live/dead assay and implemented a custom image analysis method to quantify the number of organoids, organoid sizes and the number of apoptotic, necrotic and viable cells. This image-based procedure provides valuable insights on treatment effects in living organoids.

**Conclusion:** We developed two protocols for PCa PDXO-based drug testing and provide additional read-outs with our image-based procedure. Both procedures might well be customized for PDX- and patient-derived organoids from various cancer types.

**No conflict of interest.**

119

(PB109)

**Patient-derived xenografts and organoids recapitulate castration-resistant prostate cancer with sustained androgen receptor signaling**

A. Van Hemelryk<sup>1</sup>, I. Tomljanovic<sup>2</sup>, D. Stuurman<sup>1</sup>, C.M.A. de Ridder<sup>1</sup>, W.J. Teubel<sup>1</sup>, S. Erkens-Schulze<sup>1</sup>, H. J. G. van de Werken<sup>1</sup>, M. van Royen<sup>3</sup>, M. Grudniewska<sup>2</sup>, G.W. Jenster<sup>1</sup>, W.M. van Weerden<sup>1</sup>. <sup>1</sup>Erasmus MC Cancer Institute, Urology, Rotterdam, Netherlands; <sup>2</sup>GenomeScan BV, GenomeScan, Leiden, Netherlands; <sup>3</sup>Erasmus MC Cancer Institute, Pathology, Rotterdam, Netherlands

**Introduction:** Castration-resistant prostate cancer (CRPC) is a lethal form of advanced prostate cancer (PCa), that remains reliant on reactivated and often highly augmented AR signaling. Improving therapeutic strategies is crucial to maximize patient survival, but requires comprehensive testing on robust and representative preclinical models. Patient-derived xenografts (PDXs) from CRPC patients on contemporary therapies are scarce and provide an incomplete representation of CRPC heterogeneity. Complementing our existing PDX panel, we now introduce a new set of five AR-positive (AR+) PDXs and matching PDX-derived organoids (PDXOs) obtained from heavily pretreated CRPC patients.

**Material and Methods:** A total of 38 PCa tumor samples were implanted subcutaneously into intact male mice. In parallel, we developed a workflow to create organoids from PCa xenografts. PDXs and corresponding PDXOs were extensively characterized by means of histopathology, RNA sequencing and microarray analysis. Genomic and transcriptomic profiles were compared to original tumors and independent cohorts of CRPC patients. AR signaling status was evaluated using expression levels of genes defining the pathway and effect of bilateral orchiectomy was assessed in PDXs, while PDXOs were exposed to anti-androgen treatment (enzalutamide). Responses of PDXs and PDXOs to taxane treatment (docetaxel and cabazitaxel) were evaluated and retrospectively compared to matching patient responses.

**Results and Discussion:** We developed five new CRPC PDXs, two of which were derived from the same patient at different disease stages, and generated matching PDXOs. All are high-grade AR+ adenocarcinomas that express PSA, with one PDX-PDXO pair displaying a cribriform growth pattern mixed with ductal features, all reflecting donor patient tumors. Concordance of transcriptomic profiles between native tumors, PDXs and PDXOs further validated model consistency. Across PDXs, we confirmed the presence of common PCa-associated genomic alterations, including losses and gains of *TP53*, *PTEN*, *RB1* and *MYC*. *TMPRSS2-ERG* gene fusion was identified in one and *AR* amplification in four CRPC PDXs. The continued reliance on AR signaling was preserved across the entire set and we observed tumor regression upon surgical castration followed by tumor regrowth after reintroducing testosterone. PDXs and PDXOs accurately reflected matching patient responses to anti-androgen and taxane treatment, providing perspectives for individualized drug response profiling and patient stratification.

**Conclusion:** This new set of CRPC PDXs and matching PDXOs, that faithfully reproduces key characteristics and behavior of CRPC patient tumors, constitutes a reliable and unlimited resource for in-depth studies of treatment-induced, AR-driven resistance mechanisms and for tumor-specific drug testing in late stage castration-resistant disease.

**No conflict of interest.**

120

(PB110)

**Modeling of cell cycle response to cyclin-dependent kinase 12 (CDK12) inhibition**

S. Stein<sup>1</sup>, L. Martial<sup>2</sup>, J. Elaassais-Schaap<sup>2</sup>, P. Perera<sup>3</sup>, S. Alnemy<sup>3</sup>, D. LaPlaca<sup>4</sup>, D. Moebius<sup>4</sup>, S. Hu<sup>3</sup>, W. Dworakowski<sup>5</sup>. <sup>1</sup>Syros Pharmaceuticals, Computational Biology, Cambridge, USA; <sup>2</sup>PD-value, Pharmacometrics, Utrecht, Netherlands; <sup>3</sup>Syros Pharmaceuticals, Cell and Molecular Biology, Cambridge, USA; <sup>4</sup>Syros Pharmaceuticals, Medicinal Chemistry, Cambridge, USA; <sup>5</sup>Syros Pharmaceuticals, Preclinical Pharmacology, Cambridge, USA

**Background:** *In vitro* studies have shown that CDK12 inhibition (CDK12i) leads to DNA damage accumulation, cell cycle arrest, and mitotic defects which result in antiproliferation. *In vitro* modeling and translation to *in vivo* can elucidate the PK-PD-efficacy relationship of CDK12i and subsequently simulate the efficacy of new dosing regimens. The goal of this work was to develop a mechanistic model to describe the effect of CDK12i on *in vitro* proliferation using H1048 cells, and subsequently translate the model to predict *in vivo* tumor growth inhibition (TGI) in an H1048 CDX (Cell Line-Derived Xenograft) model.

**Methods:** Total cell count, Brdu staining, and Annexin-V/PI staining data was used to describe the effect of CDK12i on antiproliferation, cell cycle arrest, and apoptosis, respectively. Model development decisions were made using goodness-of-fit criteria, with a focus on bias minimization and physiological plausibility. The *in vitro* model was translated to *in vivo* using the ratio of the *in vivo* vehicle arm and *in vitro* DMSO treated growth rates as a scaling factor. The translated *in vitro-in vivo* predictions were compared to observed *in vivo* TGI data.

**Results:** The best fitting *in vitro* model was a four compartment ordinary differential equations model. It consisted of three cell cycle compartments in a loop: G0/G1, from which cells go into S, from which cells go into G2/M. From G2/M, cells re-entered the cell cycle in G0/G1, reflecting cell division upon mitosis. Cells could go into a fourth compartment (apoptosis) from S or G2/M. Two drug effects were included: an Emax-effect on the rate constant from G2/M to G0/G1, representing the effect of CDK12i on G2/M cell cycle arrest, and an Emax-effect out of G2/M, representing the effect of CDK12i on cell death from G2/M. The chosen model structure was based on model fit criteria, as the probability of transition into apoptosis from each phase of the cell cycle and the drug effect on rate constants were not known a priori. The EC50 values were estimated to be 11 nM for the G2 arrest Emax model and 1900 nM for the G2/M cell death Emax model. 11 nM is close to the antiproliferative EC50 of the compound while 1900 nM is much higher than any clinically relevant dose, suggesting that CDK12i causes antiproliferation primarily through G2/M arrest. Finally, the *in vivo* translated model closely predicted TGI in the H1048 CDX model and captured the effect of drug holidays.

**Conclusions:** We developed a cell cycle model describing the effects of CDK12i on *in vitro* antiproliferation and translated it to describe *in vivo* TGI. The final model suggests that CDK12i causes G2/M arrest and that cells enter apoptosis primarily from G2/M. The translated model was able to predict *in vivo* TGI and the impact of drug-holidays, suggesting that it can be used to predict *in vivo* efficacy of alternative dosing regimens.

**No conflict of interest.**

121

(PB111)

**Systematic evaluation of label-free protein quantification pipelines in 12 mouse syngeneic models**

B. Mao<sup>1</sup>, K. Xiao<sup>2</sup>, X. Chen<sup>1</sup>, J. Zhu<sup>2</sup>, H. Gu<sup>2</sup>, S. Guo<sup>1</sup>. <sup>1</sup>Crown Bioscience Inc., Data Science & Bioinformatics, SuZhou, China; <sup>2</sup>PTM Biolabs, Proteomic Service Department, HangZhou, China

**Background:** The widespread application of omics technologies in the past two decades has significantly expanded our knowledge of cancer biology. Proteins act as the link between genetic code and phenotype and can better reflect the dynamic state of a cell. With rapid advances in the field of proteomics, especially the label-free proteomics quantification technology powered by LC-MS/MS, it is now a routine to characterize and quantify thousands of proteins in tumor samples in a timely manner. Data-dependent acquisition (DDA) has been the workhorse for bottom-up proteomics within the past few years, however, it suffers from a high percentage of missing data originating from its stochastic nature. With this, data-independent acquisition (DIA) has gained increasing popularity in the field of bottom-up proteomics, due to its higher reproducibility and improved data completeness. In this study, bottom-up proteomics was used to profile the proteome for samples from 12 widely used mouse syngeneic models, and a systematic evaluation of the performance of different label-free protein quantification pipelines was conducted.

**Methods:** A total of 120 tumor samples were prepared for 12 mouse syngeneic models in two batches. Five tumor samples were collected per model when the tumor volume reached ~500 mm<sup>3</sup> (batch one) and ~1000 mm<sup>3</sup> (batch two). All samples were analyzed by DDA using MaxQuant software, and three samples from each model of batch two were analyzed by DIA using Spectronaut 15.0 software. Seven protein abundance matrices were generated from different label-free protein quantification pipelines, based on different combinations of parameters, quantification algorithms, and data acquisition methods. Missing data analyses, sample similarity analyses, and mRNA: protein correlation analyses were conducted to evaluate the quality of protein abundance data.

**Results:** DIA outperformed DDA in many aspects, including data coverage, data reproducibility, discrimination power among models, and mRNA: protein correlation. More specifically, the number of proteins with no missing data in all samples by DIA far outnumbered that of DDA, and the missing data percentage of DIA was much lower than that of DDA. On average DIA had a smaller coefficient of variation for protein abundance measurement in a biological replicate unit. Further, greater differentiation of samples from different models was observed with DIA than DDA. Finally, the average mRNA: protein correlation of DIA was slightly higher than that of DDA.

**Conclusion:** A protocol was developed to evaluate the quality of protein abundance data, and it was found that DIA offers a more comprehensive picture of the proteome in a panel of different models than DDA with better data reproducibility.

**No conflict of interest.**

**122** (PB112)  
**Establishment of RET inhibitor-induced resistant patient-derived colorectal cancer xenograft models**

L. Hua<sup>1</sup>, L. Chen<sup>1</sup>, J. Huang<sup>1</sup>, X. Chen<sup>1</sup>, S. Guo<sup>1</sup>, J. Wang<sup>1</sup>. <sup>1</sup>Crown Bioscience Inc., San Diego, CA, USA; Suzhou, China

**Background:** Rearranged during transfection (RET), a transmembrane receptor tyrosine kinase, is involved in multi-system tissue development which includes nervous, hematopoietic, and gastrointestinal systems. Activating RET alteration, induced by gene fusions or point mutations, has been discovered in several different solid tumor types including thyroid cancer, non-small cell lung cancer (NSCLC), breast cancer, and colorectal cancer. Recently, two RET-specific tyrosine kinase inhibitors (TKIs), selipercatinib (LOXO-292) and pralsetinib (BLU-667), were approved by the FDA for the treatment of thyroid cancer and NSCLC. Despite the encouraging efficacy of these RET inhibitors, acquired resistance, such as solvent-front RET G810R/S/C mutations has limited their clinical benefits. Therefore, to better investigate novel therapeutic strategies which can overcome the acquired resistance, we established patient-derived xenograft (PDX) colorectal cancer models with drug-induced resistance.

**Methods:** CR2518, a colorectal cancer PDX model with a CCDC6-RET fusion gene, was implanted subcutaneously and treated with LOXO-292 at 3 mg/kg, twice daily, for 116 days. Recurrent tumors were isolated, cryopreserved and their gene mutation was analyzed by RNA sequencing (RNA-seq) and verified by PCR. The tumors harboring different mutations were transplanted into the mice, and the tumor bearing mice with mean tumor volumes of 150–200 mm<sup>3</sup> were treated with LOXO-292 at 3 mg/kg or 10 mg/kg, twice daily, for 21 days. The changes in tumor volume over time were used to evaluate anti-tumor efficacy *in vivo*.

**Results:** LOXO-292 vigorously inhibited tumor growth and complete regression was seen in all ten mice on day 63 after the treatment in model CR2518. However, tumor re-growth was observed in nine out of ten mice from day 63 onwards. The RNA-seq data demonstrated that the acquired gatekeeper RET V804M mutation was found in 7 out of 9 tumors, and 4 of them co-occurred with an acquired solvent front RET G810S mutation. Additionally, homozygous mutation of RET G810S was in the other two tumors. Furthermore, the growth of the tumors with RET V804M mutation could be still suppressed upon LOXO-292 treatment at 3 mg/kg and 10 mg/kg in mice. Whereas, the tumors with RET G810S mutation became resistant to LOXO-292 treatment even when the dosing level was increased to 10 mg/kg *in vivo*.

**Conclusion:** The successfully established colorectal cancer PDX models with RET inhibitor-induced mutation could become a useful tool for the development of next generation RET inhibitors.

**No conflict of interest.**

**123** (PB113)  
**Omomyc downregulates MYC transcriptional signature in preclinical models of solid tumours and shows long half-life in tumour tissue**

S. Martínez Martín<sup>1</sup>, S. López-Estévez<sup>1</sup>, L. Foradada<sup>1</sup>, J. Kaur<sup>2</sup>, E. Serrano<sup>2</sup>, Í. González-Larreategui<sup>2</sup>, F. Giuntini<sup>2</sup>, S. Casacuberta-Serra<sup>1</sup>, H. Thabussot<sup>1</sup>, V. Castillo Cano<sup>1</sup>, L. Nonell<sup>3</sup>, L. Soucek<sup>1,2,4,5</sup>, M.E. Beaulieu<sup>1</sup>. <sup>1</sup>Peptomyc S.L., Biomarkers, Barcelona, Spain; <sup>2</sup>Vall d'Hebron Institute of Oncology VHIO, Models of Cancer Therapies, Barcelona, Spain; <sup>3</sup>Vall d'Hebron Institute of Oncology VHIO, Bioinformatics Unit, Barcelona, Spain; <sup>4</sup>Universitat Autònoma de Barcelona, Department of Biochemistry and Molecular Biology, Barcelona, Spain; <sup>5</sup>Institució Catalana de Recerca i Estudis Avançats, iCREA, Barcelona, Spain

**Background:** The expression and function of the MYC family of oncoproteins are tightly regulated in normal cells, but it becomes deregulated in up to 70% of human cancers through a variety of mechanisms, functioning as a master modulator of the cancer transcriptome. Despite the broad therapeutic utility anticipated for a clinical MYC inhibitor, MYC remains considered undruggable, and so far, no direct MYC inhibitor has been approved for clinical use.

Omomyc is a first-in-modality recombinant mini-protein that entered into a Phase I/IIa clinical trial in March 2021 to evaluate its safety and efficacy. Omomyc relies on a unique mechanism of action (MoA), acting as a

dominant-negative of the MYC protein: it competes with the MYC/MAX dimers by forming homo- and heterodimers and sequestering MYC away from its target genes on DNA. In this work, we aimed at describing the transcriptional reprogramming exerted by Omomyc supporting target engagement in preclinical models of various solid tumours.

**Materials and methods:** We used 2 cell lines of each lung cancer (A549, H441), colorectal cancer (SW480, DLD-1) and breast cancer (MDA-MB-231, MX-1). We treated the cells *in vitro* with 10, 20 and 30 µM of Omomyc for 24 and 120 h and analysed cell proliferation and gene expression by RNAseq. We also assessed Omomyc's efficacy at 25, 50 and 75 mg/kg after 3 weeks of intravenous (iv), weekly treatments in subcutaneous xenograft mouse models of each cell line. Finally, we analysed the transcriptome of *in vivo* tumours by RNAseq after 24 h or 22 days of treatment. Importantly, to characterise the PK/PD relationship, we quantified the amount of functional Omomyc present in tumour tissue homogenates (fresh-frozen and paraffin-embedded) and serum of the treated mice using a targeted proteomic approach.

**Results:** All the cell lines treated with Omomyc showed the shutdown of MYC transcriptional signature, both at 24 and 120 h, confirming the on-target activity *in vitro*. Moreover, all the Omomyc-treated xenografts showed reduced tumour growth and MYC transcriptional shutdown *in vivo* as well. Importantly, quantification of functional Omomyc revealed that 2 h after iv administration, higher concentrations of the drug were reached in the tumours compared to serum, and persisted at least 4 times more concentrated in the tumour tissue at 72 h after dosing. In accordance to Omomyc's MoA, there was no correlation between MYC levels and the response to MYC inhibition.

**Conclusions:** Our results show evidence of the long-lasting half-life of functional Omomyc in tumour tissues, *in vivo* target engagement and therapeutic utility of this pan-MYC inhibitor in lung, colon and breast cancer models. They also shed light on potential predictive biomarkers of response to Omomyc treatment, bringing insights for the clinical path fulfilment of this cutting-edge therapeutic modality.

**Conflict of interest:**

Other Substantive Relationships: S. Martínez-Martín, S. López-Estévez, H. Thabussot, V. Castillo Cano are employees of Peptomyc S.L. L. Foradada and S. Casacuberta-Serra are employees and shareholders of Peptomyc S.L. L. Soucek and M-E. Beaulieu are co-founders and shareholders of Peptomyc S.L.

**124** (PB114)  
**Defining activity and patient selection of a novel CDK7 inhibitor, GTAEXS-617, through AI-supported primary cancer tissue profiling**

M. Somlyay<sup>1</sup>, E. Durinkova<sup>1</sup>, J. Besnard<sup>2</sup>, O. Barbeau<sup>2</sup>, J. Le Coz<sup>1</sup>, M. Senekowitsch<sup>1</sup>, B. Ergüner<sup>1</sup>, K. Hackner<sup>3</sup>, L. Dzurillova<sup>4</sup>, E. Petru<sup>5</sup>, J. Lafleur<sup>6</sup>, J. Singer<sup>7</sup>, T. Füreder<sup>8</sup>, R. Paveley<sup>9</sup>, J. Joseph<sup>10</sup>, F. Aswad<sup>11</sup>, T. Winkler-Penz<sup>1</sup>, R. Sehlke<sup>1</sup>, C. Boudesco<sup>1</sup>, G. Vladimer<sup>1</sup>. <sup>1</sup>Exscientia, Translational Research, Vienna, Austria; <sup>2</sup>Exscientia, Design, Oxford, United Kingdom; <sup>3</sup>Karl Landsteiner University of Health Sciences, Health Sciences, Krems, Austria; <sup>4</sup>National Oncological Institute, Department of Oncology, Bratislava, Slovak Republic; <sup>5</sup>Medical University of Graz, Department of Gynecology, Graz, Austria; <sup>6</sup>Ordensklinikum Linz- Barmherzige Schwestern, Gynecology Department, Linz, Austria; <sup>7</sup>Krems University Hospital, Clinical Department of Internal Medicine, Krems, Austria; <sup>8</sup>Medical University of Vienna, Clinical Department of Internal Medicine, Vienna, Austria; <sup>9</sup>Exscientia, Translational Research, Oxford, United Kingdom; <sup>10</sup>GT Apeiron, Biology, San Francisco, USA; <sup>11</sup>GT Apeiron, Biology, San Francisco, USA

**Background:** Dual inhibition of CDK4/6 has become a mainstay treatment for several cancers, including HR-positive/HER2-negative breast cancer. CDK7 represents another potentially attractive CDK target that could combine the cell cycle inhibition found in CDK4/6 inhibitors with inhibition of transcription. We have generated a highly potent, selective and bioavailable inhibitor of CDK7, GTAEXS-617 ('617).

CDK7 is expressed in both normal and diseased tissue, thus understanding expression, sensitivity profiles and effects of CDK7 inhibition on cancer and non-transformed cells (e.g. stromal or immune) is crucial to elucidate MOA and determine the therapeutic window. In order to identify those patients more likely to benefit from CDK7 inhibition and '617 therapy in particular, we have used machine learning and other approaches in part to analyse multiparameter response in heterogeneous patient tissue samples.

**Materials and Methods:** To achieve full understanding of the potency and activity of '617, including versus other CDK7 and CDK4/6 inhibitors, we deployed disease relevant primary sample model systems from, for instance, ovarian, breast, lung and MCL patients that represent the cancer microenvironment. Single cell ex vivo functional screening combined with

transcriptomics after CDK7 perturbation in disease relevant primary human cancer samples helps reveal cancer-specific effects and patient selection methods. A translatable high content imaging platform amenable to primary human material supported by deep learning driven image analysis is used for all functional profiling.

**Results:** Primary cancer samples from various indications had a broad differential sensitivity to '617, with specific sensitivity in high grade ovarian cancer versus low grade. Ex vivo cancer cell sensitivity differences in various ovarian cancer grades, as identified by correlation of phenotypic response to differential single cell transcriptomics after '617 perturbation, indicates a potential stratification point that could be used for patient enrichment in clinical trials. Further, '617 displayed less cytotoxic effects on the immune compartment than other CDK7 and CDK4/6 inhibitors.

**Conclusions:** We used single cell functional profiling and transcriptomics to begin to maximise our understanding of '617 effect with the goal of enriching likely responding patient groups. We've described approaches which enable the rapid assessment of new targeted therapies in primary human disease samples containing host immune cells, together with functional data.

#### Conflict of interest:

Ownership: MS, ED, JB, MS, OB, JIC, BE, RP, TWP, RS, CB, GIV are shareholders and employees of Exscientia. FA and JJ are shareholders and employees of GT Aperia.

## POSTER SESSION

### Radiation Interactive Agents

125 (PB115)  
**Targeting nuclear HER3-AKT cascade improves radiotherapy of non-small cell lung cancer**

M. Toulany<sup>1</sup>, M. Iida<sup>2</sup>, L. Konstanze<sup>1</sup>, J.P. Coan<sup>2</sup>, K. Shayan<sup>1</sup>, P.M. Harari<sup>2</sup>, D.L. Wheeler<sup>2</sup>. <sup>1</sup>University of Tuebingen, Division of Radiobiology and Molecular Environmental Research- Department of Radiation Oncology, Tuebingen, Germany; <sup>2</sup>University of Wisconsin in Madison, Department of Human Oncology, Madison, USA

**Background:** Double-strand breaks (DSB) are the most lethal type of DNA damage induced by ionizing radiation (IR) that are repaired either by non-homologous end joining (NHEJ) throughout the cell cycle or by homologous recombination (HR) during the S phase and G2 phase. The repair of IR-induced DSB through NHEJ and HR is partially dependent on AKT. AKT must be present and activated in the nucleus immediately after irradiation to initiate the described DSB repair through the fast NHEJ repair process. We investigated the subcellular distribution of AKT1 induced by IR and the role of the epidermal growth factor receptor (EGFR)/HER family members on the activation of nuclear AKT1.

**Materials and methods:** Plasmid-based overexpression and siRNA transfections as well as the pharmacological inhibitors were applied to analyze the subcellular distribution of AKT1 and the role of HER family receptor members on the phosphorylation of nuclear AKT in non-small cell lung cancer (NSCLC) cells *in vitro*.  $\gamma$ H2AX foci assay was applied to investigate the role of nuclear AKT activating signaling pathway on DSB repair. A mouse tumor NSCLC xenograft model was used to study the impact of signaling pathway activating nuclear AKT on the radiation response *in vivo*.

**Results:** GFP-tagged exogenous AKT1 (GFP-AKT1) was detected in the nucleus 24 h after transfection and the nuclear accumulation was not modified by IR. Nuclear translocation of GFP-AKT1 was inhibited by the inhibitors of phosphatidylinositol 3-kinase and AKT. IR and HER3 ligand induced activation of endogenous AKT levels in both subcellular fractions. Activation of nuclear AKT after either of these stimuli was not associated with nuclear translocation of AKT1. IR-induced phosphorylation of nuclear AKT was primarily dependent on HER3 expression and EGFR tyrosine kinase activity. In line with the role of AKT1 in DSB repair, the HER3 neutralizing antibody patritumab as well as HER3-siRNA diminished DSB repair *in vitro*. Combination of patritumab with radiotherapy improved the effect of radiotherapy on tumor growth delay in a xenograft model.

**Conclusions:** IR-induced activation of nuclear AKT occurs in the nucleus that is mainly dependent on HER3 expression in NSCLC. Thus, targeting HER3 in combination with radiotherapy may provide a logical treatment option for investigation in selected NSCLC patients.

**No conflict of interest.**

## POSTER SESSION

### Tumour Immunology and Inflammation

126 (PB116)  
**Immunomodulatory effects of low piperine fractional Piper nigrum extract on breast cancer prevention**

N. Mad-Adam<sup>1</sup>, P. Graidist<sup>1</sup>, J. Saetang<sup>1</sup>, T. Rattanaburee<sup>1</sup>, T. Tanawattanasuntorn<sup>1</sup>, S. Dokduang<sup>1</sup>, S. Taraporn<sup>1</sup>, C. Chompunud Na Ayudhya<sup>1</sup>. <sup>1</sup>Prince of Songkla University, Biomedical Sciences and Biomedical Engineering, Songkhla, Thailand

**Background:** *Piper nigrum*, black pepper, has various biological effects such as anti-microbial, anti-inflammatory and anti-cancer activities. A crude extract of *P. nigrum* named low piperine fractional *Piper nigrum* extract (PFPE) has been reported for anti-tumor and anti-tumor immunity on breast cancer. PFPE also had an ability on cancer prevention. However, the mechanism of action of PFPE on cancer prevention has not been elucidated yet. Here, we evaluated the immunomodulatory role of PFPE on the prevention of breast cancer in mammary tumor rat model.

**Material and methods:** Female Sprague-Dawley rats, 45 days old (virgin) were divided into 6 groups, including normal, control, vehicle (MCT and vitamin E) and PFPE at doses of 50, 100 and 150 mg/kg BW. Rats were injected with 250 mg/kg BW of NMU at 50 and 80 days old and fed with 100  $\mu$ g/kg BW of estradiol after 7 days of 2nd NMU injection for 10 days. The PFPE was orally administered after 5 days of the 1st NMU injection, 3 times per week for 91 days. The blood from lateral tail vein was collected for cytokine study at 15 and 61 days after PFPE treatment. At the end of the experiment, rats were sacrificed and collected blood by cardiac puncture for investigation of blood parameters, ROS production, cytokines, chemokines and immune cell types. Internal organs were weighed, and tumor tissues were collected for histology study.

**Results:** The cancer preventive effects of PFPE at a dose of 50, 100 and 150 mg/kg BW were 71.43, 71.43 and 100%, respectively. Meanwhile vehicle prevented breast cancer at 28.57%. There were no significant changes in organ/body weight ratio and blood parameters, except for alkaline phosphatase at a dose of 150 mg/kg BW. For the histological study, tumors of the control rats were invasive ductal carcinoma, while the rats treated with PFPE at doses of 50 and 100 mg/kg BW were ductal carcinoma *in situ*. In addition, PFPE treatment at a dose of 100 and 150 mg/kg BW represented amount of ROS higher than non-treated and vehicle groups. PFPE at doses of 50 and 150 mg/kg BW suppressed cytokines and chemokines compared to control and vehicle groups at 15 days after PFPE treatment. Moreover, PFPE at a dose of 100 mg/kg BW was the most effective dose at 61 and 91 days after treatment. Interestingly, all doses of PFPE stimulated IFN- $\gamma$  at the endpoint of experiment. PFPE at doses of 100 and 150 mg/kg BW significantly promoted type 1 T helper cells and inhibited type 2 T helper cells and regulatory T cells compared to non-treated and vehicle groups.

**Conclusions:** These results indicate that PFPE at doses of 100 and 150 mg/kg BW had efficacy on immunomodulation in cancer prevention through the regulation of ROS, Th1/Th2/Treg and cytokine/chemokine production. However, PFPE at a dose of 150 mg/kg BW should be carefully used for a long time due to its adverse effect on liver function.

**No conflict of interest.**

127 (PB117)  
**Using patient-derived xenografts as sources of 3D tumor sphere cultures to study autologous tumor-infiltrating lymphocytes in metastatic uveal melanoma**

V. Sah<sup>1,2</sup>, J. Karlsson<sup>3</sup>, V. Bucher<sup>1,2</sup>, R. Olofsson Bagge<sup>1,2</sup>, L. Ny<sup>2,4</sup>, L. Nilsson<sup>3</sup>, J. Nilsson<sup>1,2,3</sup>. <sup>1</sup>Sahlgrenska Center for Cancer Research, Department of Surgery- University of Gothenburg, Gothenburg, Sweden; <sup>2</sup>Sahlgrenska University Hospital, Institute of Clinical Sciences, Gothenburg, Sweden; <sup>3</sup>Harry Perkins Institute of Medical Research, Melanoma Discovery- University of Western Australia, Perth, Australia; <sup>4</sup>Sahlgrenska Center for Cancer Research, Department of Oncology- University of Gothenburg, Gothenburg, Sweden

**Introduction:** Uveal melanoma (UM) is a rare form of melanoma, but the most common primary malignancy of the eye. 50% of patients with UM develop metastasis, mainly to the liver, with a median survival of less than a year. Immune checkpoint inhibitors are markedly less effective in patients with the uveal form as compared to the cutaneous form of melanoma. Adoptive cell therapy (ACT) has not been extensively studied clinically or pre-

clinically in UM. There has been a lack of robust ex vivo screening models and very few patient-derived xenograft (PDX) mouse models. Here we develop a 3D ex vivo tumor sphere coculture platform using PDX samples and their autologous tumor-infiltrating lymphocytes (TILs).

**Material and Methods:** UM metastases from ten patients were found to grow when implanted subcutaneously in NOG mice. The PDXs were used to generate tumors from which we cultured tumor spheres, in ultra-low attachment U-bottom wells, and cocultured them with ex vivo expanded autologous or MART1-specific HLA-matched allogenic TILs. The coculture was analysed using ELISA and flow cytometry (FACS) to look at markers of T cell activity. Single-cell RNA sequencing was performed on biopsies and TILs. Immunohistochemistry was used to compare biopsies from PDXs and patients. Using Incucyte, 3D image quantification was performed, showing interactions and effects on tumor spheres after coculture with TILs.

**Results:** UM patient tumors utilized for this study were of choroidal origin, 70% being liver mets and remainder skin mets. All PDXs correlated with the histopathological and molecular characteristics of original patient tumors. All samples had BAP1 mutations, 90% had GNA11/GNAQ with some having additional CYSLTR2 or CDKN2A mutations and 10% had PLCB4 and SF3B1 mutations. Degranulation (CD107a+) and activation (41BB+) with FACS was observed for 30% of all coculture samples, supported by comparative Granzyme B activity with ELISA. Single-cell sequencing of biopsies and TILs, as well as TCR sequencing of the “activated” TILs allowed for a deeper characterization of clonal expansion of tumor-reactive TILs. 3-D image-based analysis showed interactions between tumor spheres and TILs and further quantified differences in fluorescently labelled spheres post TILs treatment.

**Conclusion:** These results demonstrate that our tumor sphere platform is effective in studying TILs from metastatic UM samples. The platform is a powerful tool for visualizing and quantifying tumor-TIL interactions, and can aid in identifying immunological mechanisms that could be clinically translatable. It also serves as a valuable platform to screen for means to improve TIL function, i.e., by genetic engineering. To further study autologous TILs therapy in-vivo, we have developed few orthotopic UM liver metastasis NOG-IL2 PDX models, which can be utilised after the tumor sphere experiments.

**No conflict of interest.**

**128** (PB118)  
**NUC-3373 induces DAMPs release from NSCLC cells potentiating a favourable immunogenic microenvironment**

B. Kaghazchi<sup>1</sup>, I.H. Um<sup>1</sup>, J. Bré<sup>1</sup>, D.J. Harrison<sup>1</sup>, O.J. Read<sup>1</sup>. <sup>1</sup>University of St Andrews, School of Medicine, St Andrews, United Kingdom

**Background:** Immune checkpoint inhibitors (ICIs) exert their anticancer effects by modulating the interaction between tumour and immune cells. ICIs are more active in ‘hot’ tumours characterised by high density of tumour infiltrating lymphocytes (TILs). The immune cell contexture (cell type, density and spatial location) of the tumour microenvironment (TME) influences the outcome of such interactions. Damage-associated molecular patterns (DAMPs), including cell-surface calreticulin (CRT), adenosine triphosphate (ATP) and high mobility group box 1 protein (HMGB1), have been shown to govern immune contexture and lead to immunogenic cell death (ICD). Existing chemotherapies are known to induce ICD *in vitro*, turning immunologically ‘cold’ tumours ‘hot’. NUC-3373 has previously been shown to induce DAMPs in colorectal cancer cells and potentiate ICD. We hypothesise that DAMPs govern the immune cell contexture in tissue from patients with NSCLC adenocarcinoma. We also investigate NUC-3373-mediated DAMPs release and potentiation of ICD in co-cultures of lung cancer cells and peripheral blood mononuclear cells (PBMCs).

**Methods:** Tumour cell morphology and population were analysed in samples from 162 chemotherapy-naive NSCLC adenocarcinoma patients (stage I-IIA). In a sub-cohort (n = 60), multiplex immunofluorescence was performed utilising lymphocytes and DAMPs panels. Infiltration and spatial analyses performed using HALO® software. NSCLC cell lines A549 (adenocarcinoma) and Nx002 (squamous) were treated with sub-IC<sub>50</sub> dose of NUC-3373. Cell surface CRT and PD-L1 were measured by flow cytometry, ATP vesicles stained with quinacrine and HMGB1 assessed by immunofluorescence and ELISA. NSCLC cells exposed to NUC-3373 or DMSO for 24 hours prior to addition of PBMCs then treated with pembrolizumab and cultured up to 72 hours. Cell confluence and viability were determined by automated cytometry analysis and Sulforhodamine B assay, respectively.

**Results:** Significantly longer overall survival (OS) was demonstrated in the immune-high vs -low patients (p = 0.02). In the sub-cohort, 63% and 55% of CD8<sup>+</sup> cytotoxic T cells and 55% and 38% CD20<sup>+</sup> B cells were found in CRT<sup>high</sup> and HMGB1<sup>high</sup> areas, respectively. Distribution of CD8<sup>+</sup> T cells around CRT<sup>low</sup> cancer cells was sparse. NUC-3373 induced the release of

DAMPs (CRT, ATP, HMGB1) and cell surface expression of PD-L1 in both cell lines. In NUC-3373-treated co-cultures, ICD was observed and further potentiated by the addition of pembrolizumab.

**Conclusion:** In untreated NSCLC, DAMPs within the TME are associated with high density of TILs and longer OS. NUC-3373, a potent TS inhibitor, has the potential to modulate the immune contexture in NSCLC. With the ability to induce DAMPs and ICD, NUC-3373 is an attractive combination partner for ICIs in NSCLC.

**Conflict of interest:**

Corporate-sponsored Research: NuCana plc

Other Substantive Relationships: Oliver James Read and Jennifer Bré are full-time NuCana employees and David James Harrison is a part-time NuCana employee.

**129** (PB119)  
**MYC inhibition by OMO-103 induces immune cell recruitment in preclinical models of NSCLC and modulates the cytokine and chemokine profiles of Phase I patients showing stable disease**

S. Casacuberta Serra<sup>1</sup>, S. Martínez-Martín<sup>1</sup>, Í. González-Larreategui<sup>2</sup>, S. López-Estévez<sup>1</sup>, T. Jauset<sup>1</sup>, M. Zacarías-Fluck<sup>2</sup>, D. Massó-Vallés<sup>1</sup>, G. Martín<sup>2</sup>, L. Foradada<sup>1</sup>, J. Grueso<sup>2</sup>, E. Serrano<sup>2</sup>, H. Thabussot<sup>1</sup>, V. Castillo Cano<sup>1</sup>, J.R. Whitfield<sup>2</sup>, J. Morales<sup>1</sup>, M. Niewel<sup>1</sup>, M.E. Beaulieu<sup>1</sup>, L. Soucek<sup>1,2,3,4</sup>. <sup>1</sup>Peptomyc, Peptomyc, Barcelona, Spain; <sup>2</sup>Vall d’Hebron Institute of Oncology VHIO, Models of Cancer Therapies, Barcelona, Spain; <sup>3</sup>Institució Catalana de Recerca i Estudis Avançats ICREA, Institució Catalana de Recerca i Estudis Avançats ICREA, Barcelona, Spain; <sup>4</sup>Universitat Autònoma de Barcelona, Universitat Autònoma de Barcelona, Bellaterra, Spain

**Background:** Despite the promise of targeted therapies and immunotherapy, many cancer patients do not respond to treatment and are still in need of effective therapeutic options. We propose a revolutionary strategy based on the inhibition of MYC, a central molecule that drives multiple aspects of tumor progression and immune evasion. Although MYC has long been considered undruggable, we have demonstrated the safety and dramatic therapeutic potential of its inhibition using a MYC dominant negative, termed Omomyc. We showed that the Omomyc mini-protein abrogates tumor progression in a KRAS-driven Non-Small Cell Lung Cancer (NSCLC) mouse model, modulates chemokine/cytokine profiles and recruits T cells to the tumor site. These results have granted further development of the Omomyc mini-protein towards ongoing Phase I/IIa clinical trials (MYCure).

**Materials and Methods:** We used a well-characterized Kras<sup>G12D</sup> transgenic NSCLC mouse model, a syngeneic Kras<sup>G12V</sup>/p53<sup>KO</sup> NSCLC mouse model and PBMC-humanized KRAS and EGFR-driven xenograft mouse models. Tumor growth was measured by microCT or caliper measurements. Immune cell infiltration was evaluated by immunohistochemistry and flow cytometry. In addition, patient samples were obtained from the ongoing Phase I study and soluble immune modulators were measured by Luminex®.

**Results:** Here we show for the first time that, in our preclinical models, the infiltrating T cells consequence of Omomyc treatment are mainly CD4<sup>+</sup> T cells expressing PD-1, Tim-3, OX-40 and 4-1BB, suggesting that Omomyc induces the expansion of this tumor-reactive cell population. Interestingly, mice treated intranasally with Omomyc display higher proportions of Th1-Th17 hybrid population, effector memory T cells, cytolytic NK cells and activated dendritic cells. Importantly, this immune stimulatory effect is also observed upon systemic intravenous Omomyc administration in a p53/KRAS-mutated NSCLC model. Finally, we confirmed that Omomyc treatment also induces CD4<sup>+</sup> and/or CD8<sup>+</sup> T cell recruitment in PBMC-humanized xenograft lung cancer models independently of their driving mutation. Most notably, immune engagement was also seen in Phase I patients receiving OMO-103 and showing stable disease after 9 weeks of treatment. In particular, they display a cytokine signature that was not observed in patients with progressive disease. In addition, OMO-103 treatment also modified serum levels of other soluble immune modulators, including *bona fide* MYC targets. Of note, none of the patients showed anti-drug antibodies throughout the treatment.

**Conclusions:** Our findings support the therapeutic opportunity to induce a potent antitumor immune response in NSCLC by pharmacological MYC inhibition with Omomyc. In addition, they suggest that OMO-103 can also induce immune activation in patients displaying stable disease.

**Conflict of interest:**

Ownership: L. Soucek and ME. Beaulieu are co-founders of Peptomyc S.L. Board of Directors: L. Soucek and ME. Beaulieu are members of the BoD of Peptomyc S.L.

Other Substantive Relationships: S. Casacuberta-Serra, S. López-Estévez, M F. Zacarías-Fluck, L. Foradada, J. R. Whitfield, M. Niewel, M.E. Beaulieu and L. Soucek are shareholders of Peptomyc S.L.  
S. Casacuberta-Serra, S. Martínez-Martín, S. López-Estévez, L. Foradada, J. Grueso, H. Thabussot, V. Castillo Cano, J. Morales, M. Niewel, M.E. Beaulieu and L. Soucek are employees of Peptomyc S.L.

130 (PB120)

### Characterization of KRAS-driven NSCLC cell lines with diverse mutational landscape and assessment of their response to MYC inhibition

Í. González-Larreátegui<sup>1</sup>, L. Vera<sup>2</sup>, F. Giuntini<sup>1</sup>, S. Martínez-Martín<sup>3</sup>, J. Grueso<sup>1</sup>, S. López<sup>3</sup>, E. Serrano del Pozo<sup>1</sup>, H. Thabussot<sup>3</sup>, I. Macaya<sup>2</sup>, M.E. Beaulieu<sup>3</sup>, S. Vicent<sup>2,4,5</sup>, S. Casacuberta-Serra<sup>3</sup>, L. Soucek<sup>1,3,6,7</sup>. <sup>1</sup>Vall d'Hebron Institute of Oncology VHIO, Ed. Cellex, Barcelona, Spain; <sup>2</sup>Program in Solid Tumors and Biomarkers, Center for Applied Medical Research CIMA, Pamplona, Spain; <sup>3</sup>Peptomyc S.L., Ed. Cellex, Barcelona, Spain; <sup>4</sup>IdisNA, Navarra Institute for Health Research, Pamplona, Spain; <sup>5</sup>CIBERONC, Centro de Investigación Biomédica en Red de Cáncer, Pamplona, Spain; <sup>6</sup>ICREA, Institució Catalana de Recerca i Estudis Avançats, Barcelona, Spain; <sup>7</sup>UAB, Universitat Autònoma de Barcelona, Barcelona, Spain

**Introduction:** Lung cancer is the second most common cancer type both in males and females and the leading cause of cancer death worldwide. Inside lung cancer, Non-Small-Cell Lung Cancer (NSCLC) represents around 85% of the cases, where KRAS is the leading mutated oncogene (~25%) and confers poor prognosis and a high risk of tumor recurrence. Subsets of mutant KRAS NSCLC have been described based on the presence of concurrent mutations in tumor suppressor genes (TSGs), being the most common TP53, KEAP1 and LKB1 (also called STK11). Their mutation frequency is noteworthy and negatively affects survival and response to treatments, especially immunotherapies (IO). The MYC oncogene is a key transcription factor downstream of KRAS and it is usually amplified or deregulated in the majority of NSCLC, not only promoting tumor progression but also orchestrating tumor immune evasion and resistance to IO, all features that make it a promising target in these specific tumors. Although MYC was long considered undruggable, our lab has designed the first direct MYC inhibitor, called Omomyc. Here, we aim to determine how the different TSGs mutations affect the MYC network in a KRAS-mutated context and study their impact on the response to the Omomyc mini-protein, which offers a pharmacological approach to inhibit MYC in KRAS-driven NSCLC.

**Methodology:** We used KRAS Lung Adenocarcinoma (KLA) isogenic cell lines modified by CRISPR/Cas9 technology in order to obtain the knockout for TRP53, STK11 or KEAP1 gene. MYC and MAX levels were determined by western blot (WB) and sensitivity to Omomyc by proliferation and metabolic assays. For *in vivo* studies, cells were injected subcutaneously into C57BL/6J and the hybrid F1 mice obtained from the crossing of C57BL/6 and 129/Sv strains.

**Results:** MYC basal levels were increased in the mutant cell lines compared to the parental one. Although KEAP1-deficient cells showed slower *in vitro* growth, they presented faster *in vivo* growth, especially compared to KLA-STK11, which often did not give rise to tumors in syngeneic C57BL/6J mice. The change of strain to the C57BL/6 × 129/Sv provided a better model for the KLA cell lines, which were all able to grow *in vivo* while maintaining the other TSGs-mutant differences. Importantly, Omomyc significantly reduced *in vitro* cell growth and changed the cell cycle profile of all KLA cell lines. Even more remarkably, systemic MYC inhibition in C57BL/6 × 129/Sv mice also displayed therapeutic efficacy *in vivo* and changed the tumor immune microenvironment in KRAS-mutated tumors.

**Conclusions:** Loss of TSGs increases MYC levels in a KRAS-mutated context. Independently of MYC levels, all cell lines respond to a similar extent to MYC inhibition. Thus, MYC inhibition could provide a potential pharmacological approach for all KRAS-driven NSCLC.

#### Conflict of interest:

Ownership: L. Soucek and M.E. Beaulieu are co-founders of Peptomyc S.L. Board of Directors: L. Soucek and M.E. Beaulieu are members of the BoD of Peptomyc S.L.

Corporate-sponsored Research: S. Vicent discloses receiving research funding from Roche and Revolution Medicines. None of the disclosed information applies to the current project.

Other Substantive Relationships: S. Martínez-Martín, S. López, H. Thabussot, M.E. Beaulieu, S. Casacuberta-Serra and L. Soucek are employees of Peptomyc S.L.

S. López, M.E. Beaulieu, S. Casacuberta-Serra and L. Soucek are shareholders of Peptomyc S.L.

131 (PB121)

### The PKM2 activator and molecular glue TP-1454 modulates tumor-immune responses by destabilizing T-regulatory cells

S. Sommakia<sup>1</sup>, Y. Matsumura<sup>1</sup>, C. Allred<sup>1</sup>, S. Pathi<sup>1</sup>, E. Tyagi<sup>1</sup>, J. Foulks<sup>2</sup>, A. Siddiqui<sup>3</sup>, S. Warner<sup>4</sup>. <sup>1</sup>Sumitomo Pharma Oncology, Translational Research, Lehi, USA; <sup>2</sup>Sumitomo Pharma Oncology, Discovery Biology and Translational Research, Lehi, USA; <sup>3</sup>Sumitomo Pharma Oncology, Chemistry, Lehi, USA; <sup>4</sup>Sumitomo Pharma Oncology, US Research, Lehi, USA

**Background:** Pyruvate kinase is an important enzyme that catalyzes the last step of glycolysis. The M2 isoform (PKM2) is important for balancing respiration and biosynthesis, which can be achieved by switching between the highly active tetrameric form and the less active dimeric form through allosteric metabolite binding. In addition to its role in metabolic regulation, the dimeric form of PKM2 can translocate to the nucleus, altering transcription to enhance cancer cells' ability to grow and evade immune detection. Targeting PKM2 activation presents an opportunity to potentially reprogram the tumor-immune microenvironment (TME). TP-1454 is a potent PKM2 activator achieving PKM2 activation with low nanomolar concentration in biochemical assays (AC50 = 10 nM). TP-1454 has an acceptable preclinical safety profile and is currently in a Phase I clinical trial (NCT04328740).

**Materials and Methods:** PKM2 activity was measured using a colorimetric assay. PKM2 tetramerization and Foxp3 protein stability was assayed using western blots. *In vivo* activity of TP-1454 alone and in combination with checkpoint inhibitors (CPI) was tested in multiple syngeneic mouse models. Flow cytometry was used to conduct immunophenotyping of immune cells in the TME and to test regulatory T cell (Treg) polarization. Treg proliferation was assessed in a Cell Trace Violet Assay. Mass spectrometry was conducted to identify changes in metabolite levels. Foxp3 post-translational modifications were tested using a Foxp3-Flag expressing HEK293 cell line.

**Results:** TP-1454 treatment increased PKM2 activity *in vitro* and *in vivo* and showed a dose-dependent increase in PKM2 tetramer formation. Oral administration of TP-1454 resulted in substantial [KK1] [SS2] antitumor activity as a single agent (up to 42% tumor growth inhibition compared to vehicle) and in combination with CPI (100% complete response, 58% increase in mean survival compared to CPI alone) in multiple syngeneic mouse models. *In vitro* treatment of various immune cell types with TP-1454 resulted in differential PKM2 activation. Oral administration of TP-1454 treatment reduced intratumoral CD4<sup>+</sup> Foxp3<sup>+</sup> Treg levels as assessed by Flow cytometry immunophenotyping. *In vitro* treatment with TP-1454 showed a reduction in Treg polarization but not proliferation. Human peripheral blood mononuclear cells (PBMC) treated with TP-1454 showed a decrease in glucosamine-6-phosphate (G6P), which is reported to stabilize Foxp3 via the O-linked β-N-acetylglucosamine (O-GlcNAc) post-translational modification. *In vitro* treatment of HEK293 cells with TP-1454 reduced O-GlcNAc-Foxp3 levels and resulted in faster Foxp3 degradation.

**Conclusions:** These findings suggest a novel mechanism to regulate the TME with a PKM2 activator in preclinical models and should be investigated further in clinical trials.

#### Conflict of interest:

Corporate-sponsored Research: Employment

132 (PB122)

### CENP-E inhibitor potently activates cGAS-STING pathway through misaligned chromosome-mediated micronucleation after mitotic slippage

R. Kamata<sup>1</sup>, Y. Hakozaiki<sup>1</sup>, Y. Kashima<sup>2</sup>, T.Y. Morita<sup>1</sup>, P. Lu<sup>3</sup>, A. Ohashi<sup>1</sup>. <sup>1</sup>National Cancer Center Japan, Exploratory Oncology Research & Clinical Trial Center, Kashiwa, Japan; <sup>2</sup>The University of Tokyo, Computational Biology and Medical Sciences- Graduate School of Frontier Sciences, Kashiwa, Japan; <sup>3</sup>Frederick National Laboratory for Cancer Research, Cancer Research Technology Program, Maryland, USA

**Background:** cGAS-STING, which monitors cytosolic DNA and triggers innate immune response, has recently attracted attention as a molecular target to sensitize cancer to immune therapies. Micronuclei generated by aberrant mitosis are known to profoundly activate the cGAS-STING pathway in cancer cells when they leak into the cytoplasm. We have validated that small-molecule inhibitors targeting centromere-associated protein-E (CENP-E) generate micronuclei through chromosome misalignment and mitotic slippage. This suggests that CENP-E inhibitors (CIs) have potential to activate the cGAS-STING pathway in cancer cells at concentrations well below those used for a directly cytotoxic chemotherapeutic agent. The aims of this study is (1) to elucidate the potential that micronucleus formation by CIs activates the cGAS-STING pathway in cancer cells that may be rendered

more susceptible to immunotherapeutic treatment and (2) to develop a novel workflow integrating structure and AI-based modeling approaches to accelerate the discovery of novel CIs with desirable ADMET properties.

**Material and Methods:** (1) Misaligned chromosome and (2) micronucleus formation caused by CI treatment in cancer cells were determined using a microscope. (3) Downstream factors indicative of cGAS-STING pathway activation were measured by immunoblotting. (4) Reporter assays for IRF and NF- $\kappa$ B were performed. (5) Novel CI candidates will be identified from ultra-large chemical databases using the novel AI-based prediction and optimization approaches followed by the iterative generative molecular design.

**Results:** The CI treatment caused chromosome misdistribution in cancer cells. In addition, micronuclei were formed in the cells. Immunoblotting revealed that CI markedly increased phosphorylation of TBK1 and IRF3, consistent with micronucleus formation. Furthermore, IRF-Lucia and NF- $\kappa$ B-SEAP reporter activity assays revealed that both IRF and NF- $\kappa$ B were significantly activated in a time-dependent manner in CI-treated cells but not by the control.

**Conclusions:** The CI generates micronuclei and activates the cGAS-STING pathway in cancer cells. In our previous studies, transcriptome analysis has also revealed increased gene clusters involved in (1) the cytoplasmic DNA-sensing pathway, (2) the cytokine-cytokine receptor interaction pathway, and (3) the Toll-like receptor signaling pathway. Together, these findings suggest that the novel CI being researched have potential to induce immunological activation in cancer cells, which may convert tumors from cold to hot, making them more susceptible to treatment in the tumor microenvironment, while minimizing the side effects. The process of discovering immunomodulatory CIs will be accelerated using the novel AI-based workflow. That also benefits by reducing time and costs and identifying potential risks early on.

#### Conflict of interest:

Corporate-sponsored Research: AO was an employee of Takeda Pharmaceutical Company, Ltd. AO reported paid consulting or advisory roles for Ono Pharmaceutical Company Ltd., Craif Inc., and GEXVal Inc. out of this study. AO receives research fundings from Astellas Pharma Inc., Astellas Pharma Global Development Inc., and Daiichi Sankyo Company, Ltd. out of this study.

Other Substantive Relationships: NCI Contract No. 75N91019D00024

## POSTER SESSION

### Other

133

(PB123)

#### Transition to the new EU CTIS Portal for Regulatory Clinical Trial Submissions: VHIO's Start-Up Unit Analysis

A. Matres<sup>1</sup>, N. Carballo<sup>1</sup>, Y. Bernabé<sup>1</sup>, A. Martínez<sup>1</sup>, A. Silverio<sup>1</sup>, I. Depares<sup>1</sup>, I. Cidoncha<sup>2</sup>, M. Beltran<sup>1</sup>, I. Braña<sup>3</sup>, E. Élez<sup>3</sup>, M. Díez<sup>3</sup>, E. Muñoz<sup>3</sup>, C. Saura<sup>3</sup>, A. Oaknin<sup>3</sup>, T. Macarulla<sup>3</sup>, J. Carles<sup>3</sup>, E. Felip<sup>3</sup>, J. Tabernero<sup>4</sup>, E. Garralda<sup>3</sup>, S. Pérez-Pujol<sup>1</sup>. <sup>1</sup>VHIO, Clinical Trials Office, Barcelona, Spain; <sup>2</sup>VHIO, Pharmacy Department, Barcelona, Spain; <sup>3</sup>VHIO, Oncology Department, Barcelona, Spain; <sup>4</sup>VHIO, Oncology Department, Barcelona, Spain

**Background:** The Start-up Unit at Vall Hebron Institute of Oncology (VHIO) Clinical Trials Office was created to meet the needs of a growing number of proposals, aiming to homogenize tasks for all Clinical Trials (CT).

On 31st January 2022, the new European Portal under the EU Regulation 536/2014 for CT submissions (Clinical Trials Information System, CTIS) became available. During 2022, applicants may choose either the Country specific portal or the new CTIS portal for submissions. In 2023, all applicants must use CTIS. On 2025 all ongoing CT must have transitioned to CTIS. The objective of this work is to review all Regulatory Authorities (RA) submissions of VHIO's new CT proposals performed in 2022 through CTIS and gather potential challenges in this innovative process.

**Materials/Methods:** During 2022, RA submissions have been analyzed by the Start-Up Unit, including CT proposals received in 2021 and 2022. The Platform used for submission, either Portal de Ensayos Clínicos con Medicamentos from the Agencia Española del Medicamento (AEMPS) or CTIS, has been determined for each CT. All submissions performed through CTIS have been further assessed collecting feedback from the staff in charge of the process. Specifically, training received, difficulty of use and impact in internal processes have been considered.

**Results:** A total of 100 RA submission requests were received from 1st January 2022 to 15th June 2022: 64 CT from 2021 and 36 CT from 2022. RA submission was confirmed for 70% of the CT, only 11% being performed through the new CTIS portal. According to CT Phase, 50% were phase I CT

and represented an 11% out of all phase I CT submissions. The other 50% were phase II/III CT and represented a 12% of all phase II/III submissions.

Regarding quarterly distribution of CTIS submissions, 0 were performed in Q1 vs. 8 in Q2. Monthly distribution was: 5 submissions in April, 1 in May and 2 in June 2022.

Considering type of sponsor: 75% of CTIS submissions were performed by Biotech (BC) vs. 12.5% by Pharmaceutical Companies (PC) and 12.5% by Academia (AC).

Active requesting revealed an intention of submission through CTIS for 5 additional CT from 2022. Four were phase I (2 sponsored by BC and 2 by PC) vs. 1 Phase II/III (sponsored by PC). 100% of surveyed teams agreed CTIS was a user-friendly platform, however 75% reported an impact in their internal working manner. Only a 50% received internal company-related training for CTIS use, but all stated EMA provided appropriate trainings and manuals accessible for all users.

**Conclusion:** Out of 70 RA submissions initiated during 2022 only 11% have been performed through CTIS, mostly by BC. An increasing trend to use the CTIS as the year progresses has been observed. Overall and according to the feedback collected, this new initiative feels promising facilitating the submission process for CT in the European Countries.

#### No conflict of interest.

134

(PB124)

#### Loss of MNRR1 inhibits spheroid formation and improves survival in an ovarian cancer mouse syngeneic model

H. Chehade<sup>1</sup>, N. Purandare<sup>2</sup>, A. Fox<sup>1</sup>, R. Gogoi<sup>1</sup>, S. Aras<sup>2</sup>, L. Grossman<sup>2</sup>, G. Mor<sup>1</sup>, A. Alvero<sup>1</sup>. <sup>1</sup>Wayne State University, Department of Obstetrics and Gynecology, Detroit, USA; <sup>2</sup>Wayne State University, Center for Molecular Medicine and Genetics, Detroit, USA

**Background:** Cancer progression requires mechanisms that support proliferation and metastatic capacity. Detached cells must resist anoikis and concurrently acquire metabolic flexibility to survive the limiting oxygen and nutrients during transit to secondary sites. MNRR1 (CHCHD2) is a bi-organellar protein, which in the mitochondria can bind to Bcl-xL to enhance its pro-apoptotic function, or to respiratory chain complex IV (COXIV) to improve mitochondrial respiration. In the nucleus, it promotes the expression of genes involved in mitochondrial biogenesis and stress responses. Given these, we hypothesize that MNRR1 may be a relevant targetable driver to curtail the metastatic spread of ovarian cancer.

**Methods:** MNRR1 was knocked-out (KO) in mCherry-expressing TKO mouse ovarian cancer cells using CRISPR-Cas9 (TKO R1 KO). Effect on the transcriptome was determined by RNA sequencing, Gene Ontology enrichment analysis, and qPCR. Proteins were quantified by western blot. Cells were injected intra-peritoneally (i.p.) in C57BL/6 mice (n = 8) and tumor growth was quantified by using mCherry fluorescence as measure for tumor burden.

**Results:** KO of MNRR1 in the TKO cell line resulted in the differential expression of 3,691 genes. Eleven out of the top 25 differentially regulated Biological Processes are associated with cellular locomotion. Network analysis showed 11 genes, which are associated with focal adhesion and extra-cellular matrix (ECM). *Thbs4* was the most differentially expressed ( $p = 1 \times 10^{-6}$ ; FC = -8.97) followed by *Col1a1* ( $p = 1 \times 10^{-6}$ ; FC = -3.7). qPCR validated the RNA sequencing data and showed that *Thbs4* and *Col1a1* are indeed significantly down-regulated in TKO R1 KO cells compared to the TKO parental cell line ( $p < 0.0001$  and  $p = 0.024$ , respectively) and rescued upon re-expression of wild-type MNRR1. When cultured in ultra-low attachment (ULA) conditions, we did not observe a significant difference in cell viability but instead observed a difference in morphology. Whereas TKO parental cell line formed densely packed spheroids, TKO R1 KO cultures in ULA grew as single non-aggregated cells. I.p. injection of TKO R1 KO cells in mice resulted in significant delay in tumor growth ( $p = 0.0125$ ), development of ascites ( $p = 0.04$ ), and, more importantly, improved survival ( $p = 0.0385$ ) compared to parental TKO cells.

**Conclusion:** We demonstrate that, in addition to its anti-apoptotic and metabolic function, MNRR1 is required for a focal adhesion and ECM repertoire that can support spheroid formation. The loss of this function is sufficient to delay tumor kinetics, curtail carcinomatosis, and improve survival in a syngeneic ovarian cancer mouse model. These results support the value of targeting MNRR1 to improve survival of ovarian cancer patients.

#### No conflict of interest.

135 (PB125)  
**18F-Fluoropivalate PET/MRI: imaging of treatment naïve patients and patients treated with radiosurgery**

S. Islam<sup>1</sup>, M. Inglese<sup>1</sup>, P. Aravind<sup>1</sup>, T. Barwick<sup>1</sup>, J. Wang<sup>1</sup>, K. O'Neill<sup>2</sup>, A. Waldman<sup>2</sup>, M. Williams<sup>1</sup>, E.O. Aboagye<sup>1</sup>. <sup>1</sup>Imperial College London, Surgery & Cancer, London, United Kingdom; <sup>2</sup>Imperial College London, Brain Sciences, London, United Kingdom

**Background:** Approximately 20–40% of patients with cancer will develop metastatic cancer to the brain during the course of their illness. The brain niche imposes metabolic constraints on tumour cells that metastasise to the organ involving utilisation of short chain fatty acids (SCFAs) in the presence of glucose (Mashimo et al Cell 2014). We developed <sup>18</sup>F-fluoropivalate (FPiA), for imaging SCFA transcellular flux and showed high uptake in orthotopic human brain tumours in mice. In humans, FPIA was found to have favourable dosimetry - 0.0154 mSv/MBq. We hypothesised that FPIA uptake will be high in metastases regardless of primary tumour of origin and will decrease with treatment. In this interim analysis we ask a) whether FPIA uptake is higher over background in cerebral metastases, and b) whether Stereotactic Radiosurgery (SRS) impacts FPIA uptake at early time points (4–8 weeks) when changes in imaging outcome can influence future patient management; but for which a third of patients show pseudoprogression on magnetic resonance imaging (MRI) (Patel et al Am J Neuroradiol 2011).

**Methods:** We performed FPIA-PET/MRI in patient with one or more cerebral metastases from different primary tumour of origin: breast, lung, melanoma and colorectal cancer. There were two cohorts of patients, treatment naïve and SRS treated (4–8 weeks post treatment). We present analysis of the first 17 scans (16 treatment naïve lesions and 8 radiotherapy treated lesions).

**Results:** High contrast images were seen at the 60 min time-frame after radiotracer injection. The maximum standardised uptake (SUVmax) within lesions compared to the mean SUV of contralateral brain (SUVmean) was found to differ markedly: Mean ± SEM of 1.54 ± 0.11 vs 0.47 ± 0.04 (p < 0.0001). The calculated Tumour-to-Background ratio (TBR; SUVmax in tumour/SUVmean in contralateral brain) ranged between 1.73 to 6.07 (Mean ± SEM of 3.85 ± 0.33) supporting the qualitative assertion of high image contrast in patients regardless of cancer of primary origin. Both the highest and lowest TBR values were derived from patients who presented with lung cancer primary tumours. TBR was lower in the cohort that received radiotherapy 2.92 ± 0.26 (p = 0.074) and comparatively, dynamic contrast enhanced (DCE)-K<sub>ep</sub> - symmetric exchange rate of MRI contrast agent across the capillary wall - was markedly lower in the same group.

**Conclusion:** FPIA PET shows high uptake regardless of primary tumour of origin, indicating that the tracer can be used to monitor cerebral metastases. At the time when only half of patients in the treatment group has completed their assessment, there was a trend towards lower uptake of the radiotracer at early time points after initiating radiotherapy. The decrease in FPIA may be due in part to decreases in cell viability or capillary wall changes.

Funding from UK Medical Research Council.

**Conflict of interest:**

Ownership: None  
 Advisory Board: EA is an advisor to RadioPharm Theranostics  
 Board of Directors: None  
 Corporate-sponsored Research: None  
 Other Substantive Relationships: None

136 (PB126)  
**ALRN 6924 induces cell cycle arrest in bone marrow stem cells and hair follicles with dose-dependent degree and duration of effects after a single infusion in healthy volunteers**

S. Henkelman<sup>1</sup>, C. Voors-Pette<sup>2</sup>, W. Aalders<sup>2</sup>, A. de Jong<sup>1</sup>, R. Brugman<sup>1</sup>, K. Randall<sup>3</sup>, B. Will<sup>4</sup>, U. Steidl<sup>4</sup>, M. Aivado<sup>3</sup>, V. Vukovic<sup>3</sup>, A. Annis<sup>3</sup>. <sup>1</sup>QPS Netherlands BV, Bioanalytical, Groningen, Netherlands; <sup>2</sup>QPS Netherlands BV, Clinical, Groningen, Netherlands; <sup>3</sup>Aileron Therapeutics, Inc., Research, Boston, USA; <sup>4</sup>Albert Einstein College of Medicine, Medicine, New York, USA

**Background:** ALRN-6924 is a cell-permeating, stabilized alpha-helical peptide that binds to endogenous p53 inhibitors MDMX and MDM2, thereby activating p53 and its transcriptional target p21 to cause cell cycle arrest (CCA). This effect is limited to cells with wild-type, functional p53. For cancer patients with tumors bearing mutated p53, ALRN-6924 treatment selectively induces CCA in normal cells, allowing chemotherapy to preferentially target p53-mutant cancer cells that are actively cycling.

**Materials and methods:** A Phase 1 study in healthy volunteers is being conducted to evaluate ALRN-6924 pharmacokinetics (PK) and pharmacodynamics (PD). In Part 1 (37 subjects; Voors-Pette et al, ESMO 2021) it was shown that a 1-hour intravenous (IV) ALRN-6924 infusion was safe, well tolerated, and transiently upregulates p21 in human bone marrow (BM) cells with minimal signal for apoptosis. In Part 2, we aim to directly measure dose-dependent CCA in the BM as well as in hair follicles (HFs) in female subjects across a range of doses by 1-hour IV infusion and 3-minute bolus IV injection.

ALRN-6924 was administered as a single IV infusion or bolus injection at 0 (placebo), 0.3, 0.6, or 0.9 mg/kg to cohorts of 3 to 5 subjects. Subjects were evaluated for safety and tolerability. Plasma and serum samples were obtained to determine PK and levels of macrophage inhibitory cytokine-1 (MIC-1), a biomarker of p53 activation. BM was sampled 12 hours post-dose to directly measure CCA by flow cytometry in CD34+, lineage-negative BM stem cells. Occipital scalp skin was sampled by 2 mm punch biopsy for p21 immunohistochemistry in HFs.

**Results:** As of June 20, 2022, 42 subjects (ages 18–59; 100% female) were enrolled and evaluated in Part 2. Subjects experienced only mild, transient adverse events (AEs), with nausea/vomiting as the most frequent related AEs. The degree and duration of serum MIC-1 elevation was dose-dependent. At 12 hours post-dose, the proportion of cycling BM stem cells was significantly reduced at all dose levels, while blinded pathology review suggested ALRN-6924-dependent p21 induction in anagen-phase HFs. Safety profiles, PK and PD were similar for both bolus and infusion.

**Conclusions:** ALRN-6924 shows a favorable safety profile for use as a chemoprotection agent. CCA measured in BM supports prevention of chemotherapy-induced neutropenia, thrombocytopenia, and anemia, while HF results support chemoprotection for alopecia. Administration by IV bolus may simplify dosing vs. the current 1-hr infusion clinical regimen. The dose-dependent degree and duration of effects support development of a universal treatment schedule for broad use across cancer indications and types of chemotherapy.

**Conflict of interest:**

Ownership: Manuel Aivado, Vojislav Vukovic, and Allen Annis are employees and shareholders of Aileron Therapeutics  
 Advisory Board: Ulrich Steidl is a member of the Scientific Advisory Board of Aileron Therapeutics  
 Other Substantive Relationships: Britta Will and Kevin Randall are consultants to Aileron Therapeutics

137 (PB127)  
**Representation of young adult(19–29 y) and elderly(>75 y) patients populations in an early drug development unit**

M. Vieito Villar<sup>1</sup>, K. Rojas<sup>1</sup>, B. Roger<sup>1</sup>, V. Cristina<sup>1</sup>, I. Braña<sup>1</sup>, J. Lostes<sup>1</sup>, G. Alonso<sup>1</sup>, V. Galvao<sup>1</sup>, O. Saavedra<sup>1</sup>, H. Oberoi<sup>1</sup>, M. Oiveira<sup>1</sup>, M. Gonzalez<sup>1</sup>, A. Oaknin<sup>1</sup>, E. Felip<sup>1</sup>, E. Elez<sup>1</sup>, C. Saura<sup>1</sup>, J. Carles<sup>1</sup>, T. Macarulla<sup>1</sup>, E. Garralda<sup>1</sup>, J. Tabernero<sup>1</sup>. <sup>1</sup>Vall d'Hebron Institute of Oncology VHIO, Medical Oncology, Barcelona, Spain

**Background:** 0.88% of patients(pts) diagnosed of cancer in Spain are 20–29 years old and 45.77% are >70 y old at diagnosis. Lower inclusion in clinical trials is a barrier to improve survival in both young-adult (AYA) and older pts. Underrepresentation of elderly pts, who might be at higher risk for toxicity, hinders the applicability of RP2D recommendations, and recent FDA recommendations (FDA-2019-D-5572) highlight the necessity of including elderly pts in dose-seeking studies. Meanwhile, lack of referral of AYA pts delays research in tumors more prevalent in AYAs, such as sarcoma and CNS tumors.

**Material and Methods:** Pts referred to Vall de Hebron Institute of Oncology Early Drug Development Unit between 2019 and 2021 were analyzed. Clinical variables included: age, sex, primary tumor location, clinical trial inclusion and type of clinical trial.

**Results:** A total of 1218 pts were analyzed, of which 580(48.53%) were included in at least 1 early clinical trial. Median age of the overall population was 61 y, with similar results in patients included in clinical trials(62 y) or not (60 y). Ages of patients included in clinical trials ranged from 22 to 92. Elderly pts(>75 y) represented 9.1% of the population visited and 8.89% of the included in at least 1 clinical trial, AYA pts represented 1.47% of patients visited and 1.% of the patients included. While >75 y pts were included in a similar percentage as other patients(46.90% vs 49.44%) AYA pts were matched to a clinical trial in only 33.33% of cases. (Fisher's p-value = 0.06) Sex distribution in >75 y pts and AYAs was similar (60.17% and 61.11%) while in the general population males were 50.90%(NS). 674 pts were offered at least 1 molecular analysis technique, 47.8% of elderly patients and 28.6% of AYA patients(NS). Elderly pts were numerically overrepresented in immunotherapy trials, and underrepresented in ADC, cytotoxic and targeted treatment trials(p = 0.21). AYA pts were overrepresented in clinical trials with epigenetic agents and underrepresented in immunotherapy, clinical trials(p <



0.01). Primary tumor location in pts >75 y was colorectal(28.82%), other gastrointestinal tumors(19.81%) and head and neck(14.41%) vs sarcoma (38.88%), CNS(27.77%) and other gastrointestinal(11.1%) in AYA pts. In the overall population colorectal (24.38%), other gastrointestinal tumors (18.14%) and breast cancer pts (10.91%) predominated.

**Conclusions:** Compared to patients between 29 and 74 y, elderly pts are underrepresented in the population referred to early clinical trials and AYAs have the expected prevalence. While elderly pts that are referred to our unit are included in clinical trials in a percentage similar to patients 29–74, AYA patients are included only in 33.3% of cases and are specially under-represented in immunotherapy trials. One potential barrier of access is the high frequency of “cold” tumors in AYA pts

**No conflict of interest.**

**138** (PB128)  
**ERK3/MAPK6 has a dual role as pro-and anti-tumorigenic in Triple-Negative Breast Cancer**

S. Morazzo<sup>1,2</sup>, S. Fernandes<sup>1</sup>, M. Cassani<sup>1</sup>, J.O. De La Cruz<sup>1</sup>, G. Forte<sup>1</sup>.  
<sup>1</sup>International Clinical Research Center- St Anne's University Hospital, Center for Translational Medicine, Brno, Czech Republic; <sup>2</sup>Masaryk University, Faculty of Medicine, Brno, Czech Republic

Extracellular-regulated kinase 3 (ERK3) - an atypical mitogen-activated protein kinase (MAPK), coded by the MAPK6 gene - is overexpressed in breast cancer (BC), strongly correlating with poor patient survival. However, the mechanisms by which ERK3 contributes to BC remain unknown. Therefore, this study aims to elucidate the role of ERK3 in breast cancer progression, especially in aggressive triple-negative BC subtype (TNBC).

For that purpose, BT549, a type of TNBC cell line, was transfected with siRNA against MAPK6 (ERK3-KD) or the corresponding scramble (ERK3 WT) 48 hours (h) prior to any assay. The transfection efficiency was evaluated by immunoblotting and the cells analysed for a variety of functional assays. These include: (1) motility capacity investigated by scratch assay and chemotaxis cell migration; (2) proliferation rate; (3) cellular adhesion ability to different types of extracellular matrix (ECM). In addition, the expression of different epithelial-to-mesenchymal (EMT) markers was evaluated by western blot. Lastly, to determine the effect of ERK3 on cellular chemoresistance, various drugs (e.g. doxorubicin, paclitaxel) were tested.

Our results reveal that ERK3-KD in BT549 increases cell migration at 8 h and 20 h but has no effect on the chemotaxis cell migration assay. Also, ERK3-KD does not affect the proliferation rate, which allows us to discard the proliferation effect in the scratch assay. These findings suggest that ERK3 might regulate collective cell migration rather than individual cell migration. This is of particular importance, since it has been reported that collective cell migration is more common in metastatic BC. This effect can be further investigated by spheroid invasion assay. We also observed a reduction in the cell anchoring to diverse ECM proteins, especially for fibronectin and laminin, indicating that ERK3 promotes adhesion to different types of ECM. Additionally, ERK3-KD increases the expression of EMT markers, such as ZEB-1, SNAIL and SLUG indicating that ERK3 might be involved in the regulation of EMT/MET processes. Finally, ERK3-KD increased chemosensitivity to doxorubicin and paclitaxel. These findings are in accordance with a previous study done in lung cancer, in which ERK3 increased chemoresistance by activating DNA damage repair mechanisms. Further studies will help clarify ERK3 role in drug resistance, such as exploring the activation of specific survival pathways.

Altogether, this study shows that ERK3 is an important regulator of different processes involved in TNBC, such as migration, EMT, cellular adhesions to ECM and chemoresistance. The dual role of ERK3 as both anti- and pro-tumorigenic brings new evidence to the complexity of cancer mechanisms and should be further elucidated, to understand if and how ERK3 can be used as a potential biomarker or therapeutic target in BC.

**No conflict of interest.**

**139** (PB129)  
**The anion channel GPR89 is a novel oncogene associated with tumour specific dependency in breast cancer**

R. Ferro<sup>1</sup>, A. Carroll<sup>1</sup>, A. Mendes-Pereira<sup>2</sup>, V. Reen<sup>2</sup>, I. Roxanis<sup>1</sup>, S. Annunziato<sup>3</sup>, J. Jonkers<sup>3</sup>, N. Liv<sup>4</sup>, J. Alexander<sup>1</sup>, J. Quist<sup>2</sup>, M. Pardo<sup>5</sup>, T.I. Roumeliotis<sup>5</sup>, J.S. Choudhary<sup>5</sup>, D. Weekes<sup>1</sup>, P. Marra<sup>2</sup>, R. Natrajan<sup>1</sup>, A. Grigoriadis<sup>2</sup>, S. Haider<sup>1</sup>, C.J. Lord<sup>1</sup>, A.J. Tutt<sup>1</sup>. <sup>1</sup>Institute of Cancer Research, The Breast Cancer Now Toby Robins Research Centre, London, United Kingdom; <sup>2</sup>King's College London, The Breast Cancer Now Research Unit, London, United Kingdom; <sup>3</sup>The Netherlands Cancer Institute, Division of Molecular Pathology, Amsterdam, Netherlands; <sup>4</sup>University Medical Centre Utrecht, Centre for Molecular Medicine, Utrecht, Netherlands; <sup>5</sup>Institute of Cancer Research, Functional Proteomics, London, United Kingdom

**Background:** Identification of targetable biology in breast cancer is an unmet need, particularly for triple negative breast cancer (TNBC) where patient outcome is poor and there are few clinically approved targeted therapies. Here, we identify the anion channel GPR89, to be a novel breast cancer oncogene relevant in TNBC and other breast cancer subtypes.

**Materials and Methods:** We analyzed GPR89 subcellular localization using immunofluorescence, subcellular fractionation, and electro-microscopy techniques. We developed reporter cell lines to determine the pH of the endoplasmic reticulum (ER) and used assays to define ion homeostasis. We used siRNA- shRNA- and CRISPRn- mediated gene perturbation to determine the function of GPR89 in malignant and non-malignant cells and breast cancer organoids. We used a genetically engineered mouse model of breast cancer to study the effects of GPR89 on tumor development *in vivo* and mass spectrometry to analyze GPR89 associated tumor proteomes and the GPR89 interactome.

**Results:** We found that whilst GPR89 is localized in the Golgi apparatus in non-malignant cells, localization extends to the ER in breast tumor cells. Tumor cells with ER localization also displayed addition to GPR89, whereas those with Golgi-only expression did not. In delineating the underlying biology of this relationship, we found that MYC activation changes the localization of GPR89 from Golgi-only to Golgi plus ER. When located in the ER, GPR89 modulated ER luminal pH and facilitated the unfolded protein response, limiting the otherwise deleterious effects on cell fitness of MYC-driven ER stress. Using electron microscopy, we also found that GPR89 is localized to the ER-side of mitochondria associated membranes in tumor cells, where it interacts with the voltage dependent anion channel VDAC2 and drives pro-tumor fitness by rewiring the metabolism towards glycolysis. Finally, we found that GPR89 overexpression accelerates TNBC tumorigenesis in murine mammary tumors with ectopic expression of *Myc*, suggesting that GPR89 facilitates *Myc*-driven oncogenesis.

**Conclusions:** The voltage-dependent anion channel GPR89 is a novel breast cancer oncogene that co-operates with *Myc* to support tumorigenesis. Selective GPR89 dependency is associated with extended localization of GPR89 to the ER, revealing a novel drug target and potential patient selection biomarker.

**No conflict of interest.**

**27 October 2022**

**10:00–17:00**

**POSTER SESSION**

**Apoptosis inducers**

**140** (PB020)  
**Inhibition of Fas Receptor Endocytosis Sensitizes Cancer Cells to Fas-induced Apoptosis**

C. Kural<sup>1</sup>, M. Kural<sup>2</sup>, L. Niklason<sup>2</sup>. <sup>1</sup>Ohio State University, Physics, Columbus, USA; <sup>2</sup>Yale School of Medicine, Anesthesiology, New Haven, USA

Fas (CD95/APO-1) is a transmembrane death receptor that transduces apoptotic signals upon binding to its ligand and assembling into a death-inducing signaling complex (DISC). Intracellular trafficking of Fas receptors, including recycling from endosomes to the plasma membrane, plays a vital role in ligand-induced assembly of DISC. Although Fas is highly expressed in tumor cells, insufficient expression of these receptors on the cell surface makes cancer cells insensitive to the Fas-induced apoptosis. Here we show that inhibition of endocytosis increases the formation of Fas microaggregates on the plasma membrane and sensitizes cancer cells to Fas-induced

apoptosis. We have identified a clinically used vasodilator, Fasudil, that slows down endocytosis by increasing plasma membrane tension. Fasudil enhanced apoptosis in cancerous cells when combined with exogenous soluble Fas ligand (FasL), whereas the synergistic effect was substantially weaker in nonmalignant cells. Additionally, the FasL and Fasudil combination prevented glioblastoma cell growth in embryonic stem cell-derived brain organoids and induced tumor regression in a xenograft U87 tumor model in nude mice. Our results demonstrate that FasL treatment has strong potential as an apoptosis-directed cancer therapy when the formation of Fas microaggregates is augmented by slowing down endocytosis dynamics.

#### Conflict of interest:

Other Substantive Relationships: Laura Niklason is a founder, shareholder, President, and CEO of Humacyte, Inc and serves on Humacyte's Board of Directors. Mehmet Kural is shareholder and employee of Humacyte, Inc.

#### 141 (PB021)

##### Novel iron-mediated cell death (Ferroptosis) inducer, HSB-1216, suppress acute myeloid leukemia growth

S. Kharbanda<sup>1</sup>, S. Liu<sup>1</sup>, S. Tiwari<sup>2</sup>, A. Mohammad<sup>2</sup>, E. Weisberg<sup>1</sup>, H. Singh<sup>2</sup>, R. Stone<sup>1</sup>. <sup>1</sup>Dana Farber Cancer Institute, Medical Oncology, Boston, MA, USA; <sup>2</sup>Indian Institute of Technology-Delhi, Biomedical Engineering, New Delhi, India

Acute myeloid leukemia (AML) is a heterogeneous and intrinsically resistant myeloid stem cell neoplasm, occurring in about 14 000 patients in the US annually. AML is characterized by the unbridled proliferation of myeloid progenitor cells and a block in normal differentiation.

Unfortunately, despite recent advances in the treatment, the prognosis is poor for almost all older adults and half of patients under age 60. Thus, novel effective therapies are urgently needed. Leukemic stem cells (LSCs) represent a subset of the leukemic cell population contributing to leukemia relapse and are relatively refractory to conventional treatments. Studies have shown that Salinomycin selectively kills stem cells. Salinomycin activated iron-mediated cell death (FERROPTOSIS) and leads to production of reactive oxygen species (ROS). To reduce toxicity as well as to achieve slow and sustained delivery of Salinomycin, we have generated novel biodegradable QUATRAMERTM polymeric nanoparticles (HSB-1216) (Hillstream Biopharma Inc.) that permits intracellular delivery of this agent. Treatment of human AML cell line MOLM-14 with HSB-1216 was associated with significant cell death (IC50 of 0.5  $\mu$ M). Diverse AML cell lines including FLT-ITD-positive AML; p53-mutant positive AML; NRAS-mutant AML [Mv4-11; HL-60; Kasumi, SKNO-1, KG-1, MOLM-13, NB4, THP-1, OCI-AML-3] were similarly sensitive to HSB-1216 (IC50 between 0.25 to 2.0  $\mu$ M; ROS-dependent killing). Colony assays with these cell lines demonstrated that HSB-1216 significantly decreases clonogenic survival of AML cells. HSB-1216 potently kills both Venetoclax-resistant and FLT-3-inhibitor-resistant AML cell lines. Moreover, the combination of HSB-1216 and decitabine synergistically inhibits the growth of AML cells. The data support the efficacy of HSB-1216 as an anti-leukemic at non-hemotoxic concentrations. Taken together, these results demonstrate an effective method for sustained delivery of Salinomycin, a potent leukemic stem cell inhibitor and highlight its potential for the treatment of R/R AML.

#### Conflict of interest:

Ownership: Equity ownership in Hillstream Biopharma Inc  
Advisory Board: SAB member

#### 142 (PB022)

##### Loss of SALL2 in colorectal cancer correlates with Wnt pathway activation, a new mechanism involving SALL2-dependent AXIN2 transcriptional regulation.

A. Quiroz<sup>1</sup>, C. Mardones<sup>1</sup>, J. Navarrete<sup>1</sup>, V. Fica<sup>2</sup>, A. Salas<sup>2</sup>, M. Oscare<sup>3</sup>, C. Delgado<sup>4</sup>, A. Castro<sup>1</sup>, R. Pincheira<sup>1</sup>. <sup>1</sup>Universidad de Concepción, Bioquímica y Biología Molecular, Concepción, Chile; <sup>2</sup>Universidad de Concepción, Farmacología, Concepción, Chile; <sup>3</sup>Universidad de Concepción, Coloproctología, Concepción, Chile; <sup>4</sup>Hospital Guillermo Grant Benavente, Anatomía Patológica, Concepción, Chile

**Background:** SALL2 is a developmental transcription factor involved in the regulation of cell proliferation, migration, and survival. Massive data analyses of cancer versus normal tissues indicate that SALL2 mRNA is significantly decreased in colorectal cancer (CRC), a cancer type characterized by hyperactivation of the Wnt pathway. Interestingly, our previous ChIP-seq analyses suggested that SALL2 regulates genes associated with the Wnt pathway, including the negative regulator AXIN2. Currently, SALL2 function

and its relationship with the Wnt/ $\beta$ -catenin pathway in colorectal cancer is unknown.

**Material and Methods:** SALL2 expression and markers of proliferation (Ki67) and disease progression ( $\beta$ -catenin) were evaluated in a tissue array of 130 human samples from Guillermo Grant Benavente's Hospital by immunohistochemistry. Several CRC cell models with gain and loss of SALL2 function and a HEK293 doxycycline SALL2 inducible model were used to characterize the relationship between SALL2 and the Wnt pathway. The  $\beta$ -catenin activity was evaluated by immunofluorescence and subcellular fractionation experiments. The effect of SALL2 on AXIN2 transcriptional activity was evaluated by qPCR, luciferase reporter, and Chromatin immunoprecipitation assays. Finally, the apoptotic response of CRC cells was measured using apoptotic markers expression and Annexin-V/Iodide propidium flow cytometry assay.

**Results:** Immunohistochemistry showed that SALL2 expresses in normal colon epithelium and the stroma, decreases in adenoma, and is absent in CRC. Besides, the nuclear SALL2 expression decreases during progression to CRC, and the absence of SALL2 in CRC correlates with  $\beta$ -catenin in the migratory front. These results were confirmed by subcellular fractionation experiments. SALL2<sup>-/-</sup> (SW480, HT29, and CCD-841-CoN) compared to SALL2<sup>+/+</sup> models showed higher levels of nuclear  $\beta$ -catenin, suggesting that SALL2 inhibits the Wnt pathway. Consistently, a positive correlation was found between SALL2 expression and the expression of AXIN2, a negative Wnt pathway regulator. In addition, doxycycline-dependent SALL2 induction in HEK293 SALL2<sup>-/-</sup> cells increased the AXIN2 promoter activity, suggesting a transcriptional regulation by SALL2. Finally, we showed that the SALL2-AXIN2 axis is necessary for the XAV939-induced apoptosis of SW480 cells. XAV939 is a potent, small-molecule inhibitor of the Wnt pathway.

**Conclusions:** We demonstrated that SALL2 expresses in the normal colon epithelium and stroma, but its expression decreases during CRC progression. Besides, SALL2 suppressed Wnt/ $\beta$ -catenin signaling by increasing AXIN2 transcription. Since AXIN2 is a negative regulator of the Wnt pathway, loss of SALL2 could contribute to CRC progression and therapy response.

No conflict of interest.

#### 143 (PB023)

##### Features of poorly primed apoptotic subpopulations identified using functional measurements of apoptotic priming and multiplexed immunofluorescence on single cells

E. Lecky<sup>1</sup>, A. Mukerji<sup>1</sup>, R. German<sup>1</sup>, G. Stone<sup>1</sup>, J.R. Lin<sup>2</sup>, K. McQueeny<sup>1</sup>, K. Ng<sup>1</sup>, E. Sicsinska<sup>1</sup>, P. Sorger<sup>2</sup>, A. Letai<sup>1</sup>, P. Bholra<sup>1</sup>. <sup>1</sup>Dana Farber Cancer Institute, Medical Oncology, Boston, MA, USA; <sup>2</sup>Harvard Medical School, Systems Biology, Boston, MA, USA

A proposed reason for resistance or relapse following chemotherapy are pre-existing populations of tumor cells that are relatively insensitive to cell death. The purpose of this study is to identify molecular features of pre-treatment tumor cells that are relatively insensitive for apoptosis. Performing both phenotypic apoptotic measurements and multiplexed molecular measurements on the same cancer cell with single-cell resolution is an appealing strategy to identify pre-existing features of cells that are poorly primed for apoptosis. Nonetheless, functional measurement of apoptosis and subsequent multiplexed molecular measurement on the same single cell is challenging owing to the proteases and nucleases that are activated during apoptosis.

Here, we develop and validate real-time BH3 profiling (RT-BP), a functional and live single cell measurement of pre-treatment apoptotic sensitivity that occurs upstream of apoptotic protease and nuclease activation. On the same single cells, we perform Cycling Immunofluorescence (CyCIF), which enables multiplexed immunofluorescence of more than 30 proteins.

Using cultured cells, and acute cultures of colon patient derived xenograft (PDX) models, we identify Bak protein expression as a univariate correlate of apoptotic priming and find that subpopulations which are poorly primed for apoptosis may correspond to specific stages of the cell cycle. In colon PDX models, we identify features of subpopulations that are poorly primed for apoptosis which may be targeted by pre-clinical therapeutics. Finally, we develop and validate linear and random forest models of single cell apoptotic sensitivity based on multiplexed immunofluorescence measurements.

These results indicate that there are several non-genetic features of tumor subpopulations that are poorly primed for apoptosis. We anticipate that our technology can be broadly applied to primary human tumors and can potentially be used to develop therapeutic strategies to kill subpopulations that are poorly primed for apoptosis.

**Conflict of interest:**

Ownership: PKS has equity in Glencoe Software, Applied Biomath, and RareCyte Inc. AL is an equity holder of Flash Therapeutics. Advisory Board: PKS is a member of the SAB or Board of Directors of Glencoe Software, Applied Biomath, and RareCyte Inc. PKS is also a member of the SAB of NanoString. PKS is a consultant for Montai Health and Merck. A.L. has consulted for AbbVie, Novartis, and Astra Zeneca. AL is an advisor for Dialectic Therapeutics, Zentalis Pharmaceuticals, and Anji Onco. KN has consulted for or advised Seattle Genetics, Array Biopharma, BiomX, X-Biotix Therapeutics, Bicara, Bayer, Lilly, and Tarrex Biopharma. Corporate-sponsored Research: A.L. has received research support from AbbVie, Novartis, and Astra Zeneca. KN has received research funding from Pharmavite, Evergrande Group, Revolution Medicines, Janssen, Genentech/Roche, Gilead Sciences, Celgene, Trovogene, and Tarrex Biopharma.

**POSTER SESSION****Combination Therapies**

144

(PB024)

**Combination treatment with EGFR inhibitors and doxorubicin synergistically inhibits proliferation of MDA-MB 231 breast cancer cells**

B. Abrahams<sup>1</sup>, D. Hiss<sup>2</sup>. <sup>1</sup>University of the Free State, Basic Medical Sciences, Bloemfontein, South Africa; <sup>2</sup>University of the Western Cape, Medical Biosciences, Cape Town, South Africa

**Background:** The activation of epidermal growth factor receptor (EGFR) and its associated signal transduction pathways play an important role in regulating cell proliferation and survival. EGFR is also often overexpressed in triple negative breast cancer (TNBC), an aggressive cancer with the poor prognosis due to the lack of effective treatments and a higher chance of recurrence. To examine the potential for combination treatment for TNBC, in this study we investigated the synergistic potential of EGFR inhibitor (EGFRi) with doxorubicin (DOX) in MDA-MB 231 triple negative breast cancer cells, *in vitro*.

**Materials and methods:** In this study we employed the MTT assay to evaluate cytotoxicity of an investigational tyrosine kinase inhibitor EGFRi and DOX individually and in combination at equimolar drug concentrations over 72 h. Apoptosis was confirmed using the Caspase -3/7 assay and Real Time-qPCR was used to quantify the expression levels of EGFR. Statistical analysis for the cytotoxicity assays were performed by non-linear regression analysis to determine the best-fit IC<sub>50</sub> estimates and corresponding 95% confidence intervals (95% CI) for EGFRi and DOX. Drug-drug interactions were assessed using the Combenefit software tool based on Loewe additivity and Bliss independence models and Apoptosis and RT-qPCR using One-way ANOVA.

**Results:** The EGFRi had a greater time-dependent potency than DOX after 24 and 48 h exposure intervals, with IC<sub>50</sub>'s 23.60 μM and 7.05 μM versus 111.40 μM and 344.40 μM, respectively.

The combination treatment of EGFRi with DOX at 72 h demonstrated significant cellular inhibition with a recorded IC<sub>50</sub> of 0.46 μM. Synergistic drug interactions were observed at 48 h and 72 h, with a Bliss synergy score of 44 recorded at 72 h. Apoptosis was induced by EGFRi treatment at concentrations of 1 μM (p = 0.007), 10 μM (p = 0.004) and 100 μM (p = 0.032). DOX induced apoptosis at low concentrations of 0.1 μM (p = 0.008) and 1 μM (p = 0.024). Expression of EGFR was significantly (p < 0.001) downregulated by EGFRi and DOX as well as in 1:1 concentration combination in MDA-MB-231 cells.

**Conclusion:** Our results demonstrate EGFRi's profound potential in eliciting synergistic drug interactions with DOX, that translated in enhanced growth inhibition, apoptosis induction and successful downregulation of EGFR expression in MDA-MB 231 cells. Our findings highlight the importance of multi-agent therapies over single agent monotherapy as a treatment strategy that enhances efficacy while minimizing adverse effects such as drug toxicity and its ability to render useful future clinical paradigms.

**No conflict of interest.**

145

(PB025)

**Vertical inhibition of the MAPK pathway as potential treatment strategy in NRAS-mutant melanoma**

L. Briker<sup>1</sup>, M. Johnson<sup>2</sup>, A. Kamal<sup>2</sup>, R. Dummer<sup>1</sup>, M. Levesque<sup>1</sup>, O. Eichhoff<sup>1</sup>. <sup>1</sup>University Hospital Zurich, Dermatology, Zurich, Switzerland; <sup>2</sup>SpringWorks Therapeutics, Translational Sciences, Stamford, Connecticut, USA

**Background:** Metastatic melanoma is the most aggressive form of skin cancer. Worldwide incidences of melanoma continue to rise, ranking melanoma as the sixth most common cancer. A large proportion of melanomas carry mutations in the mitogen-activated protein kinase (MAPK) signaling pathway leading to hyper-activation and proliferation. Driver mutations in BRAF V600(50%) and NRAS Q61(20%) are commonly found. FDA-approved kinase inhibitors that directly target BRAFV600E-mutated tumors have shown dramatic and long-lasting clinical efficacy, but relapses do occur. By comparison, treatment of tumors containing NRAS mutations have relied on inhibition of the downstream target of NRAS, MEK, as no current therapies that directly target mutant NRAS are available. Although targeting MEK has improved progression-free survival, response rates of only 20% were reported. Collectively, these data suggest that vertical inhibition of the MAPK in NRAS mutated melanoma could result in synergistic benefits. Importantly, proof of concept experiments using the pan-RAF dimer inhibitor lifirafenib and the selective MEK1/2 inhibitor mirdametinin have previously been shown to increase antitumor activity in RAS-mutated solid tumors.

**Material and methods:** The combinatorial effects of mirdametinin with the pan-RAF dimer inhibitor lifirafenib or BGB-3245 were evaluated in a cohort of 14 primary and patient-derived melanoma cell lines harboring NRAS Q61 mutations. After treatment addition, two-dimensional combination effects were assessed and kinase and target gene inhibition were evaluated. To correlate the findings from these *in vitro* cultures, PDX mouse models were subsequently tested for effects on tumor inhibition and response duration after combination therapy with pan-RAF/MEK inhibitors.

**Results:** Results from this study showed significant therapeutic effects on NRAS Q61 mutated melanoma cell lines through combination of mirdametinin with either pan-RAF inhibitor both *in vitro* and *in vivo*. Vertical inhibition through combination therapy with the MEK and RAF inhibitors resulted in greater inhibition of MAPK pathway activity compared to either monotherapy alone. In addition, the inhibitory effect of the newly developed pan-RAF inhibitor BGB-3245 was greater compared to lifirafenib when used as a single agent. Correlative *in vivo* studies are currently underway. Strikingly, preliminary observations from the *in vivo* studies suggest that the combination of panBRAF inhibitors with a MEK inhibitor prolonged the duration of response *in vivo*.

**Conclusion:** These data support the evaluation of MAPK pathway vertical inhibition through combination of MEK and panRAF inhibitors for treatment of patients with RAS mutations. Lastly, NRAS Q61 may serve as a prospective biomarker for patient stratification in trials assessing the combination of MEK and pan-RAF inhibitors in mutant melanoma.

**Conflict of interest:**

Corporate-sponsored Research: Luzia Briker, Reinhard Dummer, Ossia Eichhoff

146

(PB026)

**The DNA repair pathway as a therapeutic target to synergize with trastuzumab deruxtecan, an anti-HER2 antibody-drug conjugate**

J. Lee<sup>1</sup>, K. Kida<sup>2</sup>, H. Liu<sup>1</sup>, Y.J. Gi<sup>1</sup>, G. Manyam<sup>3</sup>, J. Wang<sup>3</sup>, A. Multani<sup>4</sup>, L. Huo<sup>5</sup>, D. Tripathy<sup>1</sup>, N. Ueno<sup>1</sup>. <sup>1</sup>UT MD Anderson Cancer Center, Breast Medical Oncology, Houston, USA; <sup>2</sup>St. Luke's International Hospital, Breast Surgical Oncology, Tokyo, Japan; <sup>3</sup>UT MD Anderson Cancer Center, Bioinformatics & Comp Biology, Houston, USA; <sup>4</sup>UT MD Anderson Cancer Center, Genetics, Houston, USA; <sup>5</sup>UT MD Anderson Cancer Center, Pathology, Houston, USA

**Background:** Anti-HER2 antibody-drug conjugates (HER2-ADCs) have improved survival outcomes for HER2-overexpressing (HER2+) breast cancer (BC) patients. However, intrinsic or acquired resistance to anti-HER2 therapies remains a clinical challenge for HER2+ metastatic breast cancer (mBC). We sought to identify resistance mechanisms to anti-HER2 therapy and potential novel therapeutic targets to overcome resistance.

**Materials and Methods:** We generated trastuzumab emtansine (T-DM1) or trastuzumab deruxtecan (T-DXd)-resistant SUM190 and HCC1954 HER2 + BC cell lines by continuous treatment. HER2 amplification or over-expression in the original and resistant cell lines was determined using FISH, digital PCR, and Western blotting, and cDNA microarray was used to profile

signaling networks in the resistant cell lines. To identify potential synergistic partners for enhancing the efficacy of T-DXd, we performed non-biased synthetic lethal RNAi screening. We validated combination effects using *in vitro* proliferation assays and tumor assessment in xenograft mouse models. To investigate genetic aberrations after anti-HER2 therapies, we used next-generation sequencing to analyze biopsy samples collected before and after treatment from patients with HER2+ mBC whose disease progressed during anti-HER2 therapy including T-DM1.

**Results:** We found genetic and other alterations such as loss of HER2 gene amplification and protein expression, truncation of the HER2 gene region, and DNA repair or damage pathway activation in our HER2-ADC-resistant HER2+ BC cell lines. The pathway analysis identified the DNA repair pathway as a potential target canonical pathway to enhance the efficacy of T-DXd in HER2-ADC-resistant HER2+ BC cell lines. The combination of T-DXd with ATR inhibitor elimusertib led to significant cell death of the resistant cell lines *in vitro* ( $p < 0.05$ ). Further, the combination of T-DXd with elimusertib induced tumor shrinkage of up to 95% ( $p < 0.01$ ) in T-DM1-resistant xenograft models and significantly reduced tumor growth by up to 75% in T-DXd-resistant xenograft models ( $p < 0.05$ ) compared to single agents.

To further confirm our preclinical findings, we analyzed ten patient tumor samples after anti-HER2 therapy, including T-DM1; we found amplification of DNA repair-related genes (TOP2A, RAD21) and transcription regulators (ZNF217, ZNF703, WHSC1L1, KDM5A) in 2 patients. We also found reduced HER2 gene amplification or protein expression in 4 patients.

**Conclusions:** Our findings demonstrate that the DNA repair pathway contributes to HER2-ADC resistance. Targeting the path (e.g., with ATR inhibitors) can reverse the diminished efficacy of T-DXd in HER2+ mBC preclinical models. Our data support clinical trials combining a T-DXd and ATR inhibitor for patients with HER2+ mBC with HER2-ADC monotherapy resistance (i.e., NCT04704661).

#### Conflict of interest:

Corporate-sponsored Research: Naoto Ueno has received a research grant from Daiichi Sankyo (Tokyo, Japan).

147

(PB027)

#### Combination Therapy with Poly-gamma-glutamic Acid and Anti-PD-1 Results in Synergistic Therapeutic Effects against Cancers

J.C. Choi<sup>1</sup>, K.S. Hahm<sup>1</sup>, D.Y. Lee<sup>1</sup>, Y.C. Park<sup>1</sup>. <sup>1</sup>BL Corporation, Center of Research and Development, Yongin-si, South Korea

**Background:** Combinatorial therapeutic strategies based on innate immunity have the potential to enhance the treatment efficacy of cancer therapies. We have been demonstrated that poly- $\gamma$ -glutamic acid ( $\gamma$ -PGA) has a potent innate immune modulating activities including natural killer cell activation and interferon secretion through Toll-like receptor 4 and may be a useful mean for immunotherapeutic as reported previously. The programmed death protein 1 (PD-1) plays a critical part in downregulating immune responses and limiting immunogenic response in T cells. Here, we report the anti-cancer effects of  $\gamma$ -PGA combined with PD-1 blockade in murine colon adenocarcinoma and murine melanoma.

**Material and methods:** It was performed to evaluate the *in vivo* combinatorial anti-cancer effects by oral administration of  $\gamma$ -PGA and intraperitoneal injection of anti-PD-1 in C57BL/6N mice transplanted with MC38 cell, a colorectal cancer cell. And the another study was carried out to examine the synergistic therapeutic efficacy by  $\gamma$ -PGA and anti-PD-1 against B16F10 melanoma tumor model in mice.

**Results:** Combination therapy with  $\gamma$ -PGA and anti-PD-1 produced significantly longer tumor growth delay than other treatment and almost completely inhibited melanoma tumor growth, and also the improved long-term survival rate was shown compared to  $\gamma$ -PGA or anti-PD-1 alone. Similar experiment was performed in melanoma tumor and the result shows that co-treatment with  $\gamma$ -PGA and anti-PD-1 significantly prolonged survival rate compared with anti-PD-1 alone in MC38 tumor model and dramatically reduced MC38 tumor growth but had no synergistic effect. The results showed that the survival rate of the combinatorial treatment was superior to anti-PD-1 alone.

**Conclusions:** Based on the resistance mechanism of PD-1 blockade with low response rates in many patients,  $\gamma$ -PGA treatment having an innate immune modulating activity combined with anti-PD-1 can induce stronger anti-tumor immunity and destroy the target cancer cells. In this study, oral administration of  $\gamma$ -PGA with intraperitoneal injection of anti-PD-1 dramatically inhibited tumor growth and enhanced the survival rate in MC38 and B16F10 tumor-bearing mice. The study demonstrates that the tumor microenvironment was controlled by administration of  $\gamma$ -PGA, thus results in exertion of immune checkpoint inhibitor. These data provide a strong preclinical evidence for a novel combinatorial therapeutic strategy that can be assessed in prospective clinical trials.

No conflict of interest.

148

(PB028)

#### Combination of CDK12 inhibition and olaparib enhances genomic instability in cancer models

S. Alnemy<sup>1</sup>, N. Rajagopal<sup>2</sup>, P. Perera<sup>1</sup>, R. Shawgo<sup>1</sup>, W. Dworakowski<sup>3</sup>, D. LaPlaca<sup>4</sup>, J. Carulli<sup>1</sup>, C. Chuaqui<sup>4</sup>, S. Hu<sup>1</sup>, D. Moebius<sup>4</sup>, <sup>1</sup>Syros Pharmaceuticals, Discovery Biology, Cambridge, USA; <sup>2</sup>Syros Pharmaceuticals, Computational Biology, Cambridge, USA; <sup>3</sup>Syros Pharmaceuticals, Pharmacology, Cambridge, USA; <sup>4</sup>Syros Pharmaceuticals, Chemistry, Cambridge, USA

**Background:** CDK12 has emerged as an attractive cancer target due to its role in transcription and regulation of DNA repair. It has been proposed that the loss of CDK12 function is synthetic lethal with PARP inhibition. Here, we assessed the combination effect of Compound A, a potent and selective CDK12 inhibitor, with olaparib, a PARP1/2 inhibitor, in both BRCA WT and mutant models.

**Material and Methods:** Cellular assays: p-Ser2, p-Ser5, RNA pol II,  $\gamma$ H2AX, BRCA1 and 53BP1 signals were assessed 24 hrs after compound treatment via immunofluorescence assays. Cell proliferation was determined using Cell Titer Glo after 120–168 hrs compound treatment. Apoptosis was measured by Caspase Glo 3/7 luminescence signal after 24–48 hrs of compound treatment. Cell cycle profile was evaluated with EdU, anti-p-Histone H3 (S10), and FxCycle violet stain using flow cytometry analysis following 24–48 hrs of treatment. Micronuclei formation was measured using Hoechst DNA stain via microscopy after 24–48 hrs. Mouse xenograft: Balb/c mice were implanted subcutaneously with MDA-MB-436 or MDA-MB-468 cells and randomized for treatment with test drug(s) or vehicle when tumors reached 150–200 mm<sup>3</sup>. Mice were dosed BID with Compound A and QD with olaparib as single agent and in combination through oral administration for 4 weeks continuously, after which the mice were observed for 2 weeks.

**Results:** Compound A selectively inhibited Ser2 phosphorylation over Ser5 on PolII CTD, suggesting on-target activity for CDK12. Transcriptional analysis showed that compound A treatment preferentially impacted genes involved in homologous recombination relative to other DNA damage repair pathways. Compound A in combination with olaparib increased DNA damage burden with preferential reduction of BRCA1 recruitment over 53BP1. Compound A demonstrated enhanced cellular growth inhibition and apoptosis when combined with olaparib, in both BRCA WT and mutant cell lines. Combination treatment also increased G2 arrest and micronuclei formation compared to single agent treatment. *In vivo*, combination treatment either slowed tumor growth or resulted in regression in BRCA WT and mutant CDX models, respectively, compared to single agent.

**Conclusions:** Compound A showed enhanced combination effect with a PARP inhibitor, olaparib, *in vitro*, with no difference in sensitivity between BRCA mutant or BRCA WT cell lines. However, *in vivo* results showed increased effects in BRCA mutant models compared to BRCA WT. These data suggest that the mechanism by which Compound A sensitizes cancer cells to olaparib is primarily through the accumulation of unresolved DNA damage, leading to G2/M arrest, genomic instability, and subsequent apoptosis. This supports the rationale to test combinations of Compound A and PARPi in a clinical setting.

#### Conflict of interest:

Ownership: Syros Pharmaceuticals

Board of Directors: Peter Wirth, SRINIVAS AKKARAJU, M.D., PH.D., MARK ALLES, DEBORAH DUNSIRE, M.D., S. GAIL ECKHARDT, M.D., MARSHA H. FANUCCI, AMIR NASHAT, PH.D., PHILLIP SHARP, PH.D., NANCY SIMONIAN, M.D., RICHARD A. YOUNG, PH.D.

149

(PB029)

#### Omomyc as a novel therapeutic strategy against metastatic triple-negative breast cancer, alone and in combination with the standard of care

F. Giuntini<sup>1</sup>, D. Massó-Vallés<sup>2</sup>, Í. González-Larreategui<sup>1</sup>, H. Thabusso<sup>2</sup>, J. Kaur<sup>1</sup>, M. Zacarías-Fluck<sup>1</sup>, S. Casacuberta-Serra<sup>2</sup>, S. Martínez-Martín<sup>2</sup>, L. Foradada-Felip<sup>2</sup>, E. Serrano<sup>1</sup>, G. Martín-Fernández<sup>1</sup>, V. Castillo Cano<sup>2</sup>, S. López-Estévez<sup>2</sup>, V. Serra<sup>1</sup>, J. Whitfield<sup>1</sup>, M.E. Beaulieu<sup>2</sup>, L. Soucek<sup>1,2</sup>. <sup>1</sup>Vall d'Hebron Institute of Oncology VHIO, Preclinical & Translational Research Program, Barcelona, Spain; <sup>2</sup>Peptomyc SL, Peptomyc SL, Barcelona, Spain

**Background:** Triple-Negative Breast Cancer (TNBC) represents 15–20% of breast cancers and, despite several advances in treatment options, surgery, radio- and cytotoxic chemotherapy are still the norm to delay cancer progression and prolong life. The MYC oncogene is amplified or deregulated

in most cancer types, and indeed in breast cancers. In particular, TNBC has disproportionately elevated MYC as compared to other breast cancers.

Omomyc is a MYC dominant negative that has shown potent antitumor activity in multiple cancer cell lines and mouse models, regardless of their tissue of origin or driver mutations, by impacting on several of the hallmarks of cancer. We recently demonstrated that the Omomyc mini-protein exerts antitumor and antimetastatic activity in metastatic breast cancer models *in vitro* and *in vivo*.

Importantly, Omomyc is currently being investigated in a Phase I/IIa clinical trial as monotherapy, however the next step will be to explore its efficacy in combination with the standard of care. In the case of TNBC, current first and second line therapies include cytotoxic chemotherapy (anthracyclines and taxanes), immune checkpoint blockade (for tumors with elevated PD-L1 expression) and PARP inhibitors (for tumors with BRCA1/2 mutations). There is strong evidence that elevated MYC levels are responsible for the resistance to several therapies, including but not limited to PARP inhibitors, chemotherapy and immunotherapy.

**Material and methods:** Microarray analysis was performed on the TNBC cell line MDA-MB-231 treated with the Omomyc mini-protein to identify its effect on gene expression. Additionally, a set of TNBC cell lines were characterized in terms of their response to Omomyc alone, and in combination with Olaparib (PARPi) or Paclitaxel (a taxane) through synergy matrices.

**Results:** Here, we show that Omomyc downregulates programs involved in homologous recombination (HR) and BRCA1/2 deficiency. At the gene level, treatment with Omomyc significantly reduces the expression of RAD51, PARP1 and other DDR- and HR-related genes in MDA-MB-231. Also, we found synergistic efficacy data of Omomyc combined with Olaparib or Paclitaxel *in vitro* in multiple TNBC cells. We plan to select the most promising cell lines to further study these combination therapies in mice carrying cell-derived xenografts and eventually try them in patient-derived xenografts.

**Conclusions:** Taken together, these experiments broaden our understanding of the role of MYC in TNBC and the mechanism of action of the Omomyc mini-protein, while also validating its efficacy as monotherapy or combined with current standard of care treatments, providing the rationale for the use of these potential combinations in a clinical setting.

#### Conflict of interest:

Ownership: L. Soucek and M. Beaulieu is a cofounder and shareholder of Peptomyc, a company focused on developing Myc inhibitors for cancer treatment.

Other Substantive Relationships: M.F. Zacarias Fluck reports other from Peptomyc S.L. outside the submitted work. L. Foradada reports personal fees from Peptomyc S.L. during the conduct of the study personal fees from Peptomyc S.L. outside the submitted work. S. Martínez-Martín reports personal fees from Peptomyc S.L. during the conduct of the study personal fees from Peptomyc S.L. outside the submitted work. S. Casacuberta-Serra reports personal fees from Peptomyc S.L. during the conduct of the study personal fees from Peptomyc S.L. outside the submitted work in addition, S. Casacuberta-Serra has a patent to EP19382194 pending. V. Castillo Cano reports other from Peptomyc S.L. outside the submitted work. S. López-Estévez reports personal fees from Peptomyc SL during the conduct of the study personal fees from Peptomyc S.L. outside the submitted work. J.R. Whitfield reports Shareholder in Peptomyc. L. Soucek has a patent to EP13382167.8 issued. No other disclosures were reported.

150

(PB030)

#### MEKi-based combination strategies for targeting KRAS-driven cancer

K. Kostyrko<sup>1</sup>, M. Hinkel<sup>1</sup>, P.E. Traexler<sup>1</sup>, D. Arnold<sup>1</sup>, G. Melo-Zaininger<sup>1</sup>, D. Gerlach<sup>1</sup>, R. Ruzicka<sup>1</sup>, R. Jacob<sup>1</sup>, A. Baum<sup>1</sup>, H. Lu<sup>2</sup>, C.P. Vellano<sup>2</sup>, J.R. Marszalek<sup>2</sup>, T.P. Heffernan<sup>2</sup>, U. Tontsch-Grunt<sup>1</sup>, M.H. Hofmann<sup>1</sup>.  
<sup>1</sup>Boehringer Ingelheim RCV GmbH & Co KG, Cancer Research, Vienna, Austria; <sup>2</sup>The University of Texas MD Anderson Cancer Center, TRACTION Platform, Houston, USA

**Background:** KRAS is one of the most frequently mutated oncogenes in human cancer. Recent successes with KRAS G12C-specific inhibitors are changing the treatment paradigm in this subset of cancer patients. An alternative strategy is targeting downstream KRAS effectors, such as MEK. However, MEK inhibitors have historically proven unsuccessful as monotherapy in KRAS mutant cancers, highlighting the need for combinatory approaches.

One possibility is the combination of MEK and SOS1 inhibition, which may overcome adaptive resistance to MEKi by blocking SOS1-mediated reactivation of MAPK signaling. Another promising approach is to combine MEKi with inhibitors of Bromodomain and extra-terminal (BET) proteins. While BET inhibitors exhibit broad anti-tumor activity in preclinical cancer models, BETi monotherapy demonstrated only moderate clinical activity.

Resistance to BETi has been, at least partially, attributed to MAPK pathway upregulation, suggesting that a combination with MEKi may help to overcome resistance.

**Material and Methods:** Here, we present BI 3011441, a potent and selective inhibitor of human MEK1/2. Using *in vitro* assays, we compare BI 3011441 to other clinical stage MEK inhibitors. We also combine BI 3011441 with BI 1701963 and BI 894999 - two potent, selective, and orally bioavailable inhibitors of SOS1 and BET, respectively. Both combinations are tested *in vitro* and/or *in vivo* across a panel of KRAS mutant pancreatic ductal adenocarcinoma (PDAC), colorectal cancer (CRC) and non-small cell lung cancer (NSCLC) models.

**Results:** BI 3011441 efficiently inhibits ERK phosphorylation in cell-based assays and demonstrates the strongest *in vitro* growth inhibition in a panel of BRAF or KRAS mutant cell lines among the MEK inhibitors tested. *In vivo*, BI 3011441 leads to a dose-dependent modulation of MAPK pathway, which translates into anti-tumor activity in xenograft models of KRAS-driven cancer.

The combination of BI 3011441 with SOS1i BI 1701963 synergistically decreases MAPK signaling resulting in enhanced efficacy in xenograft models, including NSCLC, CRC and PDAC. In NSCLC models this combination results in 10% of partial responses (PR) and 70% of stable disease (SD) as defined by modified Response Evaluation Criteria In Solid Tumors (mRECIST). In PDAC and CRC models the combination leads to 30% and 43% of SD, respectively.

When combined with clinically relevant concentrations of BETi BI 894999, BI 3011441 strongly decreases *in vitro* proliferation and induces apoptosis in KRAS mutant cancer cells. Synergy is observed in 17 out of 44 cell lines across different indications and harboring different KRAS mutations.

**Conclusions:** In summary, we show that combining BI 3011441 with SOS1 or BET inhibitors may lead to improved responses in KRAS mutant tumors, likely by circumventing MAPK pathway-related adaptive resistance.

#### Conflict of interest:

Other Substantive Relationships: The authors are either employees or have financial relationships with Boehringer Ingelheim.

151

(PB031)

#### Combination therapy with decitabine and olaparib in poly(ADP-ribose) polymerase inhibitor (PARPi) resistant high grade serous ovarian cancer

A. Shafa<sup>1</sup>, X. Hou<sup>2</sup>, L. Wang<sup>3</sup>, S.J. Weroha<sup>2</sup>. <sup>1</sup>Mayo Clinic, Gynecologic Oncology, Rochester, USA; <sup>2</sup>Mayo Clinic, Oncology, Rochester, USA; <sup>3</sup>Mayo Clinic, Molecular Pharmacology and Experimental Therapeutics, Rochester, USA

**Background:** Recurrent high grade serous ovarian cancer (HGSOC) is incurable and lethal. Therefore, novel drug combinations are critically needed for this patient population. DNA methyltransferase inhibitors (DNMTi) can cause DNA damage, which activates poly(ADP-ribose) polymerase (PARP) and leads to PARP trapping. Additionally, DNMTi are incorporated into replicating DNA, which causes DNMT-DNA adducts that are then degraded. Therefore, the novel drug combination of DNMTi decitabine and PARP inhibitor (PARPi) olaparib were tested in preclinical HGSOC models.

**Materials and methods:** RNA sequencing was performed on 300 patient samples of HGSOC to determine high versus low expression of DNA methyltransferases (DNMTs). Twenty-nine samples were selected for *ex vivo* 3D culture testing with titrating concentrations of DNMTi decitabine and PARPi olaparib. In preparation for *in vivo* studies, the maximum tolerated dose was determined.

**Results:** RNA sequencing demonstrated varying expression of DNMT1, DNMT3A, and DNMT3B. In *ex vivo* 3D culture, about 10% (3/29) of the models demonstrated a synergistic drug effect of decitabine and olaparib. Of these three, one was known to be PARPi resistant in animal studies, and thus was selected for patient-derived xenograft (PDX) *in vivo* studies. Prior to pursuing PDX *in vivo* studies, maximum tolerated dose testing was performed, which demonstrated that female SCID-bg mice tolerated the drug combination with less than 20% weight loss and overall good health condition scores.

**Conclusions:** Synergy was observed in a subset of HGSOC tumors by *ex vivo* drug testing. Importantly, this combination has activity in a PARPi-resistant, BRCA wildtype, homologous recombination proficient HGSOC tumor, which represents the genotypic and phenotypic characteristics of most HGSOCs. This drug combination was also well-tolerated in female SCID mice.

**No conflict of interest.**

152 (PB032)  
**NUAK1 directly induces Akt signaling and substrate specificity, promoting cancer cell survival**

M. Palma<sup>1</sup>, E. Riffo<sup>1</sup>, V. Coliboro<sup>1</sup>, J.L. Gutierrez<sup>1</sup>, R. Pincheira<sup>1</sup>, A. Castro<sup>1</sup>.  
<sup>1</sup>Universidad de Concepción, Biochemistry and Molecular Biology, Concepción, Chile

**Background:** NUAK1 is a serine/threonine kinase member of the AMPK $\alpha$ -family, whose high expression is associated with poor prognosis. However, NUAK1 regulation and functions in cancer remain poorly characterized. Here, we investigated NUAK1's role in cancer signaling.

**Materials and Methods:** We performed a bioinformatic analysis of TCGA to study the correlation between NUAK1 expression and the expression of EGFR and Akt phosphorylation in several cancers. We mainly performed the studies on breast and colon cancer cell lines. Pharmacological or shRNA-dependent inhibition of NUAK1 demonstrated its role in the EGFR and insulin-dependent signaling. *In vitro* kinase assays were performed to demonstrate the direct phosphorylation of Akt by NUAK1, and proximity ligation assays demonstrated the association of NUAK1 with Akt in cancer cells. Cell fractionation and immunofluorescence studies analyzed NUAK1 subcellular localization, and qPCR studies demonstrated its role in the Akt/FOXO1/3a axis. We used 2D and 3D cultures for cell survival studies and monitored cell death using commercial kits.

**Results:** Based on public TCGA data, we reported that NUAK1 expression correlates with EGFR expression and the Akt phosphorylation at Ser-473 in several cancers. Using pharmacological inhibition and shRNA-dependent silencing, we found that NUAK1 activates the Akt signaling, regulating FOXO1/3a and GSK3 $\beta$  phosphorylation but not TSC2 phosphorylation. Mechanistically, NUAK1 interacts with Akt and directly phosphorylates it at Ser-473. Comparing NUAK1 and mTOR inhibition revealed an Akt-dynamic activation and -substrate specificity depending on its phosphorylation by NUAK1 or mTORC2. The Akt-substrate specificity could be directly associated with NUAK1 co-localization with early endosomes. Functionally, the NUAK1/Akt/FOXO1/3a axis reduced p21CIP1 and p27KIP1 expression but induced FoxM1 expression. Additionally, our study identified that NUAK1 promotes cancer cell survival in a growth factor-dependent manner, and its inhibition potentiates the effect of MK-2206, an Akt inhibitor.

**Conclusion:** We demonstrated that NUAK1, in contrast to other AMPK-related members, regulates cancer signaling via direct Akt phosphorylation. Thus, targeting NUAK1, either alone or combined with Akt inhibitors, may be effective in cancers with hyperactivated Akt signaling.

**Funding:** ANID/Fondecyt 1191172 and 1201215

No conflict of interest.

153 (PB033)  
**Using Tipifarnib to prevent resistance to targeted therapies in oncogene-addicted tumors**

C. Delahaye<sup>1</sup>, M. Brachais<sup>1</sup>, R. Gence<sup>1</sup>, A. Doussine<sup>1</sup>, S. Figarol<sup>1</sup>, E. Clermont<sup>2</sup>, A. Casanova<sup>2</sup>, A. Pradines<sup>2</sup>, J. Mazières<sup>3</sup>, G. Favre<sup>1</sup>, O. Calvayrac<sup>1</sup>.  
<sup>1</sup>Centre de Recherches en Cancérologie de Toulouse-Inserm- CNRS- Université de Toulouse- Université Toulouse III-Paul Sabatier- Toulouse- France, Cell Signalling- Oncogenesis and Therapeutics SIGNATHER, Toulouse, France; <sup>2</sup>Institut Universitaire du Cancer de Toulouse IUCT-OncoPole, Institut Claudius Regaud- Laboratory of Medical Biology and Oncogenetics, Toulouse, France; <sup>3</sup>Institut Universitaire du Cancer de Toulouse IUCT-OncoPole, Toulouse University Hospital- CHU- Hôpital Larrey, Toulouse, France

**Purpose:** Targeted therapies can provide impressive responses in oncogene-addicted tumors, but are almost never curative due to the inevitable emergence of resistance. In this context, Drug-Tolerant Cells (DTC) have emerged as a new relevant concept which could explain the very first step of drug resistance, particularly in non-small cell lung cancers (NSCLC) and metastatic melanoma. We recently discovered that the farnesyltransferase inhibitor (FTI) tipifarnib can prevent the emergence of resistance to tyrosine kinase inhibitors in EGFR-mutant NSCLC *in vitro* and *in vivo*, by interfering with several key factors of the adaptive response, such as Rho GTPases and cell division-related proteins (Figarol *et al.*, BioRxiv 2022). Here, we report that co-treatment with tipifarnib can also prevent relapse to targeted therapies in other oncogenic settings such as KRAS-G12C and ALK-translocated NSCLC or BRAF-mutant melanoma, suggesting a common vulnerability of DTC to the FTI tipifarnib.

**Experimental design:** H3122 (EML4-ALK NSCLC), H23 and Calu-1 (KRAS-G12C NSCLC), and A375 (BRAF-V600E metastatic melanoma) cell lines were treated with 1  $\mu$ M lorlatinib, sotorasib or dabrafenib, respectively,

alone or in combination with 1  $\mu$ M tipifarnib. Cells were previously transduced by the FUCCI (fluorescence ubiquitination cell cycle indicator) system to monitor the cell cycle dynamics in real time during the adaptive response. Signalling pathways affected by the treatments were determined by Western Blot. *In vivo* studies using KRAS-G12C- and EML4-ALK-derived NSCLC PDx are ongoing.

**Results:** All the cell lines tested displayed an initial response to their corresponding monotherapy, characterized by an accumulation in G1 within the first 48 h, followed by a more or less intense cell death depending on the cell line. Similar to what was observed in EGFR-TKI-treated NSCLC, some cells, referred to as "early escapers," could escape G1 and progress through S/G2 during the initial response phase, progressively giving rise to resistant proliferative clones. Co-treatment with tipifarnib prevented relapse in all the models tested by impairing mitosis of S/G2 early escapers and promoting apoptosis. As in EGFR-mutant models, response to the different monotherapies invariably involved activation of the p27/pRb pathway, RhoB over-expression, and formation of actin stress fibers, which appeared to be hallmarks of the drug-tolerant state most likely responsible for the susceptibility of DTC to tipifarnib.

**Conclusion:** Our data provide a strong biological rationale for the development of combinations with targeted therapies and tipifarnib in the clinic.

**Conflict of interest:**

Corporate-sponsored Research: Julien Mazieres reports personal fees from Astra Zeneca, BMS, MSD, Novartis, Amgen, and grants from Roche, Astra Zeneca, Pierre Fabre, BMS.

Olivier Calvayrac received sponsored research funding from Kura Oncology.

154 (PB034)  
**Identification of an effective chemotherapy and DNA damage response inhibitor combination for diffuse large b cell lymphoma**

A. Chan<sup>1</sup>, A. Anbuselvan<sup>1</sup>, S.S. Upadhyayula<sup>1</sup>, S. Jemimah<sup>1</sup>, P. Jaynes<sup>1</sup>, M.M. Hoppe<sup>1</sup>, J.D. Wardyn<sup>1</sup>, J. Goh<sup>1</sup>, G. Bertolazzi<sup>2</sup>, M. Foiani<sup>3,4</sup>, M.J. O'Connor<sup>5</sup>, E.K. Chow<sup>1,6,7,8,9,10</sup>, C. Tripodo<sup>2</sup>, A.D. Jayasekharan<sup>1,6,11,12</sup>.  
<sup>1</sup>Cancer Science Institute of Singapore, National University of Singapore, Singapore, Singapore; <sup>2</sup>Tumor Immunology Unit, University of Palermo, Palermo, Italy; <sup>3</sup>FOM, The FIRG Institute of Molecular Oncology, Milan, Italy; <sup>4</sup>Department of Oncology and Hematology-Oncology, University of Milan, Milan, Italy; <sup>5</sup>Oncology R&D, AstraZeneca, Cambridge, UK; <sup>6</sup>NUS Center for Cancer Research N2CR, Yong Loo Lin School of Medicine- National University of Singapore, Singapore, Singapore; <sup>7</sup>KYAN Therapeutics, Singapore, Singapore, Singapore; <sup>8</sup>Department of Pharmacology, Yong Loo Lin School of Medicine- National University of Singapore, Singapore, Singapore; <sup>9</sup>N.1 Institute for Health, National University of Singapore, Singapore, Singapore; <sup>10</sup>Institute for Digital Medicine WisDM, Yong Loo Lin School of Medicine- National University of Singapore, Singapore, Singapore; <sup>11</sup>Department of Medicine, Yong Loo Lin School of Medicine- National University of Singapore, Singapore, Singapore; <sup>12</sup>Department of Haematology-Oncology, National University Cancer Institute- National University Health System, Singapore, Singapore, Cooperative Study Groups

**Background:** Chemotherapy forms the backbone of treatment for Diffuse Large B Cell Lymphoma (DLBCL); however, <~20% of tumors are chemoresistant. Inhibitors of the DNA damage response (DDR) show promise as chemosensitizers. We therefore set up an *in-vitro* screen to identify an optimal chemotherapy-DDR inhibitor (DDRI) combination in a panel of DLBCL cell lines.

**Material and Methods:** To achieve this, we harnessed Quadratic Phenotypic Optimization Platform (QPOP), an experimental-analytic method built to identify potent drug combinations. 6 DDRis (to ATR, ATM, CHK1/2, DNA-PK, WEE1, PARP) and 6 routinely used chemotherapy agents were selected for the screen. After identifying the most effective combination using a cell viability assay, we investigated the mechanism of synergy. We observed pathway activation by western blot; apoptosis by Annexin V staining; and cell cycle disruption by flow cytometry with EdU, Propidium iodide, and phospho-Histone H3 staining. To explore the underlying mechanism of synergy, we performed RNA sequencing.

**Results:** From the combination screen, ATR inhibitor, AZD6738, and chemotherapeutic drug, Gemcitabine (A+G), was the most effective combination across multiple DLBCL cell lines, including Gemcitabine-resistant cell lines. Using two gemcitabine-resistant DLBCL cell lines as models, we investigated the mechanism of A+G synergy. Inhibition of ATR abrogates the G2M checkpoint, causing cells with gemcitabine-induced DNA damage to enter mitosis and die through mitotic catastrophe. We confirmed that the combination reduced cell viability, affected Chk1 phosphorylation,

and promoted apoptosis. However, only a small proportion of cells enter mitosis after A+G treatment and cells were primarily arrested in G1 phase with blockade of entry into S phase. Pathway analysis by RNA seq revealed that several cell-cycle and DNA replication-related pathways were suppressed in the combination setting. Interestingly, the transcriptome of A+G treated cells revealed a reversal of a gene expression signature characteristic of dark zone (DZ) biology. The DZ signature reflects a gene expression program associated with B-cells in the DZ of the germinal centre and is enriched in poorly prognostic DLBCL.

**Conclusions:** Taken together, we have identified a chemotherapy-DDRI drug combination, AZD6738 and Gemcitabine, which is effective in killing DLBCL cells *in-vitro*, including cells that are resistant to Gemcitabine. The mechanism of synergy is not likely to be through mitotic catastrophe, but may potentially involve a cell cycle state reflecting the suppression of a B-cell specific transcriptional program regulating the DZ-LZ transition. Importantly, the reversal of the DZ gene expression signature by the combination indicates its potential utility as a treatment option for these lymphomas that exhibit this poor-prognostic gene signature.

#### Conflict of interest:

Advisory Board: ADJ: Consultancy fees from Turbine Ltd, AstraZeneca, Antengene, Janssen MSD and IQVIA  
Corporate-sponsored Research: ADJ: Research funding from Janssen and AstraZeneca  
Other Substantive Relationships: ADJ: Travel funding from Perkin Elmer

155

(PB035)

#### Derazantinib, an inhibitor of fibroblast growth factor receptors 1–3, increases the efficacy of paclitaxel combined with a VEGFR2-antibody in murine syngeneic tumor models

P. Mcsheehy<sup>1</sup>, M. El-Shemery<sup>1</sup>, L. Kellenberger<sup>2</sup>, H. Lane<sup>1</sup>. <sup>1</sup>Basilea Pharmaceutica International, Cancer Biology, Basel, Switzerland; <sup>2</sup>Basilea Pharmaceutica International, Research, Basel, Switzerland

**Background:** Derazantinib (DZB) is an oral fibroblast growth factor receptor (FGFR) inhibitor with clinical activity in intrahepatic cholangiocarcinoma. DZB is also in a phase-2 trial for gastric cancer (GC), where it is combined with the current standard-of-care (SoC) paclitaxel and the VEGFR2-antibody (Ab), ramucirumab. Kinase assays and cellular and *in vivo* data indicate significant activity of DZB against two other important targets in oncology, CSF1R and VEGFR2. Here, using three different syngeneic tumor models grown orthotopically or subcutaneously in mice, we have explored the efficacy and tolerability of combining DZB with paclitaxel and a murine VEGFR2-Ab.

**Materials and Methods:** Female Balb/c mice were used to host three different models: the breast tumors 4T1 and EMT6 both grown orthotopically in the mammary fat pad, and colon MC38 grown subcutaneously. When the mean tumor size was at least 80 mm<sup>3</sup>, mice were treated with vehicles (po, ip and iv), DZB alone (35 or 75 mg/kg, po, qd), paclitaxel (15 mg/kg, iv, qw) or the VEGFR2-Ab, DC101 (10 mg/kg, ip, 2qw). Treatments continued until individual tumors reached 1500 mm<sup>3</sup>, when mice were culled and tumors ablated for formalin-fixing and paraffin-embedding. Efficacy ( $\Delta T/C$ ) was determined a) by the change in tumor-volume at the day of first culling, and b) median time to 1500 mm<sup>3</sup> to allow longer treatment study in the very fast-growing models of EMT6 and MC38. The 4T1 model was stopped after 3-weeks to allow quantification of metastases by counting lung nodules. The combination interaction was assessed formally as synergy/additivity/antagonism by the Clarke-Combination-Index (CCI). Tolerability was assessed by the %-change in body-weight.

**Results:** MTD studies using non-tumor bearing mice over 3 weeks showed that half the full dose of DZB (35 mg/kg, po, qd) could be combined with the full doses of paclitaxel and DC101 (Triple-combination). In the 4T1 model, the Triple significantly increased efficacy compared to the SoC of paclitaxel-DC101 in the primary tumor ( $\Delta T/C$ s: 0.25 and 0.6 respectively) and also reduced the lung weight and metastases. In the EMT6 model, the Triple was more efficacious than the SoC against the primary tumor ( $\Delta T/C$ s: 0.42 and 0.86 respectively). The CCI for these breast tumor models indicated an additive effect, and the Triple also gave increased efficacy compared to the other two doublets (paclitaxel-DZB and DZB-Ab). The MC38 model is still ongoing. In these models the Triple was well tolerated with mice showing similar final body-weight changes compared to the other groups including the vehicle-group.

**Conclusions:** DZB is well-tolerated when combined with paclitaxel and a VEGFR2-Ab in murine syngeneic models, and shows an additive effect in the orthotopic breast models. These data support the ongoing clinical trial with DZB in GC (FIDES-03, NCT04604132).

No conflict of interest.

Abstracts, 34th EORTC-NCI-AACR Symposium

156

(PB036)

#### KRASG12C Inhibitor, VRTX126 in combination with Tyrosine Kinase Inhibitor, leads to pronounced and effective response in G12C-mutated cancers

U.K. Surampudi<sup>1</sup>, P.K. Bhavar<sup>1</sup>, P.P. Sarma<sup>2</sup>, A.R. Kshirsagar<sup>2</sup>, R. Kar<sup>2</sup>. <sup>1</sup>VRise Therapeutics Inc., Research & Development, Cambridge, USA; <sup>2</sup>VeGen Therapeutics Pvt. Ltd., Research & Development, Hyderabad, India

**Background:** KRASG12C mutation occurs in about 13% of NSCLC, 4% of colorectal and ~2% of patients with other solid tumors. Despite of significant progress made with KRASG12C inhibitors, limited clinical benefit was bestowed in reported data, which is otherwise is expected from these selective agents. Treatment with a KRASG12C inhibitor does lead to initial oncoprotein signaling inhibition but has been reported to be accompanied with reactivation of alternative MAPK pathway, including bypassing inhibition without actually affecting target inactivation. Given the multiple factors leading to acquired resistance reported by this class of inhibitors, co-targeting through a combination of KRASG12C inhibitor with TKIs or other downstream/upstream inhibitors of MAPK pathway is imperative and is expected to provide sustained and more durable response in patients with KRASG12C mutations.

**Methods:** VRTX126, was recently reported as a potent and selective inhibitor of KRASG12C with an IC<sub>50</sub> of 0.7 nM (pERK, H358). Here, we report synergistic effect of VRTX126 with Afatinib (a tyrosine kinase inhibitor) in an MTT based cell viability assay, using 96-well plate platform in a dose response matrix. Additionally, *in vivo* combinability of VRTX126 and Afatinib was ascertained in a Xenograft model of NCI-H358 using Female Balb/c Nude Mice. Protein Western blot analysis and Immunohistochemistry (IHC) for downstream KRAS pathway markers were also determined in cell lysates and tumor samples. Long read sequencing, to understand the mechanistic transcriptomic signature profile and the mechanism of crosstalk of intersecting pathways has also been investigated at both *in vitro* and *in vivo* settings.

**Results:** Dose response matrix in H358 cell lines indicated several fold reduction in IC<sub>50</sub> of Afatinib in combination with VRTX126. VRTX126 (15 mg/kg/QD) with Afatinib (12.5 mg/kg/QD) exhibited significant (>80%) tumor growth inhibition (TGI), indicating a significant reduction in the effective dose of Afatinib when used in combination with VRTX126, in this model. A pronounced suppression of biomarkers (pERK, pS6 and DUSP6) and IHC analysis indicated complete inhibition of KRAS-mediated pathway demonstrating desired downstream signal modulation.

**Conclusions:** *In vitro* study using a combination matrix of VRTX126 and Afatinib indicated synergistic effect leading to a significant dose reduction of TKI which was further confirmed in *in vivo* settings. This paves way for safely combining VRTX126 with multiple precision medicines, including TKIs at significantly lower doses.

No conflict of interest.

158

(PB038)

#### RVU120, a small molecule inhibitor of CDK8/19 kinases, enhances rituximab-driven NK cells-mediated cytotoxicity both in vitro and in vivo

E. Białopiotrowicz-Data<sup>1</sup>, K. Dziedzic<sup>2</sup>, P. Podkalicka<sup>3</sup>, K. Grycuk<sup>2</sup>, A. Golas<sup>3</sup>, I. Dolata<sup>2</sup>, S. Chmielewski<sup>4</sup>, Z. Pilch<sup>5,6,7</sup>, D. Nowis<sup>5,7</sup>, P. Juszczynski<sup>1</sup>, T. Rzymiski<sup>8</sup>. <sup>1</sup>Institute of Hematology and Transfusion Medicine, Department of Experimental Hematology, Warsaw, Poland; <sup>2</sup>Ryvu Therapeutics, Biology, Cracow, Poland; <sup>3</sup>Ryvu Therapeutics, *In vivo* Pharmacology, Cracow, Poland; <sup>4</sup>Ryvu Therapeutics, Translational Research, Cracow, Poland; <sup>5</sup>Medical University of Warsaw, Laboratory of Experimental Medicine, Warsaw, Poland; <sup>6</sup>Me.CRO, Me.CRO, Białystok, Poland; <sup>7</sup>Medical University of Warsaw, Department of Immunology, Warsaw, Poland; <sup>8</sup>Ryvu Therapeutics, Biology, Kraków, Poland

**Background:** NK cells act as one of the most important immunosurveillance mechanisms eliminating cancer cells. NK cells recognize Fc portions of antibodies binding to surface antigens of cancer cells and release cytotoxic granules and cytokines. Antibody-dependent cell-mediated cytotoxicity (ADCC) is one of the major NK-dependent killing mechanisms, activated for example by therapeutic monoclonal antibodies, such as the anti-CD20 antibody rituximab. NK cell activity is attenuated by STAT1 (S727) phosphorylation, mediated by the CDK8 kinase. Here we show results of combination therapy of anti-CD20 antibody rituximab with a clinical stage CDK8/19 small molecule inhibitor RVU120.

**Material and methods:** The effect of RVU120 or rituximab as well as their combination on human NK cells was tested *in vitro* in a co-culture cell killing assay using effector NK cells isolated from healthy donors and a panel of CD20-positive diffuse large B-cell lymphoma (DLBCL) cell lines as target

Poster Session (27 October 2022)

cells. The impact of RVU120 on the expression of LAMP1 (CD107a) degranulation marker on NK cells surface was assessed by flow cytometry. Pharmacokinetic/pharmacodynamic (PKPD) experiments were performed for RVU120 in immunocompetent naïve BALBc and C57BL6 mice. Finally in vivo effects of RVU120 and rituximab individually and in combination, in continuous and intermittent treatment schemes were tested in Rag2<sup>-/-</sup> mice inoculated with Raji CD20+ cell line. Ex vivo analyses were performed using a co-culture cell killing assay with murine splenocytes and YAC-1 cell line as a target population. NK cell phenotype was monitored in blood throughout the study, and in blood and spleens at the end of the experiment.

**Results:** In vitro cell killing assay demonstrated that treatment with RVU120 in combination with rituximab causes upregulation of LAMP1 surface level and increases NK cell cytotoxicity against CD20-positive DLBCL cell lines. Short-term treatment of naïve immunocompetent mice results in increased maturation and activated cytotoxic phenotype of NK cells, confirmed by ex vivo co-culture cell killing assay. Chronic, continuous administration of RVU120 was less effective and showed signs of NK cell exhaustion, both in vitro and in vivo. In Raji tumour bearing mice, RVU120 was not effective, whereas rituximab caused significant inhibition of tumour growth. Combined therapy of RVU120 with rituximab was well tolerated by animals and resulted in complete tumour regressions. NK cells isolated from animals treated by the combination confirmed the highest cytotoxic potential on cancer cells ex vivo.

**Conclusions:** RVU120 significantly increases rituximab-driven ADCC, resulting in complete tumour regression. This combination strategy may be useful for enhancing anti-cancer effects of other antibodies and antibody-drug conjugates, potentially leading to deep clinical responses.

#### Conflict of interest:

Ownership: Ryvu Therapeutics

### 159 (PB039) A combination vertical inhibition approach with inhibitors of SHP2 and ERK provides improved activity in KRAS-mutant pancreatic and colorectal cancer models

C. Hindley<sup>1</sup>, A. Biondo<sup>1</sup>, J. Brothwood<sup>1</sup>, K.H. Dao<sup>2</sup>, N. Kandola<sup>1</sup>, J. Lyons<sup>1</sup>, Y. Nakatsuru<sup>3</sup>, T. Smyth<sup>1</sup>, S. Wagner<sup>1</sup>, N. Wallis<sup>1</sup>, K. Hearn<sup>1</sup>. <sup>1</sup>Astex Pharmaceuticals, 436 Cambridge Science Park, Cambridge, United Kingdom; <sup>2</sup>Astex Pharmaceuticals, Inc., Pleasanton, California, USA; <sup>3</sup>Taiho Pharmaceutical Co., Ltd, Tsukuba, Ibaraki 300-2611, Japan

**Background:** Inhibitors of the MAPK pathway are approved therapeutic agents with a high initial response rate, however single agent use of MAPK inhibitors in the clinic is often limited by resistance. Resistance commonly occurs through mechanisms which result in reactivation of MAPK signaling, such as activation of receptor tyrosine kinases (RTKs). Vertical pathway combination strategies are therefore of interest for addressing resistance through pathway reactivation. Src homology region 2-containing protein tyrosine phosphatase 2 (SHP2) is a key regulator of the MAPK pathway downstream of RTKs and upstream of RAS, whilst ERK1/2 (ERK) is the final node of the kinase cascade.

We have previously presented data on a large-scale combination cell panel screen using the combination of ASTX029, a dual-mechanism ERK inhibitor which is currently undergoing clinical development in a Phase 1/2 trial in advanced solid tumors (NCT03520075), with an inhibitor of SHP2 that we developed using structure-guided drug design. We observe an enhanced response when inhibiting both ERK and SHP2 in combination in vitro and in vivo in KRAS mutant pancreatic ductal adenocarcinoma (PDAC) and colorectal cancer (CRC) models.

**Material and methods:** The combination cell panel screen composition and analysis have been previously presented. Select KRAS-mutant PDAC and CRC cell lines were used for validation and further assessment by colony formation assays and western blotting. In vivo activity was assessed using subcutaneous xenografts established in immunocompromised mice.

**Results:** The cell panel screen revealed an enhanced response to the combination in a wide range of indications, including KRAS-mutant PDAC and CRC cell lines. Combination synergy was confirmed in short- and long-term in vitro assays in a representative sample of these cell lines. In vivo treatment of xenograft tumors with a single dose of the combination resulted in a greater decrease in markers of MAPK signaling (e.g. pRSK, pERK) and a greater increase in markers of apoptosis (e.g. cleaved PARP) over treatment with either single agent. Treatment with the combination more effectively inhibited the growth of KRAS-mutant xenograft tumors in vivo, such as KRAS<sup>G12C</sup>-mutant Mia-PaCa2 xenografts, when compared to either single agent. Combination anti-tumor activity was observed using different dose schedules and at different dose levels, suggesting that the combination could be dosed in a flexible manner while retaining activity.

**Conclusions:** These data support our hypothesis that the combination of SHP2 and ERK inhibitors enhances inhibition of cell growth over the single

agents in KRAS-mutant PDAC and CRC cell lines. Our data provide a strong rationale for the use of a vertical inhibition approach with SHP2 and ERK inhibitors in KRAS-mutant PDAC and CRC and warrants further investigation in the clinic.

#### Conflict of interest:

Other Substantive Relationships: All co-authors are employees of the organisations indicated.

### 160 (PB040) The AXL inhibitor, TP-0903, reverses EMT and shows activity in non-small cell lung cancer preclinical models

R. Joe<sup>1</sup>, Y. Matsumura<sup>1</sup>, A. Siddiqui<sup>2</sup>, J. Foulkes<sup>3</sup>, M. Beg<sup>4</sup>, J. Thompson<sup>5</sup>, N. Yamamoto<sup>6</sup>, A. Spira<sup>7</sup>, J. Sarantopoulos<sup>8</sup>, J. Melear<sup>9</sup>, Y. Lou<sup>10</sup>, C. Lebedinsky<sup>11</sup>, J. Li<sup>11</sup>, A. Watanabe<sup>11</sup>, S. Warner<sup>12</sup>. <sup>1</sup>Sumitomo Pharma Oncology, Translational Biology, Lehi, USA; <sup>2</sup>Sumitomo Pharma Oncology, Chemistry, Lehi, USA; <sup>3</sup>Sumitomo Pharma Oncology, Discovery and Translational Biology, Lehi, USA; <sup>4</sup>UT Southwestern, Medical Oncology, Dallas, USA; <sup>5</sup>Medical College of Wisconsin, Oncology, Milwaukee, USA; <sup>6</sup>National Cancer Center Hospital, Thoracic Oncology, Tokyo, Japan; <sup>7</sup>Virginia Cancer Specialists, Medical Oncology, Fairfax, USA; <sup>8</sup>UT Health, Medical Oncology, San Antonio, USA; <sup>9</sup>Texas Oncology, Oncology, Austin, USA; <sup>10</sup>Mayo Clinic, Oncology, Jacksonville, USA; <sup>11</sup>Sumitomo Pharma Oncology, Clinical, Cambridge, USA; <sup>12</sup>Sumitomo Pharma Oncology, Research, Lehi, USA

**Background:** Adenocarcinomas frequently adopt mesenchymal properties to become metastatic, aggressive and drug-resistant. Non-small cell lung cancer (NSCLC), a leading cause of cancer-related deaths, is a well-understood cancer type to utilize an epithelial-to-mesenchymal transition (EMT) to acquire drug resistance in preclinical models. This is particularly applicable in resistance to EGFR inhibitors (e.g. osimertinib) in EGFR+ NSCLC, where resistance has been linked to EMT and increased AXL expression, a known driver of the mesenchymal phenotype. TP-0903 is a potent multi-targeted kinase inhibitor shown to reverse the mesenchymal phenotype through AXL inhibition and other mechanisms in preclinical models. TP-0903 and osimertinib have shown synergistic activity in the EGFR+ H1650 xenograft model. TP-0903 is currently being evaluated in combination with EGFR inhibitors in EGFR+ NSCLC patients (NCT02729298).

**Materials and Methods:** To investigate in vitro cytotoxicity and EMT markers in mutant EGFR NSCLC cell lines, H1650 and H1675, CellTiter Glo assay and western blots were performed, respectively. In a Phase I clinical trial, patients with EGFR+ NSCLC and recent progression following a best response of SD, PR, or CR per RECIST v1.1 on E2 lines of oral TKIs were treated with TP-0903 once daily for 21 out of 28 days plus (add-on) EGFR TKI to evaluate safety and preliminary antitumor activity.

**Results:** In an in vitro cytotoxicity assay, TP-0903 resulted in IC50 values of 193.3 nM and 40.15 nM in H1650 and H1975 cell lines, respectively. TP-0903 reduced SNAIL expression in H1650 and H1975. TP-0903 reduced SLUG expression and the combination treatment synergized to reduce SNAIL and SLUG expression to a further extent in H1975. Additional cell viability and EMT markers will be evaluated in NSCLC cell lines and patient-derived samples.

As of April 22, 2022, 22 patients (median age 64 y, 64% women, 59% white and 32% Asian, median 2 [range, 1–7] prior lines, 18 had osimertinib as last line) were treated with TP-0903 (3 at 37 mg flat dose, or 19 at 50 mg flat dose) as an add-on to EGFR inhibitor. The overall response rate (ORR) by investigator is 1 (4.5%) partial response (PR) and 13 (59%) stable disease (SDs), with 6 SDs for >6 months. Disease control rate (DCR) is 64%. One pt with EGFR exon 19 deletion who progressed on osimertinib has an ongoing PR for 3+ years. The most common TEAEs were nausea, vomiting and diarrhea, majority were mild and manageable with supportive care.

**Conclusions:** TP-0903 was active and suppressed EMT marker expression in mutant EGFR cell lines. TP-0903 added to osimertinib in unselected resistant EGFR+ NSCLC patients showed intriguing signals of activity that deserves further investigation, the safety profile was manageable.

#### Conflict of interest:

Advisory Board: Dr. Muhammad Beg - Ipsen, Array Biopharma, AstraZeneca/MedImmune, Cancer Commons, Legend Biotech, and Foundation Medicine. Dr. Noboru Yamamoto - Eisai, Takeda, Otsuka, Boehringer Ingelheim, Cimic, Chugai  
Corporate-sponsored Research: Dr. Muhammad Beg - Bristol-Myers Squibb, AstraZeneca/MedImmune, Merck Serono, Five Prime Therapeutics, Genentech, Immunesensor, and Tolero Pharmaceuticals. Dr. Alexander Spira - Sumitomo Pharma Oncology. Dr. Noboru Yamamoto - Astellas, AstraZeneca, Chugai, Eisai, Taiho, BMS, Pfizer, Novartis, Eli Lilly, AbbVie,



Daiichi-Sankyo, Bayer, Boehringer Ingelheim, Kyowa-Hakko Kirin, Takeda, ONO, Janssen Pharma, MSD, MERCK, GSK, Sumitomo Dainippon, Chiome Bioscience, Otsuka, Carma Biosciences, Genmab, Shionogi  
Other Substantive Relationships: Dr. Jonathan Thompson – Speaker's Bureau - AstraZeneca.

**161** (PB041)  
**HNSCCs overexpressing wild-type HRAS are sensitive to combined tipifarnib and alpelisib treatment**

H. Soifer<sup>1</sup>, V. Mishra<sup>1</sup>, S. Malik<sup>2</sup>, A. Smith<sup>2</sup>, S. Chan<sup>2</sup>, L. Kessler<sup>2</sup>, F. Burrows<sup>2</sup>, M. Leoni<sup>3</sup>, A. Saunders<sup>3</sup>, S. Dale<sup>3</sup>. <sup>1</sup>Kura Oncology, Diagnostics, San Diego, USA; <sup>2</sup>Kura Oncology, Translation Research, San Diego, USA; <sup>3</sup>Kura Oncology, Clinical Development, Boston, USA

**Background:** Understanding the interplay between novel molecular drivers is critical to optimize biomarker-driven clinical studies for patients with recurrent/metastatic head and neck squamous cell carcinoma (R/M HNSCC). This study used real world data, in vitro signaling, phenotypic assays and xenograft models to investigate HRAS overexpression, PIK3CA mutation and amplification as targets for combination therapy with tipifarnib, a farnesyl transferase inhibitor, and alpelisib, a PI3Ka inhibitor.

**Methods:** Real world clinical and genomic data (RWD) from >1000 patients with HNSCC with NGS and whole transcriptome RNAseq at Tempus Labs was used to determine the prevalence of PIK3CA and HRAS biomarkers. A CLIA-validated IHC assay was developed to assess HRAS expression in FFPE tissue.

**Results:** In a RWD dataset of >1000 HNSCC tumors, ~45% harbored an actionable PIK3CA and/or HRAS biomarker: PIK3CA mutation and amplification: 20% and 5.6%, respectively; HRAS mutations, 4.7%; and HRAS overexpression (defined as HRAS expression 1 standard deviation above the mean), ~15%. Since HRAS-MAPK and PI3K-AKT-mTOR signaling cascades are two interdependent, frequently dysregulated pathways in HNSCC, we explored if dual inhibition of these pathways with tipifarnib and alpelisib would be an effective anti-tumor strategy in these defined genetic subtypes. As reported previously in PIK3CA-dysregulated models, the combination synergistically induced cytotoxicity in HNSCC cell lines with HRAS overexpression relative to HRAS-low cell lines. siRNA-mediated depletion of HRAS and RHEB demonstrated that these farnesylated targets are essential to tipifarnib-mediated inhibition of mTOR and the compensatory reactivation of MAPK and mTOR pathways induced by alpelisib monotherapy. In vivo, combination therapy induced deeper antitumor responses in HNSCC PDXs with HRAS overexpression ± co-occurring mutations in PIK3CA. We validated an HRAS IHC assay to CAP/CLIA standards to investigate HRAS overexpression as a potential biomarker of response. In 46 HNSCC tumors selected to match patients in ongoing trials, 16/46 (35%) displayed intense and widespread HRAS staining, equivalent to a tumor proportion score ≥50. The preclinical and mechanistic data showing antitumor activity of the targeted combination regimen and an ability to prescreen patients for HRAS overexpression by IHC prompted the opening of KO-TIP-013, a P1/2 trial of tipifarnib plus alpelisib in HNSCC patients who failed prior therapy (NCT04997902).

**Conclusions:** Nearly half of HNSCC tumors harbor genomic alterations that suggest dependence on dysregulation of HRAS-MAPK and PI3K-AKT-mTOR pathways. Preclinical data point to a mechanistic synergy between tipifarnib and alpelisib in PIK3CA- and HRAS-dysregulated HNSCC that may overcome the lack of efficacy observed in monotherapy trials with these agents.

**Conflict of interest:**

Ownership: All authors are employed by Kura Oncology

**162** (PB042)  
**The effects of Aurora Kinase inhibition on thyroid cancer growth and sensitivity to MAPK-directed therapies**

H. Hicks<sup>1</sup>, V. Espinoza<sup>1</sup>, J. Lund<sup>1</sup>, L. Pike<sup>2</sup>, N. Pozdnyev<sup>1</sup>, R. Schweppe<sup>1</sup>. <sup>1</sup>University of Colorado Anschutz Medical Campus, Endocrinology, Aurora, USA; <sup>2</sup>University of Colorado Anschutz Medical Campus, Pharmaceutical Sciences, Aurora, USA

**Background:** Advanced papillary thyroid cancer (PTC) and anaplastic thyroid cancer (ATC) are the leading causes of endocrine cancer death. Mutations in the MAP kinase (MAPK) pathway are common in PTC and ATC. Recently, the combination of dabrafenib (BRAFi) and trametinib (MEKi) was approved for treatment of BRAF-mutant ATC. However, combined BRAF/MEK inhibition is rarely curative for ATC patients and has had limited responses in PTC. Here, we identify an induction of Aurora Kinase B (AURKB) in response to MEKi in cells that are resistant to combined BRAF/

MEK inhibition. We therefore hypothesize that inhibition of AURKB will sensitize cells to MAPK-directed therapies.

**Materials and Methods:** Cell signaling responses were assessed using western blots and cell growth was measured by ViCell, Cell-Titer Glo, or IncuCyte ZOOM Live Cell Imaging. Long-term cell growth was measured using clonogenic assays. Apoptosis was measured using cleaved caspase 3/7 assays. Synergy was calculated using Combination Index (CI). RNA-sequencing data was analyzed using BioJupies.

**Results:** In a panel of BRAF-mutant PTC and ATC cell lines, combined BRAFi/MEKi blocks MAPK signaling, indicated by an 83%–100% inhibition of pERK ( $p < 0.03$ ), and variably affects PI3K/AKT signaling. Combined BRAF/MEK inhibition prevents clonogenic growth and inhibits cell viability 43–80%. Calculation of CI values indicates that combined BRAF and MEK inhibition synergistically inhibits cell growth in the majority of cell lines (CI value < 0.75), but not those harboring PIK3CA mutations. To identify potential mechanisms mediating resistance, we treated four sensitive and four resistant cell lines with MEKi for 48 hrs then performed RNA-sequencing. We identified an upregulation of AURKB in cells resistant to combined BRAFi/MEKi ( $p = 3.22 \times 10^{-6}$ ) but a downregulation of AURKB in sensitive cells ( $p = 6.43 \times 10^{-10}$ ). We further found that combined AURKB inhibition with barasertib (AURKi) and MEKi enhances growth inhibition compared to combined BRAFi/MEKi, decreasing cell growth 61–91% ( $0.0002 < p < 0.04$ ). Finally, we evaluated cell growth and apoptosis in response to inhibiting different nodes of the MAPK pathway along with AURKi. We found that combined inhibition of BRAF, ERK, and AURKB has a significant effect on cell growth and apoptosis, decreasing growth 73–81% ( $p < 0.0001$ ) and increasing cleaved caspase 3/7 1.4 to 9.3-fold.

**Conclusions:** Combined inhibition of BRAF and MEK synergistically inhibits growth in a subset of BRAF-mutant PTC and ATC cell lines. However, some cell lines remain resistant to this combination and upregulate AURKB in response to MEK inhibition. Further, inhibition of multiple nodes of the MAPK pathway (BRAF, MEK, ERK) combined with AURKi significantly decreases cell growth and increases apoptosis, suggesting AURKB is a promising target to overcome resistance to inhibition of the MAPK-pathway.

**No conflict of interest.**

**163** (PB043)  
**KRAS G12C mutated NSCLC and bladder cancer xenografts treated with sotorasib and adagrasib in combination with mTOR inhibitors show improved antitumor activity of nab-sirolimus vs everolimus**

S. Hou<sup>1</sup>, J. Nieva<sup>2</sup>, N. Desai<sup>3</sup>. <sup>1</sup>Aadi Bioscience, Non-Clinical Affairs, Pacific Palisades, USA; <sup>2</sup>University of Southern California, Oncology, Los Angeles, USA; <sup>3</sup>Aadi Bioscience, Chief Executive Officer, Pacific Palisades, USA

**Background:** KRAS is frequently mutated in non-small cell lung cancer (NSCLC) and other tumor types, with KRAS G12C mutation representing ~9% of NSCLC patients. mTOR pathway is often activated in patients with KRAS mutation and contributes to adaptive resistance to KRAS inhibitors. A combination of mTOR and KRAS inhibitors may mitigate resistance. nab-Sirolimus is a novel albumin-bound nanoparticle form of mTOR inhibitor sirolimus and is approved for the treatment of locally advanced unresectable or metastatic malignant perivascular epithelioid cell tumor (PEComa). Previous nonclinical studies have shown superior antitumor activity of nab-sirolimus vs everolimus as single agent in PTEN-null bladder cancer and TSC2-deficient hepatocellular carcinoma models. Sotorasib (AMG510) is approved for the treatment of KRAS G12C-mutated locally advanced or metastatic NSCLC, and adagrasib (MRTX 849) is under review for the treatment of KRAS G12C-mutated NSCLC. This study investigated the antitumor activity of nab-sirolimus or everolimus in combination with sotorasib or adagrasib in KRAS G12C-mutated cancer xenografts.

**Material and methods:** Athymic mice bearing subcutaneous KRAS G12C and STK11-mutated NSCLC xenografts NCI-H2030 and NCI-H2122 and KRAS G12C-mutated and PTEN-null UMUC3 bladder cancer were treated with saline, mTOR inhibitors nab-sirolimus or everolimus (in NCI-H2030 and H2122) at clinically relevant and equal weekly dose of 15 mg/kg/wk, KRAS inhibitors sotorasib or adagrasib (in NCI-H2122) at 30 mg/kg/day (~16% and ~13% of respective clinical dose), alone or in combination. Tumors were harvested for analysis of downstream markers for KRAS and mTOR inhibition.

**Results:** In NCI-H2030 xenografts (n=6 tumors/group), both nab-sirolimus and everolimus as single agent demonstrated tumor growth inhibition (TGI: nab-sirolimus 68% vs everolimus 22%, P=ns). When combined with KRAS inhibitor sotorasib, there was greater activity with nab-sirolimus than with everolimus (TGI: nab-sirolimus+sotorasib 109% vs everolimus+sotorasib 53%, P=0.0008). Combining nab-sirolimus with sotorasib showed significantly greater TGI (109%) compared with single agent nab-sirolimus (68%, P=0.0102) or sotorasib (20%, P=0.0002). Similar results were seen with NCI-H2122 and UMUC3 cell lines.

**Conclusions:** Combining mTOR inhibition with KRAS G12C inhibition improves response against tumors *in vivo*. *nab*-Sirolimus showed greater potency compared to everolimus and is the preferred agent for further clinical development using this strategy.

**Conflict of interest:**

Ownership: JN: Epic Sciences, Quantgene, Indee Bio  
 ND: yes  
 Advisory Board: JN: Aadi Bioscience, Naveris, BMS, Fujirebio, Astra Zeneca, Mindmed, G1 Therapeutics  
 Board of Directors: ND: Aadi Bioscience  
 Corporate-sponsored Research: JN: Genentech, Merck  
 Other Substantive Relationships: SH: Full-time employee and shareholder of Aadi Bioscience  
 JN: Patent licensing – Cansera  
 ND: employee of AADI

**164** (PB044)

**Enhancement of anti-tumor immunity in immunogenic and immune-refractory RAS mutant tumors with tri-complex RAS(ON) inhibitors**

C. Blaj<sup>1</sup>, M. Menard<sup>1</sup>, N. Tobvis Shifrin<sup>1</sup>, K. Chen<sup>1</sup>, C. Chow<sup>1</sup>, H. Courtney<sup>1</sup>, A. Kumamoto<sup>1</sup>, T. Velilla<sup>1</sup>, J.W. Evans<sup>1</sup>, L. Lawrence<sup>2</sup>, B. Vonmelchert<sup>1</sup>, A. Kwok-Parkhill<sup>3</sup>, M. Singh<sup>1</sup>, J.A. Smith<sup>1</sup>, E. Quintana<sup>1</sup>. <sup>1</sup>Revolution Medicines, Biology, Redwood City, USA; <sup>2</sup>Revolution Medicines, Chemistry-Manufacturing and Control, Redwood City, USA; <sup>3</sup>Revolution Medicines, Program- Portfolio- and Alliance Management, Redwood City, USA

RAS mutations (RAS<sup>MUT</sup>), the most frequent oncogenic alterations in human cancers, promote carcinogenesis through sustained cellular proliferation and also shape the tumor microenvironment to allow cancer cells to evade an anti-tumor immune response. Some RAS<sup>MUT</sup> tumors are responsive to immune checkpoint inhibition but many, such as most colorectal and pancreatic cancers, are not. A rational approach to treating RAS<sup>MUT</sup> tumors likely would be to combine optimized targeted therapy, including direct inhibition of RAS<sup>MUT</sup> itself, with effective immunologic therapy.

We found that the novel tri-complex RAS(ON) inhibitors RMC-6291 (KRAS<sup>G12C</sup>) and RMC-6236 (RAS<sup>MULTI</sup>) modulated cytokine secretion and the expression of checkpoint and MHC molecules in KRAS<sup>G12C</sup> cancer cells. The covalent KRAS<sup>G12D</sup> (ON) inhibitor, RMC-9805, had similar effects in KRAS<sup>G12D</sup> cancer cells.

RMC-6236 is a potent inhibitor of RAS<sup>MUT</sup> and of RAS<sup>WT</sup>, a potential driver of tumor escape from selective inhibition of RAS<sup>MUT</sup>, and also a key signaling node in immune cells. RMC-6236 directly and selectively reduced the viability of M2 macrophages, but not M1 macrophages or pre-activated T cells, *in vitro*. All three RAS(ON) inhibitors promoted anti-tumor immunity and synergized with anti-PD1 therapy *in vivo*, driving durable complete responses and immunologic memory in RAS<sup>MUT</sup> immunogenic tumor preclinical models. While the immunologic effects of KRAS<sup>G12C</sup> inhibition have been previously described, this is the first demonstration of effective anti-tumor immunity with a targeted inhibitor of KRAS<sup>G12D</sup>.

In a classical immune refractory, immune-desert KRAS<sup>G12C</sup> NSCLC tumor model RMC-6291 decreased myeloid suppressor cells and increased T cell tumor infiltrates; however, the combination with anti-PD1 therapy had a limited additive activity, indicating that alternative approaches are required.

SHP2 is upstream of RAS and also interacts directly with PD1. SHP2 inhibitors have previously been shown to induce anti-tumor immunity in preclinical models and in the clinic via modulation of both adaptive and innate immunity. The combination of RMC-6291 with RMC-6236, or with a SHP2 inhibitor, potentiated the functionality of cytotoxic T cells and improved anti-tumor activity over KRAS<sup>G12C</sup> (ON) inhibition alone. This immunomodulatory activity was further enhanced with the triple combination therapy of RMC-6291 plus RMC-6236 and SHP2 inhibitor and translated into rapid and durable complete responses in an immune refractory tumor model, even in the absence of anti-PD1 therapy.

Effective targeting of RAS<sup>MUT</sup> in RAS-addicted cancers may enhance responses to immunologic therapies in immune-sensitive cancers such as NSCLC. In addition, it may rescue anti-tumor immune responses in classically immune-refractory RAS<sup>MUT</sup> tumors where KRAS<sup>G12D</sup> mutations predominate.

**Conflict of interest:**

Other Substantive Relationships: All authors are full time employees of Revolution Medicines.

**165** (PB045)

**Exploring the role of S-Adenosyl Methionine Decarboxylase (AMD1) in the growth, migration, metabolism and drug-combination profile of non-small cell lung cancer cells**

R. Lopez-Muñoz<sup>1</sup>, M. Muñoz-Urbe<sup>1</sup>, F. Lopez-Contreras<sup>1</sup>, N. Buelvas<sup>1</sup>, A. Martin-Martin<sup>1</sup>, R. Burgos<sup>1</sup>, P. Alarcón<sup>1</sup>. <sup>1</sup>Universidad Austral de Chile, Facultad de Ciencias Veterinarias- Instituto de Farmacología y Morfofisiología, Valdivia, Chile

Non-small cell lung cancer (NSCLC) accounts for 85% of lung cancer and is associated with the poorest prognosis and survival. Current chemotherapy against NSCLC is limited to traditional chemotherapy, with a high incidence of adverse effects.

Polyamines (putrescine, spermidine and spermine) are small polycationic alkylamines increased in patients with non-small cell lung cancer (NSCLC). Polyamines are essential for cell growth in almost every type of cancer cell. Polyamine synthesis is regulated by the activity of ornithine decarboxylase (ODC) and S-Adenosylmethionine decarboxylase (AMD1) enzymes. Whereas ODC has been extensively studied, little is known about the role of AMD1 in the metabolism of lung cancer cells. ADM1 catabolizes the synthesis of decarboxylated-S-adenosyl methionine, which, in turn, acts as an aminopropyl donor for spermidine and spermine synthesis. Thus, inhibition of AMD1 would impair the polyamine metabolism, affecting NSCLC cell proliferation.

In this work, we studied the role of AMD1 in NSCLC cells. We used two cell lines of NSCLC (H1299 and A549 cells). First, we identified AMD1 by immunoblotting. Then, we attempt to delete the AMD1 protein using a CRISPR-Cas9 system. Also, we used SAM486A, a pharmacologic inhibitor of AMD1, to explore the effect of AMD1 inhibition on NSCLC cell metabolism through untargeted GC-MS metabolomics. Also, we evaluated the migration and viability of NSCLC cells exposed to SAM486A by transwell and resazurin reduction methods. Finally, we assessed the synergistic effect of SAM486A with other polyamine inhibitors such as eflornithine (an ODC inhibitor) and MDL 72527 (a non-selective inhibitor of polyamine and spermine oxidase).

When comparing A549 and H1299 cell lines, we found that H1299 has significantly greater levels of AMD1 protein. Thus, we choose H1299 cells to delete AMD1. We got a partial deletion of AMD1 by CRISPR, but this reduction was enough to decrease cell proliferation significantly. SAM486A also decreased cell proliferation in a concentration-dependent manner in H1299 and A549 cells. Also, SAM486A decreased cell migration in both cell lines. As expected, SAM486 induced a significant accumulation of putrescine, despite not significantly decreasing spermidine levels. Finally, when we combined SAM486A with polyamine inhibitors, we found a synergistic effect with eflornithine but not with MDL 72527, suggesting that the parallel inhibition of both rate-limiting enzymes in polyamine synthesis is more efficient in reducing cell proliferation in NSCLC cells.

These results indicate that AMD1 could be an interesting target to be explored in NSCLC to look for combinatory strategies with other polyamines inhibitors or traditional chemotherapy *in vivo*. Funding: ANID-FONDECYT #1201378

**No conflict of interest.**

**166** (PB046)

**Targeting oncogenic HRAS in pediatric rhabdomyosarcoma**

P. Odeniyide<sup>1</sup>, A. Skaist<sup>2</sup>, E. Fertig<sup>2</sup>, C.A. Pratilas<sup>3</sup>. <sup>1</sup>The Sidney Kimmel Comprehensive Cancer Center at Johns Hopkins University School of Medicine, Division of Pediatric Oncology, Baltimore, USA; <sup>2</sup>The Sidney Kimmel Comprehensive Cancer Center at Johns Hopkins University School of Medicine, Department of Oncology, Baltimore, USA; <sup>3</sup>The Sidney Kimmel Comprehensive Cancer Center at Johns Hopkins University School of Medicine, Division of Pediatric Oncology, Baltimore, USA

**Background:** Rhabdomyosarcoma (RMS) is the most common soft-tissue sarcoma of childhood, and RAS pathway mutations are the known driver mutations in the majority of fusion-negative (FN) RMS. Recent studies have demonstrated that HRAS mutations are enriched in infant cases of FN-RMS and can be associated with an aggressive clinical course and inferior outcomes. Using HRAS-mutant RMS cell lines and xenograft models, we have demonstrated that tipifarnib (farnesyl transferase inhibitor, FTI) decreases ERK signaling, decreases *in vitro* proliferation, and decreases *in vivo* tumor growth. The effects of tipifarnib can be incomplete, however, leading only to partial or short-lived responses. Limitations may be due to adaptive or acquired resistance, suggesting that HRAS-mutated FN-RMS may be sensitive to pathway inhibition with combination therapy that prevents or delays the emergence of adaptive resistance. Trametinib (MEKi) inhibits

tumor growth in xenograft models of FN-RMS but has only modest activity as a single agent, potentially due to the release of negative feedback and activation of upstream signaling. The efficacy of inhibition with FTI and MEKI has not been previously explored in RAS-driven FN-RMS.

**Materials and Methods:** We examined the transcriptional effects of tipifarnib in FN-RMS cell lines using bulk RNA-sequencing to identify therapeutic vulnerabilities that may be exploited by RAS-directed therapies. Additionally, we utilized in vitro cellular proliferation assays, soft agar colony-forming assays, and immunoblot to evaluate the effects of tipifarnib in combination with trametinib on cell growth, differentiation, and signaling via RAS effector pathways.

**Results:** Analysis of RNA sequencing data revealed downregulation of ERK transcriptional output genes upon treatment with tipifarnib, confirming the critical role of the MEK-ERK pathway in mediating the response to farnesyltransferase inhibition. We, therefore, tested tipifarnib in combination with trametinib in HRAS-mutant FN-RMS cell lines and observed additive dose-dependent 2D and 3D growth inhibition in response to the combination. In HRAS-mutant cells, tipifarnib and trametinib more potently reduced ERK phosphorylation than either drug individually, indicating effective RAS pathway inhibition. Additionally, we found that the combination of tipifarnib and trametinib induced myosin heavy chain expression in HRAS-mutated cell lines, suggesting both inhibition of proliferation and promotion of myogenic differentiation.

**Conclusions:** Our data suggest that the combination of the FTI tipifarnib and the MEK inhibitor trametinib is active in models of HRAS-driven FN-RMS and may represent an effective therapeutic strategy for a genomically-defined subset of patients with FN-RMS.

**No conflict of interest.**

**167** (PB047)  
**Combination synergy of FGFR inhibitors with other therapeutic agents in FGFR-deregulated cancer models**

N. Zhang<sup>1</sup>, B. Shen<sup>1</sup>, J. Shi<sup>1</sup>, Z. Chen<sup>1</sup>. <sup>1</sup>Abbisko Therapeutics, Biology, Shanghai, China

**Background:** Benefitting from the emerging role of comprehensive genomic profiling in the era of precision medicine, genomic aberrations (amplification, mutation and fusion) of fibroblast growth factor (FGF) receptor (FGFR) are frequently found in multiple solid tumors. FGFR selective inhibitors targeting these alterations showed inspiring clinical benefits. Currently three FGFR inhibitors have been approved as monotherapy to treat locally advanced or metastatic urothelial carcinoma with FGFR2/3 alterations (erdafitinib) and unresectable cholangiocarcinoma with FGFR2 fusions (pemigatinib and infigratinib) through accelerated approval process. Despite the beneficial effects of FGFR inhibitors in clinic, the limited antitumor spectrum and the potential drug resistance are major concerns. Hence, combination with other therapeutic agents to overcome these limitations are needed. Here we describe a cellular-based study to identify the potential combination partners for both pan-FGFR and FGFR4 selective inhibitors.

**Materials and methods:** We tested a set of small molecule inhibitors that targeting the components related to FGFR pathway, including but not limited to PI3Ki, AKTi, mTORi, SHP2i, SOS1i, MEKi, CDK4/6i and METi, in cellular combination experiments with a pan-FGFR inhibitor ABSK091 (formerly AZD4547) or a FGFR4 selective inhibitor ABSK011 for various FGFR-deregulated models, including endometrial cancer cells harboring FGFR2 mutations, gastric cancer cells with FGFR2 amplification and overexpression, bladder cancer cells bearing FGFR3 fusion and hepatocellular carcinoma (HCC) cells with FGF19 amplification and overexpression. Cell growth inhibition was measured and synergistic effect was analyzed.

**Results:** Synergistic effects on cell growth inhibition were observed in ABSK091 in combination with several agents including copanlisib, MK2206, onataserib, SHP099, TNO155, BI3406. When evaluating agents in combination with ABSK011 in HCC models, we found that several MAPK pathway inhibitors showed synergy while inhibitors targeting PI3K-AKT pathway did not show such effect. Enhanced downstream signaling inhibition were confirmed in these synergistic combinations, which were consistent with cell growth inhibition results.

**Conclusions:** Our findings suggest that FGFR selective inhibitors in combination with broad target therapeutic agents may offer additional therapeutic benefits in various FGFR-deregulated cancers.

**No conflict of interest.**

**168** (PB048)  
**Evidence of synergetic efficacy of radioisotope nano-carrier drugs with immunotherapy**

S.S. Oh<sup>1</sup>, M.K. Joung<sup>1</sup>, K.R. Choi<sup>1</sup>, J.S. Han<sup>1</sup>, Y.S. Park<sup>1</sup>, H.S. Jang<sup>2</sup>.  
<sup>1</sup>ZTIBIOSCIENCES, R&D Team, Suwon, South Korea; <sup>2</sup>ZTIBIOSCIENCES, Chief Executive Officer, Suwon, South Korea

**Background:** Since immunotherapy first emerged as a novel, safe, and effective cancer therapeutic, it was expected to bring a new era against cancer. Yet, it has fallen short against solid tumors, one of the most common causes of death, due to immune cell's limitation in penetrating tumor masses.

To compensate for traditional cancer therapy, many methods have emerged such as antibody drug conjugates (ADC), which was challenged by reactive resistance, and radioisotope therapy (RIT), which have faced limitations in delivery. Yet, with innovative binding improvements, we may now have a solution. Based on the iron oxide material-based nano-carrier's radioisotope-binding technology, our drug is capable of delivering the payload to the target without losing the isotopes. It also functions as a platform interchangeably compatible with all types of radioisotopes and targeting ligands.

Moreover, nano-carrier technology holds tremendous potential for improving immunotherapeutic efficacy in cancer patients. In contrast to conventional oncological immunotherapies, we can design nanomaterials to trigger specific tumoricidal effects, thereby improving immune cell accessibility to major sites of metastasis and optimizing antigen presentation and inducing a persistent immune response in tissues such as bone, lungs, and lymph nodes.

**Materials and methods:** Efficacy tests were carried out in female balb/c-nu mice. Subcutaneous xenograft tumor models were created by implanting ovarian/triple negative breast cancer cells to the right flank of test animals. Resulting tumors were monitored and measured using a caliper for three to five weeks. Synergetic anti-cancer effects of radioisotope nano-carrier drugs with PD-1/PD-L1 inhibitors were observed.

**Results:** Our test results demonstrated that the combination of immunotherapy and radionuclide nano-carrier (iron oxide) drugs have synergetically higher efficacy compared to single treatment. This experiment showed higher anti-cancer efficiency and direct in-vivo effects from the nano-carrier drugs. We have verified that this can intensely affect tumor cells, in the xenograft mice models, at non-clinical level, also increasing its survival rate. Amongst the tested cell lines, mice that were treated with combined therapy, had higher rates of tumor growth inhibition and regression with no significant toxicity observed.

**Conclusions:** We have found promising potential of our radionuclide nano-carrier (iron oxide) based drug to be the next generation solution to immunotherapy for solid cancers. Based on the results of the in-vivo test, we have verified the efficacy of the combined effects of radionuclide nano-carrier based drug+immunotherapy. with precision targeting and secure delivery of the payload (radioisotopes) by the nano-carrier to the objective solid cancer cells, the drugs were able to reach high precision efficacy.

**No conflict of interest.**

**169** (PB049)  
**Ornithine decarboxylase as a new target for improving the effect of KRAS-G12C inhibitors in non-small cell lung cancer cells**

A. Martin<sup>1</sup>, N. Buelvas<sup>1</sup>, C. Guzman<sup>1</sup>, S. Guzman<sup>1</sup>, M. Mansilla<sup>1</sup>, R. Lopez Muñoz<sup>1</sup>. <sup>1</sup>Universidad Austral de Chile, Facultad de Ciencias Veterinarias- Instituto de Farmacología y Morfología, Valdivia, Chile

Non-small cell lung cancer (NSCLC) is the deadliest and most prevalent form of lung cancer. Mutations in the Kirsten rat sarcoma viral oncogene (KRAS) homolog gene exist in 20–30% of NSCLC and are associated with a poor prognosis and a high risk of cancer recurrence. Also, the G12C point mutation in KRAS is considered a driver mutation in NSCLC.

Adagrasib and sotorasib are novel small pharmacological inhibitors of the KRASG12C protein, showing efficacy against KRASG12C-mutated tumors, including NSCLC. However, these drugs can induce acquired tumor resistance throughout secondary mutations in KRAS or increase the activity of signaling pathways related to cancer cell survival. So, it is necessary to have a deeper understanding of the metabolic implications of KRAS inhibition to find combined therapies that improve the response of these inhibitors and avoid the appearance of resistance.

The polyamines (putrescine, spermidine, and spermine) are small molecules essential for cancer proliferation and survival that are increased in almost all types of cancer, including NSCLC. Ornithine decarboxylase (ODC), the rate-limiting enzyme in polyamine synthesis, is regulated at the transcription level by the KRAS-MAPK-MYC axis and is a known target of c-MYC. Therefore, the increased downstream activity of KRAS leads to the

accumulation of c-MYC protein resulting in ODC overexpression. Thus, this work aimed to study the relationship between the presence of KRASG12C mutation and the expression and activity of ODC in NSCLC cells, in order to find a new combination strategy throughout the use of KRASG12C inhibitors with eflornithine, an ODC inhibitor.

We used four NSCLC cell lines with different mutations in the codon 12 of KRAS: H358 (G12C), A549 (G12S), CORL-L23 (G12V) and H1299 (KRASwt). We measured ODC levels and the KRAS-ERK pathway phosphorylation by immunoblotting. Cell proliferation was evaluated by clonogenic assay with crystal violet stain. Cell viability assays were performed by resazurin reduction. Drug combination studies were performed using the Bliss independence model and the COMBENEFIT software.

We found that ODC levels are significantly increased in H358 cells. As expected, sotorasib and adagrasib inhibited the MAPK pathway in H358 cells, which correlates with the downstream inhibition of KRAS signaling. Both sotorasib and adagrasib reduced ODC levels in H358 cells and were significantly more potent in H358 cells. In addition, eflornithine (a specific ODC inhibitor) showed a higher effect in H358 cells when compared with the other NSCLC cell lines. Finally, synergism was observed when using sotorasib and adagrasib in combination with eflornithine. These results suggest that the combination between a KRASG12C inhibitor and an ODC inhibitor would lead new therapeutic strategies against KRASG12C-mutated tumors. Funding: FONDECYT-ANID #1201378 grant.

**No conflict of interest.**

170

(PB050)

### Polyamine transport inhibition with AMXT-1501 synergizes with cisplatin in HNSCC

A. Yassin-Kassab<sup>1</sup>, R.A. Harbison<sup>2</sup>, N. Wang<sup>3</sup>, M. Burns<sup>4</sup>, G. Delgoffe<sup>5</sup>, U. Duvvuri<sup>3</sup>. <sup>1</sup>University of Pittsburgh, Otolaryngology, Pittsburgh, USA; <sup>2</sup>Johns Hopkins University, Otolaryngology, Baltimore, USA; <sup>3</sup>University of Pittsburgh, Otolaryngology, Pittsburgh, USA; <sup>4</sup>Aminex Therapeutics, Kenmore, USA; <sup>5</sup>University of Pittsburgh, Immunology, Pittsburgh, USA

**Background:** Head and neck squamous cell carcinoma (HNSCC) is a devastating disease that has a generally poor prognosis. Cisplatin-based therapies remain the standard of care for these patients, however, many patients experience acute toxic effects and develop resistance to treatment. Polyamine metabolism has been shown to promote the growth of cancer cells. AMXT-1501 is a compound in clinical trials that inhibits polyamine transport, therefore we chose to use the combination of cisplatin and AMXT-1501. We sought to investigate whether inhibition of polyamine transport could synergize with cisplatin in HNSCC to increase cancer cell cytotoxicity.

**Methods:** Cell proliferation was measured and IC50 values were obtained in syngeneic mouse head and neck cell lines, MOC2, MEER PD-1 resistant, and TAB2 cells after treatment with cisplatin and AMXT-1501. Synergy was determined by administering cisplatin and AMXT-1501 at a ratio of 1:10. We used a DCFDA assay to measure relative ROS changes in the combination of cisplatin and AMXT-1501 compared to either treatment alone. Flow cytometry using annexin V staining was used to measure the percentage of cells undergoing apoptosis in the combination treatment compared to either treatment alone. Finally, xenograft experiments were performed in C57 black mice to test the efficacy of the combination *in vivo*.

**Results:** The combination of cisplatin and AMXT-1501 results in a synergistic effect on HNSCC cell lines. The combination treatment increases ROS production by about 3-fold compared to cisplatin treatment alone. The combination of treatments also significantly increases the percentage of cells undergoing apoptosis. The combination treatment *in vivo* resulted in 84% tumor growth inhibition in MEER PD-1 resistant cells and 90% tumor growth inhibition in MOC2 cells, which was significantly greater than either treatment individually.

**Conclusion:** Polyamine transport inhibition with AMXT-1501 enhances the cytotoxic effects of cisplatin *in vitro* and *in vivo* in HNSCC.

**No conflict of interest.**

171

(PB051)

### The PKMYT1 inhibitor RP-6306 has synergistic efficacy with carboplatin in CCNE1 amplified tumor models

J. Fourtounis<sup>1</sup>, D. Gallo<sup>1</sup>, A. Roulston<sup>2</sup>, R. Stocco<sup>1</sup>, G. Martino<sup>2</sup>, S. Fournier<sup>2</sup>, E. Aguado<sup>3</sup>, R. Kryczka<sup>2</sup>, V. Bhaskaran<sup>2</sup>, S. Morris<sup>1</sup>, C.G. Marshall<sup>4</sup>.

<sup>1</sup>Repare Therapeutics Inc., Biology, Montreal, Canada; <sup>2</sup>Repare Therapeutics Inc., Pharmacology, Montreal, Canada; <sup>3</sup>Repare Therapeutics Inc., Clinical Biomarkers and Diagnostics, Boston, USA; <sup>4</sup>Repare Therapeutics Inc., Clinical PMO, Boston, USA

**Background:** PKMYT1 is an essential mitotic checkpoint kinase in cancer cells with amplification of the replication stress-inducing gene CCNE1. RP-6306 is a first-in-class highly potent and selective PKMYT1 inhibitor currently in clinical trials as a single agent (NCT04855656) and in combination with gemcitabine and irinotecan-based therapy (NCT05147350 and NCT05147272). PKMYT1 inhibition combined with replication stress induces premature mitosis that ultimately kills cells by induction of catastrophic DNA damage. Platinum-based chemotherapies also induce replication stress via a variety of mechanisms, and they have found broad use in the clinic, including ovarian cancer where CCNE1 amplification is relatively frequent and platinum efficacy is limited. Here we investigate the combination of carboplatin with RP-6306 in CCNE1-amplified tumor settings to understand the potential for synergy that could be further tested in clinic.

**Methods and Results:** We demonstrate that combining carboplatin with the PKMYT1 inhibitor RP-6306 is synergistic in several preclinical models of CCNE1-amplified cancer. *In vitro*, strong synergistic effects are observed in a CCNE1-amplified ovarian model using low concentrations of carboplatin in cell growth inhibition assays. *In vivo*, this synergy manifests as regressions in an OVCA3 xenograft model at well-tolerated doses while single agent carboplatin or RP-6306 at the same doses shows growth inhibitory effects. Finally, we describe a mechanistic model for the effective combination of RP-6306 with carboplatin measuring the mitotic marker phospho-Histone H3 and DNA damage marker  $\gamma$ H2AX.

**Conclusions:** Together, these results provide a strong rationale for clinical development of this combination in CCNE1-amplified cancer that has therapeutic potential across several solid tumor types where platins are used.

**Conflict of interest:**

Other Substantive Relationships: All the authors of this abstract are employees of Repare Therapeutics Inc.

172

(PB052)

### Interactions between BRD4 short, LOXL2, and MED1 drive cell cycle transcription in triple-negative breast cancer

L. Pascual Reguant<sup>1</sup>, T.V. Tian<sup>2</sup>, D. Datta<sup>3</sup>, D. Cianferoni<sup>4</sup>, S. Kourtis<sup>4</sup>, A. Gañez-Zapater<sup>4</sup>, C. Cannata<sup>4</sup>, Q. Serra-Camprubi<sup>2</sup>, L. Espinar<sup>4</sup>, M. Guirola<sup>4</sup>, J. Querol<sup>2</sup>, A. Miró-Canturri<sup>5</sup>, J. Arribas<sup>2</sup>, L. Serrano<sup>4</sup>, S. Peiró<sup>2</sup>, S. Sdelci<sup>4</sup>. <sup>1</sup>CRG, Gene Regulation- Stem Cells and Cancer, Barcelona, Spain; <sup>2</sup>VHIO, Barcelona, Spain; <sup>3</sup>ISGLOBAL, Barcelona, Spain; <sup>4</sup>CRG, Barcelona, Spain; <sup>5</sup>IMIM, Barcelona, Spain

**Background:** Triple-negative breast cancer is the most aggressive breast cancer subtype. On top of the fact that for triple-negative breast cancer there are no effective therapeutic strategies, it also very often develops resistance to chemotherapy and metastasizes to distal organs, condemning patients to death. One strategy to circumvent the insurmountable anticancer drug resistance is the development of efficient combinatorial approaches targeting multiple key cancer proteins. Recently, it has been shown that the inhibition of either BRD4 or LOXL2 dampens breast cancer proliferation, having a more pronounced effect on the triple-negative subtype. Here, we seek to investigate whether the simultaneous inhibition of BRD4 and LOXL2 can be explored as a novel triple-negative breast cancer therapy.

**Material and Methods:** To develop this study, we have integrated multiple techniques including synergy assays, transcriptomics, epigenomics, and *in vivo* mouse experiments.

**Results:** We first demonstrate that the combinatorial inhibition of LOXL2 and BRD4 with small molecules effectively synergizes to reduce triple-negative breast cancer cell growth *in vitro* and *in vivo*. We further reveal that mechanistically, the synergism is mediated by the direct interaction of the short isoform of BRD4 with LOXL2. Such interaction, which happens in the nucleus, is required to promote the formation of BRD4 and MED1 transcriptional foci and to guarantee the expression of early cell cycle genes. In agreement with these findings, both the pharmacological and transcriptional repression of LOXL2 lead to G1-S cell cycle arrest, loss of BRD4 and MED1 nuclear foci, and downregulation of cell cycle-associated gene expression in triple-negative breast cancer cells.

**Conclusion:** Our results indicate that the interaction between LOXL2 and BRD4 short isoform is fundamental for the proliferation of triple-negative breast cancer and that the simultaneous inhibition of both proteins holds potential for the treatment of this unmet medical need.

**No conflict of interest.**

173 (PB053)  
**Combination of KRASG12C(ON) and SHP2 inhibitors overcomes adaptive resistance and enhances anti-tumour immunity**

P. Anastasiou<sup>1</sup>, J. Boumelha<sup>1</sup>, E. Mugarza<sup>1</sup>, S. Rana<sup>1</sup>, C. Moore<sup>1</sup>, M. Molina Arcas<sup>1</sup>, J. Downward<sup>1</sup>. <sup>1</sup>Francis Crick Institute, Downward Lab, London, United Kingdom

**Background:** Oncogenic mutations in KRAS are a major cause of non-small cell lung cancer (NSCLC) and are associated with poor prognosis. Clinical use and approval of KRAS<sup>G12C</sup> mutant-specific inhibitors, targeting the GDP-bound inactive (OFF) state, have shown promising results in KRAS<sup>G12C</sup>-mutant NSCLC patients. However, inevitably therapy resistance occurs, and responses are short-lived. Several resistance mechanisms have been described, including upstream pathway reactivation and occurrence of secondary RAS pathway mutations. Therefore, combination therapies are required to overcome resistance. In this study we combine a novel covalent tricomplex KRAS<sup>G12C</sup>(ON) inhibitor, RM-029, which targets the GTP-bound active state, with the SHP2 inhibitor RMC-4550 and analyse if treatment can result in favorable changes in the immune tumor microenvironment (TME) which can lead to adaptive anti-tumor immune responses.

**Materials and methods:** In vivo experiments were performed using transplantable KRAS-mutant lung cancer mouse models of varying immunogenicities. Tumours were generated either subcutaneously or orthotopically (via tail-vein injections) and treated with KRAS<sup>G12C</sup>(ON) inhibitor RM-029 and/or the SHP2 inhibitor RMC-4550. Four doses of anti-PD1 were administered within 2 weeks. Changes in the TME were measured by FACS or quantitative PCR.

**Results:** In vitro, RM-029 exhibited higher potency for inhibition of cell viability than the KRAS<sup>G12C</sup>(OFF) inhibitor MRTX849 in human NSCLC cell lines. However, treatment with RM-029 still resulted in RAS pathway reactivation which was blocked upon coincubation with the SHP2 inhibitor RMC-4550.

In an immune-infiltrated, anti-PD1 sensitive model of KRAS<sup>G12C</sup> driven lung cancer, single agent treatments improved overall survival of mice. The combination of the KRAS<sup>G12C</sup>(ON) inhibitor with a SHP2 inhibitor improved responses, and addition of anti-PD1 as a third agent further enhanced effects of the targeted therapies, resulting in complete tumour eradication in most mice. Furthermore, both KRAS<sup>G12C</sup>(ON) and SHP2 inhibition, alone and in combination, induced significant remodelling of the lung TME, including infiltration and activation of T cells.

Single agent and combination treatments promoted similar TME remodelling and prolonged survival in an immune-excluded, anti-PD1 resistant model of KRAS<sup>G12C</sup> driven NSCLC. Combined KRAS<sup>G12C</sup>(ON) and SHP2 inhibition sensitized immune-excluded tumours to anti-PD1 blockade which resulted in durable responses in this anti-PD1 refractory model.

**Conclusion:** Overall, these preclinical data show that both KRAS<sup>G12C</sup>(ON) and SHP2 inhibitors induce significant remodelling of the TME while their combination blocks RAS pathway reactivation, increasing tumour responses and sensitising immune evasive tumours to anti-PD1 blockade.

**Conflict of interest:**

Corporate-sponsored Research: Compounds and funding were kindly provided by Revolution Medicines (Redwood City, CA).

174 (PB054)  
**A novel BAD phosphorylation inhibitor combined with EGFR tyrosine kinase inhibitors in EGFR-mutant lung adenocarcinoma treatment**

X. Zhang<sup>1</sup>, C. Shu<sup>2</sup>, P. Huang<sup>2</sup>, V. Pandey<sup>3</sup>, P.E. Lobie<sup>3</sup>. <sup>1</sup>Shenzhen Bay Laboratory, The Institute of Biopharmaceutical and Health Engineering iBHE, ShenZhen, China; <sup>2</sup>Tsinghua Shenzhen International Graduate School, Tsinghua Berkeley Shenzhen Institute, ShenZhen, China; <sup>3</sup>Tsinghua Shenzhen International Graduate School, Institute of Biopharmaceutical and Health Engineering, ShenZhen, China

**Background:** The approval and use of epidermal growth factor receptor-tyrosine kinase inhibitors (EGFR-TKIs) in EGFR-mutant NSCLC has been a breakthrough in clinic. The activation of compensatory pathways of PI3 K/AKT and/or MEK/MAPK modulates cell survival and drug resistance of lung adenocarcinoma (LUAC). As a convergent downstream signaling node and

the determinant, BAD is a potential target to inhibit cell survival and to overcome EGFR TKI resistance in LUAC treatment.

**Material and methods:** We determined the relevance of phosphorylation of BAD at serine (S) 99 in LUAC and utilized a novel small-molecule inhibitor of pBADs99 combined with EGFR-TKIs in TKI sensitive and resistant LUAC models treatment, respectively.

**Results:** Herein we show that the relative BAD phosphorylation level is frequently higher in LUAC tumors which is associated with poor clinical outcome. pBADs99 was also found increased in the EGFR-TKI resistant cells, and that high levels of pBADs99 in LUAC cells correlates with poor therapeutic responses and cancer stem like cell (CSC) and epithelial mesenchymal transition (EMT) properties. PI3 K/AKT signaling pathway plays an important role in acquired EGFR-TKIs resistance in LUAC converging on BAD phosphorylation at Serine 99. Targeting BAD phosphorylation at Serine 99 induce cell apoptotic death and decreased CD44 related CSC and EMT properties in LUAC. Furthermore, we demonstrated that combined treatment with NPB and EGFR-TKIs in both sensitive and resistant EGFR-mutant LUAC models have a synergistic efficacy *in vitro*, *ex vivo* and *in vivo*.

**Conclusions:** Pharmacologically inhibiting BAD phosphorylation at Serine 99 is functionally relevant to both TKI sensitivity and resistance in LUAC treatment regardless of EGFR mutation or pathways involved in the drug resistance. Combination of EGFR-TKI and NPB is a rational and feasible treatment strategy for delaying and overcoming acquired resistance in LUAC.

**No conflict of interest.**

175 (PB055)  
**Abemaciclib drug combination screening with other targeted therapies in complex multicellular tumor spheroids**

T. Dexheimer<sup>1</sup>, T. Silvers<sup>1</sup>, R. Delosh<sup>1</sup>, J. Laudeman<sup>1</sup>, R. Reinhart<sup>1</sup>, C. Ogle<sup>1</sup>, Z. Davoudi<sup>1</sup>, E. Jones<sup>1</sup>, N. Coussens<sup>1</sup>, R. Parchment<sup>1</sup>, J. Morris<sup>2</sup>, M. Kunkel<sup>2</sup>, J. Wright<sup>2</sup>, N. Takebe<sup>2</sup>, J. Doroshov<sup>2</sup>, B. Teicher<sup>2</sup>. <sup>1</sup>Frederick National Laboratory for Cancer Research, Applied and Developmental Research Directorate, Frederick, USA; <sup>2</sup>National Cancer Institute, Division of Cancer Treatment and Diagnosis, Bethesda, USA

Drug combinations are frequently used to improve clinical efficacy, to minimize toxicity, and to reduce the development of resistance. Here, we investigated the growth inhibitory activity of the CDK4/6 inhibitor abemaciclib in combination with other targeted agents. Twelve well-characterized patient-derived cancer cell lines from the NCI Patient-Derived Models Repository (<https://pdmr.cancer.gov/models/database.htm>) and seven established cell lines from the NCI-60 human tumor cell line panel were grown as multicellular 3D complex spheroids. The complex spheroids, a mixture of tumor cells (60%), endothelial cells (25%), and mesenchymal stem cells (15%), were established for three days before drug(s) were added. All agents were tested at concentrations up to their reported clinical C<sub>max</sub> values and cell viability for each individual drug treatment and drug combination was assayed using CellTiter-Glo 3D after seven days of drug exposure. Abemaciclib had modest activity as a single agent. The combination of abemaciclib with the MEK inhibitor selumetinib or the ERK inhibitor ravoxertinib resulted in additive and/or synergistic cell killing in several of the cell lines screened. The KRAS G12C selective inhibitor sotorasib in combination with abemaciclib was active in the two KRAS G12C variant containing cell lines. The most effective combination for abemaciclib was with the CDK2/7/9 inhibitor BMS-387032, which achieved greater than one log of cytotoxicity in the majority of the complex spheroid models. There was also a high correlation among responses to the combination of abemaciclib and selumetinib in two patient-derived cell lines grown as complex spheroids, one patient-derived organoid line, and matching patient-derived xenograft models. This project was funded in part with federal funds from the NCI, NIH, under contract no. HHSN2612015000031.

**No conflict of interest.**

176

(PB056)

**The NEDD8 pathway as a therapeutic target in HER2-amplified colorectal cancer**F. Invrea<sup>1</sup>, A. Carugo<sup>2</sup>, S. Arena<sup>3</sup>, G. Draetta<sup>2</sup>, A. Bardelli<sup>4</sup>, E. Medico<sup>3</sup>.<sup>1</sup>Candiolo Cancer Institute- FPO-IRCCS, Laboratory of Oncogenomics, Candiolo, Italy; <sup>2</sup>MD Anderson Cancer Center, University of Texas, Houston, USA; <sup>3</sup>Candiolo Cancer Institute- FPO-IRCCS, University of Torino, Candiolo, Italy; <sup>4</sup>University of Torino, Oncology, Torino, Italy

**Background:** Colorectal cancer (CRC) is a heterogeneous disease with a wide spectrum of clinical outcomes, from indolent resectable disease to aggressive-metastatic cases. Primary and acquired resistance limits the efficacy of available treatments, and the identification of effective drug combinations is needed to further improve patients' outcomes. We previously found that the NEDD8-activating enzyme inhibitor pevonedistat induced tumor stabilization in preclinical models of poorly differentiated, clinically aggressive CRC resistant to available therapies. To identify drugs that can be effectively combined with pevonedistat, we performed a "drop-out" loss-of-function synthetic lethality screening with a shRNA library covering 200 drug-target genes in four different CRC cell lines. Screening hits were then validated. Multiple screening hits were found to be involved in the EGFR signaling pathway, suggesting that, rather than inhibition of a specific gene, interference with the EGFR pathway at any level could be effectively leveraged for combination therapies based on pevonedistat. Exploiting both BRAF-mutant and RAS/RAF wild-type CRC models, we validated the therapeutic relevance of our findings by showing that combined blockade of NEDD8 and EGFR pathways led to increased growth arrest and apoptosis both *in vitro* and *in vivo*. Pathway modulation analysis showed that compensatory feedback loops induced by single treatments were blunted by the combinations. Our results suggested possible therapeutic opportunities in specific CRC clinical settings.

**Materials and methods:** We focused on HER-2 amplified CRC cells, testing combinations of HER2/EGFR treatment with NEDD8 blockade by pevonedistat in both short-term and long-term *in vitro* assays.

**Results:** We observed significant cooperation between pevonedistat and HER-2/EGFR blockade by the trastuzumab+lapatinib combination -the current standard treatment for HER2-amplified CRC. In addition to confirming cooperation in reducing colony formation *in vitro*, we explored the effect of pevonedistat on long-term persisters, i.e., cell surviving to several weeks of HER2/EGFR blockade. Interestingly, we observed a marked decrease of cell colonies when pevonedistat was added to persisters survived to three weeks of trastuzumab+lapatinib treatment.

**Conclusions:** These results unveil the possibility of testing *in vivo* the addition of pevonedistat subsequently to tumor stabilization or reduction by HER2/EGFR blockade, to promote further tumor regression.

No conflict of interest.

177

(PB057)

**BLU-945 or BLU-701 as single agents versus their combination with osimertinib in EGFR L858R driven tumor models**L. Tavera<sup>1</sup>, J. Campbell<sup>2</sup>, A. Dhande<sup>1</sup>, T. Dineen<sup>2</sup>, M. Iliou<sup>1</sup>, T. Rouskin-Faust<sup>1</sup>, E. Rozsahegy<sup>1</sup>, C. Conti<sup>1</sup>. <sup>1</sup>Blueprint Medicines Corporation, Biology, Cambridge, USA; <sup>2</sup>Blueprint Medicines Corporation, Chemistry, Cambridge, USA

**Background:** The most common activating *EGFR* mutations (*EGFRm*) in non-small cell lung cancer (NSCLC) are exon 19 deletions (ex19del) and L858R substitutions. EGFR tyrosine kinase inhibitors (TKIs) as first-line (1L) therapy have improved outcomes in *EGFR*-driven advanced NSCLC; however, treatment resistance eventually occurs. Patients with *EGFR* L858R-driven advanced NSCLC (39% of all *EGFR* mutations in NSCLC) have shorter progression-free survival than those with *EGFR* ex19del, suggesting a significant unmet need. BLU-945 and BLU-701 are investigational, reversible, selective, orally available TKIs optimized for use as single-agent or combination therapy to suppress activating and on-target resistance *EGFR* mutants while sparing wild-type *EGFR*. *In vivo* studies have shown antitumor activity of BLU-945 against *EGFR* L858R, L858R/C797S, L858R/T790M and *EGFRm*/T790M/C797S mutants, and BLU-701 against *EGFRm* and *EGFRm*/C797S mutants. Combination of BLU-945 and BLU-701 has also shown *in vivo* activity in *EGFRm*/C797S-driven mutant NSCLC. Combining BLU-945 or BLU-701 with osimertinib could potentially enable superior coverage of frequent on-target resistance mechanisms as well additional potency on the primary *EGFR* activating mutations. Central nervous system (CNS) metastases are an ongoing challenge in NSCLC. BLU-701 has already shown preclinical CNS activity; and both BLU-945 and BLU-701 are currently being investigated for potential treatment or prevention of CNS metastases. Due to poorer outcomes in patients with

*EGFR* L858R-driven advanced NSCLC treated with osimertinib, and the inevitability of treatment resistance, studies were conducted to evaluate the activity of BLU-945 or BLU-701 in combination with osimertinib in prolonging duration of response (DOR) in preclinical NSCLC tumor models driven by the L858R mutation.

**Material and Methods:** The antitumor activity of BLU-945 or BLU-701, as single agents or in combination with osimertinib was evaluated in *EGFR* L858R-driven tumor models.

**Results:** Administration of single-agent BLU-945 or BLU-701 resulted in tumor growth inhibition in *EGFR* L858R-driven PDX models. BLU-945 in combination with osimertinib resulted in prolonged DOR and survival when compared with BLU-945 or osimertinib as single agents. BLU-701 in combination with osimertinib resulted in superior tumor growth inhibition compared with BLU-701 or osimertinib as single agents.

**Conclusions:** The *in vivo* antitumor activities of BLU-945 and BLU-701 as single agents suggest both BLU-945 and BLU-701 have the potential to be used as 1L therapy in patients with *EGFR* L858R-driven NSCLC. The superior *in vivo* antitumor activity of BLU-945 or BLU-701 in combination with osimertinib in prolonging the DOR or increasing tumor growth inhibition in these models may have clinical application in improving outcomes of patients with *EGFR* L858R-driven NSCLC in 1L settings.

**Conflict of interest:**

Other Substantive Relationships: Tavera L, Dhande A, Dineen T, Iliou M, Rouskin-Faust T, Rozsahegy E, Conti C: Employee and/or equity holder of Blueprint Medicines Corporation.

178

(PB058)

**Characterizing mechanisms of resistance to BRAF and MEK inhibitors in cancers with Class 2 BRAF mutations: uncovering novel therapeutic opportunities**M. Riaud<sup>1</sup>, M. Biondini<sup>2</sup>, E. Cianfarano<sup>3</sup>, E. Rousselle<sup>3</sup>, J. Maxwell<sup>3</sup>, I. Soria-Bretones<sup>1</sup>, P. Tai<sup>3</sup>, H. Wang<sup>1</sup>, P.M. Siegel<sup>2</sup>, D.W. Cescon<sup>4</sup>, A. Spreafico<sup>4</sup>, A. A. N. Rose<sup>1</sup>. <sup>1</sup>Lady Davis Institute- Segal Cancer Centre, Jewish General Hospital, Montreal, QC, Canada, Gerald Bronfman Department of Oncology, McGill University, Montreal, QC, Canada, Montreal, Canada; <sup>2</sup>Goodman Cancer Research Institute, McGill University, Montreal, QC, Canada, Department of Medicine, McGill University, Montreal, QC, Canada, Montreal, Canada; <sup>3</sup>Lady Davis Institute, Segal Cancer Centre, Jewish General Hospital, Montreal, QC, Canada, Division of Experimental Medicine, Montreal, Canada; <sup>4</sup>Princess Margaret Cancer Centre, University Health Network, Toronto, Ontario, Canada, Department of Medicine, University of Toronto, Toronto, ON, Toronto, Canada

**Background:** BRAF mutations are identified in many advanced cancers. Despite the curative approaches developed with targeted therapies (BRAF and/or MEK inhibitors (BRAFi and MEKi)) for patients with V600 (Class 1) BRAF mutant cancers, optimal strategies for oncogenic non-V600 BRAF mutant tumors have not been established. Class 2 BRAF mutations are oncogenic non-V600 mutations that signal as RAS-independent dimers. Clinical data supports efficacy of BRAFi+MEKi in some Class 2 BRAF mutant tumors – but this strategy may not be as effective as it is for Class 1 BRAF mutant tumors. Therefore, we sought to identify molecular mechanisms of therapeutic resistance to BRAFi+MEKi in Class 2 BRAF mutant tumors. The goal of this work is to identify and test novel targeted therapy regimens that could be more beneficial to patients.

**Material and Methods:** We determined the IC50 for binimetinib (MEKi) and encorafenib (BRAFi) (B+E) in a panel of cell lines with BRAF Class 1 (n = 4) or Class 2 (n = 5) mutations using clonogenic assays. By passaging cells in B+E for several months, we developed several cell lines with Class 2 BRAF mutations (MDA-MB-231, FM95, H2087) that have acquired resistance to B+E. RNA-sequencing with KEGG Pathway Enrichment Analysis and immunoblots were used to characterize RNA and protein-level between parental and resistant cells. Two independent Class 2 BRAF mutant melanoma Patient derived xenograft (PDXs) were used to evaluate treatment efficacy *in vivo*.

**Results:** The IC50 for B+E was significantly higher for cancer cells with Class 2 BRAF mutations vs. Class 1 BRAF mutations. KEGG enrichment analysis of B+E resistant cells identified genes involved in cell cycle as one of the most significantly differentially expressed pathways in B+E resistant cells. D and E cyclins as well as CDK6 expression and Rb phosphorylation was higher in B+E resistant cells. The addition of the CDK4/6 inhibitor (palbociclib) significantly enhanced B+E mediated growth inhibition in Class 2 BRAF mutant cancer cells (22RV1, HMV-II, H2087, FM95, MDA-MB-231) *in vitro* and in two independent BRAF L597S mutant melanoma xenografts (GCRC-Mel1, GCRC2015) *in vivo*. However, the addition of palbociclib to B+E was insufficient to inhibit growth in cells that had already established resistance to B+E.

**Conclusions:** Class 2 BRAF mutant cancer cells are less sensitive to BRAFi+MEKi than Class 1 BRAF mutant cancer cells. We have identified an effective and novel therapeutic approach for non-V600 BRAF mutant cancers that forestalls BRAF+MEK inhibitor resistance in these cells. Ongoing research aims to characterize the mechanisms that govern CDK4/6-pRb hyper-activation in B+E resistant Class 2 tumors. These data provide rationale for the clinical development of novel therapeutic strategies patients with Class 2 BRAF mutant metastatic cancers.

**No conflict of interest.**

179 (PB059)

**The combination of the metabolite-based targeted therapies ADI-PEG20 and GC7 are a promising strategy for the treatment of malignant pleural mesothelioma**

J. Carpentier<sup>1</sup>, P. Szlosarek<sup>1</sup>, S.A. Martin<sup>2</sup>. <sup>1</sup>Barts Cancer Institute, Center for Biomarkers and Biotherapeutics, London, United Kingdom; <sup>2</sup>Barts Cancer Institute, Center for Cancer Cell and Molecular Biology, London, United Kingdom

**Background:** Malignant pleural mesothelioma (MPM) is a highly aggressive cancer with less than a 10% 5-year survival rate. Arginine deprivation using pegylated arginine deiminase (ADI-PEG20) is a promising anti-metabolite strategy for MPM cells deficient in the arginine biosynthetic enzyme ASS1. However, resistance to ADI-PEG20 in MPM is a significant problem and is characterized in part by reprogramming of the urea and polyamine metabolism pathway. We sought to identify a targeted metabolism-based therapy to overcome the emerging resistance and increase the efficiency of ADI-PEG20 treatment for MPM patients.

**Material and methods:** New models of ADI-PEG20 resistance were generated by constant exposure of MPM cell lines to arginine deprivation for 6 months. ADI-PEG20 resistant and sensitive MPM cell models were treated with a panel of polyamine targeting molecules to identify potent candidate for a combination therapy with ADI-PEG20. Metabolome alterations were studied by targeted metabolomics and glucose flux analyses.

**Results:** Our results confirmed the up-regulation of ASS1 expression from between 50 and 3000-fold alongside altered polyamine enzyme expression upon generation of ADI-PEG20 resistance. Treatment of ADI-PEG20 resistant cell lines with a range of different polyamine inhibitors demonstrated that ADI-PEG20 resistant cell lines were highly sensitive to the spermidine-analog GC7. Moreover, the combination of GC7 and ADI-PEG20 prevented the emergence of resistant cells *in vitro*. Metabolomic analysis revealed that GC7 treatment significantly impaired the TCA cycle. We observed a significant synergistic effect of GC7 and ADI-PEG20 in both ADI-PEG20 sensitive and resistant cell lines in 2D and 3D cell culture models.

**Conclusions:** Our findings provide novel insights into a polyamine targeted therapy that could prevent resistance to ADI-PEG20 treatment. This targeted combination of GC7 with ADI-PEG20 has the potential to improve outcomes in patients with MPM and other arginine-auxotrophic cancers displaying ASS1 heterogeneity.

**No conflict of interest.**

180 (PB060)

**Neratinib plus dasatinib has pre-clinical efficacy against HER2-positive breast cancer**

N. Conlon<sup>1</sup>, S. Roche<sup>1</sup>, F. O'Neill<sup>1</sup>, J. Meiller<sup>1</sup>, A. Browne<sup>1</sup>, L. Breen<sup>1</sup>, L. O'Driscoll<sup>2</sup>, M. Cremona<sup>3</sup>, B. Hennessy<sup>3</sup>, J. Crown<sup>4</sup>, D. Collins<sup>1</sup>. <sup>1</sup>Dublin City University, National Institute for Cellular Biotechnology, Dublin, Ireland; <sup>2</sup>Trinity College Dublin, School of Pharmacy and Pharmaceutical Sciences, Dublin, Ireland; <sup>3</sup>Royal College of Surgeons in Ireland, Department of Molecular Medicine, Dublin, Ireland; <sup>4</sup>St Vincent's University Hospital, Department of Medical Oncology, Dublin, Ireland

**Background:** HER2-targeted therapies have revolutionised the treatment of HER2-positive breast cancer. However, *de novo* resistance or the emergence of acquired resistance is a persistent clinical problem. The aim of this study was to investigate neratinib, an irreversible pan-HER inhibitor, in combination with the multi-kinase inhibitor dasatinib, currently used to treat certain leukemias, as a new treatment option for patients with HER2-targeted therapy resistant HER2-positive breast cancer.

**Material and methods:** The anti-proliferative effect of neratinib in combination with dasatinib was examined in a panel of 20 breast cancer cell lines, including HER2-positive, estrogen receptor-positive, triple negative, and acquired HER2-targeted therapy resistant models. Reverse phase protein array (RPPA), live-cell fluorescent imaging, and Western blotting were employed to examine the mechanism of action of the drug combination.

The safety and efficacy of neratinib plus dasatinib was examined *in vivo* in HCC1954 xenografts in BALB/c nude mice.

**Results:** Neratinib plus dasatinib was highly effective against HER2-positive and triple negative breast cancer cell lines. While neratinib alone was effective at clinically relevant concentrations in 10 cell lines tested and single agent dasatinib was only effective in 4 of the cell lines, the addition of dasatinib significantly enhanced neratinib response in 11 of 20 cell lines. This included overcoming neratinib resistance in 4 acquired neratinib-resistant cell lines. In HER2-targeted therapy-naive cell lines, the drug combination was most effective against cell lines that were less responsive to HER2-targeted therapies in general. Neratinib plus dasatinib was well tolerated *in vivo* and had a prolonged anti-tumour effect against HCC1954 xenografts. RPPA analysis showed comprehensive inhibition of the HER-family signalling pathway and induction of apoptosis, which was confirmed by fluorescent microscopy.

**Conclusions:** These *in vitro* and *in vivo* data provide the preclinical evidence for the efficacy of neratinib plus dasatinib against HER2-positive breast cancer. This combination warrants clinical investigation.

**Conflict of interest:**

Ownership: JC - OncoMark, OncoAssure (stocks)  
Advisory Board: JC - AstraZeneca, MSD, Novartis  
Corporate-sponsored Research: JC and DC - Puma Biotechnology Inc  
Other Substantive Relationships: JC - Pfizer, AstraZeneca, MSD (travel), Daiichi Sankyo, Roche (conference registration fee), Cepheid (consultancy)

181 (PB061)

**Spatial transcriptomics analysis of co-targeted PIM and PI3 K/mTOR in multikinase inhibitor and single kinase inhibitor combination-treated patient-derived prostate cancer explants**

U. Okoli<sup>1</sup>, G. Akman<sup>1</sup>, V. Thavarajah<sup>1</sup>, L. M. Carmona Echeverria<sup>1</sup>, J. Griffin<sup>2</sup>, S.R. Ohayi<sup>3</sup>, A. Freeman<sup>4</sup>, A. Haider<sup>1</sup>, G. Shaw<sup>5</sup>, A.N. Sridhar<sup>6</sup>, J. Kelly<sup>1</sup>, B. Simpson<sup>7</sup>, H. Pye<sup>1</sup>, J. Crompton<sup>1</sup>, H. Whitaker<sup>1</sup>, U. Cheema<sup>1</sup>, S. Heavey<sup>1</sup>. <sup>1</sup>University College London, Division of Surgery and Interventional Science, London, United Kingdom; <sup>2</sup>Sheffield Teaching Hospitals NHS Foundation Trust, Histopathology Department, Sheffield, United Kingdom; <sup>3</sup>Enugu State University Teaching Hospital, Department of Histopathology, Enugu State, Nigeria; <sup>4</sup>University College London Hospitals NHS Foundation Trust, Department of Histopathology- UCL Hospital, London, United Kingdom; <sup>5</sup>University College London, Academic Department of Surgery- University College London, London, United Kingdom; <sup>6</sup>University College London Hospitals NHS Foundation Trust, University College London Hospital, London, United Kingdom; <sup>7</sup>University College London, University College London, London, United Kingdom

Prostate cancer is a multifocal heterogeneous disease that remains the second leading cause of male death worldwide. These deaths are caused mainly by metastasis. Moreover, PIM and PI3 K/mTOR pathways are frequently dysregulated in prostate cancer, and may lead to an invasion, increased metastasis and decreased survival. However, the interconnection of these pathways has been shown to mediate anti-tumour drug resistance. Furthermore, current treatments exhibit issues with toxicity. The novel preclinical multikinase PIM/PI3 K/mTOR inhibitor, AUM302, versus clinical trial investigated - a combination of the PI3 K/mTOR inhibitor BEZ235 (Dactolisib) and PIM inhibitor, AZD-1208 has been analyzed in our laboratory using a cohort of cancer explants emanating from our PEOPLE: PatiEnt prOstate samPLes for rEsea ch study and our current SCREEN study. This cohort has a high Gleason grade score of  $\geq 8$ . Therefore, this study aims to assess the adequacy of the prostate cancer ex vivo models and the efficacy and mechanism of action of the drugs. Using the Nanostring GeoMX DSP technology, we aim to analyze the spatial molecular profile of the co-targeted therapy treated ex vivo models to decipher the effects of heterogeneity on the co-targeted therapies efficacy. Tissue microarrays of co-targeted treated thirty ex vivo 3 mm cores derived from 5 patients will be analyzed. Morphology markers, including PAN CK positive and PAN CK negative, will be used to guide the selection of 300 regions of interest (ROI) comprising benign and tumours. ROI will be segmented and profiled using immunofluorescence. The morphological markers will define these segments into areas of illumination (AOIs) using a combination of the absence or presence of  $\alpha$ SMA and pSTAT3. The AOIs will generate multiple expression profiles for the related ROI. We intend to use this flexible, high-dimensional spatial profiling to identify the spatial genomic signatures and phosphorylation sites in cancer-targeted therapies. Our findings will contribute to understanding how the spatial landscape of the tumour microenvironment enhances the efficacy of anti-tumour drugs and what subset of patients are more likely to benefit from such therapy.

**No conflict of interest.**

## POSTER SESSION

## Cytotoxics (including Antimetabolites, Anthracyclin, Alkylating agents, Aurora kinases, Polo-like kinase, Topoisomerase inhibitors, Tubulin-binding compounds)

182

(PB062)

### N-1,2,3-Triazole-Isatin derivatives in lymphoma cell lines

E. Gaudio<sup>1</sup>, C. Tarantelli<sup>1</sup>, C.S. Marques<sup>2</sup>, H. Ekeh<sup>1</sup>, M. Carmelo<sup>1</sup>, A.J. Burke<sup>3</sup>, F. Bertoni<sup>4</sup>. <sup>1</sup>Faculty of Biomedical Sciences- USI, Institute of Oncology Research, Bellinzona, Switzerland; <sup>2</sup>Institute for Research and Advanced Studies- University of Évora, Associated Laboratory for Green Chemistry of the Network of Chemistry and Technology, Évora, Portugal; <sup>3</sup>University of Coimbra- Pólo das Ciências da Saúde, Faculty of Pharmacy, Coimbra, Portugal; <sup>4</sup>Institute of Oncology Research, Institute of Oncology Research, Bellinzona, Switzerland

**Background:** Molecular hybrid constructs are an interesting approach to merge individual pharmacophores with different mechanisms of action, potentially decreasing side effects. The 1,2,3-triazole unit is present in many bioactive compounds and it is characterized by its ability to be stable towards hydrolysis to increase the compounds lipophilicity. Hybrids containing this pharmacophore together with isatin and its analogues have shown a wide spectrum of potential therapeutic activities, also against cancer. Burke et al. have recently reported new N-1,2,3-triazole-isatin hybrids with *in vitro* anti-tumor activity in solid tumor cell lines (RSC Medicinal Chemistry 2022; EP3400938). Here, we present the *in vitro* anti-lymphoma activity and structure activity relationships (SAR) of 9 N-1,2,3-triazole-isatin hybrids.

**Methods:** Anti-proliferative activity assessed by 3-[4,5-dimethylthiazol-2yl]-2,5-diphenyl tetrazolium bromide (MTT) assay at 72 h. Cell cycle assessed by FACS. IC<sub>50</sub> values defined as the concentrations corresponding to 50% viability inhibition.

**Results:** Cell lines derived from diffuse large B-cell lymphoma (DLBCL) of the germinal center B-cell-like (GCB) type (DOHH-2, VAL) and of the activated B-cell-like (ABC) type (OCI-LY-10, SU-DHL-2) were exposed to increasing concentrations of 9 chemically modified oxindole derivatives (Table 1). While 6 compounds did not show any activity at concentrations <20 µM, compounds (1a-c) were active, with IC<sub>50</sub>s lower in ABC- than in GCB-DLBCL. Specifically, compound (1c), which carries a methyl group in the 5-position of the aromatic ring of the isatin scaffold, was the most active. The chiral non-racemic N-1,2,3-triazole-oxindole derivatives (2) did not show activity. Compounds (1a) and (1c) (10 µM; OCI-LY-10; 48, 72 h) induced an accumulation of cells in the sub-G<sub>0</sub> phase, suggestive of the induction of cell death, slightly higher with (1c) than with (1a), in agreement with the IC<sub>50</sub>s. In terms of SAR, compounds with the free carbonyl unit in the 3-position, i.e. (1a)-(1c) gave the best results against the ABC-DLBCL cell lines. Since both (1a) and (1c) were more active than (1b), the N-benzyl unit might also be important in determining anti-tumor activity.

Table 1. Chemically modified oxindole derivatives and their IC<sub>50</sub> values obtained in DLBCL cell lines. Compound names according to Burke et al., RSC Medicinal Chemistry 2022. IC<sub>50</sub> values in µM.

Compound	DOHH2	VAL	OCI-LY-10	SU-DHL-2
(1a)	>20	>20	10	0.75
(1b)	>20	>20	7	15
(1c)	10	>20	5	0.75
(S)-(2a)	>20	>20	>20	>20
(R)-(2b)	>20	>20	>20	19
(R)-(2d)	>20	>20	>20	>20
(S)-(2f)	>20	>20	>20	>20
(S)-(2i)	>20	>20	>20	>20
(R)-(2j)	>20	>20	>20	>20

**Conclusions:** *In vitro* anti-tumor activity in ABC-DLBCL models was observed for specific N-1,2,3-triazole-isatin hybrids, indicating that their structures represent the starting point to design compounds with stronger activity. *AJB* and *FB*: co-senior authors.

#### Conflict of interest:

Ownership: Patent EP3400938

183

(PB063)

### The antimetabolite KAT/3BP has *in vitro* and *in vivo* anti-lymphoma activity

C. Tarantelli<sup>1</sup>, F. Spriano<sup>1</sup>, E. Civanelli<sup>1</sup>, A.J. Arribas<sup>1</sup>, L. Aresu<sup>2</sup>, G. Risi<sup>1</sup>, O. Kayali<sup>1</sup>, A. Stathis<sup>3</sup>, Y.H. Ko<sup>4</sup>, F. Bertoni<sup>1</sup>. <sup>1</sup>Faculty of Biomedical Sciences- USI, Institute of Oncology Research, Bellinzona, Switzerland; <sup>2</sup>University of Turin, Department of Veterinary Sciences, Grugliasco TO, Italy; <sup>3</sup>Ente Ospedaliero Cantonale, Oncology Institute of Southern Switzerland, Bellinzona, Switzerland; <sup>4</sup>NewG Lab Pharma, Inc., KoDiscovery, LLC, Baltimore, Maryland, USA

**Background:** Reprogramming of cellular metabolism is one of the hallmarks of cancer (Hanahan, 2022), thus representing an important therapeutic target. 3-bromopyruvate (3BP or KAT/3BP) is a small, highly reactive molecule formed by the bromination of pyruvate (Ko et al, 2012). The very high similarity of its structure with pyruvic acid and lactic acid is the basis of its mechanism of action as an anti-cancer agent. Indeed, 3BP enters cancer cells via monocarboxylic acid transporters and it can then inhibit glycolysis and oxidative phosphorylation process. KAT/3BP has received FDA Orphan Drug Designation for different solid tumors and is about to enter the early controlled clinical evaluation. Here, we present *in vitro* and *in vivo* assessments of KAT/3BP in lymphoma models.

**Materials and Methods:** Cell lines were exposed to increasing concentration of KAT/3BP by MTT assay for 72 h. Apoptosis and cell cycle were evaluated by FACS. BALB/c mice (A20 cells in the left flank; 5 mice/group) were treated (4 weeks on, 1 off) with: oral (PO) and intratumoral (IT) vehicles, PO KAT/3BP [2.5 (low), 10 mg/kg (high)], IT KAT/3BP [0.5 (low), 2 mM (high)], PO-low/IT-low, PO-high/IT-high.

**Results:** KAT/3BP showed dose-dependent anti-proliferative activity in cell lines derived from diffuse large B-cell lymphoma (DLBCL; n = 8) and mantle cell lymphoma (MCL; 4), with median IC<sub>50</sub> s of 8 µM and 5.5 µM, respectively. The compound was also tested in marginal zone lymphoma (MZL; 2) cell lines and in their derivatives with acquired resistance to idelalisib (2), ibrutinib (1), and copanlisib (1). 3BP was equally active in parental and resistant cell lines. KAT/3BP (5 µM, 72 h) was able to induce strong apoptosis in cell lines (1 DLBCL, 1 MCL) already after 24 h of treatment.

An *in vivo* pilot experiment using the murine syngeneic model (A20 lymphoma cells, BALB/c mice) confirmed the *in vitro* observed anti-tumor activity. All mice in the control groups died after nearly 20 days. A tumor reduction compared to the control vehicle was observed in all the treatment groups based on slope values extrapolated by a linear regression model. In particular, PO-high KAT/3BP lead to complete tumor reduction in 3/5 mice (2 still alive at D92, 1 dead at D36). After D26, also 1 mouse in IT-low and 1 in PO-low/IT-low survived and showed reduced tumor mass. Peripheral and focal tumor necrosis was seen in the tumor in PO-high/IT-high, PO-high, and IT-high (1 each). Necrosis was more extensively observed at histology in IT-high and PO-high/IT-high groups.

**Conclusions:** KAT/3BP showed *in vitro* activity in MCL, DLBCL, and MZL, including models resistant to PI3 K/BTK inhibitors. *In vivo* activity was also seen in a syngeneic mouse model. KAT/3BP induced apoptosis *in vitro* and necrosis *in vivo*.

\*CT, FS: Equally contributed

#### Conflict of interest:

Advisory Board: Gilead, AbbVie, Janssen, AstraZeneca, MSD, BMS/Celgene, Roche, Mei Pharma, Astra Zeneca, Celltrion Healthcare, Incyte, Kite/Gilead  
Corporate-sponsored Research: Celgene, Roche, Janssen, Acerta, ADC Therapeutics, Bayer AG, Cellestia, CTI Life Sciences, EMD Serono, Helsinn, Immunogen, Menarini Ricerche, NEOMED Therapeutics 1, Nordic Nanovector ASA, Oncology Therapeutic Development, PIQUR Therapeutics AG, Gilead, AbbVie, Janssen  
Other Substantive Relationships: Work supported by Ko Discovery LLC.

184

(PB064)

### Transcriptome and computational analysis assess the anti-tubulin activity of [1,2]oxazole derivatives in lymphoma

M. Barreca<sup>1</sup>, V. Spanò<sup>1</sup>, R. Rocca<sup>2</sup>, R. Bivacqua<sup>1</sup>, A. Maruca<sup>2</sup>, A. Montalbano<sup>1</sup>, M.V. Raimondi<sup>1</sup>, C. Tarantelli<sup>3</sup>, E. Gaudio<sup>3</sup>, L. Cascione<sup>3</sup>, A. Rinaldi<sup>3</sup>, R. Bai<sup>4</sup>, A. Prota<sup>5</sup>, A.C. Abel<sup>5</sup>, M. Steinmetz<sup>5</sup>, S. Alcaro<sup>6</sup>, E. Hamel<sup>7</sup>, F. Bertoni<sup>3</sup>, P. Barraja<sup>1</sup>. <sup>1</sup>University of Palermo, Department of Biological- Chemical- and Pharmaceutical Sciences and Technologies STEBICEF, Palermo, Italy; <sup>2</sup>Università Magna Græcia di Catanzaro, Net4Science srl, Catanzaro, Italy; <sup>3</sup>Faculty of Biomedical Sciences- USI, Institute of Oncology Research, Bellinzona, Switzerland; <sup>4</sup>Frederick National Laboratory for Cancer Research- National Cancer Institute- National



Institutes of Health, Molecular Pharmacology Branch- Developmental Therapeutics Program- Division of Cancer Treatment and Diagnosis, Frederick, USA; <sup>5</sup>Paul Scherrer Institut, Division of Biology and Chemistry, Villigen PSI, Switzerland; <sup>6</sup>Università Magna Graecia di Catanzaro, Dipartimento di Scienze della Salute, Catanzaro, Italy; <sup>7</sup>Molecular Pharmacology Branch- Developmental Therapeutics Program- Division of Cancer Treatment and Diagnosis, Frederick National Laboratory for Cancer Research- National Cancer Institute- National Institutes of Health, Frederick, USA

**Background:** Anti-tubulin agents are widely used in the treatment of lymphoma and are included in important chemotherapy schemes (R-CHOP, ABVD, BEACOP) as well as in the innovative therapeutic approaches utilizing antibody-drug conjugates (ADCs) such as brentuximab vedotin and polatuzumab vedotin. Recently, we have devoted our efforts to the investigation of a large family of [1,2]oxazole-based derivatives that showed anti-proliferative activity in several lymphoma models, with IC<sub>50</sub> values between the low micromolar and nanomolar range. High inhibition of tubulin polymerization due to strong interactions with colchicine-binding site was confirmed by computational studies and colchicine binding to tubulin. We now present the transcriptome changes induced by the best candidate of this family (SIX2-F).

**Material and methods:** To unravel gene expression changes, MINO cell line was exposed to DMSO or to 100 nM of compound for 8, 12 and 24 hours and transcripts changes analyzed by RNA-Seq. The binding mode to colchicine-binding site was elucidated by X-ray crystallographic studies, using a T2R-TTL protein complex composed of two  $\alpha$ -tubulin (T2) dimers, the stathmin-like protein RB3 (R) and tubulin tyrosine ligase (TTL). Each tubulin dimer in the complex contained an accessible colchicine site, termed  $\beta$ 1 and  $\beta$ 2. Finally, docking poses and molecular dynamics simulations (MDs) were generated towards the 4O2B PDB model.

**Results:** The gene expression changes caused by SIX2-F revealed a significant upregulation of genes related either to spindle and microtubule assembly and to G2/M transition. The top upregulated genes were CCNB1 (cyclin B1), CCNB2 (cyclin B2), AURKA (aurora kinase A), PLK1 (Polo-like kinase 1), CENPA (centromere protein A), CENPE (centromere protein E) and BIRC5 (survivin), while genes involved in transcription and DNA replication were downregulated. In T2R-TTL-ligand structure, a large, compound shaped difference density within the binding site was observed for SIX2-F, proving that the ligand was bound. In particular, the  $\beta$ 17 and  $\alpha$ T5 loops were flipped to accommodate the compound. Docking calculations confirmed that SIX2-F well-fitted the colchicine-binding pocket (G-Score = -9.71 Kcal/mol), directing the methoxybenzyl moiety towards C241. The complex was further stabilized by means of several hydrophobic interactions with the residues A180, L242, L248, L250, L252, L255, A316, I317 and A354.

**Conclusions:** Transcriptome changes induced by SIX2-F in lymphoma overlapped with those reported for other microtubule inhibitors. These data, further supported by its docking poses and interactions with the crystal structure of tubulin, validated its activity as anti-tubulin agent and confirmed SIX2-F as promising candidate for further studies for the treatment of refractory lymphomas.

#### Conflict of interest:

Ownership: Patent

#### 185 (PB065)

##### NUC-3373 is a potent TS inhibitor and induces DNA damage in NSCLC cancer cells regardless of histological subtype

B. Kaghazchi<sup>1</sup>, A.L. Dickson<sup>1</sup>, G. Zickuhr<sup>2</sup>, D.J. Harrison<sup>1</sup>, J. Bré<sup>1</sup>.

<sup>1</sup>University of St Andrews, School of Medicine, St Andrews, United Kingdom;

<sup>2</sup>University of St Andrews, School of Biology, St Andrews, United Kingdom

**Background:** Non-small cell lung cancer (NSCLC) represents >80% of lung cancer cases and is the leading cause of cancer mortality. It is comprised of three histological subtypes: adenocarcinoma (50–65%), squamous cell carcinoma (30–40%) and large cell carcinoma (5–15%). The majority of NSCLCs do not harbour actionable mutations, so treatment options include immune checkpoint inhibitors (ICIs) alone or in combination with chemotherapies. ICI/chemotherapy combinations have resulted in significant overall survival benefit compared to chemotherapy alone in both adenocarcinoma and squamous histology. The thymidylate synthase (TS) inhibitor 5-FU has limited clinical utility in NSCLC; attributed to the high levels of 5-FU degrading enzyme dihydropyrimidine dehydrogenase (DPD). Pemetrexed, also a TS inhibitor, is the backbone therapy for first- and second-line adenocarcinoma but is not recommended in squamous histology due to high basal TS expression. NUC-3373, a phosphoramidate transformation of FUDR, is resistant to breakdown by DPD and generates high intracellular levels of the active anti-cancer metabolite fluorodeoxyuridine

monophosphate (FUDR-MP or FdUMP) and is a potent inhibitor of TS. We hypothesise that NUC-3373 inhibits TS and causes DNA damage in NSCLC, regardless of histological subtype.

**Methods:** TS protein complex formation was measured by western blot in adenocarcinoma (A549, Calu3) and squamous (Nx002, Cx140) lung cancer cell lines treated with NUC-3373, following immunocytochemistry to assess basal TS. FUDR-MP, dUMP levels (surrogate of TS inhibition) and incorporation of FdUTP into DNA (FUDR as surrogate) were assessed by LC-MS/MS. DNA damage was assessed by immunofluorescence using p-Chk1 and  $\gamma$ -H2AX as markers of strand breaks. 5-FU and pemetrexed were used as positive controls.

**Results:** Consistent with the literature, squamous cell lines had higher basal TS expression than adenocarcinoma. NUC-3373 promotes formation of TS ternary complexes (60–84% of total TS) at sub-IC<sub>50</sub> doses in all lung cancer cell lines. NUC-3373 generated high intracellular levels of the TS-inhibiting metabolite FUDR-MP, resulting in increased levels of dUMP, up to 4.5- and 3.3-fold higher than 5-FU and pemetrexed at equimolar doses, respectively. NUC-3373 treatment led to FdUTP incorporation into DNA and subsequent DNA damage in both adenocarcinoma and squamous subtypes.

**Conclusion:** NUC-3373 is a potent inhibitor of TS in both adenocarcinoma and squamous NSCLC cells. Furthermore, NUC-3373 causes extensive DNA damage, likely owing to the high intracellular generation of FUDR-MP and incorporation of FdUTP into DNA. These data indicate that NUC-3373 may be an effective treatment for NSCLC, regardless of histological subtype.

#### Conflict of interest:

Corporate-sponsored Research: NuCana plc

Other Substantive Relationships: Jennifer Bré is a full-time NuCana employee. David James Harrison and Alison Louise Dickson are part-time NuCana employees.

#### 186 (PB066)

##### HORMAD1 drives spindle assembly checkpoint defects and sensitivity to multiple mitotic kinases

C. Walker<sup>1</sup>, D. Weekes<sup>1</sup>, G. Torga<sup>1</sup>, J. Quist<sup>2</sup>, J. Trendell<sup>2</sup>, L. Hitchens<sup>2</sup>, A. Martin<sup>1</sup>, K. Davidson<sup>1</sup>, G. Kollarovic<sup>1</sup>, A. Grigoriadis<sup>2</sup>, J. Pines<sup>3</sup>, S. Pettitt<sup>4</sup>, C. Lord<sup>1</sup>, A. Tutt<sup>1</sup>. <sup>1</sup>Institute of Cancer Research, Breast Cancer Now Toby Robins Research Centre, London, United Kingdom; <sup>2</sup>Kings College London, Breast Cancer Now Research Unit, London, United Kingdom; <sup>3</sup>Institute of Cancer Research, Division of Cancer Biology, London, United Kingdom; <sup>4</sup>Institute of Cancer Research, Division of Breast Cancer, London, United Kingdom

**Background:** The study aimed to identify and target effects associated with HORMAD1 expression in breast cancer cells.

**Materials and methods:** Isogenic cell line models with inducible HORMAD1 expression were used to identify dependencies induced by HORMAD1 expression.

**Results:** Expression of HORMAD1, a gene whose function is best understood in meiosis, is usually restricted to germ-line cells but becomes aberrantly expressed in 60% of triple-negative breast cancers (TNBCs), where a clearly bimodal distribution of expression is associated with signatures of genomic instability. Here, we report that HORMAD1 expression in mitotic cells leads to defects in the spindle assembly checkpoint (SAC). These defects were observed despite functional MAD2-dependent SAC activity, and were instead a consequence of an interaction with and disruption of the chromosome passenger complex, leading to decreased Aurora B signalling. HORMAD1-driven SAC defects were also associated with excessive chromosome instability and cellular sensitivity to MPS1, Aurora B and BUB1 inhibitors, all of which are of great clinical interest in TNBC.

**Conclusions:** Our data demonstrate that aberrant HORMAD1 expression in cancer leads to SAC defects, and highlights several therapeutic targets for a large subset of breast cancers that express HORMAD1. This may also be relevant in a wider group of high clinical need cancers that similarly demonstrate bimodal HORMAD1 expression.

#### Conflict of interest:

Ownership: CJL has stock in: Tango, Ovibio, Enedra Tx., Hysplex ANJT has stock in: InBiomotion

Advisory Board: CJL: Syncona, Sun Pharma, Gerson Lehrman Group, Merck KGaA, Vertex, AstraZeneca, Tango, 3rd Rock, Ono Pharma, Artios, Abingworth, Tesselate. ANJT: Pfizer, Vertex, Artios, Prime Oncology, InBiomotion, Gilead,

Corporate-sponsored Research: CJL: AstraZeneca, Merck KGaA, Artios

ANJT: Medivation AstraZeneca, Pfizer, Vertex, Artios, Prime Oncology

## POSTER SESSION

## Epigenetic Modulators (HDAC Bromodomain modulators, EZH2)

188

(PB068)

### Updated Findings and Biomarker Analysis From the Ongoing Phase 1 Study of Enhancer of Zeste Homolog 2 (EZH2) Inhibitor CPI-0209 in Patients With Advanced Solid Tumors

K.P. Papadopoulos<sup>1</sup>, M. Gutierrez<sup>2</sup>, L.R. Duska<sup>3</sup>, L. Gandhi<sup>4</sup>, A. Bommi-Reddy<sup>5</sup>, E. Adams<sup>5</sup>, J. Jauch-Lembach<sup>6</sup>, D.W. Rasco<sup>1</sup>. <sup>1</sup>START – San Antonio, Clinical Research, San Antonio, TX, USA; <sup>2</sup>Hackensack University Medical Center, John Theurer Cancer Center, Hackensack, NJ, USA; <sup>3</sup>University of Virginia, Obstetrics and Gynecology, Charlottesville, VA, USA; <sup>4</sup>Dana-Farber Cancer Institute, Center for Cancer Therapeutic Innovation, Boston, MA, USA; <sup>5</sup>Constellation Pharmaceuticals, Inc., a MorphoSys company, Boston, MA, USA; <sup>6</sup>MorphoSys, Ag, Planegg, Germany

**Background:** CPI-0209 is an investigative oral, small-molecule, second-generation, selective inhibitor of enhancer of zeste homolog 2 (EZH2), a histone methyltransferase and the catalytic subunit of polycomb repressive complex 2, which is frequently overexpressed in cancers and correlates with poor prognosis. In Phase 1, the dose of 350 mg once daily (QD) in 28-day cycles was selected for the initiation of Phase 2 based on pharmacokinetic (PK) and safety data from dose escalation. Here, we report updated Phase 1 findings from the ongoing Phase 1/2 study of CPI-0209 as monotherapy in patients (pts) with advanced tumors (NCT04104776).

**Methods:** Pts were enrolled in a 3 + 3 design to receive CPI-0209 QD in 28-day cycles.

The primary objective was to determine the maximum tolerated dose and/or recommended Phase 2 dose. Secondary objectives were to evaluate safety, PK and pharmacodynamics, and preliminary clinical activity. Exploratory objectives were to assess molecular features from peripheral tissues and tumor biopsies. Samples were analyzed via next-generation sequencing (NGS) and immunohistochemistry (IHC) for molecular features including mutational and copy number status, and gene expression profile (genes of interest included *ARID1A* and *BAP1*) to determine correlation with efficacy or novel biomarkers.

**Results:** As of May 2, 2022, 41 pts received  $\geq 1$  dose of CPI-0209 (safety-evaluable set) at 50 mg (n = 4), 100 mg (n = 6), 137.5 mg (n = 6), 187.5 mg (n = 6), 225 mg (n = 7), 275 mg (n = 4) and 375 mg (n = 8) QD. No dose-limiting toxicities (DLTs) were observed at dose levels 50–275 mg QD. One DLT was observed in the 375 mg cohort: Grade 4 thrombocytopenia on Cycle 1 Day 18. Safety profile was consistent with that previously reported (Lakhani, et al. ASCO 2021; Abstract #3104). Median duration of treatment was 63 days. Efficacy-evaluable pts (n = 39) received  $\geq 1$  dose of CPI-0209 and had  $\geq 1$  postbaseline tumor assessment. Of 40 pts with evaluable samples, 15 had *ARID1A* alterations based on central and/or local NGS. Ten of these 15 pts had *ARID1A* loss of function (LOF) frameshift or nonsense mutations. Four of six mesothelioma pts had *BAP1* alteration/loss detected by local or central NGS/IHC. Disease control (complete response+partial response (PR)+stable disease) and PR were achieved in 16 pts (41%) and 2 pts (5.1%), respectively. One confirmed PR (treated for nine cycles) was observed in a mesothelioma pt with *BAP1* loss, confirmed by local and central NGS. One endometrial cancer patient with *ARID1A* LOF mutation detected by central tissue NGS had confirmed PR and remains ongoing on study treatment for >18 cycles to date.

**Conclusions:** Given encouraging preliminary results from Phase 1, CPI-0209 will be further assessed in six disease-specific cohorts in Phase 2. Initial signs of efficacy from Phase 1 supported the inclusion of *ARID1A* and *BAP1* as biomarkers in Phase 2.

#### Conflict of interest:

Advisory Board: KP: Basilea, Turning Point Therapeutics, Bicycle Therapeutics

LD: Genetech/Roche, Merck, Inovio Pharmaceuticals, CUE Biopharma, Regeneron

LG: Beigene, BMS, Xilio, Eisai, Mersana, Pliant, Tentarix

Board of Directors: LG: Bright Peak Therapeutics, Neximmune

Corporate-sponsored Research: KP: AbbVie, MedImmune, Daiichi Sankyo, Regeneron, Amgen, Incyte, Merck, Peloton Therapeutics, ADC Therapeutics, 3D Medicines, EMD Serono, Syros Pharmaceuticals, Mersana Jounce Therapeutics, Bayer, AnHeart Therapeutics, F-star, Linnaeus Therapeutics, Mirati Therapeutics, Tempest Therapeutics, Treadwell Therapeutics, Lilly, Pfizer, BioNTech, Bicycle Therapeutics, Kezar Life Sciences

MG: Acerta Pharmaceuticals, local PI, institutional, no financial interest  
 Arcus Biosciences, local PI, institutional, no financial interest  
 Array BioPharma, local PI, institutional, no financial interest  
 Bayer, local PI, institutional, no financial interest  
 BMS, local PI, institutional, no financial interest  
 Boehringer Ingelheim, local PI, institutional, no financial interest  
 Celgene, local PI, institutional, no financial interest  
 Checkpoint Therapeutics, local PI, institutional, no financial interest  
 Compass Therapeutics, local PI, institutional, no financial interest  
 Constellation Pharmaceuticals, local PI, institutional, no financial interest  
 Cyter, local PI, institutional, no financial interest  
 Eisai, local PI, institutional, no financial interest  
 EMD Sereno, local PI, institutional, no financial interest  
 Fate Therapeutics, local PI, institutional, no financial interest  
 GlaxoSmithKline, local PI, institutional, no financial interest  
 GSB Pharma, local PI, institutional, no financial interest  
 Incyte, local PI, institutional, no financial interest  
 Infinity, local PI, institutional, no financial interest

Johnson & Johnson, local PI, institutional, no financial interest  
 MedImmune, local PI, institutional, no financial interest  
 Merck, local PI, institutional, no financial interest  
 Moderna, local PI, institutional, no financial interest  
 NexCure, local PI, institutional, no financial interest  
 Pfizer, local PI, institutional, no financial interest

LD: Glaxo Smith Kline, Millenium, Bristol-Myers Squibb, Aeterna Zentaris, Novartis, Abbvie, Tesaro, Cerulean Pharma, Aduro Biotech, Advaxis, Syndax, Pfizer, Merck, Genetech/Roche, Morab, Morphotek, Lugwig Institute for Cancer Research, Leap Therapeutics

DR: Celgene, Eisai, Merck, Asccentage Pharma, Abbvie, Constellation Pharmaceuticals, Astex Pharmaceuticals, Compugen, Coordination Therapeutics, Glaxo Smith Kline, Gossamer Bio, Seven and Eight Biopharmaceuticals, Bolt Ingelheim, PureTech, Takeda, Kronos, Molecular Templates, Arcus Biosciences, Surface Oncology, 23andMe, Cullinan Oncology, TD2

Other Substantive Relationships: MG: Guardant Health, invited speaker, personal Projects in Knowledge, educational grant from Daiichi Sankyo, invited speaker, personal (6/2022) COTA Healthcare, stocks/shares, personal Cellularity, consultant, personal Merck, consultant, personal (6/2022)

LD: Data Safety Monitoring Committee for Inovio and Ellipses

LG: Honoraria: Tempus Stock ownership: Lilly

AB-R: Employed by MorphoSys AG. Owns stock from MorphoSys AG

EA and JJ-L: Employed by MorphoSys AG

189

(PB069)

### Ladademstat effects on neuroendocrine, inflamed and mesenchymal gene expression patterns in small cell lung cancer subtypes

N. Sacilotto<sup>1</sup>, M. M. P. Lufino<sup>1</sup>, S. Pacheco<sup>1</sup>, C. Mascaró<sup>1</sup>, R. Soliva<sup>1</sup>, J. Xaus<sup>1</sup>. <sup>1</sup>Oryzon Genomics, Research and Development, Barcelona, Spain

**Background:** Small cell lung cancer (SCLC) is a highly aggressive and lethal tumor. Rapid response to chemotherapy and radiotherapy is observed in the majority of patients, but most of them relapse within 6 to 12 months. Despite the recent addition of immunotherapy to front-line chemotherapy, the improvements in progression-free and overall survival are modest, with most deaths occurring within a year of diagnosis.

SCLC is heterogeneous and can be divided into 4 molecularly distinct subtypes based on the expression of transcription factors: SCLC-A (about 50%, characterized by high levels of ASCL1), SCLC-N (about 23%, with high levels of NEUROD1), SCLC-P (7%, high levels of POU2F3) and SCLC-I or “inflamed,” accounting for about 20% of SCLC and defined by the absence of expression of all three transcription factors and by an inflamed gene signature associated with increased T-cell infiltration, interferon signaling and epithelial-to-mesenchymal transition. Importantly, this signature has been associated with a better response to immune checkpoint inhibitor (ICI) therapies. LSD1 inhibition potentially blocks SCLC progression by activating the Notch pathway and by promoting IFN-Type I and MHC-Class I expression, leading to increased immune cell infiltration and boosting the activity of ICI in a variety of tumor models.

Herein we explore the effects of the PhII clinical stage LSD1 inhibitor iadademstat on both the viability and the gene expression pattern of cell lines from all SCLC subtypes, with special focus on the neuroendocrine and inflamed/mesenchymal gene signatures.

**Materials and Methods:** Gene expression was assessed in NCI-H510A, NCI-H146, NCI-H82, NCI-H446, NCI-H211, NCI-H526, NCI-H196 and DMS114 cell lines after 6 days of treatment with the LSD1 inhibitor iadademstat (AKA ORY-1001). A panel of neuroendocrine, Notch signaling, adaptive and innate immunity and mesenchymal genes was evaluated in response to the drug. The associated residual cell viability was also assessed after treatment.

**Results:** Iadademstat strongly reduced cell viability of SCLC-A cell lines as monotherapy marginally affecting the viability of the other sub-types.

Notch activation and the associated neuroendocrine gene repression and mesenchymal gene upregulation, together with upregulation of both native and adaptive immunity-related genes was particularly evident in the SCLC-A group. Mesenchymal and “inflamed” genes were also up-regulated in other SCLC subtypes by iadademstat treatment.

**Conclusions:** Iadademstat strongly blocks SCLC-A at a cell-autonomous level and induces a gene expression signature associated with increased response to ICI therapies in this and others subtypes. These results support exploring the combination of iadademstat and immune checkpoint inhibitors to control the neuroendocrine tumorigenic drivers and to enhance the response to immunotherapy in SCLC.

**Conflict of interest:**

Other Substantive Relationships: Natalia Sacilotto, Michele Lufino, Sarai Pacheco, Cristina Mascaró, Robert Soliva, Jordi Xaus are employees of Oryzon Genomics.

**190** (PB070)  
**Iadademstat and gilteritinib synergistically abrogate viability of both treatment-naïve and drug-resistant AML cells**

N. Sacilotto<sup>1</sup>, E.M. Strzemieczna<sup>1</sup>, S. Purcet<sup>1</sup>, C. Mascaró<sup>1</sup>, R. Soliva<sup>1</sup>, J. Xaus<sup>1</sup>. <sup>1</sup>Oryzon Genomics, Research and Development, Barcelona, Spain

**Background:** Acute myeloid leukemia (AML) is a heterogeneous and complex disease characterized by several chromosomal abnormalities and gene mutations. This translates into marked response and survival differences after treatment, being drug resistance, either primary or secondary, an additional challenge.

Lysine-specific histone demethylase 1 (LSD1) is an epigenetic enzyme that contributes to the malignant transformation event in AML by sustaining the oncogenic transformation, proliferation and maintenance of the leukemic stem cell potential. The PhII clinical stage LSD1 inhibitor iadademstat (aka ORY-1001) promotes differentiation of leukemic blasts and reduces leukemic stem cell capacity, particularly in monocytic subclones which have been related to resistance to current SoC venetoclax/HMA therapy. Activating FMS-like tyrosine kinase 3 (FLT3) mutations are detected in about one-third of AML patients, enriched in relapse/refractory patients and associated with poor prognosis.

Herein we explore the combination between iadademstat and the FLT3 inhibitor gilteritinib in both treatment-naïve and AML cells resistant to current standard-of-care therapies.

**Materials and Methods:** The viability of AML cell lines (MOLM-13: M5a FLT3-ITD; MV(4;11): M5b FLT3-ITD; OCI-AML3: M4 FLT3 WT; TF1a: M6 FLT3 WT) was assessed after 96 h treatment with iadademstat and gilteritinib, both as single agents and in combination. Additionally, drug-adapted MOLM-13 cells resistant to venetoclax, azacitidine, midostaurin or gilteritinib were tested. Synergism between both drugs was evaluated with CalcuSyn and Combenefit softwares.

**Results:** Iadademstat displayed sub-nanomolar activity as a single agent in all the cell lines and resistant sublines tested, with superior viability reductions in venetoclax- and gilteritinib-resistant cells, compared to parental cells. Gilteritinib showed potent anti-leukemic effects in FLT3-mutated cells and was less potent in FLT3 WT cells, as expected. Interestingly, the iadademstat+gilteritinib combination displayed highly synergistic effects in both FLT3-mutated and FLT3 WT cell lines. Moreover, these effects were also observed in MOLM-13 cells with acquired resistance to venetoclax, midostaurin or azacitidine.

**Conclusions:** The combination between iadademstat and gilteritinib is highly synergistic in both FLT3-mut and FLT3 WT AML cells. This synergism is also observed in FLT3-mut cells with secondary resistance to current SoC agents venetoclax, azacitidine or midostaurin. Therefore, these results support exploring the combination of iadademstat and gilteritinib in the treatment of AML patients with FLT3 mutations, including in a venetoclax/HMA- or midostaurin-relapsed/refractory setting (basis for the ongoing FRIDA clinical trial). These data also suggest that patients with WT FLT3 AML may also benefit from this combination.

**Conflict of interest:**

Other Substantive Relationships: Natalia Sacilotto, Ewelina Maria Strzemieczna, Sergi Purcet, Cristina Mascaró, Robert Soliva, Jordi Xaus are employees of Oryzon Genomics.

**191** (PB071)  
**Tazemetostat and doxorubicin in patient-derived preclinical models of epithelioid sarcoma (ES)**

S. Pasquali<sup>1</sup>, N. Arrighetti<sup>1</sup>, V. Zuco<sup>1</sup>, M. Tortoreto<sup>1</sup>, C. Soffientini<sup>1</sup>, L. Sigalotti<sup>2</sup>, R. Maestro<sup>2</sup>, S. Percio<sup>1</sup>, M. Barisella<sup>3</sup>, P. Collini<sup>3</sup>, G. Dagrada<sup>3</sup>, A.M. Frezza<sup>4</sup>, A. Gronchi<sup>5</sup>, S. Stacchiotti<sup>4</sup>, N. Zaffaroni<sup>1</sup>. <sup>1</sup>Fondazione IRCCS Istituto Nazionale dei Tumori, Department of Applied Research and Technological Development, Milano, Italy; <sup>2</sup>CRO Aviano, Unit of Oncogenetics and Functional Oncogenomics, Aviano, Italy; <sup>3</sup>Fondazione IRCCS Istituto Nazionale dei Tumori, Department of Diagnostic Pathology and Laboratory Medicine, Milano, Italy; <sup>4</sup>Fondazione IRCCS Istituto Nazionale dei Tumori, Department of Cancer Medicine, Milano, Italy; <sup>5</sup>Fondazione IRCCS Istituto Nazionale dei Tumori, Department of Surgery, Milano, Italy

**Background:** ES is an ultra-rare sarcoma characterized by the absence of INI1/SMARCB1. The activation of EZH2, consequent to loss of INI1, has been identified as relevant for therapeutic targeting. We exploited ES patient-derived xenograft (PDX) models and paired cell lines to test the activity tazemetostat plus doxorubicin and identify modifiers of tumor response and resistance.

**Material and methods:** We established two PDXs in SCID mice from two proximal-type ES characterized by INI1-deficiency due to epigenetic silencing (ES-1) or gene deletion (ES-2). Histo-morphology, IHC, and transcriptomic profile of clinical ES and paired PDXs were consistent. 2D cell lines were generated from each PDX. Tazemetostat and doxorubicin, as single-agents or in combination, were tested and maximum tumor volume inhibition percentage (max TVI%) was assessed to measure treatment activity in PDXs. Cell proliferation (Ki67-index) was evaluated at IHC and expression of proteins involved in apoptotic and autophagic response was analyzed at western blotting.

**Results:** Tazemetostat plus doxorubicin had higher effectiveness (max TVI: 95%) than single-agent doxorubicin (max TVI: 50%) or tazemetostat (max TVI: 56%). We established a post-treatment PDX model (ES-1/R) from tumors that started to re-grow roughly 3 weeks after the end of doxorubicin plus tazemetostat. After a re-challenge with the same schedules, doxorubicin was as effective as observed in the ES-1 model while a slightly lower susceptibility to tazemetostat, alone and in combination with doxorubicin, was detected (max TVI: 40 and 84%, respectively). Inherited resistance to either doxorubicin or tazemetostat or their combination was observed in the ES-2 PDX. We observed a reduction of the Ki67-index and a persistent activation of apoptosis in ES-1 but not ES-2 tumors explanted from mice after exposure to the combined treatment as well as in combination-treated in vitro cell lines. Tazemetostat with or without doxorubicin induced an autophagic response in ES-1 and ES-2 cell models. Drug combination with the autophagy inhibitor bafilomycin A, suggested a cytoprotective role for autophagy in ES-2 only. Transcriptomic analysis of untreated ES-1 and ES-2 PDXs, revealed higher expression of EMT- angiogenesis- inflammatory response- TGF $\alpha$ - and TGF $\beta$ -related signaling in ES-2 compared to ES-1. ES-2 also showed down-regulation of NSD1, a H3K36 methyltransferase whose loss was reported to confer resistance to EZH2 inhibition in SMARCB1-deficient rhabdoid tumor cells.

**Conclusions:** Tazemetostat plus doxorubicin showed synergistic anti-tumor activity in an ES tumor model, an effect that was maintained at a re-challenge in the derived post-treatment PDX. Possible determinants of resistance to this drug combination were also identified in an inherited resistant tumor model.

**Conflict of interest:**

Advisory Board: S Stacchiotti: Bayer, Bavarian Nordic, Deciphera, Daiichi, Eli Lilly, Epizyme, Karyopharm, MaxiVax, Pharmamar, Takeda

Other Substantive Relationships: S Stacchiotti: honoraria: Eli Lilly, Pharmamar travel grants: Pharmamar institutional research funding: Advenchen, Amgen Dompé, AROG, Bayer, Blueprint Medicines, Daiichi Sankyo Pharma, Deciphera, Eli Lilly, Epizyme, GSK, Karyopharm, Novartis, Pfizer, PharmaMar, SpringWorks.

AM Frezza: institutional research funding: Advenchen, Amgen Dompé, AROG, Bayer, Blueprint Medicines, Daiichi Sankyo Pharma, Deciphera, Eli Lilly, Epizyme, GSK, Karyopharm, Novartis, Pfizer, PharmaMar, SpringWorks.

A Gronchi: sponsorship or research funding: PharmaMar remuneration: Bayer, Lilly, Nanobiotix, Novartis, Pfizer, PharmaMar and SpringWorks.

192

(PB072)

**Overcoming chemoresistance in triple negative breast cancer by bromodomain inhibition**

O. Yedier-Bayram<sup>1</sup>, A. Cingoz<sup>1</sup>, A.C. Aksu<sup>1</sup>, N. Pinarbasi-Degirmenci<sup>1</sup>, B. Esin<sup>1</sup>, A. Kayabolen<sup>1</sup>, B. Cevatemre<sup>1</sup>, C. Acilan Ayhan<sup>1</sup>, M. Philpott<sup>2</sup>, A. Cribbs<sup>2</sup>, U. Oppermann<sup>2</sup>, T.T. Onder<sup>3</sup>, T. Bagci Onder<sup>3</sup>. <sup>1</sup>Koç University School of Medicine, Research Center for Translational Medicine, Istanbul, Turkey; <sup>2</sup>University of Oxford, Botnar Research Centre, Oxford, United Kingdom; <sup>3</sup>Koç University School of Medicine, Medical Biology, Istanbul, Turkey

**Background:** Triple negative breast cancer (TNBC) is an aggressive subtype of breast cancer with poor prognosis. TNBC cells do not express receptors for estrogen, progesterone or Her2, eliminating the possibility of targeted therapy applications. Therefore, current treatment option for TNBC is limited with surgery followed by conventional chemotherapy. However, acquired resistance to chemotherapy is a major challenge that is associated with relapse, which is driven by coordinated actions of genetic and epigenetic events.

**Materials and Methods:** We aimed to elucidate the roles of full spectrum of epigenetic modifiers in maintenance and reversion of chemoresistance in TNBC. To generate *in vitro* models of chemoresistant TNBC, we exposed 3 different TNBC cell lines to escalating doses of taxane (paclitaxel). Transcriptome analysis by RNA-sequencing were performed to reveal changes that regulate chemoresistance. With our custom epigenome-wide CRISPR-Cas9 library (*Epigenetic Knock-Out Library - EPIKOL*) targeting all chromatin readers, writers, erasers and associated proteins, we systematically interrogated the roles of epigenetic modifiers in chemoresistant TNBC cells. We also conducted medium scale chemical screens utilizing epigenetic probe libraries in chemoresistant cells.

**Results:** RNA sequencing on paired sensitive and chemoresistance cell lines revealed *ABCB1* upregulation as a major driver of resistance. Inhibition of the members of MLL and SWI/SNF complexes, as well as the genes related with histone ubiquitination and acetyl-mark readers re-sensitized chemoresistant cells to paclitaxel. A member of the bromodomain protein family, BRPF1, came as a common hit in our chemical screen as well as genetic screens. Knockout of BRPF1 or its chemical inhibition completely abolished paclitaxel resistance and modulated *ABCB1* expression.

**Conclusions:** Through EPIKOL screens on chemoresistant TNBC cells coupled with chemical screens, we identified novel epigenetic modifiers that are crucial for maintaining and overcoming drug resistance. Collectively, these findings provide a basis to develop combination therapies to efficiently kill chemoresistant TNBC.

**Key words:** Epigenetics, breast cancer, drug resistance

This work was supported by The Scientific and Technological Research Council of Turkey (TUBITAK) 1003- 216S461 Grant

**No conflict of interest.**

193

(PB073)

**Orally Bioavailable CBP and p300 Selective Degraders for the Treatment of AR- and ER-dependent Cancers**

S. Thiyagarajan<sup>1</sup>, C. Abbineni<sup>2</sup>, K. Chaitanya T<sup>2</sup>, I.K. Iqbal<sup>1</sup>, N. Kumar R<sup>3</sup>, A. Kumar<sup>1</sup>, P.K. Singh<sup>2</sup>, S. Mukherjee<sup>2</sup>, K. Nellore<sup>1</sup>, S. Chelur<sup>3</sup>, M. Ramachandra<sup>1</sup>, S. Samajdar<sup>4</sup>. <sup>1</sup>Aurigene Discovery Technologies Limited, Biology, Bangalore, India; <sup>2</sup>Aurigene Discovery Technologies Limited, Med Chem, Bangalore, India; <sup>3</sup>Aurigene Discovery Technologies Limited, Toxicology, Bangalore, India; <sup>4</sup>Aurigene Discovery Technologies Ltd, Med Chem, Bangalore, India

E1A binding protein (p300) and its paralog CREB binding protein (CBP or CREBBP) are ubiquitously expressed histone acetyl transferases (HAT) that act by scaffolding or as co-activator and enhancer of different transcription factors like HIF1a, BRCA-1, p53, c-Myc, Estrogen receptor (ER) and Androgen receptor (AR). CBP and p300 are multidomain proteins that harbour different functional units imperative for chromatin remodelling and transcription like Bromodomain (BD), Histone acetyl transferase (HAT) domain, KIX domain etc. These two closely related epigenetic modulators are known to play oncogenic role in variety of cancers.

In breast and prostate cancers, in addition to serving as transcriptional co-activators, CBP/p300 also acetylates AR and ER and regulates their function by enhancing stability. Therefore, unlike inhibitors a degrader of CBP and p300 is expected to show a stronger impact on the stability and transcriptional activity of both AR and ER (including mutant forms) leading to pronounced therapeutic responses by eliminating both the transcriptional co-activator and acetylation functions. Additionally, it might be possible with degraders to obtain paralog selectivity (p300 vs CBP) to achieve required pharmacological activity but with better tolerability.

In an effort to identify novel degraders of CBP and p300 for potential treatment of breast and prostate cancers, a variety of hetero bi-functional molecules were synthesized by conjugating selective CBP/p300 bromodomain binders with various E3-ligase specific ligands. Rational design approach guided by our proprietary ternary complex modeling algorithm, ALMOND (ALgorithm for MOdeling Neo substrate Degraders) resulted in the identification of structurally unique highly selective CBP/p300 degraders, which were further optimized for potency, selectivity and ADME properties.

The lead orally bioavailable CBP/p300 degrader compounds showed more pronounced cellular effects and apoptosis in multiple cancer cell lines including AR-dependent prostate and ER-dependent breast cancer cells as a single agent due to complete degradation of the targets and sustained downregulation of signaling network downstream of CBP and p300. In comparison with inhibitors, there was a remarkable and durable inhibition of the levels of AR and ER as well as their target genes observed with degraders. *In vivo* studies, including efficacy and safety assessments are planned to further understand the therapeutic potential and safety margin for these degraders. Efforts to improve paralog selectivity by modifying key interactions of CBP/p300 are also in progress.

**No conflict of interest.**

**POSTER SESSION****Immune Checkpoints**

195

(PB075)

**First-in-class anti-PVR mAb NTX1088 restores DNAM1 expression and enhances antitumor immunity**

A. Atieh<sup>1</sup>, A. Obiedat<sup>1</sup>, A. Vitenshtein<sup>1</sup>, G. Cinamon<sup>1</sup>, K. Paz<sup>2</sup>, T. Roviš<sup>3</sup>, P. Kucan<sup>3</sup>, L. Hirsli<sup>3</sup>, O. Mandelboim<sup>4</sup>, S. Jonjic<sup>3</sup>, T. Pini<sup>1</sup>. <sup>1</sup>Nectin Therapeutics, Research, Jerusalem, Israel; <sup>2</sup>Nectin Therapeutics, Management, Jerusalem, Israel; <sup>3</sup>Medri, Research, Rijeka, Croatia; <sup>4</sup>HUJI, Research, Jerusalem, Israel

NTX1088 is a humanized, hinge-stabilized IgG4 mAb that binds PVR with sub-nM affinity and blocks all known interacting receptors with a single nM EC-50. PVR (CD155), a cell surface protein, is highly upregulated on tumor cells, across multiple cancer types. PVR has been associated with worse patient outcomes, due to its role in immune suppression. PVR impact on immune cells is mediated through interaction with the key stimulatory receptor, DNAM1 (CD226), on T and NK cells, leading to internalization and degradation of DNAM1. PVR is additionally, the ligand for inhibitory immune checkpoint receptors, TIGIT and CD96. Accordingly, blocking PVR has a multi-faceted immune-stimulating role, namely, restoration of DNAM1 expression and its immune activation function, while simultaneously neutralizing TIGIT and CD96 inhibitory signals in immune cells. Importantly, DNAM1 downmodulation was recently identified as a key resistance mechanism to approved ICIs, and its restoration by NTX1088 is a unique MoA, not shared by other therapies.

*In vitro*, NTX1088, as a monotherapy, significantly increased immune cell activation, and was superior to TIGIT, CD112R, and PD1 antibody blockade, leading to superior immune-mediated tumor cell killing, IFN $\gamma$  release, and CD137 induction. Importantly only NTX1088 was able to restore DNAM1 to the surface of immune cells in all settings. Synergy was observed when NTX1088 was combined with PD1 blockers or with the anti-CD112R mAb, NTX2R13, in line with the restoration of DNAM1 expression.

Numerous humanized murine xenograft models were investigated. NTX1088 as a monotherapy exhibited robust tumor growth inhibition of the PDAC cell line, HPAFII, co-engrafted with human PBMC in NOD/SCID mice. The effect was significantly improved when NTX1088 was combined with a

PD1 inhibitor. Furthermore, a strong tumor growth inhibition by NTX1088 was observed in NSG mice engrafted with human PBMCs and the NSCLC cell line, A549, whereas TIGIT and PD1 blockers failed to impact tumor growth in this setting. Tumor-infiltrating lymphocytes, harvested from these mice, demonstrated a significantly higher prevalence of CD137+, DNAM1+, and CD8+ T cells.

In vivo toxicity and toxicokinetic studies in cynomolgus monkeys revealed that NTX1088 is well tolerated up to a high exposure level, equivalent to over 60 times the EC<sub>90</sub> values. Moreover, the ability of NTX1088 to induce non-specific cytokine release was ruled out when tested in vitro. NTX1088 has an open IND, enrolling patients with locally advanced and metastatic solid tumors NCT05378425.

**No conflict of interest.**

**196** (PB076)  
**Non-invasive biomarkers for response and survival prediction in patients with advanced solid tumours treated with immune checkpoint inhibitors (ICIs)**

K. Bernatowicz<sup>1</sup>, M. Viejto<sup>2</sup>, R. Berche<sup>2,3</sup>, G. Alonso<sup>2</sup>, V. Galvao<sup>2</sup>, H.K. Oberoi<sup>2,3</sup>, I. Braña<sup>2</sup>, O. Saavedra<sup>2</sup>, E. Muñoz-Couselo<sup>2</sup>, F. Grussu<sup>1</sup>, A. Belen<sup>3</sup>, G. Serna<sup>4</sup>, M. Rotxes<sup>2</sup>, M. Sanz<sup>2</sup>, J. Tabernero<sup>3,5</sup>, R. Toledo<sup>3,5</sup>, P. Nuciforo<sup>4</sup>, E. Garralda<sup>2,3</sup>, R. Perez-Lopez<sup>1,6</sup>. <sup>1</sup>Radiomics Group, Vall d'Hebron Hospital Campus and Institute of Oncology (VHIO), Barcelona, Spain; <sup>2</sup>Medical Oncology Department, Vall d'Hebron University Hospital, Barcelona, Spain; <sup>3</sup>Clinical Research, Vall d'Hebron Hospital Campus and Institute of Oncology (VHIO), Barcelona, Spain; <sup>4</sup>Molecular Oncology, Vall d'Hebron Hospital Campus and Institute of Oncology (VHIO), Barcelona, Spain; <sup>5</sup>Instituto de Salud Carlos III, CIBERONC, Spain; <sup>6</sup>Radiology Department, Vall d'Hebron University Hospital, Barcelona, Spain

**Background:** Optimising patient selection for cancer immunotherapy remains an unmet medical need. Non-invasive biomarkers from plasma and medical images could provide meaningful information about tumour immunophenotype and prognosis. We present exploratory biomarker data and its relation to response in advanced solid tumours.

**Material and methods:** We studied 40 patients with advanced solid tumours enrolled on the prospective translational study PREDICT with single or combinatory ICIs. We evaluated clinical, imaging and biological predictors of response at baseline, including markers derived from CT images and circulating-tumour DNA (ctDNA) from plasma. We developed a CT-radiomics signature using random survival forest (RSF) model to predict the mortality in the prospective dataset. Prognostic score was developed in the retrospective cohort of 258 patients treated with ICIs and repeated Lasso for Cox model was used for feature selection. Next, different Cox proportional-hazard (CoxPH) models were trained considering: radiomics mortality signature (RAD), tumour shedding from ctDNA, MD Anderson prognostic score containing clinical variables (PROG) and their combinations.

**Results:** 35 patients with evaluable CT images at baseline were included in the PREDICT trial since October 2020. Thirty had also plasma ctDNA quantification; missing data was imputed using RSF. Median follow-up was 10.4 months, 5 patients had PR (melanoma, lung, endometrial), 13 SD (melanoma, colon, liver) and 17 PD as best response. Median PFS was 1.9 months and median OS was 6.8 months. ORR was 14%. 3 high-importance CT-radiomics features were selected to compute the RAD, representing tumour size, shape and heterogeneity. K-M analysis showed significant differences in OS and PFS between High vs Medium vs Low RAD groups (log rank test  $p < 0.0001$ ). In multivariate analysis, tumour maximum 3D diameter was associated with shorter survival, whereas spherical and homogenous lesions (higher GLCM correlation) were associated with longer OS. Individual and integrative CoxPH model evaluations to predict OS and

PFS are presented in table 1. All models passed internal model validation using bootstrapping and calibration.

**Conclusions:** Tumour imaging phenotype assessed by CT-radiomics and ctDNA provides insights on patient response and prognosis. A limitation is small number of patients with integrated data available.

**Conflict of interest:**

Other Substantive Relationships: PREDICT study has received support from AstraZeneca. RPL is supported by a CRIS Foundation Talent Award (TALENT19-05), the FERRO Foundation, the Instituto de Salud Carlos III-Investigación en Salud (PI18/01395 and PI21/01019) and the Prostate Cancer Foundation Young Investigator Award. KB received funding from the postdoctoral fellowship Beatriz de Pinós (2019 BP).

**197** (PB077)  
**Small molecule PD-L1 inhibitor modulates expression of PD-L1 on the cell surface – a potential mechanism of blocking interaction with PD-1**

G. Weitsman<sup>1</sup>, J. Nuo En Chan<sup>1</sup>, J. Nedbal<sup>2</sup>, P.R. Barber<sup>1</sup>, A. Volgina<sup>3</sup>, C. Stevens<sup>4</sup>, S. Poland<sup>1</sup>, S. Ameer-Beg<sup>1</sup>, K. Suhling<sup>2</sup>, J. Rios-Doria<sup>4</sup>, T. Ng<sup>1</sup>. <sup>1</sup>King's College London, Comprehensive Cancer Centre, London, United Kingdom; <sup>2</sup>King's College London, Physics, London, United Kingdom; <sup>3</sup>Incyte Research Institute, Small Molecule Discovery and Preclinical Pharmacology, Wilmington, USA; <sup>4</sup>Incyte Research Institute, Biotherapeutics Research, Wilmington, USA

**Background:** Blocking the PD1-PD-L1 interaction has been shown to stimulate anti-tumour responses. Although antibody-based drugs targeting either PD-1 or PD-L1 are approved, small molecule inhibitors of PD-L1 are currently in development. A subset of these small molecule inhibitors induce the loss of cell surface PD-L1 in a time- and concentration-dependent manner. INCB090244 is a small molecule that has previously been shown to bind to PD-L1 and disrupt the PD-L1/PD-1 interaction.

**Materials and Methods:** PD-L1 homo-dimerization was detected with SEC-MALS (size-exclusion chromatography combined with multi-angle light scattering) in solution and with FRET-FLIM (Förster Resonance Energy Transfer – Fluorescence Lifetime IMaging) in live cells. Standard FRET-FLIM assay was modified for use with TIRF (Total Internal Reflection Fluorescence) to analyse PD-L1 dimerization on the cell membrane only.

**Results:** INCB090244 induced rapid cell membrane PD-L1 dimerization and removal from the cell surface via internalization. Following translocation to the intracellular compartment, the INCB090244:PD-L1 dimer complex is believed to dissociate and undergo lysosomal degradation and/or nuclear localization (data not shown) further resulting in the downregulation of PD-L1 expression. In contrast, the anti-PD-L1 antibody, atezolizumab, did not induce the dimerization or reduce expression of PD-L1 on the cell membrane. Similarly, treatment of mice bearing MDA-MB-231 tumors with INCB090244 also led to dissociation of PD-L1 homodimer, whereas atezolizumab did not have an effect.

**Conclusions:** INCB090244 transiently increased PD-L1 homodimer levels on the membrane, followed by internalisation and downregulation of PD-L1, making it unavailable for interaction with PD-1. In contrast, the anti-PD-L1 antibody atezolizumab had no effect on PD-L1 homo-dimerization and did not reduce cell surface levels of the protein.

**Conflict of interest:**

Corporate-sponsored Research: Research sponsored by Incyte Corporation  
Other Substantive Relationships: Incyte Research Institute is part of Incyte Corporation

Table (abstract: 196 (PB076))

Integrated variables	Overall survival			Progression free survival		
	C-index [95%CI]	AIC	BIC	C-index [95%CI]	AIC	BIC
RAD	0.82 [0.76–0.87]	113.37	116.48	0.81 [0.76–0.85]	139.28	142.34
ctDNA	0.58 [0.47–0.68]	136.65	138.20	0.58 [0.49–0.68]	176.29	177.85
PROG	0.68 [0.55–0.80]	133.96	140.19	0.60 [0.47–0.72]	178.92	185.14
RAD+ctDNA	0.89 [0.83–0.94]	101.28	104.39	0.89 [0.84–0.93]	123.50	126.61
RAD+PROG	0.85 [0.78–0.93]	111.53	119.31	0.85 [0.75–0.94]	144.34	152.12
RAD+ctDNA +PROG	0.85 [0.78–0.93]	113.63	122.96	0.86 [0.77–0.94]	145.33	154.67

## POSTER SESSION

## Molecular Targeted Agents 2

198

(PB078)

## Activity and safety of ipatasertib (ipat) for AKT activating mutation and/or PTEN loss/loss of function solid tumors from MyTACTIC

A. VanderWalde<sup>1,2</sup>, D.R. Spigel<sup>3</sup>, W.C. Darbonne<sup>4</sup>, W. Yu<sup>4</sup>, Y. Kim<sup>4</sup>, Z. Whitehead<sup>4</sup>, T. Szado<sup>4</sup>, D. Slater<sup>5,6</sup>, R. Zuniga<sup>5,7</sup>, E. Arrowsmith<sup>8</sup>.  
<sup>1</sup>Clinical Research, West Cancer Center and Research Institute, Germantown, TN, USA; <sup>2</sup>Clinical Development, Precision Oncology Alliance, Caris Life Sciences, Memphis, TN, USA; <sup>3</sup>Sarah Cannon Research Institute, Tennessee Oncology, Nashville, TN, USA; <sup>4</sup>US Medical Affairs Oncology, Genentech, Inc. South San Francisco, CA, USA; <sup>5</sup>Precision Medicine, OneOncology, Inc., Nashville, TN, USA; <sup>6</sup>Eastern Connecticut Hematology and Oncology, Norwich, CT, USA; <sup>7</sup>New York Cancer and Blood Specialists, Port Jefferson Station, NY, USA; <sup>8</sup>Tennessee Oncology, Chattanooga, TN, USA

**Background:** MyTACTIC (NCT04632992) is a multiarm basket study evaluating the safety/efficacy of targeted therapies as single agents or combinations in advanced unresectable/metastatic solid tumors with specific genomic alterations. We analyzed the potent oral AKT inhibitor ipat in a pan-tumor population with AKT activating mutation and/or PTEN loss/loss of function from MyTACTIC.

**Materials and Methods:** Enrolled patients (pts) were  $\geq 18$  years old and had advanced unresectable/metastatic tumors with AKT1/2/3 mutation and/or PTEN loss/loss of function alteration. Pts received ipat 400 mg/day. The primary endpoint was investigator-assessed confirmed objective response rate (cORR; complete response [CR]+partial response [PR]). Other key endpoints: disease control rate (DCR; CR+PR+stable disease or non-CR/non-progressive disease [PD]  $\geq 98$  days [28-day arms] or  $\geq 70$  days [21-day arms]); progression-free survival (PFS); duration of response (DOR); safety.

**Results:** At data cutoff (Jan 24, 2022), 26 pts with various tumor types had received ipat (AKT activating mutations, n = 5; PTEN, n = 21). Pts had a median of 3 (range 1–8) prior lines of therapy for metastatic disease. cORR was 11.5% (n = 3/26); DCR was 34.6% (n = 9/26). Median DOR was not reached (95% CI 3.7–not estimable); median PFS was 3.6 mos (95% CI 1.9–7.1). Best overall response per tumor type and AKT/PTEN status is presented in the Table. Adverse events (AEs) were consistent with the known safety profile of ipat. The most common treatment-related AEs (TRAEs) were diarrhea (65.4%) and nausea (30.8%). Grade 3 AEs were seen in 7/26 (26.9%) pts and Grade 4 AEs in 1/26 (3.8%; perirectal abscess) pt; no Grade 5 AE was seen. 2/26 pts (7.7%) had serious TRAEs: 1 pt discontinued treatment due to TRAEs.

**Conclusions:** In this small cohort, single-agent ipat showed some clinical activity in heavily pretreated pts with heterogeneous metastatic cancers. Further investigation of the role of AKT inhibition (AKTi) and potential resistance mechanisms is warranted. Given the rationale for AKTi+endocrine therapy (ET) in HR+ HER2– mBC, ipat+ET is being evaluated in the Phase 3 FINER (NCT04650581) and Phase 2 FAIM (NCT04920708) trials.

## Conflict of interest:

Ownership: W.C.D is an employee and shareholder of Roche/Genentech, Inc.

W.Y is an employee of Roche/Genentech, Inc. and owns stocks in Roche.

Y.K is an employee and shareholder of Roche/Genentech, Inc.

T.S is an employee and shareholder of Roche/Genentech, Inc.

Advisory Board: A.VW has received advisory board fees from Bristol Myers Squibb, Mirati, and consulting fees from George Clinical, Elsevier.

Other Substantive Relationships: A.VW is an employee of Caris Life Sciences.

Z.W is an employee of Rutgers University contracted by Genentech, Inc.

D.R.S reports consulting paid to the institution from Amgen, AZ, BeiGene, BMS, Curio Science, EMD Serono, Evidera, Exelixis, Genentech/Roche, GlaxoSmithKline, Intellisphere, Janssen, Jazz Pharmaceuticals, Lilly, Mirati Therapeutics, Molecular Templates, Novartis, Novocure, Pfizer, Puma Biotechnology, Regeneron, Sanofi-Aventis research grants to institution from Aeglea Biotherapeutics, Agios, Apollomics, Arcus, Arrys Therapeutics, Astellas, AZ, Bayer, BeiGene, BIND Therapeutics, BioNTech RNA Pharmaceuticals, Blueprint Medicine, Boehringer-Ingelheim, Bristol-Myers Squibb, Calithera, Celgene, CellDex, Clovis, Cyteir Therapeutics, Daiichi Sankyo, Denovo Biopharma, Eisai, Elevation Oncology, EMD Serono, Evelo Biosciences, G1 Therapeutics, Roche/Genentech, GSK, GRAIL, Hutchison MediPharma, ImClone Systems, Incyte, ImmunoGen, Ipsen, Janssen, Kronos Bio, Lilly, Loxo Oncology, MacroGenics, MedImmune, Merck, Molecular Partners, Molecular Template, Nektar, Neon Therapeutics, Novartis, Novocure, Oncologie, Pfizer, PTC Therapeutics, PureTech Health, Razor Genomics, Repare Therapeutics, Rgenix, Takeda, Tesaro, Tizona Therapeutics, Transgene, UT Southwestern, Verastem.

E.A, D.S and R.Z have no conflicts to disclose.

200

(PB080)

## Trans-(±)-kusunokinin suppresses AKR1B1: inhibition of oxidative stress and alteration of epithelial-mesenchymal transition markers on aggressive cancer

T. Tanawattanasuntorn<sup>1</sup>, T. Rattanaburee<sup>1</sup>, T. Thongpanchang<sup>2</sup>, P. Graidist<sup>1</sup>. <sup>1</sup>Prince of Songkla University, Department of Biomedical Sciences and Biomedical Engineering, Songkhla, Thailand; <sup>2</sup>Mahidol University, Department of Chemistry and Center of Excellence for Innovation in Chemistry PERCH-CIC, Bangkok, Thailand

**Background:** Trans(-)-kusunokinin, a multi-target molecule (such as CSF1R, MMP-12, HSP90- $\alpha$ , cyclinB1, MEK1, HER2 and AKR1B1), inhibited breast, cholangiocarcinoma, colon and ovarian cancer cells proliferation. In addition, natural trans(-)-kusunokinin inhibits tumor growth and migration in the rat model. However, there is no evidence to confirm the interaction and the effects of synthetic trans-(±)-kusunokinin (KU) against AKR1B1. In this work, we investigated the action of trans-(±)-kusunokinin against AKR1B1 enzyme activity consequently in the suppression of AKR1B1 and its downstream molecules.

**Material and methods:** The inhibition of aldose-reductase activity by KU was determined using an aldose reductase inhibitor screening kit. Intracellular activities of KU including cytotoxicity, drug-target interaction and oxidative stress were determined using MTT, CETSA and TBARS assays, respectively. MTT assay was performed on the breast (BT549, Hs578 T and MCF7) and ovarian cancer (A2780, SKOV3 and OVCAR3) cells. CETSA was done on high AKR1B1 expression cells (Hs578 T and

Table (abstract: 198 (PB078))

Cancer Type	Total n of pts	PR, n (mutation*, prior metastatic lines)	SD <sup>†</sup> , n (prior metastatic lines)	PD, n (prior metastatic lines)	Non-CR/non-PD, n (prior metastatic lines)	Non Evaluable, n	Missing, n
Breast	7	1 (AKT1:E17 K, 5+)		4 (range 2–5+)	1 (3)		1
Prostate	7		4 (~3–4)	2 (4; 5+)		1	
Colon	3		1 (4)	2 (3; 4)			
Colorectal	2	1 (PTEN loss, 3)		1 (2)			
Endometrial	2	1 (PTEN loss, 2)					1
Rectal	1		1 (1)				
Anal	2		1 (3)	1 (5+)			
Cervical	1		1 (2)				
Adenocarcinoma (Neck)	1						1
Grand Total, n	26	3	8	10	1	1	3

\*High-level biomarker listed for PRs only here. Protocol-allowed biomarkers included mutations and PTEN loss via IHC and/or mutation.

<sup>†</sup>6 pts had SD >4 months.

SKOV3). Hs578 T cells were treated with KU, AKR1B1 known inhibitor (epalrestat (EP)) and siRNA-AKR1B1 for 48 hrs. Finally, AKR1B1 and its downstream molecules were measured by Western blotting.

**Results:** KU inhibited aldose-reductase activity with an IC50 value of  $9.72 \pm 0.18 \mu\text{M}$  with less effectiveness than EP ( $0.77 \pm 0.01 \mu\text{M}$ ). KU exhibited the strongest cytotoxicity on Hs578 T cells which is stronger than zopolrestat, EP and cisplatin. Interestingly, KU stabilized AKR1B1 at 60°C and 75°C on SKOV3 and Hs578 T cells in a dose-dependence manner. KU also inhibited lipid peroxidation on Hs578 T in a dose-dependence manner. Moreover, KU showed a stronger ROS inhibition than EP. The suppression of AKR1B1 by KU, EP and siRNA-AKR1B1 represented the down-regulation of AKR1B1 and its downstream proteins (PKC- $\delta$ , NF- $\kappa$ B, AKT, STAT3, Nrf2, COX2, Twist2 and N-cadherin). Nevertheless, E-cadherin was up-regulated during the treatment.

**Conclusions:** In conclusion, the binding of KU with AKR1B1 caused the inhibition of AKR1B1 enzyme activity, cellular oxidative stress and migration on aggressive breast cancer.

**No conflict of interest.**

**201** (PB081)  
**Preliminary interim data of elzoventinib (TPX-0022), a novel inhibitor of MET/SRC/CSF1R, in patients with advanced solid tumors harboring genetic alterations in MET: Update from the Phase 1 SHIELD-1 trial**

D. Hong<sup>1</sup>, A. Shergill<sup>2</sup>, L. Bazhenova<sup>3</sup>, B.C. Cho<sup>4</sup>, R. Heist<sup>5</sup>, V. Moreno<sup>6</sup>, G.S. Falchook<sup>7</sup>, M. Nagasaka<sup>8</sup>, P. Cassier<sup>9</sup>, B. Besse<sup>10</sup>, D.W. Kim<sup>11</sup>, S. Yoon<sup>12</sup>, X. Le<sup>13</sup>, T. Zhao<sup>14</sup>, S. Atwal<sup>15</sup>, E. Park<sup>15</sup>, J. Lee<sup>16</sup>. <sup>1</sup>The University of Texas MD Anderson Cancer Center, Investigational Cancer Therapeutics, Houston, USA; <sup>2</sup>University of Chicago Medical Center, Medicine, Chicago, USA; <sup>3</sup>University of California San Diego Moores Cancer Center, Medical Oncology, San Diego, USA; <sup>4</sup>Yonsei Cancer Center, Yonsei University College of Medicine, Medical Oncology, Seoul, South Korea; <sup>5</sup>Massachusetts General Hospital, Cancer Center, Boston, USA; <sup>6</sup>Fundación Jiménez Díaz, Early Phase Clinical Trials, Madrid, Spain; <sup>7</sup>Sarah Cannon Research Institute at HealthONE, Drug Development, Denver, USA; <sup>8</sup>University of California Irvine, Medicine, Orange, USA; <sup>9</sup>Centre de Lutte Contre le Cancer - Centre Leon Berard, Medical Oncology, Lyon, France; <sup>10</sup>Institut Gustave Roussy, Cancer Medicine, Villejuif Cedex, France; <sup>11</sup>Seoul National University Hospital, Internal Medicine, Seoul, South Korea; <sup>12</sup>Asan Medical Center, Medical Oncology, Seoul, South Korea; <sup>13</sup>The University of Texas MD Anderson Cancer Center, Thoracic/Head and Neck Medical Oncology, Houston, USA; <sup>14</sup>Turning Point Therapeutics Inc., Biometrics-Clinical Development, San Diego, USA; <sup>15</sup>Turning Point Therapeutics Inc., Clinical Development, San Diego, USA; <sup>16</sup>Samsung Medical Center, Oncology, Seoul, South Korea

**Background:** Elzoventinib is a novel, type I tyrosine kinase inhibitor (TKI) that targets MET, SRC, and CSF1R. Genetic alterations in *MET*, including exon 14 skipping ( $\Delta\text{ex14}$ ) mutations and other oncogenic mutations, amplifications, and fusions are present in many tumor types. The Phase 1 SHIELD-1 trial (NCT03993873) is evaluating safety, pharmacokinetics (PK), and preliminary activity of elzoventinib in patients (pts) with advanced solid tumors harboring genetic *MET* alterations. An early analysis included 46 efficacy evaluable pts. Among 32 TKI-naïve pts, 8 had confirmed PRs, including 4 NSCLC, 3 gastric/GE junction adenocarcinomas, and 1 colorectal cancer (Hong DS, et al. EORTC-NCI-AACR 2021, Poster nr P225). Here we report updated data from SHIELD-1.

**Patients and methods:** Adults with advanced solid tumors harboring genetic *MET* alterations were enrolled using a 3+3 dose-escalation design with additional pt enrollment at doses where clinical activity was observed. Dose expansion at the preliminary RP2D of 40 mg QD to BID titration dose is enrolling pts and results from this portion of the study will be available for presentation. Elzoventinib was given orally in continuous 28-day cycles.

**Results:** As of 13 May 2022, 59 pts have been enrolled across 8 dose levels in the dose-escalation phase, including 33 NSCLC pts (21  $\Delta\text{ex14}$ , 9 amplifications, 3 mutations), 9 gastric cancer pts (8 amplifications, 1 fusion), and 17 pts who had other cancers with *MET* alterations. Median age was 63 (33–84) years. Median number of prior therapies was 2 (range 0–7). 39 of 59 pts (66%: 15 NSCLC; 9 gastric; 15 others) had not received a prior *MET* therapy and 20 (34%: 18 NSCLC; 1 liver; 1 pancreatic) had prior *MET* therapy. The most common adverse events (AEs) were dizziness (68%), fatigue (41%), anemia (36%), constipation (34%), lipase increase (32%). Most AEs were low-grade, with 95% of dizziness AEs being Grade 1 or 2. No events of interstitial lung disease/pneumonitis, Grade 3/4 edema, or treatment-related Grade 3/4 ALT/AST elevation were reported. Systemic exposure increased in a dose-dependent manner. Evaluation of the

recommended Phase 2 dose (RP2D) is ongoing and updated safety and efficacy analyses will be available for presentation.

**Conclusions:** Elzoventinib, a novel MET/SRC/CSF1R inhibitor, was generally well tolerated with primarily low-grade dizziness, no high-grade edema, and a favorable PK profile. The RP2D is currently under evaluation and updated safety and efficacy data will be available for presentation. A global multi-cohort Phase 2 trial of pts with *MET*-altered tumors is planned.

**Conflict of interest:**

Advisory Board: Drs. Bazhenova and Falchook: Turning Point Therapeutics, Inc.

Corporate-sponsored Research: Drs. Hong, Shergill, Heist, Moreno, Falchook, Besse, Kim: Turning Point Therapeutics, Inc.

Other Substantive Relationships: Ms. Zhao, Drs. Atwal, Park: Employment, Stock ownership – Turning Point Therapeutics, Inc.

**202** (PB082)  
**rOPCML-Fc as a potential tumor suppressive therapeutic agent for ovarian cancer**

Y. Rong<sup>1</sup>, H. Gabra<sup>2</sup>, Q. Wang<sup>3</sup>, L. Li<sup>1</sup>. <sup>1</sup>Guangxi Medical University Cancer Hospital, Department of Gynecology, Nanning, China; <sup>2</sup>Papyrus Therapeutics Inc., Preclinical Development, London, United Kingdom; <sup>3</sup>Guangxi Medical University Cancer Hospital, Research Department, Nanning, China

**Background:** Opioid binding protein/cell adhesion molecule-like (OPCML) is a tumor suppressor gene that acts at the external leaflet of the cell membrane at the lipid raft, interacting with and repressing a specific network of 9 receptor tyrosine kinases (RTKs). Here, we designed a tumor suppressive biotherapeutic molecule, an rOPCML-Fc fusion protein and evaluated the functional effects and mechanism of action of the protein in-vitro and in-vivo.

**Material and methods:** The rOPCML-Fc fusion protein was generated via stable transfection in the HEK293 expression system and subsequently purified by Ni column to high purity. The rOPCML-Fc protein was then characterized.

**Results:** We found that rOPCML-Fc powerfully inhibited invasion and migration in OVCAR3 and SKOV3 cells. Cell proliferation was suppressed through promoting apoptosis of OVCAR3 and SKOV3 cells consequent upon treatment with rOPCML-Fc. rOPCML-Fc suppressed proliferation activity of several human ovarian cancers organoids in-vitro. From a signaling perspective, rOPCML-Fc protein downregulated pHER2, pAKT and the RAF/MEK/ERK pathway in ovarian cancer cells. Finally, Intravenous rOPCML-Fc protein led to substantial regression of subcutaneous human ovarian cancer PDX in NDG mice in a dose dependent fashion and did not affect the daily activities and weight of the mice. IHC demonstrated that rOPCML-Fc was mainly enriched in tumor, without aggregation in normal mouse organs.

**Conclusions:** We conclude that intravenous rOPCML-Fc therapeutic had good targeting affinity to human ovarian cancer PDX and demonstrated substantial dose dependent efficacy in vitro and in vivo without compromising safety, suggesting that this designed biotherapeutic can be taken forward into preclinical drug development.

**No conflict of interest.**

**203** (PB083)  
**Molecular characterization of next generation AR-NTD inhibitors**

J. Obst<sup>1</sup>, C.A. Banuelos<sup>1</sup>, T. Tam<sup>1</sup>, A.H. Tien<sup>1</sup>, N.R. Mawji<sup>1</sup>, J. Wang<sup>1</sup>, M.D. Sadar<sup>1</sup>. <sup>1</sup>BC Cancer, Genome Sciences Centre, Vancouver, Canada

**Background:** Inhibition of the androgen receptor (AR) is the mainstay treatment for advanced prostate cancer. While initially effective, the disease ultimately progresses to metastatic castration-resistant prostate cancer (mCRPC), which is lethal. All current AR-targeted therapies directly or indirectly target the ligand binding domain (LBD). We have developed the EPI and sintokamide (SINT) compounds which target the AR N-terminal domain (NTD), allowing for sustained inhibition in the context of constitutively active AR-splice variants and mutations which often drive resistance to current AR-targeted therapies. Ralaniten acetate (EPI-506, NCT02606123) and next generation EPI-7386 (NCT04421222) remain the only AR-NTD inhibitors to have progressed to clinical trials. Here we characterize the molecular profile of several next generation AR-NTD inhibitors compared against traditional AR-LBD antagonist enzalutamide (ENZA).

**Methods:** LNCaP and LN95 cells treated with EPI-002, EPI-7170 or ENZA were subjected to RNA-seq to identify differences in mechanisms of action for each class of inhibitor. Data was validated using qPCR both in vitro as well as using xenografts. Protein-protein interactions with the AR following drug

treatment were identified using RIME and validated with PLA. Cell cycle and DNA damage response were assayed using flow cytometry and western blot.

**Results:** RNA-sequencing on LNCaP and AR-V7 driven LN95 cells treated with EPI-7170, EPI-002 or ENZA revealed differences in the ability of the two classes of inhibitors to de-repress androgen repressed genes. A subsequent RIME assay demonstrated that the EPI compounds preferentially inhibited AR/TBL1XR1 interaction, the latter forming a part of the NCOR1 transcriptional repression complex. The most significantly deregulated pathways associated with EPI-002 or EPI-7170 identified in a GSEA analysis were involved in cell cycle in both LNCaP (G2M pathway; FDR~0.000, mitotic spindle; FDR = 0.003) and LN95 cells (G2M pathway; FDR~0.000, mitotic spindle; FDR~0.000). Cell cycle analysis using flow cytometry revealed LN95 cells treated with the EPI compounds induced G2 arrest, while cells treated with ENZA were unaffected. Pathway analysis from RNA-seq data also indicated that the EPI compounds were superior in their ability to block DNA damage repair compared to ENZA, and cells treated with EPI compounds were sensitized to radiation treatment.

**Conclusions:** We identified clear differences in the mechanisms of action between traditional AR-LBD inhibitor enzalutamide and AR-NTD inhibitors; in terms of AR-regulated gene expression, disruptions to the cell cycle and DNA damage response. This work highlights the potential for combination therapies which utilize both classes of inhibitors. An ongoing clinical trial is currently investigating EPI-7386 in combination with enzalutamide (NCT05075577).

#### Conflict of interest:

Ownership: J.K.O., C.A.B., N.R.M., J.W., A.H.T., and M.D.S are inventors of technology which was licensed to BC Cancer by ESSA Pharma Inc. M.D.S. and C.A.B have equity in ESSA Pharma Inc.

204

(PB084)

#### TAS1440, a novel reversible LSD1 inhibitor, modulates immunosuppressive population and potentiates the antitumor efficacy of anti-PD-1 antibody therapy

T. Shibutani<sup>1</sup>, H. Fukushima<sup>1</sup>, S. Tsukioaka<sup>1</sup>, T. Machida<sup>1</sup>, A. Osada<sup>1</sup>, M. Yamada<sup>1</sup>, S. Yamashita<sup>1</sup>, S. Ohkubo<sup>1</sup>. <sup>1</sup>Taiho Pharmaceutical Co., Ltd., Discovery and Preclinical Research Division, Tsukuba, Ibaraki, Japan

**Background:** Lysine-specific demethylase 1A (LSD1/KDM1A) is a flavin adenine dinucleotide (FAD)-dependent histone demethylase that specifically modifies histone H3 lysine 4 and lysine 9. In several cancers, LSD1 has been reported to play role in cancer cell survival and growth. Therefore, LSD1 is considered to be a promising drug target. Importantly, LSD1 inhibitors are undergoing clinical development. It has been recently reported that in cancer cells, LSD1 is associated with suppression of antitumor immunity, thereby contributing to cancer cell survival through immunosuppression. However, the impact of systemic inhibition of LSD1 on antitumor immunity has not been fully analyzed. In this study, we evaluated the impact of LSD1 inhibition by TAS1440, a novel histone H3-competitive reversible LSD1 inhibitor, on systemic immune cell populations and immune-mediated antitumor activity.

**Material and methods:** The antitumor efficacy of TAS1440 and anti-PD-1 antibody was evaluated using MC38 subcutaneous implanted models in immunocompetent (C57BL/6Jcl) and immunodeficient (CB17/rlcrkdc [scid]/CrIcrIj) mice. TAS1440 and anti-PD-1 antibody were administered orally and intraperitoneally, respectively. Population and mRNA expression analyses of lymphocytes isolated from MC38 tumor-bearing C57BL/6Jcl mice or EMT6 tumor-bearing BALB/cAnCrIcrIj mice were performed using flow cytometry and qPCR, respectively.

**Results:** TAS1440 exerted antitumor activity by modulating the immunosuppressive environment. First, antitumor activity of TAS1440 against the MC38 tumors was observed in immunocompetent mice but not in immunodeficient mice. Next, flow cytometry and qPCR revealed that TAS1440 dramatically decreased the granulocytic myeloid-derived suppressor cell (gMDSC) population, and increased the CD8<sup>+</sup>T cell population in tumor and peripheral tissues. These phenomena were also observed in the EMT6 mouse model.

Finally, combined treatment with TAS1440 and anti-PD-1 antibody resulted in potent tumor growth inhibition in the MC38 model (compared to either treatment alone). The combined treatment decreased the percentage of tumor-infiltrating gMDSCs and increased the percentage of tumor-infiltrating CD8<sup>+</sup>T cells.

**Conclusions:** Our data indicate that the TAS1440 modulates the immunosuppressive tumor microenvironment by reducing gMDSCs and increasing CD8<sup>+</sup>T cells. Combined treatment with TAS1440 and anti-PD-1 antibodies can serve as a new therapeutic strategy for overcoming immunotherapy resistance.

#### No conflict of interest.

205

(PB085)

#### Anticancer activity of (±)-kusunokinin derivatives as a new HSP90 inhibitor

T. Rattanaburee<sup>1</sup>, T. Thongpanchang<sup>2</sup>, C. Chompunud Na Ayudhya<sup>1</sup>, V. Tipmanee<sup>1</sup>, P. Graidist<sup>1</sup>. <sup>1</sup>Prince of Songkla University, Department of Biomedical Sciences and biomedical engineering- Faculty of Medicine, Songkhla, Thailand; <sup>2</sup>Mahidol University- Department of Chemistry- Faculty of Science and Center of Excellence for Innovation in Chemistry, Bangkok, Thailand

**Background:** Cholangiocarcinoma (CCA) is aggressive cancer arising from the malignant transformation of biliary epithelial cells. To date, surgical resection is the only potential option for CCA patients due to CCA being often chemotherapy-resistant. Therefore, finding a new potential compound to treat CCA is necessary. Previously, synthetic (±)-kusunokinin (sKU) and its derivative (burshehennin) represented cytotoxicity effect against well-differentiated CCA (KKU-M213) and low effect on undifferentiated CCA (KKU-K100) cells. Due to the low cytotoxic effect of sKU on undifferentiated CCA, modifications of the chemical of sKU were necessary to get a new potential compound.

**Material and methods:** (±)-Kusunokinin derivatives (TPPG1-TPPG5) were modified by adding butanol and hydroxyl group at 3,4 dimethoxybenzyl butyrolactone part and 1,3-benzodioxole part, respectively. Firstly, the cytotoxicity effect was evaluated using an MTT assay on KKU-M213 and KKU-K100 cells. Cell cycle arrest, apoptosis and multicaspases activity were performed using flow cytometry. A molecular docking program was used to predict target proteins with associated CCA. Target proteins and downstream molecules were investigated by Western blotting.

**Results:** TPPG-5 represented the highest IC<sub>50</sub> values of 0.01 ± 0.001 μM and 1.53 ± 0.01 μM against KKU-M213 and KKU-K100 cells, respectively which were stronger cytotoxicity than sKU. This new compound caused cell cycle arrest at G0/G1 phase on KKU-M213 cells. Moreover, TPPG-5 also induced apoptotic cells and multi-caspase activity. Using computational prediction for the target protein, TPPG-5 stronger bound HSP90-a than EC44 (known inhibitor) and sKU. Moreover, TPPG-5 decreased HSP90-a and consequently more suppressed JAK1, STAT3, PI3 K, AKT and CyclinB1 on KKU-M213 cells than sKU.

**Conclusion:** TPPG-5 exhibited cytotoxicity against cholangiocarcinoma cells via suppression of cells cycle arrest and induction of apoptosis. HSP90-a was a possible target protein of TPPG-5. JAK1, STAT3, PI3 K, AKT and CyclinB1 were also decreased. This compound has a potential ability for cholangiocarcinoma treatment in the future.

#### No conflict of interest.

206

(PB086)

#### A novel class of Ribosome Modulating Agents (RMAs) targets ribosome heterogeneity in a subset of colorectal cancers

V. Badarinarayana<sup>1</sup>, E. Terzo<sup>1</sup>, S. Apte<sup>1</sup>, S. Padhye<sup>1</sup>, S. Rashed<sup>1</sup>, W. Austin<sup>2</sup>, M. Caponegro<sup>3</sup>, A. Reddy<sup>3</sup>, C. Wang<sup>2</sup>, R. Clark<sup>2</sup>, D. Sidransky<sup>4</sup>, V. Modur<sup>1</sup>. <sup>1</sup>Eloxx Pharmaceuticals, Biology, Watertown, USA; <sup>2</sup>Eloxx Pharmaceuticals, Chemistry, Watertown, USA; <sup>3</sup>Vindhya DataScience, Data Science, Morrisville, USA; <sup>4</sup>Johns Hopkins University School of Medicine, The Sidney Kimmel Comprehensive Cancer Center, Baltimore, USA

**Background:** Aberrant protein translation is a key driver in cancer downstream of pro-oncogenic stimuli. The aberrant protein translation is frequently carried out by ribosomes that have cancer specific alterations providing an opportunity to selectively target "oncoribosomes." Our unique synthetic chemistry generates novel macrolides that are Ribosome Modulating Agents (RMAs) capable of selectively targeting oncoribosomes. Wnt-pathway activated colorectal cancers (CRC) tend to be highly dependent on elevated protein translation capacity. These types of cancers maybe vulnerable to RMAs that selectively inhibit oncoribosomes dependent protein translation.

**Material and methods:** Cell proliferation was assessed using Cell Titer Glo assay. New protein synthesis was evaluated by metabolic labelling using L-Azidohomoalanine (AHA) followed by biotinylation and detection by Western Blot. Quantitative Mass spectrometric analysis of proteins was conducted using pulsed Stable Isotope Labeling with Amino acids in Cell culture (pSILAC) proteomics method. Cell cycle arrest and apoptosis were assessed using flow cytometry.

**Results:** We evaluated ZKN-157, a representative RMA, across a panel of 34 CRC cell lines. ZKN-157 inhibited proliferation of 24% of cell lines. Genomic analysis showed that all cell lines sensitive to ZKN-157 belonged to the Consensus Molecular Subgroup 2 (CMS2) sub-type. The anti-proliferative effect of ZKN-157 was confirmed in a panel of CMS2 patient derived



organoids while sparing normal colon organoids. Metabolic labelling showed that ZKN-157 inhibited protein translation in SW1417 (CMS2) cells but had no impact on protein translation in COLO-320DM (CMS4). Consistent with this, treatment of SW1417 [VM1] with ZKN-157 triggered nucleolar stress response resulting in cell cycle arrest and apoptosis. pSILAC proteomics showed that ZKN-157 selectively inhibited translation of a subset of proteins. The impacted proteins were enriched for proteins containing positively charged regions, particularly those involved in ribogenesis and protein translation. Finally, we show that ZKN-157 causes synthetic lethality with DNA intercalating agents, a class of chemotherapeutics that are known to inhibit ribogenesis.

**Conclusions:** ZKN-157 represents a new class of molecules that selectively inhibit protein translation in CMS2 subtype of CRC which is characterized as MicroSatellite Stable (MSS) and tends to harbor high activity of Wnt/Myc pathway. The selectivity of protein translation inhibition is further characterized by preferential effect on positively charged proteins including those involved in ribogenesis and protein translation. This novel mechanism shows synergy with traditional cytotoxic therapy to generate potential new cancer therapeutics.

#### Conflict of interest:

Ownership: Eloxix Pharmaceuticals  
Vindhya DataScience  
Advisory Board: Eloxix Pharmaceuticals  
Other Substantive Relationships: Employees of Eloxix Pharmaceuticals  
Vindhya DataScience

207

(PB087)

#### Discovery of D3S-001, a highly potent and CNS-penetrant inhibitor of KRAS G12C with rapid and sustained target engagement kinetics

J. Zhang<sup>1</sup>, J. Lu<sup>2</sup>, Z. Zheng<sup>3</sup>, J. Lu<sup>4</sup>, A. Wang<sup>5</sup>, J. Wang<sup>5</sup>, J. Chen<sup>5</sup>, H. Rui<sup>6</sup>, C. Chen<sup>5</sup>, G. Chen<sup>5</sup>. <sup>1</sup>D3 Bio, Discovery Biology, Shanghai, China; <sup>2</sup>D3 Bio, Clinical Pharmacology, Shanghai, China; <sup>3</sup>D3 Bio, Toxicology, Shanghai, China; <sup>4</sup>D3 Bio, Small Molecule CMC, Shanghai, China; <sup>5</sup>D3 Bio, Clinical Development, Shanghai, China; <sup>6</sup>D3 Bio, Translational Research, Shanghai, China

**Background:** Covalent inhibition of mutant KRAS G12C protein by locking this oncogenic driver in its inactive state is clinically efficacious. Sotorasib and adagrasib have improved overall response rates (ORR) and progression-free survival (PFS) in patients with KRAS G12C-mutant non-small cell lung cancer (NSCLC). However, achieving deeper and more durable responses remain as challenges in targeting KRAS G12C. Treatment of brain metastasis in NSCLC remains a high unmet medical need. D3S-001, currently in a phase 1 trial (NCT05410145), is designed to improve clinical outcomes by optimizing KRAS G12C target engagement (TE). Here we report its preclinical activity, selectivity, central nervous system (CNS) penetrant properties, and predicted target inhibition at dose levels under phase 1 study.

**Material and methods:** The kinetics of KRAS G12C TE was measured by GTP-RAS ELISA in tumor cells and xenografts. Covalent adduct formation with KRAS G12C protein was confirmed by LC-MS. D3S-001 selectivity was assessed by free-cysteine proteomics. Anti-proliferative effect on cancer cells was evaluated by the CTG assay. Cancer cell line- and patient-derived xenografts were utilized for *in vivo* efficacy studies. D3S-001 pharmacokinetics (PK) in plasma and cerebrospinal fluid (CSF) were investigated in beagle dogs. Human target inhibition was calculated based on human PK prediction, free drug fraction, and *in vitro* TE data.

**Results:** D3S-001 demonstrates >95% target inhibition in cells at 2 hours at 5 nM and >97% at 6 hours after a single dose of 30 mg/kg in NCI-H358 tumors. D3S-001 is highly selective with KRAS G12C being the only peptide identified by proteomic profiling. D3S-001 inhibits growth of KRAS G12C-mutant cell lines with low nanomolar IC<sub>50</sub>s while no activity is seen with non-KRAS G12C mutant cells. Daily oral administration of D3S-001 at 30 and 100 mg/kg led to complete and durable tumor regression in NCI-H358 NSCLC and CR6256 colorectal cancer models, respectively. D3S-001 demonstrates a CSF-to-plasma K<sub>p,uu</sub> value of 0.33, comparable to those of adagrasib and approved CNS-active small molecule inhibitors. Importantly, observed CSF concentrations of D3S-001 are sufficient to achieve >95% KRAS G12C TE. In phase 1, D3S-001 dose will be escalated from 50 mg to 900 mg QD. Predicted human exposures at dose levels >100 mg QD are expected to consistently achieve >95% target inhibition. At dose levels >400 mg QD, predicted exposures should achieve >95% target inhibition in CNS.

**Conclusions:** D3S-001 demonstrates rapid and near complete TE with KRAS G12C *in vitro* and *in vivo*. Its potency, selectivity, and CNS-penetrance support clinical development in patients with KRAS G12C mutation. Optimal TE predicted at clinical exposures may lead to deeper and more durable

responses in both systemic and intracranial tumors than currently available KRAS G12C inhibitors.

#### No conflict of interest.

208

(PB088)

#### Regulation of oncogenic transcription and tumor growth in pediatric cancers by the CDK9 inhibitor KB-0742

D. Saffran<sup>1</sup>, E. Poon<sup>2</sup>, G. Ibanez<sup>3</sup>, J. Nakashima<sup>4</sup>, S. Naffar-Abu Amara<sup>5</sup>, C. Noe<sup>5</sup>, T. Hood<sup>5</sup>, P. Kumar<sup>5</sup>, J. DiMartino<sup>6</sup>, F. Dela Cruz<sup>3</sup>, L. Chesler<sup>2</sup>, C.Y. Lin<sup>7</sup>. <sup>1</sup>Kronos Bio Inc., Pharmacology, San Mateo, USA; <sup>2</sup>The Institute of Cancer Research, Division of Clinical Studies, London, United Kingdom; <sup>3</sup>Memorial Sloan Kettering Cancer Center, Department of Pediatrics, New York, USA; <sup>4</sup>Certis Oncology Solutions, Chief Scientific Officer, San Diego, USA; <sup>5</sup>Kronos Bio Inc., Translational Development, San Mateo, USA; <sup>6</sup>Kronos Bio Inc., Clinical Development, San Mateo, USA; <sup>7</sup>Kronos Bio Inc., TRN Mapping, San Mateo, USA

**Background:** Disruption of transcriptional regulatory networks that drive normal cellular differentiation and development can result in oncogenic transformation and transcriptional addiction. Many pediatric sarcomas are defined by/harbor oncogenic fusion proteins, resulting from chromosomal translocations such as the *EWSR1* gene fused to an *ETS* family transcription factor (TF) gene (*FLI1* or *ERG*) in Ewing sarcoma (ES), or *PAX3/1PAX7* and *FOXO1* translocations in alveolar rhabdomyosarcoma (ARMS). In neuroblastoma, *MYCN*, a member of the *MYC* family of TFs, is often amplified and localizes to super enhancer regions, where it rewires lineage-specific transcriptional programs driving oncogenesis.

Oncogenic TFs have proven difficult to target directly; we and others have proposed targeting associated transcriptional co-regulators to inhibit their activity. CDK9 interacts with many oncogenic TFs and is essential for TF-mediated transcription elongation through phosphorylation of the C-terminal domain of RNA pol II. KB-0742 is a potent, selective, and orally bioavailable inhibitor of CDK9 currently in clinical development that shows antitumor activity in preclinical models of sarcoma and neuroblastoma.

**Materials and Methods:** Cell lines and low passage patient-derived cells (PDCs) were tested for antiproliferative effects of KB-0742, using either Cell Titer Glo (Promega) or Alamar Blue cell viability reagent (Bio-Rad). Pharmacodynamic (PD) markers of KB-0742 treatment, including phospho-SER2 (pSER2) on RNA pol II, *MYCN*, *MYC*, and cleaved poly ADP ribose polymerase (PARP), were measured by Western blot. The antitumor activity of KB-0742 was evaluated using patient-derived xenograft (PDX) models of ES and ARMS *in vivo*. Tumor samples and plasma were collected to determine PD effects and drug concentrations, respectively. The transgenic *TH-MYCN* model of neuroblastoma was used to study antitumor effects of KB-0742. All *in vivo* models were performed according to IACUC guidelines.

**Results:** KB-0742 decreased the viability of immortalized and low passage PDCs from ES, ARMS, and neuroblastoma. In neuroblastoma, cell lines with *MYCN* amplification were more sensitive to KB-0742 treatment. KB-0742-treated neuroblastoma cells had decreased pSER2, loss of expression of *MYCN* and *MYC*, and an induction of cleaved PARP. KB-0742 treatment of a *TH-MYCN* transgenic mouse model resulted in regression of established tumors. In PDX models of ES and ARMS, KB-0742 treatment inhibited tumor growth. Analysis of tumor samples revealed decreases in pSER2 and expression and function of the oncogenic TFs.

**Conclusions:** CDK9 targeting by KB-0742 inhibits growth of multiple pediatric tumor types by modulating the expression and activity of key oncogenic TFs. KB-0742 is being evaluated in a phase I dose-escalation trial in patients with relapsed or refractory solid tumors or NHL (NCT04718675).

#### Conflict of interest:

Ownership: CN, CYL, DCS, PK, and SN-AA report stock ownership in Kronos Bio, Inc. JD reports stock ownership in Kronos Bio, Inc., and Bristol-Myers Squibb Company. JN reports stock ownership in Certis Oncology Solutions. TH reports stock ownership in Kronos Bio, Inc., and NanoString Technologies.

Advisory Board: FDC reports uncompensated consultancy for Kronos Bio, Inc., Shasqi, Inc., Y-mAbs Therapeutics, Inc., Biosplice Therapeutics, Inc., Daiichi Sankyo Co., Ltd., and Sanofi-Aventis U.S., LLC.

Corporate-sponsored Research: CN, CYL, DCS, JD, PK, SN-AA, and TH report employment at Kronos Bio, Inc.

Other Substantive Relationships: FDC reports institutional research support from Eisai Co., Ltd.

209

(PB089)

**Update from the ongoing phase 1/2 registrational trial of repotrectinib: results in TKI-naïve and TKI-pretreated patients with NTRK fusion-positive advanced solid tumors (TRIDENT-1)**

B. Besse<sup>1</sup>, C. Springfield<sup>2</sup>, C. Baik<sup>3</sup>, A. Hervieu<sup>4</sup>, B. Solomon<sup>5</sup>, V. Moreno<sup>6</sup>, L. Bazhenova<sup>7</sup>, K. Goto<sup>8</sup>, Y.C. Kim<sup>9</sup>, S. Lu<sup>10</sup>, M. Sun<sup>11</sup>, D. Trone<sup>12</sup>, S. Thama<sup>12</sup>, B.C. Cho<sup>13</sup>, A. de Langen<sup>14</sup>, S. Popat<sup>15</sup>, J. Wolf<sup>16</sup>, D. Moro-Sibilot<sup>17</sup>, J. Fang<sup>18</sup>, A. Drilon<sup>19</sup>. <sup>1</sup>Institut Gustave Roussy, Villejuif, France; <sup>2</sup>Heidelberg University Hospital- National Center for Tumor Diseases, Medical Oncology, Heidelberg, Germany; <sup>3</sup>University of Washington School of Medicine- Seattle Cancer Care Alliance- Fred Hutchinson Cancer Research Center, Seattle, USA; <sup>4</sup>Centre Georges-François, Dijon, France; <sup>5</sup>Peter MacCallum Cancer Center, Melbourne, Australia; <sup>6</sup>Fundación Jiménez Díaz - START Madrid, Madrid, Spain; <sup>7</sup>University of California Moores Cancer Center, San Diego, USA; <sup>8</sup>National Cancer Center Hospital East, Chiba, Japan; <sup>9</sup>Chonnam National University Medical School- and CNU Hwasun Hospital, Hwasun-gun, South Korea; <sup>10</sup>Shanghai Chest Hospital, Shanghai, China; <sup>11</sup>Jinan Central Hospital, Jinan, China; <sup>12</sup>Turning Point Therapeutics Inc, San Diego, USA; <sup>13</sup>Yonsei Cancer Center- Yonsei University College of Medicine, Seoul, South Korea; <sup>14</sup>Netherlands Cancer Institute, Amsterdam, Netherlands; <sup>15</sup>The Royal Marsden NHS Foundation Trust, London, United Kingdom; <sup>16</sup>Centrum für Integrierte Onkologie- Uniklinik Köln, Cologne, Germany; <sup>17</sup>Centre Hospitalier Universitaire de Grenoble-Alpes, La Tronche, France; <sup>18</sup>Beijing Cancer Hospital, Beijing, China; <sup>19</sup>Memorial Sloan Kettering Cancer Center- Weill Cornell Medical College, New York, USA

**Background:** Repotrectinib is a selective, highly potent, next-generation ROS1 and TRK inhibitor that is currently under evaluation in the global registrational phase 1/2 TRIDENT-1 trial. Early clinical data from the TRIDENT-1 trial was presented in a plenary session at the 2021 AACR-NCI-EORTC conference. Repotrectinib was generally well tolerated. In NTRK fusion-positive tyrosine kinase inhibitor (TKI)-naïve (expansion cohort [EXP-5]) and TRK TKI-pretreated (EXP-6) patients with advanced solid tumors, confirmed overall response rates (cORR) per investigator assessment were 41% (95% CI: 18–67) and 48% (95% CI: 27–69), respectively. Efficacy was also observed in patients whose cancers developed solvent front mutations following prior TRK TKI treatment, with investigator-assessed cORR of 62% (95% CI: 32–86).

**Materials and methods:** TRIDENT-1 (NCT03093116) is an ongoing trial enrolling patients whose cancers harbor a ROS1 or NTRK gene fusion. Patients enter 1 of 6 defined EXPs based on cancer type and prior therapy. The primary efficacy endpoint is cORR by Blinded Independent Central Review using RECIST v1.1. Safety and tolerability are also assessed.

**Results:** The data cutoff for the present safety analysis was 11 February 2022. All treated patients were evaluable for safety (n = 380). The most common (>35% of patients) treatment-emergent adverse events (TEAE) were dizziness (60%), dysgeusia (48%), and constipation (35%). The majority (76%) of reported dizziness cases were grade 1 and no events of dizziness led to treatment discontinuation. Most treatment-related AEs (TRAE) were grade 1 or 2. Grade ≥3 TRAEs were observed in 21% of patients; no grade 5 TRAEs were observed. Dose reductions and discontinuations due to TEAEs were reported in 32% and 10% of patients, respectively. Safety results in patients with NTRK fusion-positive advanced solid tumors were similar to those in the overall population. Updated safety and efficacy data for NTRK fusion-positive TKI-naïve (EXP-5) and TKI-pretreated (EXP-6) patients will be available for presentation.

**Conclusions:** In the ongoing registrational phase 1/2 TRIDENT-1 trial, repotrectinib generally was well tolerated in 380 patients. The most common TEAE was low-grade dizziness. Updated efficacy and safety data from this ongoing trial will be presented.

**Conflict of interest:**

Ownership: Chul Cho Stock or stock options: TheraCanVac Inc, Gencurix Inc, Bridgebio therapeutics, KANAPH Therapeutic Inc, Cyrus therapeutics, Interpark Bio Convergence Corp. Denise Trone Turning Point Therapeutics Employee Sanjay Thama Turning Point Therapeutics Employee and Stock or Stock Options Alexander Drilon Stock or stock options: Treeline Bio Advisory Board: Byoung Chul Cho KANAPH Therapeutic Inc, Bridgebio therapeutics, Cyrus therapeutics Guardant Health, Joseah BIO. Luydmila Bazhenova Personal Fees Turning point therapeutics, Daiichi, BMS, Janssen, Merck, Regeneron, Bayer, Takeda, Boehringer Ingelheim, Novartis, Genentech, Sanofi, AstraZeneca, Blueprint, Mirati Alexander Drilon Melendi 14ner/Elevation Oncology Novartis Pfizer Loxo/Bayer/Lilly Repare RX Janssen Amgen MonteRosa Benjamin Solomon Roche, Novartis, AstraZeneca, Pfizer, Lilly Amgen, BMS, Merck, Takeda, Beigene

Board of Directors: Byoung Chul Cho Gencurix Inc, Interpark Bio Convergence Corp.

Other Substantive Relationships: Byoung Chul Cho Research Funding: Novartis, Bayer, AstraZeneca, MOGAM Institute, Dong-A ST, Champions Oncology, Janssen, Yuhan, Ono, Dizal Pharma, MSD Abbvie, Medpacto, GInnovationEli Lilly, Blueprint medicines, Interpark Bio Convergence Corp. Royalty: Champions Oncology. Consulting fees: Novartis, AstraZeneca, Boehringer-Ingelheim, Roche, BMS, Ono, Yuhan, Pfizer, Eli Lilly, Janssen, Takeda, MSD, Janssen, Medpacto, Blueprint medicines. Founder: DAAN Biotherapeutics

Luydmila Bazhenova Research Funding: Beyondspring Personal Fees: ORIC

Sanjay Popat Personal Fees: Amgen, AstraZeneca, Bayer, Beigene, Blueprint, BMS, Boehringer Ingelheim Daiichi Sankyo, Guardant Health, Incyte, Jansse, Lilly, Merck Serono, MSD, Novartis, Roche, Takeda, Pfizer, Seattle Genetics, Turning Point Therapeutics, Xcovery Payment for honoraria Personal Fees: AstraZeneca, Bayer, Guardant Health, Janssen, Merck Serono, Roche, Takeda, Pfizer Payment for expert testimony Personal Fees: Roche, Merck Serono Leadership role (Unpaid): British Thoracic Oncology Group, ALK Positive UK, Lung Cancer Europe, Ruth Strauss Foundation, Mesothelioma Applied Research Foundation, ETOP-IBCSG Partners Foundation Board

Adrianus de Langen Grants: BMS, MSD, Boehringer, AstraZeneca Non-Financial Support: Merck Serono, Roche

Christina Baik Grants: Hanmi Pharmaceutical, Trident Pharmaceuticals, Daiichi Sankyo, AbbVie, Orchard Therapeutics, AstraZeneca Pharmaceuticals, Hoosier Cancer Research Network, Array, Loxo, Janssen, Blueprint Medicines, Rain Therapeutics, TP therapeutics, Lilly Oncology Consulting fees: Silverback Therapeutics, AstraZeneca, Blueprint Medicines, Daiichi, Takeda, TP Pharmaceuticals, Guardant Health, Regeneron

Koichi Goto All support for present manuscript: Turning Point Therapeutics, Inc. Grants: Amgen Inc.

AstraZeneca K.K., Bayer Yakuhin, Ltd., Boehringer Ingelheim Japan, Inc., Bristol-Myers Squibb K.K., Blueprint Medicines Corporation., Chugai Pharmaceutical Co., Ltd., DAICHI SANKYO Co., Ltd.

Eisai Co., Ltd., Eli Lilly Japan K.K., Haihe Biopharma Co., Ltd., Ignyta, Inc., Janssen Pharmaceutical K.K.,

KISSEI PHARMACEUTICAL CO., LTD., Kyowa Kirin Co., Ltd., Life Technologies Japan Ltd., Loxo Oncology, Inc.,

MEDICAL & BIOLOGICAL LABORATORIES CO., LTD., Merck Biopharma Co., Ltd., Merus N.V., MSD K.K., NEC Corporation, Novartis Pharma K.K.,

Ono Pharmaceutical Co., Ltd., Pfizer Japan Inc., Sumitomo Dainippon Pharma Co., Ltd., Spectrum Pharmaceuticals, Inc., Sysmex Corporation., Taiho Pharmaceutical Co., Ltd., Takeda Pharmaceutical Co., Ltd. Payment

for honoraria Personal Fees: Amgen Inc., AstraZeneca K.K., Bayer HealthCare Pharmaceuticals Inc., Boehringer Ingelheim Japan, Inc., Bristol-Myers Squibb K.K., Chugai Pharmaceutical Co., Ltd., DAICHI SANKYO Co., Ltd., Eisai Co., Ltd., Eli Lilly Japan K.K., Guardant Health

Inc., Janssen Pharmaceutical K.K., Kyowa Kirin Co., Ltd., Life Technologies Japan Ltd., Medpace Japan K.K. Merck Biopharma Co., Ltd., MSD K.K., Novartis Pharma K.K., Ono Pharmaceutical Co., Ltd., Otsuka

Pharmaceutical Co., Ltd., Pfizer Japan Inc., Taiho Pharmaceutical Co., Ltd., Takeda Pharmaceutical Co., Ltd.

Meili Sun: No conflicts to report

Jian Fang: No conflicts to report

Shun Lu: No conflicts to report

Alexander Drilon All support for present manuscript: Pfizer Exelixis GlaxoSmithKlein Teva Taiho PharmaMar

Royalty: Wolters Kluwer Consulting fees: ArcherDX Abbvie BergenBio Hengrui Therapeutics Blueprint Medicines Ignyta/Genentech/Roche

AstraZeneca MORE Health Tyra Biosciences Loxo/Bayer/Lilly Pfizer Nuvalent Merus AXIS Medscape Liberum Med Learning PeerView EPG

Health JNCCN/Harborside Ology Clinical Care Options TouchIME Entos Treeline Prelude Applied Pharmaceutical Science, Inc mBrace i3 Health

Payment for honoraria Personal Fees: Ignyta/Genentech/Roche Loxo/Bayer/Lilly Takeda/Ariad/Millennium TP Therapeutics AstraZeneca Pfizer

Blueprint Medicines Helsinn Beigene BergenBio Hengrui Therapeutics Exelixis Tyra Biosciences Verastem MORE Health Abbvie 14ner/Elevation

Oncology ArcherDX Monopteros Novartis EMD Serono Medendi Repare RX Nuvalent Merus Chugai Pharmaceutical Remedica Ltd mBrace AXIS EPG

Health Harborside Nexus Liberum RV More Ology Amgen TouchIME Janssen Entos Treeline Bio Prelude Applied Pharmaceutical Science, Inc

AI/CE I3 Health MonteRosa John Hopkins Lung Cancer Research Other financial or non-financial interests: Boehringer Ingelheim Food/Beverage:

Merck, Puma, Merus Copyright: Selpercatinib-Osimertinib (filed/pending)

Besse Benjamin Grants (to institution): 4D Pharma, Abbvie, Amgen, Aptitude Health, AstraZeneca, BeiGene, Blueprint Medicines, Boehringer Ingelheim,

Celgene, Cergentis, Chugai pharmaceutical, Cristal Therapeutics, Daiichi-Sankyo, Eli Lilly, Eisai, Genzyme Corporation, GSK, Inivata, IPSEN,

Janssen, Onxeo, OSE immunotherapeutics, Pfizer, Roche-Genentech, Sanofi, Takeda, Tolero Pharmaceuticals, Turning Therapeutics  
 Benjamin Solomon Payment for honoraria: Roche AstraZeneca, Pfizer, Amgen, Takeda  
 Christoph Springfield Payment for honoraria: MSD  
 Young Chul Kim Research Grant: AstraZeneca, Boehringer Ingelheim  
 Payment for honoraria: AstraZeneca, Roche, Amgen, Yuhan, Johnson & Johnson, Boehringer Ingelheim, Novartis, Pfizer  
 Alice Hervieu All support for present manuscript: Provision of study materials, funding, medical writing  
 Denis Moro-Sibilot Consulting fees: BMS, MSD Payment for honoraria: Roche AstraZeneca Support for attending meetings and/or travel: Roche Jürgen Wolf Consulting fees/Payment for honoraria/ Support for attending meetings and/or travel/Participation on a data safety monitoring board or advisory board: Amgen, AstraZeneca, Bayer, Blueprint, BMS, Boehringer-Ingelheim, Chugai, Daiichi Sankyo, Janssen, Lilly, Loxo, Merck, MSD, Novartis, Nuvalent, Pfizer, Roche, Seattle Genetics, Takeda, Turning Point, BMS, Janssen Pharmaceutica, Novartis, Pfizer  
 Victor Moreno Consulting fees: Roche, Bayer, Pieris, BMS, Janssen, Basilea, Regeneron/Sanofi, BMS, Bayer. Nanobiotix Other financial or non-financial interests: Principal Investigator – Institutional Funding: AbbVie, AceaBio, Adaptimmune, ADC Therapeutics, Aduro, Agenus, Amcure, Amgen, Astellas, AstraZeneca Bayer Beigene Biolvent International AB, BMS, Boehringer, Boehringer, Boston, Celgene, Daiichi Sankyo, DEBIOPHARM, Eisai, e-Terapeutics, Exelisis, Forma Therapeutics, Genmab, GSK, Harpoon, Hutchison, Immuteq, Incyte, Inovio, Iovance, Janssen, Kyowa Kirin, Lilly, Loxo, MedSir, Menarini, Merck, Merus, Millennium, MSD, Nanobiotix, Nektar, Novartis, Odonate Therapeutics, Pfizer, Pharma Mar, PharmaMar, Principia, PsiOxus, Puma, Regeneron, Rigontec, Roche, Sanofi, Sierra Oncology, Synthon, Taiho, Takeda, Tesaro, Transgene, Turning Point Therapeutics, Upshersmith.

## 210 Targeting survivin with the small molecule sepantronium bromide (YM-155) in esophageal cancer (PB090)

P. Phatak<sup>1</sup>, J. Donhaue<sup>1</sup>. <sup>1</sup>Birmingham VA Medical Center and University of Alabama at Birmingham, Surgery, Birmingham, USA

**Background:** Survivin is a member of the Inhibitor of Apoptosis (IAP) protein family, and is involved in the regulation of cell division and in the inhibition of apoptosis. Although survivin is not expressed in most normal human tissues, it has shown to be upregulated in many human cancers, including esophageal cancer. Based on its differential expression in normal and malignant tissues and its critical role in regulating cell survival, survivin is an attractive candidate for targeted therapy. One of the most promising therapeutic approaches for targeting survivin is the suppression of its transcription by the small molecule inhibitor sepantronium bromide (YM-155). This agent has demonstrated anti-tumor efficacy in multiple malignancies, but its role in esophageal cancer has not been evaluated. The goal of this study is to determine the efficacy of YM-155 against a broad panel of esophageal cancer cell lines.

**Material and methods:** Studies were performed in human esophageal cancer lines TE7, TE10, OE21, and SK-GT-4 and in the esophageal epithelial cell line hESO. mRNA expression levels of both survivin and XIAP, another IAP family member, were measured by real-time PCR. Protein expression was examined by Western blot. Cellular viability following exposure to YM-155 was assessed by MTT assay. Survivin promoter activity was measured by luciferase reporter assay.

**Results:** Endogenous survivin mRNA and protein levels are markedly increased in the panel of esophageal cancer cell lines compared hESO cells. YM-155 treatment effectively reduces survivin mRNA and protein expression in all four cell lines with minimal effect on XIAP expression. All four esophageal cancer cell lines are exquisitely sensitive to YM-155, with ranges of IC<sub>50</sub> and IC<sub>90</sub> concentrations found to be lower than those reported in other malignant cell lines. Exposure of SK-GT-4 cells to either the IC<sub>50</sub> or IC<sub>90</sub> concentration of YM-155 results in a significant decrease in survivin promoter activity.

**Conclusions:** Survivin is overexpressed in esophageal cancer cell lines. Survivin mRNA and protein levels are markedly decreased in these cells following treatment with YM-155. In addition, all the examined cell lines are markedly sensitive to YM-155 exposure, which reduces survivin promoter activity in a dose-dependent manner. Our result suggest that YM-155 is an interesting therapeutic agent to target survivin for esophageal cancer treatment.

**No conflict of interest.**

Abstracts, 34th EORTC-NCI-ACR Symposium

## 211 A novel class of Ribosome Modulating Agents (RMAs) target MYC driven SCLC and synergize with DNA intercalating agents (PB091)

V. Badarinarayana<sup>1</sup>, M. Brait<sup>2</sup>, E. Terzo<sup>1</sup>, D.G. Lima<sup>2</sup>, M.T. Ugurlu<sup>2</sup>, S. Apte<sup>1</sup>, S. Padhye<sup>1</sup>, S. Rashed<sup>1</sup>, W.F. Austin<sup>3</sup>, C. Wang<sup>3</sup>, M. Caponegro<sup>4</sup>, R.B. Clark<sup>3</sup>, D. Sidransky<sup>2</sup>, V. Modur<sup>1</sup>. <sup>1</sup>Eloxx Pharmaceuticals, Biology, Watertown, USA; <sup>2</sup>Johns Hopkins University School of Medicine, The Sidney Kimmel Comprehensive Cancer Center, Baltimore, USA; <sup>3</sup>Eloxx Pharmaceuticals, Chemistry, Watertown, USA; <sup>4</sup>Vindhya DataScience, Data Science, Morrisville, USA

**Background:** SCLC has a very poor prognosis and limited treatment options. Genomic studies in SCLC show that MYC isoforms are key oncogenic drivers in a majority of SCLC tumors. As a result, these tumors tend to have high proliferation and protein translation rates. We hypothesized that ribosome modulating agents (RMAs) that selectively inhibit protein translation may show activity in these MYC driven cancers prompting us to test these novel RMAs and understand their effects in SCLC models.

**Material and methods:** Cell lines were purchased from ATCC and cell proliferation was measured using Deep Blue Cell Viability™ Kit (Biologend) based on the resazurin reagent. Fluorescence (excitation 544 nm, emission 590 nm) was measured after 2 h of incubation at 37°C. IC 50, GI50, and LD 50 were calculated according to the NCI-60 Human Tumor Cell Lines Screen study. Cell lines were treated with drugs at various concentrations in alone or combination for 96 or 120 hours. DMSO or water was used as a control vehicle. Carboplatin, Paclitaxel, Etoposide, Doxorubicin, Lurbinectedin, and Mitomycin C were purchased from different companies. All drugs were dissolved in DMSO or water according to the manufacturer's guidelines. We used Combobenefit software (Cancer Research UK Cambridge Institute) for the analysis of combinatorial drug studies. New protein synthesis was evaluated by metabolic labelling using L-Azidohomoalanine (AHA) followed by biotinylation and detection by Western Blot.

**Results:** We tested ZKN-217, a representative RMA, across a panel of 40 SCLC cell lines. Treatment with ZKN-217 resulted in cytotoxic response in 45% of the SCLC lines. We identified 175 genes that are differentially expressed between sensitive and insensitive cell lines. Gene signature analysis identified gene sets enriched in the sensitive cell lines including genes involved in ribogenesis, protein translation, mitochondrial translation, and c-MYC target genes. Using metabolic labelling studies, we identified that ZKN-217 selectively inhibited protein translation in NCI-H446 (sensitive) but not in NCI-H526 (insensitive) cells. Consequently, treatment with ZKN-217 triggered an apoptotic response in the NCI-H446. We then evaluated the impact of ZKN-217 in combination with standard of care drugs used to treat SCLC. We found that ZKN-217 and the DNA intercalating agents Doxorubicin and Mitomycin C had a synergistic effect.

**Conclusions:** ZKN-217 represents a new class of molecules that selectively inhibit protein translation in a subset of SCLC characterized by high c-MYC activity and high rates of ribogenesis. Furthermore, ZKN-217 demonstrated synergy with current standard of care DNA intercalating drugs.

### Conflict of interest:

Ownership: Eloxx Pharmaceuticals  
 Vindhya DataScience  
 Advisory Board: Eloxx Pharmaceuticals  
 Other Substantive Relationships:  
 Employees of Eloxx Pharmaceuticals  
 Vindhya DataScience

## 212 NVL-330 is a selective, brain-penetrant inhibitor of oncogenic HER2 exon 20 insertion mutations in preclinical models (PB092)

K.L. Andrews<sup>1</sup>, Y. Sun<sup>1</sup>, B. Gerard<sup>1</sup>, A. Tangpeerachaikul<sup>1</sup>, S. Mente<sup>1</sup>, R.A. Kemper<sup>1</sup>, C.M. Martin<sup>1</sup>, N.E. Kohl<sup>2</sup>, J.C. Horan<sup>1</sup>, H.E. Pelish<sup>1</sup>. <sup>1</sup>Nuvalent, Inc., Discovery, Cambridge, USA; <sup>2</sup>Kohl Consulting, Discovery, Wellesley, USA

**Background:** HER2 exon 20 insertion mutations (exon20ins) are oncogenic driver mutations detected in 1~3% of non-small cell lung cancer (NSCLC) patients in the US. Currently, there are no FDA- or EMA-approved targeted therapies for these patients. Development of small molecule inhibitors for HER2 exon20ins has been limited by off-target inhibition of closely related wild-type EGFR, which can lead to adverse events and dose-limiting toxicities including skin rash and gastrointestinal toxicity. In addition, activity in the central nervous system (CNS) is needed, since ~20% of HER2 exon20ins NSCLC patients present with accompanying brain metastases at the time of diagnosis. Novel HER2 inhibitor NVL-330 was designed for

Poster Session (27 October 2022)

coverage of HER2 exon20ins, selectivity over structurally related wild-type EGFR, and activity in the CNS.

**Material and Methods:** NVL-330 was profiled using phospho-HER2 assays in NCI-H1781 cells (HER2 G776del insVC; HER2<sup>YVMA</sup>) and Ba/F3 cells overexpressing HER2 A775\_G776 insYVMA (HER2<sup>YVMA</sup>), a phospho-EGFR assay in A431 cells (wild-type EGFR), and a viability assay in Ba/F3 HER2<sup>YVMA</sup> cells. Kinome profiling was conducted using the PhosphoSens<sup>®</sup> platform. Pharmacokinetic, pharmacodynamic, and efficacy studies were performed in mice subcutaneously implanted with NCI-H1781 cells or patient-derived xenograft (PDX) CTG-2543. Cellular efflux ratio was determined using an MDCK-hMDR1 permeability assay. The unbound brain-to-plasma partitioning ratio (K<sub>p,uu</sub>) was determined at one hour after oral 10 mg/kg dosing in Wistar-Han rats and adjusted by fraction unbound.

**Results:** NVL-330 inhibited cellular phosphorylation of HER2<sup>YVMA</sup> and HER2<sup>VC</sup> mutants, two major types of HER2 exon20ins, as well as the proliferation of Ba/F3 HER2<sup>YVMA</sup> cells, with IC<sub>50</sub> values <20 nM. By comparison, NVL-330 modestly inhibited the phosphorylation of wild-type EGFR with IC<sub>50</sub> >70-fold higher. In addition, NVL-330 was kinase selective; in a panel of 376 wild-type kinases, it did not inhibit any off-target kinases by >50% at 3 μM. *in vivo*, NVL-330 induced tumor regression at well-tolerated doses in an NSCLC PDX harboring HER2<sup>YVMA</sup>. NVL-330 also dose-dependently suppressed phospho-HER2 in xenograft tumors, supporting on-target activity. Finally, NVL-330 demonstrated good brain penetration as evidenced by rodent K<sub>p,uu</sub>, as well as a favorable efflux ratio.

**Conclusions:** NVL-330 is a wild-type EGFR-sparing, brain-penetrant small-molecule inhibitor of HER2 exon20ins in preclinical models, demonstrating the potential to address a medical need for HER2 exon 20 insertion mutant NSCLC patients.

#### Conflict of interest:

Advisory Board: NEK is a scientific advisor of Nuvalent, Inc. Other Substantive Relationships: KLA, YS, BG, AT, SM, RAK, CMM, JCH and HEP are employees and stockholders of Nuvalent, Inc.

#### 213 (PB093) Flotillin-1 Palmitoylation as a Mediator of Breast Cancer Metastasis

B. McClellan<sup>1</sup>. <sup>1</sup>University of Texas at Austin, Nutritional Sciences, Austin, Texas, USA

**Background:** Breast Cancer metastasis results in the majority of cancer related mortality. Flotillin-1 is overexpressed in numerous solid tumors and has been demonstrated to contribute to invasion and metastasis in breast cancer. Though its expression alone has been associated with metastasis, there has yet to be any investigation as to how certain post-translational modifications can affect its metastatic capabilities. Flotillin-1 is modified through palmitoylation, a post-translational modification essential for protein stability, processing, and localization. By generating a palmitoylation defective mutant of flotillin-1, we have demonstrated that flotillin-1 palmitoylation contributes to its stability and metastatic capabilities in both 3D and *in vivo* models of invasion and metastasis.

**Materials and Methods:** Flotillin-1 wild type or palmitoylation defective C-34A mutants were expressed in stable flotillin-1 knockdown MDA-MB-231 and SUM-159 triple negative breast cancer cells. These cells were subjected to 2D invasion chambers and 3D collagen invasion assays. Further, both wild type and C34A expressing cells were used for experimental lung metastases in mice by tail vein injection. 2-bromopalmitate (50 μM) was used as a chemical palmitoylation inhibitor and MG-132 (10 μM) for proteasomal inhibition.

**Results:** Invasion in stable knockdown cells was restored by re-expression of flotillin-1, but not by follitillin-1 C34A. We further observed a significant decrease in lung metastasis in flotillin-1 C34A cells compared to wild type flotillin-1. Flotillin-1 C34A expression led to a significant decrease in protein stability, which was restored by MG-132.

**Conclusion:** Flotillin-1 palmitoylation contributes to its stability and subsequent metastatic capabilities in breast cancer cells and experimental metastasis models. Thus, flotillin-1 palmitoylation could be a promising target for breast cancer metastasis.

#### No conflict of interest.

#### 214 (PB094) Covalent FGFR inhibitor futibatinib exhibits sustained antitumor effects compared with ATP-competitive inhibitors by being less prone to on-target resistance

H. Sootome<sup>1</sup>, H. Muraoka<sup>1</sup>, Y. Aoyagi<sup>1</sup>, M. Kato<sup>1</sup>, H. Hirai<sup>2</sup>. <sup>1</sup>Taiho Pharmaceutical Co., Ltd., Translational Research, Ibaraki, Japan; <sup>2</sup>Taiho Pharmaceutical Co., Ltd., Discovery and Preclinical Research, Ibaraki, Japan

**Background:** Futibatinib is a next-generation covalent FGFR1-4 inhibitor. Kinase inhibitors are subject to drug resistance due to acquired mutations of their target kinase, which limits the duration of response in patients. Here we compared the time to emergence of drug resistance caused by FGFR2 kinase mutations between futibatinib and reversible ATP-competitive FGFR inhibitors.

**Methods:** A library with random amino acid mutations in two regions (#1 and #2) of the kinase domain of FGFR2 was transfected as TEL-FGFR2 fusion into a Ba/F3 cell line, resulting in FGFR2-dependent cell growth. Using this as a model system for clonal selection, cells were exposed to futibatinib, pemigatinib and erdafitinib, and cell count measured over time. Surviving drug resistant clones were isolated and sequenced to determine the kinase domain mutations.

**Results:** The emergence of resistant clones due to mutations in FGFR2 kinase domain occurred most rapidly in the pemigatinib (100 nM)-treated cells with 8 days from cell seeding to >500-fold increase in resistant cells compared to 2 days in the control group. In erdafitinib (100 nM) treated cells, the T500 (time to reach 500-fold cell count) was 17 days. In contrast, no resistant cells to futibatinib (40 & 100 nM) appeared during the measurement period leading to a T500 of greater than 35 days. At the concentration that completely inhibits the proliferation of Ba/F3 cells expressing wild-type FGFR, treatment of the library-transfected cells with pemigatinib (12 nM), erdafitinib (12 nM), and futibatinib (3 nM) resulted in an average (n = 2) of 93, 27, and 13 resistant clones in region #1, respectively, and 28, 21 and 1 clones in region #2, respectively. Sequencing of the resistant clones for these three FGFR inhibitors identified mutations at the following key amino acid residues: N550, E566 and K642 (regulatory triad), V565 (gatekeeper region), and K660 (activation loop); these were also identified previously in patients who developed resistance to pemigatinib, infiratinib, and Debio1347. For further analysis, 10 FGFR2 mutations (N550D/K, V563L, V565I/L, E566A/G, K642I/R and K660M) were selected those with ≥5 clones identified as resistant to any of the tested drugs. Among them, futibatinib inhibited 8 mutants and erdafitinib inhibited 5 mutants at half-maximal effective concentrations (IC<sub>50</sub>'s) comparable to that with wild-type FGFR; pemigatinib activity against all FGFR mutants was attenuated by ≥5-fold vs wild-type.

**Conclusions:** Futibatinib, a covalent FGFR1-4 inhibitor, exhibited sustained antitumor effects compared to ATP-competitive inhibitors with fewer and later onset of acquired FGFR2 kinase resistance mutations. These data may potentially explain the numerically favorable differences in duration of response for futibatinib compared with ATP-competitive FGFR inhibitors for treatment of cholangiocarcinoma patients.

#### No conflict of interest.

#### 215 (PB095) OQL036 topical gel inhibits the skin toxicity associated with 5-fluorouracil/capecitabine: results from in vitro and in vivo preclinical studies

L. Chen<sup>1</sup>, W. Li<sup>1</sup>, K. Fang<sup>1</sup>, S. Liu<sup>2</sup>, J. Wu<sup>1</sup>, J. Luo<sup>3</sup>, R. Tyler<sup>4</sup>, S. Zhang<sup>5</sup>. <sup>1</sup>OnQuality Pharmaceuticals, Research, Shanghai, China; <sup>2</sup>OnQuality Pharmaceuticals, Research, Shanghai, China; <sup>3</sup>OnQuality Pharmaceuticals, Chief Scientific Officer, Shanghai, China; <sup>4</sup>OnQuality Pharmaceuticals, Medical and Clinical, Fort Collins, CO, USA; <sup>5</sup>OnQuality Pharmaceuticals, Chief Executive Officer, Shanghai, China

**Background:** Hand-Foot Syndrome (HFS) is a dermatological toxicity induced by capecitabine (CAP)/fluorouracil (5FU). HFS is related to damage of palmar/plantar epidermal/dermal cells by 5FU, and inflammation-mediated by cyclooxygenase-2 pathways. We hypothesize applying OQL036 a topical gel prodrug metabolizing to thymidine (TdR) and naproxen (NAP) may alleviate HFS toxicity associated with CAP/5FU.

**Methods:** To test the protective effect on 5FU (20 μM) cell toxicity, an aneuploid immortal keratinocyte cell line (HaCaT) was co-administered with dose-ranging concentrations of NAP, TdR, or dTNAP (thymidine conjugated with naproxen). Viability was determined after 48 h by a cell counting kit-8 assay. To test the prophylaxis of TdR or dTNAP on 5FU toxicity, HaCaT cells were incubated with TdR, or dTNAP at dose-ranging concentrations with 5FU (20 μM@48 h, 5 μM@72 h). Cell proliferation was determined by a

CyQUANT assay. Sprague-Dawley rats (SDR) (n = 32) were given CAP (QD, 4000 mg/kg), topical study gel (OQL036 or vehicle), and divided into 3 groups (G): G1 CAP solvent (CS)+vehicle gel (VG, n = 8); G2, CAP+VG (n = 12), and G3 CAP+OQL036 (n = 12). BALB/c mice (n = 32) were given CAP (QD, 1000 mg/kg), topical gel, and divided into 3 groups: G1 CS+VG (n = 8); G2, CAP+VG (n = 12), and G3 CAP+OQL036 (n = 12). SDR and BALB/c were monitored daily for HFS.

**Results:** 5FU reduced HaCaT cell viability to 33.9% of control and coadministration of TdR at 25, 50, 100, & 200  $\mu$ M increased viability by 22.3, 31.1, 53.3, & 51.4% and dTNAP at 3.1, 6.3, 12.5, 25, 50, 100, & 200  $\mu$ M increased viability by 29.4, 39.4, 53.7, 64.0, 70.1, 78.1, & 59.0%, respectively. NAP had no effect. Incubating of HaCaT with vehicle control (VC) and adding 5FU for 48 h or 72 h reduced cell proliferation by 62.2% & 76.2%. Pretreatment with TdR or dTNAP (both @ 0.8–66.7  $\mu$ M) showed dose-response reductions of 5FU toxicity (TdR 16.7–24.7% @ 48 h and 20.2–28.2% @ 72 h ( $p < 0.05$ –0.001); dTNAP 8.7–3.6% @ 48 h & 9.3–31.2% @ 72 h ( $p < 0.05$ –0.001). SDR treated with QD OQL036 vs. VG delayed development of HFS grade  $\geq 1$  ( $17 \pm 0.8$  vs.  $22 \pm 2.9$  days,  $p < 0.001$ ). OQL036 treated SDR also had reduced overall mean HFS grade vs. VG over the study period ( $0.3 \pm 0.2$  vs.  $0.7 \pm 0.1$  grade,  $p < 0.0001$ ). BALB/c treated with QD OQL036 vs. VG had similar time to onset of HFS at Day 4; however, OQL036- vs. VG-treated mice had a reduced overall mean HFS grade vs. VG over study days 4–16 ( $2.6 \pm 1.3$  vs.  $4.1 \pm 1.3$ , grade,  $p < 0.05$ ).

**Conclusion:** In vitro studies showed both TdR and dTNAP are effective at reducing the 5FU-induced toxicity in HaCaT cells. In animal studies, daily topical application of the prodrug gel, OQL036, releasing thymidine and naproxen delayed the onset of HFS and was effective in reducing the severity of CAP-induced HFS.

#### Conflict of interest:

Ownership: OnQuality Pharmaceuticals

Shiyi Zhang, Founder & CEO

Jie Lou, Co-founder & CSO

Other Substantive Relationships: OnQuality Pharmaceuticals Employees

Liping Chen, Wenxi Li, Kun Fang, Shilan Liu, Jiahui Wu, Robert Tyler

217

(PB097)

#### A preclinical toxicology and pharmacology study of OQL051, a gut-restricted CDK4/6 inhibitor for the prophylaxis of chemotherapy-induced diarrhea

W. Zeng<sup>1</sup>, W. Li<sup>1</sup>, S. Liu<sup>1</sup>, L. Chen<sup>1</sup>, R. Tyler<sup>2</sup>, H. Tang<sup>3</sup>, J. Luo<sup>4</sup>, S. Zhang<sup>5</sup>.

<sup>1</sup>OnQuality Pharmaceuticals, Research, Shanghai, China; <sup>2</sup>OnQuality Pharmaceuticals, Medical and Clinical, Fort Collins, CO, USA; <sup>3</sup>OnQuality Pharmaceuticals, Clinical and Medical, Seattle, USA; <sup>4</sup>OnQuality Pharmaceuticals, Chief Scientific Officer, Shanghai, China; <sup>5</sup>OnQuality Pharmaceuticals, Chief Executive Officer, Shanghai, China

**Background:** Chemotherapy-induced diarrhea (CID) from fluorouracil (5FU) and irinotecan (IRI, rate 50–80%) leads to therapy interruption/discontinuation and disruption of the intestinal microbiome. Cyclin-dependent kinase 4/6 inhibitors (CDK4/6i) induce a “pharmacological quiescence” with transient dosing. OQL051, a gut-restricted CDK4/6i, decreases chemotherapy-induced histological damage to the intestinal wall and reduces CID. We studied OQL051’s toxicology, maintenance of the microbiome, and the impact on tumor growth.

**Methods:** Rats, 20 female, 20 male, 6–7 weeks of age were studied for 8 days. OQL051 was orally administered once daily (100, 250, or 500 mg/kg) for 7 days. Mortality, clinical observations, body weight, and food consumption were recorded daily during treatment. Hematology, coagulation, serum chemistry, gross pathology, and histopathological examination (14 tissue/organ panel including stomach, duodenum, jejunum, and colon) was conducted at D8. Blood was collected from 3 to 5 animals on D1 and D7 at predose, 0.25, 1, 2, 4, 8, and 24 h post-dose to determine the concentration of OQL051. BALB/c mice were subcutaneously injected with  $10^6$  CT-26 cells (undifferentiated colon carcinoma cell line), given oral OQL051 (25 mg/kg) or control (CON) at a tumor vol. of  $30 \sim 50$  mm<sup>3</sup>, then 6 h later, injected with irinotecan (IRI, 70 mg/kg)/IRI-CON. At a tumor vol.  $200 \sim 400$  mm<sup>3</sup> mice were injected with anti-PD-1 mAb (200  $\mu$ g)/mAb-CON. Tumor vol. was determined routinely with calipers. The GI tract was sampled for microbiome analysis. Microbiome DNA library (NEBNext® Ultra™ II DNA Kit) was used for sequencing on an Illumina NovaSeq platform.

**Results:** No drug-related mortality or adverse events (AEs) were observed across all dose levels. One female rat had an intussusception event at 250 mg/kg; however, no histopathological abnormality was observed. Compared to vehicle control OQL051 at all doses studied showed no effect on body weight, food intake, hematology, coagulation, serum chemistry, gross pathology, or histopathological examination. In particular, OQL051 being concentrated in the gut showed no histopathological changes in the stomach, duodenum, jejunum, or colon. Microbiome diversity was

maintained in OQL051- vs. CON-treated mice, and tumor volume was less in OQL051+IRI+anti-PD-1 vs. CON+IRI+anti-PD-1 ( $p = 0.035$  @ 28 days).

**Conclusion:** OQL051 safety was confirmed as there were no drug-related AEs observed for OQL051 repeat doses up to 500 mg/kg/day for 7 days. CDK 4/6 inhibitor common AEs (neutropenia, leukopenia, thrombocytopenia, anemia, diarrhea, nausea, ALT) were absent indicating a low systemic exposure. The previously observed decrease in intestinal wall damage and CID from chemotherapy led to the maintenance of the gut microbiome and potentially enhanced the efficacy of chemotherapy plus immunotherapy anti-tumor efficacy at reducing tumor volume.

#### Conflict of interest:

Ownership: Shiyi Zhang, Founder, CEO

Jie Lou, Co-founder, CSO

Hong Tang, Co-founder, CMO

Other Substantive Relationships: Wenqin Zeng, employee; Wenxi Li, employee; Shilan Liu, employee; Liping Chen, employee; Robert Tyler, employee.

218

(PB098)

#### Preclinical activity of NVL-655 in patient-derived models of ALK cancers, including those with lorlatinib-resistant G1202R/L1196M compound mutation

T. Fujino<sup>1</sup>, L. Nguyen<sup>1</sup>, S. Yoda<sup>1</sup>, M. Yu<sup>2</sup>, H. Mizuta<sup>3</sup>, L. Bigot<sup>3</sup>, C. Nobre<sup>3</sup>, A. Tangpeerachakul<sup>4</sup>, H.E. Pelish<sup>4</sup>, L. Friboulet<sup>3</sup>, J. Lee<sup>5</sup>, B. Cho<sup>5</sup>, A.N. Hata<sup>1</sup>. <sup>1</sup>Massachusetts General Hospital, Center for Cancer Research, Boston, USA; <sup>2</sup>Yonsei University College of Medicine, Department of Research Support, Seoul, South Korea; <sup>3</sup>Gustave Roussy, Inserm U981-University Paris-Saclay, Villejuif, France; <sup>4</sup>Novartis, Discovery, Cambridge, USA; <sup>5</sup>Yonsei University College of Medicine, Division of Medical Oncology, Seoul, South Korea

**Introduction:** Five tyrosine kinase inhibitors (TKIs) have been approved for treatment of ALK-positive non-small cell lung cancer (NSCLC), including first- (crizotinib), second- (ceritinib, alectinib, and brigatinib), and third- (lorlatinib) generation therapies. Durability of response is limited partly by emergence of ALK resistance mutations. The most frequent ALK mutations after relapse on first- and second-generation ALK TKIs are L1196M and G1202R, respectively, together representing 20–40% of resistance cases. ALK G1202R tumors treated with lorlatinib have relapsed by acquiring compound mutations such as G1202R/L1196M and G1202R/T1151M, which confer resistance to all approved ALK TKIs. To address this medical need, we reported the discovery of NVL-655: a brain-penetrant TKI that selectively inhibits ALK and ALK resistance mutants over TRKB. Avoiding TRKB is advantageous as its inhibition has been linked to neurological adverse events and dose-limiting toxicities. Here we demonstrate the preclinical activity of NVL-655 in patient-derived models, including from patients who progressed on prior ALK TKIs.

**Methods:** EML4-ALK fusion cell lines were established from NSCLC patients: MGH026-1, MGH048-1, and MGH064-1 (treatment-naïve); MGH045-1 (L1196M post-crizotinib); MGH953-4 and YU-1077 (G1202R post-alectinib); MGH9037-2 (G1202R post-brigatinib); MGH953-7 (G1202R/L1196M post-lorlatinib); and MR448re (G1202R/T1151M post-lorlatinib). Murine xenografts were generated from YU-1077 tumors, MR619 cholangiocarcinoma tumors (STRN-ALK G1202R post-alectinib); MGH953-7 tumors; and MR448re cell line.

**Results:** NVL-655 and lorlatinib had similar potency against cancer cell lines derived from treatment-naïve ALK patients ( $IC_{50} < 5$  nM). However, only NVL-655 retained high activity ( $IC_{50} \sim 1$  nM) against ALK G1202R cell lines derived from alectinib- or brigatinib-relapsed patients, showing substantially improved potency compared to second-generation ALK TKIs or lorlatinib ( $IC_{50} \sim 35$  nM–1.5  $\mu$ M). ALK G1202R/L1196M and ALK G1202R/T1151M cell lines derived from lorlatinib-relapsed patients were indeed resistant to lorlatinib ( $IC_{50} > 400$  nM) but highly sensitive to NVL-655 ( $IC_{50} < 5$  nM). Western blot analysis confirmed on-target engagement and inhibition of pathway signaling. Consistent with *in vitro* results, NVL-655 induced regression in ALK G1202R, G1202R/L1196M, and G1202R/T1151M xenografts derived from patient tumors.

**Conclusion:** Patient-derived cells and xenografts are among the most disease-relevant preclinical models for evaluating new therapies and drug resistance. NVL-655 showed activity in diverse patient-derived models of ALK-positive cancers, including ones that exhibited clinical resistance to prior-generation ALK TKIs. The broad preclinical activity of NVL-655 suggests potential utility as a best-in-class therapy for ALK-positive cancer patients.

#### Conflict of interest:

Advisory Board: ANH is a scientific advisor of Novartis.

Corporate-sponsored Research: TF, LN, SY, MY, HM, LB, CN, LF, JL, BC, and ANH receive sponsored research funding from Nuvalent. Other Substantive Relationships: AT and HEP are employees and stockholders of Nuvalent.

**219** (PB099)  
**The RNA-Binding Protein with Multiple Splicing (RBPMS) splice variants A and C, acts as a tumor suppressor gene in ovarian cancer**

R. Rabelo-Fernandez<sup>1</sup>, R. Noriega-Rivera<sup>2</sup>, F. Valiyeva<sup>3</sup>, P. Vivas-Mejia<sup>4</sup>.  
<sup>1</sup>University of Puerto Rico at Rio Piedras, Biology Department, San Juan, Puerto Rico; <sup>2</sup>University of Puerto Rico Medical Science Campus, Department of Biochemistry, San Juan, Puerto Rico; <sup>3</sup>University of Puerto Rico Comprehensive Cancer Center, Department of Biochemistry, San Juan, Puerto Rico; <sup>4</sup>University of Puerto Rico Medical Sciences Campus, Department of Biochemistry, San Juan, Puerto Rico

RNA-Binding Protein with Multiple Splicing (RBPMS) is a member of a family of proteins that bind to nascent RNA transcripts and regulate their processing, and stability of the RNA molecules. Evidence indicates that RBPMS also control de activity of transcription factors associated with cell proliferation including AP-1 and STATs. Three major RBPMS protein splice variants have been described in the literature: RBPMSA, RBPMSB, and RBPMSC. We previously reported that reduced RBPMS levels decreased the sensitivity of ovarian cancer (OC) cells to cisplatin treatment. However, few is known about the biological role of the RBPMS splice variants in the proliferation and drug resistance in OC. We performed RT-PCR and Western blots and observed that both, RBPMSA and RBPMSC are reduced at the mRNA and protein levels in cisplatin resistant as compared with cisplatin sensitive ovarian cancer cells. The mRNA or the protein levels of RBPMSB were not detectable in any of the OC cells tested. To better understand the biological role of RBPMSA and RBPMSC, we stable transfected these two informs in the A2780CP20 cisplatin resistant OC cells and performed cell proliferation, cell migration, and invasion assays. Compared with control clones, a significant reduction in the number of colonies, and invasion were observed with both, RBPMSA and RBPMSC clones. Moreover, RBPMSA and RBPMSC clones showed reduced senescence-associated  $\beta$ -galactosidase ( $\beta$ -Gal)-levels of compared with control clones. Interestingly, RBPMSA clones were more sensitive to cisplatin treatment as compared with RBPMSC clones. RBPMSA or RBPMSC clones subcutaneously injected into female athymic nude mice formed smaller tumors as compared with control clones. Also, immunohistochemical analysis showed lower proliferation (Ki67) and angiogenesis (CD31) staining in tissue sections of RBPMSA and RBPMSC tumors compared with controls. RNAseq studies in RBPMSA and RBPMSC clones identified several downstream-RBPMS transcripts, including protein-coding genes associated with alteration of the tumor microenvironment, cancer metastasis, ribosome biogenesis with tumor suppressor capabilities. Kaplan–Meier (KM) plotter database identified clinically relevant RBPMSA and RBPMSC downstream effectors. These downstream genes will be investigated as potential targets for OC therapy. Immunoprecipitation (IP) coupled to mass spectrometry (MS) revealed that RBPMSA and RBPMSC binds to proteins including the metastasis inhibition factor (NME1) and the immunoglobulin kappa locus (IGK). Together, increased levels of both RBPMSA and RBPMSC reduce cell proliferation in ovarian cancer cells. However, only RBPMSA expression levels were associated with the sensitivity of ovarian cancer cells to cisplatin treatment. Overall, our findings indicate that RBPMSA and RBPMSC acts as tumor suppressor gene in ovarian cancer cells.

**No conflict of interest.**

**220** (PB100)  
**Discovery of INCB123667, a potent and selective cyclin-dependent kinase 2 (CDK2) inhibitor for the treatment of cyclin E dysregulated cancers**

S. Wee<sup>1</sup>, M. Ye<sup>1</sup>, Y. Lo<sup>1</sup>, M. Hansbury<sup>1</sup>, N. Shin<sup>1</sup>, M. Weber<sup>2</sup>, V. Roman<sup>1</sup>, L. Huo<sup>3</sup>, H. Skaggs<sup>4</sup>, K. Drake<sup>5</sup>, K. Kapilashrami<sup>6</sup>, K. Stump<sup>6</sup>, J. Yang<sup>6</sup>, S. Chand<sup>7</sup>, C. Timmers<sup>8</sup>, J. Hummel<sup>9</sup>, Y. Ye<sup>10</sup>, G. Zhang<sup>5</sup>, Y.O. Yang<sup>3</sup>, M. Covington<sup>11</sup>, L. Wu<sup>12</sup>, H. Koblisch<sup>13</sup>, S. Kim<sup>14</sup>. <sup>1</sup>Incyte Research Institute, Pharmacology, Wilmington, USA; <sup>2</sup>Incyte Research Institute, Biotherapeutics, Wilmington, USA; <sup>3</sup>Incyte Research Institute, dmb, Wilmington, USA; <sup>4</sup>Incyte Research Institute, Toxicology, Wilmington, USA; <sup>5</sup>Incyte Research Institute, Applied Technology - Biochemistry, Wilmington, USA; <sup>6</sup>Incyte Research Institute, Applied Technology, Wilmington, USA; <sup>7</sup>Incyte Research Institute, In vitro Pharmacology, Wilmington, USA; <sup>8</sup>Incyte Research Institute, Translational Sciences, Wilmington, USA; <sup>9</sup>Incyte Research Institute, Discovery Chemistry, Wilmington, USA; <sup>10</sup>Incyte

Research Institute, Medicinal Chemistry, Wilmington, USA; <sup>11</sup>Incyte Research Institute, Cellular Profiling & Compound Management, Wilmington, USA; <sup>12</sup>Incyte Research Institute, Medicinal Chemistry, Wilmington, USA; <sup>13</sup>Incyte Research Institute, Pharmacology, Wilmington, USA; <sup>14</sup>Incyte Research Institute, Small Molecule Discovery & Preclinical Pharmacology, Wilmington, USA

**Background:** Dysregulation of the CDK/cyclin complex causes aberrant cell cycle entry and progression that can lead to cancer. For instance, the CDK2/cyclin E complex governs the G1-S transition and overexpression of cyclin E has been associated with ovarian and breast cancers. Our initial studies have demonstrated that genetic depletion of CDK2 inhibits cell growth and survival in cancer cells overexpressing cyclin E. Furthermore, inhibition of CDK2 may be effective in cancers resistant to clinically approved CDK4/6 therapies as increased CDK2/cyclin E activity has been reported as a compensatory mechanism. Current CDK2 inhibitors are limited by off-target activity on other CDK family members, including CDK1. Here we report the identification and characterization of INCB123667, a potent and selective, orally available small molecule inhibitor of CDK2, for the treatment of cancers with high unmet medical need, such as cyclin E-amplified ovarian tumors.

**Materials and methods:** Biochemical and cell-based assays were used to determine the potency and selectivity of INCB123667. Additionally, antitumor activity was assessed in cyclin E-overexpressing cancer cell lines, and in tumor xenograft models.

**Results:** In biochemical assays, INCB123667 demonstrated sub-nanomolar inhibition of CDK2 activity and was not active against CDK1, CDK4, CDK6, CDK7, and CDK9. Selectivity of INCB123667 was confirmed across an extended panel of kinases, G protein-coupled receptors, ion channels, and transporters. In cell-based studies, INCB123667 inhibited phosphorylation of retinoblastoma (Rb), a CDK2/cyclin E substrate and key regulator of the G1-S transition. Consistent with its overall selectivity profile, INCB123667 inhibited the expression of cell cycle regulatory genes in cyclin E-overexpressed cancer cells. Furthermore, the transcriptional gene signature of INCB123667 was distinct from that reported for CDK4/6 inhibitors. In cellular assays, addition of INCB123667 resulted in G1 cell cycle arrest and cell senescence. In the OVCAR3 tumor xenograft model, which harbors cyclin E amplification, INCB123667 inhibited Rb phosphorylation and resulted in dose-dependent tumor growth inhibition along with minimal body weight loss. In the IGROV-1 model, in which cyclin E is not amplified, the same doses of INCB123667 were less effective in blocking Rb phosphorylation and inhibiting tumor growth. Notably, across in vitro and in vivo studies, cyclin E-overexpressing cancer cells were more sensitive to INCB123667 compared with cells with normal levels of cyclin E.

**Conclusions:** Our data indicate that INCB123667 is a selective and potent CDK2 kinase inhibitor that has antitumor activity in cyclin E-overexpressing cancers and tumor xenograft models. These preclinical findings support the ongoing clinical evaluation of INCB123667 as a CDK2-selective inhibitor for the treatment of cancer.

**Conflict of interest:**

Ownership: Susan Wee, Yvonne Lo, Michael Hansbury, Michael Weber, Valerie Roman, Lu Huo, Katherine Drake, Kristine Stump, Jie Yang, Saswati Chand, Cynthia Timmers, Joshua Hummel, Guofeng Zhang, Yan-ou Yang, Maryanne Covington, Sunkyu Kim: Employment and stock ownership – Incyte Corporation. Min Ye, Niu Shin, Hollie Skaggs, Kanishk Kapilashrami, Yingda Ye, Liangxing Wu, Holly Koblisch: Former employee and stock ownership – Incyte Corporation.

**221** (PB101)  
**Phase I/II study of a novel MDM-2 inhibitor (APG-115) in TP53 wild type salivary gland cancers**

A.T. Pearson<sup>1</sup>, J. Muzaffar<sup>2</sup>, E. Bellile<sup>3</sup>, F.P. Worden<sup>4</sup>, C.H. Chung<sup>2</sup>, A. Rosenberg<sup>1</sup>, E. Vokes<sup>1</sup>, M.J. Fidler<sup>5</sup>, J.C. Brenner<sup>6</sup>, Y. Zhai<sup>7</sup>, T. Fu<sup>7</sup>, R. Winkler<sup>7</sup>, P. Swiecicki<sup>4</sup>. <sup>1</sup>University of Chicago, Department of Medicine, Chicago, USA; <sup>2</sup>Moffitt Cancer Center, Department of Head and Neck-Endocrine Oncology, Tampa, USA; <sup>3</sup>Department of Biostatistics, Department of Internal Medicine, Ann Arbor, USA; <sup>4</sup>University of Michigan, Department of Internal Medicine, Ann Arbor, USA; <sup>5</sup>Rush University, Department of Internal Medicine, Chicago, USA; <sup>6</sup>University of Michigan, Department of Otolaryngology, Ann Arbor, USA; <sup>7</sup>Ascentage Pharma Group, Rockville, USA

**Background:** Malignant salivary gland cancers (SGC) are rare tumors of the head and neck with no approved therapeutics in the recurrent and/or metastatic setting. The most common histology is adenoid cystic carcinoma (ACC) and the median progression free survival (mPFS) in patients with untreated disease is 2.8 months (mo). MDM2 gene amplifications are

common in these tumors and preclinical evidence supports the activity of MDM2 inhibitors both as monotherapy and in combination with chemotherapy. APG-115 is a potent oral small molecule MDM2 inhibitor.

**Materials/Methods:** A phase 1 multicenter study was conducted to evaluate the safety and efficacy of APG-115 ± carboplatin in *TP53* wildtype (wt) SGC. Key eligibility criteria included histologically documented high grade malignant SGC, no evidence of a *TP53* mutation by genetic sequencing, and ≥20% progression by RECIST v1.1 in the preceding 12 mo. There was an initial randomized component followed by a planned single arm expansion. The primary endpoints were dose-limiting toxicity and overall response rate, secondary endpoints included PFS, duration of response, and overall survival. Data were continuously monitored and doses assigned using the time-to-event continual reassessment method. The trial design was modified to a single arm study of APG-115 monotherapy after safety meetings noted increased toxicities in the combination arm. As of 6/21/2022, 18 pts were enrolled to the monotherapy arm and 4 pts were enrolled to the combination arm. 73% of pts had ACC; 45% of pts had prior systemic therapy (40% VEGFR TKI).

**Results:** 95% (21/22) had stabilization of their previously progressive disease. A PR rate of 13% of pts on mono and 25% of patients on combo was observed. The median PFS on pts treated with mono was 11.4 mo. No DLTs were encountered in either arm. In the mono arm 72% had ≥G3 treatment related adverse events (TRAE). Common TRAEs (>30%) included: fatigue (78%), nausea (78%), vomiting (39%), thrombocytopenia (39%), and anemia (33%). In the combo arm, 100% of pts had ≥G3 TRAE. Common (>30%) TRAEs included: anemia (100%), thrombocytopenia (100%), neutropenia (75%), fatigue (75%), nausea (75%), elevated alkaline phosphatase (75%), decreased neutrophil (75%) and lymphocyte (50%) counts, and vomiting (50%).

**Conclusions:** APG-115 monotherapy demonstrates promising antitumor activity among patients with *TP53*wt SGC with an acceptable safety profile. This is the first study to evaluate the activity of MDM2 inhibition in patients with SGC. Accrual is ongoing for precise assessment of survival characteristics.

#### Conflict of interest:

Advisory Board: ATP: Has served on Advisory boards for Prelude, Ayala, Elevar research funding from Abbvie and Kura Oncology and consulting for Abbvie.

CHC: Has received honoraria from Sanofi, Merck, Brooklyn Immunotherapeutics, and Exelixis for ad hoc Scientific Advisory Board participation.

PLS: Has received honoraria from Prelude, Elevar, and Astellas for ad hoc Scientific Advisory Board participation institutional research funding for this investigator initiated trial was provided by Ascentage Pharma.

Other Substantive Relationships: YZ, TF, RW are employees of Ascentage Pharma Group.

223

(PB103)

#### Non-ATP competitive inhibition of PI3Kδ with IOA-244 shows anti-lymphoma activity

C. Tarantelli<sup>1</sup>, F. Spriano<sup>1</sup>, L. Cascione<sup>1</sup>, E. Civanelli<sup>1</sup>, E. Cannas<sup>1</sup>, A.A. Mensah<sup>1</sup>, A.J. Arribas<sup>1</sup>, A. Rinaldi<sup>1</sup>, A. Stathis<sup>2</sup>, G. Di Conza<sup>3</sup>, K. Niewola-Staszowska<sup>3</sup>, M. Lahn<sup>3</sup>, F. Bertoni<sup>1</sup>. <sup>1</sup>Faculty of Biomedical Sciences- USI, Institute of Oncology Research, Bellinzona, Switzerland; <sup>2</sup>Ente Ospedaliero Cantonale, Oncology Institute of Southern Switzerland, Bellinzona, Switzerland; <sup>3</sup>iOncura SA, Tumor Biology, Geneva, Switzerland

**Background:** Activation of PI3 K signaling, mainly mediated via PI3Kδ, is a fundamental signaling cascade in lymphomas (Tarantelli et al, 2021). IOA-244 (IOA) is a highly selective and potent PI3Kδ inhibitor with atypical non-ATP competitive activity (Johnson et al, 2019) compared to FDA-approved PI3 K inhibitors idelalisib, copanlisib and duvelisib. IOA is in phase 1 as an immunomodulatory agent for patients with melanoma, mesothelioma, non-small cell lung cancer, myelofibrosis, and follicular and peripheral T cell lymphoma (TCL) as a single agent or in combination (NCT04328844). IOA doses up to 80 mg were well tolerated in the first 16 patients (Di Giacomo et al, 2021). Here, we present the first set of data on IOA in lymphoma.

**Materials and Methods:** Cell lines were exposed to increasing concentrations of IOA and anti-proliferative activity was assessed by MTT assay at 72 h. Apoptosis and cell cycle were assessed by FACS. Poly-A RNA-Seq was performed on an Illumina system.

**Results:** IOA showed moderate dose-dependent anti-proliferative activity across 74 cell lines derived from B (n = 59) and TCL (n = 15) with IC50 <1 nM in only a few cell lines. B cell lymphomas, particularly mantle cell lymphoma (MCL) models (median AUC = 666 k; 95% CI: 979–262 k; n = 10), were more sensitive than TCL (median AUC = 956 k; 95% CI 1151–553 k; n = 15). Among TCL, cutaneous T cell lymphoma cell lines were the most sensitive. Compared to idelalisib, IOA showed similar *in vitro* anti-

proliferative activity in ten cell lines derived from MZL, DLBCL and MCL. In diffuse large B-cell lymphoma (DLBCL; n = 2) and MCL (n = 2) cell lines, IOA induced apoptosis and subG0/G1 accumulation already after 48 h at 1µM concentration.

IOA sensitivity correlated with *PIK3CD* RNA expression in all cell lines (R = -0.32; p = 0.014), as for idelalisib (R = -0.45; p = 0.053) but not for copanlisib (R < 0.1; p = 0.693). In cells derived from B-cell lymphoma, only IOA-244 correlated with *PIK3CD* (R = -0.42; p = 0.005; idelalisib R < 0.1; p = 0.992; copanlisib R < 0.1; p = 0.73).

Transcriptomic analysis by RNA-seq revealed that IOA (5 µM; 24, 48, 72 h; MCL SP53 cell line) downregulated BCR, MYD88, NF-κB, MTOR and NOTCH signaling and upregulated genes involved in cell cycle arrest (adj.P < 10<sup>-10</sup>). These changes overlapped with signatures obtained with other PI3 K and BTK inhibitors (adj.P < 10<sup>-10</sup>). The most down-regulated transcripts (n = 212; abs.fold change > 2, adj.P < 0.05) included oncogenes (*CCND2*, *TOX*, *AXL*, *SGK1*, *VEGFA*) and immune-related factors (*CCL22*, *CCL4*, *CCR1*, *CXCR3*, *CSF1*, *IL2RB*, *TNFRSF9*, *SLAMF7*, *TNF*). The up-regulated (n = 188) included proapoptotic factors (*HRK*, *BIK*), tumor suppressors (*GADD45A*, *TP63*, *BACH2*), and immune-related factors (*CXCR4*, *CTLA4*).

**Conclusions:** IOA shows moderate activity *in vitro* in lymphoma, inducing apoptosis and subG0/G1 accumulation and modulating genes involved in relevant signaling pathways and immunotolerance.

#### Conflict of interest:

Advisory Board: Gilead, AbbVie, Janssen, AstraZeneca, MSD, BMS/Celgene, Roche, Mei Pharma, Astra Zeneca, Celltrion Healthcare, Incyte, Kite/Gilead

Corporate-sponsored Research: Celgene, Roche, Janssen, Acerta, ADC Therapeutics, Bayer AG, Cellectia, CTI Life Sciences, EMD Serono, Helsinn, ImmunoGen, Menarini Ricerche, NEOMED Therapeutics 1, Nordic Nanovector ASA, Oncology Therapeutic Development, PIQUR Therapeutics AG, Gilead, AbbVie, Janssen

Other Substantive Relationships: Work supported by iOncura SA.

224

(PB104)

#### Preliminary results from HERKULES-1: a phase 1b/2, open-label, multicenter study of ERAS-007, an oral ERK1/2 inhibitor, in patients with advanced or metastatic solid tumors

J. Wang<sup>1</sup>, M. Johnson<sup>2</sup>, M. Barve<sup>3</sup>, M. Pelster<sup>2</sup>, X. Chen<sup>4</sup>, Z. Li<sup>4</sup>, J. Gordon<sup>4</sup>, M. Reiss<sup>4</sup>, S. Pai<sup>4</sup>, G. Falchook<sup>5</sup>, A. Tolcher<sup>6</sup>. <sup>1</sup>Florida Cancers Specialists/Sarah Cannon Research Institute, Drug Development Unit, Sarasota, Sarasota, USA; <sup>2</sup>Sarah Cannon Research Institute at Tennessee Oncology, Drug Development Unit, Nashville, USA; <sup>3</sup>Mary Crowley Cancer Research, Research Oncology, Dallas, USA; <sup>4</sup>Erasca Inc., Erasca Inc., San Diego, USA; <sup>5</sup>Sarah Cannon Research Institute at HealthONE, Drug Development Unit, Denver, USA; <sup>6</sup>NEXT Oncology, Oncology, San Antonio, USA

**Background:** The RAS/MAPK pathway is dysregulated in a broad range of cancers, resulting in downstream activation of ERK1/2. ERAS-007 is a novel, potent, and orally bioavailable inhibitor of ERK with a prolonged target residence time (550 min). The first-in-human Phase 1 study of ERAS-007 identified the 250 mg once weekly (QW) schedule for further evaluation based on a manageable toxicity profile and encouraging signs of clinical activity (NCT03415126). Pharmacokinetic (PK) modeling suggests that an alternative intermittent regimen (twice a day, once a week; BID-QW) is expected to have lower peak concentrations (Cmax) and similar overall PK exposures (area under the curve, AUC) compared to QW, which may improve Cmax-driven adverse events (AE) while maintaining comparable efficacy. Optimizing tolerability is particularly beneficial as combination therapies of ERAS-007 with other anti-cancer agents are being pursued.

**Materials and Methods:** HERKULES-1 is a Phase 1b/2 study evaluating ERAS-007 in patients (pts) with metastatic solid tumors refractory to standard therapies (NCT04866134). Primary objectives in Part A (dose escalation) include evaluation of safety and PK characteristics, and determination of the maximum tolerated dose of ERAS-007 administered as monotherapy on a BID-QW schedule. Secondary objectives include evaluation of tolerability and anti-tumor activity. ERAS-007 was administered at increasing dose levels of 50, 100, and 125 mg on a BID-QW schedule.

**Results:** As of the 23 May 2022 data cutoff, 23 pts were enrolled at doses of 50 (n = 4), 100 (n = 11), and 125 mg (n = 8) BID-QW. A maximum administered dose of 125 mg BID-QW was achieved; no DLTs were observed at any dose level. All grade treatment related adverse events (TRAE) occurring in ≥20% of the BID-QW treated pts included nausea (52.2%), eye disorders (52.2%), skin rash (43.5%), fatigue (39.1%), vomiting (30.4%), and diarrhea (21.7%). These AEs were mostly Grades 1 and 2. Grade ≥3 TRAEs occurring in ≥10% of patients were eye disorders (13.0%). ERAS-007 administered as a BID-QW schedule exhibited lower peak-to-trough fluctuations compared to a QW regimen. An unconfirmed

partial response was observed in a patient with KRAS G12V mutated pancreatic ductal adenocarcinoma. Updated data on safety, PK, and dose selection for ongoing studies with ERAS-007 combinations will be presented.

**Conclusions:** ERAS-007 is a potent and selective oral inhibitor of ERK1/2 with a prolonged target residence time. Intermittent dosing on a BID-QW schedule exhibited favorable PK characteristics with lower C<sub>max</sub> and similar overall PK exposure (AUC) compared to QW dosing and demonstrated a monitorable and manageable AE profile consistent with the underlying mechanism of action. This novel regimen offers an alternative schedule for combination development.

**Conflict of interest:**

Ownership: Xiaoying Chen, Jennifer Gordon, Zhengrong Li, Moshe Reiss, Sachin Pai  
Corporate-sponsored Research: Judy Wang, Melissa Johnson, Minal Barve, Meredith Pelster, Gerald Falchook, Anthony Tolcher

**225** (PB105)

**Discovery of novel small molecules that recruit DCAF11 for selective degradation of BRD4**

G. Parker<sup>1</sup>, J. Toth<sup>1</sup>, G. Leriche<sup>2</sup>, S. Fish<sup>1</sup>, A. Jamboric<sup>1</sup>, G. Blanco<sup>1</sup>, E. Daniele<sup>1</sup>, K. Steadman<sup>1</sup>, X. Li<sup>1</sup>, L. Yang<sup>1</sup>, S. Chien<sup>1</sup>, A. Dearie<sup>1</sup>, K. Chng<sup>3</sup>, E. Green<sup>2</sup>, M. Hocker<sup>2</sup>, Y. Zhang<sup>4</sup>, P. Thompson<sup>1</sup>, S. Bailey<sup>2</sup>. <sup>1</sup>Plexium, Biology, San Diego, USA; <sup>2</sup>Plexium, Chemistry, San Diego, USA; <sup>3</sup>Plexium, Discovery Technology, San Diego, USA; <sup>4</sup>Plexium, Engineering, San Diego, USA

**Background:** Targeted protein degradation (TPD) using the endogenous ubiquitin (Ub) proteasome system (UPS) is a rapidly growing drug discovery approach to eliminate pathogenic proteins. Strategies for TPD have focused on designing heterobifunctional PROTACs that utilize ligand binding to select E3 ligases (e.g., cereblon and VHL), often resulting in compounds with poor drug-like properties. Monovalent degraders represent an alternative approach, in which small molecules are designed to bind the target protein and induce its degradation through the recruitment of an E3 ligase complex. Monovalent degraders generally have better physico-chemical properties than PROTACs; however, designing compounds to induce degradation is not well precedent and relies on serendipitous discovery.

**Methods:** An E3 ligase agnostic chemical library was screened using our ultra-high throughput cell-based screening (uHTS) platform. Hits were identified by measuring protein degradation of BRD4 using immunofluorescence. A Ub pathway focused CRISPR screen was used to identify the E3 ligase responsible for compound-induced degradation of BRD4. The degradation mechanism was validated using western blot, luciferase-based protein-protein interaction (PPI) and mutational analyses. *In vitro* antitumor activity was assessed by proliferation and apoptosis assays. NOD/SCID mice were implanted sub-Q with acute myeloid leukemia (AML) xenograft model MV-4-11 and treated with compounds administered QD.

**Results:** uHTS resulted in identification of selective monovalent degraders that target the bromodomain extra-terminal (BET) protein, BRD4. Degradation series optimization produced PLX-3618, which demonstrated potent degradation of BRD4, without depleting BET family members BRD2 and BRD3. Proteasome and neddylation inhibitors confirmed degradation was mediated via the UPS, and a Ub-focused CRISPR screen identified CUL4<sup>DCAF11</sup> as the E3 complex responsible for PLX-3618 induced degradation of BRD4. PPI studies verified a BRD4/PLX-3618/DCAF11 ternary complex; BRD4 point mutational analyses provided further insights into the DCAF11-mediated degradation mechanism. Degradation of BRD4 by PLX-3618 resulted in downregulation of the MYC oncogene and potent anti-proliferative activity against a panel of tumor cell lines, with high sensitivity observed in AML. *In vivo*, PLX-3618 resulted in complete tumor regression, whereas a pan-BET inhibitor only resulted in tumor growth inhibition without regression. PK/PD analyses provided insight into the unique exposure/response profile of targeted protein degraders.

**Conclusion:** These results demonstrate the efficient discovery of novel monovalent degraders using our proprietary platform. Characterization of the degradation mechanism highlights the discovery of DCAF11 as a novel E3 ligase substrate receptor amenable to recruitment and degradation of BRD4.

**No conflict of interest.**

**226** (PB106)

**Pre-clinical In Vitro and In Vivo Characterization of a Novel EGFR Sparing ErbB2 Inhibitor with Activity Against Oncogenic ErbB2 Mutations**

M.J. Chicarelli<sup>1</sup>, K. Bouhana<sup>1</sup>, L. Cable<sup>1</sup>, M. Crow<sup>1</sup>, B. Fell<sup>1</sup>, J. Fischer<sup>1</sup>, J. Fulton<sup>1</sup>, A. Guarnieri<sup>1</sup>, R. Jalluri<sup>1</sup>, J. Robinson<sup>1</sup>, F. Sullivan<sup>1</sup>, S. Winski<sup>1</sup>, Y. Zhou<sup>1</sup>. <sup>1</sup>Cogent Biosciences, Research + Development, Boulder, USA

Oncogenic driver mutations in ErbB2 (e.g., S310F/Y, L755S, V777L, V842I) are present in a variety of tumor types including Gastric, Uterine, Urothelial Carcinoma, NSCLC, Breast, and CRC. Additionally, some of these mutations emerge as mechanisms of acquired resistance to targeted therapies. Together, this represents a novel and actionable target mutation set across solid tumor indications. Current therapies that target ErbB2 have poor potency against these mutations or are limited in their utility due to inhibition of wild type (WT) EGFR. The inhibition of WT EGFR is associated with debilitating clinical effects that include diarrhea, stomatitis, and hepatotoxicity, limiting the ability of available therapies to achieve clinical exposure levels to address these mutations. Next generation ErbB2 inhibitors that are active against ErbB2 mutations, yet spare WT EGFR, would provide improved target coverage with fewer off target side effects compared to current therapies and have the potential to exhibit superior clinical efficacy. Herein, we describe the pre-clinical *in vitro* and *in vivo* activity of a novel ErbB2 inhibitor which has potency against prevalent mutations while sparing WT EGFR.

**Conflict of interest:**

Corporate-sponsored Research: All authors are employees of Cogent Biosciences.

**227** (PB107)

**In Vivo Pre-clinical characterization of a Novel Series of FGFR2 Selective Inhibitors with Potency Against Clinically Relevant Mutations**

J. Fischer<sup>1</sup>, K. Bouhana<sup>1</sup>, M.J. Chicarelli<sup>1</sup>, J. Dahlke<sup>1</sup>, B. Fell<sup>1</sup>, J. Fulton<sup>1</sup>, A. Guarnieri<sup>1</sup>, L. Haygood<sup>1</sup>, R. Jalluri<sup>1</sup>, A. Johnson<sup>1</sup>, B. McLean<sup>1</sup>, M. Max<sup>1</sup>, R. Rieger<sup>1</sup>, J. Robinson<sup>1</sup>, M. Rodriguez<sup>1</sup>, F. Sullivan<sup>1</sup>, Y. Wang<sup>1</sup>, S. Winski<sup>1</sup>, Y. Zhou<sup>1</sup>. <sup>1</sup>Cogent Biosciences, Research + Development, Boulder, USA

Fibroblast growth factor receptor (FGFR) mutations, fusions, and rearrangements have been linked to the pathogenesis of multiple tumor types. FGFR2 alterations have emerged as oncogenic drivers across a variety of tumor types, including Cholangiocarcinoma, lung, and Uterine cancer. Approved FGFR inhibitors have demonstrated responses in patients that harbor FGFR genetic alterations but show reduced activity in patients with gatekeeper and molecular brake mutations. In addition, pan-FGFR inhibitors are associated with dose-limiting hyperphosphatemia linked to the inhibition of FGFR1. To address these issues, a novel series of reversible FGFR2 inhibitors with activity against clinically relevant mutations and selectivity over FGFR1 have been identified. The inhibition of FGFR2 phosphorylation in engineered cell lines demonstrated activity toward wild-type FGFR2, molecular brake mutations N549H/K, and gatekeeper mutations V564I/F/L. Selectivity of these inhibitors against FGFR1 and the broader kinase should lead to fewer dose limiting toxicities compared to approved FGFR inhibitors. Additionally, maintaining potency against molecular brake and gatekeeper mutations may result in significantly improved clinical response. *In vivo* characterization to be presented includes dose escalating rodent pharmacokinetics, pharmacodynamics in tumor bearing mice, and efficacy in a mouse AN3 CA tumor xenograft model. Herein, the *in vitro* and *in vivo* characterization of a representative selective reversible FGFR2 inhibitor is described.

**Conflict of interest:**

Corporate-sponsored Research: All authors are employees of Cogent Biosciences.



228

(PB108)

**Neratinib efficacy in patients with EGFR exon 18-mutant non-small-cell lung cancer: findings from the SUMMIT basket trial**

J. Goldman<sup>1</sup>, A. Martínez Bueno<sup>2</sup>, C. Dooms<sup>3</sup>, K. Jhaveri<sup>4</sup>, M.J. de Miguel<sup>5</sup>, S.A. Piha-Paul<sup>6</sup>, N. Unni<sup>7</sup>, A. Mahipal<sup>8</sup>, J.M. Suga<sup>9</sup>, C. Naltet<sup>10</sup>, A. Zick<sup>11</sup>, M. Antoñanzas Basa<sup>12</sup>, J. Crown<sup>13</sup>, Y.K. Chae<sup>14</sup>, D. DiPrimeo<sup>15</sup>, L.D. Eli<sup>16</sup>, L. McCulloch<sup>17</sup>, D. Mahalingam<sup>18</sup>. <sup>1</sup>University of California, Los Angeles, Hematology/Oncology, Santa Monica, USA; <sup>2</sup>Hospital Quirón Dexeus, Oncology, Barcelona, Spain; <sup>3</sup>University Hospitals Leuven, Respiratory Diseases, Leuven, Belgium; <sup>4</sup>Memorial Sloan Kettering Cancer Center, Breast Medicine and Early Drug Development, New York, USA; <sup>5</sup>START-CIOCC HM Sanchinarro, Medical Oncology, Madrid, Spain; <sup>6</sup>The University of Texas, MD Anderson Cancer Center, Investigational Cancer Therapeutics, Houston, USA; <sup>7</sup>The University of Texas Southwestern Medical Center, Internal Medicine, Dallas, USA; <sup>8</sup>Mayo Clinic, Medical Oncology, Rochester, USA; <sup>9</sup>Kaiser Permanente, Oncology, Vallejo, USA; <sup>10</sup>Gustave Roussy, Medical Oncology, Villejuif, France; <sup>11</sup>Hadassah Medical Center, Hebrew University of Jerusalem, Oncology, Jerusalem, Israel; <sup>12</sup>Hospital Clínico San Carlos, Oncology, Madrid, Spain; <sup>13</sup>St. Vincent's University Hospital, Oncology, Dublin, Ireland; <sup>14</sup>Northwestern University Feinberg School of Medicine- Robert H. Lurie Comprehensive Cancer Center of Northwestern University, Medicine, Chicago, USA; <sup>15</sup>Puma Biotechnology Inc., Statistical Programming, Los Angeles, USA; <sup>16</sup>Puma Biotechnology Inc., Translational Medicine and Diagnostics, San Francisco, USA; <sup>17</sup>Puma Biotechnology Inc., Clinical Sciences and Pharmacology, San Francisco, USA; <sup>18</sup>Robert H. Lurie Comprehensive Cancer Center of Northwestern University, Medicine, Chicago, USA

**Background:** The phase 2 SUMMIT basket trial (NCT01953926) demonstrated efficacy of neratinib in patients with EGFR exon 18-mutant non-small-cell lung cancer (NSCLC). Here we report the efficacy and safety of neratinib in an expanded subgroup of patients with EGFR exon 18-mutant NSCLC in SUMMIT according to prior EGFR tyrosine kinase inhibitor (TKI) treatment.

**Materials and Methods:** Eligible patients had EGFR exon 18-mutant NSCLC and ECOG performance status 0–2. Prior EGFR TKIs, chemotherapy, and checkpoint inhibitors were allowed. Enrollment of patients with stable, asymptomatic CNS metastasis was permitted. Patients received neratinib (240 mg po daily); diarrhea prophylaxis was mandatory (loperamide first 6 weeks then PRN). Key endpoints were: objective response rate (confirmed ORR, RECIST 1.1); duration of response (DOR); clinical benefit rate (CBR); progression-free survival (PFS); safety; and biomarkers.

**Results:** 29 patients were included (23 with any prior TKI, 16 with prior osimertinib, 6 with no prior TKI). Baseline characteristics: median age 65 (range 42–87) years; male/female 41%/59%; ECOG PS 0/1/2 48%/38%/14%; patients had 1–6 prior anticancer regimens. ORR was 31% overall and 26% in patients pretreated with TKIs (Table 1). Two of 7 patients with baseline CNS metastasis had a partial response (PR; median PFS 3.6 months; 95% CI 1.9–9.1 months). Long-lived responses were observed in 3 patients with G719A/X/C mutations (2 PR, 1 SD). At data cutoff, treatment was ongoing in 11 patients. The most common all-grade adverse events were diarrhea (48%), constipation (38%), and decreased appetite (31%). Diarrhea was generally low grade (10% grade 2, 10% grade 3 and no grade 4); there were no discontinuations due to diarrhea.

Table 1. Efficacy summary

	All (n = 29)	Prior TKI (n = 23)	No prior TKI (n = 6)
ORR (confirmed) <sup>a</sup>			
PR, n (%)	9 (31)	6 (26)	3 (50)
ORR, % (95% CI)	31 (15–51)	26 (10–48)	50 (12–88)
CBR <sup>b</sup>			
PR, n (%)	9 (31)	6 (26)	3 (50)
SD ≥16 weeks, n (%)	7 (24)	6 (26)	1 (17)
CBR, % (95% CI)	55 (36–74)	52 (31–73)	67 (22–96)
Median PFS <sup>c</sup>			
Months (95% CI)	7.2 (2.3–NE)	5.8 (2.3–9.2)	NE (NE–NE)

Data cut: May 2022. NE: not estimable.

<sup>a</sup>DORR: CR/PR (confirmed ≥4 weeks after response criteria initially met).

<sup>b</sup>DCBR: confirmed CR/PR+SD for ≥16 weeks.

<sup>c</sup>DKM analysis in safety population.

**Conclusion:** Neratinib monotherapy had meaningful activity in patients with EGFR exon 18-mutant NSCLC in SUMMIT; 31% of patients had a PR and most patients had prior TKIs. Rates of diarrhea were lower than seen in patients with HER2+ breast cancer and compared favorably with rates reported for other TKIs commonly used in lung cancer. Given the lack of effective treatments for patients with NSCLC and difficult-to-treat uncommon mutations after failure of EGFR TKIs, further examination of neratinib in this setting is warranted.

**Conflict of interest:**

Corporate-sponsored Research: Drs. Goldman, Martínez Bueno, Dooms, Jhaveri, de Miguel, Piha-Paul, Unni, Mahipal, Suga, Naltet, Zick, Antoñanzas Basa, Crown, Chae, Mahalingam: Puma Biotechnology, Inc. Other Substantive Relationships: Mr. DiPrimeo, Drs. Eli, McCulloch: Employment, Stock options: Puma Biotechnology, Inc.

230

(PB110)

**Efficacy signals, long-term exposure and safety data from a phase 1–2 study of a cell-penetrating peptide antagonist of CEBPβ, a novel target, in patients (pts) with refractory solid tumors**

E. Fontana<sup>1</sup>, A. Williams<sup>1</sup>, G. Falchook<sup>2</sup>, N. Lakhani<sup>3</sup>, T.R.J. Evans<sup>4</sup>, V. Gondi<sup>5</sup>, F. Iwamoto<sup>6</sup>, M. McKean<sup>7</sup>, S. Symeonides<sup>8</sup>, N. Butowski<sup>9</sup>, A. McLaren<sup>10</sup>, J. Henry<sup>2</sup>, R. Buerki<sup>5</sup>, J. Rotolo<sup>11</sup>, G. Capiaux<sup>11</sup>, R. Michel<sup>11</sup>, S. Kaeshaefer<sup>11</sup>, E. Wiegert<sup>11</sup>, A. Bexon<sup>11</sup>. <sup>1</sup>Sarah Cannon Research Institute UK, Drug Development, London, United Kingdom; <sup>2</sup>Sarah Cannon Research Institute at HealthONE, Drug Development, Denver, USA; <sup>3</sup>START Midwest, Cancer and Hematology, Grand Rapids, USA; <sup>4</sup>University of Glasgow, Institute of Cancer Sciences, Glasgow, United Kingdom; <sup>5</sup>Northwestern Medicine, Neuro Oncology, Chicago, USA; <sup>6</sup>Columbia University, Irving Medical Center, New York, USA; <sup>7</sup>Sarah Cannon Research Institute, Tennessee Oncology, Nashville, USA; <sup>8</sup>University of Edinburgh, Medical Oncology, Edinburgh, United Kingdom; <sup>9</sup>University of California, Brain Tumor Center, San Francisco, USA; <sup>10</sup>University of Glasgow, Beatson West of Scotland Cancer Centre, Glasgow, United Kingdom; <sup>11</sup>Sapience Therapeutics Inc, Drug Development, Harrison, USA

**Background:** The oncogenic transcription factor CCAAT/enhancer-binding protein β (C/EBPβ) promotes tumor survival and proliferation and inhibits differentiation. ST101 is a peptide antagonist of C/EBPβ, with anti-tumor activity in prostate cancer (PC), glioblastoma (GBM), breast cancer (BC), melanoma, and other pre-clinical models.

**Methods:** In this phase 1–2 study, phase 1 enrolled pts with various refractory solid tumors. The primary objective was to evaluate safety/tolerability of ST101 and to determine the recommended phase 2 dose. Secondary and exploratory objectives included pharmacokinetics (PK), preliminary efficacy (RECIST 1.1), and pharmacodynamic (PD) evaluation. The study used a 3 + 3 dose-escalation design, with once-weekly IV infusion dosing of ST101 at 0.5, 1, 2, 4, 6, 9 mg/kg or a flat dose of 500 mg. Phase 2 is composed of 4 cohorts: cutaneous melanoma, castration resistant PC, hormonal receptor positive BC and GBM. Enrollment in the phase 2 portion of the study is ongoing following a Simon 2 stage design.

**Results:** As of 30 June 2022, 25 pts were enrolled in phase 1 and 23 pts in phase 2. ST101 is well tolerated with substantial proliferation durations (9–90+ weeks). The most common adverse event is G1–2 histaminergic infusion-related reaction (IRR), largely pruritis, erythema, and urticaria, managed by adjusting infusion rate and use of antihistamines and leukotriene antagonists. IRRs attenuate with time, occurring in 59% pts at 1st infusion and 19% at 8th infusion. Signs of efficacy were observed in 13 pts to date (Table 1). Seven pts continue on treatment with one confirmed partial response (PR; 38% decrease in sum of target lesions) in cutaneous melanoma and one confirmed PR in GBM (71% decrease in target lesion). There is also an unconfirmed GBM PR at week 9 as of 30 June (too early for 2nd scan). Tumor biopsy analysis showed dose-proportionate staining for ST101; other PD markers are under evaluation. Population PK analysis supported a 500 mg flat dose in phase 2.

Table 1: Preliminary efficacy data

Phase	Tumor type	Dose	Response	Duration (weeks)
1	Signet ring adenoCa	0.5 mg/kg	SD	90+
1	Small bowel adenoCa	2 mg/kg	SD	18
1	Abdominal sarcoma	2 mg/kg	SD	9
1	Cutaneous melanoma	4 mg/kg	PR	68+
1	Hepatocellular carcinoma	6 mg/kg	SD	18
1	Esophageal adenoCa	6 mg/kg	SD	9
1	Cutaneous melanoma	9 mg/kg–500 mg	SD	45+
1	Uveal melanoma	500 mg (flat dose)	SD	18
1	Mucosal melanoma	500 mg (flat dose)	SD	18
2	Glioblastoma	500 mg (flat dose)	PR	18+
2	Glioblastoma	500 mg (flat dose)	Unconfirmed PR	9+
2	Cutaneous melanoma	500 mg (flat dose)	SD	18+
2	Cutaneous melanoma	500 mg (flat dose)	SD	18

**Conclusion:** ST101 demonstrated safety at all doses explored with no dose-limiting toxicities or ST101 related SAEs. This study has demonstrated evidence of efficacy across dose levels, particularly higher doses and in patients with melanoma and glioblastoma and continues to enroll in 4 indications in phase 2.

#### Conflict of interest:

Ownership: A Bexon, G Capiaux, S. Kaesshaefer, R Michel and J Rotolo own Sapience Therapeutics Inc., stock.  
Corporate-sponsored Research: All investigators have received research funding from Sapience Therapeutics Inc.

231

(PB111)

#### The Chemical Probes Portal: an enhanced public resource providing expert advice on chemical tools for cancer research

D. Sanfelice<sup>1</sup>, A. Antolin<sup>1</sup>, A. Crisp<sup>1</sup>, E. Villasclaras-Fernandez<sup>1</sup>, I. Mica<sup>1</sup>, Y. Chen<sup>1</sup>, S. Müller-Knapp<sup>2</sup>, I. Collins<sup>3</sup>, B. Al-Lazikani<sup>4</sup>, A.M. Edwards<sup>5</sup>, P. Workman<sup>3</sup>. <sup>1</sup>Institute of Cancer Research, Data Science, London, United Kingdom; <sup>2</sup>Goethe University Frankfurt, Institute of Pharmaceutical Chemistry, Frankfurt, Germany; <sup>3</sup>Institute of Cancer Research, Cancer Research UK Cancer Therapeutics Unit, London, United Kingdom; <sup>4</sup>MD Anderson Cancer Center, Therapeutics Data Science, Houston, TX, USA; <sup>5</sup>University of Toronto, Structural Genomics Consortium, Toronto, Canada

**Background:** Chemical probes, usually inhibitors, are essential tools to interrogate physiological and disease mechanisms and validate drug targets. However, to be useful, they must meet stringent criteria: evidence of potency, selectivity, cell permeability and target engagement/modulation and a 'Pharmacological Audit Trail'. Unfortunately, researchers frequently rely on the historically biased literature or use search engines or vendor catalogues, thus unwittingly selecting tools that may not be fit-for-purpose or are outdated. This results in publication of erroneous results and also in incorrect decisions in drug discovery, wasting substantial time and resources. To help researchers select the best available tools, the Chemical Probes Portal (CPP; www.chemicalprobes.org) was established in 2015 as an independent, non-profit, online resource to curate, annotate, score and document the quality of chemical probes. Here, we describe its 2021 relaunch, enhancements in usability and content, and future plans.

**Results:** Since 2021, a new enhanced version of the free, online site is available, with >750 compounds, acting on 390 targets across multiple protein families, featuring a range of chemical tools, including PROTACs and molecular glues. Probe assessment is based on reviews by a ~200-member expert panel. The new Portal has a faster, more intuitive search and easier online forms for submitting/reviewing compounds. Reviewers now benefit from automated data input from canSAR (cansarblack.icr.ac.uk), based on the medchem, pharmacology and chemical biology literature plus data from other peer-reviewed sources. The CPP also links to the complementary Probe Miner objective assessment resource (probeminer.icr.ac.uk). The new Portal features an entirely new database and backend structure to facilitate future updates. We provide new information pages, including guidelines and criteria for choosing/using well-validated compounds, e.g., guidelines for the

characterization of probes for use in animals, where suitable PK/PD properties are needed. We emphasize how best practice includes use of probes from ≥2 different chemical classes (chemotypes) acting on the same protein as well as inactive control compounds, thus mitigating risk of off-target effects. We provide a useful section on 'Historical Compounds' which highlights those compounds that have been superseded or are otherwise unsuitable for use as chemical probes.

**Conclusion:** The CPP is an invaluable community resource, enabling cancer researchers to choose the best chemical tools for their experiments. We will continue to expand toward proteome-wide coverage. We are extending our reach and impact by working with researchers and journal editors, including presentations at conferences, articles, blogs, webinars and social media, collaborating closely with the Target 2035 initiative (www.target2035.net).

#### Conflict of interest:

Ownership: DS, AC, EV-F, IM, YC, IC, PW, BA-L and AAA are/were employees of The Institute of Cancer Research (ICR), which has a commercial interest in a range of drug targets. The ICR operates a Rewards to Inventors scheme whereby employees of the ICR may receive financial benefits following the commercial licensing of a project. EV-F, AAA, BA-L and PW have been instrumental in the creation/development of canSAR and/or Probe Miner. P.W. was instrumental in the creation of the Chemical Probes Portal.

AAA is/was a consultant of Darwin Health.

BA-L is an employee of MD Anderson Cancer Center which also operates a Reward to Inventors Scheme. BA-L declares commercial interest in Exscientia and AstraZeneca. BA-L is/was a consultant/ scientific advisory board member for GSK, Open Targets, Astex Pharmaceuticals, Astellas Pharma and is an ex-employee of Inpharmatica Ltd. BA-L was instrumental in the creation of ChEMBL and is a Director of the non-profit Chemical Probes Portal. B.A.-L. is/was a consultant/scientific advisory board member for GSK, Open Targets, Astex Pharmaceuticals, and Astellas Pharma, and is an ex-employee of Inpharmatica Ltd.

P.W. is a consultant/scientific advisory board member for Alterome Therapeutics, Astex Pharmaceuticals, Black Diamond Therapeutics, CV6 Therapeutics, NextechInvest Ltd, Nuvectis Pharma, Storm Therapeutics and Vividion Therapeutics, and holds stock in Alterome, Black Diamond, Chroma Therapeutics, NextInvest, Nuvectis and Storm and is also a non-executive director of Storm a board member and executive director of the non-profit Chemical Probes Portal and a former employee of AstraZeneca. P.W. has received research funding from Astex, Cyclacel Pharmaceuticals, Merck KGaA, Nuvectis, Piramed Pharmaceuticals, Sixth Element Capital/CRT Pioneer Fund and Vernalis.

I.C. is/was a consultant to Epidarex LLP, AdoRx Therapeutics, and Enterprise Therapeutics, and is a director of the non-profit Chemical Probes Portal. I.C. has received research funding from Astex, Merck KGaA, Janssen Biopharma, Monte Rosa Therapeutics, and Sixth Element Capital/CRT Pioneer Fund. I.C. holds stock in Monte Rosa Therapeutics AG and is a former employee of Merck Sharp & Dohme.

232

(PB112)

#### Low SKP2 expression is predictive of sensitivity to an MDM2 antagonist in p53 wild-type AML

J. Kucia-Tran<sup>1</sup>, L. Bevan<sup>1</sup>, G. Chessari<sup>2</sup>, L. Fazal<sup>3</sup>, N. Ferrari<sup>4</sup>, J. Lyons<sup>4</sup>, H. Saini<sup>5</sup>, N. Wallis<sup>1</sup>, G. Ward<sup>4</sup>, M. Ahn<sup>1</sup>. <sup>1</sup>Astex Pharmaceuticals, Biology, Cambridge, United Kingdom; <sup>2</sup>Astex Pharmaceuticals, Chemistry, Cambridge, United Kingdom; <sup>3</sup>Astex Pharmaceuticals, DMPK & Preclinical Development, Cambridge, United Kingdom; <sup>4</sup>Astex Pharmaceuticals, Translational Research, Cambridge, United Kingdom; <sup>5</sup>Astex Pharmaceuticals, Molecular Sciences, Cambridge, United Kingdom

**Background:** Non-mutational aberrations of p53 function are a common event in AML. Using fragment-based drug discovery we have identified a Murine double minute 2 (MDM2) antagonist that potently activates p53 pathway. Here, we present the discovery of a novel patient selection strategy for MDM2 antagonist-induced apoptosis in wild-type p53 AML.

**Material and Methods:** Cell panel screen and bioinformatics analyses of p53 wild-type AML cell lines that undergo apoptosis following Compound 1 (MDM2 antagonist) treatment versus those that do not were employed to identify novel patient selection strategy. Correlation between low levels of SKP2 (S-Phase Kinase Associated Protein 2) and induction of apoptosis following Compound 1 treatment was tested *in vitro* using Western Blot and flow cytometry analysis. Genetic manipulation of SKP2 levels using knock-down and over-expression approaches in wild-type p53 AML cells were used to validate the role of SKP2 expression in *in vitro* and *in vivo* experiments. Finally, bone marrow-derived primary AML blasts were tested to confirm the novel patient selection strategy.

**Results:** Cell panel screen of p53 wild-type cell lines showed a wide range of sensitivity to Compound 1 suggesting that additional biomarkers are required to ensure patient stratification. Further bioinformatics analysis of apoptotic and non-apoptotic AML cancer cell lines following treatment with Compound 1 demonstrated differential gene expression levels and identified several potential predictive biomarkers. Western blot and flow cytometry analyses demonstrated that basal SKP2 expression level is lower in apoptotic AML cell lines than in non-apoptotic cells. Over-expression of SKP2 levels in MV4-11 cells reduced MDM2 antagonist-dependent cell death in previously apoptotic cell line. Similarly, SKP2 knockdown in OCI-AML3 cells increased MDM2 antagonist-induced cytotoxicity. Studies performed in mouse systemic AML model *in vivo* also demonstrated that high levels of SKP2 reduced p53 response to Compound 1. Finally, the correlation of SKP2 expression and Compound 1 sensitivity was confirmed in primary AML blasts isolated from patients.

**Conclusions:** This work demonstrates *in vitro* and *in vivo* activity of MDM2 antagonist in AML models with low basal SKP2 levels. These pre-clinical data validate low levels of SKP2 as a novel patient selection strategy in AML and support the clinical investigation of MDM2 antagonist as therapeutic strategy for the treatment of SKP2<sup>low</sup> p53<sup>wt</sup> AML.

**No conflict of interest.**

233

(PB113)

**TNG908 is a brain-penetrant, MTA-cooperative PRMT5 inhibitor for the treatment of MTAP-deleted cancer**

K. Briggs<sup>1</sup>, K. Cottrell<sup>2</sup>, A. Tsai<sup>3</sup>, M. Zhang<sup>4</sup>, M. Tonini<sup>1</sup>, S. Yoda<sup>1</sup>, S. Lombardo<sup>5</sup>, T. Teng<sup>5</sup>, C. Davis<sup>6</sup>, D. Whittington<sup>7</sup>, H. DiBenedetto<sup>8</sup>, A. Huang<sup>9</sup>, J. Maxwell<sup>1</sup>. <sup>1</sup>Tango Therapeutics, Discovery Biology, Cambridge, USA; <sup>2</sup>Tango Therapeutics, Chemistry, Cambridge, USA; <sup>3</sup>Tango Therapeutics, Discovery DMPK, Cambridge, USA; <sup>4</sup>Tango Therapeutics, Pharmacology, Cambridge, USA; <sup>5</sup>Tango Therapeutics, Functional Genomics, Cambridge, USA; <sup>6</sup>Tango Therapeutics, Clinical Pharmacology, Cambridge, USA; <sup>7</sup>Tango Therapeutics, Structural Biology, Cambridge, USA; <sup>8</sup>Tango Therapeutics, Development Operations, Cambridge, USA; <sup>9</sup>Tango Therapeutics, Chief Scientific Officer, Cambridge, USA

TNG908 is a clinical stage MTA-cooperative PRMT5 inhibitor that leverages the synthetic lethal interaction between PRMT5 inhibition and MTAP deletion. TNG908 was discovered using structure-based design following an initial high-throughput screening campaign. TNG908 is 15X selective for MTAP<sup>null</sup> cell lines over isogenic MTAP<sup>WT</sup> cell lines and has marked selectivity for MTAP-deleted cancer cell lines independent of lineage in a large, diverse cell line panel. Oral administration of TNG908 drives dose-dependent, MTAP<sup>null</sup>-selective antitumor activity in xenograft models, including durable tumor regressions in models representing glioblastoma, non-small cell lung cancer (adenocarcinoma and squamous), mesothelioma, cholangiocarcinoma, urothelial carcinoma, and others. TNG908 is brain-penetrant as exposure in the cerebrospinal fluid (CSF) approximates free, unbound plasma exposure in non-human primate studies. These data combined with strong preclinical activity in glioblastoma models strongly position TNG908 as a potential treatment of MTAP-deleted glioblastoma or solid tumor CNS metastases. A Phase 1/2 clinical trial (NCT05275478) is currently enrolling to assess safety, tolerability, and efficacy in patients with advanced or metastatic MTAP-deleted solid tumors, including non-small cell lung cancer (adenocarcinoma and squamous), mesothelioma, cholangiocarcinoma, malignant peripheral nerve sheath tumor, or in a lineage-agnostic cohort. In summary, TNG908 is a clinical stage, potent, brain-penetrant PRMT5 inhibitor with excellent drug-like properties and strong preclinical activity in multiple xenograft models that has the potential for histology-agnostic clinical development in MTAP-deleted solid tumors.

**Conflict of interest:**

Ownership: All authors are full-time employees of Tango Therapeutics and have stock and/or stock options.

234

(PB114)

**TNG462 is a potential best-in-class MTA-cooperative PRMT5 inhibitor for the treatment of peripheral MTAP-deleted solid tumors**

K. Briggs<sup>1</sup>, A. Tsai<sup>2</sup>, M. Zhang<sup>3</sup>, M. Tonini<sup>1</sup>, B. Haines<sup>3</sup>, A. Huang<sup>4</sup>, K. Cottrell<sup>5</sup>. <sup>1</sup>Tango Therapeutics, Discovery Biology, Cambridge, USA; <sup>2</sup>Tango Therapeutics, Discovery DMPK, Cambridge, USA; <sup>3</sup>Tango Therapeutics, Pharmacology, Cambridge, USA; <sup>4</sup>Tango Therapeutics, Chief Scientific Officer, Cambridge, USA; <sup>5</sup>Tango Therapeutics, Chemistry, Cambridge, USA

MTAP deletions occur in 10–15% of all human cancers, providing one of the largest precision oncology patient populations. MTA-cooperative PRMT5 inhibitors leverage the well-characterized synthetic lethal relationship between PRMT5 inhibition and MTAP-deletion. TNG908, AMG 193, and MRTX1719 are all clinical stage MTA-cooperative PRMT5 inhibitors for the treatment of MTAP-deleted solid tumors. TNG462 is an investigational stage MTA-cooperative PRMT5 inhibitor with significantly enhanced potency, selectivity and extended target coverage designed to be a best-in-class treatment for patients with peripheral MTAP-deleted cancer. *In vitro*, TNG462 is 45X selective for MTAP-deleted cancer cell lines over isogenic MTAP WT cell lines and has marked selectivity for MTAP-deleted cancer cell lines independent of lineage in a large, diverse cell line panel. TNG462 demonstrates durable PD modulation *in vitro* and *in vivo* consistent with high affinity binding to PRMT5. Oral administration of TNG462 drives dose-dependent antitumor activity including durable tumor regressions and complete responses in multiple cell line- and patient-derived xenograft models. With enhanced potency and selectivity for MTAP-deleted cancer cells, and optimized pharmacokinetic properties to extend target coverage, TNG462 has the potential for broader and deeper clinical activity in peripheral MTAP-deleted solid tumors.

**Conflict of interest:**

Ownership: All of the authors are full-time Tango employees and have stocks and/or stock options.

235

(PB115)

**Phase II trial of afatinib in patients with EGFR-mutated solid tumors excluding lung cancer: results from the NCI-MATCH ECOG-ACRIN Trial (EAY131) Subprotocol A**

K. Reckamp<sup>1</sup>, Z. Song<sup>2</sup>, S. Gettinger<sup>3</sup>, E.P. Mitchell<sup>4</sup>, J.J. Wright<sup>5</sup>, J.A. Moscow<sup>2</sup>, R.J. Gray<sup>2</sup>, V. Wang<sup>2</sup>, L.M. McShane<sup>6</sup>, L.V. Rubinstein<sup>6</sup>, D.R. Patton<sup>7</sup>, P.M. Williams<sup>8</sup>, S.R. Hamilton<sup>9</sup>, B.A. Conley<sup>10</sup>, C.L. Arteaga<sup>11</sup>, L.N. Harris<sup>10</sup>, P.J. O'Dwyer<sup>12</sup>, A.P. Chen<sup>13</sup>, K.T. Flaherty<sup>14</sup>. <sup>1</sup>Cedars-Sinai Medical Center, Medicine, Los Angeles, USA; <sup>2</sup>Dana Farber Cancer Institute- ECOG-ACRIN Biostatistics Center, Biostatistics, Boston, USA; <sup>3</sup>Yale University, Medicine, New Haven, USA; <sup>4</sup>Thomas Jefferson University Hospital, Medicine, Philadelphia, USA; <sup>5</sup>National Cancer Institute, Investigational Drug Branch- Cancer Therapy Evaluation Program- Division of Cancer Treatment and Diagnosis, Bethesda, USA; <sup>6</sup>National Cancer Institute, Biometric Research Program- Division of Cancer Treatment and Diagnosis, Bethesda, USA; <sup>7</sup>National Cancer Institute, Center for Biomedical Informatics & Information Technology, Bethesda, USA; <sup>8</sup>Frederick National Laboratory for Cancer Research, NCI Laboratory, Frederick, USA; <sup>9</sup>City of Hope National Medical Center, Pathology, Duarte, USA; <sup>10</sup>National Cancer Institute, Cancer Diagnosis Program- Division of Cancer Treatment and Diagnosis, Bethesda, USA; <sup>11</sup>UT Southwestern Simmons Cancer Center, Medicine, Dallas, USA; <sup>12</sup>University of Pennsylvania, Medicine, Philadelphia, USA; <sup>13</sup>National Cancer Institute, Early Clinical Trials Development Program- Division of Cancer Treatment and Diagnosis, Bethesda, USA; <sup>14</sup>Massachusetts General Hospital, Medicine, Boston, USA

**Background:** Molecularly targeted treatment with epidermal growth factor receptor (EGFR) tyrosine kinase inhibitors (TKIs) have prolonged survival of pts with activating EGFR mutations in non-small cell lung cancer (NSCLC). Afatinib is an ErbB family blocker that demonstrated clinical benefit in pts with NSCLC with common and uncommon activating EGFR mutations. The activity of afatinib in other tumor types with EGFR mutations is less well known. National Cancer Institute-Molecular Analysis for Therapy Choice (NCI-MATCH) Arm EAY131-A evaluated afatinib in tumors beyond lung cancer that harbored EGFR activating alterations.

**Material and methods:** Pts with advanced tumors who received prior systemic therapy were enrolled to NCI-MATCH for molecular profiling. Those with tumors other than NSCLC found to harbor actionable EGFR mutations except exon 20 insertion mutations were offered participation in subprotocol A. In this single arm, phase II trial, pts received afatinib 40-mg once daily until

disease progression or unacceptable toxicity. The primary endpoint was objective response rate (ORR). Secondary endpoints included progression free survival (PFS), 6-month PFS, overall survival (OS) and identification of predictive biomarkers.

**Results:** Nineteen pts were enrolled and 17 analyzable pts received protocol therapy. Thirteen pts had glioblastoma (GBM) with one gliosarcoma, 2 with adenocarcinoma NOS and one with adenosquamous carcinoma of the breast. *EGFR* alterations included common and uncommon mutations. The majority of pts had received  $\geq 2$  lines of prior therapy. With a median follow-up of 16.2 months, 1 complete (glioblastoma) and 1 partial response (adenocarcinoma NOS) were seen with ORR 11.8% (90% CI 2.1%–32.6%); 3 pts had stable disease. Six-month PFS was 14.1% (90% CI 4.9%–40.4%) and median OS was 9 months (90% CI, 4.6 to 14.0 months). The pt with a CR had a rare exon 18 *EGFR*-SEPT14 fusion described previously in GBM. Response is ongoing at 16 months. The pt with PR had the classic exon 19 deletion *EGFR* mutation, with duration of response of 12.8 months. Rash, diarrhea, and fatigue were the most common toxicities, most were grade 1 and 2. Grade 3 vomiting and rash were G 3-5 AEs attributed to afatinib; a grade 4 seizure was noted, but unrelated.

**Conclusions:** Afatinib had modest activity in a cohort of heavily pretreated cancer pts harboring common and uncommon *EGFR* mutations and did not meet its primary endpoint. Further evaluation of *EGFR* exon 18 fusions in glioblastoma or other cancers may be of interest. NCT02465060.

This study was coordinated by the ECOG-ACRIN Cancer Research Group (Peter J. O'Dwyer, MD and Mitchell D. Schnall, MD, PhD, Group Co-Chairs) and supported by the National Cancer Institute of the National Institutes of Health under award numbers: U10CA180820, U10CA180794, UG1CA233302, UG1CA233180, UG1CA233341, and UG1CA233337.

#### Conflict of interest:

Other Substantive Relationships: Karen L. Reckamp, receives or has received research funding to the institution from Genentech Blueprint Calithera Daiichi Sankyo Elevation Oncology Janssen serves or has served as a consultant to Amgen, AstraZeneca, Blueprint, Daiichi Sankyo, EMD Soreno, Genentech, GlaxoSmithKline, Janssen, Lilly, Merck KGA, Mirati, Seattle Genetics, Takeda, Tesaro.

Carlos L. Arteaga, receives or has received research grants from Pfizer, Lilly and Takeda holds minor stock options in Provista serves or has served in an advisory role to Novartis, Merck, Lilly, Daiichi Sankyo, Taiho Oncology, Origimed, Puma Biotechnology, Immunomedics, AstraZeneca, Arvinas, and Sanofi and reports scientific advisory board remuneration from the Susan G. Komen Foundation.

#### 236 (PB116)

##### Preclinical characterization of CNS-active, mutant-selective fourth-generation *EGFR* inhibitors with potent activity against single, double, and triple mutant *EGFR* variants including T790M and C797S

S. Zhang<sup>1</sup>, W.S. Huang<sup>2</sup>, S. Nadworny<sup>3</sup>, E. Ye<sup>4</sup>, N. Narasimhan<sup>4</sup>, C.J. Eyermann<sup>2</sup>, D. Dalgarno<sup>2</sup>, V. Rivera<sup>1</sup>, W. Shakespeare<sup>2</sup>. <sup>1</sup>Theseus Pharmaceuticals, Inc., Biology, Cambridge, USA; <sup>2</sup>Theseus Pharmaceuticals, Inc., Chemistry, Cambridge, USA; <sup>3</sup>Theseus Pharmaceuticals, Inc., Pharmacology, Cambridge, USA; <sup>4</sup>Theseus Pharmaceuticals, Inc., DMPK- Preclinical Safety, Cambridge, USA

**Background:** *EGFR* activating mutations are observed in 10–50% of NSCLC patients and the common mutations (L858R [L] and exon 19 deletions [D]) are initially sensitive to first- second- and third-generation *EGFR* inhibitors (e.g., erlotinib [1G], afatinib [2G], and osimertinib [3G], respectively). However, on-target resistance is observed in a substantial percentage of patients, with T790M (T) and C797S (C) mutations observed most frequently (post-1G/2G and post-3G, respectively). Furthermore, *EGFR* mutational heterogeneity can increase during treatment with existing inhibitors, activity against wild type (WT) *EGFR* leads to dose-limiting toxicities, and tumors commonly metastasize to the brain. We therefore set out to identify a fourth-generation (4G) *EGFR* inhibitor with 1) potent activity against all 8 major single (L and D), double (LT, DT, LC, DC), and triple (LTC, DTC) mutant variants, 2) selectivity over WT *EGFR*, and 3) central nervous system (CNS) activity.

**Materials and Methods:** In vitro drug activity was determined by assessing effects (IC50 s) in kinase assays and on tumor and BaF3 cell lines expressing WT or mutant forms of *EGFR*. Efficacy studies were conducted using engineered BaF3 and human lung cancer cells, or patient-derived models; mice were dosed orally once daily (QD) at doses that did not exceed the maximum tolerated dose.

**Results:** We have identified multiple advanced lead compounds with the profiles of a 4G *EGFR* inhibitor. A representative compound, Cmpd A, potently inhibited the kinase activity of *EGFR* L, LT, and LTC variants with IC50 s £1 nM, compared to IC50 s for osimertinib of 0.4, 0.2, and 360 nM respectively. In engineered BaF3 cells, Cmpd A inhibited viability of all 8

*EGFR* single, double, and triple mutant variants with IC50 s <12 nM, while erlotinib and osimertinib were inactive against all 4 T790M- and all 4 C797S-containing variants, respectively. Cmpd A inhibited the activity of all 8 variants with 11- to 69-fold selectivity over WT *EGFR*, which compared favorably to the 6- to 7-fold selectivity erlotinib exhibited for L and D. In vivo, Cmpd A (30–40 mg/kg QD) induced tumor regression in all 8 tumor models tested, including those containing *EGFR* single (L or D), double (LC or DT), and triple (LTC or DTC) mutant variants. Finally, Cmpd A had substantial anti-tumor activity and significantly prolonged survival in an intracranial tumor model.

**Conclusions:** We have identified potent mutant-selective and CNS-active 4G *EGFR* inhibitors. These data strongly support that inhibition of both major activating mutants, and key mutants associated with clinical resistance to all existing inhibitors - including C797S-containing variants associated with both 1st and 2nd line osimertinib failure - is achievable with a single molecule.

#### Conflict of interest:

Ownership: Employee and stock holder of Theseus Pharmaceuticals, Inc.

#### 237 (PB117)

##### A phase II study to evaluate the efficacy of regorafenib in C-KIT mutated metastatic malignant melanoma patients who have progressed on first-line treatment: A Multicenter Trial of Korean Cancer Study Group (UN-14-13)

K.H. Kim<sup>1</sup>, H.J. Lee<sup>2</sup>, S.J. Lee<sup>3,4</sup>, M. Kim<sup>5</sup>, M.S. Ahn<sup>6</sup>, M.Y. Choi<sup>7</sup>, N.R. Lee<sup>8</sup>, M. Jung<sup>1</sup>, S.J. Shin<sup>1</sup>. <sup>1</sup>Korean Cancer Study Group, Yonsei University College of Medicine, Department of Internal Medicine-Division of Medical Oncology, Seoul, South Korea; <sup>2</sup>Chungnam National University School of Medicine, Department of Internal Medicine and Cancer Research Institute, Daejeon, South Korea; <sup>3</sup>Sungkyunkwan University School of Medicine-Samsung Medical Center, Department of Medicine-Division of Hematology-Oncology, Seoul, South Korea; <sup>4</sup>Ewha Womans University College of Medicine, Department of Internal Medicine-Division of Hematology-Oncology, Seoul, South Korea; <sup>5</sup>Seoul National University Hospital-Seoul National University Cancer Research Institute, Department of Internal Medicine, Seoul, South Korea; <sup>6</sup>Ajou University School of Medicine, Department of Hematology-Oncology, Suwon, South Korea; <sup>7</sup>Inje University Busan Paik Hospital, Department of Internal Medicine-Division of Hematology-Oncology, Busan, South Korea; <sup>8</sup>Jeonbuk National University Medical School, Department of Internal Medicine-Division of Hematology and Oncology, Jeonju, South Korea

**Background:** C-KIT mutation is a therapeutic target for malignant melanoma, and C-KIT inhibitors such as imatinib have previously shown clinical efficacy. Regorafenib is a 3<sup>rd</sup> generation inhibitor of C-KIT and demonstrates high response rate in C-KIT mutated gastrointestinal stromal tumor. We evaluated the anti-tumor activity and safety of regorafenib in C-KIT mutated metastatic malignant melanoma patients who have progressed on first-line treatment.

**Material and methods:** We conducted a multicenter phase II clinical trial of regorafenib in patients with metastatic melanoma positive for C-KIT mutations whose disease progressed after at least one line of systemic treatment. C-KIT mutations were analyzed either by quantitative PCR (qPCR) method or next-generation sequencing (NGS). Patients enrolled received oral regorafenib 160 mg once daily for the 3 weeks of each 4-week cycle. The primary endpoint was disease control rate (DCR), and the secondary endpoint was safety, overall response rate (ORR), progression-free survival (PFS), and overall survival (OS).

**Results:** Between December 2014 and January 2022, 153 patients were screened for C-KIT mutation and ultimately 23 patients were enrolled and started treatment. Median age was 68 (range, 31–86), with 11 male (47.8%) and 12 female (52.2%) patients. Occurrences in melanoma subtypes included 9 (39.1%) acral, 6 (26.1%) mucosal, and 3 (13.0%) chronic sun-damaged melanomas. The DCR was 73.9%, with 2 patients (8.7%) showing complete response, 5 patients (21.7%) partial response, and 10 patients (43.5%) showing stable disease, and ORR was 30.4% (7/23 patients). Median follow-up duration was 15.2 months (95% confidential interval [CI], 10.0–21.5), and median PFS and OS were 7.0 months (95% CI, 1.5–12.5) and 16.3 months (95% CI, 12.6–19.9), respectively. Screening for C-KIT mutations found exon 11 to be the most common site (14 patients, 60.9%), with other sites including exon 13, 17, and 9 in 5 (21.7%), 5 (21.7%), 2 (8.7%) patients, respectively, and there was no difference of ORR according to the mutation site. Skin reactions including hand-foot syndrome were the most commonly reported adverse event (All grade 60.9%, G3 13.0%). Grade 3 adverse events occurred in 9 patients (39.1%), which included infection, rash, mucositis, and bone marrow suppression, and none of grade 4 toxicities nor treatment-related deaths were observed.

**Conclusion:** In metastatic malignant melanoma harboring C-KIT mutations, regorafenib in second or later line setting demonstrated significant clinical activity in patients, with ORR of 30.4% and DCR of 73.9%. Further biomarker studies with circulating tumor DNA analysis are currently underway.

**No conflict of interest.**

238 (PB118)

**Phase II study of sunitinib in tumors with c-KIT mutations: results from the NCI-MATCH ECOG-ACRIN trial (EAY131) subprotocol V**

L. Gien<sup>1</sup>, Z. Song<sup>2</sup>, A. Poklepovic<sup>3</sup>, E.A. Collisson<sup>4</sup>, E.P. Mitchell<sup>5</sup>, J.A. Zweibel<sup>6</sup>, P. Harris<sup>7</sup>, R.J. Gray<sup>2</sup>, V. Wang<sup>2</sup>, L.M. McShane<sup>8</sup>, L.V. Rubinstein<sup>8</sup>, D.R. Patton<sup>9</sup>, P.M. Williams<sup>10</sup>, S.R. Hamilton<sup>11</sup>, B.A. Conley<sup>12</sup>, C.L. Arteaga<sup>13</sup>, L.N. Harris<sup>12</sup>, P.J. O'Dwyer<sup>14</sup>, A.P. Chen<sup>15</sup>, K.T. Flaherty<sup>16</sup>. <sup>1</sup>Sunnybrook Odette Cancer Center, Gynecologic Oncology, Toronto, Canada; <sup>2</sup>Dana Farber Cancer Institute, ECOG-ACRIN Biostatistics Center, Boston, USA; <sup>3</sup>Virginia Commonwealth Univ/Massey Cancer Center, Medical Oncology, Richmond, USA; <sup>4</sup>UCSF Medical Center, Medical Oncology, San Francisco, USA; <sup>5</sup>Thomas Jefferson University Hospital, Medical Oncology, Philadelphia, USA; <sup>6</sup>National Cancer Institute, Investigational Drug Branch- Division of Cancer Treatment and Diagnosis, Bethesda, USA; <sup>7</sup>National Cancer Institute, Cancer Therapy Evaluation Program- Division of Cancer Treatment and Diagnosis, Bethesda, USA; <sup>8</sup>National Cancer Institute, Biometric Research Program- Division of Cancer Treatment and Diagnosis, Bethesda, USA; <sup>9</sup>National Cancer Institute, Center for Biomedical Informatics & Information Technology, Bethesda, USA; <sup>10</sup>National Cancer Institute, Frederick National Laboratory for Cancer Research, Frederick, USA; <sup>11</sup>City of Hope National Medical Center, Department of Pathology, Duarte, USA; <sup>12</sup>National Cancer Institute, Cancer Diagnosis Program- Division of Cancer Treatment and Diagnosis, Bethesda, USA; <sup>13</sup>Univ of TX Southwestern Medical Center, Medical Oncology, Dallas, USA; <sup>14</sup>University of Pennsylvania, Medical Oncology, Philadelphia, USA; <sup>15</sup>National Cancer Institute, Division of Cancer Treatment and Diagnosis, Bethesda, USA; <sup>16</sup>Massachusetts General Hospital, Medical Oncology, Boston, USA

**Background:** KIT mutations are common in gastrointestinal stromal tumors (GISTs) but are also found to a lesser degree in other tumor types such as mucosal melanomas, testicular seminomas or dysgerminomas. The NCI-MATCH study is a tumor agnostic platform trial enrolling patients to targeted therapies based on genomic alterations. Subprotocol V of the NCI-MATCH platform trial investigated sunitinib in patients with tumors harboring c-KIT mutations.

**Material & Methods:** EAY131-V, is an open-label, single arm, phase 2 study. Eligible patients were those with a somatic c-KIT mutation on exons 9, 11, 13, and 14. Exclusions were mutations on exons 17, 18 which are reported to have resistance to sunitinib. Excluded tumor types were GIST, renal cell carcinoma, and pancreatic neuroendocrine tumors which have a known response to sunitinib. Patients received sunitinib 50 mg orally daily for 4 weeks with 2-week rest, until disease progression or unacceptable toxicity. The primary endpoint was objective response rate (ORR); secondary endpoints were progression-free survival (PFS) at 6 months, PFS, and toxicities.

**Results:** Between November 1, 2016, and May 21, 2020, 10 patients were enrolled, 9 were analyzable. Median age was 62 years (range 30–76), 77.8% received 2 lines of systemic therapy, while 22.2% received >3 lines. The most common tumor type was melanoma (44%), followed by squamous cell carcinoma of the lung or thymus (33%). There were 2 partial responses (PRs), both in squamous cell carcinomas, with an ORR of 22.2% (90% CI 4.1%–55%) and stable disease in 44%. Estimated 6-month PFS was 33.3% (90% CI 15.4%–72.4%). The 2 PRs had a PFS of 8 months and 10.8 months, respectively. Grade 3–4 toxicities at least possibly related to treatment occurred in 5 patients and included a thromboembolic event (n = 1), skin infections (n = 2), and lymphopenia (n = 2). This arm of the study was closed in 2022 based on low accrual, despite an amendment for additional actionable mutations. Prevalence of eligible c-KIT mutations after screening 5540 patients was estimated at 0.13%.

**Conclusions:** In this study, sunitinib monotherapy for c-KIT mutations did not meet the primary endpoint for response, but in this small sample size a potential signal cannot be ruled out. Estimated rates of c-KIT mutations was lower than expected, impacting accrual to this arm.

This study was coordinated by the ECOG-ACRIN Cancer Research Group (Peter J. O'Dwyer, MD and Mitchell D. Schnall, MD, PhD, Group Co-Chairs) and supported by the National Cancer Institute of the National Institutes of Health under award numbers: U10CA180820, U10CA180794, UG1CA233302, UG1CA233180, UG1CA233341, and UG1CA189869. The

content is solely the responsibility of the authors and does not necessarily represent the official views of the National Institutes of Health.

**No conflict of interest.**

239 (PB119)

**Preclinical efficacy of BDTX-4933, a brain penetrant MasterKey inhibitor targeting oncogenic BRAF Class I/II/III mutations**

P.Y. Ng<sup>1</sup>, Y.C. Han<sup>2</sup>, L. Shin Ogawa<sup>3</sup>, R. Schulz<sup>4</sup>, S.N. Yang<sup>4</sup>, I. Jewett<sup>1</sup>, N. Ishiyama<sup>5</sup>, D. Romashko<sup>4</sup>, A. Salomatov<sup>6</sup>, S. Thakur<sup>5</sup>, M. Lucas<sup>7</sup>, T.A. Lin<sup>2</sup>, E. Buck<sup>4</sup>. <sup>1</sup>Black Diamond Therapeutics, Medicinal Chemistry, Cambridge, USA; <sup>2</sup>Black Diamond Therapeutics, Translational Biology, New York, USA; <sup>3</sup>Black Diamond Therapeutics, Non-clinical Development, Cambridge, USA; <sup>4</sup>Black Diamond Therapeutics, Research Biology, New York, USA; <sup>5</sup>Black Diamond Therapeutics, Computational Sciences, Toronto, Canada; <sup>6</sup>Black Diamond Therapeutics, Computational Sciences, New York, USA; <sup>7</sup>Black Diamond Therapeutics, Discovery, Cambridge, USA

**Background:** FDA-approved BRAF inhibitors target V600 (Class I) mutant monomers and are largely inactive against mutant BRAF dimers. These dimeric mutants found in many solid tumors including primary CNS tumors and brain metastases can drive RAS-independent (Class II) or RAS-dependent (Class III) oncogenic tumor growth. Furthermore, the approved BRAF inhibitors can induce paradoxical RAF activation that limits their activity. Although currently approved BRAF V600 mutation-selective inhibitors demonstrated efficacy in brain tumors and metastases when combined with MEK inhibitors in clinical trials, duration of response tends to be short partly due to limited BBB permeability. There remains a high unmet clinical need for a broad Class I/II/III BRAF inhibitor with high CNS penetrant activity for patients with RAF-dependent tumors carrying a broad spectrum of BRAF alterations.

**Materials and Methods:** The MAP platform used NGS data and a proprietary machine-learning algorithm to predict and then validate the oncogenicity of previously uncharacterized groups of oncogenic BRAF mutations across Class I/II/III and to identify small molecule MasterKey drug candidates against this spectrum of mutations. Candidates were further optimized for brain penetration properties.

**Results:** BDTX-4933 is a potent, selective, CNS penetrant BRAF Class I/II/III mutation inhibitor that targets MAP-predicted oncogenic BRAF alterations while sparing wild type BRAF with >10-fold selectivity in cell proliferation assays. BDTX-4933 inhibits the RAF-MEK-ERK signaling pathway and cell proliferation across a panel of cancer cell lines endogenously expressing Class I/II/III mutations without paradoxical RAF activation. BDTX-4933 achieves target engagement, inhibiting the BRAF signaling pathway in *in vivo* models, and anti-tumor activity across tumor models representing all three classes of BRAF mutations including NSCLC and melanoma. Preclinical data shows that BDTX-4933 achieves high CNS exposure, and results in tumor growth inhibition and survival benefit in BRAF mutant intracranial models.

**Conclusions:** BDTX-4933 has all the attributes of a best-in-class CNS penetrant BRAF inhibitor to address patients with and without CNS disease whose tumors express monomeric (Class I) or dimeric (Class II and III) BRAF mutants. BDTX-4933 achieves on-target inhibition of the RAF-MEK-ERK signaling pathway and anti-tumor activity in multiple preclinical tumor models, including intracranial models. IND-enabling studies for BDTX-4933 are underway.

**Conflict of interest:**

Ownership: Black Diamond Therapeutics

28 October 2022

10:00–15:00

POSTER SESSION

**Antibody-drug Conjugates**

240 (PB020)

**Antitumor activity of Antibody-Drug Conjugates targeting cancer-expressed EGFR in Preclinical Models**

D. Fitzgerald<sup>1</sup>, E. C. H. Ho<sup>1</sup>, E. Miller<sup>1</sup>, R. Qiu<sup>1</sup>, A. Antignani<sup>1</sup>. <sup>1</sup>NCI/NIH, Laboratory of Molecular Biology, Bethesda, USA

**Background:** The epidermal growth factor receptor (EGFR) plays a key role in the growth and survival of many human tumors of epithelial origin. The monoclonal antibody, 40H3, targeting overexpressed EGFR and the truncated form EGFR variant III (EGFRvIII) on tumor cells, was conjugated

to small molecules with potent cytotoxic activity, generating five antibody-drug conjugates (ADCs). Their lethality for tumor cells was evaluated *in vitro* and *in vivo*.

**Materials and methods:** ADC construction: Purified 40H3 antibody was conjugated to five different payloads: two tubulin inhibitors, monomethyl auristatin E (MMAE) and DM1, two topoisomerase inhibitors, SN38 and irinotecan (DXd1) and a PBD dimer (SG-3199).

**Binding assay:** The binding affinity constants of the various 40H3-based ADCs were determined against the His-tagged EGFR peptide loop (aa 287–302) immobilized on Ni-NTA biosensors with the Octet Red96 analyzer.

**Bystander assay:** Cocultured F98npEGFRVIII and F98 cells were treated with media, free payload (SG-3199), 40H3 antibody, 40H3-tesirine or IgG-tesirine at the indicated concentrations. After 48 hours, the cells were labeled with cetuximab-PE and SYTOX™ Red viability dye and then analyzed for bystander killing by flow cytometry.

**In vivo studies:** MDA-MB-468 or BT-20 tumor xenografts were treated with unmodified 40H3 antibody or 40H3-tesirine. Tumor volumes and mouse weights were measured at least three times weekly.

**Results:** The five ADCs retained antigen binding activity of the unmodified 40H3 antibody. They showed a potent cytotoxicity on a panel of EGFR-expressing cells including three triple negative breast cancer lines. Cell killing was correlated to the number of binding sites for the 40H3 antibody. The 40H3 conjugate with the PBD dimer (40H3-tesirine) was the most active killing agent and it also exhibited bystander killing of cells not expressing human EGFR. Moreover, *in vivo*, on two different models of tumor xenografts, treatment with 40H3-tesirine achieved complete remissions.

**Conclusions:** The 40H3 antibody is a valid delivery agent for toxic payloads. Among the five ADCs, 40H3-tesirine showed the highest cytotoxic effect toward EGFR-expressing tumor cells *in vitro* and *in vivo*.

**No conflict of interest.**

#### 241 (PB021) Development of a novel antibody-drug conjugate targeting both CEACAM5 and CEACAM6

K. Arias<sup>1</sup>, C. Enos<sup>2</sup>, M. Spear<sup>1</sup>, D. Austin<sup>1</sup>, R. Almofeez<sup>1</sup>, S. Kortchak<sup>1</sup>, L. Pincus<sup>1</sup>, Y. Kwon<sup>3</sup>, C. Gelber<sup>1</sup>. <sup>1</sup>Stromatis Pharma, Stromatis Pharma, Manassas, USA; <sup>2</sup>Eastern Virginia Medical School, Department of Dermatology, Norfolk, USA; <sup>3</sup>Leidos, Vaccine- Immunity and Cancer Directorate, Frederick, USA

**Background:** Carcinoembryonic antigen cell adhesion molecule (CEACAM) family members 5 and 6 are tumor-associated antigens frequently upregulated in epithelial cancers, including pancreatic ductal adenocarcinoma (PDAC) and colorectal cancer (CRC), where they contribute to invasion, metastasis, survival, resistance to chemotherapy, and immune escape. CT109 is a novel antibody with dual specificity for both CEACAM5 and 6, mediated by binding to a shared glycoepitope. CT109 exhibits a high affinity (in the single nM range) to the target. Recently CEACAM6 was identified as a novel immune checkpoint. To further develop CT109, *in vitro* and *in vivo* characterization of the antibody-drug conjugate (ADC), CT109-SN-38, was performed.

**Materials and Methods:** Immunoblots were performed against recombinant CEACAM5/6 and lysates of PDAC and CRC cell lines to assess the specificity of CT109. Immunohistochemistry (IHC) was also performed to establish the expression prevalence in epithelial cancers and confirm specificity. Internalization kinetics were assessed by pHrodo conjugation and flow cytometry in two PDAC cell lines. ADC IC<sub>50</sub> values were determined in the antigen-expressing PDAC line, BxPC-3, and non-expressing line, PANC-1, using CellTiter Glo. Effects of CT109-SN-38 *in vivo* were performed in a heterotopic xenograft model in nude mice that received triweekly injections of CT109-SN-38 for three weeks.

**Results:** CT109 binds to both cell surface and recombinant CEACAM5 and CEACAM6 in immunoblots. CT109 exhibits remarkable specificity in IHC with high expression prevalence in CRC and PDAC cores (3/3 cores). CT109 is internalized in antigen-expressing, but not in non-expressing, PDAC cells with a half-maximal localization to low pH compartments of 24 hours. *In vitro*, CT109-SN-38 and auristatin conjugates exhibit robust killing of antigen-expressing cells. *In vivo*, CT109-SN-38 mediates specific tumor-killing, resulting in reduced tumor volumes (through day 50,  $p < 0.001$ ) and reduced tumor burden below baseline in a subset of mice (2/10 mice).

**Conclusions:** CT109, as a novel anti-CEACAM5/6 antibody, binds to a high proportion of CRC and PDAC lines and cores. However, binding to CEACAMs 5 and 6 does not compromise specificity in IHC, with no observed staining of normal tissues. While GPI-linked proteins are canonically viewed as slowly or non-internalizing antigens, CT109 is nonetheless internalized. It mediates a dose-dependent cytotoxic effect *in vitro* as an SN-38, monomethyl auristatin (MMA) F, and MMAE conjugate. CT109-SN-38 similarly exhibits a dose-dependent effect in reducing tumor growth in a

heterotopic PDAC tumor xenograft model, with 2/10 mice exhibiting tumor regression throughout the study. Further preclinical and clinical development of CT109-SN-38 is warranted.

#### Conflict of interest:

Ownership: Dr. Cohava Gelber has partial ownership and is a shareholder of Stromatis Pharma.  
Board of Directors: Dr. Cohava Gelber is a co-chairperson and founder of Stromatis Pharma.

#### 242 (PB022) Relationship between the intratumor pharmacokinetics and antitumor effect of the payload eribulin in the novel antibody–drug conjugate MORAb-202

S. Koganemaru<sup>1</sup>, H. Fuchigami<sup>2</sup>, H. Tsugawa<sup>2</sup>, Y. Kuboki<sup>1</sup>, K. Furuuchi<sup>3</sup>, T. Uenaka<sup>3</sup>, T. Doi<sup>1</sup>, M. Yasunaga<sup>2</sup>. <sup>1</sup>National Cancer Center Hospital East, Department of Experimental Therapeutics, Kashiwa, Japan; <sup>2</sup>National Cancer Center, Exploratory Oncology Research and Clinical Trial Center, Kashiwa, Japan; <sup>3</sup>Eisai Inc., Epochal Precision Anti-Cancer Therapeutics EPAT, Exton, USA

**Background:** Antibody–drug conjugates have the potential to improve antitumor activity through specific targeting of tumor cells, using antibodies attached to a cytotoxic payload, compared with the payload alone.

**Material and methods:** MORAb-202 (farletuzumab ecteribulin) is an antibody–drug conjugate composed of the humanized antifolate receptor-alpha (FR $\alpha$ ) monoclonal antibody, farletuzumab, conjugated to eribulin by a cathepsin B-cleavable linker. In this preclinical study, we investigated the relationship between the antitumor effect and the intratumor pharmacokinetics of the potent cytotoxic microtubule inhibitor payload, eribulin, as part of MORAb-202, compared with eribulin alone, using FR $\alpha$ + and FR $\alpha$ - human cancer models.

**Results:** MORAb-202 treatment showed a statistically significant antitumor effect in the tumor xenograft model with high-FR $\alpha$  expression, even at doses that did not indicate an antitumor effect in the equivalent eribulin- or antibody-treated groups ( $P < 0.05$ ). In the xenograft models with high-FR $\alpha$  expression, the maximum concentration of intratumor eribulin was 10-fold higher with MORAb-202 treatment, when dosed at equivalent eribulin levels, than with eribulin treatment alone. Also in the xenograft models with high-FR $\alpha$ -expression, with eribulin treatment, the maximum concentration was reached within 12 hours after administration and was below the detection limit at 72 hours, while with MORAb-202 treatment, the concentration was almost saturated 24 hours after administration and remained so until 144 hours after administration.

**Conclusions:** MORAb-202 notably increased intratumor accumulation and sustained tumor-release of eribulin (payload) compared with dosed eribulin alone. Thus, MORAb-202 is expected to have a more-potent antitumor effect compared with eribulin alone.

#### Conflict of interest:

Corporate-sponsored Research: Eisai Inc. - Shigehiro Koganemaru  
Other Substantive Relationships: Employees of Eisai Inc. - Keiji Furuuchi and Toshimitsu Uenaka

#### 243 (PB023) Evaluation of in vitro/in vivo bystander effect and immunogenic cell death induction by MORAb-202 (farletuzumab ecteribulin)

K. Furuuchi<sup>1</sup>, J. Fulmer<sup>1</sup>, K. Rybinski<sup>1</sup>, A. Soto<sup>1</sup>, B. Drozdowski<sup>1</sup>, T. Uenaka<sup>1</sup>. <sup>1</sup>Eisai Inc., Epochal Precision Anti-Cancer Therapeutics EPAT, Exton, USA

**Background:** MORAb-202 is an antibody–drug conjugate (ADC) consisting of farletuzumab, a humanized anti-folate receptor-alpha (FR $\alpha$ ) monoclonal antibody, conjugated to eribulin as a payload. MORAb-202 targets eribulin to tumor cells expressing FR $\alpha$  and is being investigated in clinical trials in patients with solid tumors. In the dose-escalation part of a first-in-human phase 1 study, partial response was observed beginning at MORAb-202 0.3 mg/kg. To evaluate the antitumor activity of MORAb-202, we investigated its biological mechanism, focusing on its bystander effect and ability to induce immunogenic cell death (ICD).

**Methods:** The bystander effect of MORAb-202 was further characterized in an *in vitro* coculture system of the FR $\alpha$ - HL60 and FR $\alpha$ + IGROV1 cell lines. Analyses included: 1) different ratios of FR $\alpha$ - cells from ~0.5–2-fold against FR $\alpha$ + cell line; 2) time-dependent bystander effect from 48 to 96 hours; 3) cell cytotoxicity of the FR $\alpha$ - cells in the presence of supernatant recovered from coculture condition; 4) bystander effect of anti-FR $\alpha$ -sulfopSPDB-DM4 (FR $\alpha$ -DM4). *In vitro* induction of ICD by eribulin and by MORAb-

202 was examined in breast cancer (BC) cell lines. In vivo ICD induction was examined in OV CDx and TNBC PDx models. Post-dose tumor samples from OV CDx and TNBC PDx models were analyzed by IHC/IF staining against HMGB1, HSP90, and F4/80 as ICD markers.

**Results:** A consistent in vitro bystander effect of MORAb-202 was observed from 48 to 96 hours. Endpoint supernatant recovered from the coculture exhibited cell cytotoxicity in FR $\alpha$ - cells, suggesting that released eribulin is liable for the observed bystander effect. FR $\alpha$ -DM4 failed to induce a bystander effect; its off-target effect was greater than MORAb-202. Both eribulin and MORAb-202 elicited in vitro ICD induction of calreticulin and HMGB1 in human BC cell lines.

In in vivo studies, MORAb-202 (12.5 mg/kg) treatment on OV CDx had durable tumor shrinkage; eribulin treatment (1.0 mg/kg) showed tumor regrowth. HSP90 staining from MORAb-202- and eribulin-treated tumors showed enhanced intensity from day 1 after treatment, while no HSP90 enhancement was observed in vehicle-treated tumor. HMGB1 staining from MORAb-202- and eribulin-treated tumors showed intensified cytoplasmic and membrane translocation from the nuclei, from day 1; no translocation of HMGB1 staining was observed in vehicle control. A lower dose of MORAb-202 (5 mg/kg) in TNBC PDx was examined, and enhanced staining and translocation of HMGB1 in all tumors treated with MORAb-202 was observed. Additionally, MORAb-202 treatment-accumulated macrophages (F4/80) were found in tumors.

**Conclusion:** MORAb-202 exhibited a strong in vitro bystander effect with a limited off-target effect, while FR $\alpha$ -DM4 failed to show a bystander effect with a higher off-target effect. MORAb-202 induced ICD in both in vitro and in vivo settings.

#### Conflict of interest:

Other Substantive Relationships: Employees of Eisai Inc. - Brian Drowdzowski, James Fulmer, Keiji Furuuchi, Katherine Rybinski, Allis Soto, and Toshimitsu Uenaka

244

(PB024)

#### Phase I Biomarker Analysis Results of MORAb-202 (Farletuzumab Ecterbibulin) Effects on Vascular Remodeling and Immune Modulation in Patients With Ovarian Cancer

Y. Zhang<sup>1</sup>, S. Li<sup>1</sup>, T. Uenaka<sup>2</sup>, K. Furuuchi<sup>2</sup>, K. Yonemori<sup>3</sup>, T. Shimizu<sup>4</sup>, S. Nishio<sup>5</sup>, M. Yunokawa<sup>6</sup>, K. Matsumoto<sup>7</sup>, K. Takehara<sup>8</sup>, K. Hasegawa<sup>9</sup>, Y. Hirashima<sup>10</sup>, H. Kato<sup>11</sup>, Y. Otake<sup>12</sup>, T. Miura<sup>12</sup>, J. Matsui<sup>13</sup>. <sup>1</sup>Eisai Inc., Department of Translational Science, Nutley, USA; <sup>2</sup>Eisai Inc., Epochal Precision Anti-Cancer Therapeutics EPAT, Exton, USA; <sup>3</sup>National Cancer Center Hospital, Department of Breast and Medical Oncology, Tokyo, Japan; <sup>4</sup>National Cancer Center Hospital, Department of Experimental Therapeutics, Tokyo, Japan; <sup>5</sup>Kurume University School of Medicine, Department of Obstetrics and Gynecology, Fukuoka, Japan; <sup>6</sup>Cancer Institute Hospital, Department of Gynecologic Oncology, Tokyo, Japan; <sup>7</sup>Hyogo Cancer Center, Division of Medical Oncology, Hyogo, Japan; <sup>8</sup>National Hospital Organization Shikoku Cancer Center, Department of Gynecologic Oncology, Ehime, Japan; <sup>9</sup>Saitama Medical University International Medical Center, Department of Gynecologic Oncology, Saitama, Japan; <sup>10</sup>Shizuoka Cancer Center, Department of Gynecology, Shizuoka, Japan; <sup>11</sup>Hokkaido Cancer Center, Department of Gynecologic Oncology, Hokkaido, Japan; <sup>12</sup>Eisai Co. Ltd., Department of Japan and Asia Clinical Development, Tokyo, Japan; <sup>13</sup>Eisai Inc., Oncology Business Group, Nutley, USA

**Background:** MORAb-202 is an antibody–drug conjugate consisting of the humanized anti-folate receptor-alpha (FR $\alpha$ ) monoclonal antibody, farletuzumab, and the potent microtubule dynamics inhibitor, eribulin. It is highly stable in systemic circulation and releases eribulin in the targeted cells. While MORAb-202 is cytotoxic to FR $\alpha$ -expressing cancer cells, it also exerts cytotoxic bystander effects on adjacent tumor and stromal cells, as well as noncytotoxic bystander effects on the tumor microenvironment (TME) in preclinical models. Eribulin was reported to modulate the TME to potentially enhance antitumor activity via effects such as vascular remodeling in both preclinical and clinical studies. One purpose of this exploratory biomarker study was to evaluate MORAb-202-induced pharmacological effects in patients with ovarian cancer (OC) to examine its clinical mechanism of action (MoA).

**Methods:** In Study 101 (NCT03386942), 94 exploratory serum protein markers were analyzed in samples from 58 patients with OC. Samples were collected predose on day 1 of treatment cycles 1–6 and at the end of treatment; then analyzed using Luminex or Simoa assays. Any markers that had >30% of data points out of analytical ranges were excluded from the analysis. For each marker at each time point, percentage changes from

baseline value were computed and 1-sample Wilcoxon signed-rank test was used to evaluate statistical significance.

**Results:** Of 94 markers assessed, 54 were significantly altered versus baseline at  $\geq 1$  timepoint post-MORAb-202 dosing ( $P < 0.05$ ), including endothelial cell markers and other factors with functions in vascular remodeling (eg, increases in endoglin, ICAM1, PECAM-1, TIE-2, PLGF, SDF-1, VEGF, VEGF-D, VCAM-1, MMP3, and PDGF-BB; decreases in ANG-2 levels). The data provide evidence of vascular remodeling with MORAb-202 and are consistent with effects in the TME reported with eribulin and changes of vascular remodeling serum biomarkers in patients treated with the liposomal formulation of eribulin. Further, many markers altered after MORAb-202 dosing were associated with immune responses such as IFN $\gamma$ -mediated responses and macrophage activation (eg, increases in IP-10, MIP-1 $\beta$ , RANTES, IL-18, IL-12p40, IL-6, BLC, TARC, and PARC; decreases in MCP-1 levels).

**Conclusions:** These biomarker changes are suggestive of vascular remodeling by MORAb-202 in patients with OC, causing a possible noncytotoxic bystander effect secondary to released eribulin or soluble factors in the TME. MORAb-202 treatment may also potentially modulate immune responses in patients. Further research is being carried out in the MORAb-202 201 study (NCT04300556) to explore the MoA of MORAb-202.

#### Conflict of interest:

Advisory Board: Kan Yonemori - Novartis, Eisai, AstraZeneca, Chugai, Takeda, Genmab, OncXerna.

Corporate-sponsored Research: Kan Yonemori - Research support (to institution): MSD, Daiichi-Sankyo, Astrazeneca, Taiho, Pfizer, Novartis, Takeda, Chugai, Ono, Sanofi, Seattle Genetics, Eisai, Eli Lilly, Genmab, Boeringer Ingelheim, Kyowa Hakko Kirin, Nihon Kayaku, Haihe. Toshio Shimizu - Research funding: Novartis, Eli Lilly, Daiichi-Sankyo, AbbVie, Bristol-Myers Squibb, Eisai, AstraZeneca, Pfizer, Loxo Oncology, Takeda Oncology, Incyte, Chordia Therapeutics, 3D-Medicine, Symbio Pharma. Mayu Yunokawa - Research funding: MSD, Eisai, AstraZeneca, Merck, Chugai Pharma, NanoCarrier, Takeda. Koji Matsumoto - Research funding: Daiichi Sankyo, MSD, Novartis, ICON Clinical Research, Chugai Pharma, AstraZeneca, Ono Pharmaceutical, ICON Clinical Research, Eli Lilly SA. Kosei Hasegawa - Research funding: Ono Pharmaceutical, Daiichi Sankyo, Merck.

Other Substantive Relationships: Employees of Eisai, Inc. - Keiji Furuuchi, Shuyu Li, Junji Matsui, Toshimitsu Uenaka and Yan Zhang. Employees of Eisai Co. Ltd. - Yohei Otake and Takuma Miura. Kan Yonemori - Honorarium for lecture: Pfizer, Eisai, AstraZeneca, Eli Lilly, Takeda, Chugai, Fuji Film Pharma, MSD, Boeringer Ingelheim, Ono, Daiichi-Sankyo. Toshio Shimizu - Consultancy/Advisory: AbbVie, Daiichi-Sankyo, Takeda Oncology. Speakers' bureau: Eli Lilly, AbbVie, Chugai Pharmaceutical Co., Taiho, InvesntisBio. Mayu Yunokawa - Honorarium: MSD, Eisai, AstraZeneca, Merck, Chugai Pharma, Takeda. Koji Matsumoto - Honorarium: Chugai Pharma, MSD, Kyowa Kirin, Takeda, Pfizer, Kaken Pharmaceutical, Eli Lilly SA. Kosei Hasegawa - Consultancy: MSD K.K, Kaken Pharmaceutical. Honorarium: MSD K.K, Daiichi Sankyo, Chugai Pharma, AstraZeneca, Eisai, Kyowa Kirin, Takeda. Yasuyuki Hirashima - Speaker's bureau: Chugai Pharma, Takeda, MSD, AstraZeneca.

245

(PB025)

#### Archival vs fresh tumor samples for assessing the gene expression of NaPi2b and immune-related genes in the Phase 1b study of Upifitab Rilsodotin (UpRi) in platinum-resistant ovarian cancer

M. Lu<sup>1</sup>, P. Shaw<sup>1</sup>, D. Richardson<sup>2</sup>, E. Hamilton<sup>3</sup>, P. Bernardo<sup>4</sup>, C. Bradshaw<sup>5</sup>, A. Tolcher<sup>6</sup>, R. Mosher<sup>1</sup>. <sup>1</sup>Mersana Therapeutics, Translational Medicine, Cambridge, USA; <sup>2</sup>Stephenson Cancer Center- OU Health, Gynecologic Oncology, Oklahoma City, USA; <sup>3</sup>Sarah Cannon Research Institute-Tennessee Oncology, Gynecologic Oncology, Nashville, USA; <sup>4</sup>Mersana Therapeutics, Biometrics, Cambridge, USA; <sup>5</sup>Mersana Therapeutics, Biostatistics, Cambridge, USA; <sup>6</sup>NEXT Oncology, Clinical Research, San Antonio, USA

**Background:** Upifitab rilsodotin (UpRi; XMT-1536) is an investigational first-in-class antibody drug conjugate (ADC) targeting NaPi2b, a sodium-dependent phosphate transport protein broadly expressed in solid tumors and in approximately two-thirds of high-grade serous ovarian cancer (HGSOC) patients, with limited expression in normal tissue. Efficacy and safety data from a Phase 1b single-agent trial of UpRi in HGSOC was presented earlier this year (Richardson et al, SGO 2022). Archival tumor tissue and/or fresh biopsy (if medically feasible) were collected in this Ph 1 trial (NCT03319628) to compare the gene expression levels of NaPi2b and other genes of interest in archival vs fresh tumor samples in patients with platinum-resistant ovarian cancer.

**Material and methods:** Gene expression was analyzed by Nanostring (770 immune-focused genes from IO360 panel + 30 customized ADC-

related genes). The gene expression data were available in 92 archival tumor samples with 89 samples collected from non-lymph node locations and 40 fresh tumor samples with 22 samples collected from non-lymph node locations. Data from paired archival and fresh samples were available in 22 patients, of which 12 pairs were collected from non-lymph node locations. Students' t-tests were used in the statistical analysis.

**Results:** Differential gene expression profiles between samples collected from lymph node and non-lymph node locations were observed. The gene expression level of NaPi2b/SLC34A2 was not different between archival and fresh tumor samples. Excluding samples collected from lymph node, genes involved in antigen presentation showed decreased expression in fresh tumors compared to archival tumors.

**Conclusions:** The RNA level of NaPi2b remains stable between archival and fresh samples, suggesting that NaPi2b is a lineage marker whose expression level may not change over time and that a new biopsy may not be required for the determination of NaPi2b status, sparing patients from risks associated with repeated sample collection. Antigen presentation genes showed decreased expression in fresh samples, suggesting tumors may evade immune surveillance during disease progression. Clinical trial information: NCT03319628.

**Conflict of interest:**

Advisory Board: Debra Richardson  
Corporate-sponsored Research: Anthony Tolcher  
Other Substantive Relationships: Min Lu, Pamela Shaw, Patti Bernardo, Chelsea Bradshaw, Rebecca Mosher are employees of Mersana Therapeutics.

**246** (PB026)

**The anti-CD205 antibody drug conjugate MEN1309/OBT076 shows synergistic activity in combination with the monoclonal antibody rituximab in diffuse large B cell lymphomas**

C. Tarantelli<sup>1</sup>, E. Civanelli<sup>1</sup>, E. Gaudio<sup>1</sup>, A. Stathis<sup>2</sup>, G. Merlino<sup>3</sup>, M. Binaschi<sup>4</sup>, F. Bertoni<sup>5</sup>. <sup>1</sup>Faculty of Biomedical Sciences- USI, Institute of Oncology Research, Bellinzona, Switzerland; <sup>2</sup>Ente Ospedaliero Cantonale, Oncology Institute of Southern Switzerland, Bellinzona, Switzerland; <sup>3</sup>Menarini Group, Menarini Ricerche S.p.A, Firenze, Italy; <sup>4</sup>Menarini Group, Menarini Ricerche S.p.A, Florence, Italy; <sup>5</sup>Institute of Oncology Research, Institute of Oncology Research, Bellinzona, Switzerland

**Background:** MEN1309/OBT076 is an antibody drug conjugate (ADC) consisting of an anti-CD205 monoclonal antibody (moAb) conjugated to the DM4 maytansine derivative via a cleavable N-succinimidyl-4-(2-pyridyldithio) butanoate linker (Merlino et al, 2019), currently in phase 1 (NCT04064359). CD205 expression is prevalent in different tumor types, including hematological malignancies, where MEN1309 has potent *in vitro* and *in vivo* anti-tumor activity (Gaudio et al, 2020). Here, we extend the observed synergism the anti-CD20 moAb rituximab (Gaudio et al, 2020), using a schedule with lower dose of MEN1309.

**Materials and Methods:** Xenografts were established by injecting OCI-LY-10 lymphoma cells ( $15 \times 10^6$  cells/mouse) into the left flanks of female NOD-SCID mice. Mice were divided in 4 groups of 6 animals each and were treated with MEN1309 (1 mg/kg IV, D1, 12, 21, 28), or rituximab (5 mg/kg IV, same days as MEN1309), or MEN1309 plus rituximab (M+R; same schedule as single agents; MEN1309 2.5 mg/kg IV plus rituximab 5 mg/kg IV at D37, D50), or with vehicle only (IV, as single agents). Three mice per group were sacrificed 4 h after the first treatment (early termination), and processed for the expression of CD20 and CD205 by immunoblotting.

**Results:** Single agents and combinations (MEN1309, rituximab, M+R) were more active than controls, with M+R as the most active. No statistically significant differences could be observed in terms of tumor weight, but after D35 only mice treated with M+R were still alive ( $P < 0.001$ ). All single agents and control groups had to be sacrificed at earlier time points due to tumor volumes beyond the limit of 2000 mm<sup>3</sup>. Treatments were well tolerated by mice and body weight loss was not detected.

Differently from previous *in vitro* results (Gaudio et al, 2020), both CD205 and of CD20 protein levels in the xenografts decreased 4 h after the first dose of MEN1309, rituximab and M+R compared to control. The strongest decrease was seen in M+R for CD205 and with MEN1309 and M+R for CD20. A downregulation of CD20 and CD205 was also observed in xenografts taken at the end of the previous experiment with higher dose of MEN1309 2.5 mg/kg plus rituximab 5 mg/kg.

**Conclusions:** The *in vivo* experiment based on a low dose of MEN1309 (1 mg/Kg) showed an increased survival for animals treated with the combination M+R, in line with previously reported benefit using higher dose of MEN1309 (2.5 mg/Kg). In immunoblotting analyses of xenografts samples, a downregulation of CD205 and CD20 was observed, especially after exposure to M+R, suggesting that the treatments might lead to

degradation of their target receptors, perhaps due to ubiquitination as reported with anti-Her2 antibodies and with rituximab itself.

**Conflict of interest:**

Ownership: patent  
Corporate-sponsored Research: Menarini Ricerche S.p.A.  
Other Substantive Relationships: Employment (Menarini Group)

**247** (PB027)

**Preclinical studies of the bispecific MUC1xEGFR antibody drug conjugate M1231 in EGFR mutant NSCLC**

J. Codony-Servat<sup>1</sup>, J. Dotterweich<sup>2</sup>, M.A. Molina-Vila<sup>1</sup>, R. Román<sup>1</sup>, A. Giménez-Capitán<sup>1</sup>, E. Aldeguer<sup>1</sup>, S. Rodríguez<sup>1</sup>, C. Kneuhl<sup>2</sup>, R. Rosell<sup>3</sup>. <sup>1</sup>Pangaea Oncology- Quirón-Dexeus University Hospital, Oncology Laboratory, Barcelona, Spain; <sup>2</sup>Merck Healthcare KGaA, TIP Oncology & Immuno-Oncology, Darmstadt, Germany; <sup>3</sup>Hospital Germans Trias i Pujol, Cancer Biology & Precision Medicine Program Laboratory, Badalona, Spain

**Background:** M1231 is a bispecific antibody drug conjugate (ADC) targeting tumor-associated mucin 1 (MUC1) and epidermal growth factor receptor (EGFR). Concurrent binding leads to ADC internalization and trafficking to lysosomes where the hemisterlin-related cytotoxic payload is enzymatically cleaved from the ADC. The released payload interferes with microtubule dynamics and subsequently kills the tumor cells.

EGFR kinase activating mutations are common in non-small cell lung cancer (NSCLC) adenocarcinoma and resistance to EGFR tyrosine kinase inhibitors (TKIs) frequently develops in patients with NSCLC that expresses mutant EGFR. MUC1 and EGFR are both overexpressed in NSCLC. Therefore, the bispecific MUC1xEGFR ADC M1231 may be an effective treatment option for patients with EGFR mutant NSCLC and high unmet medical need.

**Material and Methods:** Cell viability was analyzed after M1231 treatment in EGFR mutant NSCLC cell lines, including TKI resistant lines, using an assay measuring cell metabolic activity. The effect of M1231 on cell cycle was investigated using fluorescence-activated single cell sorting and western blotting. MUC1 and EGFR expression was analyzed by western blotting and immunohistochemistry (IHC). In addition, cell viability was evaluated after the combination of M1231 with the EGFR-TKIs afatinib or osimertinib.

NSCLC patient samples (pre-treatment and/or after EGFR-TKI treatment progression) were analyzed by IHC for MUC1 and EGFR expression.

**Results:** M1231 potentially inhibited cell viability of EGFR mutant and TKI resistant NSCLC cell lines with subnanomolar to single digit nanomolar IC<sub>50</sub> values. According to DNA content analysis and western blotting, M1231 treatment led to an arrest at G2/M phase that was accompanied by an increase in phospho-histone H3 levels. The combination of afatinib or osimertinib with M1231 enhanced inhibition of cell viability in several cell lines.

Most of the NSCLC tumor samples from patients prior to and post EGFR-TKI treatment relapse showed MUC1 and EGFR protein expression by IHC.

**Conclusions:** M1231 induces G2/M arrest and potentially inhibits cell viability in a range of EGFR mutant NSCLC cell lines, including those resistant to TKIs. MUC1 and EGFR were consistently expressed in NSCLC tumors after EGFR-TKI relapse. These findings indicate that NSCLC patients developing EGFR-TKI resistance under treatment may benefit from a bispecific MUC1xEGFR ADC like M1231.

**Conflict of interest:**

Corporate-sponsored Research: Jordi Codony-Servat, Miguel Angel Molina-Vila, Ruth Román, Ana Giménez-Capitán, Erika Aldeguer, Sonia Rodríguez, Rafael Rosell  
Other Substantive Relationships: Julia Dotterweich is employee of Merck Healthcare KGaA, Darmstadt, Germany shareholder of Merck KGaA. Christine Kneuhl is employee of Merck Healthcare KGaA, Darmstadt Germany shareholder of Merck KGaA and Aveo Oncology.



248

(PB028)

### Design and development of an innovative, safe, and highly potent E1 ubiquitin-activating enzyme inhibitor CPL-410-005 conjugate in anticancer therapy

F. Mitula<sup>1</sup>, M. Równicki<sup>1</sup>, J. Pieczykolan<sup>1</sup>, T. Kornatowski<sup>1</sup>, M. Marczak<sup>1</sup>, A. Moroz<sup>2</sup>, P. Pietrow<sup>2</sup>, M. Mroczkiewicz<sup>2</sup>, R. Piast<sup>1</sup>, D. Dąbrowski<sup>1</sup>, M. Górka<sup>1</sup>, O. Abramczyk<sup>1</sup>, M. Wieczorek<sup>3</sup>, D. Popiel<sup>1</sup>. <sup>1</sup>Celon Pharma S.A., Preclinical Department, Kazuń Nowy, Poland; <sup>2</sup>Celon Pharma S.A., Medicinal Chemistry Department, Kazuń Nowy, Poland; <sup>3</sup>Celon Pharma S.A., Pre- and Clinical Department, Kazuń Nowy, Poland

**Introduction:** Targeting ubiquitin-proteasome system (UPS) has emerged as a rational approach in the treatment of human cancer. The therapeutic potential of this pathway has been validated by the clinical successes of bortezomib – the first proteasome inhibitor drug implemented in the therapy of multiple myeloma and mantle cell lymphoma. However, the treatment of solid tumors remains challenging, mostly due to poor tumor-selective drug delivery and low therapeutic efficacy. Previously, we reported on the development of novel potential therapeutic – CPL-410-005 – a non-selective, cell permeable, inhibitor of ubiquitin-activating enzyme (E1). To allow specific targeting of CPL-410-005 to solid tumor cells and thus reduce off-target effects, we developed targeted antibody-drug conjugates (ADC) made from a humanized anti-HER2 antibody conjugated with derivatives of CPL-410-005.

**Material and method:** Two CPL-410-005 derivatives, CPL-410-077 and CPL-410-082, were designed and synthesized for preparation of ADCs. The general synthetic scheme incorporated a cleavable glycosidase-sensitive trigger unit to allow intracellular release of the final cytotoxic agent after endocytosis of the ADC. Conjugates of the anti-HER2 prepared with CPL-410-077 and CPL-410-082 were characterized *in vitro* for the interaction with the extracellular domain of human HER2 using a surface plasmon resonance and for stability in buffer and culture media using reversed phase chromatography–mass spectrometry (RP-HPLC). Next, their cytotoxicity and selectivity were evaluated in two human adenocarcinoma models with high expression of HER2: ovarian (SKOV-3) and breast (SKBR-3) using CellTiter-Glo 2.0 Assay. As a control we used human embryonic kidney cell line (HEK-293) with minimal HER2 expression.

**Results and discussion:** Yields obtained for bioconjugations were above 85%. Analytical characterization by denaturing RPLC–MS confirmed efficient conjugation and homogeneity of the conjugates. Conjugates showed improved cellular uptake, selectivity, and anticancer activity compared to unconjugated CPL-410-005 derivatives in the HER2 receptor overexpressing cancer cells. The cytotoxic activity was displayed only upon cleavage of the carbohydrate linker. Additionally, HEK293 cells were not affected by conjugates in concentrations required for cytotoxic effect in tested adenocarcinoma cell lines. This implies enhanced safety by reducing off-target side effects compared to free CPL-410-005 and unconjugated CPL-410-005 derivatives.

**Conclusion:** The anti-HER2-CPL-410-077 and anti-HER2-CPL-410-082 conjugates provide significant and selective antitumor effects against human adenocarcinoma. Presented results support further preclinical validation for the validation of anti-HER2-drug conjugates and ubiquitin-proteasome system inhibitors in cancer therapy.

**No conflict of interest.**

249

(PB029)

### Identification of Nectin-4 Specific Monoclonal Antibodies Using a High-throughput Flow Cytometry Screening System

L. Pincus<sup>1</sup>, A. Raghad<sup>1</sup>, M. Spear<sup>1</sup>, D. Austin<sup>1</sup>, K. Arias<sup>1</sup>, C. Gelber<sup>1</sup>. <sup>1</sup>Stromatis Pharma, Stromatis Pharma, Manassas, USA

**Background:** Nectin-4 has recently emerged as a highly valuable therapeutic target. This is due to its overexpression in epithelial cancers, including ovarian, breast, colorectal, lung, and pancreatic, while exhibiting limited expression in normal adult tissue. This overexpression is functionally significant for tumor progression, making Nectin-4 an ideal target for potential cancer therapeutics. Using a high-throughput flow cytometry-based antibody screening procedure, wherein antibody binding to native cell-expressed Nectin-4 is assessed concomitantly with off-target binding, multiple antibodies were identified. These antibodies will be used to generate novel antibody-drug conjugates (ADC) targeting Nectin-4 with significant therapeutic potential in Nectin-4-expressing cancers.

**Materials and Methods:** A Nectin-4 expressing cell line was established in HEK293 T cells by transduction with a Nectin-4 lentivirus, followed by limiting dilution cloning. In order to discriminate the Nectin-4 expressing cells by flow cytometry barcoding screening method, the HEK293T-Nectin-4 expressing cell population was stained with a fluorescently labeled

proliferation marker and then pooled with the non-labeled, non-expressing parental HEK293 T cells. To identify hybridomas secreting Nectin-4 antibodies, hybridoma supernatant was added to a mixed population of Nectin-4<sup>+</sup> and Nectin-4<sup>-</sup> cells and detected using a fluorescently labeled mouse-specific secondary antibody. Positive hybridoma clones were identified based on the selective staining of only the HEK293T-Nectin-4 positive population. This method eliminates antibodies that target non-specific cell-surface antigens by identifying hybridomas that nonspecifically stain parental HEK293 T cells. A flow cytometer with autosampler capabilities was used for high-throughput screening.

**Results:** Utilization of this efficient screening method allowed the discrimination of thousands of hybridomas and identified numerous antibodies that recognize specific epitopes of the antigens expressed by live cells in their native conformation, eliminating antibodies to nonspecific cell surface antigens and non-native epitopes. Selected monoclonal antibodies will be further characterized and subsequently developed into antibody-drug conjugates directed against Nectin-4.

**Conclusion:** Several Nectin-4 targeting antibodies were identified using an antigen-expressing cell-based flow cytometry screening technique. This technique exclusively identifies high-specificity antibodies and is compatible with high-throughput screening. These results are significant given the recent emergence of Nectin-4 as a potential prognostic cell surface biomarker and promising therapeutic target in solid tumors.

#### Conflict of interest:

Ownership: Dr. Cohava Gelber is a founder of Stromatis Pharma and owns stock in the company.

Board of Directors: Dr. Cohava Gelber is co-chairperson of the Stromatis Pharma Board of Directors.

250

(PB030)

### Targeting acidosis to improve immunotherapy in a pancreatic ductal adenocarcinoma model

B. Victorasso Jardim Perassi<sup>1</sup>, D. Abrahams<sup>2</sup>, P. Irrera<sup>1</sup>, C. Whelan<sup>3</sup>, M. Beatty<sup>4</sup>, S. Byrne<sup>4</sup>, D. Longo<sup>5</sup>, K. Gaspa<sup>6</sup>, S. Pilon-Thomas<sup>4</sup>, A. Ibrahim Hashim<sup>1</sup>, C. Böhler<sup>6</sup>, R. Gillies<sup>1</sup>. <sup>1</sup>Moffitt Cancer Center, Cancer Physiology, Tampa, USA; <sup>2</sup>University of South Florida, Comparative Medicine, Tampa, USA; <sup>3</sup>University of Illinois, Biological Sciences, Chicago, USA; <sup>4</sup>Moffitt Cancer Center, Immunology, Tampa, USA; <sup>5</sup>Institute of Biostructures and Bioimages, National Research Council, Turin, Italy; <sup>6</sup>Helix BioPharma Corp., Helix BioPharma Corp., Toronto, Canada

**Background:** Solid tumors are acidic due to the combination of high rates of glycolysis with poor perfusion. The consequent establishment of the acidosis state leads to an immunosuppressive mechanism in the tumor microenvironment, inhibiting T-cell activation and leading to tumor growth. We previously showed that neutralization of tumor acidity using sodium bicarbonate could be additive or synergistic with checkpoint blockade (anti-PD1 and anti-CTLA4) in pre-clinical models. However, the buffer therapy phase I/IIa clinical trials failed due to poor patient compliance. Thus, the overall aim of the current work is to test clinically translatable alternative agents to bicarbonate to neutralize tumor acidity and improve pancreatic ductal adenocarcinoma (PDAC) response to immune checkpoint blockade. In this study, we test L-DOS47, a targeted urease immunoconjugate designed to directly neutralize tumor acidity that has been shown to be well-tolerated in phase I/IIa trials. L-DOS47 binds carcinoembryonic antigen cell adhesion molecule 6 (CEACAM6), a cell surface protein highly expressed in GI and lung cancers, which allows urease to cleave endogenous urea into two NH<sub>4</sub><sup>+</sup> and one CO<sub>2</sub> and raise local pH.

**Material and Methods:** Immunocompetent mice were inoculated orthotopically with KPC961 cells transfected to express human CEACAM6, and after 7 days, mice were randomized into groups with equal tumor volume averages to initiate therapies. Mice were treated with anti-PD1 (300 µg/twice a week) in combination with L-DOS47 (90 µg/kg/twice a week) or bicarbonate (200 mmol/L chronically in drinking water). Control groups included L-DOS47, bicarbonate, and anti-PD1 monotherapies, in addition to the no therapy group. Tumor volumes were measured weekly by ultrasound imaging. Two experimental designs were performed to assess therapies efficacy: First by monitoring tumor growth changes up to day 28, and second by analyzing overall survival with an endpoint tumor volume of 750 mm<sup>3</sup>.

**Results:** Combination of L-DOS47 or bicarbonate with anti-PD1 showed great efficacy in delaying tumor growth and tumor regression was observed in both therapy groups. Survivorship comparisons using Log-Rank test showed a survival benefit for anti-PD1 compared to control (p = 0.003), bicarbonate (p = 0.01) and L-DOS47 (P = 0.04), and for bicarbonate+anti-PD1 compared to control (p = 0.01). However, the greatest survival benefit was observed for the L-DOS47+anti-PD1 group, with 50% of mice alive 10 weeks after starting therapies, in comparison with 0% of mice alive in the control group (p =

0.0008), 12.55% in the L-DOS47 ( $p = 0.02$ ) and 40% in the anti-PD1 monotherapy group ( $p = 0.57$ ).

**Conclusion:** This study shows that neutralizing acidic tumor pH strengthens the response to immune checkpoint blockade in the PDAC model.

**No conflict of interest.**

251 (PB031)

**An exatecan derivative based linker-payload platform leads to ADC products with promising anti-tumor efficacy and potential low interstitial lung disease (ILD) risk**

S. Lin<sup>1</sup>, R. Shi<sup>2</sup>, B. Li<sup>1</sup>, Y. Qiu<sup>2</sup>, H. Hua<sup>1</sup>, Y. Zhang<sup>1</sup>. <sup>1</sup>Duality Biologics, Research and Development, Shanghai, China; <sup>2</sup>Duality Biologics, Research and Development, New Jersey, USA

**Background:** Camptothecins-based payload ADCs are attracting attentions as a promising anti-tumor modality. One of the most advanced linker-payload combinations approved and in development is Deruxtecan, which was used in a series of ADCs, including DS-8201, DS-1062, U3-1402, etc. These Dxd ADCs have shown clinical benefits in multiple solid tumors. However, life-threatening ILD can occur in 10–13% of patients treated with DS-8201. There is an interest to develop camptothecin-based ADCs that pose lower ILD risk.

**Material and Methods:** A novel linker-payload combination L101P1003 was developed, that consists of an exatecan derivative payload P1003, a tetrapeptide linker and a maleimide moiety. DB-1303 is a HER2 ADC composed of trastuzumab biosimilar conjugated with L101P1003. The *in vitro* activity of P1003 was evaluated in multiple cancer cell lines. The pharmacokinetics of P1003 was assessed *in vitro* and *in vivo*. The safety profile of P1003 was assessed in rats and monkeys. The *in vitro* and *in vivo* activity, pharmacokinetics as well as toxicity of DB-1303 in monkey were evaluated.

**Results:** P1003 showed comparable cellular activity as Dxd, 2–3-fold less potent in EC50. Unlike Dxd, P1003 is neither a substrate of cytochrome P450 enzymes, nor a substrate of BCRP or P-gP. DB-1303 showed comparable anti-proliferation activity to DS-8201 in HER2 high and medium cell lines (NCI-N87 and JIMT-1). In HER2 low PDX models, DB-1303 showed comparable efficacy to DS-8201 at the same doses. P1003 is well tolerated in animals. DB-1303 confirmed a highest non-severely toxic dose (HNSTD) of 80 mg/kg without any observation of ILD related features in pulmonary tissues in cynomolgus. Literature reports indicated that the pulmonary observations in toxicology study in cynomolgus were highly correlated with the ILD in clinic and were suspected to be related with the non-specific internalization and Dxd release in macrophages infiltrated into pulmonary tissues. To explain if the differences in toxicological findings between DB-1303 and DS-8201 are due to the difference in payload release profile, a tumor cell culture assay was developed. After incubation of the ADCs with tumor cells or monocytes at the same concentration for 48 hours, the free payload level in the culture media was detected by LC-MS/MS. In a HER2 high expressing NCI-N87 cell line, the payload level of DB-1303 was comparable to DS-8201, while in a monocyte cell line, THP-1, much lower payload release was observed for DB-1303 than DS-8201. In addition, compared to DS-8201, DB-1303 was much more stable in human plasma in a 14-day experiment.

**Conclusions:** The differences in ADC plasma stability and payload release profile from non-specific tissue may partially explain the improved safety of ADCs with linker-payload L101P1003. Currently, DB-1303 is under clinical evaluation (ClinicalTrials.gov Identifier: NCT05150691).

**No conflict of interest.**

252 (PB032)

**DB-1303, a HER2-targeting ADC with a novel DNA topoisomerase I inhibitor, demonstrates a promising safety profile and anti-tumor efficacy with differentiation from DS-8201a**

S. Lin<sup>1</sup>, Y. Zhang<sup>1</sup>, B. Li<sup>1</sup>, R. Shi<sup>2</sup>, Y. Qiu<sup>2</sup>, H. Hua<sup>1</sup>. <sup>1</sup>Duality Biologics, Research and Development, Shanghai, China; <sup>2</sup>Duality Biologics, Research and Development, New Jersey, USA

**Background:** DB-1303 is a novel antibody-drug conjugate comprised of trastuzumab biosimilar, enzymatically cleavable peptide-linker, and a proprietary topoisomerase I inhibitor P1003. It is designed to have high plasma stability, low free payload in circulation and wide therapeutic index. Herein, we describe the preclinical profile of DB-1303, including efficacy, pharmacokinetics, and safety.

**Material and Methods:** *In vitro* cell growth inhibition and *in vivo* antitumor activities of DB-1303 were evaluated in several Her2-low tumor cell lines and xenograft models. Tumor-bearing mice were used to assess

pharmacokinetic and pharmacodynamic characteristic of DB-1303. The mechanism of action for the efficacy was also evaluated. Plasma stability of DB-1303 was determined with rat, monkey, and human plasma. Pharmacokinetic and safety profiles of DB-1303 were evaluated in cynomolgus monkeys.

**Results:** *In vitro*, DB-1303 selectively binds to and is endocytosed into the lysosome of HER2-positive cells. DB-1303 causes G2/M cell cycle arrest, induces DNA damage, and inhibits cell proliferation in HER2-expressing cells. Importantly, DB-1303 showed inhibitory activity to Her2 low-expressing CAPAN-1 (pancreatic cancer) and Ishikawa (endometrial cancer) cell lines. Under a coculture condition of HER2-positive KPL-4 cells and HER2-negative MDA-MB-468 cells *in vitro*, DB-1314 inhibited the proliferation of both cells, demonstrating its bystander effect.

*In vivo*, DB-1303 induced dose-dependent tumor growth inhibition and tumor regression in T-DM1-resistant JIMT-1 xenograft model, HER2 low-expressing Ishikawa xenograft and two HER2-low breast cancer PDX models. A single dosing of DB-1303 in NCI-N87 tumor-bearing mice induced significant DNA damage in tumors, and the  $C_{max}$  of payload in tumor tissues was about 45-fold higher than that in peripheral blood.

Pharmacokinetics and safety profiles of DB-1303 were favorable and the highest non-severely toxic dose was 80 mg/kg in cynomolgus monkey study with Q3W dosing of 3 repeated doses. It's worth noting that, unlike DS-8201a, no interstitial pneumonia was observed in monkeys during the dosing period and recovery period. The payload P1003 poses very low risk of drug-drug interaction. Following administration of DB-1303, systemic P1003 exposure was low and P1003 was cleared rapidly.

**Conclusions:** DB-1303 exhibited potent antitumor activity in both HER2 positive and HER2 low tumor models with a wide therapeutic window. The stable linker in circulation and fast clearance of P1003 may contribute to the superior safety profile of DB-1303. These studies suggest the potential of DB-1303 to address unmet medical needs in HER2 expressing cancers, especially in HER2 low cancers. At the time of presentation, a first-in-human phase 1/2 study in patients with advanced solid tumors is in progress (NCT05150691).

**No conflict of interest.**

253 (PB033)

**The Trop-2-targeting antibody drug conjugate DB-1305 has higher anti-tumor activity and a potentially better safety profile compared with DS-1062**

Y. Zhang<sup>1</sup>, B. Li<sup>1</sup>, R. Shi<sup>2</sup>, Y. Qiu<sup>2</sup>, C. Zhong<sup>1</sup>. <sup>1</sup>Duality Biologics, Research and Development, Shanghai, China; <sup>2</sup>Duality Biologics, Research and Development, New Jersey, USA

**Background:** Trop-2 is a well validated oncology therapeutic target. DB-1305 is an antibody drug conjugate designed by conjugating an anti-Trop-2 antibody with a novel topoisomerase I inhibitor P1021 via an enzymatically cleavable tetrapeptide linker.

**Material and Methods:** To characterize DB-1305 and the payload P1021, thorough studies were performed including *in vitro* functional assays, *in vivo* efficacy and PK/PD studies with murine CDX models, as well as PK/TK and GLP toxicity studies in monkeys and rats.

**Results:** The results show that *in vitro*, DB-1305 selectively bound to Trop-2-positive cells and was endocytosed into their lysosomes. DB-1305 led to Trop-2-dependent cytotoxicity in Trop-2-expressing cells but not Trop-2-negative cells in a concentration-dependent manner. DB-1305 demonstrated tumor cell proliferation inhibition activities comparable to or stronger than DS-1062 produced in-house, as well as intriguingly displayed a stronger bystander killing effect.

*In vivo*, DB-1305 showed strong anti-tumor activity in mouse models of MDA-MB-468, COLO205 and DMS-53, with significantly higher efficacy compared with DS-1062. In Trop-2 negative SHP77 model, DB-1305 did not suppress tumor growth, indicating the dependence of DB-1305 activity on Trop-2 expression. The PK/PD study performed by treatment of DB-1305 in the MDA-MB-468 model demonstrated substantially increased ratios of P1021 exposure (AUC) to the exposure of DB-1305-total antibody or DB-1305-ADC in the tumor than in serum, suggesting that P1021 is effectively released in the tumor.

The pharmacokinetics parameters of DB-1305 (total antibody, ADC, and released payload) were obtained from the PK/TK studies in monkeys. The PK/TK profile of P1021 was assessed in rats in addition to the PK/TK study of DB-1305 in monkeys. The exposure levels of DB-1305 and P1021 had no obvious gender difference and no apparent accumulation in monkeys and rats. The systemic exposure  $AUC_{0-last}$  and  $C_{max}$  of ADC showed similar values to those of total antibody, and both parameters were increased approximately dose proportionally from 1 mg/kg to 10 mg/kg. Particularly, in monkeys, the peak concentration of P1021 in the DB-1305 10 mg/kg group was reduced to 1/171 compared with the P1021 0.14 mg/kg (equivalent to

the molar mass of P1021 in 10 mg/kg DB-1305), while the  $t_{1/2}$  was prolonged from 0.651 h to 194 h. DB-1305 was well tolerated in the GLP toxicity studies in Cynomolgus monkeys with the highest non-severely toxic dose (HNSTD) of 80 mg/kg, which is significantly higher than HNSTD of 30 mg/kg for DS-1062.

**Conclusions:** Taken together, this study has demonstrated higher efficacy and a potentially better safety profile of DB-1305 compared with DS-1062, supporting further clinical development of DB-1305 and indicating the great potential of DB-1305 in the treatment of Trop-2-positive cancers.

**No conflict of interest.**

255

(PB035)

**Efficacy and pharmacokinetics of EGFR-targeted antibody-drug conjugates following convection-enhanced delivery in mice with glioblastoma xenografts**

J. Sarkaria<sup>1</sup>, J. Griffith<sup>2</sup>, K. Porath<sup>3</sup>, J.H. Oh<sup>2</sup>, K. Bakken<sup>3</sup>, W. Zhang<sup>2</sup>, D. Burgenske<sup>3</sup>, T. Feldsien<sup>4</sup>, D. Lefebvre<sup>4</sup>, E. Reilly<sup>5</sup>, W. Elmquist<sup>2</sup>. <sup>1</sup>Mayo Clinic, Radiation Oncology, Rochester, Minnesota, USA; <sup>2</sup>University of Minnesota, Pharmaceutics- Brain Barrier Research Center, Minneapolis, MN, USA; <sup>3</sup>Mayo Clinic, Radiation Oncology, Rochester, MN, USA; <sup>4</sup>AbbVie Inc, Development Sciences, North Chicago, IL, USA; <sup>5</sup>AbbVie Inc, Discovery Oncology, North Chicago, IL, USA

**Purpose:** Antibody-drug conjugates (ADCs) provide specific delivery of potent toxins to cancers. Unfortunately, the clinical benefits of these powerful therapeutics have not been realized in glioblastoma (GBM). The blood brain barrier (BBB) in GBM can limit distribution of ADCs into tumor tissue. To bypass the BBB, we tested convection enhanced delivery (CED) infusion of ADCs into orthotopic GBM patient derived xenografts.

**Methods:** Two EGFR-targeted ADCs with a similar antibody backbone but different toxins were compared: depatuzumab mafodotin (Depatux-M) has a monomethyl auristatin F (MMAF) toxin, which is not cell permeant once released, and Losatuzumab vedotin (ABBV-221) has a cell permeant monomethyl auristatin E (MMAE) toxin. Efficacy was evaluated in three GBM PDX models with amplified/mutant EGFRviii. Bioluminescence imaging and survival were used to evaluate efficacy. MMAE levels were quantified using LC-MS/MS, and NeuN immunostaining was used to evaluate neuronal cell loss.

**Results:** Efficacy was compared across models following treatment with Depatux-M and ABBV-221 delivered in three serial CED infusions (21 days apart) or seven intraperitoneal (IP) injections (7 days apart). The median survivals by treatment group are shown in the table. For the two more mature studies, the data demonstrate a consistent enhancement in survival with CED infusion of Depatux-M (60 mg) or ABBV-221 (66 mg) as compared to IP injection (5 mg/kg). CED infusion of C57BL6 non-tumor bearing mice at the therapeutic dose levels of Depatux-M and ABBV-221 were well tolerated and had no impact on NeuN+ neuronal density. At much higher concentrations, CED of 740 mg Depatux-M also had no effect on Neu+ cell density, while CED with 274 mg ABBV-221 resulted in marked loss of NeuN+ cell density and lethal toxicity by 5 days. Following CED infusion of 570 ng of free MMAE, toxin levels were relatively stable over a four-hour sampling period with an AUC of 3860 ± 311 h\*ng/g in the infused right hemisphere compared to 2.4 ± 0.6 h\*ng/mL in plasma. A similar brain exposure profile was observed following CED of 60 mg ABBV-221 with AUC for total MMAE of 3073 ± 635 h\*ng/g and free MMAE of 311 ± 131 h\*ng/g. Surprisingly, relatively high plasma exposure was observed following CED with total MMAE of 2924 ± 449 h\*ng/mL, while free MMAE was below the limit of quantitation.

Treatment	Median survival, days		
	GBM6	GBM39	GBM108
AB095 – CED	49	20	NR
AB095-MMAF – CED	>80	58	18.5
Depatux-M – IP	57	68	NR
Depatux-M – CED	>80	>100	NR
AB095-MMAE – CED	57	19	NR
ABBV-221 – IP	53	>100	NR
ABBV-221 – CED	>80	>100	NR

**Conclusions:** CED of either Depatux-M or ABBV-221 can extend survival in EGFR amplified GBM PDXs. However, high concentrations of ABBV-221 are associated with increased neuronal cell loss and toxicity as compared to Depatux-M, suggesting a broader therapeutic window for the latter ADC.

**No conflict of interest.**

256

(PB036)

**A Phase 1 study of the anti-tissue factor antibody-drug conjugate XB002 in patients with advanced solid tumors (JEWEL-101): initial results from the dose-escalation stage**

S. Ulahannan<sup>1</sup>, M.L. Johnson<sup>2</sup>, H. Park<sup>3</sup>, A. Vandross<sup>4</sup>, S. Uttamsingh<sup>5</sup>, J. Li<sup>6</sup>, M. Syed<sup>7</sup>, A. Tolcher<sup>8</sup>. <sup>1</sup>Sarah Cannon Research Institute/Tennessee Oncology, Department of Hematology/Oncology, Nashville, TN, USA; <sup>2</sup>Sarah Cannon Research Institute/Tennessee Oncology, Department of Lung Cancer Research, Nashville, TN, USA; <sup>3</sup>Washington University, Department of Medicine, St Louis, MO, USA; <sup>4</sup>NEXT Oncology, Department of Medical Oncology, Austin, TX, USA; <sup>5</sup>Exelixis, Inc., Department of Clinical Science, Alameda, CA, USA; <sup>6</sup>Exelixis, Inc., Department of Clinical Pharmacology, Alameda, CA, USA; <sup>7</sup>Exelixis, Inc., Department of Clinical Development, Alameda, CA, USA; <sup>8</sup>NEXT Oncology, Department of Clinical Research, San Antonio, TX, USA

**Background:** XB002 is an antibody-drug conjugate (ADC) composed of a high-affinity tissue factor (TF)-directed human monoclonal antibody conjugated to a novel cytotoxic payload, Zymelink Auristatin. TF, a transmembrane protein, functions as a FVIIa receptor, initiating the extrinsic coagulation cascade. TF is also expressed in multiple tumor types. XB002 demonstrated antitumor activity in pre-clinical studies across multiple tumor types and did not perturb coagulation. Presented here are initial results from the dose-escalation stage of the JEWEL-101 study with XB002 in advanced solid tumors.

**Materials and methods:** This phase 1, open-label, multicenter, first-in-human trial (NCT04925284) consists of dose-escalation and tumor-specific cohort-expansion stages. Pts ≥18 years with advanced solid tumors and limited treatment options are being enrolled. Pts must have ECOG PS 0–1 and adequate organ function. In the dose-escalation stage, cohorts of 3–12 pts are being enrolled using an interval 3+3 design. The primary objective for this stage is to determine the maximum tolerated dose (MTD) and recommended dose (RD) of XB002.

**Results:** At cutoff on 13 May 2022, 15 pts were enrolled across four dose levels (XB002 IV Q3W): 0.16 mg/kg (n = 3); 0.5 mg/kg (n = 3); 1.0 mg/kg (n = 6); 1.5 mg/kg (n = 3). Median age was 63 years (range 45–79); 67% had an ECOG PS of 1. Median prior lines of non-radiation anticancer therapy was 3 (range 2–8). No dose-limiting toxicity was observed; an MTD/RD has not yet been determined. The most common reason for treatment discontinuation was radiographic progression (n = 8).

All pts had a treatment-emergent adverse event (TEAE), but no grade 4 or 5 TEAEs were seen. All 5 (33%) grade 3 TEAEs were unrelated to XB002. No bleeding events or peripheral neuropathy were observed.

All treatment-related AEs (TRAEs) were grade ≤2 and resolved prior to next dose: these included ocular toxicities (n = 2, grade 1 dry eyes and grade 2 conjunctivitis in the same pt at 1.0 mg/kg and grade 2 conjunctivitis at 1.5 mg/kg), fatigue and nausea (n = 2 each, all grade 1), and chills, peripheral edema, skin infection, and vomiting (n = 1 each, all grade 1). Two serious AEs unrelated to XB002 occurred with 1.0 mg/kg (COVID-19 pneumonia and diarrhea).

Pharmacokinetic (PK) analysis showed that XB002  $C_{max}$  and AUC increased with increasing dose. Total antibody and intact ADC PK were similar, suggesting XB002 is stable in vivo. Free payload levels were over 300-fold lower than intact ADC at all doses (<0.5 ng/mL).

**Conclusions:** XB002 Q3W was well tolerated at multiple dose levels with manageable TRAEs, all grade ≤2 including ocular toxicities, and no bleeding events or neuropathy. PK analysis revealed appropriate exposure with very low levels of free payload. Dose-escalation is ongoing and updated data will be presented.

**Conflict of interest:**

Ownership: Shailaja Uttamsingh, Jing Li, and Mustafa Syed: Exelixis. Anthony Tolcher: Pyxis (Inst).

Advisory Board: Susanna Ulahannan: Array BioPharma Bayer Eisai Incyte Syros Pharmaceuticals Exelixis. Research Funding - Abbvie (Inst) Adlai Nortye (Inst) ArQule (Inst) Astex Pharmaceuticals (Inst) AstraZeneca (Inst) atreca (Inst) Boehringer Ingelheim (Inst) Bristol-Myers Squibb (Inst) Celgene (Inst) CicloMed (Inst) Erasca, Inc (Inst) evelo biosciences (Inst) Exelixis (Inst) G1 Therapeutics (Inst) GlaxoSmithKline (Inst) Igm Biosciences (Inst) Incyte (Inst) Klus Pharma (Inst) MacroGenics (Inst) Merck (Inst) Mersana (Inst) OncoMed (Inst) Pfizer (Inst) Regeneron (Inst) Revolution Medicines (Inst) Synmore biologics (Inst) Takeda (Inst) Takeda (Inst) Tarveda Therapeutics (Inst) Tempest Therapeutics (Inst) Tesaro (Inst) Vigeo Therapeutics (Inst). Melissa Johnson: Abbvie (Inst) Amgen (Inst) Astellas Pharma (Inst) AstraZeneca (Inst) Axelia Oncology (Inst) Black Diamond Therapeutics (Inst) Boehringer Ingelheim (Inst) Bristol-Myers Squibb (Inst) Calithera Biosciences (Inst) CytomX Therapeutics (Inst) Daiichi Sankyo (Inst) EcoR1 Capital (Inst) Editas Medicine (Inst) Eisai (Inst) EMD Serono (Inst) G1 Therapeutics (Inst) Genentech/Roche (Inst) Genmab (Inst) GlaxoSmithKline

(Inst) Gritstone Bio (Inst) IDEAYA Biosciences (Inst) ITeos Therapeutics (Inst) Janssen Oncology (Inst) Lilly (Inst) Merck (Inst) Mirati Therapeutics (Inst) Oncorus (Inst) Regeneron (Inst) Ribon Therapeutics (Inst) Sanofi (Inst) Turning Point Therapeutics (Inst) WindMIL (Inst).

Anthony Tolcher: AbbVie (Inst) Aclaris Therapeutics (Inst) Adagene (Inst) Agenus (Inst) Aro Biotherapeutics (Inst) Asana Biosciences (Inst) Ascentage Pharma (Inst) Aximmune (Inst) Bayer (Inst) Biinvent (Inst) BluPrint Oncology (Inst) Boehringer Ingelheim (Inst) Daiichi Sankyo, Inc. (Inst) Deka Biosciences (Inst) Eleven Biotherapeutics (Inst) Elucida Oncology (Inst) EMD Serono (Inst) Gilde Healthcare (Inst) HBM Partners (Inst) HiberCell (Inst) IDEA Pharma (Inst) Ikena Oncology (Inst) Immunering (Inst) Immunome (Inst) Immunomet (Inst) IMPACT Therapeutics (Inst) Janssen (Inst) Jazz Pharmaceuticals (Inst) Karma Oncology (Inst) Lengo Therapeutics (Inst) Lilly (Inst) Mekanistic Therapeutics (Inst) Menarini (Inst) Mersana (Inst) Mirati Therapeutics (Inst) Nanobiotix (Inst) NBE Therapeutics (Inst) Ocellaris Pharma (Inst) Partner Therapeutics (Inst) Pelican Therapeutics (Inst) Pfizer (Inst) Pieris Pharmaceuticals (Inst) Pierre Fabre (Inst) Pyxis (Inst) Ryvu Therapeutics (Inst) Seattle Genetics (Inst) Senti Biosciences (Inst) SK Life Sciences (Inst) Sotio (Inst) Spirea (Inst) Sunshine Guojian (Inst) Transcenta (Inst) Transgene (Inst) Trillium Therapeutics (Inst) Vincerx Pharma (Inst) Zentalis (Inst) ZielBio (Inst) Zymeworks (Inst).

Corporate-sponsored Research: Melissa Johnson: Abbvie (Inst) Acerta Pharma (Inst) Adaptimmune (Inst) Amgen (Inst) Apexigen (Inst) Arcus Biosciences (Inst) Array BioPharma (Inst) Artios (Inst) AstraZeneca (Inst) Atreca (Inst) BeiGene (Inst) BerGenBio (Inst) BioAtla (Inst) Black Diamond Therapeutics (Inst) Boehringer Ingelheim (Inst) Calithera Biosciences (Inst) Carisma Therapeutics (Inst) Checkpoint Therapeutics (Inst) Corvus Pharmaceuticals (Inst) Curis (Inst) CytomX Therapeutics (Inst) Daiichi Sankyo (Inst) Dracen (Inst) Dynavax Technologies (Inst) Elicio Therapeutics (Inst) EMD Serono (Inst) Erasca, Inc (Inst) Exelixis (Inst) Fate Therapeutics (Inst) Genentech/Roche (Inst) Genmab (Inst) Genocera Biosciences (Inst) GlaxoSmithKline (Inst) Gritstone Bio (Inst) Guardant Health (Inst) Harpoon (Inst) Helsinn Healthcare (Inst) Hengrui Pharmaceutical (Inst) Hutchison MediPharma (Inst) IDEAYA Biosciences (Inst) IGM Biosciences (Inst) Immunocore (Inst) Impact Therapeutics (Inst) Incyte (Inst) Janssen (Inst) Jounce Therapeutics (Inst) Kadmon (Inst) Kartos Therapeutics (Inst) Lilly (Inst) Loxo (Inst) Lycera (Inst) Memorial Sloan-Kettering Cancer Center (Inst) Merck (Inst) Merus (Inst) Mirati Therapeutics (Inst) NeolmmuneTech (Inst) Neovia Oncology (Inst) Novartis (Inst) Numab (Inst) Nuvalent, Inc. (Inst) OncoMed (Inst) Pallean Pharmaceuticals (Inst) Pfizer (Inst) PMV Pharma (Inst) Rain Therapeutics (Inst) RasCal (Inst) Regeneron (Inst) Relay Therapeutics (Inst) Revolution Medicines (Inst) Ribon Therapeutics (Inst) Rubius Therapeutics (Inst) Sanofi (Inst) Seven and Eight Biopharmaceuticals (Inst) Shattuck Labs (Inst) Silicon Therapeutics (Inst) Stem CentRx (Inst) Syndax (Inst) Takeda (Inst) Tarveda Therapeutics (Inst) TCR2 Therapeutics (Inst) Tempest Therapeutics (Inst) Tizona Therapeutics, Inc. (Inst) Tmunity Therapeutics, Inc. (Inst) Turning Point Therapeutics (Inst) University of Michigan (Inst) Vyriad (Inst) WindMIL (Inst) Y-mAbs Therapeutics (Inst).

Haeseong Park: Ambrx (Inst) Amgen (Inst) Aprea Therapeutics (Inst) Array BioPharma (Inst) AstraZeneca (Inst) Bayer (Inst) BeiGene (Inst) BJ Bioscience (Inst) Bristol-Myers Squibb (Inst) Daiichi Sankyo (Inst) EMD Serono (Inst) Five Prime Therapeutics (Inst) Genentech (Inst) Gilead Sciences (Inst) GlaxoSmithKline (Inst) Gossamer Bio (Inst) ImmuneOncia (Inst) Immunomedics (Inst) Incyte (Inst) Jounce Therapeutics (Inst) Lilly (Inst) MabSpace Biosciences (Inst) MacroGenics (Inst) MedImmune (Inst) Medivation (Inst) Merck (Inst) Millennium (Inst) Mirati Therapeutics (Inst) Novartis (Inst) Oncologie (Inst) Pfizer (Inst) PsiOxus Therapeutics (Inst) Puma Biotechnology (Inst) Regeneron (Inst) Roche (Inst) Seattle Genetics (Inst) Synermore Biologics (Inst) Taiho Pharmaceutical (Inst) TopAlliance Biosciences (Inst) Turning Point Therapeutics (Inst) Vedanta Biosciences (Inst) Vertex (Inst) Xencor (Inst).

Andrae Vandross: Mabwell (Shanghai) (Inst) Abbvie (Inst) Astra Zeneca (Inst) Aminex Therapeutics (Inst) Ascentage Pharma (Inst) Asana Bio (Inst) BioOneCure (Inst) BJ Bioscience Inc (Inst) Elpiscience Biopharma (Inst) Nanjing Immunophages Biotech (Inst) Chugai Pharmaceuticals (Inst) Lygen Biopharma (Inst) NGMBio (Inst) Zhuhai Yufan Biotechnologies (Inst) siRNAomics (Inst) Sorrento therapeutics (Inst) Exelixis (Inst) Xilio (Inst) ZielBio (Inst).

Anthony Tolcher: - AbbVie (Inst) ABL Bio (Inst) Adagene (Inst) ADC Therapeutics (Inst) Agenus (Inst) Aminex (Inst) Amphivena (Inst) Apros Therapeutics (Inst) Arcellix (Inst) ARMO BioSciences (Inst) Arrys Therapeutics (Inst) Artios (Inst) Asana Biosciences (Inst) Ascentage Pharma (Inst) Astex Pharmaceuticals (Inst) Basilea (Inst) Bioinvent (Inst) Birdie (Inst) BJ Bioscience (Inst) Boehringer Ingelheim (Inst) Boston

Biomedical (Inst) CStone Pharmaceuticals (Inst) Daiichi Sankyo, Inc. (Inst) Deciphera (Inst) eFFECTOR Therapeutics (Inst) EMD Serono (Inst) Gilead Sciences (Inst) GlaxoSmithKline (Inst) ImmuneOncia (Inst) Inhibrx (Inst) Innate Pharma (Inst) Janssen Research & Development (Inst) K-Group Beta (Inst) Kechow Pharma (Inst) Kiromic (Inst) Merck Sharp & Dohme (Inst) Mersana (Inst) Mirati Therapeutics (Inst) Naturewise (Inst) NBE Therapeutics (Inst) NextCure (Inst) Nitto BioPharma (Inst) Odonate Therapeutics (Inst) ORIC Pharmaceuticals (Inst) Pfizer (Inst) Pieris Pharmaceuticals (Inst) Qilu Puget Sound Biotherapeutics (Inst) Samumed (Inst) Seattle Genetics (Inst) Shanghai HaiHe Pharmaceutical (Inst) Spring Bank (Inst) Sunshine Guojian (Inst) Symphogen (Inst) Syndax (Inst) Synthorx (Inst) Takeda (Inst) Tizona Therapeutics, Inc. (Inst) Zymeworks (Inst).

Other Substantive Relationships: Melissa Johnson: Travel, Accommodations, Expenses - Abbvie AstraZeneca Genentech Incyte Merck Pfizer Sanofi.

Haeseong Park: Travel, Accommodations, Expenses - Bayer Daiichi Sankyo Vedanta Biosciences.

Anthony Tolcher: Employment - Next Oncology. Leadership - Next Oncology. Expert Testimony - Immunogen. Travel, Accommodations, Expenses - Sotio (Inst).

Shailaja Uttamsingh, Jing Li, and Mustafa Syed: Employment: Exelixis.

## 257

(PB037)

### Treatment of Cholangiocarcinoma with a Humanized Anti-Claudin-1 Monoclonal Antibody

M. Muller<sup>1,2</sup>, Z. Nehme<sup>1,2</sup>, N. Röhlen<sup>1,2</sup>, F. Juehling<sup>1,2</sup>, E. Crouchet<sup>1,2</sup>, P. Pessaux<sup>1,2,3</sup>, E. Felli<sup>1,2,3</sup>, L. Goyal<sup>4</sup>, M. Meyer<sup>5</sup>, R. Iacone<sup>5</sup>, A. Toso<sup>5</sup>, N. Bardeesy<sup>4</sup>, C. Schuster<sup>1,2</sup>, L. Maily<sup>1,2</sup>, T. Baumert<sup>1,2,3,6</sup>. <sup>1</sup>Institut de Recherche sur les Maladies Virales et Hépatiques, Inserm- U1110, Strasbourg, France; <sup>2</sup>University of Strasbourg, University of Strasbourg, Strasbourg, France; <sup>3</sup>Institut Hospitalo-Universitaire- Pôle Hépat-Digestif, Hôpitaux Universitaires De Strasbourg, Strasbourg, France; <sup>4</sup>Department of Medicine- Division of Oncology- Massachusetts General Hospital, Harvard Medical School, Boston, USA; <sup>5</sup>Alentis Therapeutics, Alentis Therapeutics, Basel, Switzerland; <sup>6</sup>Institut Universitaire de France, Institut Universitaire de France, Paris, France

**Background:** Cholangiocarcinoma (CCA) is an adenocarcinoma of the hepatobiliary system showing an alarming rise in incidence and mortality with unsatisfactory treatment options. Claudin-1 (CLDN1) is a transmembrane protein involved in epithelial tight junctions and is also expressed non-junctionally mediating cell plasticity and signaling. However, its functional role in CCA pathogenesis and progression is unknown. We have previously developed a highly specific monoclonal antibody (mAb) targeting exposed non-junctional CLDN1 exhibiting an excellent safety profile in non-human primates. Here, we aimed to explore the role of CLDN1 as an oncogenic driver and therapeutic target in intra- and extrahepatic CCA.

**Material and methods:** Comprehensive CLDN1 expression analyses were performed to evaluate CLDN1 as a target for treatment of CCA. Proof-of-concept studies using CLDN1 mAbs were performed in state-of-the-art cell line-derived and patient-derived xenograft mouse models, as well as in human CCA cell lines. Single-cell and bulk RNA sequencing, and proteomics were applied to investigate tumor cell fate and signaling in vivo.

**Results:** Comprehensive analyses of CLDN1 protein and RNA expression in CCA patient tissues revealed a marked and significant upregulation of CLDN1. Single-cell RNA sequencing of the CCA microenvironment revealed strong expression in tumor cells showing EMT, cell cycle and interferon response signature, uncovering CLDN1 as a therapeutic target. Targeting exposed non-junctional CLDN1 by highly specific mAbs resulted in a significant and robust antitumoral effect in vivo across cell line-derived and patient-derived xenograft models for intra- and extrahepatic CCA. Functional studies in cell-based models of CCA showed that CLDN1 mAbs markedly and significantly suppressed migration and invasion of tumor cells. Mechanistically, treatment with CLDN1 mAb suppressed Notch1, Src, and Hippo-YAP signaling - key signal transduction pathways implicated in CCA development and progression.

**Conclusions:** Collectively, these results provide robust pre-clinical proof-of-concept for CLDN1-specific mAbs to treat CCA and set the stage for its clinical development.

**No conflict of interest.**

## POSTER SESSION

## Cancer Genomics

258

(PB038)

**SORT1 with oncogenic potential associated hypomethylation and promotes tumor progression in hepatocellular carcinoma**

H.R. Ahn<sup>1</sup>, J.A. Son<sup>1</sup>, J.H. Weon<sup>2</sup>, G.O. Baek<sup>2</sup>, M.G. Yoon<sup>2</sup>, J.E. Han<sup>2</sup>, S.S. Kim<sup>2</sup>, J.Y. Cheong<sup>2</sup>, M. Kwon<sup>3</sup>, J.W. Eun<sup>3</sup>, H.J. Cho<sup>2</sup>. <sup>1</sup>Ajou University School of Medicine and Graduate School of Medicine, Gastroenterology, Suwon, South Korea; <sup>2</sup>Ajou University School of Medicine, Gastroenterology, Suwon, South Korea; <sup>3</sup>Asan Medical Center- University of Ulsan College of Medicine, Otorhinolaryngology-Head and Neck Surgery, Seoul, South Korea

**Background:** Hepatocellular carcinoma (HCC) is the one of the most common cancers and lethal diseases in the world. SORT1 is a neuronal type-1 membrane protein and member of the Vps10p-domain receptor family, which was most abundantly expressed in neuronal cells. However, SORT1 effect on HCC progression remains unclear in hepatocellular carcinoma.

**Material and methods:** Analysis of various public omics datasets revealed that SORT1 is overexpressed in HCC. Next, we performed the enrichment of SORT1-related genes in TCGA and network analysis of SORT1-related protein-protein interactions. When examining the regulatory mechanism of SORT1, we observed a negative correlation between SORT1 methylation status and mRNA expression in the TCGA\_LIHC dataset. The cg16988986 CpG island in the SORT1 5' promoter region was hypomethylated in HCC compared to matched non-tumor samples.

**Results:** In this study, we first identified that SORT1 was significantly overexpressed in HCCs compared to non-tumor tissues and was clinically related with prognosis in the Cancer Genome Atlas liver hepatocellular carcinoma project (TCGA\_LIHC) dataset and GSE114564 dataset. SORT1 knockdown suppressed cell growth and proliferation of HCC cells, and reduced the metastatic potential of HCC cells. We observed that targeted inactivation of SORT1 suppressed cell cycle proteins and caused apoptotic cell death of HCC cells. Also, we found a inverse correlation between DNA methylation and gene expression of SORT1. Although SORT1 methylation was significantly downregulated according to HCC tumor stage, SORT1 expression was significantly upregulated.

**Conclusions:** We identified that SORT1 is significantly overexpressed and hypomethylated in HCC and we suggest that the inactivation of SORT1 might be one of the candidates for the therapeutic target for HCC.

**No conflict of interest.**

259

(PB039)

**CDK11 is a selective dependency in neuroblastoma harboring loss of chromosome 1p36**

M. Guenther<sup>1</sup>, Y. Wei<sup>1</sup>, S. Stein<sup>1</sup>, A. D'Ippolito<sup>1</sup>, D. Farouq<sup>1</sup>, D. Moebius<sup>1</sup>, J. Marineau<sup>2</sup>, E. Cooper<sup>2</sup>, C. Chuaqui<sup>2</sup>, J. Carulli<sup>1</sup>, E. Olson<sup>1</sup>. <sup>1</sup>Syros Pharmaceuticals, Biology, Cambridge, USA; <sup>2</sup>Syros Pharmaceuticals, Chemistry, Cambridge, USA

**Background:** Neuroblastoma is the most common infant cancer and exhibits frequent deletion of chromosome 1p36 in the high-risk setting. We sought to identify key dependencies and drug targets driving high-risk neuroblastoma cell growth.

**Materials and methods:** We used targeted shRNA-mediated gene ablation to identify and validate CDK11 as a drug target in SK-N-BE(2) cells. Used CDK11 nanoBRET assay, radiometric kinase activity assay catalyzed by recombinant kinases, and cDNA complementation using exogenous WT CDK11, inhibitor resistant CDK11<sup>G579S</sup> and kinase deficient CDK11<sup>K467M</sup> to determine CDK11 target engagement and activity. Total RNA-seq was deployed to define splicing modulation upon CDK11 perturbation and genome-wide CRISPR-Cas9 screening to define synthetic lethal interactions upon CDK11 perturbation.

**Results:** We discovered that CDK11 (CDC2L1/CDC2L2) is frequently deleted of one copy at chromosome 1p36 and is a deep dependency in high-risk neuroblastoma cells harboring 1p36 Loss-of-heterozygosity ( $\Delta$ 1p36). We show that CDK11 loss-of-function via genetic or chemical inhibition preferentially impedes proliferation of  $\Delta$ 1p36 tumor cells vs WT 1p36 tumor cells. Reconstitution of wild-type CDK11 levels in  $\Delta$ 1p36 tumor cell lines rendered neuroblastoma cells resistant to CDK11 inhibitors whereas kinase-deficient CDK11 did not, suggesting a dosage requirement for CDK11 kinase function in  $\Delta$ 1p36 neuroblastoma cells. Chemical inhibition of CDK11 kinase activity in  $\Delta$ 1p36 tumor cells induces intron-retention splicing defects at mRNA processing and export genes, indicating a core role for CDK11 in RNA metabolism. A genome-wide CRISPR screen for synthetic lethality with CDK11 inhibitors revealed that cognate cyclin CCNL1 and a set of core splicing regulators collaborate with CDK11 to enforce neuroblastoma tumor cell growth.

**Conclusions:** Together, our findings identify CDK11 as a druggable vulnerability and potential therapeutic target for high-risk neuroblastoma patients exhibiting  $\Delta$ 1p36.

**Conflict of interest:**

Other Substantive Relationships: All authors are employees of Syros Pharmaceuticals.

260

(PB040)

**Discovery of Essential microRNA in Prostate Cancer Cells**

J. Chow<sup>1</sup>, D. K. C. Lee<sup>1</sup>, K. Chen<sup>1</sup>, N. Fu<sup>1</sup>, I. Grigore<sup>1</sup>, M.M. Gabra<sup>1</sup>, L. Salmena<sup>1,2</sup>. <sup>1</sup>University of Toronto, Department of Pharmacology and Toxicology- Faculty of Medicine, Toronto, Canada; <sup>2</sup>University Health Network, Princess Margaret Cancer Centre, Toronto, Canada

**Background:** Prostate cancer (PCa) is the most common cancer in men worldwide. Tumour progression is highly variable: most tumours will remain "dormant" negating a need for treatment, but some will progress and become metastatic resulting in extremely poor prognosis. Despite the introduction of new treatments, metastatic PCa remains lethal and incurable. This is invariably due to the onset of castration-resistance in advanced cases producing a more aggressive tumour with increased metastatic potential. microRNA (miRNA) are small non-coding RNA that can regulate diverse gene networks simultaneously. Due to their wide-ranging effects, we hypothesize that miRNA can promote PCa progression and aggressive phenotypes. Thus an extensive investigation of miRNA function in PCa is necessary, and does not yet exist.

**Methods:** We previously developed a new and improved version of the miRNA CRISPR Knockout library called miRKOv2 to comprehensively discover miRNA that regulate PCa growth. We performed a dropout CRISPR-Cas9 screen with miRKOv2 in Cas9+ DU145 cells, and identified essential miRNA using the Bayesian Analysis of Gene Essentiality (BAGEL) algorithm. We then performed preliminary validation of screen results using proliferation assays that measured PCa cell growth over 10–12 days.

**Results:** Precision-recall analysis demonstrated reliable performance of our screen. In total, 35 essential miRNA were identified using a 10% FDR cutoff (see Table 1). Experimental validation demonstrated that miR-483 is required for growth in PCa cells over a 10 day growth assay. Tracking of Indels by Decomposition (TIDE) analysis confirmed successful indel formation at the miR-483 genomic locus. While miR-483-5p has previously been reported as a promoter of PCa cell proliferation and invasion, the role of miR-483-3p in PCa remains undefined. Interestingly, both mature strands are similarly expressed in DU145 cells, which could suggest a role for both in PCa.

**Conclusion and Future Directions:** We identified miR-483 as an essential gene from a CRISPR-Cas9 dropout screen using our novel miRKOv2 library. Further exploration into roles for miR-483-3p and miR-483-5p in PCa and cross-validation in other PCa cell lines, including 22Rv1 and PC3, is ongoing to cover the breadth of PCa genomic backgrounds. Furthermore, molecular targets of miR-483-3p and miR-483-5p will be elucidated and characterized for their roles in PCa growth.

**No conflict of interest.**

Table 1. (abstract: 260 (PB040)). The 35 essential miRNA identified in a dropout screen using the miRKOv2 library.

miR-1181	miR-5001	miR-624	miR-6780a	miR-4716	miR-6779	miR-6736
miR-1226	miR-320a	miR-4505	miR-7108	miR-5010	miR-3160-2	miR-93
miR-4448	miR-4533	miR-185	miR-3185	miR-939	miR-132	miR-340
miR-6501	miR-663a	miR-3127	miR-5187	miR-6872	miR-1286	miR-642a
miR-130b	miR-636	miR-449a	miR-6738	miR-7973-2	miR-648	miR-483

261

(PB041)

**Molecular characterization of canine follicular and medullary thyroid carcinomas**

D. Duval<sup>1</sup>, S. Das<sup>1</sup>, S. Schlemmer<sup>2</sup>, R. Idate<sup>1</sup>, B.I. Lee<sup>3</sup>, D. Regan<sup>4</sup>, D. Thamm<sup>1</sup>, S. Lana<sup>1</sup>. <sup>1</sup>Colorado State University, Clinical Sciences, Fort Collins, USA; <sup>2</sup>University of Georgia, Pathology, Athens, USA; <sup>3</sup>Colorado State University, Cell and Molecular Biology Graduate Program, Fort Collins, USA; <sup>4</sup>Colorado State University, Microbiology- Immunology- and Pathology, Fort Collins, USA

**Background:** Thyroid tumors represent 1–3% of canine cancers with most tumors classified as follicular carcinomas. Medullary carcinomas arising from c-cells are less frequently diagnosed in both dogs and humans. In comparison, papillary thyroid carcinomas are the most common type of human thyroid cancer (70–80%) with follicular thyroid cancer diagnosed in 10–15% of cases. Medullary carcinomas are 2% of human cases and 20% of these are associated with inherited gene mutations in *RET*. Human papillary and follicular carcinomas frequently bear activating mutations in *BRAF* and *NRAS*.

**Materials and Methods:** To determine if canine and human thyroid tumors share molecular characteristics, we conducted whole exome (WES) and RNA sequence analysis of canine thyroid tumors. We used whole exome capture (Agilent Sure Select V2) to sequence 27 thyroid tumors and matched normal genomic samples and ribosomal RNA depleted total RNA was sequenced from 30 tumors. The tumors were histologically typed as solid, follicular compact, or follicular, diagnosed as carcinomas or adenocarcinomas, and contained >70% tumor tissue.

**Results:** For the WES, 150 bp paired end reads (Illumina) were mapped against CanFam3.1 using BWA and short variants were called and annotated with Mutect2 and VEP tools. Average depth of sequencing was 212 ± 27. RNAseq reads were mapped against CanFam3.1 with STAR and normalized counts were generated with DESeq2. Protein coding somatic variants per tumor ranged from 17 to 346 (total 2181). Known cancer genes with somatic mutations in 2 or more tumors were *SALL4*, *HSP90AA1*, *MEN1*, *SFPQ*, *LEPROTL1*, *CDK4*, *RAD17*, *MGAM*, *NOTCH4*, and *RANBP2*. No somatic variants were identified in *BRAF* or *NRAS*, although individual variants of unknown impact were identified in *KRAS*, *ARAF*, and *RASA1*. Individual tumors also had variants in *TSHR* and *THRAP3*. Hierarchical clustering of gene expression data separated the tumors into 2 groups: C1 and C2. Differential gene expression analysis between these groups identified high expression (>1000-fold change) of calcitonin transcripts in C1, suggesting that the C1 cluster is comprised of medullary thyroid carcinomas. Notable among the upregulated genes in C1 relative to C2 were: *FOXA1*, *SCG5*, *RET*, *ERBB4*, *NTRK1*, *WNK2*, and *MUC1*. Upregulated genes in C2 included: *FGFR2*, *MECOM*, *PAX8*, *ERBB2*, *GRM3*, *AR*, *SMO*, *IGF2BP2*, and *SOCS1*. Pre-ranked gene set enrichment analysis (GSEA) identified the “Hallmark KRAS signaling UP” and “GOBP Regulation of Membrane Potential” pathways enriched in C1, while enrichment for C2 was limited, with “GOBP thyroid hormone generation” being the most significant.

**Conclusions:** These data suggest that medullary thyroid carcinomas in the dog, like their human counterparts, may be driven by RET signaling. In contrast, follicular tumors in dogs show limited reliance on RAS/RAF signaling for oncogenic progression.

No conflict of interest.

263

(PB043)

**A small RNA signature from extracellular vesicles in patient plasma correlates with recurrence or progression of high-grade gliomas**

J.H. Han<sup>1</sup>, K. Attwood<sup>1</sup>, J. Roy<sup>2</sup>, A. Weeks<sup>1</sup>. <sup>1</sup>Dalhousie University, Division of Neurosurgery, Halifax, Canada; <sup>2</sup>Dr. Georges-L.-Dumont University Hospital Centre, Atlantic Cancer Research Institute, Moncton, Canada

**Background:** Glial cell-derived tumours of the central nervous system make up the largest group of brain tumours. Most are high-grade gliomas (HGG) and are universally fatal despite multimodal therapy. With a suspected HGG, surgery is undertaken for tumour de-bulking and to make a definitive diagnosis. While the tumour genetics provides some insight on prognosis, it rarely changes decision-making, nor does it predict recurrence. In managing patients with HGG, predicting recurrence, or differentiating between pseudo-progression (radiation necrosis) and true tumour progression would be invaluable in improving overall prognosis. Characterizing small RNA (sRNA) expression profiles from plasma-derived extracellular vesicles (EVs) over the course of a patient's treatments, may allow for patient-specific treatment modifications and improve outcomes.

Our objectives were to identify a unique small RNA (sRNA) signature from isolated EVs that could be correlated with the longitudinal, clinical status of the respective patient and the imaging characteristics of the tumour on

routine follow up MRI and to evaluate differentially expressed sRNA identified from stable vs. progressed patient samples.

**Materials and Methods:** Adult patients with suspected HGG were enrolled. Blood samples obtained longitudinally from just prior to surgery, during surgery, 2-weeks post-surgery, at recurrence, and with routine surveillance imaging.

Plasma EVs were isolated using Vn96 capture from HGG patients peri-operatively and with routine, follow-up surveillance imaging. Small RNA sequencing was conducted and unsupervised hierarchical clustering of sRNA signatures were completed. Expression profiles were grouped longitudinally with the clinical status of patients.

**Results:** Cluster analysis of nine HGG patients, has revealed a sRNA signature that is able to distinguish between tumours showing evidence of progression and those remaining stable over time. Those samples obtained from patients where a clinical diagnosis of tumour progression or pseudo-progression were uncertain, were found to cluster into progression vs. stable signatures.

Annotation of differentially expressed sRNAs identified from stable vs. clinically progressed patients include small nuclear RNA, ribosomal RNA, and microRNA among others. Examples of miRNA species we have identified correspond to previously identified miRNA, which have been ascribed functional significance to GBM aggressiveness and progression.

**Conclusion:** To date, we have enrolled 26 patients with HGG with over 100 longitudinal blood draws, which represents one of the largest prospective, longitudinal cohorts in HGG liquid biopsy research

These preliminary findings demonstrate the potential utility of sRNA profiling of plasma-derived EVs obtained from patients with HGG as non-invasive biomarkers for recurrent/progressive disease or stability/pseudo-progression.

No conflict of interest.

264

(PB044)

**In vivo CRISPR screening to identify modulators of cancer metabolism-based therapy response**

I. García Cao<sup>1</sup>, C. Stephan-Otto Attolini<sup>2</sup>, J. Espinosa Carrasco<sup>3</sup>, F. Supek<sup>1</sup>, A.R. Nebreda<sup>1</sup>, T.H. Stracker<sup>4</sup>. <sup>1</sup>Institute for Research in Biomedicine IRB Barcelona- The Barcelona Institute of Science and Technology, Cancer Science Program, Barcelona, Spain; <sup>2</sup>Institute for Research in Biomedicine IRB Barcelona- The Barcelona Institute of Science and Technology, Biostatistics and Bioinformatics Unit, Barcelona, Spain; <sup>3</sup>Centre for Genomic Regulation CRG- The Barcelona Institute of Science and Technology, Bioinformatics and Genomics, Barcelona, Spain; <sup>4</sup>National Cancer Institute NCI- Center for Cancer Research, Radiation Oncology Branch, Bethesda, USA

**Background:** Altered cell metabolism is an established hallmark of cancer. A common feature of the altered metabolism in cancer cells is the increased glucose uptake and conversion to lactate through aerobic glycolysis (“Warburg effect”). However, in addition to aerobic glycolysis, it is now clear that mitochondrial metabolism is also essential for tumor cell proliferation. We aim to exploit the metabolic alterations in cancer cells following the hypothesis that aberrant mitochondrial metabolic pathways are potential molecular targets for the development of novel cancer treatments.

**Material and methods:** We have performed a combination of biochemical approaches, *in vitro* studies in cultured human cancer cells and *in vivo* assays (xenografts) to assess the anti-tumoral effect of a novel drug targeting key mitochondrial enzymes [CPI-613 (*devimistat*), *Comerstone Pharmaceuticals*]. We have carried out an *in vivo* genome-wide CRISPR-Cas9-based screening to identify modulators of the treatment response.

**Results:** The altered mitochondrial cancer cell metabolism represents a potential therapeutic target for cancer treatment. Mitochondria provide both energy and building blocks that cancer needs to support growth. Here we show that the metabolic drug CPI-613, targeting two key mitochondrial enzymes of the Krebs cycle, is able to reduce the growth of different human colon cancer cell lines harboring different genetic mutations. This finding suggests that aberrant energy metabolism could be a common feature of cancer cells. The effectiveness of the treatment was also demonstrated *in vivo*, as CPI-613 reduces tumor growth in a xenograft model of colorectal cancer. In order to gain insight about the mechanism of action, identify target genes that increase the effectiveness of the treatment, and also reveal possible resistance mechanisms, we set up an *in vivo* CRISPR screening taking advantage of the use of genome-wide CRISPR-Cas9 libraries. Modulators of the treatment response include genes implicated in mitochondrial function, antioxidant response, and chromatin remodellers. The final goal is to identify potential targets to enhance metabolism-based anticancer drugs action and efficacy, as well as biomarkers that would predict drug resistance for future therapeutic interventions.

**Conclusions:** Targeting mitochondrial metabolism is a promising therapeutic strategy to treat a wide variety of cancers. CPI-613, a first-in-class drug selectively targeting altered tumor mitochondrial metabolism, is effective in colon cancer treatment both *in vitro* and *in vivo* studies. By performing an *in vivo* genome-wide CRISPR-Cas9-based screening we have identified potential modulators of the treatment response. This data is of clinical relevance for novel combination therapies and personalized medicine approaches in cancer treatment.

**No conflict of interest.**

**265** (PB045)  
**Predictive impact of ARID1A status in solid tumors**

S. Daniel Ampanattu<sup>1</sup>, G. Ahmed<sup>1</sup>, B. Thapa<sup>1</sup>, A. Janardan<sup>2</sup>, A. Vallejos<sup>3</sup>, B. Taylor<sup>3</sup>, D. Huayang<sup>4</sup>, A. Szabo<sup>4</sup>, B. George<sup>1</sup>. <sup>1</sup>Medical College of Wisconsin, Hematology and Oncology, Milwaukee, USA; <sup>2</sup>Medical College of Wisconsin, Medicine, Milwaukee, USA; <sup>3</sup>Medical College of Wisconsin, Biomedical Informatics, Milwaukee, USA; <sup>4</sup>Medical College of Wisconsin, Biostatistics, Milwaukee, USA

**Background:** Mutations in the gene encoding AT- Rich Interactive Domain-containing protein 1A (*ARID1A*) occur in several cancer types with varying frequency. The predictive impact of *ARID1A* mutations on platinum-based chemotherapy and immunotherapy have been investigated retrospectively, yielding conflicting results. We report our analysis on the predictive impact of *ARID1A* status – mutated (MUT) versus (vs.) wild type (WT) – in metastatic solid tumor patients who were exposed to platinum-based chemotherapy and immunotherapy.

**Materials and Methods:** Our institutional database was interrogated to identify adult patients with metastatic solid tumors who had comprehensive genomic profiling performed between January 2011 to May 2022 and met with following eligibility criteria (i) *ARID1A* status -MUT vs. WT- available (ii) had exposure to platinum-based chemotherapy or immunotherapy (iii) reliable treatment data available. Platinum-based chemotherapy treatment was defined as exposure to systemic doses of cisplatin, carboplatin, or oxaliplatin either as a single agent or in combination with other chemotherapy agents. Immunotherapy treatment was defined as exposure to anti-programmed death-1 receptor (PD-1) agents, anti-programmed death ligand-1 (PD-L1) agents, or anti-cytotoxic T-lymphocyte-associated protein 4 (CTLA-4) agents either as a single agent or in combination.

**Results:** We identified 135 patients that met inclusion criteria - the median age at diagnosis was 64 years, 77 (57%) were female, and 87 (64%) were *ARID1A* mutated. The most common cancer types were colorectal (N = 19; 14%), lung (N = 19; 14%), urothelial (N = 16; 12%), and gastroesophageal (N = 14; 10%). The probability of *ARID1A* MUT vs. WT patients remaining on platinum-based chemotherapy at 6, 12, and 24 months since treatment initiation were 25.5% vs. 23.1%, 11.2% vs. 15.4%, and 3.37% vs. 5.13% respectively (p = 0.7). The probability of *ARID1A* MUT vs. WT patients remaining on immunotherapy at 6, 12, and 24 months since treatment initiation were 31.3% vs. 33.3%, 25.0% vs. 18.5%, and 10.4% vs. 14.8%, respectively (p = 0.4). The median duration of platinum-based chemotherapy and immunotherapy exposure in *ARID1A* MUT vs WT patients were 2.5 months vs. 3.5 months and 3.7 months vs. 2.5 months, respectively.

**Conclusions:** There were no differences in duration of exposure to platinum-based chemotherapy or immunotherapy based on *ARID1A* MUT vs WT status suggesting its lack of predictive impact for these therapies. Since genomic alterations have a context dependent impact – both prognostic and predictive – larger analyses powered to identify the histology specific impact and therapeutic relevance of *ARID1A* status are warranted.

**Conflict of interest:**

Corporate-sponsored Research: Research Support for : Roche/Genentech (Inst), Taiho Oncology (Inst), Boehringer Ingelheim (Inst), Toray (Inst), NGM Biopharma (Inst), Hutchison Medipharma (Inst), Mirati Therapeutics (Inst), Trishula Therapeutics (Inst), Glyconex (Inst), Helix Biopharma (Inst), Pfizer (Inst), Sirnaomics (Inst)

Other Substantive Relationships: Consultant for Ipsen, Bristol Myers Squibb, Exelixis, Foundation Medicine, Terumo Interventional Systems, Taiho Oncology, Boston Scientific, Roche/Genentech, Pfizer

**266** (PB046)  
**Evaluating the performance of two NGS-based copy number aberration detection tools in patient-derived organoids**

W. Qian<sup>1</sup>, S. Guo<sup>2</sup>. <sup>1</sup>Crown Bioscience, Inc., NGS, San Diego, USA; <sup>2</sup>Crown Bioscience, Inc., Data Science & Bioinformatics, San Diego, USA

**Introduction:** NGS sequencing technology, including whole genome sequencing (WGS) and whole exome sequencing (WES), has become a primary tool to study genetic variants of tumors. Many tools have been developed for NGS-based copy number aberration (CNA) detection including software GATK (Broad Institute) and CopyWriteR, which both demonstrate reliable performance. GATK software can be applied to WES and WGS data, using target region depth and germline mutation allele frequency for copy number detection. CopyWriteR software uses only WES data, leveraging on the off-target region depth. In this study the advantages and disadvantages of these two tools are compared.

**Methods:** CNA of 23 pairs of patient-derived organoid (PDO) models were analyzed using WGS data with the GATK software, and 18 pairs of PDO models using WES data with both the GATK and CopyWriteR software. CNA was inferred in the presence and absence of paired WGS and WES-based CNA results were compared to evaluate the influence of NGS data type. The WES-based CNA data by GATK and CopyWriteR were compared to evaluate the two algorithms.

**Results:** The number of amplified/deleted regions and genes are comparable for the three combinations (GATK + WGS, GATK + WES, and CopyWriteR + WES) when matched controls were used. WES-based combination detected significantly more CNA events in the absence of matched controls when compared to WGS-based combination. GATK software was prone to unexpected results when the WES capture efficiency was not equal in library preparation. CopyWriteR software missed the presence of some highly amplified genes.

**Conclusions:** WGS data was found to be a superior source for CNA detection when compared to WES data. CopyWriteR software has shortage on detection of high gene amplification events and for WES data, with uneven exon capture rate, it demonstrated superior performance over GATK. These results suggest it is integrating the WES-based results from both software.

**No conflict of interest.**

**267** (PB047)  
**Consensus analysis of associated target-biomarker pairs in cancers**

E. Jeong<sup>1</sup>, S. Yoon<sup>1</sup>. <sup>1</sup>Sookmyung Women's University, Department of Biological Sciences, Seoul, South Korea

The heterogeneity of cancers limits the reproducibility of anticancer target-biomarker associations in diverse cohorts or sample groups. Here, we carried out consensus analyses of cancer omics data to find improved consistency (reproducibility) of prognostic power of biomarkers and anticancer potential of targets. Overall, ~74% of prognostic RNA expression in patient samples were exclusively found in a single lineage, and most of them did not pass the cross-validation within the given lineage. Prognostic RNA expression (i.e., biomarker) showing subtype consensus within the lineage, also tend to exhibit high consensus in other lineages. In the analysis of the association between CRISPR knockout and RNA expression data in cell lines, the lineage consensus of the association between them increased the reproducibility in sh/siRNA knockdown and qPCR experiment. From this study, we found that the consensus analysis was useful to prioritize reproducible target-biomarker combinations from cancer omics data. It has been implemented in Q-omics software (<http://qomics.sookmyung.ac.kr>) for general oncology and cancer research.

**No conflict of interest.**

**268** (PB048)  
**Smart software for assisting oncology and cancer research**

S. Jeong<sup>1</sup>, E. Jeong<sup>1</sup>, S. Yoon<sup>2</sup>. <sup>1</sup>Sookmyung Women's University, Biological Sciences, Seoul, South Korea; <sup>2</sup>Sookmyung Women's University, Department of Biological Sciences, Seoul, South Korea

Increased multi-level omics data have enabled data-driven studies on cancer drugs, targets and biomarkers. Thus, it is necessary to develop comprehensive tools for oncologists and cancer scientists to carry out extensive data mining without computational expertise. Mutations, gene/protein expression, patient survival, immune score (tumor infiltrating cells), drug screening and RNAi (shRNA and CRISPR) screening data on patient samples and cell lines, were integrated from TCGA, GDSC, CCLE, NCI, DepMap, etc. into Q-

omics software. Analyses are guided by smart systems for the quick finding of significant associations between data pairs. Furthermore, unique consensus scoring methods based on multiple statistical tests using varied sample (or lineage) selection, enriches robust cross-associated pairs in the hit list for successful experimental validation. Q-omics provides simple and powerful tools for all areas of oncology and cancer research. The latest version of Q-omics software is available at <http://qomics.sookmyung.ac.kr>.

**No conflict of interest.**

**269** (PB049)  
**Development of a rapid and fully automated Idylla™ assay for qualitative detection of mutations in the PIK3CA and AKT1 gene in advanced breast cancer FFPE samples**

T. Piofczyk<sup>1</sup>, K. Covens<sup>1</sup>, T. Adriany<sup>1</sup>, M. Petruskeviciute<sup>2</sup>, B. Lopez-Jimena<sup>2</sup>, D. De Vega<sup>2</sup>, C. Roesl<sup>2</sup>, M. Kavanagh-Williamson<sup>2</sup>, J. Wuyts<sup>1</sup>, T. Forster<sup>2</sup>, J. Campos<sup>2</sup>, D. Daems<sup>1</sup>, C. Claxton<sup>2</sup>, P. Wasson<sup>2</sup>, S. Metsu<sup>1</sup>, A. Smith<sup>2</sup>, G. Maertens<sup>1</sup>. <sup>1</sup>Biocartis NV, Development, Mechelen, Belgium; <sup>2</sup>LifeArc, Diagnostics, Nine, Edinburgh, United Kingdom

**Background:** Breast cancer (BC) is the second most common cancer in the world with over 1.67 million new cases yearly. 30% of women with early breast cancer develop metastatic breast cancer (MBC). Despite advances in treatment strategies, MBC remains largely incurable and is the primary cause of over 600 000 deaths annually worldwide.

PIK3CA mutations are the most common alteration on the PI3K/AKT/mTOR pathway, occurring in 20 to 40% of BC cases. Today, these cases can be treated with PI3K inhibitors, while for AKT1 positive tumors, promising therapeutic drugs are in the pipeline. Hence, identifying the presence of these mutations with tumor profiling tests will help characterize cancer patients who are likely to benefit from targeted agents and improve patient outcome.

Medical research charity LifeArc and Biocartis have joined efforts to co-develop an easy-to-use, rapid and fully automated sample-to-result assay to detect PIK3CA and AKT1 mutations starting from tumor FFPE biopsies on Biocartis' Idylla™ system, allowing decentralized fast clinical decision making.

**Materials and methods:** Advanced BC FFPE samples with characterized PIK3CA and AKT1 mutations were purchased from BioIVT, Biomarker Solutions, and Indivumed and tested using a prototype version of the Idylla™ assay for qualitative detection of 13 PIK3CA mutations (N345K, C420R, E542K, E545K, E545G, E545D [1635G>T], E545A, Q546K, Q546R, Q546E, H1047R, H1047L, H1047Y) and 1 AKT1 mutation (E17K). Following sensitivity (LOD) and specificity assessment, preliminary reproducibility testing was performed on a representative subset of advanced BC FFPE samples (n = 31) in triplicate.

**Results:** Analytical validation studies using synthetic targets indicate an LOD of <5% mutant allelic frequency for all PIK3CA and AKT1 mutations.

During initial performance evaluation, 31 FFPE breast cancer samples covering the most prevalent PIK3CA and AKT mutations, were tested with the prototype PIK3CA/AKT1 assay on the Idylla™ system. The obtained results demonstrated 100% concordance for presence or absence of PIK3CA and AKT1 mutations previously characterized by the biobanks using Next Generation Sequencing (NGS). All results were obtained within 150 minutes, starting from one 20 µm or two 10 µm FFPE slices.

	frequency in breast cancer (Solar1 trial)	concordance (observed/expected)	concordance %
WT	64%	15/15	100%
N345K	5.5%	12/12	100%
E542K	10.7% (18%)	12/12*	100%
E545K	17.5% (31%)	18/18	100%
H1047R	35.0% (52%)	30/30*	100%
H1047L	4.0%	3/3	100%
E17K	6.3%	6/6	100%
TOTAL		96/96	100%

\*one sample was known to have two co-occurring mutations.

**Conclusions:** The rapid and fully automated prototype PIK3CA/AKT1 Idylla™ assay offers great sensitivity and shows 100% concordance with previously obtained NGS results. Further verification studies are ongoing.

**No conflict of interest.**

**270** (PB050)  
**Comparative pan-cancer transcriptomics reveals that aberrant expression of long non-coding RNAs define cancers, tumor progression and immune cell exclusion**

M.C. Wasson<sup>1</sup>, J. Brown<sup>1</sup>, J. Venkatesh<sup>1</sup>, P. Marcato<sup>1,2</sup>. <sup>1</sup>Dalhousie University, Department of Pathology, Halifax, Canada; <sup>2</sup>Dalhousie University, Department of Microbiology & Immunology, Halifax, Canada

**Background:** Long non-coding RNAs (lncRNAs) are emerging targets for the diagnosis and therapeutic treatment of cancer. lncRNAs are non-protein-coding transcripts that regulate gene expression through epigenetic mechanisms mediated through binding of DNA, small RNAs and proteins. They exhibit high tissue- and context-specific expression, marking them as attractive biomarkers for cancer treatment or detection. Of the over 18 000 lncRNAs identified in the genome, the vast majority remain completely uncharacterized, limiting our understanding of the role of this group of non-coding RNAs in cancer.

**Methods:** To gain insight into the relative impact of lncRNAs in cancer progression in comparison to mRNAs, we conducted parallel bioinformatic analyses of 12 727 lncRNAs and 18 500 mRNAs utilizing patient tumour expression from The Cancer Genome Atlas and survival data in 20 cancer types.

**Results:** Our study determined that lncRNAs exhibit distinct expression patterns across cancers based on tissue of origin. Further, through conducting survival analyses for each lncRNA and mRNA over the 20 cancer datasets, we determined which are significantly associated with patient outcomes. This revealed that lncRNAs impact patient survival at similar proportions to mRNAs. Additionally, we found that the function of lncRNAs is highly cancer-dependent, with some lncRNAs playing oncogenic roles in some cancers while exhibiting benign functions in others. Our results indicate that lncRNAs enriched in tumour tissues are more likely to be associated with worse survival, while those depleted in tumor tissues are more likely to be associated with better survival. CIBERSORTx, a machine learning algorithm which estimates proportions of the heterogeneous cell populations within the tumor microenvironment, revealed that the expression of many lncRNAs is significantly associated with an immune suppressive environment.

**Conclusion:** This study demonstrates that lncRNAs are clinically relevant players in the progression of cancer and merit further investigation as potential therapeutic targets.

**No conflict of interest.**

**271** (PB051)  
**Clinical actionability and therapy selection for advanced NSCLC patients tested using comprehensive genomic profiling**

B. Bapat<sup>1</sup>, R. Weerasinghe<sup>2</sup>, R. Meng<sup>3</sup>, A. Dowdell<sup>3</sup>, S.C. Chang<sup>2</sup>, B. Schroeder<sup>4</sup>, C. Bifulco<sup>5</sup>, B. Piening<sup>5</sup>. <sup>1</sup>illumina, Inc., Health Economics and Outcomes Research, Portland, USA; <sup>2</sup>Providence Health, Research Accelerator, Portland, USA; <sup>3</sup>Providence Health, Earle A Chiles Research Institute, Portland, USA; <sup>4</sup>illumina, Inc., Market Access, San Diego, USA; <sup>5</sup>Providence Health, Genomics, Portland, USA

**Background:** Comprehensive genomic profiling (CGP) enables physicians to recommend advanced cancer treatments at the individual level by identifying patients that are likely and unlikely to benefit from targeted therapy or immunotherapy (IO). We assessed the utility of CGP-based testing for identifying biomarkers associated with approved therapies, and therapies in precision medicine basket clinical trials (CT) across a large cohort of advanced NSCLC patients in the Providence health system.

**Methods:** Advanced cancer patients were tested utilizing the Providence CGP workflow between 2019 and 2021. Clinical actionability was assessed for patients based on OncoKB Tier 1 AMP/ASCO/CAP categorization: FDA recognized (Level 1), standard of care (Level 2), and standard of care predictive of resistance to an FDA approved drug (Level R1). CT matching was assessed based on enrollment criteria for ASCO-TAPUR, NCI-MATCH and My Pathway CTs at time of testing. Systemic therapy post CGP-testing was assessed among patients whose care was managed at Providence post CGP testing. Pooled electronic medical record and genomic data were curated and standardized.

**Results:** 466 advanced NSCLC cancer patients were tested with CGP and followed up for cancer care management at Providence, 49% were female, 83% were white, and median age was 69 years. 59% (277) had at least 1 actionable biomarker for an approved and/or guideline recommended targeted therapy (based on OncoKB levels 1,2, R1), and 61% were eligible for at least 1 of 3 basket trials.



Of the CGP tested patients, 9% did not receive any cancer directed therapy and/or received only supportive care. Patients were treated using the following systemic therapies in line following CGP testing: chemotherapy only (97[21%]), chemotherapy + IO (140 [30%]), IO only (83 [18%]), targeted therapy in community setting (91 [20%]), targeted therapy in CT setting (7 [2%]), and off label use of targeted therapy (2 [0.4%]). Of 91 patients who received targeted therapy, 84 (92%) had an associated oncogene while 7 (8%) were treated based on approved NSCLC-specific indications.

**Conclusions:** CGP results in high proportion of patients eligible for both on-label therapies and for genomically-informed clinical trials. Moreover, comprehensive detection of both targeted and IO biomarkers simultaneously leads to optimal treatment selection.

#### Conflict of interest:

Ownership: Bela Bapat and Brock Schroeder are employees of Illumina, Inc. Corporate-sponsored Research: Brian Piening is recipient of a research grant from Illumina Inc.

## POSTER SESSION

### Functional Genomics

272 (PB052)  
**Hepsin promotes breast tumor growth signaling via TGF beta-EGFR axis**

T. Tervonen<sup>1</sup>, D. Belitskin<sup>1</sup>, P. Munne<sup>1</sup>, S. Pant<sup>1</sup>, J. Anttila<sup>1</sup>, K. Belitskina<sup>2</sup>, J. Pouwels<sup>1</sup>, J. Klefström<sup>3</sup>. <sup>1</sup>University of Helsinki, Translational Cancer Medicine Research Program- Research Programs Unit- Faculty of Medicine, Helsinki, Finland; <sup>2</sup>North Estonia Medical Centre, Pathology Department, Tallinn, Estonia; <sup>3</sup>Helsinki University Hospital, Finnish Cancer Institute & FICAN South, Helsinki, Finland

**Background:** Hepsin, a type II transmembrane serine protease encoded by *HPN* gene, is commonly overexpressed in prostate and breast cancer. Hepsin protein is stabilized by Ras-MAPK pathway signaling, and downstream, this protease regulates the degradation of extracellular matrix components and activates growth factor pathways, including hepatocyte growth factor and transforming growth factor (TGF) beta pathway. The significance of the hepsin-dependent signaling on cell proliferation and tumor growth is still partially unclear.

**Material and methods:** We used engineered breast cancer cell lines, WAP-Myc; *Hpn*<sup>-/-</sup> breast cancer mouse model, and patient-derived explant cultures from breast tumors to illuminate the role of hepsin in signaling on breast cancer cell proliferation and tumor growth.

**Results:** We made orthotopic transplantation into syngeneic wild-type recipient mice from isolated WAP-Myc; *Hpn*<sup>-/-</sup> mammary tumor cells. The resulting mammary tumors had decreased size both in primary and metastatic site in comparison to tumors derived from WAP-Myc; *Hpn*<sup>+/+</sup> tumor cells. This decreased growth was accompanied by downregulation of total epidermal growth factor receptor (EGFR) protein levels as well as reduction in EGFR signaling and TGF beta signaling. In addition, we showed that in 3D culture overexpression of hepsin induced TGF beta 1 and EGFR signaling-dependent cell proliferation, while PDECs treated with hepsin inhibiting antibodies and small molecules had decreased EGFR and TGF beta signaling activity and less cell proliferation marker expression.

**Conclusions:** This study demonstrates a role for hepsin as a regulator of cell proliferation and tumor growth through TGF beta and EGFR pathways, warranting consideration of hepsin as a potential indirect upstream target for therapeutic inhibition of TGF beta and EGFR pathways in cancer.

No conflict of interest.

273 (PB053)  
**Comparison of biomarker selection methods in high-dimensional genomic data**

Y. Wang<sup>1</sup>, S. Guo<sup>1</sup>. <sup>1</sup>Crown Bioscience, Data Science & Bioinformatics, San Diego, USA

**Background:** High-dimensional genomic data are indispensable in drug research and development. Genomic data-based biomarker discovery provides comprehensive insights to drug mechanism of action and efficacy prediction. However, it faces the difficulty of selecting suitable signature genes from several thousand or more genes with highly fluctuating and often tightly correlated expression patterns. This study aims to compare the performance of three recent signature gene selection algorithms in several large in vitro cell assays.

**Methods:** Drug response datasets of irinotecan, cetuximab, pelitinib, gefitinib, erlotinib and KRAS (G12C) inhibitor-12 were obtained from the Genomics of Drug Sensitivity in Cancer (GDSC). Cell line gene expression data were gathered from our internal dataset of 20,432 genes, with 1,068 cell lines, across 23 tissues. The three algorithms evaluated were Stable Iterative Variable Selection (SIVS), Precision Lasso (PL) and Whitening Lasso (WL). Efficacy variance between different cancer types (ANOVA p-value) and prediction accuracy of drug efficacy were calculated to evaluate the results.

**Results:** The accuracy of PL predictions was more positively correlated with the number of genes than SIVS and WL. The number of signature genes was limited from 5 to 50 and the most precise results were obtained for all drugs with 30 to 50 genes composite biomarkers. The PL, WL and SIVS methods separately selected 30, 17 and 6 genes as composite biomarkers for irinotecan with an accuracy of 85.7%, 78.2% and 87.3% respectively, in the training set. In validation set, the prediction accuracy of the SIVS panel was the highest at 83.1%. For erlotinib, SIVS, WL and PL picked out 22, 23 and 32 genes as the best composite biomarker with an accuracy of 73%, 83% and 76.8%, respectively. Overall, composite biomarkers selected by SIVS was the superior choice in four of six drugs. In most cases, these three algorithms took less time than 100 iterations of Boruta under the same conditions.

**Conclusions:** Compared with PL and WL, the SIVS method appears to obtain a higher prediction accuracy with a relatively smaller number of genes in this research. PL tended to select many more signature genes than SIVS and WL to yield comparable performance. Overlapping signature genes between the three algorithms was generally low, including for genes belonging to same molecular pathways. The cost and practicality of in vivo experiments would have made it difficult to select a large number of cancer types, drug response, and gene expression data. Therefore, selecting the best predictive composite biomarker in vitro screening for in vivo validation can significantly reduce costs and accelerate the early drug development process.

No conflict of interest.

274 (PB054)  
**Characterisation of adaptive responses of cancer cells to oxaliplatin by analysis of leading edge genes from genes set enrichment analysis**

K. Bigot<sup>1,2</sup>, M. Robin<sup>1,3,4,5</sup>, A. Djiane<sup>6</sup>, L. Heron-Milhavet<sup>6</sup>, L. Bréhélin<sup>4</sup>, M. Bini<sup>7</sup>, C. Gongora<sup>1</sup>, D. Tosi<sup>1,3,5</sup>. <sup>1</sup>Institut de Recherche en Cancérologie de Montpellier, Résistance aux traitements et thérapies innovantes, Montpellier, France; <sup>2</sup>Centre Hospitalier Universitaire de Montpellier, Lapeyronie, Montpellier, France; <sup>3</sup>Fondazione Gianni Bonadonna, Research, Milan, Italy; <sup>4</sup>LIRMM- Univ Montpellier, cnrs, Montpellier, France; <sup>5</sup>Institut du Cancer de Montpellier, Unité d'essais cliniques précoces, Montpellier, France; <sup>6</sup>Institut de Recherche en Cancérologie de Montpellier, Croissance épithéliale et cancer, Montpellier, France; <sup>7</sup>Istituto Nazionale Tumori, Fondazione IRCCS, Milan, Italy

**Background:** Oxaliplatin (OXA) is a third-generation platinum based chemotherapy used in the treatment of colorectal cancer (CRC). We recently showed by gene set enrichment analysis (GSEA) that subactive doses of OXA induce adaptive changes in CRC cell lines, with preservation of cell viability (Tosi *et al*, ASCO Annual Meeting 2022, abstr. #3091). In particular, a widespread negative enrichment of gene sets involved in DNA repair was detected both at 24 and at 48 hours, with a far greater negative enrichment at 48 hours, which suggest a commitment of cancer cell to a major limitation of DNA repairing capability following a DNA damaging insult. To untangle the fine tuning of these adaptive responses, we performed an in-deep analysis of the subsets of genes (referred to as the leading edge) that contributed the most to the statistical significance of the corresponding gene sets.

**Material and methods:** We analysed previously generated GSEA data from RNAseq profiling of CRC cell line HCT116 treated in vitro for 24 or 48 hours with OXA at low, ineffective concentration (0.5 mM, corresponding to the IC10). We used *pathview* and *SBGNview* R packages to perform extensive pathway-based data mapping and visualization.

**Results:** The analysis of leading edge genes shows that CRC cells develop a complex and organized response to low-dose oxaliplatin treatment. This adaptive response include a transcriptome rewiring consisting in (i) an increase of mRNA of cyclin D and CDK4/6 and a concomitant reduction of several genes implicated in the control of all other cell cycle phases, (ii) a progressive reduction of mRNA of genes coding for several DNA replication machinery components, in particular DNA polymerase alpha-primase complex, MCM complex, clamp loader and RPA, (iii) a reduction in the mRNA of genes of different pathways of DNA repair machinery, in particular short and long patch base excision repair complexes, MutS homolog (MSH) family genes and Rad51 paralogs, (iv) an increase in

mRNA of proapoptotic factor genes and membrane receptors involved in apoptosis induction, including TRAIL, Fas and TNFR.

**Conclusion:** This analysis suggests that cancer cell adaptive response to low-dose OXA promotes the transition of cell population toward the G1/S transition, while blocking further progression in cellular cycle and decreasing DNA replication and DNA repair capabilities. This may confer a selection advantage to cells with fewer OXA-induced DNA damages and favour the DNA integrity of cell population. Rewired cell pathways could constitute a suitable target to improve the antitumor activity of low-dose oxaliplatin. Experimental confirmation of these data is needed.

**No conflict of interest.**

## POSTER SESSION

### DNA Repair Modulation (including PARP, CHK, ATR, ATM)

275 (PB055)

#### Large genome rearrangement of BRCA1/2 in BRCA mutation negative ovarian cancer patients

M.H. Kim<sup>1</sup>, H.J. Jung<sup>1</sup>, B.J. Kim<sup>1</sup>, H. Kim<sup>2</sup>, S.I. Park<sup>3</sup>, S.Y. Ryu<sup>1</sup>. <sup>1</sup>Korea Cancer Center Hospital- KIRAMS, Ob/Gyn, Seoul, South Korea; <sup>2</sup>Korea Cancer Center Hospital- KIRAMS, Laboratory Medicine, Seoul, South Korea; <sup>3</sup>Dongnam Institute of Radiological and Medical Sciences, Ob/Gyn, Busan, South Korea

**Background:** We performed large genomic rearrangement (LGR) analysis of BRCA1/2 in ovarian cancer patients who were negative for BRCA1/2 as a result of the Next Generation Sequencing (NGS) analysis to determine the prevalence and the characteristics of the mutations.

**Material and methods:** We studied patients with epithelial ovarian cancer diagnosed at Korea Cancer Center since 2008, who have confirmed germline BRCA through Next generation sequencing (NGS) test at our hospital. Among patients with BRCA mutation negative, we preferentially selected patients with a family history of HRD-related cancer. We commissioned the Green Cross Medical Foundation for complex ligation-dependent probe amplification (MLPA) analysis of blood samples from selected patients. We mapped the mutation site through long-range PCR in the DNA of the sample in which the large genomic rearrangement (LGR) mutation was detected through Medical Foundation for complex ligation-dependent probe amplification (MLPA) analysis.

**Results:** We performed MLPA analysis on blood samples from a total of 36 BRCA-negative ovarian cancer patients. As a result of MLPA analysis, a LGR mutation of BRCA was identified in one patient's blood sample. The LGR mutation was confirmed in a patient with stage 2 ovarian cancer, and a mutation was confirmed in BRCA1. The detection rate of BRCA mutation through MLPA analysis of our institute was 2.8%.

**Conclusions:** This study showed a higher result than the BRCA mutation detection rate through MLPA of previous papers of South of Korea. High risk ovarian cancer patients with NGS-negative results should be considered for LGR detection. The importance of this MLPA analysis could be confirmed, and it can be expected that the rationale for PARP inhibitor treatment for germline BRCA-negative patients and improvement of treatment results can also be expected. The detection of more BRCA1/2 mutations in patients of ovarian cancer is important for efforts to provide targeted therapy.

**No conflict of interest.**

277 (PB057)

#### PPP2R1A missense mutations as a novel biomarker of response to ATR inhibitors in ARID1A mutant ovarian clear cell carcinoma

J. Stewart<sup>1</sup>, J. Baxter<sup>1</sup>, D. Zatreanu<sup>1</sup>, R. Brough<sup>1</sup>, F. Song<sup>1</sup>, A. Konde<sup>1</sup>, D. Krastev<sup>1</sup>, J. Alexander<sup>1</sup>, R. Natrajan<sup>1</sup>, S. Banerjee<sup>2</sup>, P. Stephen<sup>1</sup>, C. Lord<sup>1</sup>. <sup>1</sup>Institute of Cancer Research, CRUK Gene Function Laboratory, London, United Kingdom; <sup>2</sup>Royal Marsden NHS Trust, Gynaecology Unit, London, United Kingdom

**Introduction:** Ovarian clear cell carcinoma (OCCC) is characterised by a high prevalence of ARID1A mutations and chemotherapy resistance. We previously found that loss of ARID1A causes ATR inhibitor (ATRi) sensitivity, a finding that led to the Phase 2 ATARI clinical trial (NCT04065269). We aim to identify novel genetic determinants of ATRi response in ARID1A-mutant OCCC.

**Materials and methods:** A genome wide CRISPR knockout (CRISPRn) screen was performed in ARID1A mutant OCCC TOV21G cells. CRISPR prime gene-editing was used to introduce PPP2R1A p.R183 mutations. *In vitro* and *in vivo* ATRi sensitivity was assessed in PPP2R1A isogenic models. Cell cycle analysis was performed via flow cytometry. Mass spectrometry based phosphoproteomic profiling was performed in the PPP2R1A isogenic models in the presence and absence of ATRi.

**Results:** A CRISPRn screen in ARID1A mutant OCCC cells identified protein phosphatase 2 (PP2A) complex subunits as ATRi response genes. In OCCC, PPP2R1A missense mutations cause amino acid substitutions at residue p.R183. Characterisation of a cohort of OCCC primary tumours revealed a higher prevalence of structural subunit (PPP2R1A) mutations than previously reported (52%) which frequently co-occurred with ARID1A mutations. ARID1A-mutant OCCC cells with heterozygous PPP2R1A p. R183P or p.R183W mutations both enhanced ATRi sensitivity *in vitro* and *in vivo*.

The most profound cell-cycle defects caused by PPP2R1A missense mutation was an ATRi-induced reduction in active S phase and premature mitotic entry. ATRi exposure in PPP2R1A mutants increased 53BP1 bodies, a biomarker of residual DNA damage in mitosis.

Phospho-proteomic profiling of PPP2R1A mutant OCCC cells revealed the selective increase in phosphorylation of Lysine Deficient Protein Kinase 1 (WNK1) following ATRi exposure, as well as increased phosphorylation of the WNK1 substrate Oxidative Stress Response Kinase 1 (OSR1). Depletion of WNK1 rescued ATRi sensitivity and S phase defects in PPP2R1A mutant cells suggesting a novel role for this kinase.

**Conclusions:** The ability of PPP2R1A missense mutations to enhance ATRi sensitivity in tumours cells with pre-existing ARID1A mutations suggests that the co-occurrence of these mutations may be better predictors of ATRi sensitivity than either mutation alone. Increased phosphorylation of WNK1 may drive ATRi sensitivity in PPP2R1A mutant cells.

#### Conflict of interest:

Advisory Board: CL: Syncona, Sun Pharma, Gerson Lehman Group, Merck KGaA, Vertex, AstraZeneca, Tango, 3rd Rock, Ono Pharma, Artios, Abingworth, Tesselate, Dark Blue Therapeutics. Has stock in: Tango, Ovibio, Enedra Tx., Hysplex, Tesselate.

SB: Amgen, Astrazeneca, Genmabs, GSK, Immunogen, MSD, Merck Sereno, Mersana, Oncxerna, Seagen, Shattuck Labs.

Corporate-sponsored Research: CL: AstraZeneca, Merck KGaA, Artios.

SB: Astrazeneca, GlaxoSmithKline.

278 (PB058)

#### CDK12 loss leads to replication stress and sensitivity to combinations of the ATR inhibitor camonsertib (RP-3500) with PARP inhibitors

J. Setton<sup>1</sup>, D. Gallo<sup>2</sup>, D. Glodzik<sup>3</sup>, B. Kaiser<sup>2</sup>, S. Braverman<sup>1</sup>, T. Ubhi<sup>4</sup>, S. Fournier<sup>5</sup>, P. Selenica<sup>6</sup>, N. Laterre<sup>7</sup>, A. Roulston<sup>5</sup>, G. Brown<sup>4</sup>, S. Morris<sup>2</sup>, J. Reis-Filho<sup>6</sup>, M. Zimmermann<sup>2</sup>. <sup>1</sup>Memorial Sloan Kettering Cancer Center, Department of Radiation Oncology, New York, USA; <sup>2</sup>Repare Therapeutics Inc., Cancer Biology, Saint-Laurent, Canada; <sup>3</sup>Harvard Medical School, Department of Biomedical Informatics, Boston, USA; <sup>4</sup>University of Toronto, Donnelly Centre for Cellular and Biomolecular Research- Department of Biochemistry, Toronto, Canada; <sup>5</sup>Repare Therapeutics Inc., Pharmacology, Saint-Laurent, Canada; <sup>6</sup>Memorial Sloan Kettering Cancer Center, Department of Pathology, New York, USA; <sup>7</sup>Repare Therapeutics Inc., SNIPRx Target Discovery Platform, Saint-Laurent, Canada

**Background:** Loss-of-function (LOF) alterations in Cyclin-Dependent Kinase 12 (CDK12) are found across tumors, including metastatic prostate (~5%) and serous ovarian (~3%) cancers. While initial data suggested that CDK12 LOF compromises DNA repair by homologous recombination (HR), there is burgeoning evidence questioning this notion. CDK12-deficient tumors lack genomic features indicative of HR-deficiency (HRD) and instead harbor large tandem duplications thought to originate from DNA replication stress of unknown etiology. Cancers carrying CDK12 LOF alterations also do not respond to chemotherapy or poly-ADP-ribose polymerase inhibitors (PARPi) nearly as well as HRD tumors. Therefore, defining the nature of the genome instability in CDK12 LOF-driven cancers could help develop new targeted therapeutic solutions for these patients and represent pressing unmet medical needs.

**Methods:** CDK12-null cell lines, generated using CRISPR/Cas9, were characterized for their DNA repair capacity and genomic instability. CRISPR-enabled chemogenomic screening was used to identify therapeutic vulnerabilities in the CDK12-deficient models. PARPi/ATRi monotherapy and combination efficacy was tested in multiple CDK12-deficient mouse xenografts. Next generation sequencing-based analysis of genomic signatures is being performed in cell line models and in human tumor samples harboring CDK12 LOF.

**Results:** *CDK12*-null cells did not show HR deficiency and were considerably less sensitive to single-agent PARPi compared to HR-deficient controls. *CDK12*-null cells, however, displayed a reduction in G1-phase CDT1 levels and chromatin-bound MCM helicase, resulting in a prolonged S-phase indicative of ongoing replication stress. Genomes of human *CDK12* deficient cancers showed the expected pattern of tandem duplications, highlighting a potential mechanistic link between defective origin licensing and *CDK12*-associated genomic features. The presence of replication stress suggested that *CDK12* deficiency may exacerbate sensitivity to ATR inhibitors (ATRI), including the highly potent and selective ATRI camonsertib (RP-3500). We profiled available chemogenomic CRISPR screening data identifying genes that modulate sensitivity to RP-3500. These data revealed that *CDK12* LOF leads to profound sensitivity to camonsertib, especially in combination with PARPi. These observations were further validated in cell viability assays and *CDK12*-deficient mouse xenografts at doses that were sub-therapeutic as single agents and well tolerated in combination.

**Conclusions:** The work reports on novel evidence supporting the hypothesis that *CDK12* LOF does not lead to HRD, but rather causes aberrant DNA replication origin licensing. Our findings suggest that *CDK12* biallelic LOF mutations may result in a therapeutic vulnerability to ATRI/PARPi, potentially leading to a new therapeutic approach to tumors with *CDK12* LOF.

#### Conflict of interest:

Ownership: Repare Therapeutics (MZ, JRF, SM, AR, NL, SF, BK, DG, DG).  
Paige.AI (JRF).  
Advisory Board: Repare Therapeutics (JRF, GB, TU).  
Volition RX (JRF).  
Personalis (JRF).  
Paige.AI (JRF).  
Roche Tissue Diagnostics (JRF).  
Ventana Medical Systems (JRF).  
Novartis (JRF).  
Genentech (JRF).  
MSD (JRF).  
Daiichi Sankyo (JRF).  
InVicro (JRF).  
Board of Directors: Grupo Oncoclinicals (JRF).  
Corporate-sponsored Research: Repare Therapeutics.  
Other Substantive Relationships: Repare Therapeutics - current or former full time employees (MZ, SM, AR, NL, SF, BK, DG, DG).  
Goldman Sachs - personal consulting fees (JRF).  
Personalis - personal consulting fees (JRF).  
Eli Lilly - personal consulting fees (JRF).

#### 279 (PB059)

##### ATR inhibitor camonsertib (RP-3500) suppresses early-stage erythroblasts by mediating ferroptosis

M. Levy<sup>1</sup>, G.B. Ferraro<sup>2</sup>, M. Planoutene<sup>1</sup>, L. Li<sup>2</sup>, Y. Han<sup>3</sup>, L. Varicchio<sup>1</sup>, S. Fournier<sup>2</sup>, X. An<sup>3</sup>, S.J. Morris<sup>4</sup>, M. Koehler<sup>5</sup>, R. Hoffman<sup>1</sup>, A.J. Fretland<sup>5</sup>, A. Roulston<sup>1</sup>, Y.Z. Ginzburg<sup>1</sup>. <sup>1</sup>The Tisch Cancer Institute, Icahn School of Medicine at Mount Sinai, New York, NY, USA; <sup>2</sup>Repare Therapeutics Inc, Pharmacology, Saint-Laurent, QC, Canada; <sup>3</sup>Lindsley F. Kimball Research Institute, New York Blood Center, New York, NY, USA; <sup>4</sup>Repare Therapeutics Inc, Discovery Research, Saint-Laurent, QC, Canada; <sup>5</sup>Repare Therapeutics Inc, Clinical, Cambridge, MA, USA

**Background:** Ataxia telangiectasia mutated and Rad3-related kinase (ATR) mediates cellular response to replication stress and DNA damage. Camonsertib is a potent and selective ATR inhibitor with strong pre-clinical efficacy, promising clinical activity (NCT04497116) but results in rapid monocytopenia leading to dose limiting anemia potentially implicating a disturbance in iron homeostasis. Pre-clinically, dosing 3 days on/4 off mitigates anemia without compromising efficacy, allowing reticulocyte regeneration between doses. High iron requirements are uniquely essential for heme synthesis during erythropoiesis, specifically increasing erythroblast vulnerability to iron-dependent reactive oxygen species (ROS) and potential for iron-mediated oxidative DNA damage. We thus explore iron-mediated mechanisms of anemia induction in response to RP-3500.

**Methods and Results:** In mice, early bone marrow erythroblast depletion is noted 24 hours post camonsertib treatment. This depletion is reversible with erythroblast regeneration after 2–4 days off treatment. *In vitro*, during human CD34+ cell differentiation to erythroblasts, we show that ROS concentration is highest in early-stage erythroblasts and does not correlate with the degree of apoptosis. Next, we demonstrate altered expression of iron-related genes in erythroblasts: mRNA expression of ferritin (*FTH* and *FTL*), *PCBP1*, *NCOA4*, and *TFR2a* increases and *TFRC* decreases during erythroblast differentiation *in vitro*, confirming reliance on iron trafficking during erythropoiesis. When erythroblasts are treated with camonsertib, proliferation and differentiation are decreased in a dose dependent manner.

Specifically the proportion of early-stage erythroblasts decrease, while ROS concentration and *NCOA4* expression increase and *FTH* expression in treated cells decrease; all consistent with enhanced ferroptosis. Erythropoietin (EPO) supplementation does not alter erythroblast proliferation, differentiation, apoptosis, or ROS levels in camonsertib treated cells. Finally, the addition of ferristatin-1, intended to block ferroptosis, decreases ROS, increases apoptosis, and prevents a dose-dependent decrease in early-stage erythroblasts in culture. This is the first evidence that ATR inhibitor treatment suppresses erythropoiesis via ferroptosis in early-stage erythroblasts.

**Conclusions:** These results demonstrate that camonsertib-induced anemia is reversible. High levels of ROS, characteristic of early erythroblasts, may increase their susceptibility to ATR inhibition, mediated by increased ferroptosis. Although supplemental EPO does not alleviate the erythroid vulnerability to camonsertib, intermittent dosing allows for erythroid cell recovery, minimizing anemia while maintaining efficacy. Ongoing mechanistic studies will be discussed in the context of supportive therapeutic strategies to minimize camonsertib induced anemia.

#### Conflict of interest:

Ownership: GBF, LL, SF, SJM, MK, AJF and AR are employees of Repare Therapeutics, shareholders and have stock options.  
Corporate-sponsored Research: RH and YZG receive sponsored research funding from Repare Therapeutics.

#### 281 (PB061)

##### Ku-DNA binding inhibitors modulate the DNA damage response in response to DNA double-strand breaks

P. Mendoza-Munoz<sup>1</sup>, N.S. Gavande<sup>2</sup>, P.S. VanderVere-Carozza<sup>1</sup>, K.S. Pawelczak<sup>3</sup>, J.R. Dynlacht<sup>4</sup>, J.E. Garrett<sup>4</sup>, J.J. Turchi<sup>1,3,5</sup>. <sup>1</sup>Indiana University- School of Medicine, Medicine, Indianapolis, IN, USA; <sup>2</sup>Wayne State University College of Pharmacy and Health Sciences, Pharmaceutical Sciences, Detroit, MI, USA; <sup>3</sup>NERx Biosciences, Inc., Indianapolis, IN, USA; <sup>4</sup>Indiana University, School of Medicine, Radiation Oncology, Indianapolis, IN, USA; <sup>5</sup>Indiana University- School of Medicine, Biochemistry and Molecular Biology, Indianapolis, IN, USA

**Background:** The DNA-dependent protein kinase (DNA-PK) plays a critical role in the non-homologous end joining (NHEJ) double-strand break (DSB) repair pathway and the DNA damage response (DDR). Consequently, blocking DNA-PK kinase activity is being pursued as a therapeutic strategy for the treatment of cancer in combination with ionizing radiation (IR). Towards developing a new class of DNA-PK inhibitors, our laboratory previously reported the development of Ku-DNA binding inhibitors (Ku-DBis) that act via inhibition of DNA-PK catalytic kinase activity by blocking the Ku-DNA interaction. Ku-DBis display nanomolar activity *in vitro*, possess cellular DNA-PK and NHEJ inhibitory activity, and sensitize non-small cell lung cancer (NSCLC) cells to DSB generating chemotherapeutics bleomycin and etoposide.

**Material and Methods:** Using multiple NSCLC cell lines possessing mutations in specific DDR genes we interrogated the molecular mechanism involved in cellular sensitization to DSBs as a function of Ku-DBis treatment. We employed multiple cellular viability assays coupled with Western blot and immunofluorescence determination of DDR pathway activation to assess how specific alteration in the DDR pathway impact Ku-DBi activity.

**Results:** Our findings demonstrate that Ku-DBi treatment in combination with DNA DSB-inducing agents (bleomycin or IR), showed a significant reduction of autophosphorylation events of DNA-PKcs at the S2056 cluster compared to DNA DSB-inducing agent alone. In addition, analysis of phospho-ATM and phospho-p53 protein levels in these NSCLC cell lines suggested activation of the ATM pathway as a function of Ku-DBi treatment followed by bleomycin, evidenced by an increase of phosphorylation of ATM at Ser1981, and a modest increase of p53 phosphorylation at Ser15. Our results demonstrate that Ku-DBis block DNA-DSB dependent DNA-PKcs autophosphorylation, resulting in potentiating cellular sensitivity to bleomycin and IR, and a likely effect on the ATM-dependent signaling pathway.

**Conclusions:** In this study, we demonstrate that chemical inhibition of the Ku-DNA interaction potentiates the cellular effects of bleomycin and IR via p53 phosphorylation through the activation of the ATM pathway. This response is concomitant with a reduction in DNA-PKcs autophosphorylation events at the S2056 cluster (pS2056). These data are consistent with Ku-DBis possessing a novel mechanism of action that abrogates autophosphorylation of DNA-PKcs to impact DSB repair and potentially DDR signaling, becoming in a promising approach as part of an anticancer therapeutic strategy in combination with DNA DSBs-inducing agents.

**No conflict of interest.**

282

(PB062)

**Optimization of treatment schedule for the ATR inhibitor elimusertib (BAY 1895344) in preclinical tumor models**

A. Wengner<sup>1</sup>, L. Ehresmann<sup>1</sup>, N. Guthof<sup>2</sup>, S. Osterberg<sup>1</sup>, B. Ploeger<sup>3</sup>, A. Wiedmann<sup>1</sup>, G. Wilkinson<sup>1</sup>. <sup>1</sup>Bayer AG, RED Oncology, Berlin, Germany; <sup>2</sup>Bayer AG, RED Oncology, Boston, USA; <sup>3</sup>Bayer AG, RED Pharmacometrics Modeling, Berlin, Germany

**Background:** ATR kinase is a critical component of the DNA damage response (DDR) machinery. Elimusertib, a potent and selective ATR inhibitor, has demonstrated efficacy in preclinical tumor models as monotherapy and synergistic antitumor activity in combination with DNA damage inducing as well as DNA repair compromising therapies. Elimusertib monotherapy revealed clinical benefit in patients with advanced solid tumors carrying DDR defects (Yap et al. Cancer Discovery 2021; Yap et al. AACR Annual Meeting 2022). Hematologic toxicities are common side effects associated with this class of drug and are clinically dose-limiting. We explored alternative dosing schedules in preclinical tumor models to mitigate hematologic toxicity and inform clinical dosing schedule optimization.

**Methods:** The previously determined MTD schedule for elimusertib monotherapy in preclinical mouse models was a twice daily application of 40 or 50 mg/kg for 3 days followed by 4 days treatment break (BID 3on/4off). Alternative dosing schedules were tested, including continuous treatment with elimusertib once or twice daily (QD, BID) or applied twice daily for 3 days followed by 11 days treatment break (BID 3on/11off). Antitumor activity and tolerability were assessed in direct comparison to the clinically relevant schedule 3on/4off in models of different indications with a focus on hematological toxicity.

**Results:** In the tumor xenograft models Hs746T (gastric cancer), 22Rv1 (prostate cancer), REC-1 (mantle cell lymphoma), HCC1806 (TNBC), HT-29 (CRC) elimusertib showed good antitumor activity upon dosing with 60 mg/kg BID 3on/11off. The efficacy was comparable or better than observed with 40 mg/kg BID 3on/4off treatment. Importantly, the 3on/11off schedule induced less hematological effects than the 3on/4off treatment. The 3on/11off schedule impacted to a lesser extent the red blood cell counts as well as Hb level in peripheral blood and bone marrow aspirates. In contrast, daily continuous treatment substantially worsened hematological toxicities and reduced antitumor activity compared to 3on/4off.

**Conclusion:** We demonstrate in preclinical tumor models that elimusertib monotherapy twice daily treatment for 3 days followed by an extended treatment break of 11 days improves overall safety profile by reducing hematologic toxicity while maintaining or enhancing antitumor efficacy due to improved tolerability. Herewith, the basis was given to test this schedule in the ongoing Ph1 clinical trial of elimusertib. Preliminary clinical data with 3on/11off schedule are consistent with the expected improvement in the safety profile showing less hematologic toxicity at a comparable cumulative exposure vs the 3on/4off schedule (Yap et al. AACR Annual Meeting 2022). Elimusertib is currently being evaluated as single agent and in multiple combination studies (NCT03188965, NCT04267939, NCT04095273).

**Conflict of interest:**

Other Substantive Relationships: All authors are employees of Bayer AG.

283

(PB063)

**Replication protein A targeted therapy: In vivo anticancer activity and cellular target engagement**

J. Turchi<sup>1</sup>, P. VanderVere-Carozza<sup>2</sup>, K. Pawelczak<sup>3</sup>. <sup>1</sup>Indiana University School of Medicine, Medicine and Biochemistry & Molecular Biology, Indianapolis, USA; <sup>2</sup>Indiana University School of Medicine, Medicine, Indianapolis, USA; <sup>3</sup>NERx Biosciences, Research, Indianapolis, USA

**Background:** Replication protein A (RPA) plays essential roles in DNA replication, repair, recombination and the DNA-damage response (DDR). Retrospective analysis of lung cancer patient data demonstrates high RPA expression as a negative prognostic biomarker for overall survival in smoking-related lung cancers. These observations are consistent with the increase in RPA expression serving as an adaptive mechanism that allows tolerance of the genotoxic stress resulting from carcinogen exposure.

**Materials and methods:** We have employed chemical synthesis, *in vitro* analyses and *in vivo* xenograft studies to assess mechanism of action, cellular engagement and therapeutic activity of RPA-targeted agents.

**Results:** We have discovered, developed and characterized a novel small molecule RPA inhibitor (RPAi) NERx-329 that blocks the RPA-DNA interaction. We have optimized formulation for *in vivo* analyses and cellular engagement studies. NERx 329 elicits single agent *in vitro* anticancer activity across a broad spectrum of cancers which allowed the identification of genetic predictors of RPAi efficacy. A genetic knock out screen also identified

additional genetic alterations that increase RPAi activity. A series of these genetic models were pursued and results demonstrate specific genetic alterations increase RPAi activity *in vitro* and *in vivo*. Chemical RPA inhibition is shown to potentiate the anticancer activity of a series of DDR inhibitors as well as traditional DNA damaging cancer therapeutics. The analysis of cell cycle, chromatin-bound RPA and DDR pathway activation demonstrate on-target cellular engagement of RPA by NERx-329.

**Conclusions:** These data demonstrate that targeting the RPA-DNA interaction elicits a state of chemical RPA exhaustion that results in *in vivo* anticancer activity. In addition, specific genetic predictors of RPAi sensitivity have been identified which will allow the selection of patient populations likely to benefit from RPA-targeted therapeutics.

**Conflict of interest:**

Ownership: JJT is a cofounder of NERx Biosciences.

Board of Directors: JJT and KSP serve on the NERx Biosciences BoDs.

**POSTER SESSION****Drug Delivery**

284

(PB064)

**Ultrasound-induced cavitation enhances therapeutic efficacy of AXL-targeting ADC leading to improved survival in a human xenograft model of renal cancer**

M. Masiero<sup>1</sup>, E. Vojtasova<sup>1</sup>, P. Boulos<sup>2</sup>, F. Zammarchi<sup>3</sup>, P. van Berkel<sup>4</sup>, C. Crake<sup>2</sup>, C. Coviello<sup>2</sup>, C. Rowe<sup>1</sup>. <sup>1</sup>OxSonic Therapeutics, Research and Development, Oxford, United Kingdom; <sup>2</sup>OxSonic Therapeutics, Engineering, Oxford, United Kingdom; <sup>3</sup>ADC Therapeutics, Pharmacology, London, United Kingdom; <sup>4</sup>ADC Therapeutics, Research and Development, London, United Kingdom

**Background:** Antibody-drug conjugates (ADCs) are a new class of anti-tumor agents that combine the targeting specificity of monoclonal antibodies (mAbs) with the cell killing ability of powerful cytotoxic molecules.

However, poor penetration of drugs into solid tumors, including mAbs, is a well-recognized barrier to effective therapy as this strongly limits the number of tumor cells targeted by the therapeutic agent. A novel non-invasive approach to tackle this problem is ultrasound-mediated drug delivery using co-infused cavitation nuclei, which shows promise as a way to pump more drug (including mAbs/ADCs) into and throughout tumors.

The purpose of this study was to test a suboptimal single dose of mipasetamab uzoptirine (ADCT-601), an ADC targeting the AXL protein, in combination with ultrasound-induced cavitation in a preclinical mouse model of renal cancer.

**Material and methods:** SCID mice were injected subcutaneously with SN12C human renal cancer cells and when tumors reached an average size of 150 mm<sup>3</sup>, animals were divided into 6 cohorts (N = 6–7 mice each): a) PBS (vehicle control); b-c) B12-PL1601 (control ADC) at 0.3 mg/kg ± cavitation; d-e) ADCT-601 at 0.3 mg/kg ± cavitation; f) ADCT-601 at 1 mg/kg (efficacious dose). Cavitation nuclei and drug agent were administered intravenously just before ultrasound application from the OxSonic SonoCart system (ultrasound parameters: fc = 0.5 MHz; 8000cycles; PRF = 0.5 Hz; PRFP = 1–2.9 MPa variable). Ultrasound amplitude was set according to the cavitation monitoring method (passive acoustic mapping [PAM]) to be within 0.1–0.5 nJ/pulse for 10 minutes of treatment. Mice were culled when tumors' width + length passed the value of 24 mm.

**Results:** Results indicated that cavitation was achieved in the desired range for all ultrasound groups. Following treatment, 2 groups (ADCT-601 at 1 mg/kg and ADCT-601 at 0.3 mg/kg + cavitation) showed significant tumor growth delay, ultimately leading to a significant improvement in survival when compared to all other groups. No significant difference between the high and the low ADCT-601 dose with cavitation was observed, indicating that the combination enhanced potency by 3.3-fold.

**Conclusions:** Cavitation-enhanced delivery of ADCT-601 has a strong effect on xenograft tumor growth leading to a significant increase in survival. This was demonstrated for a suboptimal ADC dose, indicating that ultrasound-mediated drug delivery could be used to reduce the administered dose while preserving therapeutic efficacy. These preclinical data warrant further evaluation of this promising combination in the clinic.

**Conflict of interest:**

Ownership: Massimo Masiero, Erika Vojtasova, Paul Boulos, Calum Crake, Christian Coviello and Cliff Rowe own OxSonic Therapeutics share options. Christian Coviello also owns OxSonic Therapeutics shares. Francesca Zammarchi and Patrick van Berkel own ADC Therapeutics shares.

Other Substantive Relationships: Massimo Masiero, Erika Vojtasova, Paul Boulos, Calum Crake, Christian Coviello and Cliff Rowe are OxSonic Therapeutics employees. Christian Coviello is also OxSonic Therapeutics co-founder. Francesca Zammarchi and Patrick van Berkel are ADC Therapeutics employees.

**285** (PB065)  
**Using Fluorescence Cross Correlation Spectroscopy to Monitor and Quantify Drug Target Occupancy in Cells, Tissues and Patient Biopsies**

F. Becker<sup>1</sup>. <sup>1</sup>Intana Bioscience GmbH, Research, Planegg, Germany

Fluorescence Cross Correlation Spectroscopy (FCCS) is a singly molecule sensitive method to analyze molecular interactions.

The approach has been employed in the past by Intana to set up high throughput screens, based on affinity or enzymatic activities. Similarly, we have investigated the formation and assembly of large protein complexes and studied complex targets as channels, transporters and even GPCRs.

Among many other advantages, FCCS allows measurements in cellular lysates, bypassing protein purification and retaining the physiological environment. Consequently, assay development is straight forward and allows tackling also demanding targets.

With this study we aimed to quantify the absolute drug target occupancy in cell in order to correlate the ratio of inhibited target molecules to the physiological, i.e. therapeutic effect.

In order to measure unlabeled drugs and targets without purification of either binding partner for subsequent analysis Intana has set up an FCCS based assay format making use of fluorescent antibodies to label targets without interfering with drug target interactions and fluorescent tracer to quantify the unoccupied fraction of targets.

For this samples are processed to cellular lysates using proprietary protocols and co-incubated with 2 different antibodies, carrying 2 different fluorescent labels and binding independently on 2 epitopes on the target. By this the total concentration of targets in the lysate can be precisely quantified.

In a second step a fluorescent tracer molecule, which binds into the same pocket as the drug of interest is added to the lysate to quantify all unoccupied targets. In addition, a fluorescent antibody directed against the target is added for increase sensitivity. Knowing the exact concentration of targets in the sample and the concentration of targets that is bound to the tracer yields a precise quantification of target occupancy in the sample.

Our approach was tested in cells, tissues, xenograft tumors and clinical patient samples. Data can help to guide cellular and animal experiments and to correlate or stratify patient responses to drug treatments.

**Conflict of interest:**

Ownership: Intana Bioscience GmbH, siTOOLS Biotech GmbH, Alpine Antiviral GmbH.

**286** (PB066)  
**Therapeutic potential of systemically delivered breast cancer specific modified mRNA**

M. Žak<sup>1,2,3</sup>, J. Yoo<sup>1,2,3</sup>, L. Zangi<sup>1,2,3</sup>. <sup>1</sup>Icahn School of Medicine at Mount Sinai, Cardiovascular Research Institute, New York, USA; <sup>2</sup>Icahn School of Medicine at Mount Sinai, Black Family Stem Cell Institute, New York, USA; <sup>3</sup>Icahn School of Medicine at Mount Sinai, Department of Genetics and Genomic Sciences, New York, USA

Triple negative breast cancer (TNBC) presents the worst prognosis among breast cancers with a 40% mortality rate within 5 years from diagnosis. Due to the molecular characteristics of TNBC, cytotoxic chemotherapy remains the main treatment. An efficient targeted therapeutic approach is needed to improve treatment outcome with reduced toxicity. Here we developed a novel system that enables systemic delivery of modified mRNA (modRNA) specifically to TNBC cells. We transiently expressed therapeutic genes or modRNA-encoded antibodies (modRNabs) in 4T1 mouse model of TNBC.

Breast cancer Specific Modified mRNA Translation System (SMRTs) allows gene expression in 4T1 breast cancer cells based on their microRNA (miR) profile. SMRTs contains two modRNAs; the first carrying a Cas6 gene with a specific anti-miR sequence, and the second carrying a gene of interest with a Cas6 recognition site (hairpin) which enables expression of Cas6 only in cells that do not contain 4T1-specific miRs. In non-4T1 cells, the Cas6 cleaves the modRNA at the hairpin, preventing expression of the gene of

interest. However, in breast cancer cells, 4T1-specific miRs attach to an anti-miR sequence causing degradation of modRNA carrying Cas6 gene which in turn allows expression of the gene of interest. For systemic delivery, therapeutic or reporter modRNA was encapsulated in lipid nanoparticles (LNP) and visualized using bioluminescence (BL) imaging. To assess tumor growth inhibition, Pip4k2c alone or in combination with anti-CTLA-4 modRNab was intravenously injected into female BALBc mice bearing 4T1 tumors every 3 days for a total of 5 injections.

Four out of five of the designed nGFP SMRTs showed expression in 4T1 breast cancer cells and significant decrease in the mouse mammary gland epithelial cell line *in vitro*. *in vivo*, direct injection of Luciferase (Luc) SMRTs into the 4T1 mammary gland tumor and contralateral femur muscle showed expression in the tumor and significant decrease in the muscle of BALBc mice. Similar BL signal in the tumor was seen when Luc modRNA or Luc SMRTs encapsulated in LNP were delivered systemically. However, in mice injected with Luc SMRTs, BL signal significantly decreased in the liver ( $p < 0.0001$ ), spleen ( $p = 0.0009$ ) and kidney ( $p = 0.0306$ ). Therapeutically, Pip4k2c SMRTs with anti-CTLA-4 modRNab significantly inhibited tumor growth when compared to non-treated mice ( $p = 0.0002$ ) or Luc SMRTs injected mice ( $p = 0.0032$ ).

SMRTs allow breast cancer specific gene translation *in vitro* and *in vivo*. SMRTs encapsulated in LNP allow efficient systemic delivery and breast cancer specific expression of therapeutic genes. modRNA can be used for efficient production of therapeutic monoclonal antibodies. We are confident that SMRTs constructs can be created for other tumor cell types, and that such system can be widely used for cancer therapeutics.

**No conflict of interest.**

**287** (PB067)  
**Investigation of a novel radionuclide carrier for targeted radionuclide therapy**

Y. Yu<sup>1</sup>, S.S. Oh<sup>1</sup>, K.R. Choi<sup>1</sup>, A. Kim<sup>1</sup>, Y.S. Park<sup>1</sup>, H.S. Jang<sup>2</sup>. <sup>1</sup>ZTIBIOSCIENCES, R&D Team, 107- Gwanggyo-ro- Yeongtong-gu- Suwon-si- Gyeonggi-do, South Korea; <sup>2</sup>ZTIBIOSCIENCES, Chief Executive Officer, 107- Gwanggyo-ro- Yeongtong-gu- Suwon-si- Gyeonggi-do, South Korea

**Background:** In internal radiation therapy of cancer, optimal targeting ligand and type of therapeutic radionuclide must be considered carefully for effective treatment. In addition, optimal ligand and nuclide type may vary depending on diverse parameters characterizing the tumor. Thus, for use in various cancers, there is a need for the development of a carrier that can firmly bind to a variety of nuclides. Here we introduce a biocompatible iron oxide nano radionuclide carrier. By reacting nanoparticles and nuclides using our conjugate synthesizer, it is possible to bind near-permanently nuclides to our nanocarriers.

**Material and methods:** To test the carrier's biocompatibility, particles were labeled with a fluorescence dye and injected intravenously into female CD-1 mice. Mice were anesthetized and carrier biodistribution was recorded. In addition, to test the carrier's radionuclide binding capabilities, carriers were radiolabeled with radioactive iodine and injected intravenously in CD-1 mice that were anesthetized and scanned using single-photon emission computed tomography (SPECT). Ligand-mediated cellular uptake of the carriers was demonstrated per iron content in human origin cancer cells qualitatively through Prussian blue staining and quantitatively by ICP-MS.

**Results:** As a result of biodistribution studies, carriers circulated through the body during initial time points were rapidly excreted through the kidney and could be detected in the bladder at 3 hours post-injection. Rapid excretion of carriers allows for lowered whole-body radiation toxicity. SPECT data showed stable distribution of radioactive iodine throughout the whole body. Given that the normal distribution of free radioiodine is for it to accumulate in the thyroid, such a result is evidence of firm binding of nuclides to the carrier. Ligand-receptor-mediated cellular uptake of nanocarriers increased dose-dependently up to 24 hours post-treatment.

**Conclusions:** Here we have introduced a biocompatible radionuclide carrier. Its biodistribution and near-permanent nuclide binding properties make it an admirable platform for targeted radionuclide therapy. Further *in vivo* studies have been carried out to test the carrier's application for treating triple-negative breast cancers (TNBC) and platinum-resistant ovarian cancers using <sup>131</sup>I and folic acid targeted ligands.

**No conflict of interest.**

288 (PB068)

**Eliminating the Immunotoxicity of Interleukin-12 through Protease-Sensitive Masking**

J. Ishihara<sup>1</sup>, A. Mansurov<sup>2</sup>, J. Hubbell<sup>2</sup>. <sup>1</sup>Imperial College London, Bioengineering, London, United Kingdom; <sup>2</sup>University of Chicago, Pritzker school of molecular engineering, Chicago, USA

**Background:** Checkpoint inhibitor (CPI) immunotherapy demonstrates modest efficacy against immunologically 'cold' or immune-excluded tumors, therefore needs another approach for majority of patients. Although interleukin-12 (IL-12) is a promising antitumor cytokine that enables activation and recruitment of immune cells into tumors, its widespread use in the clinic has been hindered due to severe immune-related adverse events (irAEs). An ideal IL-12 therapy would restrict the proinflammatory effects of IL-12 to the tumor site, while limiting its exposure in the periphery.

**Method:** Here, we solved the IL-12 toxicity challenge by exploiting the preferential overexpression of proteases (Matrix Metalloproteinases, Serine Proteases) in the tumor to engineer tumor-selective, masked IL-12. A IL-12RB1 receptor-based masking domain was fused to IL-12 p35 domain via a protease-cleavable linker.

**Result:** Recombinant fusion of masking domain to IL-12 prevented IL-12 from signaling systemically, whereas proteolytic cleavage of the linker domain by tumor-associated enzymes restored the biological activity of IL-12. We demonstrate that intravenously (i.v.) administered, masked IL-12 produces strong therapeutic effects through remodeling the immune-suppressive microenvironment and renders CPI-resistant tumors responsive, while systemic irAEs are eliminated, boosting the therapeutic index of this promising cytokine. In several solid tumour models, the therapeutic effects of masked IL12 were similar to its unmasked wild-type form, yet its toxicity was as low as saline injections. Masked IL-12 synergised with anti-PD-1 antibody for efficacy. We found that addition of human tumour lysates, and not adjacent healthy tissue lysates, cleaved off the mask, induced significant IFN $\gamma$  production and STAT4 phosphorylation, similar to wild-type IL-12. We made fully humanized masked IL-12 molecule already.

**Conclusion:** Masking approach to IL-12 may solve the toxicity issue of IL-12 observed in 1990s clinical trials, while maintaining extremely high anti-tumor effects in immunologically cold tumors.

**Conflict of interest:**

Ownership: Shareholder of ArrowImmune Inc.

Other Substantive Relationships: Consultant of Libo pharma.

289 (PB069)

**The ABCB1/ABCG2 inhibitor elacridar is a more potent pharmacoenhancer compared to tariquidar for treatment of intracranial tumors with small molecule drugs**

O. Van Tellingen<sup>1</sup>, A. Lentzas<sup>1</sup>, S. Zuidema<sup>1</sup>, C. Çitirikkaya<sup>1</sup>, N. Venekamp<sup>1</sup>, J. Beijnen<sup>1</sup>. <sup>1</sup>Netherlands Cancer Institute, Pharmacology, Amsterdam, Netherlands

**Background:** The blood-brain barrier (BBB) is a major hurdle to successful pharmacotherapy of brain tumors. ABCB1 and ABCG2 are efflux transporters that are expressed in brain tumor vessels and reduce the uptake of many small molecule drugs. Elacridar and tariquidar are both dual ABCB1 and ABCG2 inhibitors. We aim to improve pharmacotherapy of brain cancer by concomitant use of potentially effective drugs with elacridar. Since tariquidar has mostly been used to assess the effects of ABC-transporters on brain uptake in human studies with PET tracers, we decided to compare both agents in our rodent models. We determined the relationship between the plasma concentration of the inhibitor and the brain-to-plasma (B/P) ratio of substrate drugs.

**Materials and methods:** We used *Abcg2;Abcb1a/b* double knockout (DKO), *Abcb1a/b* KO, *Abcg2* KO and wild-type mice receiving a cocktail of 7 model drugs at a fixed low dose in combination with elacridar or tariquidar at a range of doses. Drugs were given by 3-h infusion. DKO mice are the reference for complete inhibition, while single KO mice allow interrogation of the remaining transporter in case of dual substrate drugs. Brain and plasma levels were measured by LC-MS/MS.

**Results:** Complete inhibition of *Abcb1* by elacridar was achieved when the plasma level is about 1.0  $\mu$ M. However, a much higher plasma level (>4  $\mu$ M) of tariquidar was needed. Inhibition of *Abcg2* is more difficult. For erlotinib and palbociclib about 1.0  $\mu$ M of elacridar was sufficient, but other more profound *Abcg2* substrate drugs (e.g. vemurafenib and afatinib) never reached the B/P ratios achieved in reference DKO mice, even not at 4  $\mu$ M.

Strikingly, tariquidar was not able to even marginally enhance the brain uptake of ABCG2-substrate drugs in *Abcb1a/b* KO mice.

The B/P ratio of elacridar in DKO mice was 6. Elacridar improved its own brain distribution in WT mice, achieving steady-state B/P ratios at plasma level above 1.4  $\mu$ M. The B/P ratio of tariquidar in DKO mice was about 2. The B/P ratio in WT and *Abcb1a/b* KO mice was 0.3 and did not increase even at plasma concentration >8  $\mu$ M. Only in *Abcg2* KO mice, the B/P ratio increased to levels in DKO mice at tariquidar plasma levels of > 6  $\mu$ M. It appears that the efflux of tariquidar by *Abcg2* at the BBB severely compromises the usefulness of tariquidar as a pharmacoenhancer for brain delivery.

**Conclusions:** Thus, elacridar is a much more potent inhibitor of *Abcb1a/b* and *Abcg2* at the BBB. Elacridar can act as a pharmacoenhancer of ABCB1 substrate drugs and weaker ABCG2 substrates, but is not suited for brain delivery of drugs that are profound ABCG2 substrates. Tariquidar will enhance the brain penetration of ABCB1 substrates, but full inhibition is only achieved at levels above those reported in human subjects. Tariquidar completely fails to inhibit ABCG2 at the BBB.

**No conflict of interest.**

**POSTER SESSION****Drug Design**

290 (PB070)

**Discovery and characterization of potent and selective AXL receptor tyrosine kinase inhibitor AB801**

D. Miles<sup>1</sup>, S. Paprcka<sup>2</sup>, C. Foley<sup>1</sup>, S. Qu<sup>1</sup>, M. Lamani<sup>1</sup>, S. Paladugu<sup>1</sup>, H.T. Huang<sup>3</sup>, N. Tibrewal<sup>4</sup>, A. Chen<sup>4</sup>, J. Kulusich<sup>4</sup>, S. Garrido-Shaqfeh<sup>4</sup>, P. Fabila<sup>4</sup>, S. Sridhar<sup>2</sup>, S. Liu<sup>5</sup>, D. Swinarski<sup>5</sup>, X. Zhao<sup>4</sup>, E. Fernandez-Salas<sup>2</sup>, D. Green<sup>4</sup>, L. Jin<sup>3</sup>, M. Leleti<sup>1</sup>. <sup>1</sup>Arcus Biosciences, Chemistry, Hayward, USA; <sup>2</sup>Arcus Biosciences, Biology, Hayward, USA; <sup>3</sup>Arcus Biosciences, Drug Metabolism and Pharmacokinetics, Hayward, USA; <sup>4</sup>Arcus Biosciences, Discovery Pharmacology, Hayward, USA; <sup>5</sup>Arcus Biosciences, Pharmacology, Hayward, USA

**Background:** AXL receptor tyrosine kinase (AXL) is a transmembrane protein that is overexpressed in a variety of tumors and correlates with poor prognosis in cancer patients. AXL is expressed in cancer and stromal cells and has been implicated in the development of resistance to chemotherapy, targeted therapies & immunotherapies. Activation of AXL by its ligand, growth arrest specific protein 6 (GAS6), or ligand-independent dimerization facilitates AXL phosphorylation, initiates signaling cascades that promote cancer cell proliferation, survival, and an immunosuppressive microenvironment. Here we present the discovery and characterization of a novel, highly potent and selective AXL inhibitor, AB801.

**Materials and methods:** The potency and specificity of AB801 against AXL and other kinases were determined using a panel of HTRF® KinEASE-TK assays. The effects of AB801 on AXL were further assessed by p-AXL ELISA utilizing HEK293T cells transiently transfected with NanoLuc®-tagged AXL. Kinome selectivity was determined through a competition binding assay utilizing DNA-tagged kinases. Pharmacokinetics were evaluated in preclinical species. AB801 was also characterized in routine in vitro safety assays, including hERG inhibition.

**Results:** The novel AXL inhibitor AB801 is potent, reversible, and selective. AB801 exhibits a double-digit picomolar inhibitory constant and retains significant activity in 100% human serum cell-based assays. Additionally, good selectivity was observed against MERTK, TYRO3, and the overall kinome. Importantly, the molecule does not show significant inhibition of the major CYP450 isoforms or the hERG potassium channel. Studies in preclinical species demonstrate a favorable pharmacokinetic profile, consistent with a projected once-a-day oral administration in humans.

**Conclusions:** AXL inhibition is a promising therapeutic mechanism for impairing the growth and metastasis of chemotherapy- and immunotherapy-resistant tumors. AB801 exhibits improved potency, selectivity, and safety profiles compared to other AXL inhibitors currently advancing through clinical development.

**Conflict of interest:**

Ownership: Shareholder(s) in Arcus Biosciences

Other Substantive Relationships: Current employees of Arcus Biosciences.

291 (PB071)

**Improved binding affinity and pharmacokinetics enables sustained degradation of BCL6 *in vivo***

A. Harnden<sup>1</sup>, R. Huckvale<sup>1</sup>, K.M. Cheung<sup>1</sup>, O. Davis<sup>1</sup>, O. Pierrat<sup>1</sup>, R. Talbot<sup>1</sup>, G. Box<sup>1</sup>, M. Bright<sup>1</sup>, A. Akpinar<sup>1</sup>, D. Miller<sup>1</sup>, A. Hayes<sup>1</sup>, E. Gunnell<sup>2</sup>, Y.V. Le Bihan<sup>2</sup>, R. Burke<sup>1</sup>, V. Kirkin<sup>1</sup>, R. Van Montfort<sup>2</sup>, F. Raynaud<sup>1</sup>, O. Rossanese<sup>1</sup>, B. Bellenie<sup>1</sup>, S. Hoelder<sup>1</sup>. <sup>1</sup>The Institute of Cancer Research, Cancer Therapeutics, London, United Kingdom; <sup>2</sup>The Institute of Cancer Research, Cancer Therapeutics/Division of Structural Biology, London, United Kingdom

**Background:** The transcriptional repressor BCL6 is an oncogenic driver often found to be deregulated in lymphoid malignancies. We report the optimisation of our previously reported benzimidazolone molecular glue type degrader CCT369260 to CCT373566, a highly potent probe suitable for sustained depletion of BCL6 *in vivo*.

**Materials and methods:** Key to discovering CCT373566 were two design approaches: 1) careful, property focused optimisation of the piperidine moiety to reduce lipophilicity whilst maintaining the ability to degrade BCL6 in cells, 2) replacing the benzimidazolone of CCT369260 with a potent tricyclic quinolinone core that showed significantly tighter binding to the BCL6 BTB domain. *In vitro* and *in vivo* profiling will be demonstrated, including application to xenograft models of lymphoma.

**Results:** During this optimisation, we observed sharp degradation SAR, where subtle structural changes conveyed the ability to induce degradation of BCL6. Our resulting lead degrader CCT373566 has improved pharmacokinetics and activity compared to CCT369260. CCT373566 showed modest *in vivo* efficacy in a lymphoma xenograft mouse model following oral dosing.

**Conclusions:** CCT373566 represents an excellent tool to probe the function of BCL6 in human cancer cells and xenograft models.

**No conflict of interest.**

292 (PB072)

**Development of selective MCL-1 heterobifunctional degraders**

T. Tomczyk<sup>1</sup>, J.M. Arencibia<sup>1</sup>, M. Milewicz<sup>1</sup>, D. Trębicka<sup>1</sup>, J. Skalska<sup>1</sup>, K. Poniatowska<sup>1</sup>, J. Adamczyk<sup>1</sup>, K. Wójcik<sup>1</sup>, S. Cottens<sup>1</sup>, P. Kowalczyk<sup>1</sup>, P. Dobrzański<sup>1</sup>, M. Biśta<sup>1</sup>, K. Brach<sup>1</sup>, M. Świtalska-Drewniak<sup>1</sup>, A. Tracz<sup>1</sup>, M. Pastok<sup>1</sup>, K. Górecka-Minakowska<sup>1</sup>, K. Chrzanowska<sup>1</sup>, T. Takagi<sup>1</sup>, M. Walczak<sup>1</sup>. <sup>1</sup>Captor Therapeutics Inc., R&D Department, Wrocław, Poland

**Background:** MCL1 is a member of the Bcl-2 family that plays a key role in cellular homeostasis through the regulation of apoptosis as well as other less characterized functions. The growing recognition of MCL-1 role in cancer cell survival and its association with the development of anticancer drug resistance makes it an attractive target for cancer therapy. Several inhibitors have been developed during the past decade and some of them have entered clinical trials, but no drugs have been approved for clinical use so far. Targeted protein degradation using heterobifunctional degraders has emerged as a novel therapeutic modality in drug discovery. This technology has many potential advantages over traditional inhibitors, e.g. reduced side effects and drug resistance, extended duration of action, elevated selectivity, and the opportunity to target “undruggable” proteins.

In this study, we report the development of the first-in-class MCL-1 bifunctional degraders with *in vivo* PD effect.

**Material and Methods:** Compounds’ affinity to CRBN (Cereblon), an E3 ligase, and to MCL-1 was determined by FP and SPR, respectively. AlphaLISA and HTRF were utilized to confirm ternary complex formation.

Cell viability was assessed by CellTiter-Glo Assay. Apoptosis induction and changes in mitochondrial membrane potential were assessed by flow cytometry using Annexin/PI and TMRE staining, respectively. Targeted protein degradation in cells treated with compounds in the absence or presence of apoptosis inhibitor was assessed by WB.

The mechanism of action of the compounds was confirmed in cancer cells pre-treated with proteasome or NEDD8-Activating Enzyme inhibitors, or CRBN-targeting siRNA, and then treated with the compounds. MCL-1 abundance and expression of apoptosis markers were confirmed by WB.

PK studies were conducted in CD1 mice and Sprague Dawley rats, and PD studies in CB-17 SCID mice xenografted with MV4–11 cells.

**Results:** Synthesized compounds bind CRBN and MCL-1 with high affinity, form a ternary complex *in vitro* and induce the degradation of MCL-1 in cells, which is caspase- and proteasome-dependent and leads to apoptosis induction. This series of compounds showed a nM range cytotoxic activity in haematological cancer cell lines with the best compounds having an IC50 <100 nM. Moreover, MCL-1 degradation *in vivo* can be

achieved by IP administration leading to the initiation of the programmed cell death.

**Conclusions:** Our compounds have a broad cytotoxic activity toward cultured human cancer cells and a promising *in vivo* pharmacokinetic profile. Our data indicate that targeting MCL-1 by employing bifunctional degraders represents a potentially new and effective strategy for cancer treatment.

**No conflict of interest.**

293 (PB073)

**HR-LiP, a novel structural proteomics approach for the prediction of small molecule drug-protein binding events**

D. Redfern<sup>1</sup>, N. Beaton<sup>1</sup>, J. Adhikari<sup>2</sup>, R. Bruderer<sup>1</sup>, R. Tomlinson<sup>2</sup>, L. Wrobel<sup>3</sup>, S.M. Hill<sup>3</sup>, D.C. Rubinsztein<sup>3</sup>, Y. Feng<sup>1</sup>, I. Cornella-Taracido<sup>2</sup>, L. Reiter<sup>1</sup>. <sup>1</sup>Biognosys AG, RnD, Schlieren, Switzerland; <sup>2</sup>Cedilla Therapeutics, RnD, Cambridge, MA, USA; <sup>3</sup>University of Cambridge, Dept. of Medical Genetics, Cambridge, United Kingdom

**Background:** High resolution profiling of drug-protein interactions and binding mechanisms remains a major hurdle during lead selection and optimization. A key milestone in structure-based drug design is compound binding site identification and characterization. Structure-activity relationship (SAR) studies utilize a number of techniques such as nuclear magnetic resonance, x-ray crystallography and cryo-electron microscopy to address these hurdles but they are labor, time and cost intensive. Although mass spectrometry holds promise for such studies, to date only hydrogen-deuterium exchange has been extensively utilized. Further, SAR studies are often complicated by protein size (i.e. large proteins and/or multimers) and location (i.e. membrane proteins), which can lead to protocol adaptations (e.g. recombinant protein fragment) that can introduce artifacts. HR-LiP (high-resolution limited proteolysis) is a high-throughput, high-resolution approach that utilizes peptide-level resolution to characterize drug-protein interactions.

**Methods:** Mechanically sheared cell lysate overexpressing target proteins of interest was incubated with compound at multiple concentrations. Next, LiP was performed using proteinase K. After quenching this digestion, lysate was trypsin digested to peptides for mass spectrometry analysis. The resulting peptides were analyzed quantitatively using data-independent acquisition (DIA)-MS.

**Results:** Two well-characterized drug target proteins, bromodomain-containing protein 4 (BRD4) and transitional endoplasmic reticulum ATPase (VCP), were selected for analysis as they represent both difficult targets for structural biology (size and oligomerization respectively). BRD4 was targeted with a well characterized inhibitor (JQ1), while VCP investigated for binding with a known autophagy activator (not known to bind VCP previously). Using HR-LiP we identify the binding site of the BRD4 inhibitor JQ1 in the full-length protein, which is typically too large to be used directly in with conventional methods. Further, we confirm binding of the autophagy activator to VCP at a site known to increase VCP activity. For both compounds tested, our data are in good accordance with orthogonal data obtained by other structural protein approaches including HDX-MS and click chemistry-based chemoproteomics.

**Conclusions:** We demonstrate that HR-LiP can be used to dissect small molecule-protein binding events, including compound binding site prediction for protein targets classically considered to be difficult and time intensive. Further, we show that this data can be used to shed light on the biological mechanisms driving a phenotypic response. Given its biological power, broad applicability and ease of implementation, we envision the use of HR-LiP as a routine approach for target validation and lead optimization in small molecule drug discovery pipelines.

**No conflict of interest.**

294 (PB074)

**Development of a Novel IGF2BP1 Inhibitor as Metastasis-Specific Therapeutic Agent**

A. Singh<sup>1</sup>, V. Singh<sup>2</sup>, N. Wallis<sup>3</sup>, O. Elimelech<sup>3</sup>, F. Oberman<sup>3</sup>, A. Ramos<sup>4</sup>, J. Yisraeli<sup>3</sup>, V. Spiegelman<sup>2</sup>, A. Sharma<sup>1</sup>. <sup>1</sup>The Pennsylvania State University, Pharmacology, Hershey, USA; <sup>2</sup>The Pennsylvania State University, Pediatrics, Hershey, USA; <sup>3</sup>Hebrew University Hadassah Medical School, Department of Developmental Biology and Cancer Research, Jerusalem, Israel; <sup>4</sup>University College London, Division of Biosciences, London, United Kingdom

IGF2BP1 is a multifunctional RNA-binding protein that regulates the stability, localization and translation of its mRNA targets. High levels of IGF2BP1 expression have been shown to be associated with poor prognosis in

patients with variety of cancer types. Given the correlation between elevated IGF2BP1 expression and poor clinical outcomes, the specific activation of IGF2BP paralogs in a wide variety of cancers, and the effectiveness of preventing metastasis in animal models by reducing IGF2BP1 activity, therapies directed at inhibiting IGF2BP1 function constitute a potentially powerful approach for fighting cancer. In addition, IGF2BP1's pleiotropic effect on multiple pro-tumorigenic and pro-metastatic pathways make it a promising target, as this may avoid the development of resistance, associated with targeted agents in general. Furthermore, specific inhibitors of IGF2BP1 are expected to have minimal side effects since: i) IGF2BP1 is expressed at very low levels in normal adult tissues, and ii) adult mice with an inducible whole-mouse knockout of IGF2BP1 are healthy. To identify an efficient IGF2BP1 inhibitor, a fluorescent polarization (FP)-based high throughput screen of over 27,000 small molecules was performed, and the most promising candidates were further validated in an array of *in vitro* and cell-based assays leading to the identification of a lead compound, "7773," that selectively inhibited IGF2BP1 RNA binding and a variety of its cellular functions. To further optimize "7773" and create more selective, effective and safe small-molecule inhibitors of IGF2BP1 that could be developed clinically as cancer therapeutics, we conducted an SAR study based on the lead "7773" structure. Novel 27 compounds were designed and synthesized and evaluated for IGF2BP1 inhibition using our novel cell-based split-luciferase assay, which led to the identification of 6 compounds that performed similar or better than "7773". Cell-based wound healing assay revealed that one of these selected compounds, AVJ16, was especially (>14 times than "7773") effective in inhibiting cell migration in H1299 cell line that express high levels of endogenous IGF2BP1, but not in LKR-M cells that express very low levels of IGF2BP1. The specificity of AVJ16 was further confirmed in LKR-M cells that ectopically express IGF2BP1 – these cells become sensitive to AVJ16 upon overexpression of IGF2BP1 (but not GFP). Together our data provide strong evidence for AVJ16 to be effective and selective in inhibiting IGF2BP1 function by interfering with its ability to bind target RNAs.

**No conflict of interest.**

## POSTER SESSION

### Drug Resistance and Modifiers

295 (PB075)  
**Cancer-associated fibroblast-derived SPP1 is a potential target for overcoming sorafenib and lenvatinib resistance in hepatocellular carcinoma**

H.R. Ahn<sup>1</sup>, J.W. Eun<sup>2</sup>, J.H. Yoon<sup>3</sup>, J.A. Son<sup>1</sup>, J.H. Weon<sup>2</sup>, G.O. Baek<sup>2</sup>, M.G. Yoon<sup>2</sup>, J.E. Han<sup>2</sup>, M. Kwon<sup>4</sup>, S.S. Kim<sup>2</sup>, J.Y. Cheong<sup>2</sup>, H.J. Cho<sup>2</sup>.  
<sup>1</sup>Ajou University School of Medicine and Graduate School of Medicine, Gastroenterology, Suwon, South Korea; <sup>2</sup>Ajou University School of Medicine, Gastroenterology, Suwon, South Korea; <sup>3</sup>The Catholic University of Korea, Pathology, Seoul, South Korea; <sup>4</sup>Asan Medical Center- University of Ulsan College of Medicine, Otorhinolaryngology-Head and Neck Surgery, Seoul, South Korea

**Background:** Cancer-associated fibroblasts (CAFs) play an important role in the induction of chemo-resistance. The objectives of this study were to clarify the mechanism underlying CAF-mediated sorafenib/lenvatinib resistance and identify a novel therapeutic target to overcome resistance to sorafenib/lenvatinib in hepatocellular carcinoma (HCC).

**Material and methods:** Whole transcriptome sequencing (WTS) data of nine pairs of CAFs and para-cancer fibroblasts (PAFs) were analyzed to identify key molecules that induce resistance to tyrosine kinase inhibitors (TKIs). *In vitro* and *in vivo* experiments were performed to validate selected targets and related mechanisms. Plasma SPP1 expression levels prior to sorafenib/lenvatinib treatment as well as progression-free survival (PFS) and overall survival (OS) of an advanced HCC cohort (n = 42) were evaluated using Kaplan-Meier analysis.

**Results:** Co-culturing CAFs and HCC cells significantly reduced the responsiveness of HCC cells to sorafenib/lenvatinib, *in vitro* and *in vivo*. Systematic integrative analysis of the WTS data of CAFs/PAFs and publicly available gene expression data indicated that CAF-derived SPP1 (CAF-SPP1) was suitable for use as a candidate molecule to induce sorafenib/lenvatinib resistance. An evaluation of the mechanisms involved indicated that CAF-SPP1 increased phosphorylation of PKC $\alpha$ , which then activated

RAF-ERK1/2-STAT3 and PI3K-AKT-mTOR in HCC cells. SPP1 inhibitors reversed [Author1] CAF-induced sorafenib/lenvatinib resistance *in vitro* and *in vivo*. Patients showing high plasma SPP1 prior to sorafenib/lenvatinib treatment exhibited significantly poor PFS (P = 0.005) and OS (P = 0.041).

**Conclusions:** CAF-SPP1 enhances sorafenib/lenvatinib resistance in HCC by alternatively activating oncogenic pathways via PKC $\alpha$  phosphorylation. Inhibition of CAF-SPP1 may be utilized as a therapeutic strategy against TKI-resistance in HCC. Plasma SPP1 level prior to TKI treatment shows potential as a promising biomarker for predicting sorafenib/lenvatinib response in advanced HCC patients.

**No conflict of interest.**

296 (PB076)  
**Cellular hormone metabolism is critical for canonical androgen receptor antagonist activity**

R. Narayanan<sup>1</sup>, S. Ponnusamy<sup>1</sup>, W. Effah<sup>1</sup>, T. Thiyagarajan<sup>1</sup>, D.J. Hwang<sup>2</sup>, Y. He<sup>2</sup>, J.B. Breitmeyer<sup>3</sup>, G.F. Kaufmann<sup>3</sup>, D.D. Miller<sup>2</sup>. <sup>1</sup>University of Tennessee Health Science Center, Medicine, Memphis, USA; <sup>2</sup>University of Tennessee Health Science Center, Pharmaceutical Sciences, Memphis, USA; <sup>3</sup>Oncternal Therapeutics Inc., Medicine, San Diego, USA

**Background:** Second-generation androgen receptor (AR) antagonists and an androgen synthesizing enzyme inhibitor have become the standard of care for advanced prostate cancer (PCa). Clinically-approved AR antagonists bind to the AR ligand binding domain (LBD) and competitively inhibit AR function. Dual action AR inhibitors (DAARIs), which bind to the N-terminal domain (NTD) of the AR inhibit AR signaling and lead AR protein degradation, have been identified by our group as potential therapeutics for PCa. Despite initial response to AR antagonist therapy, PCa often evolves treatment resistance via various mechanisms. Delineating mechanisms of resistance might identify new therapeutic targets and treatment options, thus, ultimately benefitting PCa patients. The objective of this study was to investigate and compare the role of androgen metabolism on the activity of LBD-binding AR antagonists and DAARIs in PCa cells.

**Materials and methods:** The DAARIs UT-34 (ONCT-534) and UT-105 were synthesized in our laboratory. Cells were grown as three-dimensional organoids and were treated for 4–28 days. Tumor xenograft studies were performed under UTHSC ACUC-approved protocols. All experiments were performed with n = 4 samples and experiments were repeated to ensure reproducibility. Data were analyzed using appropriate statistical tools.

**Results:** Levels of androgen-inactivating glucuronidating enzymes UGT2B 15, 17, and 28 were significantly lower in AR-antagonist enzalutamide (ENZA)-resistant PCa cells compared to ENZA-sensitive PCa cells *in vitro*. Expression of UGT2B enzymes was induced by LBD-binding AR with maximum stimulation observed on day 7. This induction was lost by day 21 and rather the expression was then inhibited. Induction of UGT2Bs corresponded with inhibition of AR signaling pathway and vice versa, suggesting that UGT2Bs activation could be an important step for the anti-tumor activity of AR antagonists. DAARIs UT-34 and UT-105 did not induce the expression of UGT2Bs and continuously inhibited AR signaling via an UGT2B-independent mechanism. Knock-down of UGT2Bs diminished LBD-binding AR antagonist activity. In PCa xenografts where AR antagonists failed to induce the UGT2Bs they failed to inhibit PCa tumor growth. On the other hand, DAARIs effectively inhibited tumor growth by ~100% even in the absence of UGT2Bs stimulation.

**Conclusion:** These studies establish the importance of UGT2B enzyme induction and subsequent inactivation of androgens as a prerequisite for the anti-tumor activity of competitive AR antagonists in PCa. Furthermore, UGT2Bs and modulation of their activities might represent new therapeutic targets and strategy. AR NTD-binding DAARIs, that act independently of UGT2Bs provide sustained strong anti-tumor activity and may provide new future treatment options for advanced PCa resistant to LBD-binding AR antagonists.

**Conflict of interest:**

Ownership: James B. Breitmeyer, Gunnar F. Kaufmann, Ramesh Narayanan.

Corporate-sponsored Research: Ramesh Narayanan, Duane D. Miller. Other Substantive Relationships: Ramesh Narayanan (consultant Oncternal Therapeutics Inc.).

Suriyan Ponnusamy, Dong-Jin Hwang, Yali He, Duane D. Miller, and Ramesh Narayanan are inventors in DAARI technology and receive royalties.

Work was funded by NCI R01 CA229164 and Oncternal Therapeutics.



297

(PB077)

**CAR T cells in marginal zone lymphoma (MZL) models with acquired resistance to PI3K and BTK inhibitors**

S. Wang<sup>1</sup>, A.J. Arribas<sup>2</sup>, C. Tarantelli<sup>2</sup>, A. Pradier<sup>1</sup>, E. Zucca<sup>2</sup>, D. Rossi<sup>2</sup>, F. Simonetta<sup>1</sup>, F. Berton<sup>2</sup>. <sup>1</sup>Geneva University Hospitals- University of Geneva, Division of Hematology- Department of Oncology- and Translational Research Centre in Onco-Haematology, Geneva, Switzerland; <sup>2</sup>Faculty of Biomedical Sciences- USI, Institute of Oncology Research, Bellinzona, Switzerland

**Background.** MZLs are characterized by an indolent course with median survival over 10 years. However, relapses/progressions are common and if they occur during the first 2 years, they heavily impact the median survival. Among the 23 relapsed/refractory/MZL patients treated with the anti-CD19 CAR-T cells axicabtagene ciloleucel (Axi-Cel), the overall response rate was 83% with 73% of complete responses (Jacobson, Lancet Onc 2022; Neelapu, ASH2021). We previously presented MZL-derived models with secondary resistance to BTK/PI3K inhibitors, observing, in some of the resistant cells, an increase in CD19 levels and higher sensitivity to the anti-CD19 loncastuximab tesirine antibody drug conjugate (Arribas, ASH2019, ENA2019, Haematologica 2022). Here, we tested CAR-T cells with costimulatory receptors CD28 or 4-1BB (28z CAR-T and BBz CAR-T), representative of Axi-Cel and tisagenlecleucel (Tisa-Cel), respectively, in these models.

**Methods:** CD19-specific 28z CAR-T and BBz CAR-T produced from 4 healthy donors with retroviral vectors. Transduction efficacy evaluated by protein L staining. MZL models of secondary resistance to PI3K/BTK inhibitors and their parental cells cocultured for 48 h with CAR-T cells (1:1 E: T ratio) after adjusting for transduction efficacy. CAR-T cell-mediated cytotoxicity (CX) calculated as percentage of cell death compared to tumor cells cultured alone. CD19 expression determined by flow cytometry (protein) and RNA-Seq (RNA).

**Results.** We first tested 28z CAR-T and BBz CAR-T against the VL51 cell line and in the 2 derivatives, resistant to various PI3K inhibitors and ibrutinib, respectively. Median CX against parental was 24% and 29% with 28z or BBz CAR-T, respectively. CX was significantly increased against PI3K resistant cells, with a median CX of 62% after coculture with 28z CAR-T and 55% with BBz CAR T cells. Ibrutinib resistant VL51 cells displayed an even higher sensitivity to CAR-T cell killing, with a median CX of 68% after co-culture with 28z CAR-T and 79% with BBz CAR-T cells. Differently from VL51, both parental Karpas1718 and PI3K resistant derivative were equally sensitive to CAR-T cells, with a median 28z CAR-T CX of 72% against parental and 72% against PI3K resistant Karpas1718. Similar results were observed after coculture with BBz CAR-T cells (median CX 67% against parental and 66% against PI3K resistant Karpas1718). The results agreed with CD19 levels, higher in Karpas1718 (parental and derivative) and in the resistant VL-51 derivatives than in parental VL51.

**Conclusions:** Anti-CD19 28z and BBz CAR-T showed maintained or even increased *in vitro* antitumor activity in MZL models after acquisition of secondary resistance to PI3K/BTK inhibitors. The data support exploring CD19 directed therapeutic modalities for MZL patients.

FS, FB: co-senior authors. Work supported by Barletta and Henriette Meyer Foundations.

**Conflict of interest:**

Advisory Board: Gilead, AbbVie, Janssen, AstraZeneca, MSD, BMS/Celgene, Roche, Mei Pharma, Astra Zeneca, Celltrion Healthcare, Incyte, Kite/Gilead.

Corporate-sponsored Research: Celgene, Roche, Janssen, Acerta, ADC Therapeutics, Bayer AG, Cellectia, CTI Life Sciences, EMD Serono, Helsinn, ImmunoGen, Menarini Ricerche, NEOMED Therapeutics 1, Nordic Nanovector ASA, Oncology Therapeutic Development, PIQUR Therapeutics AG, Gilead, AbbVie, Janssen.

298

(PB078)

**Identifying the INPP4B-lysosome signaling axis as a putative target in acute myeloid leukemia**

K. Chen<sup>1</sup>, J.F. Woolley<sup>2</sup>, D.K.C. Lee<sup>1</sup>, C.M.P. Melo<sup>1</sup>, G.T. Saffi<sup>1</sup>, A. He<sup>3</sup>, S. Dhir<sup>1</sup>, J.T.S. Chow<sup>1</sup>, R.J. Botelho<sup>4</sup>, L. Salmena<sup>1</sup>. <sup>1</sup>University of Toronto, Pharmacology and Toxicology, Toronto, Canada; <sup>2</sup>University of Liverpool, Pharmacology and Therapeutics, Liverpool, United Kingdom; <sup>3</sup>University of Toronto, Molecular Genetics, Toronto, Canada; <sup>4</sup>Toronto Metropolitan University, Chemistry and Biology, Toronto, Canada

**Background:** Acute myeloid leukemia (AML) is an aggressive blood cancer characterized by impaired hematopoiesis and accumulation of functionally immature myeloblasts. Previously, we characterized the lipid phosphatase,

INPP4B, as a prognostic marker for poor outcomes in AML. High expression levels of INPP4B in AML was associated with poor patient survival and chemoresistance. We recently demonstrated that knockout of *Inpp4b* in *MLL-AF9* murine leukemias resulted in a less aggressive disease phenotype. RNA sequencing revealed a disproportionate reduction in numerous lysosomal gene transcripts in *Inpp4b*-/- leukemias; these include cathepsins and other lysosomal specific proteases. Notably, increased lysosomal biogenesis and activation of lysosomal signaling networks are emerging hallmarks of AML. Together, these data support the hypothesis that INPP4B may drive AML progression and chemoresistance through the regulation of lysosomal functions.

**Methods:** To further these findings, we assessed lysosomal properties in AML cell lines and *MLL-AF9* leukemia models using LysoTracker-Red, DQ-BSA-Green and the Magic Red Cathepsin B Assay. We also examined lysosomal biogenesis by qPCR to assess the levels of lysosomal gene transcripts upon INPP4B overexpression. Additionally, the consequences of lysosomal inhibition with Lys05 on AML cell survival, differentiation and colony formation potential were studied.

**Results:** INPP4B-overexpressing AML cells led to elevated levels of LysoTracker-Red, DQ-BSA-Green and Magic Red fluorescence, whereas the opposite was true for INPP4B-knockdown cells. qPCR analysis revealed that high INPP4B levels increased expression of key lysosomal genes, *LAMP1*, *CTSB*, *CTSD*, *ATP6V1H*, *ATP6V1D*, and *MCOLN1*. Together these data suggest that INPP4B expression promotes lysosomal biogenesis and functions. Lastly, colony formation assays demonstrated that lysosomal inhibitors reduced colony formation potential and promoted leukemia differentiation in an *Inpp4b*-dependent manner.

**Conclusion:** Our findings suggest that INPP4B is involved in lysosomal biogenesis and lysosomal proteolytic functions, both of which maintain aggressive leukemia phenotypes. Therefore INPP4B may also serve as a biomarker of disease outcome, and response to lysosomal inhibition. Future analyses aim to uncover how INPP4B expression in AML controls lysosomal mechanisms and biology and to test therapeutic strategies to exploit this pathway.

**No conflict of interest.**

299

(PB079)

**Epithelial-Mesenchymal plasticity mediates acquired resistance to eribulin in breast cancer**

C. Bellio<sup>1</sup>, E. Zamora<sup>2</sup>, C. Saura<sup>2</sup>, V. Serra<sup>1</sup>, B.A. Littlefield<sup>3</sup>, J. Villanueva<sup>1</sup>. <sup>1</sup>Vall d'Hebron Institute of Oncology VHIIO, VHIIO - Cellex, Barcelona, Spain; <sup>2</sup>Vall d'Hebron Univ. Hospital, Breast Cancer Program, Barcelona, Spain; <sup>3</sup>Eisai Inc., Eisai Inc., Cambridge, MA, USA

**Background:** A major obstacle in the fight against cancer is the development of drug resistance in response to therapy. Metastatic Breast Cancer (MBC) is extremely difficult to cure, mainly because it is driven by tumor cell sub-populations characterized by an increased capacity of adaptation to various stresses. Emerging evidence suggests that the epithelial-mesenchymal transition (EMT) program contributes to drug resistance. Therefore, our hypothesis is that tumor cell plasticity mediates tumor progression and acquired resistance to cancer drugs in breast cancer, and it could be an effective approach for cancer therapeutics.

**Material and methods:** In this project, we first characterized both the cellular and molecular effects induced by the chronic treatment of BC cells (MCF7 and MDA-MB-231) with approx. an IC80 dosage of eribulin, focusing on Snail as a driver of EM-plasticity to escape the action of eribulin. Then we studied by RT-PCR expression the up-regulation of several ABC-transporters as mediators of the acquired resistance mechanism. Finally, we performed a 3D organoids drug screening of several ABC-transporters inhibitors (Verapamil, Elacridar, Tariquidar) to find a possible combinational therapy to overcome eribulin resistance.

**Results:** We observed that after one week of eribulin treatment, approx. 80% of the initial cells die. For about 3 weeks, the remaining cells stay in a quiescence drug-tolerant persister state (DTP). Then, after approx. 1 month from the initial treatment, a subpopulation of cells starts growing in the presence of IC80 of the drug. These drug-resistant (DR) cells are highly chemoresistant to increasing concentrations of eribulin, and they maintain their morphology and chemoresistance characteristics even when the drug is removed for weeks, confirming a non-reversible drug-resistant phenotype. Interestingly, both MCF7 and MDA-MB-231 DR populations strongly upregulated the expression of the EMT-TF Snail. Moreover, RT-PCR expression analysis of several ABC-transporters confirmed up-regulation of ABCB1, ABCG2, and ABCA1 transporters in DR cells. Finally, DR cells treated with drug combinations of eribulin with different ABC-inhibitors (Verapamil, Elacridar, Tariquidar) regain sensitivity to eribulin.

**Conclusions:** These results provide evidence linking EM-plasticity to acquired resistance to eribulin through a Snail-driven mechanism mediating

the up-regulation of specific ABC transporters. We expect that our work will lead to new therapeutic tools, where combinations of eribulin with ABC-transporters inhibitors will increase the success in the treatment of MBC patients.

#### Conflict of interest:

Other Substantive Relationships: Bruce A. Littlefield is a full-time employee of Eisai Inc.

### 300 (PB080)

#### Adaption of Osteosarcoma Tumor Cells to ATG7 Knockout and Autophagy Deficiency is Dependent on Parental Cell Line and does not Sensitize Cells to Doxorubicin

D. Gustafson<sup>1</sup>, L. Viola<sup>1</sup>, K. Banks<sup>1</sup>, S. Witta<sup>1</sup>, S. Das<sup>1</sup>, D. Duval<sup>1</sup>, K. Van Eaton<sup>1</sup>. <sup>1</sup>Colorado State University, Flint Animal Cancer Center, Fort Collins, USA

**Background:** Autophagy inhibitors such as hydroxychloroquine (HCQ) are an active area of research in cancer therapy due to the role autophagy plays in tumor cell survival during physiologic and pharmacologic stress. Recent studies have suggested that tumor cell survival following ATG7 knockout is dependent on NRF2 expression leading to stress responses including macropinocytosis. Characterization of tumor cell adaption to autophagy inactivation is a critical step in understanding how these cells may become resistant to clinical use of autophagy inhibitors. Recently, we have focused on the role of autophagy in the survival and drug response of osteosarcoma. Canine osteosarcoma (cOSA) is recognized as being similar to human osteosarcoma in terms of molecular, pathological and clinical features and to serve as a surrogate for the rarer human form in dogs that develop the disease.

**Materials and Methods:** Validated and dual RFP/GFP labelled cOSA cell lines (Abrams, D17, Gracie, OSA8) were transfected with Cas9 and guide RNAs targeting GFP and ATG7 and resulting RFP only cells screened for loss of ATG7 and functional autophagy by Western Blotting for ATG7 and LC3I/LC3II conversion. Three ATG7-deficient clones were identified for each cell line for subsequent studies. Measures of tumor cell proliferation and death in response to growth conditions and drug treatment were done by live cell imaging of RFP and YOYO-1 labelled cells using an INCUCYTE ZOOM<sup>o</sup>. Lysosomal volume and macropinocytosis were determined using LysoTracker<sup>o</sup> and uptake of Dextran-FITC, respectively. RNA was isolated from select ATG7-deficient clones for each cell line and RNASeq analysis performed.

**Results:** Three ATG7-deficient clones were identified for each cell line. Response to low serum conditions varied across the deficient cell lines in a parental-dependent manner as did response to doxorubicin. Changes in lysosomal volume and upregulation of macropinocytosis were observed in some, but not all clones and these observed phenotypic changes were consistent with changes in lysosomal and macropinocytosis related gene expression in the RNASeq data. Interestingly, the ATG7-deficient clones maintained a similar sensitivity to HCQ and LysoV as the parental lines suggesting a disconnect between functional autophagy and sensitivity to drugs that inhibit autophagy by inhibiting lysosomal fusion.

**Conclusions:** The results from these studies show that ATG7-deficient cOSA cells have drug sensitivities similar to those of the parental line from which they were derived for both HCQ, LysoV and doxorubicin. ATG7-deficiency also leads to changes in lysosomal volume and macropinocytosis activity that are varied across cell lines as well as changes in gene expression. These results will help in understanding tumor cell response to autophagy inhibition and how cell of origin can influence these responses.

No conflict of interest.

### 301 (PB081)

#### The first-in-class WASP activator EG-011 is active in lymphoma and multiple myeloma cell lines resistant to FDA approved compounds

F. Spriano<sup>1</sup>, A.J. Arribas<sup>1</sup>, C. Tarantelli<sup>1</sup>, G. Sartori<sup>2</sup>, E. Gaudio<sup>1</sup>, C. Driessen<sup>3</sup>, F. Bertoni<sup>1</sup>. <sup>1</sup>Faculty of Biomedical Sciences- USI, Institute of Oncology Research, Bellinzona, Switzerland; <sup>2</sup>Faculty of Biomedical Sciences- USI, Institute of Oncology Research, Bellinzona, Switzerland; <sup>3</sup>Cantonal Hospital St. Gallen, Clinics for Medical Hematology and Oncology, St. Gallen, Switzerland

**Background:** One of the major causes of failure to achieve cure in cancer patients is the development of resistance to the drugs after an initial response. EG-011 is the first-in-class Wiskott-Aldrich syndrome protein (WASP) activator (Spriano et al, AACR 2022) with anti-tumor activity in hematological cancers (Gaudio et al, AACR 2019). Here, we assessed EG-

011 in the context of cellular models of secondary resistance to FDA approved agents: marginal zone lymphoma (MZL) cell lines resistant to PI3K and BTK inhibitors and multiple myeloma (MM) cell lines resistant to proteasome inhibitors.

**Methods:** MZL and MM cell lines were exposed to a large range of concentrations of EG-011 as single agent for 72 h, followed by MTT and after 4 h SDS to stop the reaction. The day after, plates were read using a Cytation 3 multimode plate reader (Biotek) and IC50s were calculated. IC50 was defined as the drug concentration giving 50% of proliferating cells compared to vehicle treated cells.

**Results:** We first tested EG-011 in models of secondary resistance to FDA approved PI3K and BTK inhibitors from splenic MZL cell lines (Arribas et al, ASH 2019, ENA 2020, Haematologica 2022). The anti-tumor activity of EG-011 was maintained in the resistant cell line derived from the MZL VL51 with secondary resistance to ibrutinib (IC50: 500 nM in both parental and resistant), while it was higher in the MZL model with resistance to PI3Kdelta inhibitor derived from VL51 (IC50: 100 nM). The copanlisib-resistant MZL VL51 (IC50: 2 µM) and Karpas1718 idelalisib-resistant (5 nM) showed a slightly decreased sensitivity to EG-011 (Karpas1718 parental, IC50: 1 nM).

We then assessed the lack of cross resistance with proteasome inhibitors in MM cell lines with acquired resistance to this class of agents (Besse et al, Leukemia 2018, Haematologica 2019; Brünnert et al, BBA Mol Basis Dis 2019). The AMO-1 carfilzomib resistant cell line showed an IC50 to EG-011 treatment that was more than 20 times lower than the carfilzomib sensitive parental cell line (IC50: 250 nM vs 6 µM). The L363 bortezomib resistant line showed an IC50 around ten times lower than the sensitive parental cell lines (IC50: 1 vs 12 µM). A 4-fold increase in sensitivity was observed in both RPMI-8266 bortezomib resistant and in RPMI-8266 carfilzomib resistant cells compared to parental (IC50: 2.5 vs 10 µM for both models).

**Conclusions:** These data indicate that the first-in-class WASP activator EG-011 was active also after acquisition of resistance to different FDA approved agents such as PI3K, BTK and proteasome inhibitors in MZL and MM models.

#### Conflict of interest:

Ownership: Patent

### 302 (PB082)

#### Improving responses to dual PI3K/BCL2 inhibition in lymphomas: results of a pharmacological screen with over 1,400 compounds

A. Arribas<sup>1</sup>, M. Chiappa<sup>2</sup>, S. Napoli<sup>1</sup>, E. Cannas<sup>1</sup>, L. Cascione<sup>1</sup>, F. Spriano<sup>1</sup>, C. Tarantelli<sup>1</sup>, D. Rossi<sup>1</sup>, E. Zucca<sup>3</sup>, A. Alimonti<sup>1</sup>, A. Stathis<sup>4</sup>, G. Damia<sup>2</sup>, M. Broggin<sup>2</sup>, F. Bertoni<sup>1</sup>. <sup>1</sup>Faculty of Biomedical Sciences- USI, Institute of Oncology Research, Bellinzona, Switzerland; <sup>2</sup>IRCCS, Laboratory of Molecular Pharmacology, Milan, Italy; <sup>3</sup>Faculty of Biomedical Sciences- USI, Oncology Institute of Southern Switzerland, Bellinzona, Switzerland; <sup>4</sup>Oncology Institute of Southern Switzerland, Oncology Institute of Southern Switzerland, Bellinzona, Switzerland

**Background:** Copanlisib, a pan-PI3K inhibitor with stronger activity against the alpha and delta isoforms, is Food and Drug Administration (FDA) approved for the treatment of patients with relapsed or refractory follicular lymphoma, and it is has shown clinical activity in other indolent lymphomas including marginal zone lymphoma (MZL). Preclinical studies have demonstrated strong synergism of copanlisib and BCL2 inhibitor venetoclax in different lymphomas (Tarantelli Blood Adv 2020). A phase 1 study has explored this specific combination (NCT03886649), while others have explored similar schemes based on dual PI3K and BCL2 targeting. We have previously reported a model of resistance to copanlisib/venetoclax developed by prolonged exposure to copanlisib (Arribas ENA 2020). Here, we present the data from a large pharmacological screen with over 1400 compounds in this MZL model.

**Methods:** Copanlisib/venetoclax-resistant cells were exposed to DMSO or a library of 1443 FDA-approved compounds at 5 µM dose, as single or in combination with 1 nM copanlisib +50 nM venetoclax for 72 hours (hr). Spatial and intra- and inter-plates effects were corrected. Values were then normalized to control (DMSO). Either highly active compounds as single agent (cell viability <30%) or inhibitors with improved activity upon copanlisib/venetoclax combination (cell viability <50%, ratio combo/single <0.7) were selected for further validation upon copanlisib/venetoclax in resistant and parental cells (MTT assay, 72 hr). Synergy of combinations was evaluated according to the Chou-Talalay combination index (CI), as well as potency and efficacy, estimated according to the MuSyC algorithm.

**Results:** The screen identified 82 highly active compounds and 99 drugs that improved the response to copanlisib/venetoclax. These inhibitors targeted WNT, CDK, HDAC, HSP, PLK, ALDH1, AURKA, proton pump and microtubule polymerization, among others. A selection underwent further validation experiments in parental and resistant upon copanlisib/

venetoclax combination. Addition of the ALDH1 inhibitor disulfiram was beneficial in both parental and resistant cells, but especially in the latter condition with improved synergy and enhanced efficacy of copanlisib/venetoclax, overcoming the resistance. Combinations with ganetespib (HSP90), rigosertib (PLK), panobinostat (HDAC), alisertib (AURKA) and AZ1602 (WNT) were beneficial either in parental and resistant cells and improved the sensitivity to copanlisib/venetoclax in resistant cells.

**Conclusions:** In conclusion, a large pharmacological screen has identified a series of compounds that could be added to copanlisib/venetoclax in a triple combination or used in patients developing resistance to copanlisib/venetoclax. Further experiments are on-going to extend the findings to additional PI3K/BCL2 inhibitors.

Work partially supported by Swiss Cancer Research.

**No conflict of interest.**

### 303 (PB083) ISG15 as a prognostic biomarker in solitary fibrous tumour

J.L. Mondaza Hernandez<sup>1,2</sup>, D.S. Moura<sup>1,2</sup>, M. Lopez-Alvarez<sup>3</sup>, P. Sanchez-Bustos<sup>3</sup>, E. Blanco-Alcaina<sup>3,4</sup>, C. Castilla-Ramirez<sup>5</sup>, P. Collini<sup>6</sup>, J. Merino-Garcia<sup>7</sup>, J. Zamora<sup>1,2</sup>, J. Carrillo-Garcia<sup>1,2</sup>, R. Maestro<sup>8</sup>, N. Hindi<sup>1,2,9</sup>, J. Garcia-Foncillas<sup>1,9</sup>, J. Martin-Broto<sup>1,2,9</sup>. <sup>1</sup>Health Research Institute Fundacion Jimenez Diaz- Universidad Autonoma de Madrid IIS/ FJD-UAM, Oncohealth, Madrid, Spain; <sup>2</sup>University Hospital General de Villalba, ATBSarc, Madrid, Spain; <sup>3</sup>Institute of Biomedicine of Sevilla IBIS-HUVR- CSIC- Universidad de Sevilla, Oncohematology and Genetics, Sevilla, Spain; <sup>4</sup>CIBERONC- Instituto de Salud Carlos III, Non-applicable, Madrid, Spain; <sup>5</sup>University Hospital Virgen del Rocío, Pathology Department, Sevilla, Spain; <sup>6</sup>Soft Tissue and Bone Pathology- Histopathology and Pediatric Pathology Unit- Fondazione Istituto di Ricovero e Cura a Carattere Scientifico IRCCS- Istituto Nazionale Tumori, Diagnostic Pathology and Laboratory Medicine Department, Milan, Italy; <sup>7</sup>University Hospital Fundacion Jimenez Diaz- Universidad Autonoma, Pathology Department, Madrid, Spain; <sup>8</sup>Unit of Oncogenetics and Funcional Oncogenomics- Centro di Riferimento Oncologico di Aviano CRO Aviano- IRCCS National Cancer Institute, Oncogenetics and Funcional Oncogenomics, Aviano, Italy; <sup>9</sup>University Hospital Fundacion Jimenez Diaz, Medical Oncology department, Madrid, Spain

**Background:** Solitary fibrous tumour (SFT) is a rare mesenchymal malignancy that lacks robust prognostic and predictive biomarkers. Interferon-stimulated gene 15 (ISG15) is a ubiquitin-like modifier, associated with tumour progression, and with poor survival of SFT patients, as previous published by our group. Here, we describe the role of ISG15 in the biology of this rare tumour.

**Materials and methods:** ISG15 expression was assessed by immunohistochemistry in tissue microarrays from SFT patients and tested for correlation with progression-free survival and overall survival (OS). The effects of ISG15 knockdown or induction were investigated for cancer stem cell (CSC) characteristics and for drug sensitivity in unique *in vitro* models of SFT.

**Results:** The prognostic value of ISG15 for OS was validated at protein level in malignant SFT patients, prospectively treated with pazopanib and enrolled in GEIS-32 trial. In SFT *in vitro* models, ISG15 knockdown lead to a decrease in the expression of CSC-related genes, including *SOX2*, *NANOG*, *ALDH1A1*, *ABCB1* and *ABCC1*. Likewise, ISG15 downregulation decreased the clonogenic/ tumoursphere-forming ability of SFT cells, while enhancing apoptotic cell death after doxorubicin, pazopanib or trabectedin treatment in 3D cell cultures. The regulation of CSC-related genes by ISG15 was confirmed after inducing its expression with interferon- $\beta$ 1; ISG15 induction upregulated 1.28- to 451-fold the expression of CSC-associated genes.

**Conclusions:** ISG15 is a prognostic factor in malignant SFT, regulating the expression of CSC-related genes and CSCs maintenance. Our results suggest that ISG15 could be a novel therapeutic target in SFT, which could improve the efficacy of the currently available treatments.

**Conflict of interest:**

Other Substantive Relationships: D.S.M. reports institutional research grants from PharmaMar, Eisai, Immix BioPharma and Novartis outside the submitted work travel support from PharmaMar, Eisai, Celgene, Bayer and Pfizer. NH reports grants, personal fees and non-support from PharmaMar, research grants from Eisai, Immix BioPharma and Novartis outside the submitted work and re-search funding for clinical studies (institutional) from PharmaMar, Eli Lilly and Company, AROG, Bayer, Eisai, Lixte, Karyopharm, Deciphera, GSK, Novartis, Blueprint, Nektar, Forma, Amgen and Daichi-Sankyo. J.M.-B. reports research grants from PharmaMar, Eisai, Immix BioPharma and Novartis outside the submitted work honoraria for advisory board participation and expert testimony from PharmaMar, honoraria for

advisory board participation from Eli Lilly and Company, Bayer and Eisai and research funding for clinical studies (institutional) from PharmaMar, Eli Lilly and Company, AROG, Bayer, Eisai, Lixte, Karyopharm, Deciphera, GSK, Novartis, Blueprint, Nektar, Forma, Amgen and Daichi-Sankyo. All other authors declare that there is no conflict of interest.

### 304 (PB084) Pharmacological screening identified promising combination partners in marginal zone lymphoma models with secondary resistance to BTK and PI3K inhibitors

A. Arribas<sup>1</sup>, S. Vultaggio<sup>2</sup>, A. Andronache<sup>2</sup>, M. Robusto<sup>2</sup>, D. Fancelli<sup>2</sup>, E. Cannas<sup>1</sup>, F. Spriano<sup>1</sup>, C. Tarantelli<sup>1</sup>, D. Rossi<sup>3</sup>, E. Zucca<sup>3</sup>, A. Stathis<sup>3</sup>, M. Varasi<sup>2</sup>, C. Mercurio<sup>2</sup>, F. Bertoni<sup>1</sup>. <sup>1</sup>Faculty of Biomedical Sciences- USI, Institute of Oncology Research, Bellinzona, Switzerland; <sup>2</sup>The AIRC Institute of Molecular Oncology, Experimental Therapeutics Program, IFOM ETS, Milan, Italy; <sup>3</sup>Oncology Institute of Southern Switzerland, Oncology Institute of Southern Switzerland, Bellinzona, Switzerland

**Background.** Marginal zone lymphoma (MZL) is an indolent yet incurable B-cell malignancy. Two BTK inhibitors, ibrutinib and zanubrutinib, are FDA approved for relapsed/refractory MZL patients. PI3K inhibitors have also shown clinical activity although their use has been recently reduced due to toxicities. We have previously reported a model of resistance to BTK/PI3K inhibitors developed by prolonged exposure to the PI3K-delta inhibitor idelalisib (Arribas, ASH2019). Here, we present the data from a large pharmacological screen with over 1,500 compounds in this MZL model.

**Methods:** Models with secondary resistance were developed by continuous exposing the cell line Karpas1718 and its derivative with resistance to BTK/PI3K inhibitors (Arribas, ASH2019). Parental Karpas1718 and resistant derivative were exposed to DMSO or a library of 1722 compounds at five doses (from 5 nM to 50  $\mu$ M at 1:10 dilution) for 72 hours (hr). Spatial and intra- and inter-plates effects were corrected. Z-factor was then calculated between negative (DMSO) and positive (Panobinostat IC100) controls. Highly active compounds with IC50 <100 nM in both parental and resistant were selected for further validation by combination with idelalisib or ibrutinib (MTT assay, 72 hr). Synergy of combinations was evaluated according to the Chou-Talalay combination index (CI), as well as potency and efficacy, estimated according to the MuSyC algorithm.

**Results.** The screening identified 34 highly active compounds as single agents in both parental and resistant. The identified molecules targeted apoptosis, cell cycle, DNA damage, epigenetics, cancer stemness, and metabolism processes. Among these, we selected compounds that might be easier to be used in the clinical setting for further testing in combination with ibrutinib and idelalisib. Addition of ALDH1 inhibitor disulfiram, the PLK inhibitor rigosertib or HSP90 inhibitor ganetespib recovered sensitivity to ibrutinib and improved the potency of the BTK inhibitor in resistant but not in the parental cells. Adding disulfiram, rigosertib, ganetespib, the dual PI3K-HDAC inhibitor fimepinostat (CUDC-907) or the CDK4/6 inhibitor palbociclib was of benefit (additivity or synergism) in both parental and resistant cells.

**Conclusions:** Our results identified combination partners for BTK and PI3K inhibitors. Targeting of PLK, HSP90, ALDH1, HDAC and CDK4/6 appeared as possible therapeutic approaches to be further assessed in MZL as single agents and in combination.

AA, SV, AA, MR: equally contributed. Work partially supported by the Fondazione ticinese per la ricerca sul cancro. Experimental Therapeutic Program work is supported by a generous donation to IFOM from Ravelli Family.

**No conflict of interest.**

### 305 (PB085) Differentiating Ensartinib from Lorlatinib and Alectinib for first line use in an ALK+ non-small cell lung cancer preclinical model (ResCu)

L. Hill<sup>1</sup>, M. Gadde<sup>1</sup>, V. Ruiz<sup>1</sup>, D. Alabduljabbar<sup>1</sup>, C. Bulow<sup>1</sup>, N. Goldner<sup>1</sup>, G. Selvaggi<sup>2</sup>. <sup>1</sup>resistanceBio, Oncology, San Carlos, USA; <sup>2</sup>Xcovery Holdings, Inc, Oncology, Miami, USA

**Background:** The objective of this study was to determine whether Ensartinib with its high potency and resistance suppressing properties creates a more favorable treatment profile when used as first-line therapy in ALK+ non-small cell lung cancer compared to two other ALK inhibitors, Alectinib and Lorlatinib.

**Materials and Methods:** The ResCu system, a novel culturing system, allows for long term culture of cells without the need for passaging, allowing determination of treatment resistance that can develop over time in a physiologically relevant system that conserves the resistance pathways found in patients. Two ALK-dependent lung adenocarcinoma cell lines,

H3122 and H2228 were used to derive starting populations for this study. Using ResCu, we drove resistance to three ALK inhibitors: alectinib, lorlatinib, and ensartinib by using a clinically equivalent dose.

A colony-forming-based assay of cells evolving in ResCu provided an indication of time to therapeutic resistance. The evolved cells were characterized for cross-sensitivity and resistance to a representative panel of 21 drugs. Cell viability was assessed by luminescence after 7 days of exposure to these secondary drugs.

**Results:** The ResCu system developed resistant cell populations by evolutionary steering of H3122 and H2228 cell lines treated with ensartinib, alectinib, and lorlatinib. Genetic background had a significant effect on which ALK<sub>i</sub> exhibited the most durable response. The H2228 derived cell population became resistant to alectinib and lorlatinib by 14 days while ensartinib remained effective for at least 42 days. In contrast, H3122 derived cells became resistant to all ALK inhibitors tested by 14 days.

Rate of cross-resistance generation also varied between ALK inhibitors. Alectinib led to the highest levels of cross-resistance to other ALK<sub>i</sub>, approximately 3× higher. Lorlatinib led to highest levels of cross-resistance to other drug classes. Treatment with lorlatinib led to resistance in 13 other drug classes. Ensartinib led to least cross-resistance to ALK<sub>i</sub> and other drug classes. While the H3122 derived cells more rapidly evolved ALK<sub>i</sub> resistance, first line treatment with ensartinib sensitized them to lorlatinib, extending overall response to ALK<sub>i</sub>.

**Conclusion:** The ResCu system developed two ALK<sub>i</sub> resistant cell populations from distinct genetic backgrounds under physiologically relevant conditions. In one of the two genetic background ensartinib response was durable for greater than 42 days compared to 14 days with alectinib and lorlatinib. Alectinib led to the most cross-resistance to other ALK<sub>i</sub> while lorlatinib led to the most cross-resistance to other drug classes in both backgrounds. Biomarkers of ALK<sub>i</sub> escape and cross-resistance were derived from RNA-seq, and we are currently validating these alterations against clinical samples.

#### Conflict of interest:

Ownership: None.

Advisory Board: None.

Board of Directors: None.

Corporate-sponsored Research: resistanceBio provided sponsored research services to Xcovery Holdings, Inc.

306

(PB086)

#### Reversal of resistance to docetaxel and cabazitaxel in prostate cancer cells with ritonavir

E. Van Der Putten<sup>1</sup>, K. Wosikowski<sup>2</sup>, C. Freund<sup>1</sup>, J. Beijnen<sup>3</sup>. <sup>1</sup>Modra Pharmaceuticals, Development, Amsterdam, Netherlands; <sup>2</sup>Wosikowski Consulting, Consulting, Poing, Germany; <sup>3</sup>Netherlands Cancer Institute - Antoni van Leeuwenhoek, Department of Pharmacy & Pharmacology, Amsterdam, Netherlands

**Background:** The taxanes docetaxel and cabazitaxel are indicated for treatment of metastatic castration-resistant prostate cancer (mCRPC). Resistance to docetaxel often develops during treatment, which can be due to an increased efflux of docetaxel via P-glycoprotein (P-gp) from the intracellular site of action. Ritonavir is an inhibitor of both cytochrome P4503A4 (CYP3A4) and P-gp. In this study we investigated whether ritonavir could improve the efficacy of docetaxel through inhibition of P-gp in docetaxel-resistant prostate cancer cells.

**Methods:** Prostate cancer cell lines DU-145 and 22Rv1 were exposed to increasing doses of docetaxel to generate resistant sublines, DU145-DOC10 and 22Rv1DOC8 respectively. Gene expression of the resistant clones was compared to that of the parental cell lines. The parental cell lines and the docetaxel resistant cell lines were treated with several drug combinations in an 8\*2 matrix 3D tumor clonogenic assay. The following drug combinations were tested: docetaxel/ritonavir, docetaxel/elacridar and cabazitaxel/ritonavir. The IC50 values of single agent drugs and drug combinations as well as combination effects between drugs (using a Bliss independence dose-response evaluation) were determined in all cell lines.

**Results:** The most differentially upregulated gene in the resistant cell lines was ABCB1 (P-gp). Western blotting showed that both resistant cell lines

expressed more P-gp than the parental cell lines. A comparison of the observed docetaxel and cabazitaxel IC50 values has been summarized in the below table.

We found that docetaxel resistance conferred cross-resistance to cabazitaxel. With the addition of 10 μM ritonavir (DU-145DOC10) and 32 μM ritonavir (22Rv1DOC8) the cytotoxicity of docetaxel and cabazitaxel returned to the level of observed in the parental cell lines. A similar experiment with the specific P-gp inhibitor elacridar showed that a concentration of 0.3 μM was sufficient to reverse docetaxel resistance to the same level as in the parental cell lines, confirming this as an important mechanism-of-action. In DU-145-DOC10 and 22Rv1DOC8 cells strong synergistic effects were seen of the docetaxel/ritonavir as well as the cabazitaxel/ritonavir combination, in contrast to the lack of synergy seen in the parental cell lines with these combinations.

**Conclusions:** We demonstrated the potential for the combination of docetaxel and ritonavir to reverse or offset resistance to docetaxel (and, by implication due to its cross-resistance, also to cabazitaxel), primarily mediated through inhibition of P-gp. This provides a strong rationale to clinically test these taxanes in combination with ritonavir in patients with mCRPC.

#### Conflict of interest:

Ownership: Jos Beijnen is a shareholder of Modra Pharmaceuticals.

Board of Directors: Colin Freund and Eric van der Putten are directors of Modra Pharmaceuticals.

307

(PB087)

#### Targeting the exosome biogenesis pathway to overcome daratumumab resistance in hematological cancers

N. Mustafa<sup>1</sup>, M.I. Azaman<sup>2</sup>, W.J. Chng<sup>1,2,3</sup>. <sup>1</sup>National University of Singapore, Yong Loo Lin School of Medicine, Singapore, Singapore; <sup>2</sup>Cancer Science Institute of Singapore, Cancer Science Institute of Singapore, Singapore, Singapore; <sup>3</sup>National University Hospital, Department of Hematology-Oncology, Singapore, Singapore

**Background:** Daratumumab is a monoclonal antibody that targets CD38, which is highly expressed in lymphoid tumour cells. Daratumumab-based combinations have been incorporated as frontline therapy for multiple myeloma, and is well tolerated in clinical trials for other blood cancers. However, responses are heterogeneous and development of treatment resistance inevitable. Therefore, elucidation and targeting of mechanisms which can overcome daratumumab resistance is essential for the optimization of therapeutic response in patients.

**Materials & Methods:** Isogenic daratumumab resistant (dara R) and sensitive (dara S) cancer cell lines were developed by the stepwise increase of dara concentrations in complement serum. *In vivo*, mice tumour was designated "R" where it enlarges with prolonged dara treatment while "S" tumors remain similar to volume at treatment initiation. RNA sequencing was performed, genes dysregulated analyzed and validated by qRT-PCR and immunoblotting. Exosomes were isolated by differential ultracentrifugation and quantified and visualized by Particle Metrix Zetaview and electron microscopy. Effect of targeted siRNA knockdown and drug efficacy was measured via CTG (Promega) viability assays.

**Results:** RNAseq revealed an enriched expression of genes mediating exosome biogenesis and secretion in dara R models. Alix, TSG101 and Rab27b protein expression was indeed upregulated and elevated levels of exosomes detected in the dara R tumour microenvironment. The growth of dara S cells is enhanced in a co-culture with dara R cell lines and sensitivity to dara-induced CDC was reduced upon addition of dara R exosomes thereby suggesting a role for exosomes in promoting resistance. We thus hypothesized that targeting the exosomal pathway may successfully overcome the survival of dara R cells. Neticonazole and ketoconazole have been identified as selective inhibitors of exosomal biogenesis in a drug repurposing study for advanced cancers. Interestingly, dara R cell lines were more strongly suppressed by azole treatment than dara S cell lines. Immunoblot analysis showed that azole treatment at identical concentrations resulted in a more extensive downregulation of Alix, Rab27b and CD81 protein expression in dara R than dara S cells. Additionally, depletion of Alix and Rab27b protein expression via siRNA knockdown induced cell death

Table (abstract: 306 (PB086))

	DU-145	DU-145DOC10	DU-145DOC10	22Rv1	22Rv1DOC8	22Rv1DOC8
Docetaxel IC50 (nM)	2.9	9.5	2.8*	1.3	54.6	3.0**
Cabazitaxel IC50 (nM)	0.6	1.5	0.6*	0.7	9.5	0.7**

\*with 10 μM ritonavir,

\*\*with 32 μM ritonavir.

substantiating that dara R cell lines are dependent on exosomal-mediated pathways for survival.

**Conclusion:** We demonstrate that dara resistant cancer cell lines secrete elevated levels of exosomes which mediate mechanisms promoting resistance and survival. Dara resistant cells are more sensitive to exosome biogenesis inhibitors than dara sensitive cells thereby suggesting an addiction to the exosome pathway which can be exploited therapeutically to overcome dara resistance and enhance the long term response in patients.

**No conflict of interest.**

**308** (PB088)  
**Develop selective inhibitors of drug-metabolizing enzymes CYP3A4/5 to improve cancer drug efficacy and reduce drug toxicity and resistance**

J. Wang<sup>1</sup>, C. Buchman<sup>1</sup>, J. Seetharaman<sup>2</sup>, D. Miller<sup>2</sup>, A. Huber<sup>1</sup>, J. Wu<sup>1</sup>, S. Chai<sup>1</sup>, E. Garcia-Maldonado<sup>1</sup>, C. Wright<sup>1</sup>, J. Cheng<sup>1</sup>, T. Chen<sup>1</sup>. <sup>1</sup>St. Jude Children's Research Hospital, Chemical Biology and Therapeutics, Memphis, USA; <sup>2</sup>St. Jude Children's Research Hospital, Structural Biology, Memphis, USA

**Background:** The human cytochrome P450 (CYP) CYP3A4 and CYP3A5 enzymes metabolize more than half of marketed drugs. They share high structural and substrate similarity and are often studied together as CYP3A4/5. However, they preferentially metabolize different clinically prescribed drugs. Moreover, the differential distribution and expression levels of CYP3A4 and CYP3A5 in both normal and diseased tissues can aggravate toxicity and induce resistance during treatment. Therefore, selective inhibitors of CYP3A4 and CYP3A5 are needed to distinguish their roles and serve as starting points for potential therapeutic development.

**Materials and methods:** We used biochemical and cell-based assays and high-throughput screening to discover and characterize selective inhibitors. We used X-ray crystallography to unravel the structural basis of selective inhibition.

**Results:** We discovered clobetasol propionate as the first selective inhibitor of CYP3A5 and reported the crystal structure of CYP3A5 in complex with clobetasol propionate. Supported by structure-guided mutagenesis analyses, the CYP3A5-clobetasol propionate structure showed that a unique conformation of the F-F' loop in CYP3A5 enables selective binding of clobetasol propionate to CYP3A5, thus proving the structural basis for the selective inhibition. Based on these results we performed large-scale high-throughput screening to identify additional selective inhibitors of both CYP3A4 and CYP3A5 that are suitable for chemical optimization.

**Conclusions:** It is feasible to selectively inhibit the highly homologous CYP3A4 and CYP3A5 enzymes, thus chemically validating CYP3A4 and CYP3A5 as targets for development of therapeutics to improve drug efficacy while reducing drug toxicity and resistance during treatment.

**No conflict of interest.**

**309** (PB089)  
**AB801 is a potent and selective AXL inhibitor that demonstrates significant anti-tumor activity in combination with standard of care therapeutics**

S. Paprcka<sup>1</sup>, S. Sridhar<sup>1</sup>, A. Goshayeshi<sup>1</sup>, E. Park<sup>1</sup>, S. Liu<sup>2</sup>, R. Flores<sup>2</sup>, L. Rocha<sup>2</sup>, D. Miles<sup>3</sup>, M. Lamani<sup>3</sup>, S. Cho<sup>4</sup>, N. Wang<sup>4</sup>, Y. Guan<sup>5</sup>, S. Chandrasekar<sup>5</sup>, R. Kushwaha<sup>5</sup>, S. Jafri<sup>6</sup>, A. Kaplan<sup>6</sup>, E. Stagnaro<sup>6</sup>, L. Seitz<sup>5</sup>, J. Kline<sup>2</sup>, E. Fernandez-Salas<sup>1</sup>. <sup>1</sup>Arcus Biosciences, Biology, Hayward, USA; <sup>2</sup>Arcus Biosciences, Pharmacology, Hayward, USA; <sup>3</sup>Arcus Biosciences, Chemistry, Hayward, USA; <sup>4</sup>Arcus Biosciences, Bioinformatics, Hayward, USA; <sup>5</sup>Arcus Biosciences, Biophysics, Hayward, USA; <sup>6</sup>Arcus Biosciences, Translational, Hayward, USA

**Background:** The receptor tyrosine kinase AXL, expressed in cancer, stromal, and select immune cells, has been implicated in resistance to chemotherapy, targeted therapies & immunotherapies. AXL expression correlates with poor prognosis in cancer patients. Activation of AXL can occur in a ligand-dependent manner via its ligand, growth arrest specific protein 6 (Gas6), or in a ligand-independent manner, both of which facilitate AXL phosphorylation & initiation of signaling cascades promoting cancer cell proliferation, survival, and an immunosuppressive microenvironment. Here we present the preclinical evaluation of a novel, highly potent, and selective AXL inhibitor, AB801.

**Materials and Methods:** Inhibition of AXL phosphorylation in cancer cells was evaluated by Western blot and levels of soluble and cell-surface AXL were assessed by ELISA and flow cytometry, respectively. Downstream signaling of AXL was evaluated by Western blot and qPCR. Pharmacokinetics (PK), pharmacodynamics (PD) and anti-tumor efficacy

in combination with standard of care therapies were evaluated in murine cancer models.

**Results:** AB801 inhibits both ligand-dependent and ligand-independent AXL phosphorylation. AXL phosphorylation and subsequent signaling leads to receptor internalization, thereby decreasing both surface AXL and soluble AXL levels. AB801 inhibits AXL activity in a concentration-dependent manner reducing AXL phosphorylation and increasing both surface AXL expression and soluble AXL levels. Moreover, AXL inhibition results in upregulation of cell surface proteins that mediate immune/cancer cell interaction, e.g., LFA-1. Significant anti-tumor efficacy is observed in combination with targeted therapies in several *in vivo* models. Importantly, AB801 treatment significantly reduces tumor growth after relapse to single-agent therapy.

**Conclusions:** AB801 demonstrates significant anti-tumor activity in combination with standard of care therapeutics. Selective AXL inhibition is a promising therapeutic strategy to overcome resistance to therapy.

**Conflict of interest:**

Ownership: Arcus Biosciences Shareholder  
Corporate-sponsored Research: Employee of Arcus Biosciences.

**310** (PB090)  
**Metabolic profile associated with chemoresistance in ovarian cancer cells using metabolomics**

P. Alarcon-Zapata<sup>1</sup>, A.J. Perez<sup>2</sup>, V. Ormazabal<sup>3</sup>, F.A. Zúñiga<sup>4</sup>. <sup>1</sup>Universidad de Concepción - Facultad de Farmacia, Departamento de Bioquímica Clínica e Inmunología, Concepción, Chile; <sup>2</sup>Universidad de Concepción - Facultad de Farmacia, Departamento de Análisis Instrumental, Concepción, Chile; <sup>3</sup>Universidad de Concepción, Facultad de Ciencias Biológicas, Departamento de Farmacología, Concepción, Chile; <sup>4</sup>Universidad de Concepción, Facultad de Farmacia, Bioquímica Clínica e Inmunología, Concepción, Chile

**Background:** Ovarian cancer (OvCa) is the fifth leading cause of cancer death in women worldwide and the second leading cause of death of all gynecological malignancies. Although the incidence is not that high, mortality is about 70%, due mainly to its high recurrence rate, despite chemotherapy and targeted therapy. Factors such as invasiveness, metastatic properties, and response to treatment affect disease prognosis and survival. This work uses a metabolomics approach to identify metabolites from chemoresistant and chemosensitive ovarian cancer cells.

**Material and Methods:** For metabolomics, cell extracts were analyzed via UHPLC-HR-QTOF-MS (Compact, Bruker) using a hydrophilic column (HILIC, Waters) with positive and negative electrospray ionization modes. Data were processed and analyzed with Metaboscape software (Bruker) and the Metaboanalyst online platform. Growth inhibition rate (GR50) was determined in SK-OV-3 and OVCAR-3 cells exposed to doxorubicin (DOX) and cisplatin (CDDP) using the Sulforhodamine B method.

**Results:** GR50 analysis indicated a cytotoxic effect of DOX and CDDP on OVCAR-3 cells with values of  $1.16 \pm 0.13 \mu\text{M}$  and  $25.24 \pm 0.16 \mu\text{M}$ , respectively. In SK-OV-3 cells, we observed only a cytostatic effect of both drugs with GR50 values of  $2.25 \pm 0.12 \mu\text{M}$  for DOX and  $3.49 \pm 0.12 \mu\text{M}$  for CDDP. Regarding metabolomic analysis, overall differences were observed in the metabolism of nitrogen, CoA, vitamin B5, arginine and proline, glutathione, fatty acids, and the PPP pathway. In chemoresistant SK-OV-3 cells, the differences were marked by metabolites such as 2-aminoadenosine, uridine, glutathione, and carnitine, among the most important; in chemosensitive OVCAR-3 cells, these differences were marked by metabolites such as glutamine, aspartate, N-Acetyl-L-aspartate, among others.

**Conclusions:** We identify several metabolic differences between resistant and sensitive ovarian cancer cells. The use of inhibitors for metabolic pathways associated with chemoresistance could be used as new therapeutic targets to improve drug sensitivity.

**No conflict of interest.**

**311** (PB091)  
**Mechanisms of resistance to mobocertinib in EGFR exon 20 insertion-mutant non-small cell lung cancer (NSCLC)**

S. Park<sup>1</sup>, T.M. Kim<sup>1,2</sup>, S. Kim<sup>1,3</sup>, M. Kim<sup>1,2</sup>, B. Keam<sup>1,2</sup>, D.W. Kim<sup>1,2,3</sup>, D.S. Heo<sup>1,2</sup>. <sup>1</sup>Seoul National University, Cancer Research Institute, Seoul, South Korea; <sup>2</sup>Seoul National University Hospital, Internal Medicine, Seoul, South Korea; <sup>3</sup>Seoul National University, Integrated Major in Innovative Medical Science, Seoul, South Korea

**Background:** Although mobocertinib is an approved EGFR tyrosine kinase inhibitor for advanced NSCLC with EGFR exon 20 insertion mutation, its

resistance mechanism is unknown. Here, we developed mobocertinib-resistant NSCLC models and identified a therapeutic strategy. In addition, an identified resistance mechanism was validated in a patient with NSCLC with *EGFR* exon 20 insertion mutation who received mobocertinib.

**Materials and Methods:** ENU mutagenesis screening for Ba/F3 cells expressing *EGFR* exon 20 insertion mutations was performed under the treatment of mobocertinib to identify resistance mechanisms. In addition, mobocertinib-resistant SNU-3173 cell lines harboring an *EGFR* H773insAH mutation were established by stepwise exposure to mobocertinib at 1  $\mu$ M. Ba/F3 cells expressing *EGFR* exon 20 insertion variants with C797S were generated to validate the resistance mechanism discovered through mutagenesis screening. We compared the structure and delta G values of mobocertinib docking for *EGFR*-D770insNPG without and with C797S. Furthermore, cell viability and colony forming assays were performed to identify a therapeutic strategy for *EGFR* exon 20 insertion and C797S mutations. Cell-free DNA sequencing and droplet digital PCR (ddPCR) of plasma samples in a patient with *EGFR* exon 20 insertion-mutant advanced NSCLC who received mobocertinib were performed.

**Results:** All resistant Ba/F3 clones expressing *EGFR* exon 20 insertion mutation in ENU mutagenesis screening had mutations at the *EGFR* C797 site (C797S, 96%; and C797G, 4%). Ba/F3 cells harboring *EGFR* exon 20 insertion and C797S mutations were resistant to mobocertinib, poziotinib, and TAS-6417. Mobocertinib docking simulation demonstrated delta G values for *EGFR*-D770insNPG without and with C797S were  $-10.6$  and  $-6.8$ , respectively, suggesting that binding to *EGFR*-D770insNPG/C797S was energetically unfavorable. Mobocertinib was far away from its binding pocket on *EGFR*-D770insNPG/C797S (9.1 Å) than its pocket on *EGFR*-D770insNPG (5.4 Å). In addition, combined treatments brigatinib plus cetuximab or amivantamab showed synergistic effects (combination index value < 1) on Ba/F3 cells harboring *EGFR* exon 20 insertion and C797S mutations in short-term cell viability assays and long-term colony forming assays. Furthermore, an *EGFR* C797S mutation was identified in plasma samples of an NSCLC patient with *EGFR* exon 20 insertion mutation who showed acquired resistance to mobocertinib using ddPCR. Mobocertinib-resistant SNU-3173 cell lines had higher *EGFR* amplification than parental SNU-3173 cells.

**Conclusions:** *EGFR* C797S mutation and *EGFR* amplification were identified as resistance mechanisms to mobocertinib in *EGFR* exon 20 insertion-mutant NSCLC models. Combined treatment of brigatinib plus cetuximab or amivantamab may be an effective therapeutic strategy for *EGFR* exon 20 insertion/C797S-mutant NSCLC in preclinical models.

#### Conflict of interest:

Advisory Board: T.M. Kim reports consulting or advisory roles from AstraZeneca/MedImmune, BeiGene, Hanmi, Janssen, Novartis, Roche/Genentech, Takeda, and Yuhan.

D.W. Kim reports uncompensated consultation or advisory roles from Amgen, AstraZeneca, BMS/ONO Pharmaceuticals, Daiichi-Sankyo, GSK, Janssen, Merck, MSD, Oncobix, Pfizer, SK Biopharm, and Takeda.

Corporate-sponsored Research: T.M. Kim reports research funding from Amgen, AstraZeneca/MedImmune, Boehringer-Ingelheim, BMS, Hanmi, Janssen, Merck, MSD, Novartis, Regeneron, Roche/Genentech, Sanofi, and Takeda and research funding outside the submitted work from AstraZeneca-KHIDI.

D.W. Kim reports research funding from Alpha Biopharma, Amgen, AstraZeneca/MedImmune, Boehringer-Ingelheim, BMS, Bridge BioTherapeutics, Chong Keun Dang, Daiichi-Sankyo, GSK, Hanmi, Janssen, Merck, Merus, Mirati Therapeutics, MSD, Novartis, ONO Pharmaceutical, Pfizer, Roche/Genentech, Takeda, TP Therapeutics, Xcovery, and Yuhan and laboratory research funding from InnoN.

Other Substantive Relationships: D.W. Kim reports travel and accommodation support for advisory board meeting attendance from Amgen and Daiichi-Sankyo and medical writing assistance from Amgen, AstraZeneca, Boehringer-Ingelheim, BMS, Chong Keun Dang, Daiichi-Sankyo, GSK, Pfizer, MSD, Merck, Novartis, Roche, Takeda, and Yuhan.

312

(PB092)

#### Mechanisms of resistance toward FGFR4 inhibition in hepatocellular carcinoma

N. Zhang<sup>1</sup>, B. Shen<sup>1</sup>, J. Shi<sup>1</sup>, Z. Zhu<sup>1</sup>, Y. Zhang<sup>1</sup>, H. Ying<sup>1</sup>, Z. Chen<sup>1</sup>.

<sup>1</sup>Abbisko Therapeutics, Biology, Shanghai, China

**Background:** Hepatocellular carcinoma (HCC), which accounts for up to 90% of all primary liver cancers, is a leading cause of cancer mortality worldwide. FGF19 is a gut secreted endocrine hormone that acts in liver through its unique receptor FGFR4 and co-receptor KLB, to regulate bile acid synthesis and hepatocyte proliferation. FGF19 is reported to be over-expressed and/or amplified in ~30% of HCC. Genomic and functional studies have identified FGF19 as a potential driver oncogene in HCC. Several

FGFR4 inhibitors have entered clinical trials for treating HCC patients. BLU-554 is a potent, selective, and irreversible FGFR4 inhibitor that has demonstrated preliminary efficacy as a second-line treatment in HCC patients harboring FGF19 overexpression. The observed responses, however, on average only last few months before patient relapse, suggesting likely occurrence of acquired resistance. Here, we investigated the changes that occur with long-term FGFR4 inhibition and the development of resistance in preclinical HCC models, in order to identify resistance mechanisms and possible combination strategies.

**Materials and methods:** We established resistant cell lines following long-term exposure of Huh7 with BLU-554. Proteomic, genomic and transcriptomic characterizations were performed to identify potential resistance mechanisms.

**Results:** Huh7 cells resistant to BLU-554 were generated and confirmed with insensitivity to BLU-554. In addition, the cells were also resistant to other FGFR4 inhibitors including FGF-401, H3B-6527 and erdafitinib. Genomic analysis found no mutations on the FGFR4 gene itself. Proteomic analysis revealed activation of a RTK in the BLU-554 resistant cells compared with the parental cells. Transcriptomic analysis revealed changes in gene expression and GSEA analysis revealed multiple relevant gene sets were significantly enriched in the resistant cells. We tested several inhibitors against the identified RTK pathway and found complete inhibition this pathway could restore BLU-554 sensitivity.

**Conclusions:** These data suggest the bypass activation of other RTK may contribute to acquired resistance of FGFR4 inhibition and potential combination strategy to overcome resistance.

No conflict of interest.

313

(PB093)

#### Establishment and characterization of an EGFR-mutant NSCLC XPDX model representing first-line osimertinib resistance through an acquired TRIM24-BRAF fusion

A. Moriarty<sup>1</sup>, J. Flores<sup>1</sup>, A. Stackpole<sup>1</sup>, S. Ulmer<sup>2</sup>, K. Papadopoulos<sup>3</sup>, A. Patnaik<sup>2</sup>, D. Rasco<sup>3</sup>, E. Calvo<sup>4</sup>, V. Moreno<sup>4</sup>, M. Wick<sup>1</sup>. <sup>1</sup>XenoSTART, Translational Research, San Antonio, USA; <sup>2</sup>START Center, Medical Oncology, San Antonio, USA; <sup>3</sup>START, Ph1 Research, San Antonio, USA; <sup>4</sup>START Madrid, Ph1 Research, Madrid, Spain

**Background:** Osimertinib is a third generation EGFR inhibitor approved as first-line treatment for patients with exon 19 or specific exon 21 variants. While this therapy has proven efficacy, resistance to treatment inevitably occurs in patients. One reported resistance mechanism following first-line osimertinib treatment is an acquired TRIM24-BRAF fusion. While molecular studies to identify this and other genomic alterations have been performed, no actionable in vivo model of this resistance mechanism has been widely available for testing. To this end we have established a non-small cell lung XenoSTART Patient-Derived Xenograft (XPDX) model designated ST5570 from a patient post first-line osimertinib which harbors an *EGFR* exon 19 deletion and TRIM24-BRAF fusion. This model was characterized for receptor expression, genomic alterations, and in vivo drug sensitivities toward multiple chemotherapies and targeted agents.

**Methods:** ST5570 was established from a biopsy of a recurrent lung lesion collected from a 70-year-old African-American non-smoker female following two years of osimertinib treatment. The resulting model was passaged and characterized using immunohistochemistry and genomic analysis including WES and RNA<sub>seq</sub>. In vivo studies were performed testing various chemotherapy and targeted agents; study endpoints included tumor volume and time from treatment initiation with %T/C values and tumor regression reported at study completion; a %T/C of  $\leq 20$  versus control was considered sensitive. Tumor regression (%T/C < 0) versus Day 0 tumor volume was also reported.

**Results:** Immunohistochemistry analysis of ST5570 confirmed disease morphologically similar to the patient's archival clinical sample and a distinct profile for various receptor and signaling targets. WES analysis confirmed the exon 19 deletion at aa746–750, while RNA sequencing revealed a TRIM24-BRAF gene fusion, independently confirmed using molecular studies.

In vivo, ST5570 was resistant to weekly cisplatin, paclitaxel or combination. Oral EGFR inhibitors osimertinib, afatinib or erlotinib were ineffective as was twice weekly cetuximab injections. Dabrafenib or encorafenib treatment was ineffective; however single agent trametinib resulted in tumor regressions.

**Conclusion:** We have established and characterized an EGFR-mutant NSCLC XPDX model with an acquired TRIM24-BRAF fusion sensitive in vivo to the MEK inhibitor trametinib but not BRAF or EGFR inhibitors. This model is a valuable tool to study osimertinib-resistant lung cancer.

No conflict of interest.

314

(PB094)

**Loss of RHOA impairs lenalidomide antitumor activity in mantle cell lymphoma**

J. Carvalho Santos<sup>1</sup>, N. Profitós Pelejà<sup>1</sup>, M. Caillot<sup>2</sup>, S. Sánchez Vences<sup>3</sup>, B. Sola<sup>2</sup>, M. Lima Ribeiro<sup>1,3</sup>, G. Roué<sup>1</sup>, <sup>1</sup>Josep Carreras Leukaemia Research Institute, Lymphoma Translational Lab, Badalona, Spain; <sup>2</sup>INSERM U1245- University of Caen Normandy, Microenvironment and haematological cancers, Caen, France; <sup>3</sup>Sao Francisco University Medical School, Laboratory of Immunopharmacology and Molecular Biology, Braganca Paulista, Brazil

**Background:** Mantle cell lymphoma (MCL) is a rare, aggressive and incurable subtype of B-cell non-Hodgkin lymphoma (NHL) with a median overall survival of 5–7 years. Lenalidomide is an immunomodulatory agent, with clinical activity in relapsed or refractory (R/R) MCL patients. Among other effects, lenalidomide is known to enhance the formation of immunological synapses between MCL and Lytic T/natural killer (NK) cells. The small GTPase Ras homolog family member A (RHOA) acts as a molecular switch controlling a wide variety of cellular processes such as cytoskeleton organization, cell proliferation, differentiation and migration. Recent evidences have demonstrated RHOA tumor suppressor activity in some hematological malignancies. Here we investigated its role in MCL aggressiveness and response to lenalidomide.

**Methods:** RHOA expression was analyzed by qPCR and western blot (WB) in a panel of 11 MCL and NHL cell lines. RHOA inactivation was carried out by CRISPR/Cas9-mediated gene edition in two MCL cell lines, and confirmed by WB, DNA sequencing and RHOA-GTP pulldown assay. Transcriptomic analysis was carried out by RNA sequencing and gene set expression analysis. Cell proliferation, mitotic index and cell migration/invasion were assessed by CellTiter-Glo, histone H3-pSer10 labeling and Transwell assay, respectively. Immune synapse formation was analyzed by fluorescence-based detection of effector/B cells, perforin and F-actin levels. Cell-mediated toxicity was determined in MCL co-cultures by lactate dehydrogenase (LDH) release. Effect of a twice-weekly administration of lenalidomide was evaluated in vivo in a set of MCL chick embryo chorioallantoic membrane (CAM) cell-derived (CDX, n = 2, RHOA<sup>WT</sup> vs RHOA<sup>KO</sup>) and patient-derived (PDX, n = 3) xenograft models.

**Results:** Genetic deletion of RHOA in MCL cultures elicited a 40% increase in cell proliferation, a 10-fold increase in mitotic index, and a 3-fold potentiation of cell migration. Comparative RNA-seq analysis of RHOA<sup>WT</sup> and RHOA<sup>KO</sup> subclones highlighted a crucial role of the enzyme in the regulation of migration-related gene sets. While lenalidomide enhanced T/NK cell-mediated cytotoxicity against RHOA<sup>WT</sup> cells, it exhibited minimal activity in RHOA<sup>KO</sup> co-cultures, as shown by a 30–40% decrease in immune synapse formation and a 4-fold drop in LDH release. In vivo, lenalidomide treatment failed to elicit a significant tumor growth inhibition (TGI) in RHOA<sup>KO</sup> xenografts, contrasting with the RHOA<sup>WT</sup> counterparts in which the drug triggered the formation of multiple perforin-containing immunological synapses, allowing to a 50% TGI and a 20–30% reduction in MCL metastatic properties.

**Conclusions:** These data provide the first insight into the immune-mediated mechanism of action of lenalidomide against MCL tumors through RHOA signaling, and suggest that RHOA may exert a tumor suppressor function in this disease.

**No conflict of interest.**

315

(PB095)

**Cisplatin resistance of TMEM16A overexpressing head and neck tumors and cancer models is driven by increased lysosomal flux and reversed by Hydroxychloroquine**

A. Vyas<sup>1</sup>, S. Cruz-Rangel<sup>1</sup>, J. Pacheco<sup>1</sup>, G. Hammond<sup>2</sup>, K. Kiselyov<sup>3</sup>, U. Duvvuri<sup>1</sup>. <sup>1</sup>University of Pittsburgh, Otolaryngology, Pittsburgh, USA; <sup>2</sup>University of Pittsburgh, Cell Biology, Pittsburgh, USA; <sup>3</sup>University of Pittsburgh, Biological Sciences, Pittsburgh, USA

**Background.** Squamous cell carcinoma of the head and neck (SCCHN) is the sixth deadliest tumor worldwide. Despite the advances in therapies, this disease has low cure rates. Approximately 30% of SCCHN tumors amplify chromosomal band 11q13, which harbors the ANO1 gene that encodes the calcium-activated chloride ion channel TMEM16A. TMEM16A overexpression in SCCHN is associated with poor response to cisplatin and reduced survival. The mechanisms of cisplatin resistance in TMEM16A-overexpressing tumors are unclear; finding them would suggest new combinatorial therapy targets for SCCHN.

**Materials and Methods:** Human tumors were obtained from the University of Pittsburgh Medical Center. Written informed consent was

obtained from all the patients before inclusion in the study. Lysosomal exocytosis was measured using beta-hexosaminidase activity. Cell proliferation was measured using WST-1 or crystal violet. Nonobese diabetic severe combined immunodeficiency gamma female mice (4 wk old) were implanted subcutaneously with human tumor pieces on each flank and randomized. Treatments were administered two times a week intraperitoneally. The volume of the tumors was measured three times a week. The animals were handled and euthanized in accordance with Institutional Animal Care and Use Committee guidelines.

**Results:** We find increased lysosomal biogenesis and exocytosis (lysosomal flux) in TMEM16A overexpressing human SCCHN tumors and SCCHN models: OSC19 and FaDu cell lines. TMEM16A inhibition or knockdown reduces the lysosomal flux and increases cisplatin efficacy. TMEM16A has been linked to the production of reactive oxygen species through NADPH oxidase 2 and to  $\beta$ -catenin activation, which are linked to the activation of the endolysosomal ion channel TRPML1 and Melanocyte Inducing Transcription Factor (MITF), both of which drive lysosomal biogenesis. Accordingly, MITF and TRPML1 inhibition and knockdown reduce the lysosomal flux and enhance cisplatin efficacy. A general endolysosomal inhibitor, hydroxychloroquine (HCQ), which is widely used in clinic, synergized with cisplatin in killing SCCHN PDX models.

**Conclusions:** Our data implicate lysosomal biogenesis and exocytosis as mediators of cisplatin resistance in TMEM16A overexpressing SCCHN. Mechanistically, our data link these processes to MITF and TRPML1, specifically TRPML1 activation by reactive oxygen species downstream of NADPH oxidase 2 and MITF activation downstream of  $\beta$ -catenin activation. These results uncover a new model of treatment resistance in cancer, its reversal, and a new role of TMEM16A.

**No conflict of interest.**

316

(PB096)

**Pharmaceutical reactivation of attenuated apoptotic pathways leads to elimination of drug tolerant cells after osimertinib treatment in EGFR-mutant non-small cell lung cancer**

M. Martin<sup>1</sup>. <sup>1</sup>AstraZeneca, Oncology R&D, Cambridge, United Kingdom

**Background:** Osimertinib is a tyrosine kinase inhibitor (TKI) with established clinical efficacy in non-small cell lung cancer driven by activating mutations in the epidermal growth factor receptor (EGFR). However acquired resistance develops in a majority of patients, and analysis of tumour DNA shows a highly heterogeneous landscape of genetic drivers. Intervening with combination treatments prior to resistance may eliminate a greater number of tumour cells to enhance patient benefit. Recent studies have shown that drug-tolerant persister cells (DTPs) - tumour cells which survive EGFR TKI treatment but have yet to acquire mutations allowing them to proliferate in drug – have a distinct transcriptional profile that may confer specific vulnerabilities. By definition these cells avoid apoptosis, yet little is known about how their survival is regulated.

**Materials and Methods:** We generated DTPs from a panel of EGFR-mutant cell lines and characterised their expression of genes that regulate apoptosis. Further, we screened drug compounds for their ability to induce apoptosis in established DTP cultures. Finally, we tested pro-apoptotic compounds from our DTP screen in cell populations fully resistant to osimertinib for their ability to block tumour cell growth.

**Results:** We found that paradoxically, the pro-apoptotic gene BIM was significantly upregulated in DTPs. Co-treatment of established DTPs with BH3 mimetics targeting Mcl1 or Bcl2/xL, which normally inactivate BIM, could trigger apoptosis. Further, we found that both Smac mimetics and agents targeting the YAP/TEAD transcriptional pathway could block DTP formation as an up-front combination with osimertinib, and induced apoptosis in pre-formed DTPs, which normally are highly refractory to cell death. Finally, we show that apoptosis can be maximized in cell lines with intrinsic osimertinib resistance by combining BH3 or Smac mimetics, or YAP/TEAD inhibitors, with agents that target the resistance driver in these models.

**Conclusions:** These data suggest that drug tolerant cells after osimertinib maintain their apoptotic potential, and suggest potential novel therapeutic strategies at the point of minimal residual disease or full osimertinib resistance for patients in this critical area of unmet need.

**Conflict of interest:**

Corporate-sponsored Research: All authors are employees and shareholders of AstraZeneca.

317

(PB097)

**Identification of novel therapeutic targets to overcome chemoresistance in high-grade serous ovarian cancer**

E. Christie<sup>1</sup>, C. Huang<sup>2</sup>, V. Zhang<sup>2</sup>, K. Cowley<sup>3</sup>, K. Simpson<sup>3</sup>, G. Wang<sup>2</sup>, P. Cao<sup>2</sup>, W. Wiedemeve<sup>2</sup>. <sup>1</sup>Peter MacCallum Cancer Centre, Cancer Evolution and Metastasis Program, Melbourne, Australia; <sup>2</sup>BridGene Biosciences, Research and Development, San Jose, USA; <sup>3</sup>Peter MacCallum Cancer Centre, Victorian Centre for Functional Genomics, Melbourne, Australia

High-grade serous ovarian cancer (HGSC) remains a deadly gynecologic malignancy that kills approximately 120 000 women per year worldwide. Despite initial responses to platinum and taxol-based combination therapy in the majority of patients, virtually all HGSC eventually recur as drug resistant disease with very few treatment options. Thus, it is critical to identify novel therapeutic targets and treatment modalities in chemotherapy-resistant HGSC. Here, we describe an approach that combines phenotypic screening in chemoresistant HGSC cell lines with proteome-wide profiling by mass spectrometry in order to deconvolute cellular targets of small molecule inhibitors that can overcome acquired chemotherapy resistance in HGSC.

BridGene's proprietary platform, IMTAC (Isobaric Mass Tagged Affinity Characterization), allows for the identification of protein targets bound to covalent small molecules by mass spec. In addition, we have built a library of covalent compounds with drug-like properties that can be utilized in both phenotypic screens and in combination with IMTAC proteome-wide profiling. We screened a subset of our library in two sets of paired, patient derived cell lines from HGSC patients before and after acquired drug resistance. We assessed cell viability, cell cycle distribution and morphology in sensitive and resistant cell lines and identified several compounds with enhanced activity in resistant cells. We then applied IMTAC to identify the cellular targets of these active compounds.

Taken together, the combination of functional screens using a proprietary covalent library in drug-resistant cells and target deconvolution by IMTAC has yielded novel compounds with the potential to overcome acquired drug resistance. These compounds will provide a starting point for structure activity relationship (SAR)-guided optimization to further improve their potency and selectivity. Moreover, target deconvolution by IMTAC will improve our understanding of the mechanisms underlying acquired drug resistance and identify novel therapeutic targets in chemoresistant HGSC. Our ultimate goal is to take these findings into clinical trials and improve outcomes for women with HGSC.

No conflict of interest.

**POSTER SESSION****Drug Screening**

318

(PB098)

**Stereoisomeric effects of kusunokinin isomers on CSF1R selectivity**

C. Na Ayudhya<sup>1</sup>, P. Graidist<sup>1</sup>, V. Tipmanee<sup>1</sup>. <sup>1</sup>Prince of Songkla University, Faculty of Medicine- Department of Biomedical Sciences and Biomedical Engineering, Songkhla, Thailand

**Background:** Naturally extracted *trans*(-)-kusunokinin from *P. nigrum* showed anticancer activities via binding and inhibition of CSF1R. However, the synthetic racemic mixtures of *trans*(-) and *trans*(+)-kusunokinin (*trans*(±)-kusunokinin) exhibited different effects on breast cancer cell lines. It was hypothesized that *trans*(±)-kusunokinin bind to additional molecules, including AKR1B1. Previously, we found that *trans*(-)-isomer had better relative binding energies ( $\Delta G_{\text{bind}}$ ) than *trans*(+)-isomer in every studied proteins. Chiral carbon configurations in kusunokinin may also result in *cis*(-)-isomer and *cis*(+)-isomer. Differences in stereochemistry may lead to stereoisomeric preference for target protein selection and binding mode variety among four kusunokinin isomers.

**Material and Methods:** The target of four kusunokinin enantiomers: *trans*(-), *trans*(+), *cis*(-) and *cis*(+)-isomer was investigated on 57 proteins related to the CSF1R-breast cancer progression pathway, grouped by their main functions. The potential inhibition was determined by kusunokinin isomers'  $\Delta G_{\text{bind}}$  and binding sites, compared to known inhibitors. A preferable form of kusunokinin isomers was proposed using molecular docking combined with our ranking and scoring procedure. Contributing factors of the binding pocket's stereoselectivity were observed. Aggregation of *trans*(±)-kusunokinin and *cis*(±)-kusunokinin isomers was evaluated using Molecular dynamics simulation (MD).

**Results:** *Trans*(-)-kusunokinin selectively targeted CSF1R whereas *trans*(+), *cis*(-) and *cis*(+)-isomer inhibited AKR1B1 without stereoselectivity. *Trans*(-)-kusunokinin was the most preferred isoform while *cis*(±)-kusunokinin isomers potentially targeted metastasis proteins. The proteins without stereoselectivity shared a nature of large spherical binding pockets, as well as a lack of aromatic residues within the binding sites. A narrow binding pocket of CSF1R required a planar arrangement of the binding ligand to form  $\pi$ - $\pi$  interaction with Trp550, the selective residue on juxtamembrane domain region. MD simulation highlighted the stability of *trans*(-)-kusunokinin in binding to CSF1R was better than *trans*(+)-kusunokinin. Aggregation of the two racemate pairs were found not to affected the target protein binding.

**Conclusions:** *Trans*(±)-kusunokinin inhibited breast cancer progression mainly via *trans*(-)-isoform binding to CSF1R, as well as inhibition of related molecules by *trans*(-) and *trans*(+)-isoform, including AKR1B1, CDK2, COX2, EGFR, Hsp90a, JAK3 and MNK2. Aggregation of *trans*(±)-kusunokinin and *cis*(±)-kusunokinin isomers did not affected protein selectivity. Therefore, *trans*(±)-kusunokinin was a promising selective CSF1R racemic inhibitor whereas the effects of *cis*(±)-isomer on metastasis proteins was to be further investigated.

No conflict of interest.

319

(PB099)

**Screening of NXP900 and dasatinib across 121 cancer cell lines identifies differences in their antiproliferative activity profiles**

B. King<sup>1</sup>, R.E. Hughes<sup>1</sup>, S. Navarro-Marchal<sup>1</sup>, V.G. Brunton<sup>1</sup>, E. Poradosu<sup>2</sup>, N.O. Carragher<sup>1</sup>, A. Unciti-Broceta<sup>1</sup>. <sup>1</sup>University of Edinburgh, Cancer Research UK Edinburgh Centre, Edinburgh, United Kingdom; <sup>2</sup>Nuvelctis Pharma, Discovery, Fort Lee, USA

**Background:** We have recently reported that NXP900 (a.k.a. eCF506) binds and locks SRC tyrosine kinase in its 'closed' inactive conformation, being classified as a Type I1/2A inhibitor. This conformation-selective binding mode results in the inhibition of both SRC enzymatic activity and SRC-FAK complex formation, confers superior activity towards SRC-family kinases (SFK) and a high selectivity profile over the rest of the kinome [1,2]. This contrasts with the binding mode of dasatinib, which inhibits SRC kinase activity in its 'open' conformation (Type I), thus enhancing its capacity to bind to FAK. Moreover, dasatinib inhibits additional protein kinases beyond SFK, including ABL, KIT and PDGFR $\alpha$ . Consequently, despite their similar in vitro potency against SFK, we anticipated that these mechanistically-different inhibitors could induce distinct antiproliferative effects in particular cancer cell lines where either SFK-protein interactions or alternative kinases (e.g. targeted by dasatinib's promiscuity) are important drivers of cell proliferation and survival.

**Materials and Methods:** We screened NXP900 across the Oncolines™ cell line panel (121 cancer cell lines) and compared the results with those of dasatinib (reference control, OncolinesProfiler™).

**Results:** Statistical comparison of the IC<sub>50</sub> fingerprints showed that most cancer cell lines responded similarly to both compounds (Pearson correlation coefficient = 0.56). However, seven cell lines were much more sensitive to dasatinib than to NXP900, including the chronic myeloid leukemia cells K-562 and KU812, in agreement with the highly superior potency of dasatinib against ABL. Notably, over 20 cell lines including colorectal cancer cells HCT116, RKO, SW620 and LoVo, showed significantly higher sensitivity to NXP900 compared to dasatinib (from 10- to 250-fold difference in activity).

**Conclusions:** Our results indicate that specific patient subgroups may benefit from the distinct pharmacological properties of NXP900, but not from classical FDA-approved type I SRC inhibitors. Further in-depth bioinformatic analysis are ongoing to identify predictive biomarkers associated to NXP900-specific sensitivity to inform the clinical development strategy.

**Conflict of interest:**

Ownership: EP is a founder and has shares in Nuvelctis.  
Board of Directors: EP is in the board of directors of Nuvelctis Pharma.  
Corporate-sponsored Research: Research study funded by Nuvelctis Pharma  
Other Substantive Relationships: NOC and AU-B are inventors of NXP900. Nuvelctis has commercialization rights for NXP900.

**References**

1. *Cancer Res* (2021) 81 (21): 5438–5450. <https://doi.org/10.1158/0008-5472.CAN-21-0613>
2. *Cancer Res* (2022) 82 (12\_Supplement): 3326. <https://doi.org/10.1158/1538-7445.AM2022-3326>



320

(PB100)

**A Novel Hybrid Bifunctional Alkylating Agent That Potently Suppresses the Growth of mCRC Cells Xenografts and Patient-Derived Organoids**

V. Navakanth Rao<sup>1</sup>, L. Kuo-Chu<sup>2</sup>, L. Chin-Huang<sup>3</sup>, C. Joanne Jeou-Yuan<sup>1</sup>, S. Tsann-Long<sup>1</sup>, L. Te-Chang<sup>1</sup>. <sup>1</sup>Academia Sinica, Institute of Biomedical Sciences, Taipei, Taiwan; <sup>2</sup>Chang Gung University, Department of Physiology and Pharmacology, Taipei, Taiwan; <sup>3</sup>Tzu Chi University, Department of Pharmacology, Hualien, Taiwan

**Background:** Hitherto metastatic colorectal cancer (mCRC) is the basis for the second-leading death of all cancers. As the first-line chemotherapy in mCRC treatment, an antiangiogenic combination of bevacizumab with FOLFOX4 improved the competence and overall survival (OS). We developed a new hybrid small molecule with dual properties as first-line therapy to study its synergistic effect on CRC cell lines and patient-derived organoids.

**Materials and methods:** The anti-proliferative effect was analyzed by PrestoBlue assay using CRC cell lines and CRC patient-derived organoids (PDO). Antiangiogenic property has been assessed using the docking model, molecular, *in vitro*, and *in vivo* methods. Xenografts of CRC cell lines and PDOs were tested for BO-2762 efficacy with 20 mg/kg (*i.v.*) using nude mice. For safety profiling and toxicology, the ICR mice model has been used for various pathological analyses.

**Results:** We identified ant proliferative IC<sub>50</sub> ranged between 0.5 to 4.5 μM against CRC cell lines and PDO cell lines. Subsequently, DNA damage has been observed by inter-strand cross-linking (ICL) in alkaline agarose gel and cell lines. ICL affects the cellular DNA synthesis by arresting the cell cycle at S Phase upon apoptosis. Angiogenesis inhibition occurred by inhibiting VEGFR2 activation on endothelial cells with anti-proliferative IC<sub>50</sub> of 3 μM and in the mouse as well. Based on *in vitro* analysis, metastatic and non-metastatic cells (LoVo, SW620, LS1034, and HT-29) and PDOs (T<sub>53</sub> and T<sub>112</sub>) induced xenografts have shown effective growth inhibition with 85.8%, 83.0%, 75.4%, and 44.8% respectively. PDO xenografts have shown a tremendous inhibition of more than 90% of growth reduction. Pathological analysis elaborates the effect of BO-2762 treatment by elevating γ-H2AX and CD31 expression in treated mice tumor tissues. Biosafety analysis has shown promising safety parameters in blood chemistry and pathology analysis.

**Conclusions:** BO-2762 is a potent anti-cancer agent to mCRC. The mice model indicates that BO-2762 driven bifunctional properties induced serious DNA damage and inhibited angiogenesis leading to promising inhibition of tumor growth as first-line chemotherapy properties with a satisfying safety profile.

**No conflict of interest.**

321

(PB101)

**High content screening of ovarian organoid models to accelerate anti-cancer drug discovery**

M. Hornsvelde<sup>1</sup>, M. Madej<sup>1</sup>, J. García Mateos<sup>1</sup>, G. Goverse<sup>1</sup>, M. Putker<sup>1</sup>, E. Spanjaard<sup>2</sup>, L. Price<sup>3</sup>, B. Herpers<sup>1</sup>. <sup>1</sup>Crown Bioscience, Organoid, Leiden, Netherlands; <sup>2</sup>Crown Bioscience, Bioinformatics, Leiden, Netherlands; <sup>3</sup>Crown Bioscience, In Vitro, Leiden, Netherlands

**Background:** Establishment of advanced *in vitro* ovarian cancer organoid models provides a rapid and biologically relevant platform for testing novel cancer (immune) therapies. These ovarian models, when cultured alone or in co-culture with other cell types, serve as a great tool for predicting treatment responses in patients, discriminating different drug responses, and flagging off-target effects. In this study a high throughput platform that combines 3D cultured ovarian models with phenotype-based image analysis is presented. This platform allows the measurement of clinically relevant endpoints beyond conventional cell viability, including those associated with tumor killing, growth inhibition, toxicity, different types of cell death and interactions with added immune cells.

**Methods:** A panel of genetically characterized ovarian cancer organoid models was cultured in a natural extracellular matrix scaffold to mimic *in vivo* complex biology. To investigate the effects of standard-of-care (SoC) treatments, a library of small molecules and novel targeting antibodies on tumor outgrowth, the following organoid test systems were set up: 1. Compound profiling on various ovarian cancer organoids alone or in combination with irradiation; 2. High throughput compound library screen in a panel of ovarian models; 3. Co-culture of ovarian cancer organoids with PBMCs and cancer associated fibroblasts (CAFs).

**Results:** High content 3D image analysis of ovarian organoids upon various treatments enables sensitive detection of treatment-induced and compound-specific morphological changes such as (inhibition of) growth, development, lumen formation, epithelial integrity and cell death or

discrimination of cellular interactions in a complex tumor co-culture microenvironment. Ovarian organoids with specific mutations and diverse genetic backgrounds show various sensitivity to the treatments alone or in combination with irradiation or relevant immune cells.

**Conclusions:** Our high content image analysis of *in vitro* 3D cultured organoids represents a rapid, reproducible and physiologically relevant model system for testing various candidate compounds (e.g., antibodies, antibody-drug conjugates, small molecules, oncolytic viruses or immunotherapies) that target, for example, ovarian cancer. This platform is suitable for high throughput screening in a panel of organoids but also for in-depth mode of action study in mono- or co-culture systems. Therefore, our ovarian organoid screening platform represents a significant advance on conventional *in vitro* models and helps bridge the translational gap between *in vivo* and conventional *in vitro* studies.

**No conflict of interest.**

322

(PB102)

**Cationic amphiphilic drugs as potential anticancer therapy for PDAC**

M. Živanović<sup>1</sup>, M. Selaković<sup>2</sup>, Ž. Selaković<sup>3</sup>, A. Pavić<sup>4</sup>, J. Grahovac<sup>5</sup>, B. Šolaja<sup>6</sup>, T. Srdić-Rajić<sup>7</sup>. <sup>1</sup>Institute for Oncology and Radiology of Serbia-Belgrade, Serbia, Department of Experimental Oncology and Radiology, Belgrade, Serbia; <sup>2</sup>Innovative Centre of the Faculty of Chemistry in Belgrade-Ltd., Department of Organic Chemistry, Belgrade, Serbia; <sup>3</sup>Faculty of Chemistry- University of Belgrade- Belgrade, Serbia, Department of Organic Chemistry, Belgrade, Serbia; <sup>4</sup>Institute for Molecular Genetics and Genetical Engineering- Belgrade, Department for Microbial Molecular Genetics and Ecology, Belgrade, Serbia; <sup>5</sup>Institute for Oncology and Radiology of Serbia-Belgrade, Serbia, Department of Experimental oncology, Belgrade, Serbia; <sup>6</sup>Serbian Academy of Sciences and Arts, Department of Chemistry, Belgrade, Serbia; <sup>7</sup>Institute for Oncology and Radiology of Serbia-Belgrade, Serbia, Department for experimental oncology, Belgrade, Serbia

**Introduction:** Pancreatic ductal adenocarcinoma (PDAC) is the sixth leading cause of death worldwide. PDAC carries a 5-y survival of less than 10%, as it is often diagnosed at a late stage and is widely refractory to available therapies. PDAC tumors are hypoperfused, resulting in poor nutrient delivery. To exist in this hostile microenvironment, PDAC cells rely on intracellular and extracellular scavenging pathways to acquire metabolic substrates for growth. Autophagy and other lysosome-dependent recycling pathways are aberrantly regulated in PDAC. Although autophagy modulation is an emerging therapeutic strategy for PDAC, the co-dependences induced by lysosomal inhibition have not been systematically explored. Cationic amphiphilic drugs (CADs) accumulate in lysosomes, destabilize their membranes, and can have anti-tumorigenic effects. CADs include hundreds of pharmacologic agents used to treat a broad spectrum of common diseases. The aim of this study was to investigate anti-PDAC activity of several clinically-approved and newly synthesized CADs.

**Material and methods:** Imidazoline, quinoline, and chrysene derivatives were examined. Anti-tumor activity of CADs was evaluated in human PDAC cell lines *in vitro* and in Tg(fli1:EGFP) zebrafish model *in vivo*. Effects on mitochondria, lysosomes, and autophagy flux were examined by immunofluorescent microscopy. Levels of reactive oxygen species (ROS), changes in the mitochondrial membrane potential, and induction of apoptosis by the selected CADs were evaluated by flow cytometry.

**Results:** The newly synthesized derivatives of quinoline and chrysene induced apoptosis in PDAC cells *in vitro* in the 2–10 μM range, while the only FDA-approved imidazoline with apoptotic activity was rilmenidine, at doses higher than 100 μM. Most of the tested compounds induced the expansion of the acidic compartment, as measured by acridine orange and LAMP1 staining, and modulated autophagy, as seen by LC3 staining intensity and distribution. Mitochondrial oxidative stress was induced by the tested CADs as well as the dissipation of the mitochondrial membrane potential (ΔΨ<sub>m</sub>). Ultimately, both newly synthesized CADs and rilmenidine limited the growth and spread of PANC1 cancer cells in the Tg(fli1:EGFP) zebrafish model.

**Conclusion:** Quinoline and chrysene CADs had the potential for a dual lysosome/mitochondrion targeting in PDAC cells and were inducing apoptosis almost in a nM range. While rilmenidine was less potent than newly synthesized CADs in inducing cell death *in vitro*, all the tested compounds had significant anti-tumor effects in the zebrafish model. These results imply that CADs have promising anti-PDAC effects and that effects on the other cells in the tumor microenvironment other than the cancer cells themselves have to be examined.

**No conflict of interest.**

323 (PB103)

**LiP-MS, a machine learning-based chemoproteomic approach to identify drug targets in complex proteomes**

D. Redfern<sup>1</sup>, N. Beaton<sup>1</sup>, F. Sabino<sup>1</sup>, C. Below<sup>1</sup>, R. Bruderer<sup>1</sup>, Y. Feng<sup>1</sup>, P. Castaldi<sup>2</sup>, L. Reiter<sup>1</sup>. <sup>1</sup>Biognosys AG, RnD, Schlieren, Switzerland; <sup>2</sup>Astra Zeneca, Discovery Sciences, IMED Biotech Unit, Waltham, MA, USA

**Background:** Target identification is a critical step in elucidating the mechanism of action (MoA) for bioactive compounds. For target-based and phenotypic drug discovery pipelines, extensive potential target knowledge for a lead compound provides essential insights that enable potency and selectivity optimization. The tedious process of target deconvolution for a compound often necessitates a plethora of biochemical and biophysical techniques. To expand the toolbox of unbiased target ID approaches, we developed a drug target deconvolution workflow combining limited proteolysis with quantitative mass spectrometry (LiP-MS) that exploits the drug binding phenomena of protein structural alterations and steric hindrance. Advantageously, LiP-MS's unique peptide-centric focus exploits signature peptide detection to discern ligand binding. Here we demonstrate the performance of LiP-MS using two well-characterized kinase inhibitors (KIs), an AstraZeneca CDK9 inhibitor (AZ) and Selumetinib (SE).

**Methods:** Mechanically sheared HeLa or U2OS cell lysate was incubated with compound at multiple concentrations. Next, a limited proteolytic digest was performed using proteinase K. After quenching this digestion, lysate was trypsin digested to peptides for mass spectrometry analysis. The resulting peptides were analyzed quantitatively using data-independent acquisition (DIA)-MS with Spectronaut Pulsar X.

**Results:** Herein, we use LiP-Quant to unbiasedly identify unique peptides generated by the binding of two distinct classes of kinase inhibitors in human cell lysate. For the ATP-competitive inhibitor AZ, LiP-Quant shows a strong enrichment for CDKs in the target space defined by LiP score, including CDK1, 2, 4, 6, 9 and 11A. In addition, our data indicates that this KI targets members of the CDKs with different selectivity, with CDK9 displaying the highest compound affinity (nM range). For Selumetinib, a non-competitive allosteric inhibitor, LiP-MS clearly identified the direct targets MEK1 and MEK2 as the main hits by LiP score. Both cases represent a highly specific enrichment given that we quantified > 200'000 peptides mapped to > 8'000 proteins in each of the experiments. These findings confirm our approach's ability to identify genuine drug targets regardless of drug MoA in a complex biological matrix. Importantly, in both KI target ID studies, identified LiP peptides could be successfully deployed to map compound binding site, demonstrating the potential of LiP-MS to pinpoint regions involved in drug-protein interactions.

**Conclusions:** Collectively, this data demonstrates that LiP-MS can be used to effectively identify protein drug targets and characterize the binding properties in complex proteomes independent of the compound's MoA and without compound modification or labeling. These capabilities make LiP-MS a powerful addition to the target deconvolution toolbox.

**No conflict of interest.**

324 (PB104)

**Quantitative analysis of EGFR expression and distribution upon drug treatment in colorectal organoid models**

M. Putker<sup>1</sup>, J. Garcia Mateos<sup>1</sup>, C. Del Angel Zuvirio<sup>1</sup>, L. Price<sup>2</sup>, B. Hergers<sup>1</sup>. <sup>1</sup>Crown Bioscience, Oncology, Leiden, Netherlands; <sup>2</sup>Crown Bioscience, In vitro, Leiden, Netherlands

**Background:** Human organoids are patient-derived tissues that can be expanded *in vitro* by stimulating the (cancer) stem cells with WNT pathway activators, treatment with differentiation inhibitors and by providing growth factors in an extracellular matrix environment. These organoids form three-dimensional (3D) multicellular structures that polarize and self-organize and express relevant disease-related markers, which makes an organoid biobank ideal for testing the efficacy and mode of action of compounds and antibodies across a diverse patient population. Here, our colorectal organoid biobank and high content imaging platform were used to characterize EGFR dynamics upon drug treatment.

**Methods:** An established biobank of normal colon and colorectal cancer organoid models was characterized for its sensitivity to the growth factor

EGF, EGFR-inhibitors (Cetuximab), and standard-of-care compounds. To study the distribution of the EGF receptor, antibodies followed by immunofluorescence staining were used to detect the localization and distribution upon growth factor stimulation. (Inducible) knockdown organoid models with shRNA constructs targeting EGFR were generated to validate the findings.

**Results:** The 3D organoid screening and our proprietary image analysis platform allows the in-depth detection and distinction of growth factor responses that not necessarily only relate to proliferation. By making use of this system, the sensitivity of organoid models to EGF stimulation that are independent of EGF for their outgrowth could be determined. By combining the detection of the target, EGFR, with the detection of targeting EGFR-inhibitory antibodies by immunofluorescence followed by image analysis, the redistribution of the receptor upon EGF-stimulation and in response to antibody exposure could be visualized and quantified. This revealed that EGFR is internalized in the first hours upon EGF stimulation. Along with making use of (inducible) knockdown organoids, it also revealed that different EGFR-targeting antibodies have different effects on the redistribution, internalization, and degradation of EGFR.

**Conclusions:** The high content imaging platform in combination with high throughput screening in 3D-cultured organoid models allows compound and antibody testing in physiologically relevant patient-derived models to not only study the sensitivity to novel compounds, but also for patient stratification and to study the mode of action or understand the underlying relevant biology. The outcome of this work demonstrated that organoids are versatile, multicellular structures that are highly suitable for studying the expression and redistribution of disease-relevant targets.

**No conflict of interest.**

325 (PB105)

**High-Throughput Screening Identifies Novel ROS-Inducing Small Molecules as a Therapy for Treatment-Resistant Melanoma**

C. Stoffel<sup>1</sup>, O. Eichhoff<sup>1</sup>, P. Turko<sup>1</sup>, P. Cheng<sup>1</sup>, L. Briker<sup>1</sup>, A. Dzung<sup>1</sup>, R. Dummer<sup>1</sup>, M. Levesque<sup>1</sup>. <sup>1</sup>University Hospital Zurich, Dermatology, Zurich, Switzerland

**Background:** Melanoma heterogeneity and plasticity leading to disease progression as well as the lack of targeted therapies for NRAS-mutated patients highlights the ongoing need for new treatments for these patients. Reprogramming cell energy metabolism has been recognized as an emerging hallmark of cancer. Targeting deregulated cellular energetics by reactive oxygen species (ROS) induction is in focus of research for the treatment of metastatic and resistant melanomas.

**Material & Methods:** We have employed high-throughput screening of a chemical library of 17'000 small molecules in an NRAS-mutated patient-derived melanoma cell culture derived from a metastatic site to identify ROS-inducing lead compounds that target NRAS-mutated melanoma cells.

**Results:** Rescue experiments with the antioxidant N-acetyl-L-cysteine (NAC) revealed two compounds (C8 and C37) that were rescued by NAC, induced cytoplasmic ROS as well as DNA double-strand breaks and apoptosis. Treatment of *ex vivo* tumor material from resistant and metastatic patients with our novel ROS-inducing compounds led to the inhibition of melanoma cell proliferation. Xenograft experiments showed that one hit compound (C37) decreased tumor volume *in vivo* in combination with the MEK-inhibitor binimetinib in resistant NRAS-mutated melanomas. By screening a larger cohort of cell cultures, including BRAF-mutated as well as treatment sensitive cell cultures, we found that these two compounds specifically target melanoma cells resistant to targeted therapies. We observed a correlation between high cytoplasmic ROS levels, targeted therapy resistance, and sensitivity to our two compounds. This correlation was especially significant in a cohort of NRAS-mutated melanoma cell cultures. Profiling the phosphorylation of 37 signaling kinases revealed that downregulation of the phosphorylation of the transcription factor CREB is associated with responses to our compounds.

**Conclusion:** Our data suggest that two novel compounds increase intracellular ROS levels to a deadly threshold by impairing antioxidant defense supported by CREB signaling. Strikingly, we have found two novel hit compounds effective in NRAS mutated treatment resistant melanoma *in vitro* and *in vivo*.

**No conflict of interest.**

## POSTER SESSION

## Molecular Profiling

326

(PB106)

**Identifying FGFR2 fusions/rearrangements in cholangiocarcinoma patients using a novel cfDNA algorithm for treatment with RLY-4008, a highly selective irreversible FGFR2 inhibitor**

A. Schram<sup>1</sup>, M. Borad<sup>2</sup>, V. Sahai<sup>3</sup>, S. Kamath<sup>4</sup>, R. Kim<sup>5</sup>, C.Y.A. Liao<sup>6</sup>, D.Y. Oh<sup>7</sup>, M. Ponz-Sarvisé<sup>8</sup>, J. Yachnin<sup>9</sup>, S.A. Shell<sup>10</sup>, P. Cassier<sup>11</sup>, E. Dotan<sup>12</sup>, V. Florou<sup>13</sup>, V. Moreno<sup>14</sup>, J.O. Park<sup>15</sup>, D. Tai<sup>16</sup>, O. Schmidt-Kittler<sup>17</sup>, C. Ferté<sup>18</sup>, L. Goyal<sup>19</sup>, V. Subbiah<sup>20</sup>. <sup>1</sup>Memorial Sloan Kettering Cancer Center, Medical Oncology, New York, New York, USA; <sup>2</sup>Mayo Clinic Scottsdale - PPDS, Medical Oncology, Phoenix, Arizona, USA; <sup>3</sup>University of Michigan, Gastrointestinal Medical Oncology, Ann Arbor, Michigan, USA; <sup>4</sup>The Cleveland Clinic Taussig Cancer Institute, Hematology and Medical Oncology, Cleveland, Ohio, USA; <sup>5</sup>H Lee Moffitt Cancer Center and Research Institute, Medical Gastrointestinal Oncology, Tampa, Florida, USA; <sup>6</sup>University of Chicago Medical Center, Hematology and Oncology, Chicago, Illinois, USA; <sup>7</sup>Seoul National University Hospital, Hemato-Oncology, Seoul, South Korea; <sup>8</sup>Clinica Universidad Navarra, Medical Oncology, Pamplona, Spain; <sup>9</sup>Karolinska Universitetssjukhuset Solna, Early Clinical Trial Unit, Stockholm, Sweden; <sup>10</sup>Guardant Health, Biopharma Collaborations, Palo Alto, California, USA; <sup>11</sup>Centre Léon Bérard, Medical Oncology, Lyon, France; <sup>12</sup>Fox Chase Cancer Center, Gastrointestinal Medical Oncology, Philadelphia, Pennsylvania, USA; <sup>13</sup>University of Utah - Huntsman Cancer Institute - PPDS, Oncology, Salt Lake City, Utah, USA; <sup>14</sup>START MADRID Hospital Universitario Fundacion Jimenez Diaz, Clinical Research, Madrid, Spain; <sup>15</sup>Samsung Medical Center - PPDS, Hematology/Oncology, Seoul, South Korea; <sup>16</sup>National Cancer Centre, Medical Oncology, Singapore, Singapore; <sup>17</sup>Relay Therapeutics, Translational Medicine, Cambridge, Massachusetts, USA; <sup>18</sup>Relay Therapeutics, Clinical Development, Cambridge, Massachusetts, USA; <sup>19</sup>Massachusetts General Hospital, Hematology/Oncology, Boston, Massachusetts, USA; <sup>20</sup>University of Texas MD Anderson Cancer Center, Investigational Cancer Therapeutics, Houston, Texas, USA

**Background:** *FGFR2* fusions/rearrangements (*f/r*) are a critical therapeutic target in cholangiocarcinoma (CCA). Genomic profiling based on tumor tissue is standard for CCA patients but can be challenging due to the limited specimens often obtained during diagnostic biopsies and the aggressive nature of the disease prompting clinicians to forego repeat biopsies to rapidly initiate therapy. Cell-free DNA (cfDNA) may offer a noninvasive approach to overcome these tissue limitations, however, there are technical challenges detecting the long tail of unique *FGFR2* fusion partners. We assessed the utility of a de novo *FGFR2 f/r* calling algorithm in identifying these alterations.

**Methods:** Patients with unresectable or metastatic CCA identified with an *FGFR2 f/r* by local tissue or plasma testing were enrolled in the first-in-human study of RLY-4008, a highly selective *FGFR2* irreversible inhibitor (NCT04526106). Pre-treatment samples were evaluated centrally by next generation sequencing (NGS) in tumor tissue and by Guardant360@CDx (G360) in cfDNA. A novel research-use only de novo *f/r* calling algorithm (fusion partner agnostic) was applied to the G360 test to broaden the capability of detecting *FGFR2 f/r*. The objective was to evaluate the feasibility (failure rate) and the sensitivity (percent positive agreement [PPA]) of the novel cfDNA *f/r*-calling algorithm to compare to the local and central tissue assessments for identifying *FGFR2 f/r*.

**Results:** Forty-eight CCA patients with *FGFR2 f/r* per local testing had available tumor tissue and plasma for central testing. All of these patients had *FGFR2 f/r* initially identified based on tumor tissue. *FGFR2 f/r* included 10 *FGFR2-BICC1* fusions and 38 non-*FGFR2-BICC1* fusions. Implementation of the de novo *f/r* calling algorithm increased the *f/r* calling of G360 from 30 to 38. Undetectable circulating tumor DNA occurred in one patient (2%). The PPA of research-use G360 with local results was 81% (38/47). Central tissue NGS also confirmed 38 *f/r* with a PPA of 93% (38/41) while failure due to low DNA yield or insufficient tumor content occurred in seven patients (15%). Agreement of *FGFR2 f/r* calling between the central tissue NGS and research-use G360 was 84% (31/37).

**Conclusions:** In this study, *FGFR2 f/r* detection using a novel fusion partner-agnostic cfDNA approach has an acceptable performance and is a feasible noninvasive option for screening CCA patients. These encouraging results suggest a utility of cfDNA in *FGFR2 f/r* profiling, which will be prospectively validated in the RLY-4008-101 pivotal study.

**Conflict of interest:**

Ownership: CF: Relay Therapeutics.

OSK: Relay Therapeutics.

Advisory Board: PC: OSE Immunotherapeutics.

LG: (DSMB) AstraZeneca (SAC) Alentis Therapeutics AG, Black Diamond, H3Biomedicine, Incyte Corporation, QED Therapeutics, Servier, Sirtex Medical, Taiho, Transthera, Kinnate.

SK: Exelixis, Guardant Health, Tempus.

CYAL: Incyte, Transthera, QED Therapeutics.

DYO: AstraZeneca, Novartis, Genentech/Roche, Merck Serono, Bayer, Taiho, ASLAN, Halozyme, Zymeworks, BMS/Celgene, BeiGene, Basilea, Turning Point, Yuhan, Arcus Biosciences, IQVIA.

MPS: AstraZeneca, GE.

AMS: Relay Therapeutics, Mersana.

Board of Directors: n/a.

Corporate-sponsored Research: MB: Relay Therapeutics.

JC: (all institutional funding) Bayer, GlaxoSmithKline, Janssen, Lilly, AstraZeneca, Roche/Genentech, Merck/Serono, Toray Industries, Novartis, Plexixon, Bristol Myers Squibb, Taiho, Transgene, Innate Pharma, Loxo, Blueprint Medicines, Celgene, Abbvie, Merck Sharp & Dohme.

ED: Relay Therapeutics Lilly, Pfizer, Incyte, AstraZeneca, SMP Oncology, Zymeworks, NGM Biopharmaceuticals, Ipsen, Syneos Health.

LG: (all institutional funding) Adaptimmune, Bayer, Eisai, Merck, MacroGenics, Genentech, Novartis, Incyte, Eli Lilly, Loxo Oncology, Relay Therapeutics, QED Therapeutics, Servier, Taiho, LEAP Therapeutics, Bristol Myers Squibb, Nucana.

VM: (all institutional funding/PI) AbbVie, AceaBio, Adaptimmune, ADC Therapeutics, Aduro, Agenus, Amcure, Amgen, Astellas, AstraZeneca, Bayer, Beigene, BiInvent International AB, BMS, Boehringer, Boehringer, Boston, Celgene, Daichii Sankyo, DEBIOPHARM, Eisai, e-Terapeutics, Exelixis, Forma Therapeutics, Genmab, GSK, Harpoon, Hutchison, Immunet, Incyte, Inovio, Iovance, Janssen, Kyowa Kirin, Lilly, Loxo, MedSir, Menarini, Merck, Merus, Millennium, MSD, Nanobiotix, Nektar, Novartis, Odonate Therapeutics, Pfizer, Pharma Mar, PharmaMar, Principia, PsiOxus, Puma, Regeneron, Rigotec, Roche, Sanofi, Sierra Oncology, Synthon, Taiho, Takeda, Tesaro, Transgene, Turning Point Therapeutics, Upshersmith.

DYO: (all institutional funding) AstraZeneca, Novartis, Array, Eli Lilly, Servier, BeiGene, MSD, Handok.

AMS: (all institutional) AstraZeneca, ArQule, BeiGene/Springworks, Black Diamond Therapeutics, Elevation Oncology, Kura, Lilly, Merus, Northern Biologics, Pfizer, PMV Pharma, Relay Therapeutics, Repare Therapeutics, Revolution Medicine, Surface Oncology.

ViS: Relay Therapeutics.

Other Substantive Relationships:

PC: (honoraria) ITeos Therapeutics, Amgen, Janssen (travel) Netris Pharma, Amgen, Merck Sharp & Dohme, Roche, Merck Serono, AstraZeneca/MedImmune.

ED: (consulting fees) QED, Taiho, Helsinn, Incyte, Basilea, SMP Oncology, G1 Therapeutics (honoraria) Pfizer.

CF: (employment) Relay Therapeutics.

LG: (consulting fees) Alentis Therapeutics, Genentech, Exelixis, Incyte Corporation, QED Therapeutics, Servier, Sirtex Medical, and Taiho.

VM: (consulting fees) Roche, Bayer, Pieris, BMS, Janssen, Basilea, Regeneron/Sanofi, Nanobiotix.

MPS: (consulting fees) AstraZeneca, Incyte (honoraria) Roche (travel) Incyte, BMS, AstraZeneca (medical writing support) Roche.

OSK: (employment) Relay Therapeutics.

DT: (honoraria) Ipsen, Eisai, BMS, Roche (consulting fees) Novartis, Celgene, SIRTEX, Eisai, Ipsen, Bayer, BMS (travel) AstraZeneca.

327

(PB107)

**Key Oncogenic Proteins Are Regulated By Enzyme-Driven Nitration**

I. Griswold-Prenner<sup>1</sup>, S. Hussain<sup>2</sup>. <sup>1</sup>Nitrase Therapeutics, Brisbane, USA; <sup>2</sup>Nitrase Therapeutics, Discovery, Dallas, USA

**Background:** Nitrase Therapeutics is unlocking the therapeutic potential of nitrases, a new class of enzymes discovered by the company that catalyze a post-translation modification called nitration.

**Materials And Methods:** Nitrases catalyze the post-translation modification called nitration, a process by which an NO<sub>2</sub> group is transferred from peroxynitrite to specific tyrosines on substrates (nitro-substrates). Nitration is an important modifier of protein structure, function and localization. We have identified 30 putative nitrases. To identify nitrase activity and specificity against nitro-substrates, we established nitrase biochemical activity assays. These nitrase assays consist of dose response of low nanomolar concentrations of each nitrase incubated with micromolar concentrations of peroxynitrite, the physiological cofactor for nitrases, on a 23 000 protein chip (HuProt). Nitro-substrates present on the chip are detected post-nitrase activity assay using anti-nitrotyrosine antibodies.

**Results:** Using these nitrase assays, we have discovered several nitrases that regulate nitro-substrates which have known relevance for tumor cell survival and/or tumor evasion from the immune system. For example, we have found that Nitrase #3 catalyzes nitration of Pak4. Pak4 is implicated in driving the oncogenic state as well as contributing to evasion of tumor cells from immunological cell surveillance. Nitrase#3 nitration of Pak4 increases Pak4 kinase activity. Nitrase #3 does not nitrate or regulate Pak6, suggesting inhibition of Nitrase #3 could provide a niche mechanism to selectively inhibit Pak4 activity. With this, it suggests Nitrase #3 through Pak4 activation could function by both tumor-autonomous and immune-oncology mechanisms.

Similarly, we have found that Nitrase #12 nitration activates RhoA. Nitrase #11 nitration of Bax reduces its induced pore formation/induction of cytochrome C release from the mitochondria. Inhibition of either Nitrase, therefore, could be an important mechanism to slow or inhibit progression of the oncogenic state of Nitrase#12/RhoA/Rock or Nitrase#11/Bax dependent tumors.

**Conclusions:** The inhibitors that Nitrase Therapeutics is developing target the nitrases and potentially will help slow or halt the progression of numerous diseases in which nitrases and nitro-substrates play a role, including oncology.

#### Conflict of interest:

Ownership: Irene Griswold-Prenner owns shares in Nitrase Therapeutics. Sami Hussain owns shares in Nitrase Therapeutics.

328

(PB108)

#### Expression of the sortilin 1 receptor (SORT1) in healthy and tumor tissues

G. Roy<sup>1</sup>, P. Kadekar<sup>1</sup>, L.M. Douglas<sup>1</sup>, J.C. Currie<sup>1</sup>, J. Dhillon<sup>2</sup>, G. Cesarone<sup>2</sup>, R. Siderits<sup>2</sup>, K. Kirchner<sup>2</sup>, M. Demeule<sup>1</sup>, C. Marsolais<sup>1</sup>. <sup>1</sup>Theratechnologies Inc., Medical Affairs, Montreal, Canada; <sup>2</sup>Discovery Life Sciences LLC, Immunohistochemistry, Newton, PA, USA

**Background:** Sortilin (SORT1), or neurotensin receptor-3, is a scavenging receptor in the Vacuolar Protein Sorting 10 protein (Vps10p) family. SORT1 is involved in the internalization and trafficking of its ligands through an endocytic process and is reported to play a role in cancer cell survival and progression, making SORT1 a candidate for novel drug delivery. The pattern and prevalence of SORT1 expression in different healthy and cancer tissues is still not well understood.

**Material and methods:** To gain better understanding about the expression of SORT1, screening of healthy and cancer tissue microarrays (TMAs) was undertaken using an immunohistochemistry (IHC) method. A total of 19 TMAs were screened, 4 for breast cancer (including triple-negative breast cancer (TNBC)), 3 for ovarian cancer, 2 for endometrial cancer, 3 for melanoma, 3 for colorectal cancer, 3 for pancreatic cancer and 1 for different healthy tissues. A total of 1222 cancer cores were evaluable and scored using a H-score ranging from 0 to 300, where 0 corresponds to no cell stained for SORT1, while 300 corresponds to strong SORT1 staining in all cells.

**Results:** A H-score  $\geq 100$  was observed in 88% of breast cancers (n = 195), 70% of TNBC (n = 171), 75% of ovarian cancers (n = 249), 91% of endometrial cancers (n = 76), 88% of melanomas (n = 158), 55% of colon cancers (n = 195), and 26% of pancreatic cancers (n = 178). The corresponding average H-scores were 160, 135, 142, 175, 163, 99 and 54, respectively. Sub-analyses of SORT1 expression by tumor histological subtype and grade are on-going, and additional TMAs are being screened. A total of 160 healthy tissue cores were also evaluated. Interestingly, SORT1 staining was either negative (null) or low for most healthy tissues including lung, stomach, liver, ovary, prostate, lymph node, esophagus, small intestine, cervix, skin, spleen, bone marrow and thymus. Some healthy tissues had moderate or strong staining in  $>10\%$  of cells, i.e. colonic mucosa, rectal epithelium, pancreatic islets and vessels, breast lobules, testicular spermatids and Sertoli cells, kidney tubules and cerebral neuronal cells and astrocytes.

**Conclusions:** SORT1 is currently been studied as a cancer target in a first-in-human (FIH) study of a peptide-drug conjugate (clinicaltrials.gov: NCT04706962). Overall, these results suggest that SORT1 is highly expressed in multiple tumors and is a promising target for the delivery and internalization of cancer therapeutic agents.

#### Conflict of interest:

Other Substantive Relationships: Christian Marsolais is Senior VP and Chief Medical Officer of Theratechnologies Inc., for which he sits on the executive leadership team (salary and bonus) and has shares of the company.

329

(PB109)

#### Tensin2 is a novel diagnostic marker in gastrointestinal stromal tumor, associated with gastric location and non-metastatic tumors

S. Salmikangas<sup>1</sup>, T. Böhling<sup>1</sup>, N. Merikoski<sup>1</sup>, J. Jagdeo<sup>1</sup>, M. Sampo<sup>2</sup>, T. Vesterinen<sup>2</sup>, H. Sihto<sup>1</sup>. <sup>1</sup>University of Helsinki, Department of Pathology, Helsinki, Finland; <sup>2</sup>Helsinki University Hospital/University of Helsinki, Department of Pathology, Helsinki, Finland

Gastrointestinal stromal tumor (GIST) is a rare soft tissue sarcoma, for which KIT and DOG1 are used as highly sensitive diagnostic markers. Other diagnostic markers include CD34, protein kinase C  $\theta$ , deficiency of succinate dehydrogenase complex subunit B, carbonic anhydrase II, and type I insulin-like growth factor receptor. However, most of these markers are expressed in other similar malignancies relevant for the differential diagnosis of GIST, such as leiomyomas, leiomyosarcomas or schwannomas. We found that Tensin2 (TNS2) mRNA expression is downregulated in most human cancers but overexpressed in GIST. Therefore, we investigated the role of TNS2 as a diagnostic biomarker by using immunohistochemistry in 176 GISTs and 521 other sarcomas. All GISTs expressed TNS2, having intermediate or high expression in 71.4% of the samples. The majority of other sarcomas (89.8%) were negative for TNS2, and intermediate to strong staining was only seen in 2.9% of the samples. Strong TNS2 staining associated with a gastric location (gastric 52.8% vs. non-gastric 7.2%;  $P < 0.001$ ), an absence of metastases (non-metastatic tumors 44.3% vs. metastatic tumors 5.9%;  $P = 0.004$ ), female sex (female 45.9% vs. male 33.8%;  $P = 0.029$ ) and tumors of lower risk categories (very low or low 46.9% vs. intermediate 51.7% vs. high 29.0%;  $P = 0.020$ ). TNS2 expression did not correlate with overall survival or metastasis-free survival. No associations between TNS2 expression and KIT/PDGFRA mutation status, tumor size, mitotic count, or age of the patient were detected. The results provide conclusive evidence for the value of TNS2 as a sensitive and specific diagnostic biomarker for GIST.

No conflict of interest.

330

(PB110)

#### Evaluation of membrane type 1 metalloproteinase (MT1-MMP/MMP14) expression as a prognostic biomarker in patients with solid tumours screened for a Phase I/II trial

N. Peters<sup>1</sup>, H. Morley<sup>1</sup>, S. Khalique<sup>2</sup>, S. Scalzo<sup>2</sup>, R. Patel<sup>3</sup>, U. Gunaydin<sup>3</sup>, G. Funingana<sup>4</sup>, J. Evans<sup>5</sup>, D. Papadatos-Pastos<sup>2</sup>, U. Banjeri<sup>3</sup>, B. Basu<sup>4</sup>, A. Niewiarowski<sup>6</sup>, S. Symeonides<sup>7</sup>, F. Kelly<sup>8</sup>, L. Sawretse<sup>6</sup>, C. Bacon<sup>8</sup>, M. Robinson<sup>9</sup>, T. Gelb<sup>10</sup>, S. Blakemore<sup>11</sup>, N. Cook<sup>1</sup>. <sup>1</sup>The Christie NHS Foundation Trust, Experimental Cancer Medicine, Manchester, United Kingdom; <sup>2</sup>University College London Hospital, NIHR UCLH Clinical Research Facility, London, United Kingdom; <sup>3</sup>Royal Marsden Hospital, Drug Development Unit, London, United Kingdom; <sup>4</sup>Cambridge University Hospitals NHS Foundation Trust, Experimental Cancer Medicine, Cambridge, United Kingdom; <sup>5</sup>The Beatson- West of Scotland Cancer Centre, Experimental Cancer Medicine, Glasgow, United Kingdom; <sup>6</sup>Cancer Research UK, Centre for Drug Development, London, United Kingdom; <sup>7</sup>Cancer Research UK-Edinburgh Centre, Centre for Drug Development, Edinburgh, United Kingdom; <sup>8</sup>Newcastle University, Clinical and Translational Research Institute, Newcastle Upon Tyne, United Kingdom; <sup>9</sup>Newcastle upon Tyne Hospitals NHS Foundation, NovoPath and Department of Cellular Pathology, Newcastle Upon Tyne, United Kingdom; <sup>10</sup>Bicycle Therapeutics, Bicycle Therapeutics, Massachusetts, USA; <sup>11</sup>Accent Therapeutics, Inc., Translational Medicine, Massachusetts, USA

**Background:** MT1-MMP plays an important role in pericellular proteolysis and is implicated in cancer cell migration, growth, invasion and angiogenesis. Limited evidence suggests that MT1-MMP overexpression is associated with a poor prognosis in numerous solid tumours. Using data from immunohistochemical pre-screening for a Phase 1/2 clinical trial targeting MT1-MMP (clinicaltrials.gov identifier: NCT03486730), we determined if MT1-MMP over-expression was a prognostic biomarker in selected solid tumours.

**Methods:** An analytically validated MT1-MMP immunohistochemistry assay using a commercially available antibody was developed by NovoPath (Newcastle upon Tyne) in collaboration with Cancer Research UK and Bicycle Therapeutics® and was used for clinical trial pre-screening. All patients (pts) from 5 UK sites pre-screened between 2/2020 and 2/2022 were included. Pts were considered positive (+ve) for MT1-MMP overexpression if the cancer cell membrane H score on their archival tumours was  $\geq 150$ . Overall survival (OS) was evaluated using Kaplan Meier methodology from 3 timepoints (T): date of diagnosis (T1), date of archival tissue (T2) and date of MT1-MMP testing consent (T3). Log rank analysis was used to assess for survival differences between groups.

**Results:** 284 pts were included; 26% (N = 74) MT1-MMP +ve and 74% (N = 210) MT1-MMP -ve. Pts characteristics are outlined in Table 1. At a median follow up time of 8.9 months (mos), 55% (N = 41) MT1-MMP1 +ve pts and 52% (N = 108) MT1-MMP -ve pts had died (p = 0.58). There was no statistically significant difference in median OS between MT1-MMP +ve and -ve pts at T1 (43.4 mos vs 49.8 mos p = 0.71), T2 (27.3 mos vs 33.1 mos p 0.32) or T3 (6.5 mos vs 7.2 mos p = 0.84). Subgroup analysis based on tumour or histological subgroups did not reveal a significant difference in OS at any time point for MT1-MMP +ve and -ve tumours.

Table 1: Demographic factors of pts who tested +ve and -ve for MT1-MMP overexpression.

	MT1-MMP +ve	MT1-MMP -ve	p Value*
<b>Median Age</b>	59 years	59.6 years	p = 0.93 <sup>a</sup>
<b>Gender</b>			p = 0.56 <sup>b</sup>
Male	30%(22)	33%(70)	
Female	70%(52)	67%(140)	
<b>ECOG</b>			p = 0.95 <sup>b</sup>
0-1	97% (72)	98% (206)	
2	1.5% (1)	2% (4)	
Unknown	1.5% (1)		
<b>Tumour Group</b>			p = 0.20 <sup>b</sup>
Breast	20% (15)	11.5%(24)	
Lung	22% (16)	17% (35)	
Gynaecological	16% (12)	27%(57)	
Head and Neck	12%(9)	11% (23)	
Genitourinary	8% (6)	3% (7)	
Sarcoma	12% (9)	11.5% (24)	
Gastrointestinal	5.5% (4)	9% (19)	
Melanoma	3% (2)	3% (7)	
Other	1.5%(1)	7% (14)	
<b>Histological subtype</b>			p = 0.66 <sup>b</sup>
Adenocarcinoma	34%(25)	38%(80)	
Squamous cell carcinoma	40%(30)	31%(66)	
Melanoma	3% (2)	3% (7)	
Sarcoma	12% (9)	11.5%(24)	
Small cell carcinoma	1.5%(1)	4.5%(9)	
Adenosquamous carcinoma	1.5%(1)	0.5%(1)	
Other/Unknown	8%(6)	11%(23)	

\*Comparison between MT1-MMP overexpression +ve and -ve pts.

<sup>a</sup>p value calculated using Independent T test, <sup>b</sup>p value calculated using Pearson's chi squared test.

**Conclusion:** In this study of heavily pre-treated pts, MT1-MMP expression was shown not to be a prognostic biomarker.

#### Conflict of interest:

Advisory Board: Jeff Evans has received honoraria from Bicycle Therapeutics (payable to employing institution) for advisory boards on a different compound, and support from Bicycle Therapeutics for commercial clinical trials (different compound – payable to employing institution).

B.Basu Consulting or Advisory Role - Eisai GenMab Roche

Corporate-sponsored Research: Jeff Evans holds the research grant (payable to the employing institution) from CRUK's CDD for the Glasgow Biomarkers Hub which supports biomarker studies for this, and other, CDD clinical trials.

B.Basu Research Funding – Celgene

N.Cook Research funding/educational research grants have been received by Cook's research team from AstraZeneca, Bayer, Pfizer, Orion, Taiho, Oncology, Roche, Starpharma, Eisai, RedX, UCB, Boehringer, Merck, Stemline Tarveda and Avacta.

Other Substantive Relationships: B.Basu: Speakers' Bureau - Eisai Europe

331

(PB111)

#### TP53 mutations are frequently concurrent in patients with BRAF V600E mutated solid tumors and is associated with shorter duration of response to BRAF targeted therapy

M. Eriksen<sup>1</sup>, C.W. Yde<sup>2</sup>, L.B. Ahlborn<sup>2</sup>, C. Qvortrup<sup>1</sup>, U. Lassen<sup>1</sup>, M. Højgaard<sup>1</sup>, I. Spanggaard<sup>1</sup>, K.S. Rohrberg<sup>1</sup>. <sup>1</sup>Copenhagen University Hospital, Department of Oncology, Copenhagen, Denmark; <sup>2</sup>Copenhagen University Hospital, Department of Genomic Medicine, Copenhagen, Denmark

**Background:** Duration of response to BRAF targeted therapy in patients with BRAF V600E mutated solid tumors varies considerably and no predictive biomarkers exist. The purpose of this study was to explore the association between concurrent mutations at baseline and treatment outcome in patients with BRAF V600E mutated advanced solid tumors.

**Materials and methods:** 24 patients with a BRAF V600E mutated advanced solid tumor treated with BRAF targeted therapy were included in this study. The primary tumors were colon (n = 16), lung (n = 3), neuroendocrine carcinoma (n = 2), breast (n = 1), cholangiocarcinoma (n = 1) and melanoma (n = 1). Baseline genomic profiling was done for all patients. Concurrent mutations were analyzed and interpreted using QIAGEN Clinical Insight Interpret software. Only somatic mutations were studied. Variant classification systems were used to guide interpretation of cancer associated mutations; selecting only mutations classified as "Pathogenic" or "Likely Pathogenic" to report. Clinical data were collected from electronic patient records.

A nonparametric Pearson's chi-squared test was used to estimate difference in median duration of therapy. The Kaplan-Meier method was used to estimate overall survival (OS) and the Cox proportional hazards model method was used to estimate hazard ratio and 95% confidence interval (CI).

**Results:** Mutations in the tumor suppressor gene *TP53* were the most frequent co-mutation. At baseline, 62.5% (15/24) of the patients had *TP53* mutations with 1 patient having 2 concurrent *TP53* alterations. All *TP53* mutations were predicted to be *loss-of-function* mutations and included 14 point mutations and 2 mutations consisting of 13 and 16 base pair deletions, respectively.

Median duration of BRAF targeted therapy was 32 weeks (range 8–230 weeks) in the entire cohort and therapy continued until progression of disease in all patients. We found concurrent mutation(s) in *TP53* to be associated with a median of 12.4 weeks shorter duration of response to BRAF targeted therapy (p = 0.003).

Median OS was 78.6 weeks in the group of patients without *TP53* mutation (s) at baseline and 57.1 weeks in the group of patients with concurrent *TP53* mutation(s), but this difference was not statistically significant (hazard ratio, 1.3; 95% CI, 0.54–3.2; p = 0.6).

**Conclusions:** Mutations in *TP53* were frequently detected in patients with BRAF V600E mutated advanced solid tumors. The presence of concurrent *TP53* mutations at baseline were associated with shorter duration of response to BRAF targeted therapy but did not significantly correlate to OS outcome. *TP53* mutations at baseline may contribute to the overall assessment of the expected clinical response to BRAF targeted therapy in patients with BRAF V600E mutated advanced solid tumors.

#### Conflict of interest:

Ownership: Genmab

Advisory Board: Bayer, Novartis, Amgen, MSD

Corporate-sponsored Research: BMS, GSK, Pfizer, Roche, Puma Biotechnology, MSD, Genmab, Genentech, Bristol-Myers Squibb, Orion, Loxo/Bayer, Loxo/Lilly, Cantargia AB, Symphogen, Alligator Bioscience, Incyte, AstraZeneca, Novartis, Monta Bioscience, Bioinvent, Pierre Fabre

332

(PB112)

#### Developing a preclinical CD47 IHC assay using patient-like samples for the development of a companion diagnostic for CD47-targeting treatments

X. Tu<sup>1</sup>, L. Zhang<sup>1</sup>, W. Chen<sup>1</sup>, D. Wang<sup>1</sup>, J. Guo<sup>1</sup>, H. Li<sup>2</sup>, J. Gunn<sup>3</sup>, X. An<sup>4</sup>. <sup>1</sup>Crown Bioscience Inc, Scientific Research Innovation, Taicang, China; <sup>2</sup>Hanx Biopharmaceuticals- Ltd, Research, Wu Han, China; <sup>3</sup>Crown Bioscience Inc, Scientific Research Innovation, San Diego, USA; <sup>4</sup>Crown Bioscience Inc., Scientific Research Innovation, Taicang, China

**Background:** CD47 is a receptor widely expressed in human tumors, including lymphoma, AML, and many solid tumors. It interacts with its ligand SIRPα on macrophages, also found on dendritic cells, to evade macrophage phagocytosis. CD47 is an important innate and adaptive immune checkpoint and is considered one of the most promising immuno-oncology targets since

PD-1/PDL-1. Anti-CD47 antibodies and SIRP $\alpha$  fusion proteins are currently being developed for the treatment of various cancers. It is believed that CD47 expression on the surface of cancer cells is critical to the success of these therapies and if true, CD47 could become a predictive biomarker for the treatment of cancer and/or be developed as a companion diagnostic (CDx). It is thus prudent to have a robust, practical, and relevant clinical testing assay that can measure CD47 expression in the clinic. In this study, a CD47 IHC assay that can potentially be developed as a clinical testing assay was explored using preclinical FFPE samples of patient-derived xenograft (PDX) tumor models. The models used represent diverse cancer types and heterogeneity, are consistent and renewable for assay standardization, and are characterized by both transcriptomics and pharmacological testing.

**Methods:** Tissue microarray (TMA) or FFPE slides of both lymphoma (37 PDX models) and breast cancer (38 PDX models) were prepared following standard histology procedure. A standard IHC staining protocol was performed in BondRx Automated IHC/ISH Slide Staining System (Leica) using a commercial anti-CD47 antibody (Abcam, ab218810). This was followed by whole slide imaging using the NanoZoomer NDP2.0-HT Digital Slide System (Hamamatsu) and quantified using the HALO™ image analysis software (Indica Labs), with pathologists' peer review. The CD47 IHC score was also compared to the RNA expression, determined by whole transcriptome sequencing.

**Results:** Thousands of PDX models of diverse tumor types have been created and fully characterized, including with RNA-seq and pathology data, and are accessible via Crown Bioscience's HuBase database. TMAs have also been prepared for selected disease sample panels. CD47 IHC staining of lymphoma and breast PDX TMAs or FFPE slides revealed heterogeneous expression levels of CD47 between different models or even different tumor cells within same model. In addition, IHC scores were not entirely correlated with the RNA levels of the same model.

**Conclusion:** The lack of consistency between CD47 RNA expression and protein measurement warrants further investigation into how the heterogeneity, identified by IHC assessment, could potentially correlate with the pharmacology of specific CD47 blockers thus, predicting response and setting the stage for the development of the treatment companion diagnostics.

**No conflict of interest.**

333 (PB113)

**Peroxisome Proliferator-Activated Receptor Gamma (PPARG) status defines the luminal lineage in molecular profiles of advanced urothelial cancers (UC)**

W. Motley<sup>1</sup>, S. Islam<sup>2</sup>, K. Eagle<sup>1</sup>, J. Bell<sup>2</sup>, R. Sims<sup>1</sup>, M. Bowden<sup>1</sup>. <sup>1</sup>Flare Therapeutics, Inc, Cambridge, USA; <sup>2</sup>Tempus, Inc, Chicago, USA

**Background:** About 20 000 patients are diagnosed with muscle-invasive UC annually, where the five-year survival rate is approximately 5% in metastatic cases. The transcription factor PPARG is associated with the luminal lineage subtype reflecting ~65% of all advanced UC patients. Recurrent genetic alterations in PPARG, including focal amplification, missense mutations, and fusions, as well as hotspot mutations in its obligate heterodimer, retinoid X receptor alpha (RXRA) are characteristic of this molecular subtype.

**Materials and Methods:** We analyzed tumor tissue collected from over 3000 patients with muscle-invasive UC sequenced using the Tempus xT assay (DNA-seq of 648 genes at 500x coverage; RNA-seq; 3262pt DNA, 2685pt both). Molecular classification as luminal (luminal papillary, luminal, and luminal infiltrated subtypes) or non-luminal (basal-squamous and neuronal subtypes) was performed using non-negative matrix factorization (NMF) rank 5 following the Robertson method, excluding PPARG from the gene set to eliminate the inference of bias. Mean expression was reported as Log<sub>2</sub>[TPM+1]. Mutations were reported as single nucleotide variants or insertion/deletions (Svnlndel).

**Results:** We determined that luminal-papillary (669pt), luminal (449pt), and luminal-infiltrated (621pt) UC subtypes comprised 65% of the real-world cohort, consistent with subtype distribution as reported in the Robertson TCGA data set. Higher PPARG expression was associated with luminal subtypes (7.78 Log<sub>2</sub>[TPM+1],  $p < 0.00001$ ) compared to non-luminal subtypes (5.47 Log<sub>2</sub>[TPM+1]). The prevalence of mutations in PPARG, RXRA, and fibroblast growth factor receptor 3 (FGFR3) was also significantly higher in the luminal subtype, where the frequency of PPARG amp (copy number 4–7) was 10% ( $p < 0.05$ ), PPARG Svnlndel was 2.0% ( $p = 0.8$ ),

RXRA hotspot Svnlndel was 3.3% ( $p < 0.00005$ ) and FGFR3 Svnlndel was 14% ( $p < 0.005$ ). Collectively 1 in 3 advanced UC patients in a real-world population harbored mutations in PPARG, RXRA or FGFR3. A PPARG expression threshold (7.75 Log<sub>2</sub>[TPM+1]) was derived from logistic regression comparing amplified and diploid patients, where gain of even one copy of PPARG is associated with overexpression. Many diploid patients exhibit PPARG expression (7.49 Log<sub>2</sub>[TPM+1]) comparable to amplified patients. High PPARG expression was sustained in metastatic samples (7.55 Log<sub>2</sub>[TPM+1]), and expression did not significantly vary by metastatic tissue site ( $p > 0.05$ ).

**Conclusion:** To the best of our knowledge, this represents the largest real-world dataset from patients with advanced and metastatic UC evaluated to date. Stratification of advanced UC patients based upon PPARG status as a defining feature of the luminal phenotype supports targeting of this pathway with novel agents under development.

**Conflict of interest:**

Ownership: Flare-affiliated authors are shareholders of Flare Therapeutics.

334 (PB114)

**Molecular crosstalk between NF- $\kappa$ B and NRF2 signaling affects prognosis in HPV-associated head and neck cancer**

A. Kothari<sup>1</sup>, T. Parke Schrank<sup>2</sup>, W. Gray Yarbrough<sup>2</sup>, N. Isaeva<sup>3</sup>. <sup>1</sup>University of North Carolina at Chapel Hill, Pharmacology, Chapel Hill, USA; <sup>2</sup>University of North Carolina at Chapel Hill, Otolaryngology, Chapel Hill, USA; <sup>3</sup>University of North Carolina at Chapel Hill, Pathology and laboratory medicine, Chapel Hill, USA

The incidence of head and neck squamous cell carcinoma (HNSCC) is on the rise and is expected to increase by 50% by 2030. Around half of the patient population affected are diagnosed when the tumor is at a locally advanced stage. These patients are usually treated with intense radiotherapy, leading to severe side-effects. Precision medicine would revolutionize the treatment of head and neck cancer by accurately identifying patients that are at low risk of recurrence, reduce treatment related side-effects and aid in overall improvement in quality of life of patients after treatment. This generates the need to develop biomarkers to identify patients with less aggressive tumors as candidates for treatment de-escalation.

We applied an unbiased approach (weighted gene correlation network analysis (WGCNA)) that allows detection of autocorrelated gene sets on 3 independent cohorts of HPV+ HNSCC and created 22 consensus transcriptional modules by selecting genes that grouped together in WGCNA analyses from all 3 cohorts. Interestingly, only 1 module intrinsically divided HPV+ HNSCC into 2 subtypes, displaying different mutational profiles, mutational signatures, HPV gene expression patterns, HPV integration status, and patient survival. Gene set enrichment analysis revealed that this module was enriched in NF- $\kappa$ B genes and strongly associated with NF- $\kappa$ B signaling, confirming our prior findings that defined HPV+ HNSCC subtypes by presence or absence of NF- $\kappa$ B regulators, TRAF3 or CYLD defects and by the NF- $\kappa$ B activity classifier.

We hypothesized that NF- $\kappa$ B-driven intrinsic tumor characteristics contribute to increased sensitivity of NF- $\kappa$ B active HPV+ head and neck tumors to radiation, providing patients survival benefits. Indeed, TRAF3 or CYLD deletion dramatically increased radiation sensitivity of HPV+ head and neck cancer cells. As we began to investigate mechanisms of radiation sensitization associated with TRAF3 and CYLD deletion, we found that activation of NF- $\kappa$ B significantly correlated with marked downregulation of nuclear factor erythroid 2-related factor 2 (NRF2) activity in tumors from 3 independent cohorts, as well as in HPV+ HNSCC cells that harbor constitutively active NF- $\kappa$ B due to deletion of TRAF3 or CYLD. Interestingly, TRAF3 CRISPR KO cells had lower NRF2 protein levels that were restored by MG132 treatment, indicating an involvement of KEAP1/CUL3 mediated proteasomal degradation of NRF2.

In summary, our data showcases an inverse correlation between NF- $\kappa$ B and NRF2 pathways in HPV+ HNSCC. Currently, there are no prognostic biomarkers to distinguish patients who require aggressive therapy versus those that are appropriate for reduced intensity treatment. Identification of markers distinguishing the 2 subtypes of HPV+ HNSCC (high NF- $\kappa$ B and low NRF2 activity) may serve as prognostic biomarkers to help clinicians with therapeutic decisions.

**No conflict of interest.**

335

(PB115)

**Treatment strategies based on the molecular subtypes of transformed small cell lung cancer (t-SCLC)**

S. Oh<sup>1,2</sup>, J. Koh<sup>3</sup>, T.M. Kim<sup>1,4</sup>, S. Kim<sup>1,2</sup>, J. Youk<sup>1,4</sup>, M. Kim<sup>1,4</sup>, B. Keam<sup>1,4</sup>, Y.K. Jeon<sup>1,2,3</sup>, D.W. Kim<sup>1,2,4</sup>, D.S. Heo<sup>1,4</sup>. <sup>1</sup>Seoul National University, Cancer Research Institute, Seoul, South Korea; <sup>2</sup>Seoul National University College of Medicine, Integrated Major in Innovative Medical Science, Seoul, South Korea; <sup>3</sup>Seoul National University Hospital, Department of Pathology, Seoul, South Korea; <sup>4</sup>Seoul National University Hospital, Department of Internal Medicine, Seoul, South Korea

**Background:** Small-cell transformation is one of the resistance mechanisms (4–14%) to Epidermal Growth Factor Receptor (EGFR) Tyrosine Kinase Inhibitors (TKIs) in *EGFR*-mutant lung adenocarcinomas (LADCs). Although bi-allelic inactivation of *TP53* and *RB1* is identified as the major genetic footprint of t-SCLC, the molecular driving force to the small cell transformation is still unknown. Recent studies to classify the genetic subtypes of *de novo* SCLC have guided subtype-specific treatment strategies. Here, we characterized the subtypes of nine t-SCLC cases and two t-SCLC patient-derived cell lines.

**Material and methods:** We compared RNA profiles of two t-SCLC cell lines (SNU-2962A and SNU-4505) with 57 LADC and 48 SCLC cell lines from the Cancer Cell Line Encyclopedia (CCLE). We investigated the molecular subtypes of t-SCLC and their therapeutic strategies. SNU-2962A and SNU-4505 cells were seeded in 384-well plates containing the siRNA of 709 kinases for 72hr. Furthermore, cell viability assays were performed on drugs targeting genes suggested as subtype-specific vulnerabilities in *de novo* SCLC. We also examined four subtype markers (ASCL1, NEUROD1, POU2F3, and YAP1) by immunohistochemistry (IHC) in t-SCLC tumor samples of 5 *EGFR*-mutant and 3 *EGFR* wild-type patients.

**Results:** RNA-seq results showed that the SNU-2962A cell line was classified into the NEUROD1 subtype with high expression of neuroendocrine genes and typical SCLC markers (SYP, CHGA, and NCAM1). In contrast, the SNU-4505 cell line, classified as a YAP1 subtype, has EMT characteristics with low neuroendocrine and SCLC marker expressions. A dimension reduction plot of RNA expression showed that the SNU-2962A cell line was clustered close to the NEUROD1 subtype. The SNU-4505 cell line was located close to LADC with other SCLC-YAP1 cell lines. We tested the drug sensitivities of the targets based on kinome screening and the previously proposed subtype-specific vulnerabilities. In both cell lines, PLK1 knockdown significantly reduced cell viability. SNU-2962A cell line was sensitive to bromodomain and extra-terminal (BET) inhibitors, and the apoptotic pathway was activated through Caspase signaling. SNU-4505 cell lines did not show sensitivity to the drugs tested except for paclitaxel. Subtype classification by IHC in patient samples was positive for at least one subtype marker. In most cases, ASCL1 or NEUROD1 that exhibits neuroendocrine characteristics was identified as a dominant subtype. In addition, there was no difference of subtypes, according to the *EGFR* status.

**Conclusions:** Our *in vitro* studies suggest that *EGFR*-mutant t-SCLC can be classified into subtypes like *de novo* SCLC. NEUROD1-positive SNU-2962A cell line was sensitive to BET inhibition, whereas YAP1-positive SNU-4505 cell line was only sensitive to paclitaxel, suggesting a subtype-specific therapeutic strategy in t-SCLC.

**Conflict of interest:**

Advisory Board: T.M. Kim reports advisory role or honorarium from AstraZeneca/MedImmune, Bayer, Boryung, Hanmi, Janssen, Novartis, Roche/Genentech, Sanofi, and Takeda.

D.W. Kim reports Uncompensated consultation or advisory role from Amgen, AstraZeneca, BMS/ONO Pharmaceuticals, Daiichi-Sankyo, GSK, Janssen, Meck, MSD, Oncobix, Pfizer, SK Biopharm, and Takeda

Corporate-sponsored Research: T.M. Kim reports research funding from Amgen, AstraZeneca/MedImmune, Boehringer-Ingelheim, BMS, Hanmi, Janssen, Merck, MSD, Novartis, Regeneron, Roche/Genentech, Sanofi, and Takeda.

D.W. Kim reports research funding from Alpha Biopharma, Amgen, Astrazeneca/MedImmune, Boehringer-Ingelheim, BMS, Bridge BioTherapeutics, Chong Keun Dang, Daiichi-Sankyo, GSK, Hanmi, Janssen, Merck, Merus, Mirati Therapeutics, MSD, Novartis, ONO Pharmaceutical, Pfizer, Roche/Genentech, Takeda, TP Therapeutics, Xcovery, and Yuhan and laboratory research funding from InnoN.

Other Substantive Relationships: D.W. Kim reports travel and accomodation support for advisory board meeting attendance from Amgen, Daiichi-Sankyo and medical writing assistance from Amgen, AstraZeneca, Boehringer-Ingelheim, BMS, Chong Keun Dang, Daiichi-Sankyo, GSK, Pfizer, MSD, Meck, Novartis, Roche, Takeda, and Yuhan.

336

(PB116)

**PMEPA1 has an oncogenic role in hepatocellular carcinoma in the context of TGFβ signaling: data from single cell RNAseq and transgenic models**

R. Pinyol<sup>1</sup>, C. Andreu-Oller<sup>1</sup>, M. Piqué-Gili<sup>1</sup>, R. Esteban-Fabró<sup>1</sup>, M. Bárcena-Varela<sup>2</sup>, C. Montironi<sup>3</sup>, M. Ruiz de Galarreta<sup>4</sup>, J. Peix<sup>1</sup>, J. Abril-Fornaguera<sup>1</sup>, J. Huguet-Pradel<sup>1</sup>, K.E. Lindblad<sup>2</sup>, M. Torres-Martin<sup>1</sup>, D. Sia<sup>4</sup>, A. Lujambio<sup>5</sup>, J.M. Llovet<sup>6</sup>. <sup>1</sup>IDIBAPS, Liver Cancer Translational Research Laboratory, Barcelona, Spain; <sup>2</sup>The Icahn School of Medicine at Mount Sinai, Department of Oncological Sciences, New York, USA; <sup>3</sup>Biomedical Diagnostic Center- Barcelona Hospital Clínic- University of Barcelona, 3Pathology Department & Molecular Biology CORE, Barcelona, Spain; <sup>4</sup>Icahn School of Medicine at Mount Sinai, Mount Sinai Liver Cancer Program, New York, USA; <sup>5</sup>Department of Oncological Sciences The Icahn School of Medicine at Mount Sinai, Department of Oncological Sciences The Icahn School of Medicine at Mount Sinai, New York, USA; <sup>6</sup>IDIBAPS-Hospital Clínic de Barcelona- Universitat de Barcelona- ICREA, Liver Cancer Translational Research Laboratory, Barcelona, Spain

**Background:** Transforming growth factor β (TGFβ) acts as a tumor suppressor in early stages of carcinogenesis, but promotes invasiveness, angiogenesis and immunosuppression in advanced stages. Prostate Transmembrane Protein Androgen Induced 1 (PMEPA1) negatively regulates TGFβ signaling by interacting with SMADs, and promotes TGFβ oncogenic effects in other cancers. Here, we explored the role of PMEPA1 in hepatocellular carcinoma (HCC).

**Methods:** We analyzed transcriptomic, genomic, epigenomic and clinicopathological data of a discovery cohort of 228 HCCs and a validation cohort of 361 HCCs. *PMEPA1* levels were quantified by qPCR in the discovery cohort, and *PMEPA1* overexpression was validated in 6 other publicly available cohorts (n = 916) with microarray or RNAseq data. We analyzed *PMEPA1* expression at the single-cell level using a publicly available single-cell RNAseq dataset including 16 HCCs. We inferred cell-cell interactions using CellPhoneDB. Genetically engineered mouse models were generated by hydrodynamic tail-vein injection of equal amounts of plasmids overexpressing *MYC* and *MYC+PMEPA1*. Tumors were analyzed by RNAseq and histopathological stainings.

**Results:** *PMEPA1* was overexpressed in 18% of human HCCs [FC>2; n = 203/1144], a feature associated with TGFβ signaling (p < 0.05). *PMEPA1* overexpression was associated with gene body hypermethylation (p < 0.0001). HCCs displaying both Wnt/TGFβ signaling and high *PMEPA1* (11% of cases) were significantly enriched in signatures of immune exhaustion, late TGFβ activation, tumor microenvironment (TME) response to TGFβ and active stroma (p < 0.05) as compared with HCCs with Wnt/TGFβ signalling alone (8% of cases) or *PMEPA1* overexpression alone (11% of cases). Analyses of *PMEPA1* expression at the single-cell level revealed that it is not only expressed by tumoral cells but also by stromal cells such as endothelial cells (ECs), fibroblasts and pericytes CellPhoneDB analysis revealed increased interactions between *PMEPA1*-expressing fibroblasts/tumor cells and immune suppressive cell subtypes. *in vivo*, overexpression of *MYC+PMEPA1* led to HCC development in 56% of the mice (n = 9/16) and was associated with a significantly reduced survival when compared to mice overexpressing *MYC* alone (p = 0.014), which did not develop tumors (n = 0/7). Overexpression of *PMEPA1* was confirmed at the mRNA level. The transcriptomically profiled *MYC+PMEPA1* tumors (n = 4) presented a significant enrichment in late TGFβ activation and proliferation signatures when compared to healthy livers (n = 6) and *MYC-lucOS;CTNNB1* tumors (n = 5).

**Conclusion:** *PMEPA1* upregulation is linked to TGFβ activation and an aggressive phenotype in human HCC. Overexpression of *PMEPA1* in combination with *MYC* *in vivo* led to HCC development, showing for the first time the oncogenic role of *PMEPA1* in this cancer type.

**No conflict of interest.**

337 (PB117)  
**Identification and molecular characterization of invasive lobular breast cancer models in a panel of 180 breast XPDX models**

J. Flores<sup>1</sup>, A. Moriarty<sup>1</sup>, F. Lizette<sup>1</sup>, A. Lang<sup>2</sup>, A. Rosenthal<sup>2</sup>, K. Papadopoulos<sup>3</sup>, M. Beeram<sup>2</sup>, A. Patnaik<sup>3</sup>, D. Rasco<sup>3</sup>, B. DeBerry<sup>2</sup>, M. Elmi<sup>2</sup>, R. Drenkler<sup>2</sup>, T. Hernandez<sup>4</sup>, M. Sharma<sup>5</sup>, N. Lakhani<sup>5</sup>, L. Smith<sup>2</sup>, V. Moreno<sup>4</sup>, E. Calvo<sup>4</sup>, J. Garcia-Foncillas<sup>4</sup>, M. Wick<sup>1</sup>. <sup>1</sup>XenoSTART, Translational Research, San Antonio, USA; <sup>2</sup>START Center, Medical Oncology, San Antonio, USA; <sup>3</sup>START, Ph1 Research, San Antonio, USA; <sup>4</sup>START Madrid, Ph1 Research, Madrid, Spain; <sup>5</sup>START Midwest, Ph1 Research, Grand Rapids, USA

**Background:** Invasive lobular and ductal breast tumors have distinct histologies and clinical presentation. Invasive lobular cancer (ILC) characteristics include somatic alterations in the CDH1 gene leading to loss of E-cadherin expression, low HER2 expression, frequent loss of PTEN, increased AKT expression and mutations in PIK3CA, TBX3 and FOXA1 genes. Invasive ductal cancers (IDC) express E-cadherin and more often include HER2+ cancers and ESR1 mutations. The XenoSTART Patient-Derived Xenograft (XPDX) breast cancer platform includes over 180 models spanning all subtypes characterized with immunohistochemistry (IHC) including ER $\alpha$ , PR and HER2 protein levels, genomic and transcriptomic sequencing and in vivo drug sensitivity. To further annotate our platform, we classified each breast XPDX model as ILC or IDC based on clinical history, E-cadherin staining, presence of variants in target genes and HER2 expression or amplification.

**Methods:** XPDX models were established and validated as previously described and further characterized using IHC to determine E-cadherin protein levels (Abcam a-Rabbit ab15148). Analysis was performed on WES to identify variants in CDH1, PIK3CA, TBX3, FOXA1 and PTEN. RNAseq data was used to determine expression levels of AKT and HER2. Clinical histology data was also used for ILC versus IDC classification. Resulting models classified as ILC by our analysis were histologically confirmed by a clinical pathologist.

**Results:** 180 breast models were examined by IHC and 25/180 (14%) lacked E-cadherin staining. Six of these 25 models (24%) reported CDH1 variants including deletions, frameshifts and point mutations. PIK3CA mutations, most notably H1047R, were reported in 5/25 models and FOXA1 (Q209E) was co-mutated in 2 of these models (ST2167 and ST2167/TDR). High AKT1 expression was reported in 5/25 models. While most E-cadherin-negative models were from clinically HER2 negative patients, 4/25 were from clinically HER2+ patients and corresponding models retained HER2 staining and amplification. 3/25 models were clinically classified as metaplastic and did not contain any target gene variant.

**Conclusion:** We screened 180 models in our XPDX breast cancer platform and identified at least twenty-two ILC models based on E-cadherin staining, genomics and clinical histology, and confirmed heterogeneity of this subtype of breast cancer. Additional analysis is underway to compare sensitivity of chemotherapy and targeted agents in ILC and IDC-classified breast models.

**No conflict of interest.**

339 (PB119)  
**An open-source, pathologist-in-the-loop workflow for quantitative and spatially-driven analysis of multiplexed immunohistochemistry images of the solid tumor microenvironment**

M. Zaidi<sup>1</sup>, P. Lombard<sup>1</sup>, S. Mansouri<sup>2</sup>, T. McKee<sup>3</sup>, G. Zadeh<sup>2</sup>, B. Wouters<sup>1</sup>. <sup>1</sup>University of Toronto, Medical Biophysics, Toronto, Canada; <sup>2</sup>University Health Network, MacFeeters-Hamilton Center for Neuro-Oncology Research, Toronto, Canada; <sup>3</sup>University of Toronto, Laboratory Medicine and Pathobiology, Toronto, Canada

With the recent technological advancements for highly multiplexed spatial imaging platforms, extensive studies have been performed to elucidate molecular landmarks of proliferation, immune invasion, hypoxia, and other attributes of the solid tumor microenvironment. However, many of the analysis pipelines for extracting quantitative information from these datasets offer limited windows for pathologists to interpret and provide biological meaning to results. We present an end-to-end workflow for quantitative analysis of tumor microenvironments, with an emphasis on using pathologists input for the classification of cells, quality control, and segmentation of microenvironmental structures. Here, we demonstrate the utility of this pipeline in identifying hallmarks of hypoxia in clinical glioblastoma (GBM) samples.

Sections from 35 clinical glioblastoma samples were taken and stained for a panel of markers suspected to be differentially expressed under hypoxia. The exogenous hypoxia probe pimonidazole (PIMO) was administered to the patients, and an antibody to detect this probe was included in the panel. Imaging mass cytometry (IMC) was performed to acquire multiplexed images, which were then loaded into the open-source digital pathology platform QuPath. Cells were segmented, and thresholds were set in conjunction with a pathologist to classify each cell as being positive for any of the markers included in the panel. Regional segmentation of hypoxic (PIMO+) from normoxic (PIMO-) areas was performed by training an artificial neural network on several manual annotations from the pathologist.

In total, over 423 000 cells were identified, with over half from *de novo* GBMs, with the remainder composed of recurrent GBMs, and primary IDH mutant GBM. We found significant enrichment of all four endogenous hypoxia markers (CA9, GLUT-1, HK2, and LDHA) within PIMO+ areas across all three groups ( $p < 0.05$ ). We found a statistically significant ( $p < 0.05$ ) enrichment of IBA1 cells in PIMO+ areas, whereas pSTAT3, pS6, SOX2, and Ki67 exhibited a statistically significant ( $p < 0.03$ ,  $p < 0.06$ ,  $p < 0.01$ , and  $p < 0.001$ , respectively) enrichment in PIMO- areas. Furthermore, we found a statistically significant ( $p < 0.001$ ) reduction in microvascular area across all three patient groups within PIMO+ areas.

In short, we have presented a robust, pathologist-in-the-loop digital pathology workflow for the analysis of multiplexed immunohistochemistry datasets. Using this tool to identify hallmarks of hypoxia in GBM, we observed several unique trends in gene expression patterns of both known hypoxia pathway targets, as well as a variety of immune-modulated processes. Lowering the barrier for accessibility to computational tools using open-source platforms to study the tumor microenvironment will further promote the development of novel personalized medicine therapeutics.

**No conflict of interest.**

340 (PB120)  
**Spatial transcriptomics analysis for spatial biomarker discovery in glioblastoma**

P. Lombard<sup>1</sup>, M. Zaidi<sup>1</sup>, S. Mansouri<sup>2</sup>, G. Zadeh<sup>2</sup>, B. Wouters<sup>1</sup>. <sup>1</sup>University of Toronto, Medical Biophysics, Toronto, Canada; <sup>2</sup>University Health Network, MacFeeters-Hamilton Center for Neuro-Oncology Research, Toronto, Canada

Over the past few years, the field of spatial transcriptomics has been rapidly advancing the ability of researchers to comprehensively characterize tissue organization and architecture at the single-cell or subcellular resolution. Spatial data can provide insight into cancer development and the tumor microenvironment (TME) that cannot be obtained through non-spatial modalities; insight that may aid in the development of effective therapeutic approaches. Computational methods development is essential to translate new spatial data into meaningful biological insights.

We present a computational method for analysis of spatial transcriptomics data from the tumor microenvironment of clinical glioblastoma (GBM) datasets, identifying spatially variable genes driven by metabolic gradients throughout the tissue. Our work demonstrates the ability to process spatial transcriptomics datasets for characterization of molecular heterogeneity in the TME.

Twelve sections were obtained from surgically resected glioblastoma tumor masses and were processed using the Visium® Spatial Gene Expression assay. In accordance with Visium® methodology, fresh frozen tissue sections were placed on an array of spatially barcoded oligonucleotides, each with an mRNA capture region and reverse transcription primers. Sections were stained with H&E and imaged before being permeabilized to allow mRNA to diffuse onto the chip and hybridize with the oligonucleotides. cDNA was synthesized from captured mRNA and then washed off the slide before sequencing library construction. Data from the resulting feature-barcode matrices and images of each sample were analyzed in Python using functions from the Scanpy and Squidpy packages. While most spatial transcriptomics data analysis pipelines process each sample individually, we implemented a method of sample integration such that dimensionality reduction and clustering algorithms could utilize data from across all 12 samples, while correcting for batch effects. After applying dimensionality reduction (UMAP) and Leiden clustering to the obtained sequencing libraries, the top marker genes associated with each cluster and the most spatially variable genes were identified. Cluster signatures were scored against published gene signatures and compared with patient metadata to identify biological relevance.

This work presents an integrated, end-to-end workflow for analyzing spatial transcriptomics datasets. This workflow can be used to identify clusters of cells with similar transcriptomic profiles, determine their prominent activities and functions, and compare spatial relationships between clusters



to investigate molecular trends in the tumor microenvironment. The development of computational methods is necessary to exploit the immense potential of spatial transcriptomics in the investigation of novel therapeutic strategies.

**No conflict of interest.**

## POSTER SESSION

### New Therapies in Immuno Oncology

341

(PB121)

**MCLA-129, a human anti-EGFR and anti-c-MET bispecific antibody, in patients with advanced NSCLC and other solid tumors: an ongoing phase 1/2 study**

S.H. Ou<sup>1</sup>, V. Moreno Garcia<sup>2</sup>, I. Gil Bazo<sup>3</sup>, H. Prenen<sup>4</sup>, I. Moreno<sup>5</sup>, M. Johnson<sup>6</sup>, E. Castañón Álvarez<sup>7</sup>, M. Nagasaka<sup>1</sup>, S. Adeyemi<sup>8</sup>, B. Barasa<sup>9</sup>, K. Bol<sup>10</sup>, P. Doze<sup>10</sup>, A. Engbers<sup>10</sup>, A.K. Joe<sup>10</sup>, V. Stalbovskaya<sup>8</sup>, G. Laus<sup>10</sup>, J. Call<sup>11</sup>. <sup>1</sup>University of California Irvine School of Medicine, Department of Medicine- Division of Hematology Oncology, Irvine, USA; <sup>2</sup>Start Madrid-FJD, Hospital Universitario Fundación Jimenez Diaz, Madrid, Spain; <sup>3</sup>Clinica Universidad de Navarra, Department of Medical Oncology, Pamplona, Spain; <sup>4</sup>Antwerp University Hospital, Oncology, Antwerp, Belgium; <sup>5</sup>Start Madrid-CIOCC, HM Sanchinarro University Hospital, Madrid, Spain; <sup>6</sup>Sarah Cannon Research Institute LLC, Lung Cancer Research, Tennessee, USA; <sup>7</sup>Clinica Universidad de Navarra, Department of Medical Oncology, Madrid, Spain; <sup>8</sup>Merus, Biometrics, Utrecht, Netherlands; <sup>9</sup>Merus, Translational Research, Utrecht, Netherlands; <sup>10</sup>Merus, Clinical, Utrecht, Netherlands; <sup>11</sup>START Mountain Region, Medical Oncology, Salt Lake City, USA

**Background:** MCLA-129, a novel human, EGFR/c-MET bispecific antibody, demonstrates anti-tumor activities in EGFR and/or c-MET driven tumor models via multiple mechanisms, including inhibition of ligand binding, receptor co-degradation, antibody-dependent cell-mediated cytotoxicity and antibody-dependent cell-mediated phagocytosis. MCLA-129 is being investigated in patients (pts) with advanced solid tumors in an ongoing First in Human study (NCT04868877). EGFR and c-MET are frequently mutated or overexpressed in epithelial tumors, driving ligand-independent receptor activation.

**Methods:** Pts are treated every 14 days in escalating dose levels up to 1500 mg guided by an adaptive Bayesian Logistic Regression Model following the Escalation With Overdose Control principle. The primary objective is to determine the Maximum Tolerated Dose (MTD) or Recommended Phase 2 Dose (RP2D) and secondary objectives include safety, efficacy (ORR, PFS, DOR), pharmacokinetics, cytokines and immunogenicity.

**Results:** At the data cut-off date of 8 May 2022, 20 pts were enrolled, across the 100, 300, 600, 1000 and 1500 mg cohorts. Median age was 65 years (range 43–79). Pts enrolled included: 14 pts with EGFR mutant (mt) NSCLC (3 pts L858R, 10 pts Del19, 1 pt exon 20 insertion), 3 pts with c-MET exon 14 mt NSCLC, 1 pt with c-MET amplified gastric adenocarcinoma, and 2 pts with HNSCC. All pts received prior systemic therapy. The median duration of treatment was 8 weeks (range 3.4–29.3); 11 pts were still on treatment at the cut-off date. No dose limiting toxicity was observed, and the MTD was not reached. Three SAEs have been reported. The most frequently reported AE, regardless of causality, was Infusion Related Reaction (IRR); 18 out of the 20 pts (90%) reported an IRR after the first infusion, majority of which were grade 1–2 (17 out of 18 pts, 94%). There were no treatment discontinuations due to an AE. No interstitial lung disease has been reported. All except one infusion were completed on the same day. Dose-dependent depletion of soluble EGFR and c-MET was observed. Pharmacokinetics of MCLA-129 was linear in the dose range of 600 to 1500 mg Q2W. Mean serum concentrations at 1500 mg Q2W dose are above that required for >95% target engagement of cell-bound EGFR and cMET throughout the dosing period. At the time of the cut-off date, 13 pts were evaluable for response. Preliminary anti-tumor activity has been observed, including one confirmed and one unconfirmed partial response in EGFR mt NSCLC, 4 confirmed stable disease and 38.5% (5 out of 13 pts) confirmed disease control rate.

**Conclusions:** MCLA-129 is well tolerated and has a favorable safety profile, with no reductions or discontinuations due to toxicity. Initial signals of efficacy were observed. The RP2D for dose expansion is 1500 mg every 14 days. Enrollment is ongoing into multiple dose expansion cohorts.

**Conflict of interest:**

Ownership: Turning Point Therapeutics, Elevation Oncology (Prof Ou)  
Advisory Board: Elevation Oncology (Prof Ou)  
Other Substantive Relationships: Consulting honorarium-Lilly, BeiGene, Jansen/JNJ (Prof Ou)  
Speaker honorarium-Jansen/JNJ, Pfizer, DAVA Oncology LLP (Prof Ou)

342

(PB122)

**Neutralizing antibody for S100A8/A9 soil sensing signal to prevent metastatic disease**

T. Kähkönen<sup>1</sup>, J. Halleen<sup>1</sup>, R. Kinoshita<sup>2</sup>, S. Morita<sup>3</sup>, K. Sagayama<sup>4</sup>, M. Sakaguchi<sup>2</sup>. <sup>1</sup>OncoBone Ventures Ltd, None, Nailsworth, United Kingdom; <sup>2</sup>Okayama University, Department of Cell Biology- Faculty of Medicine- Dentistry and Pharmaceutical Science, Okayama, Japan; <sup>3</sup>Okayama University, Center for Innovative Clinical Medicine, Okayama, Japan; <sup>4</sup>Okayama University, The Organization for Research Strategy and Development, Okayama, Japan

Organotropism of cancer metastasis is driven by the 'seed and soil' theory where the soil (metastatic microenvironment) provides signals to attract the seeds (cancer cells) to grow on a certain location. S100A8/A9 is a 'soil sensing signal' that binds to receptors expressed by many cancer types. We aimed to understand the role of S100A8/A9 in melanoma, breast and lung cancer, to develop a neutralizing antibody, and to provide a proof-of-concept for the antibody for inhibiting metastasis.

Cell lines were obtained from ATCC. Overexpression of S100A8/A9 receptors MCAM and NPTNβ was induced by cDNA vector and MCAM expression was silenced by a siRNA. Recombinant S100A8/A9 protein was produced in-house. Migration/invasion assays were performing with Boyden Chamber method, colony formation assay with agarose gel cultures, and the results were quantitated by counting crystal violet stained cells/colonies. mRNA expression was analyzed by qPCR. In mouse lung metastasis models, cancer cells were injected into tail vein, and lung metastases were monitored by X-ray Computed Tomography and quantitated by counting metastatic foci at endpoint. A chimeric S100A8/A9 antibody was produced in CHO-S cells by incorporating genomic sequences of heavy and light chains of a mouse monoclonal S100A8/A9 antibody to the Fab domain of human cDNA-encoded IgG2-Fc part.

S100A8/A9 was expressed in monocytes and attracted cancer cells expressing its receptors to immunosuppressed premetastatic niche. Of these receptors, MCAM was highly expressed in metastatic, but not in non-metastatic melanoma and breast cancer cells. Overexpression of MCAM in non-metastatic melanoma cells increased migration, and downregulation in metastatic cells eliminated migration, but also resulted in lost sensitivity to S100A8/A9 stimulation. In breast cancer cells, overexpression of MCAM in non-metastatic cells increased migration, which was abrogated by addition of S100A8/A9 decoy receptor to the cultures. Overexpression of MCAM induced EMT-like expression profile in the breast cancer cells. In lung cancer, overexpression of S100A8/A9 receptor NPTNβ induced anchorage independent growth, migration and invasion, which were further increased by addition of S100A8/A9 ligand to the cultures. From the produced antibodies, the clones that efficiently bound S100A8 and A9 heterodimer most effectively inhibited migration and cytokine production. The S100A8/A9 antibody effectively prevented formation of lung metastases in melanoma and breast cancer lung metastasis models.

These results demonstrate a role for S100A8/A9 and its receptors in metastasis of melanoma, breast and lung cancer. A neutralizing antibody for S100A8/A9 prevented formation of lung metastases, suggesting pharmacological inhibition of S100A8/A9 as a potential option for preventing metastatic disease.

**No conflict of interest.**

343

(PB123)

**HX301, a potent CSF1R inhibitor, suppresses tumor associated M2 macrophage (TAM), enhancing tumor immunity and causing transit tumor inhibition in syngeneic EMT-6 tumors**

X. An<sup>1</sup>, M. Zang<sup>1</sup>, L. Xiong<sup>2</sup>, H. Ke<sup>3</sup>, Y. Tao<sup>4</sup>, C. Chen<sup>3</sup>, H. Li<sup>3</sup>. <sup>1</sup>Crown Bioscience Inc., Scientific Research Innovation, Taicang, China; <sup>2</sup>Crown Bioscience Inc, In vivo, Taicang, China; <sup>3</sup>Hanx Biopharmaceuticals, Ltd, Research, Wu Han, China; <sup>4</sup>Crown Bioscience Inc, Inflammation, Taicang, China

**Background.** Tumor associated macrophage (TAM) plays important immunosuppression role within the tumor microenvironment (TME). CSF1R is a receptor tyrosine kinase (RTK) responsible for the growth, survival and polarization (toward M2) of macrophages, thus implicated in

pathogenesis of immunological disorders, as well as immuno-oncology (IO). High CSF1R expression is reported to be correlated to poorer prognosis of cancers CSF1R inhibitors (CSF1Ri), both TKIs or antibodies, have been proposed as potential cancer treatment strategy, although yet to be proven in the clinics. HX301 is a clinical stage kinase inhibitor, and also a strong CSF1Ri (IC<sub>50</sub> of ~0.7 nM) warranting further investigation for potential IO treatment of solid tumors.

**Methods:** We tested HX301 in a macrophage (human PBMC derived) differentiation/proliferation assay *in vitro* under M-CSF stimulation. We also performed pharmacodynamic (PD) study on tumor-infiltrate leukocytes (TILs) using multi-color flow cytometry, along with antitumor efficacy assessment, using EMT-6 syngeneic triple negative breast cancer (TNBC) model by daily administration of HX301 intraperitoneally (IP). EMT-6 model was selected based on the relative high TAM levels within the TME and the associated strong immune suppression role.

**Results:** Our result showed that HX301 has strong inhibitory effect with IC<sub>50</sub> of ~70 nM in an *in vitro* culture under M-CSF stimulation, confirming the agent's biological function as a CSF1Ri. During the early dose phase of the EMT-6 *in vivo* study, PD analysis of TILs demonstrated that HX301 had strong inhibition [RK1] of TAMs, accompanied with significant increases in T-TILs (both CD8<sup>+</sup> and CD4<sup>+</sup>) and NKT (at least transiently), as well as decreased T<sub>reg</sub>, suggesting HX301's role in enhancing tumor immunity. A moderate inhibition of tumor growth [RK2] also appeared to correlate with this apparent enhancement of tumor immunity during this early dose phase. Most interestingly, the treatment also caused dramatic increase of gMDSC, consistent with previous report showing depletion of TAM caused activation of cancer associated fibroblast (CAF), leading to recruitment of both gMDSC (also mMDSC) into TME to compensate the loss of immune suppression due to the depletion of TAMs. However, at the end of the study, all lineages of T-TILs (CD4<sup>+</sup>, CD8<sup>+</sup>, T<sub>reg</sub> cells) were dramatically decreased (almost disappeared), suggesting a complete loss of tumor [RK3] immunity, thus tumor growth inhibition, as indeed seen in the efficacy assessment. In another word, initial investigation in a EMT-6 model, HX301's anti-tumor activity appeared to be transient, possibly due to other compensatory immunosuppressive signals.

**Conclusions:** Our data suggest that HX301 has the potential to be explored as a new IO combination treatment strategy against solid tumors.

**No conflict of interest.**

#### 344 (PB124) Statin in combination with cisplatin makes favorable tumor-immune microenvironment for immunotherapy of head and neck squamous cell carcinoma

K. Minsu<sup>1</sup>, H. Jung<sup>2</sup>, H.J. Cho<sup>3</sup>, H.R. Ahn<sup>3</sup>. <sup>1</sup>Asan Medical Center, Otolaryngology, Seoul, South Korea; <sup>2</sup>Korea University Anam Hospital, Otorhinolaryngology, Seoul, South Korea; <sup>3</sup>Aju University Hospital, Gastroenterology, Suwon, South Korea

**Background:** Immune checkpoint inhibitors (ICIs) targeting programmed cell death 1 receptor (PD-1) or its ligand (PD-L1) improved survival in patients with advanced head and neck squamous cell carcinoma (HNSCC), and approval for its use was granted by the Food Drug Administration in the USA. However, anti-PD-1 antibodies did not significantly affect the progression-free survival rate of patients with HNSCC. Consequently, new approaches to improve treatment efficacy through the combination of conventional therapies and ICIs for the treatment of HNSCC are being investigated. The purpose of this study was to determine whether statins can enhance anticancer effects in HNSCC when used with cisplatin and act as immunogenic cell death (ICD) inducers that can be used in cancer immunotherapy.

**Material and methods:** In this study, we sought to determine whether statin use could lead to synergistic antitumor effects with cisplatin against HNSCC by analyzing data from a hospital cohort of patients who had received cisplatin-based induction chemotherapy (IC). We then reconfirmed the anticancer effect of statins in an experimental setting in relation to ICD mechanisms. Finally, we sought to determine the combined effect of cisplatin and statins against HNSCC and validate whether the combination enhanced anticancer immune responses, possibly leading to further synergistic effects if used in triple combination with ICIs.

**Results:** The pre-diagnosis use of statins in patients with HNSCC who underwent cisplatin-based IC was significantly associated with improved overall survival. Statins alone showed both *in vitro* and *in vivo* inhibitory effects against HNSCC, and synergistic antitumor effects were observed when combined with cisplatin in a syngeneic murine HNSCC model. Statins increased calreticulin exposure and endoplasmic reticulum stress-related signals in HNSCC cells. In addition, it was confirmed that statins could activate antigen-presenting cells and tumor-specific CD8<sup>+</sup> T cells with an increase in their numbers in the tumor tissues and draining lymph nodes, with

this effect showing significant improvement following the combination therapy with cisplatin. Moreover, in triple combination with both cisplatin and anti-programmed cell death 1 receptor (anti-PD-1) antibody, statins dramatically induced further tumor eradication and improved the survival of tumor-bearing mice.

**Conclusions:** Taken together, these results demonstrate that statins, administered in combination with anti-PD-1 antibody, could enhance the anticancer effect of cisplatin and potentiate the efficacy of immunotherapy for HNSCC and present a rationale for repurposing statins as an adjuvant immunotherapeutic option for HNSCC.

**No conflict of interest.**

#### 345 (PB125) STC-15, an oral small molecule inhibitor of the RNA methyltransferase METTL3, inhibits tumour growth through activation of anti-cancer immune responses associated with increased interferon signalling, and synergises with T cell checkpoint blockade

Y. Ofir-Rosenfeld<sup>1</sup>, L. Vasiliauskaite<sup>1</sup>, C. Saunders<sup>1</sup>, A. Sapetschnig<sup>1</sup>, G. Tsagkogeorga<sup>1</sup>, M. Albertella<sup>1</sup>, M. Carkill<sup>2</sup>, J. Self-Fordham<sup>2</sup>, J.B. Holz<sup>1</sup>, O. Rausch<sup>1</sup>. <sup>1</sup>Storm Therapeutics Ltd, Storm Therapeutics, Cambridge, United Kingdom; <sup>2</sup>Charles River, Charles River, Portishead, United Kingdom

**Background:** METTL3 is an RNA methyltransferase responsible for the deposition of N-6-methyladenosine (m<sup>6</sup>A) modification on mRNA and long non-coding RNA (lncRNA) targets, to regulate their stability, splicing, transport and translation. Small molecule inhibitors of METTL3 catalytic activity have previously demonstrated direct anti-tumour efficacy in models of acute myeloid leukemia (AML). Here we present pre-clinical data showing that the orally bioavailable small molecule METTL3 inhibitor STC-15 inhibits cancer growth and induces anti-cancer immunity.

**Materials & Methods:** To characterise transcriptomic changes following METTL3 inhibition, RNA sequencing studies were performed across a panel of cancer cell lines treated with STC-15. Induction of specific genes was validated by qPCR and Western Blots. The functional consequence of the upregulation of innate immune pathways was investigated *in vitro* using a co-culture system of SKOV3 ovarian cancer cells and human peripheral blood mononuclear cells (PBMC), and animal studies using subcutaneous A20 and MC38 syngeneic tumour models.

**Results:** Inhibition of METTL3 by STC-15 in cancer cell lines leads to prominent upregulation of genes associated with innate immunity, such as those in the interferon (IFN) signalling pathway. Transcription of type-I and type-III IFNs was activated following STC-15 treatment, in agreement with the expression of many Interferon Stimulated Genes (ISG). Cells treated with STC-15 accumulated double-stranded RNA (dsRNA), suggesting that activation of IFN signalling is triggered by innate pattern recognition sensors.

In an *in vitro* co-culture system, STC-15 demonstrated strong and dose-dependent enhancement of PBMC-mediated killing of cancer cells that occurred at concentrations where STC-15 caused little or no direct killing of cancer cells in the absence of PBMCs.

In MC38 colorectal and A20 lymphoma syngeneic models, oral treatment of immune-competent tumour bearing mice with STC-15 significantly inhibited tumour growth. Combination of STC-15 with anti-PD1 antibody resulted in significant tumour regression in both models, with mice remaining tumour-free until the end of study, long after treatment ceased. Even when regressed mice from the A20 model were re-challenged with a new batch of A20 cells, no new tumour growth was observed, further demonstrating the induction of durable anti-tumour immunity.

**Conclusions:** In pre-clinical cancer models, STC-15 treatment results in activation of innate immune pathways, inhibits tumour growth and enhances the anti-tumour properties of anti-PD1 therapy to generate a durable anti-tumour immune response. These data provide the rationale for the development of STC-15 both as monotherapy and in combination with checkpoint inhibition for the treatment of solid tumour malignancies. A Phase I, First-in-Human clinical trial is planned to begin in 2022.

**Conflict of interest:**

Ownership: MA is a stockholder of Storm Therapeutics. Other Substantive Relationships: YOR, LV, CS, AS, GT, MA, JBH and OR are current/former employees/consultants of Storm Therapeutics. MC and JSF are employees of Charles River.

346 (PB126)

**Preventing cystatin F proteolytic activation by cathepsin V increases cytotoxicity of effector immune cells**

E. Senjor<sup>1,2</sup>, A. Mitrović<sup>1</sup>, M. Jukić<sup>2</sup>, M. Proj<sup>2</sup>, M. Perišić Nanut<sup>1</sup>, S. Gobec<sup>2</sup>, J. Kos<sup>1,2</sup>, <sup>1</sup>Jožef Stefan Institute, Department of Biotechnology, Ljubljana, Slovenia; <sup>2</sup>University of Ljubljana, Faculty of Pharmacy, Ljubljana, Slovenia

**Background:** Granule-dependent cytotoxicity of natural killer cells and cytotoxic T lymphocytes is regulated by the proteolytic network. Cysteine cathepsins C, H and L are needed for the activation of granzymes and perforin, which initiate the killing of target cancer cells. Activity of cathepsins C, H and L is inhibited by cystatin F. Therefore, cystatin F can negatively impact the cytotoxicity of immune cells. Activity of cystatin F is regulated by expression levels, N-glycosylation and proteolytic activation. Although cystatin F is normally expressed in immune cells, its levels were found to be increased in the tumor microenvironment, where also non-immune cells express cystatin F. Due to the glycosylation, cystatin F can be translocated to endo/lysosomes or secreted and further internalized into bystander cells. In the lysosomes, cystatin F is activated from inactive dimeric form to active monomer by cathepsin V, which cleaves 15 N-terminal amino acids from cystatin F. As increased levels of cystatin F may contribute to the immunosuppressive status of the tumor microenvironment, we evaluated the effects of cathepsin V inhibition on the cytotoxicity of immune effector cells NK-92 and TALL-104.

**Materials and methods:** Molecular docking was used to evaluate interactions of small molecular compounds from commercial libraries with cathepsin V. A set of selected compounds was evaluated by enzyme kinetics for the enzyme inhibition, selectivity and reversibility of binding. The most potent, selective and reversible acting compound was tested in functional assays. The effect of cathepsin V inhibition on cystatin F activation was tested by western blot. Calcein-AM release assay was used to evaluate the effect on immune cell cytotoxicity.

**Results:** The best performing ureido methylpyridine carboxylate derivative compound, which selectively and reversibly inhibited cathepsin V, was evaluated for cystatin F activation in immune cells. The cystatin F dimer-to-monomer ratio was increased after treatment with both broad-spectrum peptidase inhibitor E-64d and after treatment with the selective reversible cathepsin V inhibitor. As expected, treatment of immune effector cells with E-64d decreased cytotoxic function, as this inhibitor impairs the activities of all cathepsins including cathepsins C, H, and L. However, treatment of cytotoxic cells with cathepsin V inhibitor, selectively preventing the activation of cystatin F, increased their cytotoxicity.

**Conclusions:** Selective inhibition of cathepsin V prevents the monomerization and activation of cystatin F. By targeting of cystatin F activating peptidase, we can reduce the detrimental effects of cystatin F on cytotoxic cells in the tumor microenvironment.

**No conflict of interest.**

347 (PB127)

**ON203: A new antibody targeting the oxidized form of macrophage migration inhibitory factor demonstrates antitumorogenic activity in preclinical models**

A. Schinagl<sup>1</sup>, B. Maurer<sup>2</sup>, G. Rossmüller<sup>1</sup>, I. Mirkina<sup>1</sup>, C. Landinger<sup>3</sup>, M. Thiele<sup>2</sup>. <sup>1</sup>OncoOne Research & Development GmbH, Biotechnology, Vienna, Austria; <sup>2</sup>OncoOne Research & Development GmbH, Biology, Vienna, Austria; <sup>3</sup>OncoOne Research & Development GmbH, Development, Vienna, Austria

**Background:** The pleiotropic cytokine macrophage migration inhibitory factor (MIF) is associated with tumor aggressiveness, metastasis, and disease progression. Due to its ubiquitous nature, MIF is considered an unsuitable target for therapeutic intervention. Oxidized MIF (oxMIF) is the disease-related, tumor-specific isoform of MIF, which undergoes a structural change enabling selective oxMIF-targeting by antibodies. We now developed ON203, a bioengineered anti-oxMIF antibody with highly improved biophysicochemical and biological properties, designed to exert better tumor retention and effector functions.

**Material and Methods:** After physicochemical characterization of the optimized anti-oxMIF antibody ON203, cell-based assays were performed to evaluate antibody-dependent cellular cytotoxicity and antibody-dependent cellular phagocytosis. Tumor penetration was assessed by infrared-labeled ON203 injected in tumor-bearing mice. Human cancer cell-line (PC3) xenografted mice and human colorectal carcinoma 3D tumoroids were treated with ON203, and efficacy was assessed either by tumor volume measurements and immunohistochemical analysis or by tumor-cell killing and immune cell composition assessment.

**Results:** ON203 demonstrated strong immune cell effector functions in reporter- and PBMC-mediated tumor cell killing assays. In xenograft models, ON203's accumulation and retention in the tumor tissue was proven and tumor volumes were significantly reduced upon treatment. Tumor cell proliferation (assessed by Ki67 staining quantification) and tumor vessel density (CD31 staining quantification) were strongly decreased in the ON203-treated tumors compared to the isotype control. Tumor-infiltrating immune cells provided further insights on the immunomodulatory therapeutic effects of ON203. Strikingly, freshly isolated tumoroids from colorectal carcinoma patients responded not only with tumor cell death, but a clear immunomodulatory effect on the tumor microenvironment in responding tumoroids was detected: ON203 activated NK and NKT cells and supported M1 polarization.

**Conclusions:** Our results demonstrate direct antitumorogenic effects of the anti-oxMIF antibody ON203 (i) by blocking the biologic function of oxMIF thereby reducing tumor cell proliferation and angiogenesis and (ii) by immunomodulation of the tumor microenvironment. In the upcoming Phase 1 trial we will evaluate ON203's safety, tolerability, pharmacokinetics, and pharmacodynamics in patients with solid tumors. ON203 bears a high potential as a standalone therapy or in rational combinations with immune checkpoint inhibitors or antiangiogenic agents in the treatment of solid tumors.

**Conflict of interest:**

Ownership: Alexander Schinagl, Michael Thiele

348 (PB128)

**Immunological profile and cytokine dynamics in head and neck cancer patients treated with radio-immunotherapy**

M. Mangoni<sup>1</sup>, G. Salvatore<sup>1</sup>, M. Sottili<sup>1</sup>, M.E. Melica<sup>1</sup>, I. Desideri<sup>1</sup>, C. Becherini<sup>2</sup>, C. Santini<sup>1</sup>, V. Salvestrini<sup>1</sup>, M. Loi<sup>2</sup>, P. Bonomo<sup>2</sup>, L. Livi<sup>1</sup>.

<sup>1</sup>University of Florence, Department of Experimental and Clinical Biomedical Sciences "Mario Serio", Firenze, Italy; <sup>2</sup>Careggi Hospital AOUC, Radiotherapy, Firenze, Italy

**Background:** We conducted a translational study on enrolled patients in a phase I/II trial of anti PD-L1 durvalumab (Du) combined with cetuximab (Ctx) and radiotherapy (RT) in locally advanced squamous cell carcinoma of the head and neck (DUCRO trial, NCT03051906). The aim was to evaluate the immunological profile and to investigate the dynamics of cytokine production in peripheral blood mononuclear cells (PBMCs).

**Material and methods:** Nine patients were enrolled. Blood samples were obtained at 3 different time points: T0 at the moment of the recruitment, T1 two weeks after the beginning of the RT and Du-Ctx therapy, and T2 three months after the last RT session, during immunotherapy. PBMCs were isolated to perform flow cytometry and ELISA analysis. Flow cytometry data analysis was performed with Flowlogic 7.3. The expression of phenotypic markers on circulating T cells and NK cells was evaluated by the percentage of positive cells. PBMCs were cultured with and without T cell stimulation anti-CD3 for 24 h. Then, the cytokine concentration for IL6, TGFβ, IL10, IFNγ and galectin1 in PBMC culture supernatants were measured in a quantitative sandwich ELISA. Statistical analysis was performed using GraphPad Prism 6.01. One-way analysis of variance (ANOVA) was performed.

**Results:** We analysed the immunophenotype of circulating total T cells (CD3+) and total NK cells (CD56+ and/or CD16+). Our results showed in all the patients a similar proportions of circulating T cells and NK cells, with a mean of 53.50% of T cells and 2.63% of NK. Flow cytometry analysis showed among T cells a higher percentage of CD4+ cells (65.57% ± 12.54) compared to CD8+(23.31 ± 13.60) (p<0.05) and among NK cells a higher percentage of CD16+ cells compared to CD56+ and CD56dim (p ≤ 0.05). The relative capacity of PMBCs for cytokine production in vitro was next addressed and cytokine dynamics evaluated. We observed a significant decrease of IL6, IFNγ and galectin1 at T1 compared to T0. Production was restored at T2 and at T1 after T cell activation with anti-CD3. Production of IL10 significantly decreased at T2 and it was not restored with anti-CD3. TGFβ production didn't show significant change at the evaluated time points.

**Conclusions:** Flow cytometry analysis showed that CD4/CD8 ratio was in the range of European general population. CD16+ NK were more represented in enrolled patient compared to health population. The dynamics of cytokine production suggests an immunomodulatory effect of combined treatment RT + Du + Ctx.

**No conflict of interest.**

349 (PB129)

**Novel, brain penetrant small molecule inhibitor of PD-L1 for targeting glioblastoma and brain metastasis**

S. Dhanalakshmi<sup>1</sup>, S. Rajagopal<sup>2</sup>, C. Gajendran<sup>1</sup>, M.N. Sadhu<sup>2</sup>, M. Zainuddin<sup>1</sup>, R. Gosu<sup>3</sup>, L. Rastelli<sup>1</sup>. <sup>1</sup>Jubilant Therapeutics Inc, Discovery Biology, Bedminster, USA; <sup>2</sup>Jubilant Therapeutics Inc, Discovery Chemistry, Bedminster, USA; <sup>3</sup>Jubilant Therapeutics Inc, Protein Chemistry, Bedminster, USA

**Background:** The PD-1/PD-L1 molecular pathway is one of the primary mechanisms of immune evasion deployed by cancer cells and anti-PD-L1 monoclonal antibodies (mAbs) restore T-cell proliferation and enhanced tumor cell killing which has been shown to result in clinically revolutionary efficacy in many tumor types. Unfortunately, this is not the case in CNS tumors where these mAbs have failed to show improved responses and survival. It appears that one of the main reasons for this is the poor brain penetrance of these mAbs and clinical evidence suggests that increasing brain penetrance results in better efficacy. Therefore, small molecule inhibitors of PD-L1 with enhanced tumor and brain penetrance could become highly valuable in CNS cancer therapy. In addition, small molecules with optimized oral bioavailability and short half-life, can address other known limitations of the PD-1/PD-L1 antibodies, including the well-known immune-breakthrough toxicities. JBI-2174 is an orally available selective small molecule inhibitor with similar binding and mechanism of action as anti-PD-L1 antibodies. JBI-2174 is highly brain penetrant and shows comparable efficacy to approved mAbs in preclinical studies.

**Materials and methods:** Structure based drug design was used to design PD-L1 inhibitors; potency of these inhibitors was assessed in an *in-vitro* TR-FRET assay. Reporter assays and ex-vivo co-culture assays were used to assess T-cell proliferation and function. Pharmacokinetics were performed in multiple pre-clinical species to derive at bioavailability and brain penetration. In vivo efficacy was assessed in mice syngeneic and orthotopic models.

**Results:** Our lead molecule JBI-2174 showed strong *in vitro* IC<sub>50</sub> of 1.5 nM in TR-FRET assay that measures interaction between PD-1 and PD-L1 and also induced dimerization of PD-L1 in cell based assay. This molecule also augmented T-cell response as measured by IFN- $\gamma$  activation in a cancer cell-PBMC based co-culture assay. Competition study between anti-PD-L1 blocking antibody and x-ray co-crystallization studies clearly demonstrate that JBI-2174 has similar finger-print on PD-L1 as the anti-PD-L1 antibodies. More importantly, JBI-2174 showed good oral bioavailability across pre-clinical species and strong and sustained brain exposure (0.66 to 2.1 fold plasma vs. brain ratio). JBI-2174 showed comparable efficacy to the anti-PD-L1 antibody Atezolizumab in hPD-L1/MC38 syngeneic and orthotopic models by oral administration. Toxicological studies conducted in non-human primates clearly show that the molecule is well tolerated at exposures much higher than efficacious exposure.

**Conclusion:** Oral administration and brain exposure of JBI-2174 provides an attractive option to be used in the treatment of glioblastoma and other solid tumors with brain metastasis. IND-enabling studies are being initiated for this compound.

No conflict of interest.

350 (PB130)

**An orally bioavailable ENPP1-selective inhibitor demonstrates superior immune preservation effects over STING agonists and confers anti-tumor efficacy in combination with other therapies in syngeneic tumor models**

X. Hu<sup>1</sup>, E. Garcia<sup>1</sup>, A. Goossens<sup>1</sup>, M. Gozo<sup>1</sup>, T. Lee<sup>1</sup>, X. Liu<sup>1</sup>, B. Le<sup>1</sup>, K. Taylor Meadows<sup>1</sup>, D. Eto<sup>1</sup>, I. Yusuf<sup>1</sup>, K. Lu<sup>2</sup>, T. Michels<sup>2</sup>, M. Kasem<sup>2</sup>, K. Marby<sup>2</sup>, M. Rowbottom<sup>2</sup>, R. Osterhout<sup>3</sup>, L. Carter<sup>4</sup>. <sup>1</sup>Gossamer Bio, Inc., Biology, San Diego, CA, USA; <sup>2</sup>Gossamer Bio, Inc., Chemistry, San Diego, CA, USA; <sup>3</sup>Gossamer Bio, Inc., Translational Medicine, San Diego, CA, USA; <sup>4</sup>Gossamer Bio, Inc., Research & Development, San Diego, CA, USA

**Background:** The cGAS-cGAMP-STING pathway plays a crucial role in both tumor and immune cells to promote anti-tumor immunity. Preclinically, synthetic STING agonists have shown promise, but have not demonstrated robust clinical efficacy potentially due to detrimental effects on immune cells which may compromise anti-tumor efficacy. ENPP1, an ectonucleotide pyrophosphatase/phosphodiesterase that catalyzes the hydrolysis of the endogenous STING agonist 2',3'-cGAMP, is a negative regulator of STING activation and its inhibition represents an alternative way to stimulate the STING pathway that would potentially spare the immune damaging effects associated with hyperactivation of STING. In addition, ENPP1-mediated hydrolysis of cGAMP and ATP generates AMP, which upon conversion to adenosine by CD73 suppresses immune cell function. Thus, an ENPP1

inhibitor is expected to restore endogenous cGAMP and STING pathway activation and reduce immunosuppressive adenosine to support effective anti-tumor immunity.

**Material and methods:** ENPP1 enzymatic, selectivity and cellular assays were used to drive a medicinal chemistry effort to identify potent, selective, and orally bioavailable ENPP1 inhibitors. The impact of key compounds on the STING pathway and the adenosine pathway were evaluated in both tumor and immune cells. The ENPP1-specific effects were demonstrated using ENPP1 knockout cells. Their anti-tumor effects were assessed in syngeneic tumor models.

**Results:** This effort led to the identification of GBD-09259 as a potent and selective ENPP1 inhibitor. GBD-09259 inhibited ENPP1 hydrolysis activity with cGAMP or ATP as a substrate in enzymatic and cellular assays. In human and murine ENPP1-expressing cancer cells, GBD-09259 restored cytosolic DNA-elicited cGAMP levels and STING pathway activation in an ENPP1-dependent fashion. In contrast to STING agonists which profoundly inhibit human T cell proliferation and survival, GBD-09259 had no inhibitory effects on T cells but increased cGAMP levels and subsequent interferon beta production. GBD-09259 had excellent oral bioavailability and *in vivo* exposure. When dosed in various syngeneic tumor models, GBD-09259 suppressed tumor growth in combination with anti-PD1 antibody or cisplatin. Gene expression and immune profiling suggest that GBD-09259 induced interferon-stimulated genes and increased immune infiltrates into the tumor microenvironment.

**Conclusions:** GBD-09259 is a potent and selective ENPP1 inhibitor that demonstrated superior immune protection compared with synthetic STING agonists. In syngeneic tumor models, GBD-09259 enhanced the efficacy of an immune checkpoint inhibitor anti-PD1 antibody and the chemotherapeutic agent cisplatin. The excellent selectivity, physicochemical properties, and pharmacokinetic profile make it a candidate for clinical development.

**Conflict of interest:**

Ownership: All authors are employees and stockholders of Gossamer Bio, Inc.

Corporate-sponsored Research: This research is being funded by Gossamer Bio, Inc.

352 (PB132)

**Subasumstat, a first-in-class inhibitor of SUMO-activating enzyme, demonstrates dose-dependent target engagement and SUMOylation inhibition, leading to rapid activation of innate and adaptive immune responses in the dose escalation portion of a phase 1/2 clinical study**

G. Saggi<sup>1</sup>, D. Stroopinsky<sup>2</sup>, A.Z. Dudek<sup>3</sup>, A.J. Olszanski<sup>4</sup>, D. Juric<sup>5</sup>, A. Dowlati<sup>6</sup>, U. Vaishampayan<sup>7</sup>, H. Assad<sup>8</sup>, J. Rodon<sup>9</sup>, J. Gibbs<sup>10</sup>, J. Green<sup>11</sup>, Z. Du<sup>12</sup>, R. Rudicell<sup>13</sup>, K. Kannan<sup>14</sup>, R. Gharavi<sup>15</sup>, A. Gomez-Pinillos<sup>16</sup>, R.J. Fram<sup>15</sup>, A. Berger<sup>17</sup>, K. Sachsenmeier<sup>13</sup>, S. Kasar<sup>17</sup>. <sup>1</sup>Takeda Development Center Americas, Inc. TDCA, Translational Oncology, Lexington, MA, USA; <sup>2</sup>Takeda Development Center Americas, Inc. TDCA, Oncology Therapeutic Area OTAU, Lexington, MA, USA; <sup>3</sup>HealthPartners Institute, Hematology and Oncology, St Paul, Minnesota, USA; <sup>4</sup>Fox Chase Cancer Center, Medical Oncology, Philadelphia, USA; <sup>5</sup>Massachusetts General Hospital Cancer Center, Department of Medicine- Harvard Medical School, Boston, USA; <sup>6</sup>University Hospitals Seidman Cancer Center and Case Western Reserve University, Oncology, Cleveland, USA; <sup>7</sup>University of Michigan, Internal Medicine Oncology, Ann Arbor, USA; <sup>8</sup>Wayne State University Karmanos Cancer Institute, Oncology, Detroit, USA; <sup>9</sup>MD Anderson Cancer Center, Investigational Cancer Therapeutics, Houston, USA; <sup>10</sup>Takeda Development Center Americas, Inc. TDCA, Quantitative Clinical Pharmacology, Lexington, MA, USA; <sup>11</sup>Takeda Development Center Americas, Inc. TDCA, Clinical Biomarker Innovation and Development, Lexington, MA, USA; <sup>12</sup>Takeda Development Center Americas, Inc. TDCA, Computational Biology, Lexington, MA, USA; <sup>13</sup>Takeda Development Center Americas, Inc. TDCA, Precision and Translational Medicine, Lexington, MA, USA; <sup>14</sup>Takeda Development Center Americas, Inc. TDCA, Oncology Therapeutic Area Unit, Lexington, MA, USA; <sup>15</sup>Takeda Development Center Americas, Inc. TDCA, Oncology Clinical Research, Lexington, MA, USA; <sup>16</sup>Takeda Development Center Americas, Inc. TDCA, Clinical Science OTAU R&D, Lexington, MA, USA; <sup>17</sup>Takeda Development Center Americas, Inc. TDCA, Oncology Precision and Translational Medicine, Lexington, MA, USA

**Background:** Subasumstat (TAK-981), a small-molecule inhibitor of SUMOylation, promotes a type-1 interferon (IFN-1) response, leading to activation of the immune system with the potential to augment antitumor immunity. Previous preclinical data suggest that subasumstat enhances antigen cross-presentation and promotes T and NK cell-dependent antitumor

responses in syngeneic mouse models. Here, we report pharmacodynamic (PD) data from the dose-escalation portion of a phase 1/2 clinical study (NCT03648372).

**Materials and Methods:** Eighty-four patients with advanced/metastatic solid tumors received subasumstat IV twice-weekly (BIW; days 1, 4, 8, 11) or once-weekly (QW; days 1, 8) in 21-day cycles. Peripheral blood (PB) samples were collected on cycle (C) 1 day (D) 1 and C1D8, pre-dose and at multiple timepoints post-end-of-infusion (EOI); skin biopsies were collected at screening and C1D8. Target engagement and levels of SUMO2/3 conjugates were assessed in PB by flow cytometry and in skin biopsies by immunohistochemistry (IHC). Immune activation was assessed in PB by flow cytometry. Plasma cytokines were assayed using MesoScale Discovery and gene expression was examined using a Nanostring panel. A custom gene signature score based on levels of seven key IFN-1 target genes was utilized.

**Results:** Subasumstat demonstrated robust target engagement and SUMOylation inhibition both in circulation (PB) and in tissue (skin), with inhibition detected in PB cells as early as 1 hour (h) post-EOI and sustained for at least 8 h. Subasumstat led to significant dose-dependent upregulation of the IFN-1 gene signature in blood and several IFN-1-induced plasma cytokines, including >100-fold increase in IP-10 and >10-fold increase in MCP-1. Importantly, subasumstat induced a significant increase in activated NK cells and activated CD8 and CD4T cells 24 h post-EOI. We also observed increased surface expression of co-stimulatory molecules CD80 and CD86 on PB monocytes and an increase in gene expression of CD86 and Siglec-1 in PB, suggesting enhanced potential for antigen presentation upon subasumstat treatment. Although target engagement and SUMOylation inhibition were detected at dose levels  $\geq 40$  mg, a consistent increase in IFN-1 signalling and immune activation was observed only at doses of  $\geq 60$  mg. Repeat dosing on QW and BIW schedules led to similar levels of target engagement and immune activation on C1D8 as on C1D1.

**Conclusions:** Subasumstat-mediated inhibition of SUMOylation led to dose-dependent activation of innate and adaptive immunity, thus supporting the hypothesized immune-activating MOA of the drug. Our findings support continued development of subasumstat for treatment of solid tumors and lymphoma. The phase 2 portion of this study is currently underway and accruing to investigate subasumstat 90 mg BIW; this dose was selected based on safety, tolerability, and PK/PD data.

#### Conflict of interest:

Ownership: Takeda Pharmaceutical Company Limited - Allison Berger, John Gibbs

Advisory Board: Peptomyc, Kelun Pharmaceuticals/Klus Pharma, Ellipse Pharma, Molecular Partners, IONCTURA - Jordi Rodon

Corporate-sponsored Research: Novartis, Spectrum Pharmaceuticals, Symphogen, BioAlta, Pfizer, GenMab, CytomX, Kelun-Biotech, Takeda-Millennium, GlaxoSmithKline, Taiho, Roche Pharmaceuticals, Hummingbird, Yingli, Bicycle Therapeutics, Merus, Curis, Bayer, AadiBioscience, Nuvation, ForeBio, BioMed Valley Discoveries, Loxo Oncology, Hutchinson MediPharma, Cellestia, Deciphera, Ideaya, Amgen, Tango Therapeutics, Mirati Linnaeus Therapeutics - Jordi Rodon

Other Substantive Relationships: Takeda employees:

Gurpanna Saggi, Alejandro Gomez-Pinillos, Dina Stroopinsky, John Gibbs, Jennifer Green, Zhou Du, Rebecca Rudicell, Karupiah Kannan, Robert Gharavi, Robert J. Fram, Allison Berger, Kris Sachsenmeier, Siddha Kasar

353

(PB133)

#### Investigating the effects of ERAP1 inhibition on antigen presentation and the tumour immune response

A. Margarido<sup>1</sup>, B. Whitton<sup>1</sup>, E. Arwert<sup>1</sup>, M. Cheeseman<sup>1</sup>, A. Kalusa<sup>1</sup>, G. Davison<sup>1</sup>, R. Salimraj<sup>1</sup>, O. Pierrat<sup>1</sup>, M. Richards<sup>1</sup>, H. dos Santos Costa<sup>1</sup>, P. Meister<sup>1</sup>, A. Hayes<sup>1</sup>, E. Reeves<sup>2</sup>, E. James<sup>2</sup>, R. Burke<sup>1</sup>, F. Raynaud<sup>1</sup>, R. Van Montfort<sup>1</sup>, J. Choudhary<sup>3</sup>, O. Rossanese<sup>1</sup>, G. Newton<sup>1</sup>. <sup>1</sup>The Institute of Cancer Research, Cancer Therapeutics, London, United Kingdom; <sup>2</sup>University of Southampton, Faculty of Medicine, Southampton, United Kingdom; <sup>3</sup>The Institute of Cancer Research, Cancer Biology, London, United Kingdom

**Background:** Antigen presentation by MHC class I is an essential mechanism of regulation against neoplastic and foreign cells. One key player in the antigen-processing pathway is the endoplasmic reticulum aminopeptidase 1 (ERAP1) enzyme, which trims peptides for presentation by MHC class I complexes on the surface of tumour cells. Modulation of this enzyme via genetic knock out/down leads to presentation of new immunogenic peptides, which can result in an immune reaction against tumour cells. The purpose of this study was to determine the feasibility of developing new chemical and biological tools to explore the therapeutic potential of ERAP1 inhibition as a new modality in immunotherapy.

**Materials and Methods:** CRISPR technology and doxycycline (Dox) inducible system were used to create ERAP1 knock-out (EKO) and knock-

down in mouse cell lines, respectively. These cell lines were implanted in syngeneic mice to track tumour growth, followed by immunohistochemistry and flow cytometry to analyse the inflammatory infiltrate. Structure-based drug design was used to develop selective inhibitors of ERAP1. ERAP1 inhibition was confirmed by a combination of biochemical and cellular assays that measure ERAP1 activity, binding affinity, and antigen presentation. To interrogate the effect of our compounds on MHC class I antigen presentation we used immunopeptidomics with TMT multiplexing on human and murine cell lines.

**Results:** The EKO mouse colorectal tumour cell line resulted in tumour rejection approximately seven days after injection, while the control tumours grew until the end point. When investigated before rejection, the EKO tumours contained higher numbers of immune cells, specifically cytotoxic T cells.

Structure based drug design was used to generate bioavailable compounds that bind in the regulatory site of ERAP1. The compounds were shown to inhibit ERAP1 in cells and modulate HPV-relevant antigen presentation.

Immunopeptidomics analysis revealed that Dox-inducible knockdown and compound treatment modulate antigen presentation, recapitulating the effects of ERAP1 KO in human and murine cell lines. Specifically, longer antigens are increased with ERAP1 inhibition in a dose dependent manner. We are currently investigating the level of immunogenicity these antigens could provide.

**Conclusions:** We have developed genetic models to evaluate ERAP1 as a therapeutic target in oncology. Moreover, we have developed encouraging small molecule ERAP1 inhibitors. Altogether, ERAP1 is a promising target to alter antigen processing, which, upon inhibition, leads to presentation of longer immunogenic peptides by MHC class I. Further work is ongoing to establish the therapeutic potential of ERAP1 inhibitors in combination with immune checkpoint inhibitors and/or radiotherapy.

**No conflict of interest.**

354

(PB134)

#### SpliceIO™ a novel AI platform for the discovery of splicing-derived immunotherapeutic targets

M. Manzanares<sup>1</sup>, H. Zurnut<sup>1</sup>, S. Gera<sup>1</sup>, A. Casili<sup>2</sup>, K. Anderson<sup>2</sup>, A. Geier<sup>3</sup>, M. Akerman<sup>2</sup>, G. Arun<sup>1</sup>. <sup>1</sup>Envisagenics, Biology Dept., New York, USA; <sup>2</sup>Envisagenics, Bioinformatic, New York, USA; <sup>3</sup>Envisagenics, Engineering, New York, USA

Alternative splicing (AS) plays a critical role in generating tumor-specific neoepitopes targetable through an arsenal of immunotherapeutic modalities. Previous studies have demonstrated tumor-promoting activity of deregulated AS isoforms and mutated splicing factors, both of which increase the yield of neoepitope-encoding AS isoforms. Therefore, the identification of AS isoforms has the potential to produce novel therapeutic targets, especially in tumor types where splicing deregulation is frequent, like breast cancer.

SpliceIO™ is Envisagenics' AI platform for AS-derived neoepitope discovery. SpliceIO uses a "predictive ensemble" approach to uncover neoepitopes that are both stably expressed and located on the extracellular membrane of cancer cells. Using SpliceIO, we have analyzed >10,000 RNA-seq samples from 5 patient cohorts covering 5 breast cancer subtypes as well as 2,647 normal RNA-seq samples from GTEx to identify tumor-specific neoepitopes present in AS transmembrane proteins.

Here, we present experimental evidence for SpliceIO-identified neoepitopes in breast cancer. We have validated RNA expression of the neoepitope-expressing transcripts in breast cancer cell lines, primary cells and breast tumor FFPE tissues using a combination of RT-PCR as well as RNA-FISH. Further, we have confirmed the expression of neoepitope-containing isoforms at the protein level using western blotting as well as proteomics. Interestingly, one such candidate is an endoplasmic reticulum protein overexpressed in TNBC tumors. The TNBC specific isoform of the protein is localized to plasma membrane in TNBC cells, suggesting that different splice isoforms of a protein can alter protein localization. This demonstrates the potential of utilizing RNA splicing for identifying many more membrane associated proteins for tumor specific targeting. The combination of computational and experimental approaches to neoepitope identification using SpliceIO allows for novel target discovery amenable for targeted immunotherapeutic development for cancer treatment and clinical care.

**Conflict of interest:**

Other Substantive Relationships: All the authors are salaried employees of Envisagenics.

355 (PB135)

**Cellular transporters as novel metabolic immune checkpoints: NGY-091, a small molecule dual MCT1/4 inhibitor for immuno oncology**

V. Sandanayaka<sup>1</sup>, S. Sharma<sup>2</sup>, N. Bowman<sup>2</sup>, J. Duffy<sup>2</sup>, S. Wijerathna<sup>2</sup>, M. Yu<sup>2</sup>, J. Escobedo<sup>2</sup>, N. Kuklin<sup>2</sup>. <sup>1</sup>Nirogy Therapeutics, Discovery & Development, Boston, USA; <sup>2</sup>Nirogy Therapeutics, Discovery, Boston, USA

**Background:** Aberrant metabolic reprogramming of malignant cells is known to drive cancer progression and metastasis. The increase in glycolytic flux in cancer cells creates a lactate-rich tumor microenvironment (TME), which tumors exploit by expanding immunosuppressive cell populations such as Tregs and MDSCs that thrive on lactate as a fuel source. Blockade of lactate export from glycolytic cancer cells, while inhibiting lactate uptake by suppressive immune cells, is a novel therapeutic strategy to treat cancer. Lactate transport in cells is predominantly mediated by MCT1 and MCT4 transporters. We have developed a compound, NGY-091, a first-in-class small molecule dual inhibitor of the MCT1 and MCT4 lactate transporters.

**Materials and Methods:** The direct cytotoxic effect of NGY-091 was examined in multiple cancer cell lines. The on-target activity of NGY-091 was validated by measuring intracellular and extracellular lactate levels. *in vivo* efficacy of NGY-091 was studied using CDX, PDX and syngeneic tumor models. Immune profiling of tumor was performed 2 weeks after treating animals with NGY-091 by flow cytometry.

**Results:** NGY-091 treatment exhibited a potent *in vitro* cytotoxicity against cancer cells with various levels of MCT1 and MCT4 expressions. NGY-091 strongly blocked lactate import through MCT1 under high lactate conditions and lactate export through MCT4 in high glucose conditions. NGY-091 treatment also inhibited pyruvate entry into the mitochondria through MPC1. Furthermore, direct *in vivo* tumor cell killing was evident in multiple human CDX and PDX models with the treatment of NGY-091. In syngeneic models of 4T1 and MC38 murine tumors, we observed significant tumor growth inhibition with NGY-091 treatment, and strong synergistic tumor reduction when treatment was combined with various immune checkpoint inhibitors. Profiling of lymphoid and myeloid cells in NGY-091 treated tumors by flow cytometry revealed a significant alteration in immune architecture suggesting activation of antitumor immunity. NGY-091 treated tumors induced a profound increase in effector T cell populations, CD8/Treg ratio, and tumor-suppressive M1 macrophages, while significantly downregulating M2 macrophages. To further investigate if NGY-091 directly alters immune cell activation and functionality *in vitro*, we treated CD4 T, CD8T, Tregs, and MDSCs in a lactate-rich culture condition, which mimicked the lactate level in the TME. NGY-091 treatment strongly increased effector CD4+ and CD8+ T cells, meanwhile it significantly reduced suppressive function of Treg and MDSCs *in vitro*.

**Conclusions:** These findings indicate the direct effect of NGY-091 on immune cells and validate the *in vivo* observations in 4T1 tumors. Therefore, NGY-091 intervenes with two key hallmarks of cancer, metabolism and immunity and provides a novel modality to therapeutically target cancer.

**Conflict of interest:**

Ownership: Nirogy Therapeutics

356 (PB136)

**Hydroxychloroquine synergizes with anti-PD-1 immune checkpoint blockade in squamous carcinoma of the head and neck**

A. Vyas<sup>1</sup>, S. Cruz-Rangel<sup>1</sup>, N. Khan<sup>1</sup>, R. Ferris<sup>1</sup>, T. Bruno<sup>2</sup>, N. Schmitt<sup>3</sup>, K. Kiselyov<sup>4</sup>, U. Duvvuri<sup>1</sup>. <sup>1</sup>University of Pittsburgh, Otolaryngology, Pittsburgh, USA; <sup>2</sup>University of Pittsburgh, Immunology, Pittsburgh, USA; <sup>3</sup>Emory University, Otolaryngology, Atlanta, USA; <sup>4</sup>University of Pittsburgh, Biological Sciences, Pittsburgh, USA

**Background:** The recent evidence shows that PD-L1 exposure on the plasma membrane is dynamically modulated. PD-L1 is delivered to the plasma membrane via the secretory pathway which involves lysosomal activity. Whereas the significance of this step is not completely understood, it provides a rationale for testing lysosomal inhibition as a means to regulate PD-L1. Limited but intriguing prior attempts at such resolution yielded mixed results, suggesting complex regulation of this process. A corollary, and a test of lysosomal and endocytic involvement in PD-L1 handling, is that the inhibition of membrane turnover in the endocytic pathway should suppress PD-L1 plasma membrane presentation and synergize with anti-PD-1 immune checkpoint blockade.

**Materials and Methods:** PD-L1 plasma membrane presentation was measured using flow cytometry with PE-Cy7 antibodies using lysosomotropic drugs. Lysosomal exocytosis was measured using beta-hexosaminidase activity. C57/Bl (4 wk old) mice were implanted subcutaneously with MOC-1 or UPCI:UDSCC:M4Tu lines on each flank and randomized. Treatments were administered two times a week intraperitoneally. The

volume of the tumors was measured three times a week. The animals were handled and euthanized in accordance with Institutional Animal Care and Use Committee guidelines.

**Results:** We find that *in vitro*, endolysosomal inhibition using the PIKfyve inhibitor apilimod or prolonged exposure to hydroxychloroquine suppresses plasma membrane presentation of PD-L1, which confirms endolysosomal involvement in PD-L1 handling. *In vivo*, in mouse models of head and neck cancers, hydroxychloroquine synergizes with anti-PD-1 therapy, causing tumor growth inhibition of 80% and dramatically increased survival ( $p < 0.001$ , log-rank test).

**Conclusions:** We conclude that by inhibiting PD-L1 turnover, hydroxychloroquine is a potent adjuvant for anti-PD-1 therapy.

**No conflict of interest.**

357 (PB137)

**A novel gut-restricted small molecule TLR2 agonist enhances immune checkpoint inhibitor efficacy in a preclinical mouse fibrosarcoma tumor model**

J. Simon<sup>1</sup>, C.J. Oalman<sup>1</sup>, P. Stern<sup>1</sup>, R.K. Senter<sup>1</sup>, M. Chien<sup>1</sup>, R. Graf<sup>1</sup>, A. Bessedé<sup>2</sup>, A.S. Campbell<sup>1</sup>. <sup>1</sup>Axial Therapeutics, Research & Development, Woburn, USA; <sup>2</sup>Explicyte, In Vivo Models, Bordeaux, France

Immune checkpoint inhibitor (ICI) therapy has revolutionized cancer treatment, but patient response remains variable. Substantial research has been focused on understanding the tumor-intrinsic and tumor-extrinsic factors underlying patient response. Recently, the gut microbiome emerged as a modulator of ICI therapy in both human patients and mouse tumor models. Antibiotic treatment has deleterious effects on ICI therapy efficacy and retrospective studies have identified microbiome signatures associated with ICI therapy responders and non-responders. Furthermore, fecal matter transplant (FMT) from ICI responders can improve the efficacy of ICI therapy in non-responders, however there is substantial variability in response that may be attributable to the imprecise nature of FMT. We identified Toll-like Receptor 2 (TLR2) as a key receptor in the gut mediating the microbial impact on host immunity and are developing novel gut-restricted small molecules that specifically engage and activate gut-resident TLR2. Compound A showed pro-inflammatory activity *in vitro*, eliciting a broad cytokine response from human and mouse macrophage-like cell lines with low nanomolar potency. Compound A significantly restored the efficacy of anti-PD1 therapy *in vivo* in a mouse tumor model where treatment with antibiotics abrogated anti-PD1 efficacy. In this model, mice bearing MCA205 fibrosarcoma tumors responded well to anti-PD1 therapy with significantly delayed tumor growth and prolonged survival. Antibiotic treatment significantly attenuated the efficacy of anti-PD1 therapy, and Compound A treatment significantly restored the efficacy of anti-PD1 therapy in the presence of antibiotics. We conclude that Compound A and related analogs have the potential to enhance ICI therapy by modulating the anti-tumor immune response via activation of TLR2 in the gut. Further mechanistic and pharmacological studies in additional tumor models are in progress.

**Conflict of interest:**

Ownership: JS, CJO, RKS, MC, RG, and ASC are employees and shareholders of Axial Therapeutics. PS is a shareholder of Axial Therapeutics.

358 (PB138)

**MDNA132 is an IL-13 Superkine selective to IL-13Rα2 with broad potential for delivery of immunotherapies to the tumor microenvironment**

A. Sharma<sup>1</sup>, M. To<sup>1</sup>, P. Gobeil<sup>1</sup>, F. Merchant<sup>1</sup>. <sup>1</sup>Medicenna Therapeutics Inc., Research and Development, Toronto, Canada

**Background:** Interleukin-13 binds two receptors. The first is the IL-13Rα1/IL-4Rα heterodimer which also responds to IL-4 ligand engagement, is broadly expressed, and is canonically associated with type-2 immune signaling. The second, IL-13Rα2, also referred to as the IL-13 decoy receptor, is negligibly expressed in normal tissues but is overexpressed in a range of cancers including pancreatic, colorectal, and lung tumors. MDNA132 is an engineered IL-13 mutein with specificity for IL-13Rα2. Herein we characterize Bi-functional SuperKine ImmunoTherapies ("BiSKITs") comprised of long-acting Fc-MDNA132 fusion constructs as proof-of-principle for targeted delivery of checkpoint inhibitors or IL-2 Superkines to IL-13Rα2-expressing tumors.

**Materials and Methods:** MDNA132 constructs fused to Fc (to improve peripheral half-life) and anti-PD1 or an IL-2 super-agonist, MDNA109FEAA (a mutein IL-2 with selective IL-2Rβγ agonist function) were characterized by

SPR. Anti-PD1 function was quantified using a cell-based PD1 blockade assay. IL-2R activity was characterized by *in vitro* signaling assay. Fc-MDNA132 localization in animals bearing IL-13R $\alpha$ 2-expressing tumors was determined by *in vivo* imaging.

**Results:** Fc-MDNA132 displayed undetectable binding to IL-13R $\alpha$ 1 and high affinity for both human and mouse IL-13R $\alpha$ 2. A MDNA132 BiSKIT incorporating anti-human or mouse PD1 antibody did not alter binding to IL-13R $\alpha$ 2. Anti-PD1-MDNA132 retained affinity for PD1 and capacity to block PDL1/PD1 signaling *in vitro*. A MDNA132 BiSKIT with MDNA109FEAA maintained affinity for IL-13R $\alpha$ 2, and the distinct MDNA109FEAA binding profile (ablated binding to IL-2R $\alpha$  and increased binding to IL-2R $\beta$ ) as well as signaling through IL-2R $\beta$  *in vitro*.

In tumor-bearing athymic mice implanted contralaterally with IL-13R $\alpha$ 2 positive (A375 and U87) and negative (A549) tumors, *in vivo* imaging demonstrated preferential localization of Fc-MDNA132 to IL-13R $\alpha$ 2-expressing tumors, illustrating the applicability of the Fc-MDNA132 platform for *in vivo* delivery of immunotherapies to the tumor microenvironment (TME).

**Conclusions:** MDNA132-based BiSKITs retain receptor binding profile and biological function of both MDNA132 and the fusion partner. MDNA132 localizes preferentially to IL-13R $\alpha$ 2 tumors in mice. These data highlight the versatility of MDNA132 and its potential to localize delivery of immunotherapeutics to the TME of cancers expressing IL-13R $\alpha$ 2.

**Conflict of interest:**

Ownership: All listed authors are employees of Medicenna Therapeutics Inc.

POSTER SESSION

**Novel Clinical Trial Design**

359

(PB139)

**Response to neoadjuvant targeted therapy in operable head and neck cancer confers survival benefit**

M. Mascarella<sup>1</sup>, T. Olonisakin<sup>2</sup>, P. Rumde<sup>3</sup>, V. Vendra<sup>3</sup>, M. Nance<sup>3</sup>, S. Kim<sup>3</sup>, M. Kubik<sup>3</sup>, S. Sridharan<sup>3</sup>, R. Ferris<sup>2</sup>, F. Moon<sup>4</sup>, D. Clayburgh<sup>5</sup>, J. Ohr<sup>4</sup>, S. Joyce<sup>4</sup>, M. Sen<sup>4</sup>, J. Herman<sup>4</sup>, J. Grandis<sup>6</sup>, D. Zandberg<sup>4</sup>, U. Duvvuri<sup>3</sup>.

<sup>1</sup>University of Pittsburgh Medical Center, Otolaryngology - Head and Neck Surgery, Pittsburgh, USA; <sup>2</sup>UMPC, Otolaryngology, Pittsburgh, USA;

<sup>3</sup>UPMC, Otolaryngology, Pittsburgh, USA; <sup>4</sup>UPMC, Oncology, Pittsburgh, USA; <sup>5</sup>OHSU, Otolaryngology, Portland, USA; <sup>6</sup>UCSF, Oncology, San Francisco, USA

**Background:** Neoadjuvant targeted therapy provides a brief, preoperative 'window of opportunity' that can be exploited to individualize cancer care based on treatment response. We investigated whether response to neoadjuvant therapy during the preoperative window confers survival benefit in patients with operable head and neck squamous cell carcinoma (HNSCC).

**Materials and Methods:** A pooled analysis of treatment naive patients with operable HNSCC enrolled in one of three clinical trials from 2009 to 2020 (NCT00779389, NCT01218048, NCT02473731). Neoadjuvant regimens consisted of EGFR inhibitors (n = 83) or anti-ErbB3 antibody therapy (n = 9) within 28 days of surgery. Clinical to pathologic stage migration was compared to overall survival (OS) while adjusting for confounding factors using multivariable Cox regression. Circulating tumor markers validated in other solid tumor models were analyzed.

**Results:** A total of 92 patients were analyzed; 76 patients had clinical stage III/IV disease with 50% (46/92) oral cavity, 24% (22/92) larynx/hypopharynx and 26% (24/92) oropharynx primaries. All patients underwent surgery following neoadjuvant therapy. Clinical to pathologic downstaging was more frequent in patients undergoing neoadjuvant targeted therapy compared to a historic cohort without neoadjuvant therapy (P = 0.048). Six patients with pathologic downstaging no longer met criteria for adjuvant treatment and were subsequently observed. Patients with pathologic downstage migration had the highest OS (89.5%, 95% CI 75.7–100) compared to those with no stage change (58%, 95% CI 46.2–69.8) or

upstage (40%, 95% CI 9.6–70.4, P = 0.003). On multivariable analysis, downstage migration remained a positive prognostic factor for OS (hazard ratio 0.22, 95% CI 0.05–0.90) while adjusting for measured confounders. Downstage migration correlated with decreased circulating tumor markers, SOX17 and TAC1 (P = 0.0078).

**Conclusions:** Brief neoadjuvant therapy achieved pathologic downstaging in a subset of patients and was associated with significantly better OS as well as decreased circulating methylated SOX17 and TAC1.

**No conflict of interest.**

POSTER SESSION

**Oncolytic Viruses and Vaccination**

360

(PB140)

**Pancreatic cancer models exhibit interferon-independent resistance mechanisms to a Morreton hybrid oncolytic vesiculovirus**

C. Dumbauld<sup>1</sup>, M. Gabere<sup>2</sup>, O. Barro<sup>2</sup>, B.M. Nagalo<sup>3</sup>, M. Borad<sup>2</sup>.

<sup>1</sup>Mayo Clinic, Immunology, Scottsdale, AZ, USA; <sup>2</sup>Mayo Clinic, Hematology, Scottsdale, AZ, USA; <sup>3</sup>University of Arkansas for Medical Sciences, Pathology, Little Rock, AR, USA

The five-year survival rate for pancreatic ductal adenocarcinoma (PDAC) remains only 10%, urging the development of novel therapeutics and combination therapies. Immune checkpoint blockade (ICB) and virotherapy have improved survival for a subset of cancer patients in recent years. However, extending the benefit to patients with PDAC has lagged. Prior studies have highlighted the role of intact type I interferon (IFN) signaling in mediating PDAC resistance to oncolytic vesicular stomatitis virus (VSV). Despite this, ongoing clinical trials utilize oncolytic VSV encoding interferon beta (IFN $\beta$ ) to increase safety, while simultaneously limiting viral efficacy.

Due to safety concerns regarding wild-type VSV's ability to infect neurons, we engineered a hybrid vesiculovirus replacing the viral surface glycoprotein (G protein) with that of Morreton virus, shown to be well-tolerated in immunocompetent mice. We characterized the oncolytic properties of the hybrid virus - VSV expressing the Morreton G protein (VMG) - in PDAC cell lines, patient-derived organoids, and a syngeneic murine model.

Cell lines were variably susceptible to VMG-induced cell death *in vitro*, independent of type I IFN or infectious viral particle production. We evaluated resistance signatures using Significance Analysis of Microarrays and RNA-Seq (SAMseq) and quantitative proteomics. Differential gene expression of sensitive and resistant cell lines showed higher expression of *HAS3* at baseline in resistant cell lines. We also performed quantitative proteomics of infected versus control sensitive (MIA-PaCa2) and resistant (CFPAC-1) PDAC cell lines. Overall, fewer proteins were differentially expressed in CFPAC-1 after infection, but we detected all five structural proteins of VMG in infected samples. IFN-related proteins were not among the most upregulated within either cell line after infection with VMG. The highest upregulated proteins in CFPAC-1 after VMG infection were PLEKHA2, PALM, and TMEM30B. Notably, PLEKHA2 has also been shown to have a role in Zika virus resistance.

We observed variability in response to VMG treatment between patient-derived organoids, although the cause remains to be determined. In the syngeneic murine model of PDAC Panc.02, we observed no tumor regression after two intratumoral injections of VMG. However, VMG administration was well tolerated, and flow cytometric analysis showed a significant increase of CD8 T cells within oncolytic virus treated tumors.

These results demonstrate oncolytic VMG shows promise in some models of PDAC, but responses can be expected to be variable in a broad patient base. It is vital to identify genetic or cellular signatures which can indicate whether a tumor will be responsive to oncolytic VMG therapy, and how to rationally combine with other treatment modalities such as ICB to overcome the elucidated mechanisms.

**No conflict of interest.**

## Author index

### A

- Aalders W., S49 (136)  
 Abbineni C., S69 (193)  
 Abdulkadir S., S36 (102)  
 Abel A.C., S65 (184)  
 Aboagye E.O., S49 (135)  
 Abrahams B., S52 (144)  
 Abrahams D., S90 (250)  
 Abramczyk O., S90 (248)  
 Abril-Fornaguera J., S120 (336)  
 Achtenberg A., S9 (16)  
 Acilan Ayhan C., S69 (192)  
 Açılan Ayhan C., S15 (43)  
 Adamczyk J., S104 (292)  
 Adams E., S67 (188)  
 Adeshina A., S12 (31)  
 Adayemi S., S122 (341)  
 Adhikari J., S104 (293)  
 Adriany T., S97 (269)  
 Aguado E., S61 (171)  
 Ahlborn L.B., S118 (331)  
 Ahmed G., S96 (265)  
 Ahn H.R., S94 (258), S105 (295),  
   S123 (344)  
 Ahn M., S83 (232)  
 Ahn M.S., S85 (237)  
 Aillard B., S19 (56)  
 Aivado M., S49 (136)  
 Ajayi B., S12 (31)  
 Akerman M., S126 (354)  
 Akman G., S64 (181)  
 Akpınar A., S104 (291)  
 Aksu A.C., S69 (192)  
 Alabduljabbar D., S108 (305)  
 Al-Ahmadie H.A., S10 (21)  
 Alarcón P., S59 (165)  
 Alarcon-Zapata P., S110 (310)  
 Albertella M., S123 (345)  
 Alcaro S., S65 (184)  
 Aldea M., S11 (22), S26 (74)  
 Aldeguer E., S89 (247)  
 Alemany C., S36 (101)  
 Alexander J., S50 (139), S99 (277)  
 Alimonti A., S107 (302)  
 Alistar A., S32 (91)  
 Al-Lazikani B., S83 (231)  
 Allen E., S16 (47)  
 Alliaga A., S16 (46)  
 Alli C., S26 (77)  
 Allred C., S47 (131)  
 Almofeez R., S87 (241)  
 Alnemy S., S43 (120), S53 (148)  
 Alonso G., S5 (7), S49 (137), S70 (196)  
 Alvero A., S48 (134)  
 Amaudrut J., S26 (77)  
 Ambrogio C., S18 (52)  
 Ameer-Beg S., S70 (197)  
 Ames T.D., S39 (110)  
 Amidon B., S40 (111)  
 Anastasiou P., S62 (173)  
 Anbuselvan A., S55 (154)  
 Anderson K., S126 (354)  
 Andreu-Oller C., S120 (336)  
 Andrews K.L., S76 (212)  
 Andronache A., S108 (304)  
 Anel A., S39 (110)  
 Angelosanto N., S23 (67)  
 Annis A., S49 (136)  
 Annunziato S., S50 (139)  
 Antignani A., S86 (240)  
 Antolin A., S83 (231)  
 Antolin Hernandez A., S25 (72)  
 Antoñanzas Basa M., S82 (228)  
 Antos A., S13 (36)  
 Anttila J., S98 (272)  
 An X., S100 (279), S118 (332),  
   S122 (343)  
 Aoyagi Y., S77 (214)  
 Apte S., S73 (206), S76 (211)  
 Aras R., S19 (53)  
 Aras S., S48 (134)  
 Aravind P., S49 (135)  
 Ardini E., S2 (3LBA), S17 (48)  
 Arena S., S63 (176)  
 Arencibia J.M., S104 (292)  
 Aresu L., S65 (183)  
 Arias K., S87 (241), S90 (249)  
 Arnold D., S54 (150)  
 Arribas A., S107 (302), S108 (304)  
 Arribas A.J., S65 (183), S80 (223),  
   S106 (297), S107 (301)  
 Arribas J., S61 (172)  
 Arrighetti N., S68 (191)  
 Arrowsmith E., S71 (198)  
 Arteaga C., S25 (73)  
 Arteaga C.A., S8 (11)  
 Arteaga C.L., S84 (235), S86 (238)  
 Arun G., S126 (354)  
 Arwert E., S126 (353)  
 Ascheid D., S11 (30)  
 Assad H., S125 (352)  
 Aswad F., S44 (124)  
 Atieh A., S69 (195)  
 Attwood K., S95 (263)  
 Atwal S., S72 (201)  
 Audia J., S33 (94)  
 Audugier-Valette C., S26 (74)  
 Austin D., S87 (241), S90 (249)  
 Austin W., S73 (206)  
 Austin W.F., S76 (211)  
 Avanzi N., S17 (48)  
 Awan A., S31 (87)  
 Azaman M.I., S109 (307)

### B

- Bacha J., S39 (109)  
 Bacon C., S117 (330)  
 Badarinarayana V., S73 (206), S76 (211)  
 Bader S., S38 (107)  
 Bae J.H., S19 (54)  
 Baek G.O., S94 (258), S105 (295)  
 Baek J., S20 (59)  
 Bagnardi V., S4 (4)  
 Bagci Onder T., S69 (192)  
 Baik C., S75 (209)  
 Bailey S., S81 (225)  
 Bai R., S65 (184)  
 Bakken K., S92 (255)  
 Balazs Z., S3 (2)  
 Balcer A., S16 (47)  
 Ball J., S23 (66)  
 Baloglu E., S40 (112)  
 Banaszak K., S15 (45)  
 Banerjee S., S99 (277)  
 Banjeri U., S117 (330)  
 Banks K., S107 (300)  
 Banuelos C.A., S72 (203)  
 Bapat B., S97 (271)  
 Barasa B., S122 (341)  
 Barbacid M., S18 (52)

\*Page numbers are followed by the abstract numbers in parentheses.



- Barbeau O., S44 (124)  
 Barber P.R., S70 (197)  
 Bárcena-Varela M., S120 (336)  
 Bardeesy N., S93 (257)  
 Bardelli A., S63 (176)  
 Barisella M., S68 (191)  
 Barraja P., S65 (184)  
 Barreca M., S65 (184)  
 Barro O., S128 (360)  
 Bart A., S9 (16)  
 Bartosik A., S15 (45)  
 Barve M., S1 (1LBA), S34 (95), S80 (224)  
 Barwick T., S49 (135)  
 Bashir A., S31 (87)  
 Basu B., S117 (330)  
 Baum A., S54 (150)  
 Baumert T., S93 (257)  
 Baxter J., S99 (277)  
 Bayle A., S11 (22)  
 Bayliffe A., S5 (6)  
 Bazhenova L., S72 (201), S75 (209)  
 Beaton N., S104 (293), S115 (323)  
 Beatty M., S90 (250)  
 Beaulieu M.E., S24 (68), S38 (106),  
 S38 (108), S44 (123), S46 (129),  
 S47 (130), S53 (149)  
 Beaumont E., S19 (56)  
 Becherini C., S124 (348)  
 Becker F., S102 (285)  
 Becker M., S12 (33), S41 (115)  
 Bedard P., S31 (87)  
 Bedke J., S12 (33)  
 Beeram M., S121 (337)  
 Begley C.G., S41 (114)  
 Beg M., S1 (2LBA), S57 (160)  
 Beijnen J., S103 (289), S109 (306)  
 Belen A., S70 (196)  
 Belitskina K., S98 (272)  
 Belitskin D., S98 (272)  
 Bellenie B., S104 (291)  
 Bellier J., S29 (84)  
 Bellile E., S79 (221)  
 Bellio C., S106 (299)  
 Bell J., S119 (333)  
 Belmonte M.A., S24 (71)  
 Below C., S115 (323)  
 Beltran M., S48 (133)  
 Bensen D., S16 (47)  
 Berche R., S70 (196)  
 Berger A., S125 (352)  
 Berger M.F., S10 (21)  
 Bernabé Y., S48 (133)  
 Bernardo P., S88 (245)  
 Bernatowicz K., S70 (196)  
 Bertolazzi G., S55 (154)  
 Bertoni F., S65 (182), S65 (183),  
 S65 (184), S80 (223), S89 (246),  
 S106 (297), S107 (301), S107 (302),  
 S108 (304)  
 Besnard J., S44 (124)  
 Besse B., S1 (2LBA), S6 (8), S11 (22),  
 S26 (74), S72 (201), S75 (209)  
 Bessede A., S127 (357)  
 Bevan L., S83 (232)  
 Bexon A., S82 (230)  
 Bhaskaran V., S61 (171)  
 Bhavar P.K., S56 (156)  
 Bhave V., S3 (3)  
 Bholia P., S51 (143)  
 Białopiotrowicz-Data E., S56 (158)  
 Biannic B., S37 (103)  
 Bifulco C., S97 (271)  
 Bigot K., S98 (274)  
 Bigot L., S78 (218)  
 Binaschi M., S89 (246)  
 Bini M., S98 (274)  
 Biondini M., S63 (178)  
 Biondo A., S57 (159)  
 Bird T., S19 (53)  
 Bisbocci M., S26 (77)  
 Bišta M., S104 (292)  
 Bittner A., S41 (115)  
 Bivacqua R., S65 (184)  
 Bi W.L., S3 (3)  
 Blair J., S38 (107)  
 Blaj C., S59 (164)  
 Blakemore S., S117 (330)  
 Blanc-Durand F., S11 (22)  
 Blanchette P., S31 (87)  
 Blanco-Alcaina E., S108 (303)  
 Blanco G., S81 (225)  
 Blank J.L., S24 (71)  
 Blaszkowska M., S23 (67)  
 Blay J.Y., S32 (91)  
 Blum Y., S9 (16)  
 Bobowska A., S15 (45)  
 Boemer U., S9 (17)  
 Böhler C., S90 (250)  
 Böhling T., S117 (329)  
 Bohnert R., S12 (33)  
 Bol K., S122 (341)  
 Bommi-Reddy A., S67 (188)  
 Bonifacio A., S27 (78)  
 Boni V., S23 (67)  
 Bonomo P., S124 (348)  
 Borad M., S116 (326), S128 (360)  
 Boran A., S21 (61)  
 Borrelli D.R., S29 (84)  
 Botelho R.J., S106 (298)  
 Boudesco C., S44 (124)  
 Bouhana K., S81 (226), S81 (227)  
 Boulos P., S101 (284)  
 Boumelha J., S62 (173)  
 Boutard N., S15 (45)  
 Bove J., S38 (106)  
 Bowden M., S119 (333)  
 Bowman N., S127 (355)  
 Box G., S35 (98), S104 (291)  
 Brachais M., S55 (153)  
 Brach K., S104 (292)  
 Bradley B., S24 (71)  
 Bradley J., S38 (107)  
 Bradshaw C., S88 (245)  
 Brail L., S34 (95)  
 Brait M., S76 (211)  
 Braña I., S48 (133), S49 (137), S70 (196)  
 Braverman S., S99 (278)  
 Bray M., S31 (87)  
 Breen L., S64 (180)  
 Bréhélin L., S98 (274)  
 Breitmeyer J.B., S105 (296)  
 Bré J., S46 (128), S66 (185)  
 Brenner J.C., S79 (221)  
 Breschi A., S23 (66)  
 Briggs K., S26 (75), S84 (233), S84 (234)  
 Bright M., S104 (291)  
 Briker L., S3 (2), S52 (145), S115 (325)  
 Broggin M., S107 (302)  
 Brooijmans N., S29 (84)  
 Brooun A., S19 (54)  
 Brothwood J., S57 (159)  
 Brotz T., S20 (59)  
 Brough R., S99 (277)  
 Brown C.V., S10 (19)  
 Brown D., S39 (109)  
 Browne A., S64 (180)  
 Brown G., S99 (278)  
 Brown J., S97 (270)  
 Bruderer R., S104 (293), S115 (323)  
 Brugman R., S49 (136)  
 Bruno T., S127 (356)  
 Brunton V.G., S113 (319)  
 Brzezicha B., S12 (32), S41 (115)  
 Brzózka K., S15 (45)  
 Bucheit A., S14 (38)  
 Bucher V., S45 (127)  
 Buchman C., S110 (308)  
 Buck E., S22 (64), S23 (66), S86 (239)  
 Buelvas N., S59 (165), S60 (169)  
 Buerki R., S82 (230)  
 Bukowinski A., S28 (82)  
 Bulow C., S108 (305)  
 Burgenske D., S92 (255)  
 Burgos R., S59 (165)  
 Burke R., S104 (291), S126 (353)  
 Burkner A.J., S65 (182)  
 Burns M., S61 (170)  
 Burn T., S16 (47)  
 Burrows F., S58 (161)  
 Butowski N., S82 (230)  
 Büttner F.A., S12 (33)  
 Byrne S., S90 (250)
- ## C
- Cable L., S81 (226)  
 Cade I., S19 (56)  
 Cadzow L., S37 (105)  
 Caffarra C., S18 (52)  
 Caillot M., S112 (314)  
 Calizo A., S17 (49)  
 Calles A., S6 (8)  
 Calles Blanco A., S26 (74)  
 Call J., S122 (341)  
 Calvayrac O., S55 (153)  
 Calvo E., S5 (7), S111 (313), S121 (337)  
 Camidge D.R., S1 (2LBA), S6 (8)  
 Campbell A.S., S127 (357)  
 Campbell E., S19 (56)  
 Campbell J., S63 (177)  
 Camphausen K., S11 (30)  
 Campos J., S97 (269)  
 Cannas E., S80 (223), S107 (302),  
 S108 (304)

- Cannatá C., S61 (172)  
 Casacuberta Serra S., S46 (129)  
 Castillo Cano V., S24 (68), S46 (129), S53 (149)  
 Cao P., S41 (114), S113 (317)  
 Capiiaux G., S82 (230)  
 Caponegro M., S73 (206), S76 (211)  
 Carballo N., S48 (133)  
 Carkill M., S123 (345)  
 Carles J., S48 (133), S49 (137)  
 Carmelo M., S65 (182)  
 Carmona Echeverria L.M., S64 (181)  
 Carpentier J., S64 (179)  
 Carragher N.O., S113 (319)  
 Carrillo-Garcia J., S108 (303)  
 Carroll A., S50 (139)  
 Carter L., S3 (1), S125 (350)  
 Carugo A., S26 (77), S63 (176)  
 Carulli J., S53 (148), S94 (259)  
 Carvalho Santos J., S112 (314)  
 Casacuberta-Serra S., S24 (68), S38 (108), S44 (123), S47 (130), S53 (149)  
 Casale E., S17 (48)  
 Casanova A., S55 (153)  
 Cascione L., S65 (184), S80 (223), S107 (302)  
 Cash T., S28 (82)  
 Casill A., S126 (354)  
 Cassani M., S50 (138)  
 Cassier P., S32 (91), S72 (201), S116 (326)  
 Castaldi P., S115 (323)  
 Castañón Álvarez E., S122 (341)  
 Castilla-Ramirez C., S108 (303)  
 Castillo Cano V., S38 (106), S44 (123)  
 Castro A., S51 (142), S55 (152)  
 Casuscilli F., S17 (48)  
 Catania C., S4 (4)  
 Cesarone G., S117 (328)  
 Cescon D., S31 (87)  
 Cescon D.W., S63 (178)  
 Cevatembre B., S69 (192)  
 Chae Y.K., S82 (228)  
 Chai S., S110 (308)  
 Chaitanya T K., S69 (193)  
 Chaligne R., S4 (5)  
 Chan A., S55 (154)  
 Chandrasekar S., S110 (309)  
 Chand S., S79 (220)  
 Chang J., S19 (53)  
 Chang Q., S27 (78)  
 Chang S.C., S97 (271)  
 Chan J., S4 (5)  
 Chan S., S58 (161)  
 Chaturvedi S., S28 (82)  
 Chaudhary O., S4 (5)  
 Cheal S., S3 (1)  
 Cheema U., S64 (181)  
 Cheeseman M., S35 (98), S126 (353)  
 Chehade H., S48 (134)  
 Chelstowska M., S23 (67)  
 Chelur S., S69 (193)  
 Chen A., S25 (73), S103 (290)  
 Chen A.P., S8 (11), S84 (235), S86 (238)  
 Chen C., S74 (207), S122 (343)  
 Chen G., S74 (207)  
 Chenge J., S110 (308)  
 Chenghao Ying C.Y., S27 (79)  
 Cheng P., S115 (325)  
 Cheng T., S20 (58)  
 Chen H., S19 (54)  
 Chen J., S74 (207)  
 Chen K., S59 (164), S94 (260), S106 (298)  
 Chen L., S44 (122), S77 (215), S78 (217)  
 Chen P., S19 (54)  
 Chen T., S110 (308)  
 Chen W., S34 (96), S38 (107), S118 (332)  
 Chen X., S43 (121), S44 (122), S80 (224)  
 Chen Y., S4 (5), S83 (231)  
 Chen Z., S10 (21), S22 (65), S60 (167), S111 (312)  
 Cheong J.Y., S94 (258), S105 (295)  
 Cherniak A., S9 (17)  
 Chesler L., S74 (208)  
 Chessari G., S83 (232)  
 Cheung K.M., S104 (291)  
 Cheung N.K., S3 (1)  
 Chiang G., S19 (54)  
 Chiappa M., S107 (302)  
 Chicarelli M.J., S81 (226), S81 (227)  
 Chicón-Bosch M., S24 (69)  
 Chien M., S127 (357)  
 Chien S., S81 (225)  
 Childs B.H., S28 (82)  
 Chin-Huang L., S114 (320)  
 Chmielewski S., S56 (158)  
 Chng K., S81 (225)  
 Chng W.J., S109 (307)  
 Cho B., S78 (218)  
 Cho B.C., S1 (2LBA), S72 (201), S75 (209)  
 Cho H.J., S94 (258), S105 (295), S123 (344)  
 Choi J.C., S53 (147)  
 Choi K.R., S60 (168), S102 (287)  
 Choi M.Y., S85 (237)  
 Choi S., S35 (99)  
 Choi W., S20 (59)  
 Chompunud Na Ayudhya C., S45 (126), S73 (205)  
 Choo Z.N., S4 (5)  
 Chopra R., S5 (6)  
 Cho S., S110 (309)  
 Choudhary J., S126 (353)  
 Choudhary J.S., S50 (139)  
 Chow C., S59 (164)  
 Chow E.K., S55 (154)  
 Chow J., S94 (260)  
 Chow J.T.S., S106 (298)  
 Christie E., S113 (317)  
 Christin J.R., S10 (21)  
 Chrzanowska K., S104 (292)  
 Chuaqui C., S53 (148), S94 (259)  
 Chu C.E., S10 (21)  
 Chung C.H., S79 (221)  
 Chung J., S28 (82)  
 Chung V., S34 (96)  
 Cianfarano E., S63 (178)  
 Cianferoni D., S61 (172)  
 Çiçek E., S15 (43)  
 Cidoncha I., S48 (133)  
 Cinamon G., S69 (195)  
 Cingoz A., S69 (192)  
 Citarella F., S26 (74)  
 Çitirikkaya C., S103 (289)  
 Civanelli E., S65 (183), S80 (223), S89 (246)  
 Clark D., S36 (101)  
 Clarke P.A., S35 (98)  
 Clark R., S73 (206)  
 Clark R.B., S76 (211)  
 Claxton C., S97 (269)  
 Clayburgh D., S128 (359)  
 Clermont E., S55 (153)  
 Cloughesy T., S32 (90)  
 Coan J.P., S45 (125)  
 Codony-Servat J., S89 (247)  
 Colaceci F., S26 (77)  
 Colajori E., S2 (3LBA)  
 Coliboro V., S55 (152)  
 Collini P., S68 (191), S108 (303)  
 Collins D., S64 (180)  
 Collins I., S83 (231)  
 Collisson E.A., S86 (238)  
 Coma S., S18 (52)  
 Conci N., S26 (74)  
 Conforti F., S4 (4)  
 Conley B., S25 (73)  
 Conley B.A., S8 (11), S84 (235), S86 (238)  
 Conlon N., S64 (180)  
 Conrad T., S41 (115)  
 Conti C., S63 (177)  
 Cook N., S117 (330)  
 Cooper E., S94 (259)  
 Cornella-Taracido I., S104 (293)  
 Corral E., S5 (7)  
 Correia S., S41 (116)  
 Cottens S., S104 (292)  
 Cottrell K., S26 (75), S84 (233), S84 (234)  
 Courtney H., S59 (164)  
 Cousin S., S26 (74)  
 Coussens N., S62 (175)  
 Covens K., S97 (269)  
 Coviello C., S101 (284)  
 Covington M., S79 (220)  
 Cowley K., S113 (317)  
 Crane C., S101 (284)  
 Cremona M., S64 (180)  
 Cribbs A., S69 (192)  
 Crisp A., S83 (231)  
 Cristina V., S49 (137)  
 Crivori P., S2 (3LBA)  
 Crompton J., S64 (181)  
 Crouchet E., S93 (257)  
 Crow M., S81 (226)  
 Crown J., S64 (180), S82 (228)  
 Cruz-Rangel S., S112 (315), S127 (356)  
 Cryan L., S24 (71)  
 Cui J., S41 (114)  
 Currie J.C., S117 (328)  
 Czuba E., S21 (62)

**D**

- Dąbrowski D., S90 (248)  
 Dacek M., S3 (1)  
 Daems D., S97 (269)  
 Dagrada G., S68 (191)  
 Dahlke J., S81 (227)  
 Dahlmann M., S12 (33)  
 Dai Y., S27 (79)  
 Dale S., S58 (161)  
 Dalgarno D., S85 (236)  
 Damia G., S107 (302)  
 Damian S., S2 (3LBA)  
 Daniele E., S81 (225)  
 Daniel Ampanattu S., S96 (265)  
 Dao K.H., S57 (159)  
 Darbonne W.C., S71 (198)  
 Das S., S11 (30), S15 (41), S95 (261), S107 (300)  
 Datta D., S61 (172)  
 Daugaard M., S39 (109)  
 Davidson K., S66 (186)  
 Davis C., S84 (233)  
 Davis O., S104 (291)  
 Davison G., S126 (353)  
 Davite C., S2 (3LBA)  
 Davoudi Z., S62 (175)  
 Dearie A., S81 (225)  
 De Haven Brandon A., S35 (98)  
 DeBerry B., S121 (337)  
 De Billy E., S35 (98)  
 DeCillis A., S7 (10)  
 de Jong A., S49 (136)  
 de Jong L., S22 (63)  
 DeLaBarre B., S33 (94)  
 Dela Cruz F., S74 (208)  
 De La Cruz J.O., S50 (138)  
 Delahaye C., S55 (153)  
 Del Angel Zuvirie C., S115 (324)  
 de Langen A., S75 (209)  
 Delgado C., S51 (142)  
 Delgoffe G., S61 (170)  
 Dellamary L., S34 (97)  
 Delosh R., S62 (175)  
 de los Rios M., S34 (97)  
 Demeule M., S117 (328)  
 de Miguel M.J., S6 (8), S82 (228)  
 Deng N., S41 (114)  
 Deninno M., S20 (59)  
 Depares I., S48 (133)  
 De Pas T., S4 (4)  
 De Pietro M.T., S2 (3LBA)  
 Depinho R., S40 (112)  
 de Ridder C.M.A., S42 (118), S43 (119)  
 Desai N., S21 (62), S58 (163)  
 Desideri I., S124 (348)  
 De Stanchina E., S27 (78)  
 De Vega D., S97 (269)  
 Dexheimer T., S62 (175)  
 Dhanalakshmi S., S125 (349)  
 Dhande A., S63 (177)  
 Dharani S., S15 (41)  
 Dhawan N., S38 (107)  
 Dhillon J., S117 (328)  
 Dhir S., S106 (298)  
 Diadziuszkzo R., S1 (2LBA)  
 DiBenedetto H., S84 (233)  
 Dicker Sagy E., S9 (16)  
 Dicker T., S9 (16)  
 Dickson A.L., S66 (185)  
 Di Conza G., S80 (223)  
 Díez M., S48 (133)  
 Di Fabio R., S26 (77)  
 DiMartino J., S74 (208)  
 Dineen T., S63 (177)  
 Ding Q., S27 (79)  
 D'Ippolito A., S94 (259)  
 DiPrimeo D., S82 (228)  
 Disconzi L., S2 (3LBA)  
 Distel M., S3 (2)  
 Divita G., S21 (62)  
 Djiane A., S98 (274)  
 Dobrzański P., S104 (292)  
 Doebele R.C., S20 (60)  
 Doger de Spéville B., S5 (7)  
 Doi T., S87 (242)  
 Dokduang S., S45 (126)  
 Dolata I., S56 (158)  
 Domingo A., S19 (56)  
 Donahue R., S5 (6)  
 Dong I., S41 (114)  
 Donhaue J., S76 (210)  
 Dooms C., S82 (228)  
 Doroshov J., S62 (175)  
 dos Santos Costa H., S126 (353)  
 Dotan E., S116 (326)  
 Dotterweich J., S89 (247)  
 Douglas L.M., S117 (328)  
 Doussine A., S55 (153)  
 Dovat S., S29 (83)  
 Dowdell A., S97 (271)  
 Dowlati A., S125 (352)  
 Downward J., S62 (173)  
 Doyle L., S25 (73)  
 Doyle L.A., S8 (11)  
 Doze P., S122 (341)  
 Draetta G., S63 (176)  
 Drake K., S79 (220)  
 Drake T., S19 (53)  
 Drenkler R., S13 (37), S14 (38), S121 (337)  
 Drescher C., S31 (89)  
 Driessen C., S107 (301)  
 Drilon A., S1 (2LBA), S6 (8), S75 (209)  
 Drozdowski B., S87 (243)  
 DuBois S.G., S28 (82)  
 Duca M., S2 (3LBA)  
 Duchateau P., S15 (41)  
 Dudek A.Z., S125 (352)  
 Dudziak R., S23 (67)  
 Du F., S27 (79)  
 Duffy J., S127 (355)  
 Dufner D., S7 (9)  
 Duke K., S29 (83)  
 Dumbauld C., S128 (360)  
 Dumbrava E.E., S7 (9), S10 (19)  
 Dummer R., S3 (2), S52 (145), S115 (325)  
 Durinikova E., S44 (124)  
 Duska L.R., S31 (89), S67 (188)  
 Duval D., S95 (261), S107 (300)

- Duvvuri U., S61 (170), S112 (315), S127 (356), S128 (359)  
 Du Z., S125 (352)  
 Dworakowski W., S43 (120), S53 (148)  
 Dymkowska M., S9 (16)  
 Dynlacht J.R., S100 (281)  
 Dziadziuszkzo R., S23 (67)  
 Dziedzic K., S56 (158)  
 Dzung A., S115 (325)  
 Dzurillova L., S44 (124)

**E**

- Eagle K., S119 (333)  
 Eathiraj S., S22 (64), S23 (66)  
 Eberhart C., S3 (3)  
 Eccles S.A., S35 (98)  
 Ecsedy J., S40 (111)  
 Eder J.P., S7 (10)  
 Edwards A.M., S83 (231)  
 Effah W., S105 (296)  
 Eheim A., S9 (17)  
 Ehler J., S19 (56)  
 Ehresmann L., S101 (282)  
 Eibler L., S3 (1)  
 Eichhoff O., S3 (2), S52 (145), S115 (325)  
 Eisert A., S26 (74)  
 Eis K., S9 (17)  
 Ekeh H., S65 (182)  
 Elaassai-Schaap J., S43 (120)  
 Elamin Y.Y., S6 (8)  
 Eleswarapu S., S33 (92), S33 (93)  
 Elez E., S49 (137)  
 Élez E., S48 (133)  
 Eli L.D., S82 (228)  
 Elimelech O., S104 (294)  
 El-Khoueiry A.B., S32 (91)  
 Elmi M., S121 (337)  
 Elmquist W., S92 (255)  
 El-Shemerly M., S56 (155)  
 Engbers A., S122 (341)  
 Enos C., S87 (241)  
 Enríquez J.A., S39 (110)  
 Ergüner B., S44 (124)  
 Eriksen M., S118 (331)  
 Erkens-Schulze S., S42 (118), S43 (119)  
 Ernst M., S13 (35)  
 Escobedo J., S127 (355)  
 Escorcia F., S11 (30)  
 Esin B., S69 (192)  
 Espinar L., S61 (172)  
 Espinoza V., S19 (57), S58 (162)  
 Esposito S., S26 (77)  
 Espinosa Carrasco J., S95 (264)  
 Esteban-Fabró R., S120 (336)  
 Eto D., S125 (350)  
 Eun J.W., S94 (258), S105 (295)  
 Evans J., S117 (330)  
 Evans J.W., S59 (164)  
 Evans T.R.J., S82 (230)  
 Eyer mann C.J., S85 (236)

**F**

Fabbrini D., S26 (77)  
 Fabila P., S103 (290)  
 Facchin C., S16 (46)  
 Fagan P., S19 (54)  
 Fairchild L., S21 (61)  
 Falchook G., S80 (224), S82 (230)  
 Falchook G.S., S72 (201)  
 Fallet V., S26 (74)  
 Faltaos D., S36 (101)  
 Fancelli D., S108 (304)  
 Fang J., S75 (209)  
 Fang K., S77 (215)  
 Farouq D., S94 (259)  
 Faulhaber N., S31 (89)  
 Favre G., S55 (153)  
 Fazal L., S83 (232)  
 Feldsien T., S92 (255)  
 Felip E., S1 (2LBA), S6 (8), S48 (133), S49 (137)  
 Fell B., S81 (226), S81 (227)  
 Felli E., S93 (257)  
 Feng Y., S104 (293), S115 (323)  
 Fernandes S., S50 (138)  
 Fernandez-Salas E., S103 (290), S110 (309)  
 Ferrara R., S26 (74)  
 Ferrari N., S83 (232)  
 Ferraro G.B., S100 (279)  
 Ferrat T., S14 (39)  
 Ferris R., S127 (356), S128 (359)  
 Ferro R., S50 (139)  
 Ferté C., S116 (326)  
 Fertig E., S59 (166)  
 Fica V., S51 (142)  
 Fidler M.J., S79 (221)  
 Figarol S., S55 (153)  
 Finan P., S19 (56)  
 Fischer J., S81 (226), S81 (227)  
 Fish S., S81 (225)  
 Fitzgerald D., S86 (240)  
 Flaherty K., S25 (73)  
 Flaherty K.T., S8 (11), S84 (235), S86 (238)  
 Flechsig S., S12 (33)  
 Flores J., S13 (37), S14 (38), S111 (313), S121 (337)  
 Flores R., S110 (309)  
 Florou V., S116 (326)  
 Fodale V., S26 (77)  
 Foiani M., S55 (154)  
 Foley C., S103 (290)  
 Foley K., S27 (79)  
 Fontana E., S82 (230)  
 Foradada-Felip L., S53 (149)  
 Foradada L., S24 (68), S38 (106), S44 (123), S46 (129)  
 Forster-Gross N., S35 (100)  
 Forster T., S97 (269)  
 Forte G., S50 (138)  
 Foster J.H., S28 (82)  
 Foster P., S20 (58)  
 Foulks J., S47 (131), S57 (160)

Fournier S., S61 (171), S99 (278), S100 (279)  
 Fourtounis J., S61 (171)  
 Fox A., S48 (134)  
 Fox E., S28 (82)  
 Fraga Timiraos A., S16 (46)  
 Fram R.J., S125 (352)  
 Freeman A., S64 (181)  
 French P.J., S42 (118)  
 Fretland A.J., S100 (279)  
 Freund C., S109 (306)  
 Frezza A.M., S68 (191)  
 Friboulet L., S78 (218)  
 Friedman G.K., S28 (82)  
 Fritsch C., S14 (39)  
 Fuchigami H., S87 (242)  
 Fuentes Antras J., S31 (87)  
 Fujino T., S78 (218)  
 Fukushima H., S73 (204)  
 Fulmer J., S87 (243)  
 Fulton J., S81 (226), S81 (227)  
 Fu N., S94 (260)  
 Funingana G., S117 (330)  
 Füreder T., S44 (124)  
 Furman W.L., S28 (82)  
 Furuuchi K., S87 (242), S87 (243), S88 (244)  
 Fu S., S7 (9), S10 (19)  
 Fu T., S79 (221)

**G**

Gabay Y., S9 (16)  
 Gabere M., S128 (360)  
 Gabra H., S72 (202)  
 Gabra M.M., S94 (260)  
 Gadde M., S108 (305)  
 Gadgeel S.M., S6 (8)  
 Gajendran C., S125 (349)  
 Gallego S., S28 (81)  
 Gallo D., S61 (171), S99 (278)  
 Gallo-Oller G., S28 (81)  
 Galvani A., S2 (3LBA), S17 (48)  
 Galvao V., S49 (137), S70 (196)  
 Ganapathy S., S37 (105)  
 Gandhi L., S31 (89), S67 (188)  
 Gañez-Zapater A., S61 (172)  
 Gao J., S14 (39)  
 Gao S.P., S10 (21)  
 Gara M., S7 (10)  
 Garcia E., S125 (350)  
 Garcia Raposo F., S19 (56)  
 Garcia-Foncillas J., S108 (303), S121 (337)  
 Garcia-Maldonado E., S110 (308)  
 Garcia Mateos J., S115 (324)  
 García Mateos J., S114 (321)  
 García-Sancho A.M., S31 (89)  
 Garmey E.G., S34 (96)  
 Garon E.B., S21 (61)  
 Garralda Cabanas E., S23 (67)  
 Garralda E., S5 (7), S17 (50), S48 (133), S49 (137), S70 (196)  
 Garrett J.E., S100 (281)  
 Garrett M., S19 (56)  
 Garrido-Shaqfeh S., S103 (290)  
 García Cao I., S95 (264)  
 Gaspar K., S90 (250)  
 Gastinne T., S31 (89)  
 Gattis B., S36 (102)  
 Gaudio E., S65 (182), S65 (184), S89 (246), S107 (301)  
 Gaudreau P.O., S31 (87)  
 Gauthier K., S20 (58)  
 Gavande N.S., S100 (281)  
 Gayle S., S7 (10)  
 Geier A., S126 (354)  
 Gelber C., S87 (241), S90 (249)  
 Gelb T., S117 (330)  
 Gence R., S55 (153)  
 Georgakopoulou A., S19 (53)  
 George B., S32 (91), S96 (265)  
 Gerard B., S76 (212)  
 Gera S., S126 (354)  
 Gerlach D., S54 (150)  
 German R., S51 (143)  
 Gettinger S., S84 (235)  
 Ghaidi F., S39 (109)  
 Gharavi R., S125 (352)  
 Gianellini L., S2 (3LBA)  
 Gianneschi N., S36 (102)  
 Gibbs J., S125 (352)  
 Gibson N., S1 (1LBA)  
 Gien L., S86 (238)  
 Gil Bazo I., S122 (341)  
 Gillies R., S90 (250)  
 Giménez-Capitán A., S89 (247)  
 Ginzburg Y.Z., S100 (279)  
 Giuliano C., S27 (78)  
 Giuntini F., S38 (108), S44 (123), S47 (130), S53 (149)  
 Gi Y.J., S52 (146)  
 Glodzik D., S99 (278)  
 Gluskin R., S9 (16)  
 Gluza K., S15 (45)  
 Gobec S., S124 (346)  
 Gobeil P., S127 (358)  
 Gogoi R., S48 (134)  
 Goh J., S55 (154)  
 Gokhale P.C., S37 (105)  
 Golas A., S56 (158)  
 Goldman J., S82 (228)  
 Goldner N., S108 (305)  
 Golfier S., S9 (17)  
 Gomez-Pinillos A., S125 (352)  
 Gondela A., S15 (45)  
 Gondi V., S82 (230)  
 Gongora C., S98 (274)  
 Gong S., S26 (75)  
 González-Larreategui Í., S44 (123), S46 (129), S47 (130), S53 (149)  
 Gonzalez M., S49 (137)  
 Goodrich D., S4 (5)  
 Goossens A., S125 (350)  
 Gopalan A., S4 (5)  
 Gordon J., S80 (224)  
 Górecka-Minakowska K., S104 (292)  
 Gore S., S7 (9)  
 Górka M., S90 (248)  
 Gorman T., S19 (56)

- Goshayeshi A., S110 (309)  
 Gosu R., S125 (349)  
 Goto K., S75 (209)  
 Gotur D., S26 (75)  
 Goverse G., S114 (321)  
 Gowda C., S29 (83)  
 Goyal L., S93 (257), S116 (326)  
 Gozo M., S125 (350)  
 Graf R., S127 (357)  
 Graham K., S9 (17)  
 Grahovac J., S114 (322)  
 Graidist P., S45 (126), S71 (200), S73 (205), S113 (318)  
 Grandis J., S128 (359)  
 Gray R., S25 (73)  
 Gray R.J., S8 (11), S84 (235), S86 (238)  
 Gray Yarbrough W., S119 (334)  
 Green D., S103 (290)  
 Green E., S81 (225)  
 Green J., S6 (8), S125 (352)  
 Greulich H., S9 (17)  
 Grevel J., S28 (82)  
 Griffin J., S64 (181)  
 Griffith J., S92 (255)  
 Grigore I., S94 (260)  
 Grigoriadis A., S50 (139), S66 (186)  
 Griswold-Prenner I., S116 (327)  
 Groen H.J.M., S21 (61)  
 Gronchi A., S68 (191)  
 Gross J., S17 (49)  
 Grossman L., S48 (134)  
 Grudniewska M., S43 (119)  
 Grueso J., S24 (68), S38 (106), S46 (129), S47 (130)  
 Grunenberger A., S21 (62)  
 Grussu F., S70 (196)  
 Gryaznov S., S30 (86)  
 Grycuk K., S56 (158)  
 Guan Y., S110 (309)  
 Guarnieri A., S81 (226), S81 (227)  
 Guenther M., S94 (259)  
 Gu H., S43 (121)  
 Guidetti M., S21 (62)  
 Guirola M., S61 (172)  
 Gu L., S26 (75)  
 Gulley J.L., S5 (6)  
 Gunaydin U., S117 (330)  
 Gunnell E., S104 (291)  
 Gunn J., S118 (332)  
 Guo F., S22 (65)  
 Guo J., S118 (332)  
 Guo S., S9 (15), S41 (114), S43 (121), S44 (122), S96 (266), S98 (273)  
 Gürgen D., S12 (33)  
 Gustafson D., S42 (117), S107 (300)  
 Guthof N., S101 (282)  
 Gutierrez J.L., S55 (152)  
 Gutierrez M., S67 (188)  
 Guzman C., S60 (169)  
 Guzman-Perez A., S29 (84)  
 Guzman S., S60 (169)  
 Gyuris J., S40 (112)
- H**
- Hackner K., S44 (124)  
 Hadar N., S31 (89)  
 Hadoux J., S11 (22)  
 HaDuong J., S28 (82)  
 Hagerman L., S31 (87)  
 Hahm K.S., S53 (147)  
 Haider A., S64 (181)  
 Haider S., S50 (139)  
 Haines B., S84 (234)  
 Hakozaiki Y., S47 (132)  
 Halleen J., S122 (342)  
 Hallsworth A., S35 (98)  
 Hamel E., S65 (184)  
 Hamilton E., S36 (101), S88 (245)  
 Hamilton S., S25 (73)  
 Hamilton S.R., S8 (11), S84 (235), S86 (238)  
 Hammond G., S112 (315)  
 Han J., S3 (1)  
 Han J.E., S94 (258), S105 (295)  
 Han J.H., S95 (263)  
 Han J.S., S60 (168)  
 Hanna D., S32 (91)  
 Hansbury M., S79 (220)  
 Han Y., S100 (279)  
 Han Y.C., S86 (239)  
 Harari P.M., S45 (125)  
 Harbison R.A., S61 (170)  
 Harnden A., S104 (291)  
 Harris L., S25 (73)  
 Harris L.N., S8 (11), S84 (235), S86 (238)  
 Harrison D.J., S46 (128), S66 (185)  
 Harris P., S86 (238)  
 Harvey R.D., S31 (89)  
 Hasegawa K., S88 (244)  
 Hata A.N., S29 (84), S78 (218)  
 Hayes A., S35 (98), S104 (291), S126 (353)  
 Haygood L., S81 (227)  
 Hays J., S25 (73)  
 He A., S106 (298)  
 Hearn K., S57 (159)  
 Heavey S., S64 (181)  
 Heffernan T.P., S54 (150)  
 Heinze K., S11 (30)  
 Heist R., S72 (201)  
 Heist R.S., S21 (61)  
 Henke E., S11 (30)  
 Henkelman S., S49 (136)  
 Hennessy B., S64 (180)  
 Henry J., S82 (230)  
 Heo D.S., S110 (311), S120 (335)  
 Herman J., S128 (359)  
 Hermsen M., S9 (17)  
 Hernandez-Guerrero T., S5 (7)  
 Hernandez T., S121 (337)  
 Heron-Milhavet L., S98 (274)  
 Herpers B., S114 (321), S115 (324)  
 Herterich S., S11 (30)  
 Hervieu A., S75 (209)  
 Hewison S., S19 (56)  
 He Y., S105 (296)  
 Heymach J., S1 (1LBA)
- Hicks H., S58 (162)  
 Hidalgo D., S40 (111)  
 Hillig R.C., S9 (17)  
 Hill L., S108 (305)  
 Hill S.M., S104 (293)  
 Hilton J., S31 (87)  
 Hindi N., S108 (303)  
 Hindley C., S57 (159)  
 Hinkel M., S54 (150)  
 Hirai H., S77 (214)  
 Hirashima Y., S88 (244)  
 Hirsl L., S69 (195)  
 Hiss D., S52 (144)  
 Hitchens L., S66 (186)  
 Hoadley W.E., S10 (19)  
 Hocker M., S81 (225)  
 Ho E.C.H., S86 (240)  
 Hoelder S., S104 (291)  
 Hoffman I., S16 (47)  
 Hoffman M.C., S19 (57)  
 Hoffmann J., S12 (32), S41 (115)  
 Hoffman R., S100 (279)  
 Hofmann J., S12 (33)  
 Hofmann M.H., S54 (150)  
 Højgaard M., S118 (331)  
 Hollebecque A., S11 (22)  
 Holliday N., S19 (56)  
 Holloway K., S19 (53)  
 Holz J.B., S123 (345)  
 Hong D., S34 (95), S72 (201)  
 Hong D.S., S7 (9), S10 (19)  
 Hong E., S37 (104)  
 Hong N.H., S37 (103)  
 Hood J., S34 (97)  
 Hood T., S74 (208)  
 Hoppe M.M., S55 (154)  
 Horan J.C., S76 (212)  
 Hornemann T., S3 (2)  
 Hornsveld M., S114 (321)  
 Horrigan S., S19 (53)  
 Hou S., S58 (163)  
 Hou X., S54 (151)  
 Hsu J., S5 (6)  
 Hua H., S91 (251), S91 (252)  
 Hua L., S44 (122)  
 Huang A., S26 (75), S84 (233), S84 (234)  
 Huang C., S41 (114), S113 (317)  
 Huang F., S28 (82)  
 Huang H.T., S103 (290)  
 Huang J., S17 (50), S44 (122)  
 Huang P., S62 (174)  
 Huang W., S41 (116)  
 Huang W.S., S85 (236)  
 Huang X.Y., S34 (96)  
 Huaying D., S96 (265)  
 Hubbell J., S103 (288)  
 Huber A., S110 (308)  
 Huckvale R., S104 (291)  
 Hudkins R., S16 (47)  
 Huff M.R., S29 (84)  
 Hughes R.E., S113 (319)  
 Huguet-Pradell J., S120 (336)  
 Hu H., S25 (72)  
 Hui R., S36 (101)  
 Hummel J., S79 (220)

Huo L., S52 (146), S79 (220)  
 Hu S., S43 (120), S53 (148)  
 Hussain S., S116 (327)  
 Hu X., S125 (350)  
 Hwang D.J., S105 (296)

**I**

Iacone R., S93 (257)  
 Ibanez G., S74 (208)  
 Ibrahim Hashim A., S90 (250)  
 Idate R., S95 (261)  
 Igartua K., S23 (66)  
 Iida M., S45 (125)  
 Iranzo Gomez P., S26 (74)  
 Ill Sims, R., S33 (94)  
 Iliou M., S63 (177)  
 Inamura K., S30 (85)  
 Inglese M., S49 (135)  
 Invrea F., S63 (176)  
 Iqbal I.K., S69 (193)  
 Irimia A., S19 (54)  
 Irrera P., S90 (250)  
 Isacchi A., S2 (3LBA), S17 (48)  
 Isaeva N., S119 (334)  
 Ishihara J., S103 (288)  
 Ishiyama N., S86 (239)  
 Islam S., S49 (135), S119 (333)  
 Issabayeva G., S37 (104)  
 Italiano A., S11 (22)  
 Ito T., S29 (84)  
 Ivy S.P., S7 (9)  
 Iwamoto F., S82 (230)  
 Iyer G., S10 (21), S25 (73)  
 Iyer K., S22 (63)  
 Iyer S., S16 (47)

**J**

Jacob R., S54 (150)  
 Jafri S., S110 (309)  
 Jagdeo J., S117 (329)  
 Jahic H., S26 (75)  
 Jalluri R., S81 (226), S81 (227)  
 Jamborcic A., S81 (225)  
 James E., S126 (353)  
 Janardan A., S96 (265)  
 Jandrig B., S12 (33)  
 Jang H.S., S60 (168), S102 (287)  
 Jang S., S35 (99)  
 Janz M., S41 (115)  
 Jauch-Lembach J., S67 (188)  
 Jauset T., S38 (108), S46 (129)  
 Jaynes P., S55 (154)  
 Jean-Claude B., S16 (46)  
 Jemimah S., S55 (154)  
 Jenster G.W., S43 (119)  
 Jeon D., S35 (99)  
 Jeong E., S96 (267), S96 (268)  
 Jeong S., S96 (268)  
 Jeon Y.K., S120 (335)  
 Jeung H.C., S37 (104)  
 Jewett I., S86 (239)  
 Jeyasekharan A.D., S55 (154)

Jhaveri K., S82 (228)  
 Jiao Z., S18 (51)  
 Ji L., S21 (61)  
 Jimeno J., S39 (110)  
 Jimenez Schumacher A., S38 (106)  
 Jin L., S20 (58), S103 (290)  
 Joanne Jeou-Yuan C., S114 (320)  
 Joe A.K., S122 (341)  
 Joe R., S57 (160)  
 Jo H., S20 (59)  
 Johnson A., S10 (19), S81 (227)  
 Johnson M., S52 (145), S80 (224),  
 S122 (341)  
 Johnson M.L., S6 (8), S92 (256)  
 John T., S34 (95)  
 Jones E., S62 (175)  
 Jones K., S35 (98)  
 Jonjic S., S69 (195)  
 Jonkers J., S50 (139)  
 Jonsson P., S29 (84)  
 Joseph J., S44 (124)  
 Joshi J., S39 (109)  
 Jossierand V., S21 (62)  
 Joung M.K., S60 (168)  
 Joyce S., S128 (359)  
 Juanola J., S38 (106)  
 Juehling F., S93 (257)  
 Jukić M., S124 (346)  
 Jung H., S123 (344)  
 Jung H.J., S99 (275)  
 Jung J., S20 (59)  
 Jung M., S85 (237)  
 Junquera C., S39 (110)  
 Juric D., S125 (352)  
 Juszczyński P., S56 (158)

**K**

Kadekar P., S117 (328)  
 Kaesshaefer S., S82 (230)  
 Kaghazchi B., S46 (128), S66 (185)  
 Kähkönen T., S122 (342)  
 Kaiser B., S99 (278)  
 Kalinsky K., S8 (11)  
 Kalkan B., S15 (43)  
 Kallius M., S11 (30)  
 Kalusa A., S126 (353)  
 Kamal A., S52 (145)  
 Kamata R., S47 (132)  
 Kamath S., S116 (326)  
 Kamburov A., S9 (17)  
 Kandola N., S57 (159)  
 Kang H., S20 (59)  
 Kang M., S23 (66)  
 Kang O.Y., S37 (104)  
 Kannan K., S125 (352)  
 Kann L., S31 (89)  
 Kansara S., S24 (71)  
 Kao S., S1 (2LBA)  
 Kapilashrami K., S79 (220)  
 Kaplan A., S110 (309)  
 Karlsson J., S45 (127)  
 Karnam K., S33 (92), S33 (93)  
 Karp D.D., S7 (9), S10 (19)  
 Kar R., S56 (156)  
 Karsai G., S3 (2)  
 Karsli-Uzunbas G., S9 (17)  
 Karthaus W., S4 (5)  
 Kasar S., S125 (352)  
 Kasem M., S125 (350)  
 Kashima Y., S47 (132)  
 Katherina H., S11 (30)  
 Kato H., S88 (244)  
 Kato M., S77 (214)  
 Katraggada M., S5 (6)  
 Kaufmann G.F., S105 (296)  
 Kaur J., S24 (68), S38 (108), S44 (123),  
 S53 (129)  
 Kavanagh-Williamson M., S97 (269)  
 Kayabolen A., S69 (192)  
 Kayali O., S65 (183)  
 Kc S., S34 (97)  
 Keam B., S110 (311), S120 (335)  
 Ke H., S18 (51), S122 (343)  
 Kellenberger L., S35 (100), S56 (155)  
 Kelly F., S117 (330)  
 Kelly J., S64 (181)  
 Kemper R.A., S76 (212)  
 Kendrew J., S19 (56)  
 Kesner A., S3 (1)  
 Kessler L., S58 (161)  
 Khalique S., S117 (330)  
 Khan N., S127 (356)  
 Kharbanda S., S51 (141)  
 Khodos I., S27 (78)  
 Kida K., S52 (146)  
 Kim A., S102 (287)  
 Kim B.J., S99 (275)  
 Kim D., S35 (99)  
 Kim D.W., S72 (201), S110 (311),  
 S120 (335)  
 Kim E., S35 (99)  
 Kim H., S99 (275)  
 Kim J., S35 (99)  
 Kim K., S10 (21)  
 Kim K.H., S85 (237)  
 Kim M., S35 (99), S85 (237), S110 (311),  
 S120 (335)  
 Kim M.H., S99 (275)  
 Kim R., S116 (326)  
 Kim S., S79 (220), S110 (311),  
 S120 (335), S128 (359)  
 Kim S.S., S94 (258), S105 (295)  
 Kim S.W., S1 (2LBA)  
 Kim T.M., S110 (311), S120 (335)  
 Kim Y., S20 (59), S71 (198)  
 Kim Y.C., S75 (209)  
 Kindler H., S31 (89)  
 King B., S113 (319)  
 King-Underwood J., S20 (59)  
 Kinoshita R., S122 (342)  
 Kirchner K., S117 (328)  
 Kirkin V., S104 (291)  
 Kirschbaum M., S17 (50)  
 Kiselyov K., S112 (315), S127 (356)  
 Klefström J., S98 (272)  
 Kleppa M.J., S40 (113)  
 Kline J., S110 (309)  
 Knuehl C., S89 (247)

- Kobelt D., S12 (33)  
 Koblisch H., S79 (220)  
 Koehler M., S100 (279)  
 Koganemaru S., S87 (242)  
 Koh J., S120 (335)  
 Kohl N.E., S76 (212)  
 Kollarovic G., S66 (186)  
 Konde A., S99 (277)  
 Konstanze L., S45 (125)  
 Kornatowski T., S90 (248)  
 Korr D., S9 (17)  
 Kortchak S., S87 (241)  
 Kos J., S124 (346)  
 Kostura M., S40 (113)  
 Kostyrko K., S54 (150)  
 Kota A., S33 (93)  
 Kothari A., S119 (334)  
 Kourtis S., S61 (172)  
 Kowalczyk P., S104 (292)  
 Ko Y.H., S65 (183)  
 Krastev D., S99 (277)  
 Krauthammer M., S3 (2)  
 Krebs S., S3 (1)  
 Kryczka R., S61 (171)  
 Krzemień D., S15 (45)  
 Kshirsagar A.R., S56 (156)  
 Kubik M., S128 (359)  
 Kuboki Y., S87 (242)  
 Kucan P., S69 (195)  
 Kucia-Tran J., S83 (232)  
 Kuklin N., S127 (355)  
 Kulusch J., S103 (290)  
 Kumamoto A., S59 (164)  
 Kumar A., S69 (193)  
 Kumar P., S74 (208)  
 Kumar R.N., S69 (193)  
 Kumar V., S31 (87)  
 Kunkel M., S62 (175)  
 Kuo-Chu L., S114 (320)  
 Kural C., S50 (140)  
 Kural M., S50 (140)  
 Kurtz K., S3 (1)  
 Kushwaha R., S110 (309)  
 Kuś K., S15 (45)  
 Kuzmic P., S29 (84)  
 Kwiatek M., S31 (89)  
 Kwok-Parkhill A., S59 (164)  
 Kwon H.S., S37 (104)  
 Kwon M., S94 (258), S105 (295)  
 Kwon Y., S87 (241)
- Lane H., S35 (100), S56 (155)  
 Lang A., S121 (337)  
 Langat P., S3 (3)  
 Langlands J., S39 (109)  
 Laniado A., S9 (16)  
 LaPlaca D., S43 (120), S53 (148)  
 Larroque A.L., S16 (46)  
 Larson S., S3 (1)  
 Lassen U., S118 (331)  
 Laterreur N., S99 (278)  
 Laudeman J., S62 (175)  
 Laus G., S122 (341)  
 Lauterwasser J., S19 (56)  
 Lawrence J., S36 (101)  
 Lawrence L., S59 (164)  
 Lawson K., S20 (58)  
 Le B., S125 (350)  
 Lebedinsky C., S57 (160)  
 Le Bihan Y.V., S104 (291)  
 Lecky E., S51 (143)  
 Le Coz J., S44 (124)  
 Lee B.I., S95 (261)  
 Lee D., S20 (59), S37 (104)  
 Lee D.K.C., S94 (260), S106 (298)  
 Lee D.Y., S53 (147)  
 Lee H.J., S85 (237)  
 Lee J., S52 (146), S72 (201), S78 (218)  
 Lee K., S35 (99)  
 Lee K.H., S1 (2LBA)  
 Lee M., S35 (99)  
 Lee N.R., S85 (237)  
 Lee S., S20 (59)  
 Lee S.J., S85 (237)  
 Lee T., S125 (350)  
 Lefebvre D., S92 (255)  
 Leleti M., S103 (290)  
 Le Moigne R., S37 (103)  
 Le Mouhaer S., S21 (61)  
 Lentzas A., S103 (289)  
 Leoni M., S58 (161)  
 Leriche G., S81 (225)  
 Letai A., S51 (143)  
 Levenets O., S15 (45)  
 Levesque M., S3 (2), S52 (145),  
 S115 (325)  
 Levy D., S20 (59)  
 Levy M., S100 (279)  
 Le X., S72 (201)  
 Liao C.Y.A., S116 (326)  
 Liao K., S20 (58)  
 Li B., S91 (251), S91 (252), S91 (253)  
 Liesa M., S40 (113)  
 Li H., S18 (51), S118 (332), S122 (343)  
 Li J., S27 (79), S57 (160), S92 (256)  
 Li L., S72 (202), S100 (279)  
 Lima D.G., S76 (211)  
 Lima Ribeiro M., S112 (314)  
 Lim B.H., S37 (104)  
 Lim H.J., S37 (104)  
 Lim S.K., S35 (99)  
 Lin B., S19 (54)  
 Lin C.Y., S74 (208)  
 Lindblad K.E., S120 (336)  
 Lindsay C., S26 (74)  
 Lin J., S1 (2LBA)
- Lin J.J., S6 (8)  
 Lin J.R., S51 (143)  
 Lin N., S36 (101)  
 Lin S., S91 (251), S91 (252)  
 Lin T.A., S86 (239)  
 Li P., S19 (54)  
 Li R., S41 (116)  
 Li S., S88 (244)  
 Li T., S3 (3)  
 Litherland K., S35 (100)  
 Littlefield B.A., S106 (299)  
 Littlewood P., S23 (67)  
 Liu A., S27 (78)  
 Liu H., S52 (146)  
 Liu J.F., S37 (105)  
 Liu K., S5 (6)  
 Liu R., S15 (42)  
 Liu S., S51 (141), S77 (215), S78 (217),  
 S103 (290), S110 (309)  
 Liu X., S125 (350)  
 Liu Z., S41 (116)  
 Livi L., S124 (348)  
 Liv N., S50 (139)  
 Li W., S77 (215), S78 (217)  
 Li X., S81 (225)  
 Li Y., S41 (116)  
 Li Z., S80 (224)  
 Lizette F., S121 (337)  
 Liebaria A., S25 (72)  
 Llovet J.M., S120 (336)  
 Lobie P.E., S62 (174)  
 Loi M., S124 (348)  
 Lombardo S., S84 (233)  
 Lombard P., S121 (339), S121 (340)  
 Lombardi Borgia A., S17 (48)  
 Longo D., S90 (250)  
 Long Ye L.Y., S27 (79)  
 Lopes G., S6 (8)  
 López-Alemán R., S24 (69)  
 Lopez-Alvarez M., S108 (303)  
 Lopez-Contreras F., S59 (165)  
 Lopez Muñoz R., S60 (169)  
 López-Estévez S., S24 (68), S38 (106),  
 S44 (123), S46 (129), S53 (149)  
 Lopez-Jimena B., S97 (269)  
 Lopez-Muñoz R., S59 (165)  
 López S., S47 (130)  
 Loponte S., S26 (77)  
 Lord C., S66 (186), S99 (277)  
 Lord C.J., S50 (139)  
 Lorient Y., S11 (22)  
 Lostes J., S49 (137)  
 Lott A., S31 (87)  
 Lou Y., S57 (160)  
 Lovati E., S27 (78)  
 Love J., S4 (5)  
 Lo Y., S79 (220)  
 Lopez Muñoz R., S60 (169)  
 Lucas M., S22 (64), S23 (66), S86 (239)  
 Lufino M.M.P., S67 (189)  
 Lugowska I., S23 (67)  
 Lu H., S54 (150)  
 Lu J., S74 (207)  
 Lujambio A., S120 (336)  
 Lu K., S125 (350)
- L**
- Lacroix L., S11 (22)  
 Ladanyi M., S27 (78)  
 Ladd B., S29 (84)  
 Lafleur J., S44 (124)  
 Lahn M., S80 (223)  
 Lakhani N., S14 (38), S82 (230),  
 S121 (337)  
 Lamani M., S103 (290), S110 (309)  
 Lam L., S42 (118)  
 Lana S., S95 (261)  
 Landlinger C., S124 (347)

- Lu M., S88 (245)  
Lund J., S58 (162)  
Luo J., S77 (215), S78 (217)  
Luo S., S41 (114)  
Lu P., S47 (132)  
Lu S., S1 (2LBA), S75 (209)  
Lv C., S27 (79)  
Lynch M., S14 (38)  
Lyons J., S57 (159), S83 (232)
- M**
- Macarulla T., S48 (133), S49 (137)  
Macaya I., S47 (130)  
Macedougall J., S38 (107)  
Machida T., S73 (204)  
Macy M., S28 (82)  
Mad-Adam N., S45 (126)  
Madej M., S15 (45), S114 (321)  
Maertens G., S97 (269)  
Maestro R., S68 (191), S108 (303)  
Magdaleno A., S28 (81)  
Magnaghi P., S17 (48)  
Mahalingam D., S82 (228)  
Mahipal A., S82 (228)  
Mahnke L., S2 (3LBA)  
Mailly L., S93 (257)  
Makower D., S36 (101)  
Ma L., S27 (79)  
Malik S., S58 (161)  
Mallender W., S26 (75)  
Mandelboim O., S69 (195)  
Mangoni M., S124 (348)  
Mansilla M., S60 (169)  
Mansouri S., S121 (339), S121 (340)  
Mansurov A., S103 (288)  
Manyam G., S52 (146)  
Manzanares M., S126 (354)  
Mao B., S43 (121)  
Maqueda-Marcos S., S24 (69)  
Marby K., S125 (350)  
Marcato P., S97 (270)  
Marco-Brualla J., S39 (110)  
Marczak M., S90 (248)  
Mardones C., S51 (142)  
Margarido A., S126 (353)  
Marineau J., S94 (259)  
Marinello A., S11 (22), S26 (74)  
Marques C.S., S65 (182)  
Marra P., S50 (139)  
Marshall C.G., S61 (171)  
Marsolais C., S117 (328)  
Marszalek J.R., S54 (150)  
Martial L., S43 (120)  
Martin A., S60 (169), S66 (186)  
Martin-Broto J., S108 (303)  
Martin C.M., S76 (212)  
Martínez A., S48 (133)  
Martínez De Mena R., S39 (110)  
Martinez E., S5 (7)  
Martínez Bueno A., S82 (228)  
Martínez-Martín S., S24 (68), S46 (129), S47 (130), S53 (149)  
Martín-Fernández G., S38 (108), S53 (149)  
Mártin-Fernández G., S24 (68)  
Martín G., S46 (129)  
Martin M., S112 (316)  
Martin-Martin A., S59 (165)  
Martino G., S61 (171)  
Martin-Romano P., S11 (22)  
Martin S.A., S64 (179)  
Martínez Martín S., S44 (123)  
Maruca A., S65 (184)  
Maruzzelli S., S2 (3LBA)  
Marzac C., S11 (22)  
Mascarella M., S128 (359)  
Mascaró C., S67 (189), S68 (190)  
Masiero M., S101 (284)  
Masilionis I., S4 (5)  
Massó-Vallés D., S38 (108), S46 (129), S53 (149)  
Mathauda-Sahota G., S36 (101)  
Matrana M., S32 (91)  
Matres A., S48 (133)  
Matsui J., S88 (244)  
Matsumoto K., S88 (244)  
Matsumura Y., S47 (131), S57 (160)  
Mattar M., S27 (78)  
Matulonis U.A., S37 (105)  
Maurer B., S124 (347)  
Mawji N.R., S72 (203)  
Max M., S81 (227)  
Maxwell J., S26 (75), S63 (178), S84 (233)  
May S., S19 (53)  
Mazières J., S55 (153)  
Mazutis L., S4 (5)  
McCann H., S35 (98)  
McCarthy C., S19 (56)  
McCarthy N., S36 (101)  
McClellan B., S77 (213)  
McCourt C., S8 (11)  
McCulloch L., S82 (228)  
McDevitt M., S3 (1)  
McKean M., S34 (95), S82 (230)  
McKee T., S121 (339)  
McLaren A., S82 (230)  
McLean B., S81 (227)  
McQueeny K., S51 (143)  
McShane L., S25 (73)  
McShane L.M., S8 (11), S84 (235), S86 (238)  
Mcsheehy P., S35 (100), S56 (155)  
Medico E., S63 (176)  
Meiller J., S64 (180)  
Meisel J., S36 (101)  
Meister P., S126 (353)  
Melear J., S57 (160)  
Melica M.E., S124 (348)  
Melo C.M.P., S106 (298)  
Melo-Zainzinger G., S54 (150)  
Mena J., S3 (2)  
Menard M., S59 (164)  
Mender I., S30 (86)  
Mendes-Pereira A., S50 (139)  
Mendoza-Munoz P., S100 (281)  
Meng R., S97 (271)  
Meniawy T., S34 (95)  
Mensah A.A., S80 (223)  
Mente S., S76 (212)  
Menz S., S9 (17)  
Mercer K., S29 (83)  
Merchant F., S127 (358)  
Merchant M., S22 (64), S23 (66)  
Mercurio C., S108 (304)  
Meric-Bernstam F., S7 (10), S7 (9), S10 (19)  
Merikoski N., S117 (329)  
Merino-Garcia J., S108 (303)  
Merlino G., S89 (246)  
Mertz J., S33 (94)  
Metro G., S26 (74)  
Metsu S., S97 (269)  
Meyer M., S93 (257)  
Meyerson M., S9 (17)  
Mezquita L., S26 (74)  
Mica I., S83 (231)  
Micallef S., S9 (16)  
Michalik K., S15 (45)  
Michel R., S82 (230)  
Michels T., S125 (350)  
Micol J.B., S11 (22)  
Miggelenbrink A., S22 (63)  
Miles D., S103 (290), S110 (309)  
Milewicz M., S104 (292)  
Milgram B.C., S29 (84)  
Miller D., S104 (291), S110 (308)  
Miller D.D., S105 (296)  
Miller D.H., S24 (71)  
Miller E., S86 (240)  
Mills G.B., S7 (9)  
Minsu K., S123 (344)  
Min Yu M.Y., S27 (79)  
Mira A., S18 (52)  
Mirkina I., S124 (347)  
Miró-Canturri A., S61 (172)  
Mishra V., S58 (161)  
Missineo A., S26 (77)  
Mitchell E., S25 (73)  
Mitchell E.P., S8 (11), S84 (235), S86 (238)  
Mitri Z., S36 (101)  
Mitrović A., S124 (346)  
Mitula F., S90 (248)  
Mitura A., S13 (36)  
Miura T., S88 (244)  
Mizuta H., S78 (218)  
Modur V., S73 (206), S76 (211)  
Moebius D., S43 (120), S53 (148), S94 (259)  
Mohamed H., S11 (30)  
Mohammad A., S51 (141)  
Mohanty S., S20 (59)  
Molina Arcas M., S62 (173)  
Molina-Vila M.A., S89 (247)  
Monaco P., S24 (69)  
Mondaza Hernandez J.L., S108 (303)  
Monette S., S3 (1)  
Montagnoli A., S2 (3LBA), S17 (48)  
Montalbano A., S65 (184)  
Montalbetti C., S26 (77)  
Montironi C., S120 (336)



Mooney L., S19 (56)  
 Moon F., S128 (359)  
 Moore C., S62 (173)  
 Morales J., S46 (129)  
 Morazzo S., S50 (138)  
 Moreno C., S13 (37)  
 Moreno Garcia V., S122 (341)  
 Moreno I., S122 (341)  
 Moreno L., S28 (81)  
 Moreno-Loshuertos R., S39 (110)  
 Moreno V., S5 (7), S72 (201),  
 S75 (209), S111 (313), S116 (326),  
 S121 (337)  
 Mor G., S48 (134)  
 Moriarty A., S13 (37), S14 (38),  
 S111 (313), S121 (337)  
 Morita S., S122 (342)  
 Morita T.Y., S47 (132)  
 Morley A., S40 (112)  
 Morley H., S117 (330)  
 Moro-Sibilot D., S75 (209)  
 Moroz A., S90 (248)  
 Morris J., S62 (175)  
 Morris M., S4 (5)  
 Morrison D., S18 (52)  
 Morris S., S61 (171), S99 (278)  
 Morris S.J., S100 (279)  
 Mortier J., S9 (17)  
 Moscow J.A., S84 (235)  
 Mosher R., S88 (245)  
 Motley W., S33 (94), S119 (333)  
 Moura D.S., S108 (303)  
 Mroczkiewicz M., S90 (248)  
 Mueller M., S19 (53)  
 Mugarza E., S62 (173)  
 Mukerji A., S51 (143)  
 Mukherjee S., S69 (193)  
 Muller F., S40 (112)  
 Müller-Knapp S., S83 (231)  
 Muller M., S93 (257)  
 Multani A., S52 (146)  
 Munne P., S98 (272)  
 Muñoz-Couselo E., S70 (196)  
 Muñoz E., S48 (133)  
 Muñoz-Urbe M., S59 (165)  
 Murali V., S24 (71)  
 Muraoka H., S77 (214)  
 Mustafa N., S109 (307)  
 Musteanu M., S18 (52)  
 Muyot L., S31 (87)  
 Muzaffar J., S79 (221)

## N

Na Ayudhya C., S113 (318)  
 Nadworny S., S85 (236)  
 Naffar-Abu Amara S., S74 (208)  
 Nagalo B.M., S128 (360)  
 Nagasaka M., S1 (2LBA), S72 (201),  
 S122 (341)  
 Nagashima T., S30 (85)  
 Naing A., S7 (9), S10 (19)  
 Nakashima J., S74 (208)  
 Nakatsuru Y., S57 (159)

Naltet C., S82 (228)  
 Nance M., S128 (359)  
 Nandigama R., S11 (30)  
 Napoli S., S107 (302)  
 Narasimhan N., S85 (236)  
 Narayanan R., S105 (296)  
 Nathanson D., S32 (90)  
 Natrajan R., S50 (139), S99 (277)  
 Navakanth Rao V., S114 (320)  
 Navarrete J., S51 (142)  
 Navarro-Marchal S., S113 (319)  
 Navarro N., S28 (81)  
 Nayak S., S37 (105)  
 Neal M., S16 (47)  
 Nebreda A.R., S95 (264)  
 Nedbal J., S70 (197)  
 Nehme Z., S93 (257)  
 Nellore K., S69 (193)  
 Nelson K., S16 (47)  
 Nevarez R., S19 (54)  
 Newton G., S126 (353)  
 Ng K., S51 (143)  
 Ngoi N., S7 (9), S10 (19)  
 Ng P.Y., S86 (239)  
 Ng T., S31 (87), S70 (197)  
 Nguyen L., S78 (218)  
 Nibbio M., S26 (77)  
 Nicotra C., S11 (22)  
 Niehues M., S9 (17)  
 Nieva J., S58 (163)  
 Niewel M., S5 (7), S46 (129)  
 Niewiarowski A., S117 (330)  
 Niewola-Staszowska K., S80 (223)  
 Niklason L., S50 (140)  
 Nilsson J., S45 (127)  
 Nilsson L., S45 (127)  
 Nir R., S40 (112)  
 Nishio S., S88 (244)  
 Nishizono Y., S30 (85)  
 Nobre C., S78 (218)  
 Noe C., S74 (208)  
 Nogai H., S23 (67)  
 Nonell L., S44 (123)  
 Noriega-Rivera R., S79 (219)  
 Nowak M., S15 (45)  
 Nowis D., S56 (158)  
 Nuciforo P., S70 (196)  
 Nuo En Chan J., S70 (197)  
 Nuvoloni S., S17 (48)  
 Ny L., S45 (127)

## O

Oaknin A., S48 (133), S49 (137)  
 Oalmann C.J., S127 (357)  
 Oberman F., S104 (294)  
 Oberoi H., S49 (137)  
 Oberoi H.K., S70 (196)  
 Obiedat A., S69 (195)  
 Obrocea M., S30 (86)  
 Obst J., S72 (203)  
 Occhino C., S16 (47)  
 O'Connor M., S22 (64), S23 (66)  
 O'Connor M.J., S55 (154)

Odeniyide P., S59 (166)  
 Odintsov I., S27 (78)  
 O'Driscoll L., S64 (180)  
 O'Dwyer P., S25 (73)  
 O'Dwyer P.J., S8 (11), S84 (235),  
 S86 (238)  
 Ofir-Rosenfeld Y., S123 (345)  
 Ogle C., S62 (175)  
 Ohashi A., S47 (132)  
 Ohayi S.R., S64 (181)  
 Oh D.Y., S17 (50), S116 (326)  
 O'Hearn E., S29 (84)  
 Oh J.H., S92 (254)  
 Ohkubo S., S73 (204)  
 Ohr J., S128 (359)  
 Oh S., S120 (335)  
 Oh S.S., S60 (168), S102 (287)  
 Oiireira M., S49 (137)  
 Okano F., S32 (91)  
 Okoli U., S64 (181)  
 Olaharski D., S19 (54)  
 Oliveira M., S40 (113)  
 Olofsson Bagge R., S46 (127)  
 Olonisakin T., S128 (359)  
 Olson E., S94 (259)  
 Olszanski A.J., S125 (352)  
 Onder T.T., S69 (192)  
 O'Neill F., S64 (180)  
 O'Neill K., S49 (135)  
 Opdam F., S1 (1LBA)  
 Oppermann U., S69 (192)  
 Ormazabal V., S110 (310)  
 Orsini P., S17 (48)  
 Osada A., S73 (204)  
 Oscares M., S51 (142)  
 Osterberg S., S101 (282)  
 Osterhout R., S125 (350)  
 Otake Y., S88 (244)  
 Ou S.H., S122 (341)  
 Ou S.H.I., S6 (8)  
 Özcan C., S15 (43)  
 Pacheco J., S112 (315)  
 Pacheco S., S67 (189)  
 Pachter J., S18 (52)  
 Padhye S., S73 (206), S76 (211)  
 Pagan E., S4 (4)  
 Pagliarini R., S29 (84)  
 Paik P., S25 (73)  
 Pai S., S80 (224)  
 Paladugu S., S103 (290)  
 Pala L., S4 (4)  
 Palma M., S55 (152)  
 Pandey V., S62 (174)  
 Pant S., S7 (9), S10 (19), S98 (272)  
 Papadatos-Pastos D., S117 (330)  
 Papadopoulos K., S13 (37), S14 (38),  
 S111 (313), S121 (337)  
 Papadopoulos K.P., S67 (188)  
 Paprcka S., S103 (290), S110 (309)  
 Parazzoli A., S17 (48)  
 Parchment R., S62 (175)  
 Pardo M., S50 (139)  
 Parikh A., S34 (95)  
 Park D., S35 (99)  
 Park E., S72 (201), S110 (309)

- Parker G., S81 (225)  
 Parke Schrank T., S119 (334)  
 Park H., S92 (256)  
 Park J., S20 (59)  
 Park J.O., S116 (326)  
 Park J.S., S37 (104)  
 Park S., S110 (311)  
 Park S.I., S99 (275)  
 Park S.J., S37 (104)  
 Park Y.C., S53 (147)  
 Park Y.H., S37 (104)  
 Park Y.S., S60 (168), S102 (287)  
 Pascual Reguant L., S61 (172)  
 Pasquali S., S68 (191)  
 Pastok M., S104 (292)  
 Patel M., S36 (101)  
 Patel P., S16 (47)  
 Patel R., S117 (330)  
 Patel V., S19 (56)  
 Paterson E., S20 (58)  
 Pathi S., S47 (131)  
 Patnaik A., S13 (37), S14 (38), S111 (313), S121 (337)  
 Patton D., S8 (11), S25 (73)  
 Patton D.R., S84 (235), S86 (238)  
 Paulitschke V., S3 (2)  
 Paveley R., S44 (124)  
 Pavić A., S114 (322)  
 Pawelczak K., S101 (283)  
 Pawelczak K.S., S100 (281)  
 Paz K., S69 (195)  
 Pearson A.T., S79 (221)  
 Pearson P., S7 (10)  
 Pe'er D., S4 (5)  
 Peiró S., S61 (172)  
 Pei X., S20 (60)  
 Peix J., S120 (336)  
 Pelish H.E., S76 (212), S78 (218)  
 Penack O., S11 (30)  
 Percio S., S68 (191)  
 Perera P., S43 (120), S53 (148)  
 Perez A.J., S110 (310)  
 Perez-Lopez R., S70 (196)  
 Pérez-Pujol S., S48 (133)  
 Perišić Nanut M., S124 (346)  
 Persad S., S4 (5)  
 Personeni N., S2 (3LBA)  
 Peskin A., S14 (38)  
 Pessaux P., S93 (257)  
 Peters N., S117 (330)  
 Petrocchi A., S26 (77)  
 Petru E., S44 (124)  
 Petruskeviciute M., S97 (269)  
 Pettitt S., S66 (186)  
 Pezo R., S31 (87)  
 Phatak P., S76 (210)  
 Phelps C., S28 (82)  
 Philpott M., S69 (192)  
 Piast R., S90 (248)  
 Picard R., S34 (95)  
 Pieczykolan J., S90 (248)  
 Piening B., S97 (271)  
 Pierrat O., S104 (291), S126 (353)  
 Pietrow P., S90 (248)  
 Piha-Paul S., S17 (50)  
 Piha-Paul S.A., S7 (9), S10 (19), S82 (228)  
 Pike L., S58 (162)  
 Pilch Z., S56 (158)  
 Pillie P.G., S10 (19)  
 Pilon-Thomas S., S90 (250)  
 Pinarbasi-Degirmenci N., S69 (192)  
 Pincheira R., S51 (142), S55 (152)  
 Pincus L., S87 (241), S90 (249)  
 Pines J., S66 (186)  
 Pini T., S69 (195)  
 Pinto N., S28 (82)  
 Pinyol R., S120 (336)  
 Piofczyk T., S97 (269)  
 Piqué-Gili M., S120 (336)  
 Pitman J., S34 (97)  
 Planoutene M., S100 (279)  
 Plawat R., S32 (90)  
 Ploeger B., S101 (282)  
 Pluard T., S36 (101)  
 Podkalicka P., S15 (45), S56 (158)  
 Poel D., S22 (63)  
 Poh A., S13 (35)  
 Poirot L., S15 (41)  
 Poklepovic A., S86 (238)  
 Pokorska-Bocci A., S9 (16)  
 Poland S., S70 (197)  
 Pollard K., S17 (49)  
 Ponce S., S11 (22), S26 (74)  
 Poniatowska K., S104 (292)  
 Ponnusamy S., S105 (296)  
 Pons G., S28 (81)  
 Ponz-Sarvisé M., S116 (326)  
 Poon E., S74 (208)  
 Popat S., S1 (2LBA), S75 (209)  
 Popiel D., S90 (248)  
 Poradosu E., S113 (319)  
 Porath K., S92 (255)  
 Pouwels J., S98 (272)  
 Powers M., S35 (98)  
 Pozdeyev N., S58 (162)  
 Pradier A., S106 (297)  
 Pradines A., S55 (153)  
 Pratilas C., S3 (3), S17 (49)  
 Pratilas C.A., S59 (166)  
 Prenen H., S122 (341)  
 Pressey J.G., S28 (82)  
 Price L., S114 (321), S115 (324)  
 Price M.R., S39 (110)  
 Prince T., S27 (79)  
 Profitós Pelejà N., S112 (314)  
 Proj M., S124 (346)  
 Prota A., S65 (184)  
 Puca F., S26 (77)  
 Pucci V., S26 (77)  
 Punkosdy G., S40 (111)  
 Punzalan B., S3 (1)  
 Purandare A., S29 (83)  
 Purandare N., S48 (134)  
 Purcet S., S68 (190)  
 Putker M., S114 (321), S115 (324)  
 Pye H., S64 (181)
- Q**
- Qian W., S9 (15), S96 (266)  
 Qiu R., S86 (240)  
 Qiu Y., S91 (251), S91 (252), S91 (253)  
 Querol J., S61 (172)  
 Quintana E., S59 (164)  
 Quiroz A., S51 (142)  
 Quist J., S50 (139), S66 (186)  
 Qureshy S., S3 (1)  
 Qu S., S103 (290)  
 Qvortrup C., S118 (331)
- R**
- Rabelo-Fernandez R., S79 (219)  
 Radzimiński A., S15 (45)  
 Raghad A., S90 (249)  
 Raimondi M.V., S65 (184)  
 Rajagopal N., S53 (148)  
 Rajagopal S., S125 (349)  
 Rajurkar M., S40 (111)  
 Ramachandra M., S69 (193)  
 Ramon J., S5 (7)  
 Ramos A., S104 (294)  
 Ramos L., S39 (109)  
 Rana S., S62 (173)  
 Randall K., S49 (136)  
 Randazzo P., S26 (77)  
 Raphael J.A., S31 (87)  
 Rasco D., S13 (37), S14 (38), S111 (313), S121 (337)  
 Rasco D.W., S67 (188)  
 Rashed S., S73 (206), S76 (211)  
 Rastelli L., S125 (349)  
 Rattanaburee T., S45 (126), S71 (200), S73 (205)  
 Rausch O., S123 (345)  
 Raynaud F., S104 (291), S126 (353)  
 Raynaud F.I., S35 (98)  
 Read O.J., S46 (128)  
 Reckamp K., S84 (235)  
 Reddy A., S73 (206)  
 Re Depaolini S., S17 (48)  
 Redfern D., S104 (293), S115 (323)  
 Reen V., S50 (139)  
 Reeves E., S126 (353)  
 Regan D., S95 (261)  
 Reig M., S2 (3LBA)  
 Reilly E., S92 (255)  
 Reilly N.M., S24 (71)  
 Reinhart R., S62 (175)  
 Reis-Filho J., S99 (278)  
 Reiss M., S80 (224)  
 Reiter L., S104 (293), S115 (323)  
 Reynaud E., S3 (1)  
 Rhein S., S12 (32)  
 Rhudy J., S7 (9)  
 Riaud M., S63 (178)  
 Richards M., S126 (353)  
 Richardson D., S88 (245)  
 Rieger R., S81 (227)  
 Riester M., S21 (61)  
 Rizzo E., S55 (152)

- Rimassa L., S2 (3LBA)  
 Rinaldi A., S65 (184), S80 (223)  
 Rios-Doria J., S70 (197)  
 Risi G., S65 (183)  
 Rivera V., S85 (236)  
 Roberti D., S2 (3LBA)  
 Robeva A., S21 (61)  
 Robin M., S98 (274)  
 Robinson J., S81 (226), S81 (227)  
 Robinson M., S117 (330)  
 Robusto M., S108 (304)  
 Rocca R., S65 (184)  
 Rocha L., S110 (309)  
 Roche S., S64 (180)  
 Rodon Ahnert J., S7 (9), S10 (19)  
 Rodón J., S125 (352)  
 Rodon L., S41 (116)  
 Rodríguez L., S13 (37)  
 Rodríguez M., S81 (227)  
 Rodríguez S., S89 (247)  
 Roesl C., S97 (269)  
 Roger B., S49 (137)  
 Röhlen N., S93 (257)  
 Rohrborg K.S., S118 (331)  
 Rojas K., S23 (67), S49 (137)  
 Roma J., S28 (81)  
 Román R., S89 (247)  
 Roman V., S79 (220)  
 Romashko D., S86 (239)  
 Rong Y., S72 (202)  
 Rose A.A.N., S63 (178)  
 Rosell R., S89 (247)  
 Rose M., S19 (57)  
 Rosenberg A., S79 (221)  
 Rosen E., S34 (95)  
 Rosenthal A., S121 (337)  
 Rossanese O., S104 (291), S126 (353)  
 Rossi D., S106 (297), S107 (302), S108 (304)  
 Rossmüller G., S124 (347)  
 Rotbein I., S9 (16)  
 Rotolo J., S82 (230)  
 Rotxes M., S70 (196)  
 Roué G., S112 (314)  
 Rouleau E., S11 (22)  
 Roulston A., S61 (171), S99 (278), S100 (279)  
 Roumeliotis T.I., S50 (139)  
 Rouskin-Faust T., S63 (177)  
 Rousselle E., S63 (178)  
 Roviš T., S69 (195)  
 Rowbottom M., S125 (350)  
 Rowe C., S101 (284)  
 Równicki M., S90 (248)  
 Roxanis I., S50 (139)  
 Roy G., S117 (328)  
 Roy J., S95 (263)  
 Rozsahegyi E., S63 (177)  
 Rubinstein L., S25 (73)  
 Rubinstein L.V., S8 (11), S84 (235), S86 (238)  
 Rubinsztein D.C., S104 (293)  
 Rudicell R., S125 (352)  
 Rui H., S74 (207)  
 Ruiz de Galareta M., S120 (336)  
 Ruiz V., S108 (305)  
 Rumde P., S128 (359)  
 Rushton M., S31 (87)  
 Russo A., S26 (74)  
 Ruzicka R., S54 (150)  
 Rybinski K., S87 (243)  
 Ryu S.Y., S99 (275)  
 Rzymiski T., S23 (67), S56 (158)
- ## S
- Saavedra O., S49 (137), S70 (196)  
 Sabanathan D., S36 (101)  
 Sabino F., S115 (323)  
 Sachsenmeier K., S125 (352)  
 Sacilotto N., S67 (189), S68 (190)  
 Sadar M.D., S72 (203)  
 Sadhu M.N., S125 (349)  
 Sadrolhefazi B., S1 (1LBA)  
 Saetang J., S45 (126)  
 Saffi G.T., S106 (298)  
 Saffran D., S74 (208)  
 Sagayama K., S122 (342)  
 Saggi G., S125 (352)  
 Sahai V., S116 (326)  
 Sah V., S45 (127)  
 Saini H., S83 (232)  
 Sakaguchi M., S122 (342)  
 Salas A., S51 (142)  
 Salguero C., S10 (19)  
 Salihi H., S13 (37)  
 Salimraj R., S126 (353)  
 Salmena L., S94 (260), S106 (298)  
 Salmikangas S., S117 (329)  
 Salomatov A., S86 (239)  
 Salom B., S17 (48)  
 Salsi E., S17 (48)  
 Salvatore G., S124 (348)  
 Salvestrini V., S124 (348)  
 Samajdar S., S69 (193)  
 Sampo M., S117 (329)  
 Sanchez-Bustos P., S108 (303)  
 Sánchez de Toledo J., S28 (81)  
 Sanchez-Martin M., S40 (111)  
 Sánchez-Serra S., S24 (69)  
 Sánchez Víneces S., S112 (314)  
 Sandanayaka V., S127 (355)  
 Sanduzzi-Zamparelli M., S2 (3LBA)  
 Sanfelice D., S83 (231)  
 Sankar N., S39 (109)  
 Sansa-Girona J., S28 (81)  
 Santana-Viera L., S24 (69)  
 Santich B.H., S3 (1)  
 Santini C., S124 (348)  
 Sanz M., S70 (196)  
 Sapetschnig A., S123 (345)  
 Sarantopoulos J., S57 (160)  
 Sarkaria J., S92 (255)  
 Sarma P.P., S56 (156)  
 Sartori G., S107 (301)  
 Sasso R., S26 (77)  
 Satala G., S15 (45)  
 Saturno G.S., S17 (48)  
 Saunders A., S58 (161)  
 Saunders C., S123 (345)  
 Saura C., S48 (133), S49 (137), S106 (299)  
 Sawretse L., S117 (330)  
 Sawyers C., S4 (5)  
 Scalabri F., S26 (77)  
 Scalzo S., S117 (330)  
 Schaeffeler E., S12 (33)  
 Scheinberg D., S3 (1)  
 Scheld D., S11 (30)  
 Schinagl A., S124 (347)  
 Schlabach M., S37 (105)  
 Schlemmer S., S95 (261)  
 Schlom J., S5 (6)  
 Schmees C., S12 (33)  
 Schmidt-Kittler O., S116 (326)  
 Schmitt C.A., S41 (115)  
 Schmitt N., S127 (356)  
 Schnell C., S14 (39)  
 Schostak M., S12 (33)  
 Schram A., S116 (326)  
 Schreck K., S3 (3)  
 Schreiber S., S3 (2)  
 Schroeder B., S97 (271)  
 Schroeder J., S9 (17)  
 Schultz N.D., S10 (21)  
 Schulz A., S28 (82)  
 Schulze V., S9 (17)  
 Schulz R., S86 (239)  
 Schuster C., S93 (257)  
 Schuster V., S19 (56)  
 Schwab M., S12 (33)  
 Schwarz D., S19 (56)  
 Schwarzer A., S40 (113)  
 Schwarzmüller A., S14 (39)  
 Schweppe R., S19 (57), S58 (162)  
 Sdelci S., S61 (172)  
 Secrist J.P., S24 (71)  
 Seetharaman J., S110 (308)  
 Segura M.F., S28 (81)  
 Sehlike R., S44 (124)  
 Seitz L., S20 (58), S110 (309)  
 Selaković Ž., S114 (322)  
 Selaković M., S114 (322)  
 Selenica P., S99 (278)  
 Self-Fordham J., S123 (345)  
 Selvaggi G., S108 (305)  
 Senekowitsch M., S44 (124)  
 Senior E., S124 (346)  
 Sen M., S128 (359)  
 Senter R.K., S127 (357)  
 Serna G., S70 (196)  
 Serra C., S25 (72)  
 Serra-Camprubi Q., S61 (172)  
 Serra J., S1 (1LBA)  
 Serrano del Pozo E., S47 (130)  
 Serrano E., S24 (68), S38 (106), S44 (123), S46 (129), S53 (149)  
 Serrano L., S61 (172)  
 Serra V., S53 (149), S106 (299)  
 Setton J., S99 (278)  
 Setty M., S4 (5)  
 Seymour L., S31 (87)  
 Shacham S., S40 (112)  
 Shafa A., S54 (151)

- Shakespeare W., S85 (236)  
 Shankavaram U., S11 (30)  
 Sharma A., S104 (294), S127 (358)  
 Sharma M., S14 (38), S121 (337)  
 Sharma S., S32 (91), S127 (355)  
 Sharma V., S19 (57)  
 Sharp S., S35 (98)  
 Shaw G., S64 (181)  
 Shawgo R., S53 (148)  
 Shaw P., S88 (245)  
 Shayan K., S45 (125)  
 Shay J., S30 (86)  
 Shell S.A., S116 (326)  
 Shen B., S60 (167), S111 (312)  
 Sheng Y., S9 (15)  
 Shenker S., S37 (105)  
 Shen M.M., S10 (21)  
 Shen W., S39 (109)  
 Shepard H.M., S27 (80)  
 Shergill A., S72 (201)  
 Shibutani T., S73 (204)  
 Shi J., S60 (167), S111 (312)  
 Shimizu T., S88 (244)  
 Shin N., S79 (220)  
 Shin Ogawa, L., S86 (239)  
 Shin S.J., S85 (237)  
 Shin Y.K., S37 (104)  
 Shi R., S91 (251), S91 (252), S91 (253)  
 Shoemaker R., S19 (54)  
 Shrishrimal S., S41 (114)  
 Shu C., S62 (174)  
 Sia D., S120 (336)  
 Sicinska E., S51 (143)  
 Siddiqui A., S47 (131), S57 (160)  
 Siderits R., S117 (328)  
 Sidransky D., S73 (206), S76 (211)  
 Siegel F., S9 (17)  
 Siegel P.M., S63 (178)  
 Siegel S., S9 (17)  
 Sigalotti L., S68 (191)  
 Sihto H., S117 (329)  
 Silverio A., S48 (133)  
 Silvers T., S62 (175)  
 Simonetta F., S106 (297)  
 Simon J., S127 (357)  
 Simpson B., S64 (181)  
 Simpson K., S113 (317)  
 Sims R., S119 (333)  
 Singer J., S44 (124)  
 Singh A., S104 (294)  
 Singh H., S51 (141)  
 Singh K., S20 (60)  
 Singh M., S59 (164)  
 Singh P.K., S69 (193)  
 Singh V., S104 (294)  
 Siteni S., S30 (86)  
 Siu L.L., S5 (6)  
 Skaggs H., S79 (220)  
 Skaist A., S59 (166)  
 Skalska J., S104 (292)  
 Skoda M., S15 (45)  
 Slater D., S71 (198)  
 Smith A., S58 (161), S97 (269)  
 Smith J.A., S59 (164)  
 Smith L., S121 (337)  
 Smith S., S22 (64), S23 (66)  
 Smolenski C., S11 (22)  
 Smyth T., S57 (159)  
 Snijder B., S3 (2)  
 Soffientini C., S68 (191)  
 Soglia J., S6 (8)  
 Soifer H., S58 (161)  
 Sola B., S112 (314)  
 Šolaja B., S114 (322)  
 Soler Agesta R., S39 (110)  
 Solit D.B., S10 (21)  
 Soliva R., S67 (189), S68 (190)  
 Solomon B., S1 (2LBA), S75 (209)  
 Somlyay M., S44 (124)  
 Sommakia S., S47 (131)  
 Somwar R., S27 (78)  
 Song F., S99 (277)  
 Song Z., S25 (73), S84 (235), S86 (238)  
 Son J.A., S94 (258), S105 (295)  
 Sootome H., S77 (214)  
 Sorensen P., S39 (109)  
 Sorger P., S51 (143)  
 Soria-Bretones I., S63 (178)  
 Soto A., S87 (243)  
 Sottili M., S124 (348)  
 Soucek L., S5 (7), S24 (68), S38 (106),  
 S38 (108), S44 (123), S46 (129),  
 S47 (130), S53 (149)  
 Sowińska M., S15 (45)  
 Spanggaard I., S118 (331)  
 Spanjaard E., S114 (321)  
 Spanò V., S65 (184)  
 Spear M., S87 (241), S90 (249)  
 Spiegelman V., S104 (294)  
 Spigel D.R., S71 (198)  
 Spira A., S57 (160)  
 Spira A.I., S6 (8)  
 Spreafico A., S63 (178)  
 Spriano F., S65 (183), S80 (223),  
 S107 (301), S107 (302),  
 S108 (304)  
 Springfield C., S1 (2LBA), S75 (209)  
 Squatrito M., S38 (106)  
 Srdic-Rajic T., S114 (322)  
 Sridhar A.N., S64 (181)  
 Sridharan S., S128 (359)  
 Sridhar S., S103 (290), S110 (309)  
 Stacchiotti S., S68 (191)  
 Stachowicz A., S15 (45)  
 Stackpole A., S111 (313)  
 Stagnaro E., S110 (309)  
 Stalbovskaya V., S122 (341)  
 Staniszewska M., S13 (36)  
 Starrett J., S16 (47)  
 Stathis A., S65 (183), S80 (223),  
 S89 (246), S107 (302), S108 (304)  
 Steadman K., S81 (225)  
 Stecklum M., S12 (32), S41 (115)  
 Stegmeier F., S37 (105)  
 Steidl U., S49 (136)  
 Steinmetz M., S65 (184)  
 Stein S., S43 (120), S94 (259)  
 Stellato C., S17 (48)  
 Stephen P., S99 (277)  
 Stephan-Otto Attolini C., S95 (264)  
 Stern P., S127 (357)  
 Stevens C., S70 (197)  
 Stewart J., S99 (277)  
 Stocco R., S61 (171)  
 Stoffel C., S3 (2), S115 (325)  
 Stone G., S51 (143)  
 Stone R., S51 (141)  
 Stopatschinskaja S., S1 (2LBA)  
 Stracker T.H., S95 (264)  
 Stroopinsky D., S125 (352)  
 Strzemieczna E.M., S68 (190)  
 Stuart D.D., S29 (84)  
 Stuckey J., S33 (94)  
 Stump K., S79 (220)  
 Stuurman D., S42 (118), S43 (119)  
 Subbiah V., S7 (9), S10 (19),  
 S116 (326)  
 Suga J.M., S82 (228)  
 Suhling K., S70 (197)  
 Sullivan F., S81 (226), S81 (227)  
 Sullivan P., S37 (105)  
 Sullivan R.J., S31 (89)  
 Sun M., S75 (209)  
 Sun Y., S6 (8), S27 (79), S76 (212)  
 Supek F., S95 (264)  
 Surampudi U.K., S56 (156)  
 Su Z., S5 (6)  
 Suzuki A., S30 (85)  
 Swanson R., S16 (47)  
 Swiecicki P., S79 (221)  
 Swinarski D., S103 (290)  
 Świtalska-Drewniak M., S104 (292)  
 Świtalska M., S13 (36)  
 Syed M., S92 (256)  
 Symeonides S., S82 (230),  
 S117 (330)  
 Szabo A., S96 (265)  
 Szado T., S71 (198)  
 Szalontay L., S28 (82)  
 Szender J., S14 (38)  
 Szlosarek P., S64 (179)
- ## T
- Tabbò F., S26 (74)  
 Tabernero J., S48 (133), S49 (137),  
 S70 (196)  
 Tagliamento M., S11 (22), S26 (74)  
 Tai D., S116 (326)  
 Tai P., S63 (178)  
 Takagi T., S104 (292)  
 Takebe N., S62 (175)  
 Takehara K., S88 (244)  
 Talbot R., S104 (291)  
 Tam T., S72 (203)  
 Tanaka H., S30 (85)  
 Tanawattanasuntorn T., S45 (126),  
 S71 (200)  
 Tan D.S.W., S21 (61)  
 Tan E.H., S19 (53)  
 Tang H., S78 (217)  
 Tangpeerachaikul A., S76 (212),  
 S78 (218)  
 Tang X., S10 (21)

Tao Y., S122 (343)  
 Tarantelli C., S65 (182), S65 (183),  
 S65 (184), S80 (223), S89 (246),  
 S106 (297), S107 (301), S107 (302),  
 S108 (304)  
 Taraporn S., S45 (126)  
 Tastanova A., S3 (2)  
 Tauriello D., S22 (63)  
 Tavera L., S63 (177)  
 Taylor B., S96 (265)  
 Taylor Meadows K., S125 (350)  
 Te-Chang L., S114 (320)  
 Teicher B., S62 (175)  
 Teng T., S84 (233)  
 Te Poele R., S35 (98)  
 Terrett N., S20 (59)  
 Tervonen T., S98 (272)  
 Terzo E., S73 (206), S76 (211)  
 Teubel W.J., S43 (119)  
 Texido G., S17 (48)  
 Thabussot H., S24 (68), S38 (106),  
 S44 (123), S46 (129), S47 (130),  
 S53 (149)  
 Thakur S., S86 (239)  
 Thamake S., S75 (209)  
 Thamm D., S95 (261)  
 Thapa B., S96 (265)  
 Thavarajah V., S64 (181)  
 Thiele M., S124 (347)  
 Thiyagarajan S., S69 (193)  
 Thiyagarajan T., S105 (296)  
 Thompson J., S57 (160)  
 Thompson P., S81 (225)  
 Thongpanchang T., S71 (200), S73 (205)  
 Tian T.V., S61 (172)  
 Tibrewal N., S103 (290)  
 Tien A.H., S72 (203)  
 Timmers C., S79 (220)  
 Tipmanee V., S73 (205), S113 (318)  
 Tirado O.M., S24 (69)  
 Tirunagaru V., S20 (60)  
 Tiwari S., S51 (141)  
 Tobin E., S37 (105)  
 Tobvis Shifrin N., S59 (164)  
 Tolcher A., S7 (10), S80 (224), S88 (245),  
 S92 (256)  
 Toledo R., S70 (196)  
 To M., S127 (358)  
 Tomczyk I., S15 (45)  
 Tomczyk T., S104 (292)  
 Tomlinson R., S104 (293)  
 Tomljanovic I., S43 (119)  
 Toniatti C., S26 (77)  
 Tonini M., S26 (75), S84 (233), S84 (234)  
 Tontsch-Grunt U., S54 (150)  
 Topolska-Woś A., S13 (36)  
 Torga G., S66 (186)  
 Torres-Martin M., S120 (336)  
 Tortoreto M., S68 (191)  
 Tosi D., S98 (274)  
 Toso A., S93 (257)  
 Toth J., S81 (225)  
 Toulany M., S45 (125)  
 Towers C., S42 (117)  
 Tracz A., S104 (292)

Traexler P.E., S54 (150)  
 Trębicka D., S104 (292)  
 Trendell J., S66 (186)  
 Tripathy D., S52 (146)  
 Tripodo C., S55 (154)  
 Troiani S., S17 (48)  
 Trombino A., S22 (64), S23 (66)  
 Trone D., S1 (2LBA), S75 (209)  
 Trucia M., S36 (102)  
 Truong S., S39 (109)  
 Tsagkogeorga G., S123 (345)  
 Tsai A., S84 (233), S84 (234)  
 Tsai F., S34 (96)  
 Tsai Y.T., S5 (6)  
 Tsang J., S32 (90)  
 Tsann-Long S., S114 (320)  
 Tsimberidou A.M., S7 (9), S10 (19)  
 Tsugawa H., S87 (242)  
 Tsukioka S., S73 (204)  
 Tu D., S31 (87)  
 TuPro C., S3 (2)  
 Turchi J., S101 (283)  
 Turchi J.J., S100 (281)  
 Turko P., S3 (2), S115 (325)  
 Tutt A., S66 (186)  
 Tutt A.J., S50 (139)  
 Tu X., S118 (332)  
 Tyagi E., S47 (131)  
 Tyler R., S77 (215), S78 (217)

## U

Ubhi T., S99 (278)  
 Uenaka T., S87 (242), S87 (243),  
 S88 (244)  
 Ueno N., S52 (146)  
 Ugurlu M.T., S76 (211)  
 Ulahannan S., S92 (256)  
 Ulmer S., S111 (313)  
 Um I.H., S46 (128)  
 Um J., S37 (104)  
 Unciti-Broceta A., S113 (319)  
 Unni N., S82 (228)  
 Upadhyayula S.S., S55 (154)  
 Uttamsingh S., S92 (256)

## V

Vaishampayan U., S125 (352)  
 Vakkalanka S., S33 (92), S33 (93)  
 Valenti M., S35 (98)  
 Valiyeva F., S79 (219)  
 Vallejos A., S96 (265)  
 Valsasina B., S17 (48)  
 Valton J., S15 (41)  
 van Berkel P., S101 (284)  
 van den Hombergh E., S22 (63)  
 Van Der Putten E., S109 (306)  
 VanderVere-Carozza P., S101 (283)  
 VanderVere-Carozza P.S., S100 (281)  
 VanderWalde A., S71 (198)  
 van der Wekken A.J., S6 (8)  
 van de Werken H.J.G., S43 (119)  
 Vandross A., S7 (10), S92 (256)

Van Eaton K., S42 (117), S107 (300)  
 van Erp N., S22 (63)  
 Van Hemelryk A., S42 (118), S43 (119)  
 Van Montfort R., S104 (291), S126 (353)  
 van Royen M., S43 (119)  
 van Royen M.E., S42 (118)  
 Van Tellingen O., S103 (289)  
 van Weerden W.M., S42 (118), S43 (119)  
 Varasi M., S108 (304)  
 Vargas D.B., S3 (1)  
 Varicchio L., S100 (279)  
 Vasiliauskaitė L., S123 (345)  
 Vasseur D., S11 (22), S26 (74)  
 Veach D., S3 (1)  
 Vecchio D., S34 (95)  
 Veeraraghavan S., S33 (93)  
 Velcheti V., S1 (2LBA)  
 Velilla T., S59 (164)  
 Vellano C.P., S54 (150)  
 Vendra V., S128 (359)  
 Venekamp N., S103 (289)  
 Venkatesh J., S97 (270)  
 Vera L., S47 (130)  
 Verge V., S11 (22)  
 Verheul H., S22 (63)  
 Verma S., S3 (1)  
 Vernier J.M., S19 (54)  
 Vesterinen T., S117 (329)  
 Vicent S., S47 (130)  
 Victorasso Jardim Perassi B., S90 (250)  
 Victorasso Jardim Perassi M., S80 (224)  
 Vieito M., S17 (50), S70 (196)  
 Vieito Villar M., S49 (137)  
 Villanona-Calero M., S17 (50)  
 Villanueva J., S106 (299)  
 Villanueva-Fernandez E., S83 (231)  
 Viola L., S42 (117), S107 (300)  
 Virginia B., S36 (101)  
 Virsik P., S37 (103)  
 Viswanadha S., S33 (92), S33 (93)  
 Viswanathan V., S3 (2)  
 Vitenstein A., S69 (195)  
 Vitoc V., S30 (86)  
 Vivas-Mejia P., S79 (219)  
 Vladimer G., S44 (124)  
 Vojnic M., S27 (78)  
 Vojtasova E., S101 (284)  
 Vokes E., S79 (221)  
 Volgina A., S70 (197)  
 Von Hoff D.D., S32 (91), S34 (96)  
 Vonmelchert B., S59 (164)  
 Voors-Pette C., S49 (136)  
 Vukovic V., S49 (136)  
 Vultaggio S., S108 (304)  
 Vyas A., S112 (315), S127 (356)

## W

Wadosky K., S4 (5)  
 Wagner S., S57 (159)  
 Walczak M., S104 (292)  
 Waldman A., S49 (135)  
 Walker C., S66 (186)  
 Walker E., S19 (56)

Wallis N., S57 (159), S83 (232), S104 (294)  
 Walther W., S12 (32), S12 (33)  
 Wang A., S74 (207)  
 Wang C., S73 (206), S76 (211)  
 Wang D., S118 (332)  
 Wang G., S41 (114), S113 (317)  
 Wang H., S63 (178)  
 Wang J., S17 (49), S18 (51), S34 (95), S44 (122), S49 (135), S52 (146), S72 (203), S74 (207), S80 (224), S110 (308)  
 Wang L., S15 (42), S54 (151)  
 Wang M., S27 (79), S36 (102)  
 Wang N., S61 (170), S110 (309)  
 Wang Q., S72 (202)  
 Wang R., S27 (79)  
 Wang S., S106 (297)  
 Wang V., S8 (11), S25 (73), S84 (235), S86 (238)  
 Wang W., S29 (84)  
 Wang Y., S27 (79), S81 (227), S98 (273)  
 Wang Z., S27 (79)  
 Ward G., S83 (232)  
 Wardyn J.D., S55 (154)  
 Warner S., S47 (131), S57 (160)  
 Warshaviak D., S40 (112)  
 Wasson M.C., S97 (270)  
 Wasson P., S97 (269)  
 Watanabe A., S57 (160)  
 Waters N., S22 (64), S23 (66)  
 Weber M., S79 (220)  
 Weekes D., S50 (139), S66 (186)  
 Weeks A., S95 (263)  
 Weerasinghe R., S97 (271)  
 Wee S., S79 (220)  
 Wegmann R., S3 (2)  
 Weigel B.J., S28 (82)  
 Weisberg E., S51 (141)  
 Weitsman G., S70 (197)  
 Wei Y., S94 (259)  
 Wei Yin W.Y., S27 (79)  
 Wendler J.J., S12 (33)  
 Wengner A., S101 (282)  
 Weon J.H., S94 (258), S105 (295)  
 Weroha S.J., S54 (151)  
 Wesolowski R., S36 (101)  
 Westin S.N., S7 (9), S10 (19)  
 Wheeler D.L., S45 (125)  
 Whelan C., S90 (250)  
 Wherry E.J., S5 (6)  
 Whitaker H., S64 (181)  
 Whitehead Z., S71 (198)  
 Whitfield J., S38 (106), S53 (149)  
 Whitfield J.R., S24 (68), S38 (108), S46 (129)  
 Whittington D., S26 (75), S84 (233)  
 Whitton B., S126 (353)  
 Wick M., S13 (37), S14 (38), S111 (313), S121 (337)  
 Wiczorek M., S90 (248)  
 Wiedemeyer W., S41 (114), S113 (317)  
 Wiedmann A., S101 (282)  
 Wiegert E., S82 (230)  
 Wijerathna S., S127 (355)

Wilkinson G., S101 (282)  
 Will B., S49 (136)  
 Williams A., S82 (230)  
 Williams M., S25 (73), S49 (135)  
 Williams P.M., S8 (11), S84 (235), S86 (238)  
 Wilson J., S33 (94)  
 Winkler-Penz T., S44 (124)  
 Winkler R., S79 (221)  
 Winski S., S81 (226), S81 (227)  
 Witta S., S107 (300)  
 Wójcik K., S104 (292)  
 Wolf J., S1 (2LBA), S21 (61), S75 (209)  
 Woolley J.F., S106 (298)  
 Worden F.P., S79 (221)  
 Workman P., S35 (98), S83 (231)  
 Wosikowski K., S109 (306)  
 Woś M., S13 (36)  
 Wouters B., S121 (339), S121 (340)  
 Wright C., S110 (308)  
 Wright J., S25 (73), S62 (175)  
 Wright J.J., S8 (11), S84 (235)  
 Wrobel L., S104 (293)  
 Wu J., S77 (215), S110 (308)  
 Wu L., S79 (220)  
 Wu Y.L., S1 (1LBA)  
 Wuyts J., S97 (269)  
 Wylie A., S37 (105)

## X

Xaus J., S67 (189), S68 (190)  
 Xiao K., S43 (121)  
 Xiong L., S122 (343)  
 Xu L., S40 (111)  
 Xu T., S4 (5)  
 Xu Y., S22 (65)

## Y

Yachnin J., S116 (326)  
 Yamada M., S73 (204)  
 Yamamoto N., S1 (1LBA), S57 (160)  
 Yamanaka Y., S30 (85)  
 Yamashita S., S73 (204)  
 Yang J., S14 (40), S34 (95), S79 (220)  
 Yang L., S81 (225)  
 Yang S., S22 (65)  
 Yang S.N., S86 (239)  
 Yang X., S27 (79)  
 Yang Y.O., S79 (220)  
 Yap T.A., S7 (9), S10 (19)  
 Yassin-Kassab A., S61 (170)  
 Yasunaga M., S87 (242)  
 Yde C.W., S118 (331)  
 Yedier-Bayram O., S69 (192)  
 Ye E., S85 (236)  
 Ye M., S79 (220)  
 Ye Q., S16 (47)  
 Ye Y., S79 (220)  
 Yi J., S34 (95)  
 Yim C.Y., S39 (110)  
 Ying H., S111 (312)  
 Ying W., S27 (79)

Yisraeli J., S104 (294)  
 Yoda S., S78 (218), S84 (233)  
 Yoh K., S1 (1LBA)  
 Yonemori K., S88 (244)  
 Yoo J., S102 (286)  
 Yoon J.H., S105 (295)  
 Yoon K.J., S35 (99)  
 Yoon M.G., S94 (258), S105 (295)  
 Yoon S., S72 (201), S96 (267), S96 (268)  
 Yoshinari T., S30 (85)  
 Youk J., S120 (335)  
 Young N., S40 (111)  
 Yuan H., S26 (75)  
 Yuan Y., S7 (9), S10 (19)  
 Yu H., S22 (65)  
 Yu M., S78 (218), S127 (355)  
 Yunokawa M., S88 (244)  
 Yusuf I., S125 (350)  
 Yu W., S71 (198)  
 Yu Y., S102 (287)

## Z

Zacarias-Fluck M., S38 (108)  
 Zacarias-Fluck M., S38 (106), S46 (129), S53 (149)  
 Zacarias-Fluck M.F., S24 (68)  
 Zadeh G., S121 (339), S121 (340)  
 Zaffaroni N., S68 (191)  
 Zaidi M., S121 (339), S121 (340)  
 Zaidi S., S4 (5)  
 Zainuddin M., S125 (349)  
 Žak M., S102 (286)  
 Zamboni N., S3 (2)  
 Zammarchi F., S101 (284)  
 Zamora E., S106 (299)  
 Zamora J., S108 (303)  
 Zandberg D., S128 (359)  
 Zangi L., S102 (286)  
 Zang M., S122 (343)  
 Zarzosa P., S28 (81)  
 Zatreanu D., S99 (277)  
 Zelichov O., S9 (16)  
 Zeng W., S78 (217)  
 Zernecke A., S11 (30)  
 Zhai B., S39 (109)  
 Zhai Y., S79 (221)  
 Zhang C., S15 (42)  
 Zhang F., S18 (51)  
 Zhang G., S79 (220)  
 Zhang J., S19 (54), S74 (207)  
 Zhang J.J., S34 (96)  
 Zhang L., S17 (49), S118 (332)  
 Zhang M., S84 (233), S84 (234)  
 Zhang N., S60 (167), S111 (312)  
 Zhang S., S77 (215), S78 (217), S85 (236)  
 Zhang V., S41 (114), S113 (317)  
 Zhang W., S26 (75), S92 (255)  
 Zhang X., S62 (174)  
 Zhang Y., S81 (225), S88 (244), S91 (251), S91 (252), S91 (253), S111 (312)

Zhao E., S32 (90)  
Zhao J., S4 (5)  
Zhao T., S72 (201)  
Zhao X., S103 (290)  
Zhao Y., S22 (65)  
Zheng Z., S74 (207)  
Zhong C., S91 (253)  
Zhou H.J., S37 (103)  
Zhou Y., S81 (226), S81 (227)

Zhu J., S43 (121)  
Zhu V.W., S6 (8)  
Zhu Y., S27 (79)  
Zhu Z., S111 (312)  
Zick A., S82 (228)  
Zickuhr G., S66 (185)  
Zihan W., S8 (11)  
Zimmermann M., S99 (278)  
Živanović M., S114 (322)

Zucca E., S106 (297), S107 (302),  
S108 (304)  
Zuco V., S68 (191)  
Zuidema S., S103 (289)  
Zumrut H., S126 (354)  
Zúñiga F.A., S110 (310)  
Zuniga R., S71 (198)  
Zweibel J.A., S86 (238)